BMR PUBLICATIONS COMPACTUS
(LENDING SECTION)
P4



111185



Geochemistry of a tropical estuary and its catchment —Broad Sound, Queensland

P. J. Cook & W. Mayo

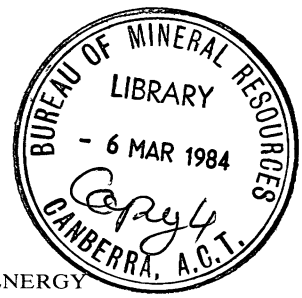
Bulletin 182

BMR
S55(94)
BUL.45
Copy 4

COVER:

False-colour composite image of Broad Sound and environs, prepared from NASA Landsat scene 1324-23280, bands 4, 5, and 7. Data obtained 12 June, 1973, satellite altitude about 920 km.

BMR PUBLICATIONS COMPACTUS
(LENDING SECTION)
04



DEPARTMENT OF NATIONAL DEVELOPMENT AND ENERGY
BUREAU OF MINERAL RESOURCES, GEOLOGY AND GEOPHYSICS

BULLETIN 182

Geochemistry of a tropical estuary and its catchment — Broad Sound, Queensland

P. J. Cook* & W. Mayo**

PART A. Geochemistry of the estuarine system

by
P. J. Cook

PART B. A numerical approach to the geochemistry of the estuarine sediments

by
W. Mayo

* Now at Research School of Earth Sciences, Australian National University, Canberra

** Now at Department of the Treasury, Canberra

AUSTRALIAN GOVERNMENT PUBLISHING SERVICE
CANBERRA 1980

DEPARTMENT OF NATIONAL DEVELOPMENT AND ENERGY
MINISTER: SENATOR THE HON. J. L. CARRICK
SECRETARY: A. J. WOODS

BUREAU OF MINERAL RESOURCES, GEOLOGY AND GEOPHYSICS
DIRECTOR: R. W. R. RUTLAND
ASSISTANT DIRECTOR, GEOLOGICAL BRANCH: J. N. CASEY

Published for the Bureau of Mineral Resources, Geology and Geophysics, by the Australian Government Publishing Service

© Commonwealth of Australia 1980

ISBN 0 642 04449.

ISSUED: SEPTEMBER 1980

Printed by Mercury-Walch 5-7 Bowen Rd, Moonah, Tasmania.

ABSTRACTS

PART A

The Broad Sound geochemical study was undertaken to determine the geochemistry of the catchment, the geochemistry of the estuarine sediments, the influence of the catchment on estuarine geochemistry, the influence of depositional environments on sedimentary geochemistry, and the hydrogeochemistry of estuarine surface waters and interstitial waters.

The catchment studies revealed normal elemental abundances. Although there are some elemental distinctions between the several constituent catchment areas, the homogenisation of sediments which takes place in Broad Sound, coupled with the influence of depositional and post-depositional processes, largely masks any effects which provenance geochemistry might have on estuarine geochemistry.

The estuarine sediments range in composition between limestones, calcareous sandstones, and non-calcareous mudstones. Elemental concentrations are similar to world average values. Most minor and trace elements are associated with the carbonate fraction (Sr, Cd, La, Y(?)) or the clay fraction (organic C, B, Cu, Pb, Zn, Sc(?), Ti, V, Cr, Fe, Co, Ni). Some elements (P, Mg) are associated with both. Fe in ferruginous coatings on carbonate nodules of the shallow-marine environment is accompanied by Mo and Mn. Absolute concentrations of trace elements give no guide to depositional environments, but the concentrations of some metals (e.g. Zn, Cr, Ni) recalculated for the non-calcareous fraction only, and ratios such as Mn/Fe, Cu/Pb, and Cu/Zn, may be useful parameters for recognising depositional environments and for establishing the location of ancient shorelines. Analyses of oyster shells in cheniers ranging in age up to about 5500 years BP indicate some trace-element depletion or concentration in calcareous shells during subaerial weathering.

The estuarine waters were found to be thoroughly mixed, both vertically and laterally, and it is only in the mangrove channels and over the supratidal flats that waters deviate significantly in composition from normal seawater; the mangrove-channel waters at low tide are interesting because of their high phosphate content, low pH, and high salinity. Interstitial waters vary considerably with the depositional environment; those of the intertidal sands have relatively low salinities, whereas the mangrove-swamp and supratidal-flat waters are highly saline. A high Mg-Ca ratio in these pore waters may be responsible for the formation of dolomite concretions in one area; phosphate-rich pore waters are believed to be responsible for some phosphatisation of the concretions.

The study has helped our understanding of geochemical processes in ancient sediments. It also highlights the importance of mangrove swamps as phosphate contributors to modern estuarine systems, and is valuable as a bench-mark against which to measure future geochemical changes in this and other tropical estuaries.

PART B

Q-mode factor analysis successfully classified the Broad Sound estuarine samples into separate sedimentary units, each representing responses to a distinct set of geological processes. Stepwise discriminant analysis and Q-technique canonical correlation analysis supported the factor analysis classification, as did Q-mode cluster analysis when the discriminatory variables identified from the stepwise discriminant analysis were used. Linking this numerical classification of the sediments with a sedimentary model based on grainsize analysis of the sediments aided the identification of differences in the geochemical processes *between* the sedimentary units. Geochemical relations *within* each sedimentary unit were interpreted using a combination of R-mode factor analysis and multiple stepwise regression. R-mode factor analysis distinguished groups of geochemically associated variables, and the groups could be interpreted geologically; multiple stepwise regression clarified the geochemical relations between the variables within each group of associated variables. R-technique canonical correlation analysis, although it supported many of the geochemical interpretations obtained using the combination of factor and regression analyses, was no substitute for this combination of techniques.

Fe and Mn are geochemically important in the Broad Sound estuary system as colloidal particles, oxide coatings on sand-sized grains, and in relict carbonate nodules in the sediments. In these three forms Fe and Mn are associated with Co, Cr, Ni, Sc, Ti, and V in the colloidal particles; with Ba, Co, Sc, and V in the oxide coatings; and with Ba, Co, Mg, Sc, Zn, and P_2O_5 in the carbonate nodules. Zn, P_2O_5, and Ti are associated with the clay fraction. Predictably, Sr and Mg substitute for Ca in biogenic carbonate, and Ti and Zr occur in the heavy-mineral fraction. Thus, the combining of a knowledge of the physical processes controlling sedimentation in Broad Sound with results of various numerical analyses applied in a logical sequence, has led to an understanding of the geochemical processes operating on a wide variety of sediment types.

PREFACE

This volume is the last in a series of three recent Bulletins dealing with estuarine studies, arising from BMR's research program on the distribution of phosphorus and associated elements in estuarine environments*. *Part A*, by Cook, takes a broad view of the geochemistry of the total estuarine system, comprising the catchment, the estuarine sediments, and the surface and pore waters. Statistical techniques are applied to some extent, but the approach adopted is essentially one of geologically-based deduction. *Part B*, by Mayo, deals with the estuarine sediments in greater detail, using more rigorous statistical and mathematical techniques to classify the sediments and to clarify the processes operating within the estuary. The two parts were written independently, use somewhat different approaches, and concentrate on different aspects of the estuarine system.

Computer listings of the original estuarine and catchment sample data sets may be obtained by writing to: Director, Bureau of Mineral Resources, P.O. Box 378, Canberra City, ACT, 2601 (see also Appendix B4).

P. J. Cook
W. Mayo

* Bulletin 178, 'Hydrology and sediments of a temperate estuary — Mallacoota Inlet, Victoria', by G. E. Reinson, was published in 1977; Bulletin 170, 'Sedimentology and Holocene history of a tropical estuary (Broad Sound, Queensland)', by P. J. Cook & W. Mayo, was published in 1978.

CONTENTS

Part A — Geochemistry of the estuarine system

	Page
INTRODUCTION	3
Acknowledgments	3
Climate	5
Previous investigations	5
GEOCHEMISTRY OF THE CATCHMENT	5
Introduction	5
Sampling scheme	5
Analytical methods	9
Statistical and computing procedures	9
Geology	9
Soils	12
Summary of geochemical results	12
Regional variations in content of trace elements and phosphate	13
Phosphate	15
Copper	15
Lead	31
Zinc	31
Cobalt	31
Nickel	31
Relationships between minor and trace elements	31
Phosphate	32
Copper, lead, zinc	32
Manganese, chromium, iron, cobalt, nickel	33
Influence of catchment geochemistry on estuary geochemistry	35
GEOCHEMISTRY OF THE ESTUARINE SEDIMENTS	38
Analytical techniques	39
The sediments of Broad Sound	40
Depositional environments	40
Grainsize variations	42
Mineralogy and petrology of the Holocene sediments	43
Major-element composition of Broad Sound sediments	43
Minor and trace-element geochemistry	45
Phosphate	47
Organic carbon	60
Magnesium	63
Strontium	66
Cadmium, lanthanum, yttrium	69
Molybdenum	69
Barium	69
Copper, lead, zinc	71
Scandium, titanium, zirconium	75
Vanadium, chromium	80
Iron, cobalt, nickel	86
Manganese	90
Geochemistry and depositional environments	90
GEOCHEMISTRY OF HOLOCENE OYSTER SHELLS	95
Analyses	95
Results	96
Variation of composition with age	96
HYDROGEOCHEMISTRY	101
Methods	101
Broad Sound waters	101
Mangrove-channel waters	104
Pore waters	108
Salinity	108
Eh and pH	110
Cations	114
Phosphate	115
IMPLICATIONS OF THE BROAD SOUND GEOCHEMICAL STUDY	117
Geochemical exploration in the Broad Sound drainage basin	117
Influence of catchment geochemistry on estuarine geochemistry	117
Trace elements as indicators of depositional environments	118
The weathering of shells	118
Phosphate deposits in the estuarine environment	119
Estuarine geochemical processes	120
REFERENCES	121

APPENDIXES

A1. Tables listing major and minor oxide composition (percent) of sediment samples from the estuary. 123

A2. Table listing physico-chemical characteristics of estuarine sediments and their expressed pore waters. 127

TABLES

A1. Mean phosphate, iron, and trace-element contents of rocks, soils, and stream sediments from the entire Broad Sound catchment, compared with world average values for various rock types. 13

A2. Means and standard deviations of phosphate, iron, and trace elements in rocks, soils, and stream sediments from the entire Broad Sound catchment (mapped bedrock units listed). 14

Page

A3. Correlation coefficients (log-transformed) for phosphate, iron, and trace-element abundances in bedrock, versus abundances in overlying soil. 15

A4. Comparisons of trace-element, phosphate, and iron means between the four local Broad Sound catchments, for bedrock, soils, and stream sediments. 15

A5. Matrix of correlation coefficients for phosphate, iron, and trace elements in rocks, soils, and stream sediments from the entire Broad Sound catchment. 32

A6. Waverley catchment: matrix of correlation coefficients for phosphate, iron, and trace elements in rocks, soils, and stream sediments. 34

A7. Herbert catchment: matrix of correlation coefficients for phosphate, iron, and trace elements in rocks, soils, and stream sediments. 35

A8. St Lawrence catchment: matrix of correlation coefficients for phosphate, iron, and trace elements in rocks, soils, and stream sediments. 36

A9. Styx catchment: matrix of correlation coefficients for phosphate, iron, and trace elements in rocks, soils, and stream sediments. 36

A10. Cu/Pb, Cu/Zn, and Pb/Zn ratios (mean values) in rocks, soils, and stream sediments, entire Broad Sound catchment. 37

A11. Fe/Mn, Co/Ni, and Fe/Ni ratios (mean values) in rocks, soils, and stream sediments, entire Broad Sound catchment. 37

A12. Mean composition (ppm) of low-carbonate sediments (less than 5% $CaCO_3$) in component estuaries, compared with Broad Sound estuary as a whole. 37

A13. Broad Sound estuary: matrix of correlation coefficients for phosphate, iron, and trace elements in fine-grained low-carbonate estuarine sediments. 37

A14. Comparisons of trace-element, phosphate, and iron means in the low-carbonate sediments of the Herbert, Styx, and Waverley estuaries. 38

A15. Mean composition (major and minor oxides) of sediment types from various depositional environments in the Broad Sound estuary. 42

A16. Worldwide average sedimentary rock compositions. 43

A17. Composition of calcareous, dolomitic, and ferruginous nodules from Broad Sound depositional environments. 45

A18. Minor and trace-element composition (ppm) of worldwide average shales, sandstones, and carbonates, compared with averages for Broad Sound estuarine sediments. 47

A19. Means and standard deviations of major and trace-element concentrations in sediments from Broad Sound depositional environments. 48

A20. Matrixes of correlation coefficients for trace elements and other components of the estuarine sediments (averages of entire Broad Sound estuary). (A) calculated from log-transformed values, (B) calculated from actual values. 50

Page

A21. Matrixes of correlation coefficients for trace elements and other components of sediments in the various depositional environments, calculated from actual values: (A) shallow-marine, (B) open-intertidal, (C) mangrove-channel, (D) mangrove-swamp, (E) supratidal-flat. 52

A22. Abundance of total organic carbon and extractable organic matter in sediments from Broad Sound depositional environments. 63

A23. Trace-element ratios in sediments from Broad Sound depositional environments. 75

A24. Ionic radii of Fe, Co, and Ni. 86

A25. Comparisons of means of trace-element compositions and other parameters of Broad Sound depositional environments. 94

A26. Mean trace-element, iron, and phosphate content of sediments in Broad Sound depositional environments, calculated on a carbonate-free basis (ppm). 94

A27. Comparisons of trace-element means in Broad Sound depositional environments, calculated on a carbonate-free basis. 95

A28. Age and composition of oyster shells, Broad Sound. 97

A29. Composition of shells of live and fossil oysters from Broad Sound *(Saccostrea* sp.) and of live oysters *(Crassostrea virginica)* from USA. 97

A30. Matrix of correlation coefficients for trace elements, phosphate, and calcium in Broad Sound oyster shells. 100

A31. Summary of physico-chemical characteristics of pore waters and associated sediments, Broad Sound (highest, lowest, and mean values). 109

A32. Gravel facies, shallow-marine environment.
A33. Sandy facies, shallow-marine environment.
A34. Sandy facies, open-intertidal environment.
A35. Muddy facies, open-intertidal environment.
A36. Mangrove-channel environment.
A37. Mangrove-swamp environment.
A38. Supratidal-flat environment.
A39. Nodules, shallow-marine environment.

} Major and minor oxide composition of sediment samples from the estuary (Appendix A1) 123

FIGURES

A1. Locality map. 4

A2. Geology and main catchments, Broad Sound drainage basin. 6

A3. Physiography of the Broad Sound drainage basin (block diagram). 8

A4. Soils of the Broad Sound drainage basin. 10

A5. Abundance histograms for P_2O_5 in stream catchments and estuarine sediments. 16

A6. Abundance histograms for Cu in stream catchments and estuarine sediments. 17

		Page
A7.	Abundance histograms for Pb in stream catchments and estuarine sediments.	18
A8.	Abundance histograms for Zn in stream catchments and estuarine sediments.	19
A9.	Abundance histograms for Co in stream catchments and estuarine sediments.	20
A10.	Abundance histograms for Ni in stream catchments and estuarine sediments.	21
A11.	Abundance histograms for Fe in stream catchments and estuarine sediments.	22
A12.	Abundance histograms for Mn in stream catchments and estuarine sediments.	23
A13.	Abundance histograms for Cr in stream catchments and estuarine sediments.	24
A14.	Distribution of P_2O_5 in the Broad Sound catchment and estuary.	25
A15.	Distribution of Cu in the Broad Sound catchment and estuary.	26
A16.	Distribution of Pb in the Broad Sound catchment and estuary.	27
A17.	Distribution of Zn in the Broad Sound catchment and estuary.	28
A18.	Distribution of Co in the Broad Sound catchment and estuary.	29
A19.	Distribution of Ni in the Broad Sound catchment and estuary.	30
A20.	Ionic radii plotted against atomic numbers.	33
A21.	Sample localities, sample numbers, and buoy positions, Broad Sound estuary.	39
A22.	Schematic relationship of tidal zones and depositional environments.	40
A23.	Distribution of depositional environments.	41
A24.	Major-oxide plot comparing Broad Sound and world average values.	44
A25.	Histograms of $CaCO_3$ abundance in estuarine depositional environments.	45
A26.	Distribution of $CaCO_3$ in estuarine sediments.	46
A27.	Plot showing relationships between mean grainsize and $CaCO_3$ content in estuarine sediments.	46
A28.	Matrix of statistically significant correlation coefficients between variables in estuarine depositional environments.	49
A29.	Abundance histograms for P_2O_5 in estuarine depositional environments.	57
A30.	Plots showing relationship of P_2O_5 with mean grainsize and $CaCO_3$, all estuarine sediments.	58
A31.	Plots showing relationship between P_2O_5 and $CaCO_3$ in the various estuarine depositional environments.	59
A32.	Plot showing relationship between P_2O_5 and gravel content in estuarine sediments.	60
A33.	Plot showing relationship between P_2O_5 and Mg (log-transformed) in estuarine sediments.	60
A34.	Plot showing relationship between mean grainsize and organic carbon in estuarine sediments.	60
A35.	Abundance histograms for Mg in estuarine depositional environments.	61
A36.	Distribution of Mg in estuarine sediments.	62
A37.	Plot showing relationship between Mg and $CaCO_3$ in estuarine sediments.	62
A38.	Abundance histograms for Sr in estuarine depositional environments.	64
A39.	Distribution of Sr in estuarine sediments.	65
A40.	Distribution of Cd in estuarine sediments.	66
A41.	Abundance histograms for Y in estuarine depositional environments.	67
A42.	Distribution of Y in estuarine sediments.	68
A43.	Abundance histograms for Ba in estuarine depositional environments.	70
A44.	Distribution of Ba in estuarine sediments.	71
A45.	Abundance histograms for Cu in estuarine depositional environments.	72
A46.	Abundance histograms for Pb in estuarine depositional environments.	73
A47.	Abundance histograms for Zn in estuarine depositional environments.	74
A48.	Abundance histograms for Ti in estuarine depositional environments.	76
A49.	Abundance histograms for Sc in estuarine depositional environments.	77
A50.	Abundance histograms for Zr in estuarine depositional environments.	78
A51.	Distribution of Ti in estuarine sediments.	79
A52.	Distribution of Sc in estuarine sediments.	80
A53.	Distribution of Zr in estuarine sediments.	81
A54.	Abundance histograms for Cr in estuarine depositional environments.	82
A55.	Abundance histograms for V in estuarine depositional environments.	83
A56.	Distribution of Cr in estuarine sediments.	84
A57.	Distribution of V in estuarine sediments.	85
A58.	Abundance histograms for Fe in estuarine depositional environments.	87
A59.	Abundance histograms for Co in estuarine depositional environments.	88
A60.	Abundance histograms for Ni in estuarine depositional environments.	89
A61.	Distribution of Fe in estuarine sediments.	91
A62.	Abundance histograms for Mn in estuarine depositional environments.	92
A63.	Distribution of Mn in estuarine sediments.	93
A64.	Locations of chenier samples.	96
A65.	Plots showing relationships of Fe with Mn and U in Holocene oyster shells.	98
A66.	Plot showing relationships between radiocarbon age of Holocene oyster shells and their content of Pb, Zn, Cu, Mn, Fe, and P_2O_5.	99
A67.	Average monthly discharge of the Isaac River at Yatton.	102
A68.	Turbidity of Broad Sound surface waters.	103
A69.	Mangrove-channel waters: relationship of P_2O_5,pH, and salinity with changing state of tide, 10-11 August 1970.	104
A70.	Mangrove-channel waters: relationship of P_2O_5 pH, and salinity with changing state of tide, 16-17 September 1970.	104
A71.	Mangrove-channel waters: relationship of P_2O_5, pH, and salinity with changing state of tide, 25-26 September 1970.	105

Page

A72. Mangrove-channel waters: relationship between phosphate content and pH. 106
A73. Schematic representation of probable groundwater movement through intertidal-supratidal sediments, and salinity variations, at high water and low water. 107
A74. Broad Sound: pore-water sample localities. 108
A75. Supratidal sediments, locality 3, Figure 74: plots showing vertical variation in pore-water geochemistry. 110
A76. Plot showing relationship of Eh to pH in expressed pore waters from the estuarine depositional environments. 111
A77. Plot showing relationship of Eh to pH in pore waters measured in situ, estuarine depositional environments. 111
A78. Plot of Eh-pH fields (measured in situ), estuarine depositional environments. 112
A79. Plot showing Eh-pH fields of expressed pore waters, estuarine depositional environments. 112
A80. Plot comparing abundance of Mg and Ca in expressed Broad Sound pore waters. 114
A81. Plot showing relationship between salinity and Mg/Ca ratio in expressed Broad Sound pore waters. 115
A82. Plot showing variation of P_2O_5 content with pH in expressed Broad Sound pore waters. 116
A83. Plot showing lack of correlation between P_2O_5 content of expressed Broad Sound pore waters and P_2O_5 content of associated sediments. 116

PLATES

A1. Geochemical sample localities, Broad Sound drainage basin (in rear pocket).
A2. Sample treatment flowsheet, Broad Sound estuary samples. facing p. 40

Part B — A numerical approach to the geochemistry of the estuarine sediments

INTRODUCTION 131

Depositional environments 131
Sampling 132
Analytical methods 132
Acknowledgements 132

NUMERICAL SAMPLE CLASSIFICATION 132

Background 132
Q-mode factor analysis classification 137
Geological interpretation 139
Statistical and mathematical check by stepwise discriminant analysis 141
Q-technique canonical correlation analysis 143
Q-mode cluster analysis 145

Page

SUMMARY STATISTICS 148

Statistics 148
Error analysis 148

INTERRELATIONS BETWEEN VARIABLES IN THE ESTUARINE SEDIMENTARY UNITS 149
Methods of data analysis 152
R-mode factor analysis 153
Multiple linear stepwise regression 154
R-technique canonical correlation analysis 154
Significance of correlation coefficients 155
Testing and equality of means 156
Mangrove-sorted-mud unit 156
Mudflat-sorted-mud unit 158
R-technique canonical correlation analysis of the mangrove and mudflat results 160
Primary-unsorted-muddy-sand unit 162
Sorted-sand unit 163
Mixed-unsorted-muddy-sand unit 165
Sorted-sandy-gravel unit 166
Unsorted-gravel unit 168

GEOCHEMICAL MODEL 170

CONCLUSIONS 171

REFERENCES 175

APPENDIXES

B1. Mathematical and statistical techniques used in the Broad Sound Study 175
(a) Factor analysis 175
Principal components analysis 175
R-mode factor analysis 175
Q-mode factor analysis 176
Limitations of Q-mode factor analysis 177
Application of Q-mode factor analysis 177
(b) Stepwise discriminant analysis 177
(c) Canonical correlation analysis 178
R-technique 178
Q-technique 179
(d) Cluster analysis 179
(e) Analysis of variance 180
(f) R-mode factor analysis 181
Broad Sound analyses 182
(g) Multiple linear stepwise regression 183
(h) References 192
B2. Sample classification into sedimentary units and depositional environments 202
B3. Frequency distribution plots (Figs. B14-21) 203
B4. Availability of data 211

TABLES

B1. Comparison of the four 'basic sedimentary units'. 134
B2. Q-mode factor scores. 137

Page

B3. Last step in stepwise discriminant analysis. 142
B4. Results of Q-technique canonical correlation analysis. 144
B5. Mean values of the variables in each sedimentary unit. 150
B6. Standard deviation values of the variables in each sedimentary unit. 152
B7. One-way-analysis-of-variance results for triplicate sampling. 153
B8. Independent variables: stepwise regression analysis. 155
B9. Summary of factor and regression analyses results, mangrove-sorted-mud unit. 157
B10. Summary of factor and regression analyses results, mudflat-sorted-mud unit. 158
B11. Comparison, of the correlations of Fe and Mn with the other chemical elements, between mangrove-sorted-mud and mudflat-sorted-mud units. 159
B12. Summary of R-technique canonical correlation analysis results, mangrove-sorted-mud unit. 160
B13. Summary of R-technique canonical correlation analysis results, mudflat-sorted-mud unit. 161
B14. Summary of factor and regression analyses results, primary-unsorted-muddy-sand unit. 162
B15. Summary of factor and regression analyses results, sorted-sand unit. 164
B16. Response regression variables having positive coefficients, sorted-sand unit. 164
B17. Summary of factor and regression analyses results, mixed-unsorted-muddy-sand unit. 165
B18. Significant correlation coefficients between trace element and grainsize parameters, mixed-unsorted-muddy-sand units. 166
B19. Summary of factor and regression analyses results, sorted-sandy-gravel unit. 167
B20. Chemical analyses of carbonate nodules (sample 70636310) and shells (sample 70636205). 167
B21. Summary of factor and regression analyses results, unsorted-gravel unit. 169
B22. Significant correlation coefficients used in interpreting the unsorted-gravel-unit results. 170
B23. Modes of occurrence of chemical elements. 172
B24. Sedimentary units: differences in chemical-element concentrations. 174
B25. Oblique factor matrix, mangrove-sorted-mud unit. 185
B26. Oblique factor matrix, mudflat-sorted-mud unit. 186
B27. Oblique factor matrix, primary-unsorted-muddy-sand unit. 187
B28. Oblique factor matrix, sorted-sand unit. 188
B29. Oblique factor matrix, mixed-unsorted-muddy-sand unit. 189
B30. Oblique factor matrix, sorted-sandy-gravel unit. 190
B31. Oblique factor matrix, unsorted-gravel unit. 191

Page

B32. Abbreviations used for the variables in Tables B33-39. 192
B33. Summary of stepwise regression analysis, mangrove-sorted-mud unit. 193
B34. Summary of stepwise regression analysis, mudflat-sorted-mud unit. 194
B35. Summary of stepwise regression analysis, primary-unsorted-muddy-sand unit. 195
B36. Summary of stepwise regression analysis, sorted-sand unit. 196
B37. Summary of stepwise regression analysis, mixed-unsorted-muddy-sand unit. 198
B38. Summary of stepwise regression analysis, sorted-sandy-gravel unit. 199
B39. Summary of stepwise regression analysis, unsorted-gravel unit. 200

FIGURES

B1. Plot of mean and standard deviation of grainsize, delineating four basic sedimentary units. 133
B2. Idealised model of Holocene non-carbonate sedimentation in Broad Sound. 135
B3. Idealised scheme of sediment movement in Broad Sound, and relation between basic sedimentary units and depositional environments. 136
B4. Triangular plot of the three normalised factor loadings from the Q-mode factor analysis. 138
B5. Triangular plot of the three normalised factor loadings, showing contrasts between sedimentary units as reflected by the variables significant in the Q-mode factor analysis. 139
B6. Frequency plot showing typical grainsize distribution of sedimentary units — *sorted sand.* 141
B7. Frequency plot showing typical grainsize distribution of sedimentary units — *sorted sandy gravel.* 143
B8. Frequency plot showing typical grainsize distribution of sedimentary units — *mixed unsorted muddy sand.* 144
B9. Frequency plot showing typical grainsize distribution of sedimentary units — *unsorted gravel.* 145
B10. Frequency plot showing typical grainsize distribution of sedimentary units — *mudflat sorted mud.* 146
B11. Plot of first two canonical variables, Q-technique canonical analysis. 147
B12. Idealised geochemical model of the Broad Sound estuarine complex, showing trace-element associations in components of the sedimentary units. 173
B13. Plots used to determine significant factor loadings in each selected 'ideal' matrix. Broken vertical lines mark cut-off value for significant factor loadings. 184

Page

B14-21. Frequency-distribution plots (entire estuary), interpolated from computer-derived histograms: 203

B14. A Mean grainsize (phi)
B Grainsize standard deviation (phi)
C Gravel (carbonate retained)
D Sand (carbonate retained)
E Mud (carbonate retained)
F Silt (carbonate retained)

B15. A Clay (carbonate retained)
B Gravel (carbonate removed)
C Sand (carbonate removed)
D Mud (carbonate removed)
E Dolomite
F Mg calcite

B16. A Calcite
B Plagioclase
C Orthoclase
D Aragonite
E Quartz
F Ba

B17. A Ca
B Co
C Cr
D Cu
E Fe
F Mg

B18. A Mn
B Ni
C Pb
D Sc
E Sr
F Ti

B19. A Va
B Y
C Zn
D Zr
E $CaCO_3$
F P_2O_5

B20. A Heavy minerals, as percentage of non-carbonate fraction.
B Opaques, as percentage of heavy minerals.
C Non-opaques, as percentage of heavy minerals.
D Zircon, as percentage of non-opaque heavy minerals.
E Epidote, as percentage of non-opaque heavy minerals.
F Tourmaline, as percentage of non-opaque heavy minerals.

B21. A Rutile, as percentage of non-opaque heavy minerals.
B Hornblende, as percentage of non-opaque heavy minerals.
C Garnet, as percentage of non-opaque heavy minerals.
D Zoisite, as percentage of non-opaque heavy minerals.

PLATES

Page

B1. Q-mode cluster analysis dendrogram, using all 29 variables. facing p. 148
B2. Q-mode cluster analysis dendrogram, using only 14 variables. facing p. 149

Page xi is blank.

Page xii is blank.

PART A

Geochemistry of the estuarine system

By

P. J. Cook

Page 2 is blank.

INTRODUCTION

As a result of stratigraphic, petrographic, and geochemical studies on the Middle Cambrian phosphate deposits of northwest Queensland in 1969, de Keyser & Cook (1972) concluded that the phosphorites were probably deposited under paralic conditions such as in a bay or estuary. Little was known about the distribution or mode of concentration of phosphorus in estuarine sediments, and consequently BMR decided to undertake its own research in order to better understand ancient sedimentary processes. Additionally, as pointed out by many authors including Lauff (1967), estuaries are important to the welfare of man generally, as they comprise vital habitats for many life forms. This is particularly so for man, as estuaries are the sites of many major towns and cities. Thus, it is important to document estuarine processes in order to minimise adverse environmental modification.

Broad Sound on the central Queensland coast, a tropical estuary (Fig. A1), and Mallacoota Inlet in eastern Victoria, a temperate estuary, were selected for study. In addition to the general contrast in climate between these two areas, the two particular estuaries were chosen because they lacked significant phosphorus input from domestic, agricultural, or industrial effluent. The study of Mallacoota Inlet was undertaken by G. E. Reinson, then of the Department of Geology, Australian National University, with the assistance of BMR, and the results were published in BMR Bulletin 178 (Reinson, 1977).

Before the Broad Sound study began, it was apparent that in order to understand mechanisms controlling the distribution of phosphorus it was necessary to study not only the phosphate levels in sediments and water but also to consider such features as water movements, grainsize, heavy minerals, clay mineralogy, biogenic activity, and the Quaternary history of the area, as well as the behaviour of major and trace elements likely to have influenced, or to be influenced by, the distribution of phosphorus. Consequently it was decided to undertake as comprehensive a study of Broad Sound as possible. A Bulletin primarily concerned with the physical processes prevailing in Broad Sound has already been published (BMR Bulletin 170, Cook & Mayo, 1978). The present Bulletin is concerned with the chemical processes, both in the estuary and in the associated drainage basin.

The work was carried out during two winter field seasons. During the first (June to October, 1970) P. J. Cook (party leader) and W. Mayo collected sediment and water samples over the estuary and adjacent areas. S. E. Smith carried out some water sampling and was responsible for analyses undertaken at the Charon Point base camp. P. M. Angus carried out detailed geochemical sampling of the Styx River catchment. During the second field season (May to August, 1971) P. J. Cook and W. Mayo carried out further sediment sampling and undertook in-situ Eh and pH measurements at selected depositional sites. Pore fluids were extracted from various sediment types. A shallow drilling program, supervised by W. A. Burgis, was also undertaken, in the Torilla Plains area at this time.

Between the two field seasons, and also later, all of these geoscientists were involved in laboratory studies. In addition, K. J. Armstrong and D. E. Hunter were responsible for all sample preparation and some of the analytical work.

ACKNOWLEDGEMENTS

The writer wishes to express his appreciation to Mr K. J. Armstrong and Mr D. E. Hunter for the outstanding manner in which they undertook both their field and laboratory work throughout the Broad Sound project. The assistance of Messrs F. L. Stevenson, G. Burgis, A. Lewis, C. Madden, M. Tratt, R. Dulski and Miss W. A. Burgis in the field was most valuable. X-ray diffraction analysis by Mr G. Berryman represented a most important contribution to the Broad Sound work. Mr D. Gibson also provided useful information on clay mineralogy. Mrs K. A. Long provided assistance with computer programming and data processing. Mr W. Mayo provided advice on all aspects of the programming; his expertise in the statistical treatment of the data was particularly valuable. The editorial comments of Mr W. Mayo, and Drs P. J. Davies, H. A. Jones, and G. E. Wilford were most helpful.

Mr S. E. Smith and Mr T. Slezak undertook a large number of elemental analyses. Mrs P. M. Angus carried out the sampling of the Styx catchment and subsequently the analysis of the Styx samples. Mr A. D. Haldane gave advice on various aspects of the study. Dr W. Ponder of the Australian Museum kindly identified a number of mollusc shells.

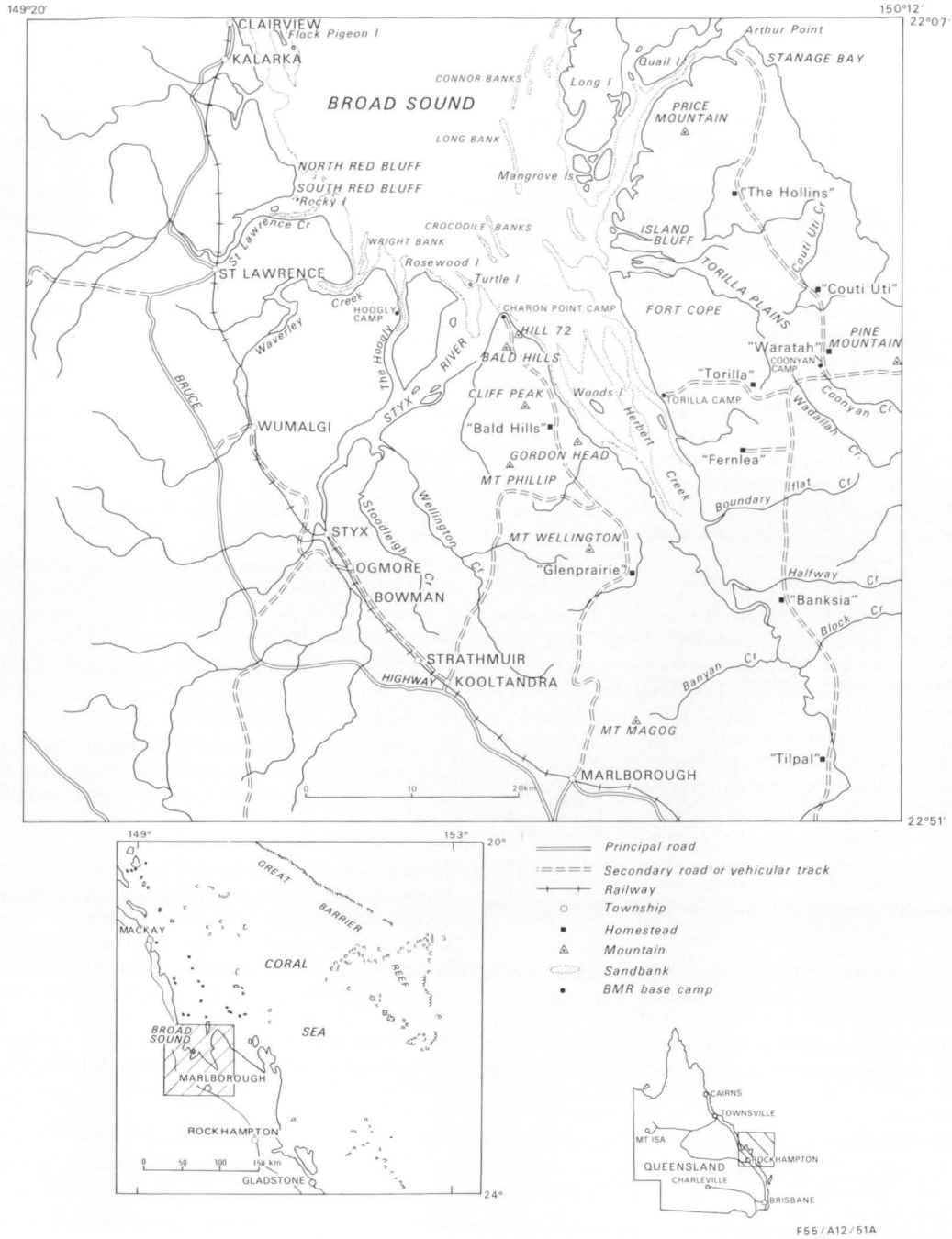


Fig. A1. Locality map.

Mr G. Oke and Mr M. Turner of the M. V. *Bali Hai* were most helpful with various phases of the investigations. The hospitality of Mr and Mrs G. Burrill of 'Bald Hills' and Mr and Mrs A. Mace of 'Torilla' was greatly appreciated by all members of the 1970 and 1971 field parties.

The figures were drawn by Miss V. Shepherd.

CLIMATE

The Broad Sound area has a sub-humid tropical climate with a marked concentration of rainfall in the summer months (Department of National Development, 1965; McAlpine, 1972). The main climatic features are summarised by Cook & Mayo (1978). The average mean temperature ranges from 27°C in January to 17°C in July. Temperatures in excess of 40°C, or below 0°C, are seldom if ever attained on the coast, but inland temperatures are more extreme. The average annual rainfall in the coastal region is about 1000 mm, most of which falls during the period November to March.

The average annual rate of evaporation at St Lawrence is about 1400 mm; consequently there is a marked annual excess of evaporation over precipitation. Only during January and February does precipitation exceed evaporation. Therefore, run-off is very slight throughout most of the year. An important feature of the rainfall pattern is that much of the rain falls during thunderstorms or tropical cyclones, resulting in marked rainfall variability from year to year. As much as 75 mm of rain in half an hour is reported to have fallen on one occasion in Kunwarara near Marlborough. Rainfall of this intensity produces catastrophic flooding in parts of the area.

Persistent but generally light winds are experienced in the Broad Sound area throughout the year. During the spring and summer months the dominant wind direction is from the northeast. As a result of the wind fetch, the area from Charon Point to the mouth of St Lawrence Creek (Fig. A1) is subjected to strong wave action in a northeasterly sea. In the autumn and winter months the wind is mainly from the southeast to southwest. The long southeasterly fetch can produce a strong southeasterly sea, but because of the configuration of the coast, this has little erosional effect on the coastline. Summer cyclonic storms with wind speeds exceeding 160 km/hour affect the Broad Sound area at times.

PREVIOUS INVESTIGATIONS

Previous geological investigations in the Broad Sound area have been concerned primarily with the Palaeozoic and Mesozoic rocks of the region. Malone, Olgers, & Kirkegaard (1969) deal briefly with the Cainozoic of the St Lawrence 1:250 000 sheet area; Kirkegaard, Shaw, & Murray (1970) show the distribution of Cainozoic sediments in the Port Clinton 1:250 000 sheet area adjacent to Broad Sound. Both these publications refer extensively to earlier reports on the Broad Sound area.

The only previous onshore work on Quaternary sediments was by Jardine (1928) who examined the Holocene marine sequence in the Torilla Plains area. Maxwell (1968) sampled the bottom sediments at a few localities at the northern end of the Sound and also briefly discussed the tidal range of the area.

A number of reports on various phases of the present investigations have already been written. These include a report by Burgis (1974) on the Cainozoic stratigraphy of the Torilla Plains area, an account of the clay mineralogy of the Quaternary sediments of Broad Sound by Gibson (1972) (now published in Cook & Mayo, 1978), and a discussion by Mayo (1972) on the formulation of grainsize analysis techniques for use with the Broad Sound sediments. In addition, Cook & Polach (1973a) report on the significance of a Holocene chenier sequence in the Styx River and Waverley Creek areas, and on the discovery of Holocene dolomites (1973b). The geochemistry of the dolomites is considered in more detail by Cook (1973). The sedimentology and Holocene history of Broad Sound and its associated drainage basins is the subject of a separate Bulletin (Cook & Mayo, 1978).

GEOCHEMISTRY OF THE CATCHMENT

INTRODUCTION

As part of the overall Broad Sound study it was considered desirable to determine the extent to which the geochemistry of an estuary is influenced by the geochemistry of its catchment. Ideally, this would have necessitated a comprehensive sampling programme of bedrock, stream sediments, and soils in the four main constituent catchments (Styx River, and St Lawrence, Waverley, and Herbert Creeks). However, because of a lack of time and personnel, only the Styx catchment was sampled extensively. Sampling in the other catchments was also limited by lack of exposure.

Sampling scheme

Drainage basin sample localities are shown in Plate A1 (in rear pocket). Owing to the rugged

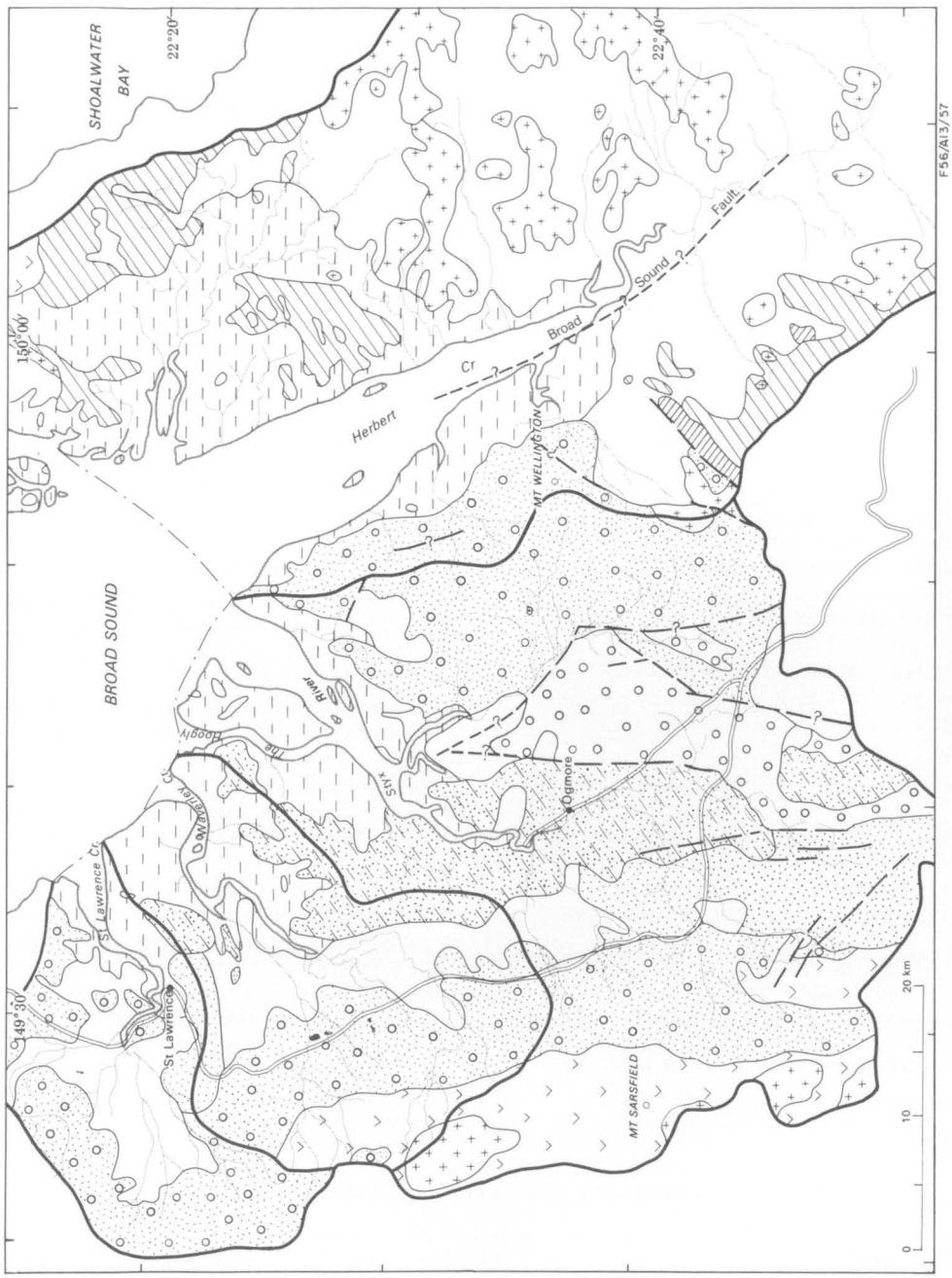
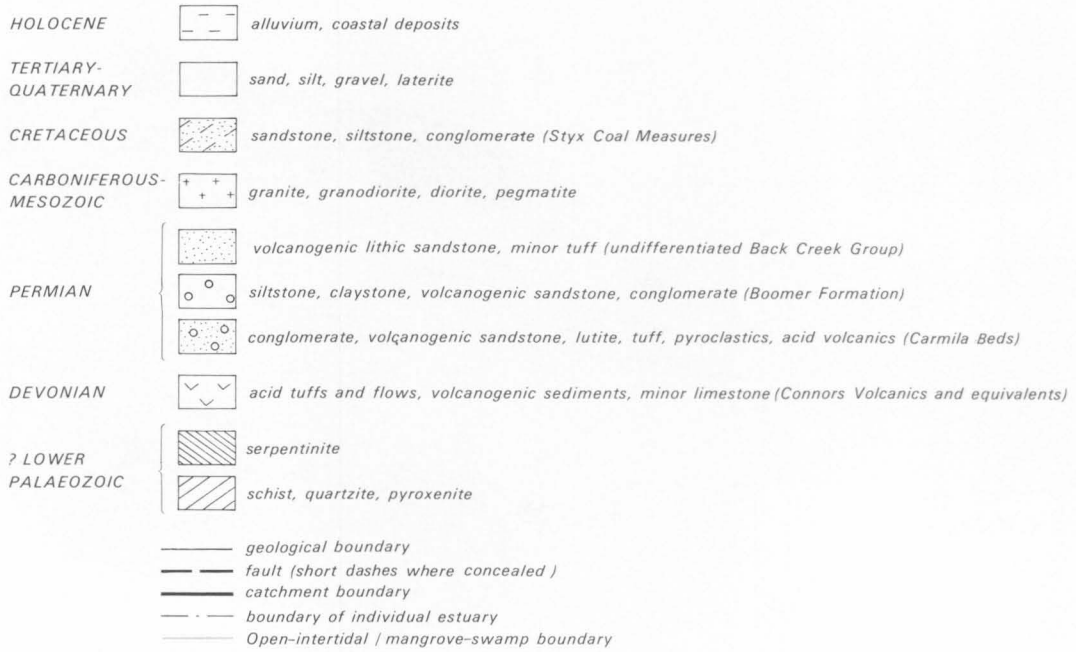


Fig. A2. Geology and main catchments, Broad Sound drainage basin (after Malone & others, 1969; Kirkegaard & others, 1970).

terrain in many areas and the limited time available, it was impossible to sample on a regular grid pattern, and of necessity sampling was commonly along tracks. In the Styx catchment, sampling was organised on the basis of geological units, with an attempted sampling density of 1 sample/3 km^2 and a minimum of 30 samples/geological unit. This ideal scheme was not achieved everywhere, owing to shortage of fresh outcrops or lack of time. In the Styx catchment, the stream-sediment samples were collected from fine material in stream banks. In the other catchments the minus-80-mesh fraction of active stream sediment was collected. Soil


HOLOCENE
alluvium, coastal deposits
TERTIARY-QUATERNARY
sand, silt, gravel, laterite
CRETACEOUS
sandstone, siltstone, conglomerate (Styx Coal Measures)
CARBONIFEROUS-MESOZOIC
granite, granodiorite, diorite, pegmatite
PERMIAN
volcanogenic lithic sandstone, minor tuff (undifferentiated Back Creek Group)
siltstone, claystone, volcanogenic sandstone, conglomerate (Boomer Formation)
conglomerate, volcanogenic sandstone, lutite, tuff, pyroclastics, acid volcanics (Carmila Beds)
DEVONIAN
acid tuffs and flows, volcanogenic sediments, minor limestone (Connors Volcanics and equivalents)
? LOWER PALAEOZOIC
serpentinite
schist, quartzite, pyroxenite
geological boundary
fault (short dashes where concealed)
catchment boundary
boundary of individual estuary
Open-intertidal / mangrove-swamp boundary

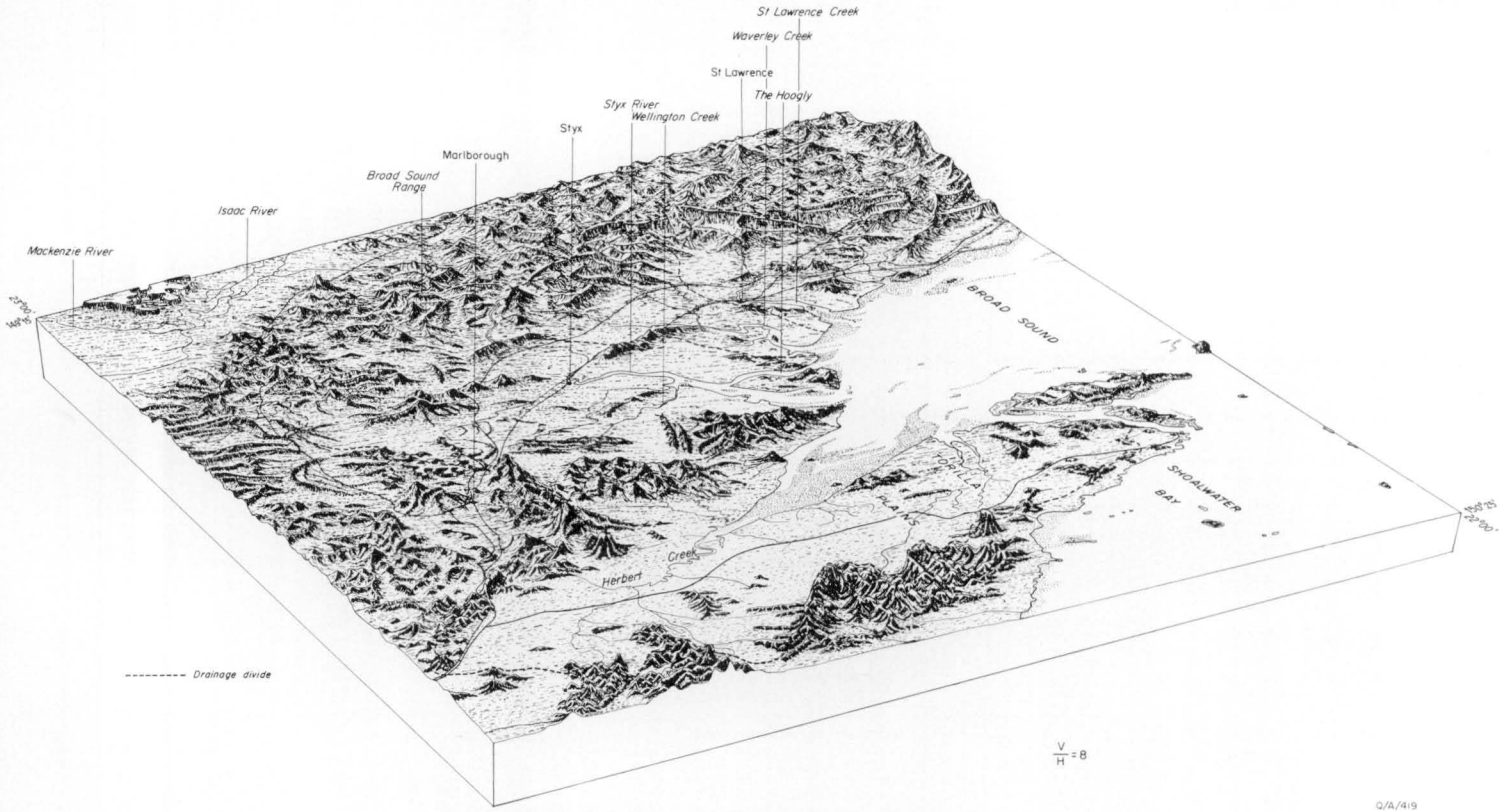


Fig. A3. Physiography of the Broad Sound drainage basin.

samples were everywhere taken from the lower part of the A horizon. Where possible, both rock and soil samples were taken from a single sampling point.

A total of 796 soil samples, 458 stream-sediment samples, and 180 rock samples were collected from the four main catchment areas.

Analytical methods

Samples from the Styx catchment were first analysed semi-quantitatively, at BMR, by emission spectroscopy. Elements sought included Ni, Cu, Pb, Ag, Au, Sb, Bi, Mo, Sn, Be, V, As, and W. The abundances of most of these elements were found to be at or below the detection limit and therefore it was decided to confine accurate analysis to Cu, Pb, Zn, Co, and Ni only, together with P_2O_5. For the St Lawrence, Waverley, and Herbert Creek catchments, Fe, Mn, and Cr were also accurately determined.

Samples were first oven-dried and then ground and split to provide 1 gram of sample, which was subjected to hydrofluoric-perchloric acid digestion. P_2O_5 was then determined colorimetrically by the phosphovanadomolybdate method. All other elements were determined by atomic absorption spectroscopy. Analyses for the Styx catchment were undertaken at BMR by P. M. Angus; analyses for the other catchments were by the Australian Mineral Development Laboratories (AMDEL).

Statistical and computing procedures

All available information on each sample, including the BMR sample registered number, the sheet and grid reference, the drainage basin, the nature of the sample (whether bedrock, stream sediment, or soil), the name of the rock unit from which the sample was obtained or which underlies the sampling point, and the trace element concentrations in ppm (P_2O_5, Cu, Pb, Zn, Co, Ni, Fe, Mn, Cr) were placed on magnetic tape prior to data manipulation.

Means, standard deviations, histograms of the frequency distribution, X-Y plots, correlation coefficients, and the equation of the regression line were determined by PROGRAM VARPLOT (Mayo & Long, 1976) on various sample groupings. Groupings were chosen primarily on the basis of sample type, the drainage basin from which the sample was obtained, or the rock unit. *t*-tests for differences between the means of the trace elements in the various catchments were also obtained from PROGRAM VARPLOT; as this test assumes equal variances, an F-test of the equality of variances preceded each *t*-test.

GEOLOGY

The Broad Sound region is structurally and stratigraphically complex. It lies on the eastern edge of the early Palaeozoic Tasman Geosyncline and the predominantly late Palaeozoic Bowen Basin, and includes the Mesozoic Styx Basin. The generalised stratigraphy of the catchment is given in Figure A2. No geological mapping was undertaken for the present study — it had previously been carried out by Malone & others (1969), and Kirkegaard & others (1970).

The Herbert catchment is located within the Marlborough and Coastal Blocks (Kirkegaard & others, 1970). The Styx and St Lawrence catchments lie mainly within the Bowen Basin, with minor portions in the Styx Basin. The Waverley catchment is almost entirely in the Styx Basin.

The oldest rocks exposed in the region are believed to be the early Palaeozoic schists, gneisses, marbles, and phyllites of the Coastal Block (Kirkegaard & others, 1970), which flank the Torilla Plains and are up to 20 000 m thick. Devonian limestones, mudstones, conglomerates, and acid volcanics are present in the north of the region and are particularly well exposed on Long Island. The serpentinites of the Marlborough area (Herbert catchment) are of uncertain age; they are believed to be early Palaeozoic but may have been block-faulted into their present position in the Early Permian.

Deposition in the area began in the Late Devonian and continued until the Late Permian. During this time, a thick volcanic and sedimentary sequence was deposited in the western half of the region including the Connors Volcanics, Carmila Beds, Boomer Formation, and undifferentiated Back Creek Group. In the Broad Sound Range this volcanogenic sequence is more than 4000 m thick. Bowen Basin sedimentation was terminated by severe folding and faulting near the end of the Permian. It was during this Permian to Mesozoic phase that many granites, granodiorites, and associated acid intrusives were emplaced in the southeast corner of the region (some have been found to be Late Carboniferous in age). Faulting and igneous activity may have continued well into the Mesozoic; many of the major structural features such as the Broad Sound Fault were probably established in this period.

The Cretaceous Styx Coal Measures were deposited in a small down-faulted basin on the west side of Broad Sound. These sediments are predominantly freshwater sandstone and mudstone with minor coal; they have a maximum thickness of 400-500 m.

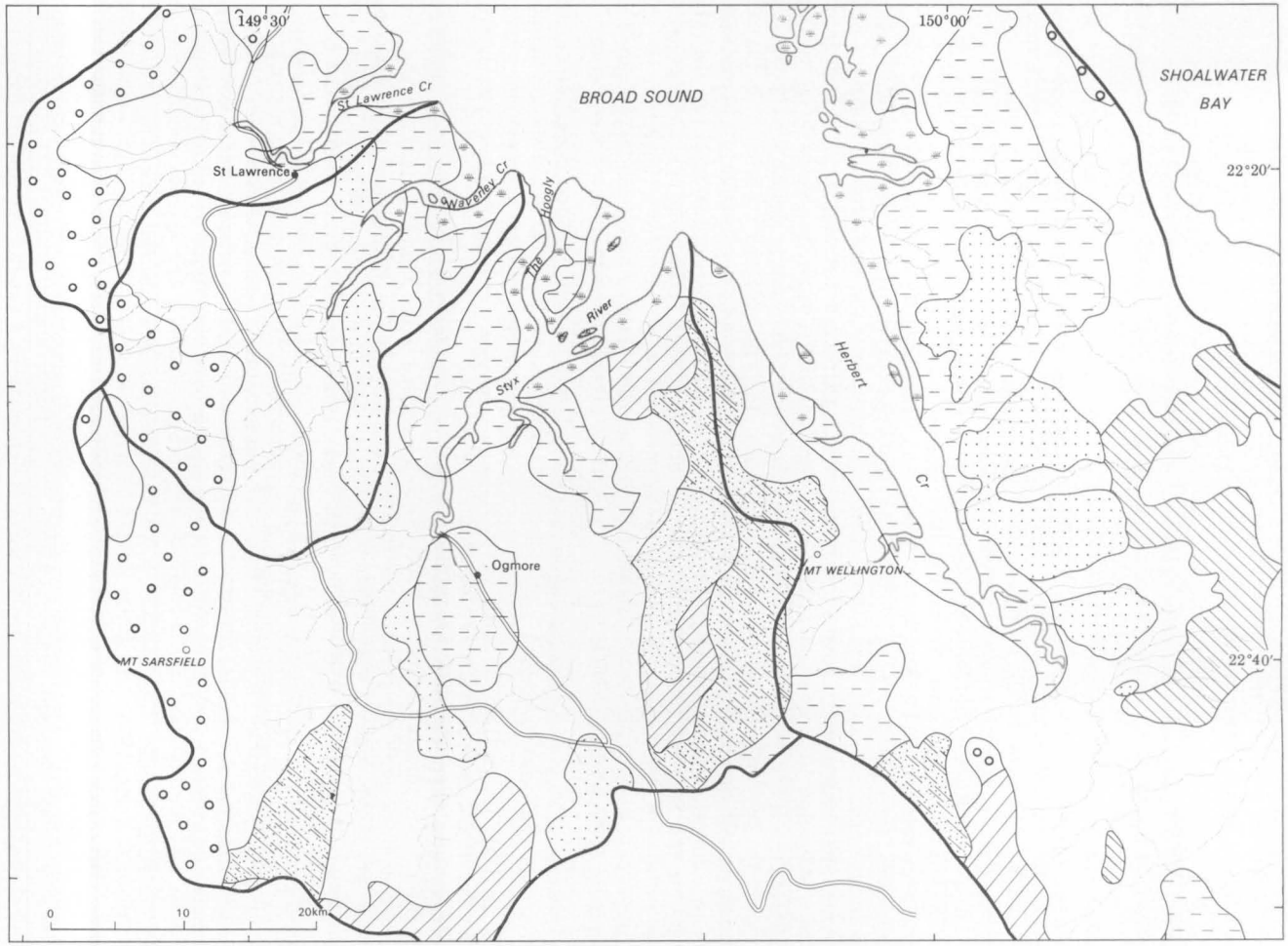
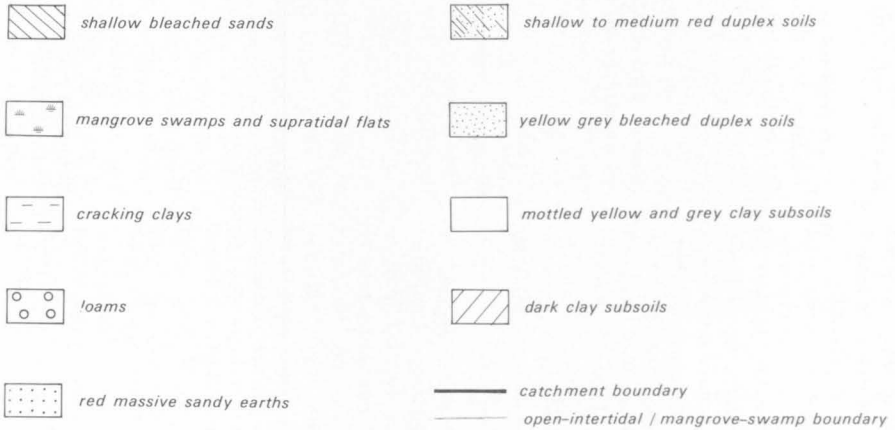


Fig. A4. Soils of the Broad Sound drainage basin (after Isbell & Hubble, 1967).


shallow bleached sands
shallow to medium red duplex soils
mangrove swamps and supratidal flats
yellow grey bleached duplex soils
cracking clays
mottled yellow and grey clay subsoils
loams
dark clay subsoils
red massive sandy earths
catchment boundary
open-intertidal / mangrove-swamp boundary

The Cainozoic stratigraphy of much of the Broad Sound region is poorly understood. It is indicated in the map (Fig. A2) as undifferentiated Tertiary-Quaternary. Thick sequences of poorly lithified colluvial conglomerates and breccias of probable Tertiary age flank the ranges on the west side of Broad Sound. The undifferentiated Cainozoic deposits on the east side comprise sand, sandstone, and conglomeratic sandstone, all showing varying degrees of lateritic weathering. Many of these deposits are believed to be Tertiary, but some, particularly the unconsolidated pale brown sands flanking parts of the Torilla Plains, are probably Quaternary. Fluvial deposits are locally developed in the upper reaches of all the river valleys. Holocene coastal deposits (discussed in detail elsewhere in this volume) are well developed around the periphery of Broad Sound, although they are comparatively thin (up to 10 m).

The physiography of the region (Fig. A3) is primarily a reflection of the geology. The broad coastal plain is mainly underlain by the Holocene coastal deposits. Landward of these are extensive low-relief areas (particularly flanking the larger rivers) which are underlain by Tertiary-Quaternary alluvial deposits. The Styx Coal Measures characteristically form low, dissected tablelands and underlie low-relief areas. On the east side of Broad Sound the Palaeozoic rocks have been extensively lateritised and form rounded hills generally rising no more than 100 m above the surrounding plains. On the west side of the Sound the ranges, which are composed mainly of Palaeozoic rocks, commonly rise to 400 m above the coastal region, reaching a maximum altitude of 500 m above sea-level in the Broad Sound Range.

The catchment areas vary markedly in their relief. Herbert Creek has both the biggest catchment area and the biggest estuary, but the relief is generally low. Because of this it is unlikely to be contributing much detritus to Broad Sound at the present time. The Waverley, St Lawrence, and Styx catchments all have considerable relief, the Styx drainage basin being the largest of the three. The Styx drainage basin probably also contributes the greatest amount of terrigenous material into the Sound at the present time.

SOILS

Except for investigations by Gunn (1972) and Burgis (1974) on the soils of the Torilla Peninsula, no detailed work has been done on the Broad Sound catchment soils and no attempt was made to map them during the present survey, though the general observation was made that there appears to be a poor correlation between soil type and the underlying bedrock.

A regional study by Isbell & Hubble (1967) indicates that there are nine major soil types in the Broad Sound drainage basin (Fig. A4). Mottled yellow and grey clay subsoils are the most widespread soils, occurring over a range of bedrock types and topography. Some other soils show a clearer correlation with geology. The massive red earths overlie early Palaeozoic metamorphics on the east side of Broad Sound, and the Cretaceous Styx Coal Measures on the west side. Loams most commonly are associated with the Connors Volcanics. The coastal cracking clays are everywhere associated with Late Holocene marine sediments (e.g. Torilla Plains). The inland cracking clays form over alluvial deposits.

SUMMARY OF GEOCHEMICAL RESULTS

The mean phosphate, iron, and trace-element compositions of the rocks, soils, and stream sediments of the catchment are given in Table A1. In general, compositions are similar to world average values given by Turekian & Wedepohl (1961), and reflect the geologically mixed nature of the drainage basin. Except for Fe, Mn, and Cr, trace-element values are highest in bedrock. If the frequency distributions are plotted as histograms (Figs. A5-13) it is apparent that all distributions for bedrock with the exception of Pb and Zn (Figs. A7, A8), are log-normal. Most distributions for soils and stream sediments are also log-normal. Wherever clear deviations from log-normality occur in a particular catchment, for example with Zn in the Styx catchment or Pb in the Waverley-St Lawrence or Styx catchments, they are evident in both the soil and stream sediment distributions. However, as such cases are rare, all values were transformed to logarithms before statistical analysis.

The various major rock units vary widely in composition (Table A2). The standard deviations also indicate wide variations within the same unit. Again, values are comparable with those given by Turekian & Wedepohl (1961) (Table A1). Although there is some tendency for high metal contents in the bedrock to be reflected in associated soils and stream sediments, the trend is not well defined.

TABLE A1. MEAN PHOSPHATE, IRON, AND TRACE-ELEMENT CONTENTS OF ROCKS, SOILS, AND STREAM SEDIMENTS FROM THE ENTIRE BROAD SOUND CATCHMENT, COMPARED WITH WORLD AVERAGE VALUES FOR VARIOUS ROCK TYPES (ppm)

	Entire Broad Sound catchment			World average values (Turekian & Wedepohl, 1961)							
	Bedrock	Soil	Stream sediments	Ultrabasic	Basaltic	Granitic high Ca	Granitic low Ca	Syenites	Shales	Sandstones	Carbonates
P_2O_5	1000	534	483	504	2520	2108	1375	1833	1604	389	916
Cu	18.4	16.3	13.9	10	87	30	10	5	45	X	4
Pb	20.1	14.7	16.4	1	6	15	19	12	20	7	9
Zn	50.8	30.3	28.9	50	105	60	39	130	95	16	20
Co	11.8	10.7	8.2	150	48	7	1	1	19	0.3	0.1
Ni	24.2	16.8	9.9	2000	130	15	4.5	4	68	2	20
Fe (%)	0.98	1.33	1.14	9.43	8.65	2.96	1.42	3.67	4.72	0.98	0.38
Mn	250	186	256	1620	1500	540	390	850	850	X	1100
Cr	7.6	28.1	10.7	1600	170	22	4	2	90	35	11

In order to establish with greater precision the extent of the bedrock-soil compositional correlation, correlation coefficients and confidence levels were determined (Table A3) for associated rock and soil samples. With P_2O_5, Pb, Co(?), and Cr, there is no significant correlation, suggesting that for these elements the composition of the bedrock has little influence on the composition of the soil. This may be a reflection of the age of the soil or the extent to which the abundance of these elements is controlled by the flora. Alternatively, in the case of P_2O_5 there may be very limited addition of phosphorus fertilisers in localised areas, although addition is negligible in the drainage basin as a whole. Generally, P_2O_5 concentrations in soils and stream sediments are lower than in bedrock.

It was pointed out earlier that the geology of the four main catchments differs. In order to determine whether such differences are reflected in the trace-element geochemistry, a log-normal distribution was assumed and *t*-tests were used to test differences between means. The results are summarised in Table A4. One result of this statistical treatment is the discovery that the geochemistry of the bedrock is more homogeneous (i.e. there are fewer significant differences between means) than the geochemistry of the soils and stream sediments. The reason for this is not apparent; it may reflect the variety of ages of the soils, or alternatively different soil types may have formed over the same rocks at different physiographic locations. Other points which may be made from Table A4 include (1) the bedrock of the Waverley and St Lawrence catchments is geochemically indistinguishable at the 95-percent confidence level; (2) trends in the bedrock (i.e. indicating that one catchment has a greater or lesser trace-element content than another) are generally repeated in the soils as well as in the stream sediments; (3) Ni and possibly Cr appear to be the best trace elements for distinguishing between catchments; (4) it may be possible to use the pattern of differences between means to distinguish between catchments and forecast the likely differences in their associated estuarine sediments.

REGIONAL VARIATIONS IN CONTENT OF TRACE ELEMENTS AND PHOSPHATE

Because of the relatively small number of bedrock and stream sampling points, only the soil values have been used to indicate regional variations (Figs. A14-19). In addition to soil values, the trace-element contents of the Broad Sound marine sediments have also been incorporated and contoured, in Figs. A14-19, though a

TABLE A2. MEANS AND STANDARD DEVIATIONS OF PHOSPHATE, IRON, AND TRACE ELEMENTS IN ROCKS (R), SOILS (S), AND STREAM SEDIMENTS (T) IN THE ENTIRE BROAD SOUND CATCHMENT (ppm)

		No. of samples	P_2O_5		Cu		Pb		Zn		Co		Ni		Fe(%)		Mn		Cr	
			mean	s.d.	mean	s.d.	mean	s.d.	mean	s.d.	mean	s.d.	mean	s.d.	mean	s.d	mean	s.d	mean	s.d.
Quaternary alluvium and sand																				
	R	26	872.3	689.9	21.6	39.9	10.3	9.7	44.3	28.2	9.5	10.1	5.2	9.1	2.67	2.64	371.2	292.9	15.0	13.4
	S	189	492.7	424.4	13.9	12.2	11.4	9.7	26.6	22.4	9.0	14.2	23.5	70.1	1.46	1.43	383.9	506.5	51.7	95.0
	T	115	452.7	481.1	10.3	12.1	9.1	10.3	23.4	19.8	6.1	8.9	6.8	14.9	1.34	1.09	322.5	682.2	20.2	40.9
Tertiary																				
	R	6	210.8	278.8	6.3	3.8	8.0	4.8	15.3	12.1	2.0	3.1	7.2	9.5	0.62	0.59	51.7	53.2	15.0	13.8
	S	13	296.5	171.1	8.2	4.3	10.8	6.4	15.3	9.0	4.0	4.5	10.1	9.3	0.22	0.38	118.8	308.5	22.7	41.1
	T	7	267.7	197.2	8.0	4.7	5.1	4.3	11.6	8.4	1.6	2.4	5.1	5.1	0.36	0.36	53.6	66.6	42.0	51.5
Styx Coal Measures																				
	R	9	1013	1051	9.2	6.7	14.3	11.5	33.0	24.2	10.1	10.4	11.9	12.7	0.39	0.65	164.4	463.7	6.7	10.9
	S	128	600.8	441.6	13.2	7.3	17.7	9.3	30.9	18.3	11.8	10.0	10.7	6.9	1.03	2.81	44.0	129.8	6.7	17.4
	T	41	383.9	220.6	10.4	8.3	21.9	28.7	25.4	16.7	7.8	6.8	9.1	9.8	0.32	0.55	20.0	44.6	1.6	3.0
Permian-Mesozoic acid igneous																				
	R	5	829.0	817.2	31.0	14.8	19.8	6.3	38.4	6.9	12.8	6.9	30.4	51.2	—	—	—	—	—	—
	S	5	208.0	64.6	5.0	3.5	2.0	2.7	5.0	3.5	2.0	2.7	6.0	5.5	0.78	0.30	153.0	70.5	120.0	37.6
	T	—	—	—	—	—	—	—	—	—	—	—	—	—	—	—	—	—	—	—
Undifferentiated Back Creek Group																				
	R	30	1379	1175.2	17.2	13.4	43.4	128.0	49.4	24.9	13.0	11.2	37.8	99.5	0.34	1.15	61.5	310.0	2.2	7.4
	S	95	507.9	306.0	17.8	11.6	15.5	10.8	34.8	18.8	10.0	7.4	15.1	14.4	0.53	2.24	44.1	271.6	2.6	9.6
	T	56	490.8	407.5	14.9	7.5	17.9	8.0	34.2	16.5	8.3	5.4	12.1	7.3	0.28	0.79	26.3	131.9	1.1	3.3
Boomer Formation																				
	R	16	1157	1205	15.1	5.7	20.6	7.8	51.8	26.1	9.8	9.7	26.1	22.6	—	—	—	—	—	—
	S	67	449.4	277.7	13.4	6.3	15.4	8.7	28.5	14.7	8.4	7.1	16.2	15.4	—	—	—	—	—	—
	T	37	286.9	135.9	12.1	3.8	19.6	14.1	26.0	10.9	7.6	4.0	14.8	7.4	—	—	—	—	—	—
Carmila Beds																				
	R	60	825.5	893.8	18.4	18.1	16.6	11.9	60.8	47.1	10.8	8.2	12.9	19.4	1.29	1.58	318.3	461.1	6.7	11.9
	S	209	545.9	336.6	19.2	18.1	16.9	10.2	33.2	15.9	12.6	10.5	14.2	23.4	1.18	2.17	228.5	467.0	6.9	13.0
	T	96	501.6	381.3	14.8	12.5	14.7	16.3	32.0	15.0	9.5	9.2	9.9	15.0	1.59	1.31	422.6	478.4	4.7	13.2
Connors Volcanics																				
	R	7	1251.7	1161.8	33.6	23.9	14.7	9.4	65.4	23.1	22.9	13.1	23.4	31.4	1.60	2.37	312.9	434.6	6.4	9.9
	S	21	578.8	343.5	20.4	12.3	14.3	8.9	32.6	14.1	18.1	13.7	22.1	38.2	0.89	1.65	229.0	457.0	4.0	6.8
	T	7	868.3	433.5	30.3	28.7	18.0	9.5	48.3	12.6	10.9	6.6	10.1	7.4	1.83	1.72	365.7	378.2	4.3	6.1
Upper Devonian																				
	R	—	—	—	—	—	—	—	—	—	—	—	—	—	—	—	—	—	—	—
	S	9	1449	1253	47.8	40.0	3.9	2.2	28.3	15.0	8.3	5.6	10.0	9.0	2.56	1.32	380.0	140.1	43.3	29.6
	T	6	2018	1728	30.0	17.0	4.2	2.0	17.5	5.2	6.7	5.2	10.0	10.5	3.35	2.89	256.7	62.5	34.2	47.7
Lower Palaeozoic metamorphics																				
	R	—	—	—	—	—	—	—	—	—	—	—	—	—	—	—	—	—	—	—
	S	17	298.8	129.5	16.5	14.2	5.3	3.7	17.9	13.8	5.0	8.5	10.3	14.5	1.95	1.45	353.8	393.1	110.0	80.7
	T	6	281.7	294.6	7.5	8.2	1.7	2.6	10.0	6.3	5.0	8.4	6.7	10.8	1.6	1.94	184.2	192.9	24.2	25.0

detailed discussion of trace-element distributions in estuarine sediments is given later. Maps have been prepared only for P_2O_5, Cu, Pb, Zn, Co, and Ni, as values are available throughout the area only for these six elements. Fe, Mn, and Cr were not determined for the Styx catchment.

Phosphate

The regional distribution of P_2O_5 is shown in Figure A14, from which it is evident that phosphate contents are high at the northern end of Broad Sound, where relict sediments predominate, and also in the muds of the supratidal flats. This pattern will be discussed later. In the catchment, the pattern of phosphate distribution is not related to any obvious geological feature, though there are similarities between the P_2O_5 and Zn (Fig. A17) distribution patterns. Highest phosphate values are most commonly found in areas of cracking clays, particularly those flooring river valleys on the west side of Broad Sound. This may be because these soils are finer grained and hence able to absorb greater amounts of phosphate. Alternatively, it may be because these are areas of greater agricultural activity where phosphate fertilisers may have been used. Conversely, the massive red earths are very low in phosphate, perhaps a result of the age of these soils and the extensive leaching associated with them.

TABLE A3. CORRELATION COEFFICIENTS (LOG-TRANSFORMED) FOR PHOSPHATE, IRON, AND TRACE-ELEMENT ABUNDANCES IN BEDROCK, VERSUS THEIR ABUNDANCES IN OVERLYING SOIL. Coefficients marked with an asterisk indicate significant correlation at a confidence level of 95 percent; $\rho = 0.3$; $t = 1.96$

P_2O_5	−0.108
Cu	0.469*
Pb	0.166
Zn	0.478*
Co	0.303
Ni	0.490*
Fe	0.403
Mn	0.535*
Cr	0.070

TABLE A4. COMPARISONS OF TRACE-ELEMENT, PHOSPHATE, AND IRON MEANS BETWEEN THE FOUR LOCAL CATCHMENTS, FOR BEDROCK, SOILS, AND STREAM SEDIMENTS. 1. Herbert catchment, 2. Styx catchment, 3. Waverley catchment, 4. St. Lawrence catchment

Catchments being compared	$-P_2O_5$	Cu	Pb	Zn	Co	Ni	Fe	Mn	Cr
Bedrock									
1 and 2	<	<	<	=	<				
1 and 3	X	=	=	=	>	>	<	=	>
1 and 4	<	=	=	=	>	>	<	<	>
2 and 3	X	X	X	=	=	>			
2 and 4	=	>	X	X	=	>			
3 and 4	X	=	=	=	=	=	=	=	=
Soils									
1 and 2	>	X	X	X	X	X			
1 and 3	<	>	<	=	=	X	<	=	>
1 and 4	=	>	<	X	<	X	X	>	>
2 and 3	<	X	>	X	X	>			
2 and 4	>	>	>	>	>	>			
3 and 4	>	<	>	X	>	>	>	>	>
Stream sediments									
1 and 2	X	X	X	X	X	X			
1 and 3	<	>	<	=	>	>	<	=	>
1 and 4	=	>	<	X	>	X	=	X	>
2 and 3	<	X	>	X	X	X			
2 and 4	=	X	>	>	>	>			
3 and 4	>	=	>	X	>	>	>	>	>

'X'.....F-test indicates different variances, thus preventing the application of a *t*-test to the means.
'1 > 2'.....*t*-test indicates the mean for the Herbert catchment is greater than the mean for the Styx catchment at a confidence level of 95-percent.
'1 < 2'.....*t*-test indicates the mean for the Herbert catchment is less than the mean for the Styx catchment at a confidence level of 95-percent.
'1 = 2'.....*t*-test indicates means for Herbert and Styx catchments are equal at a confidence level of 95-percent.

Copper

Estuarine sediments in particular are uniformly low in Cu (Fig. A15). Unlike P_2O_5, Cu is generally low in the cracking clays and high in the massive red earths, particularly on the east

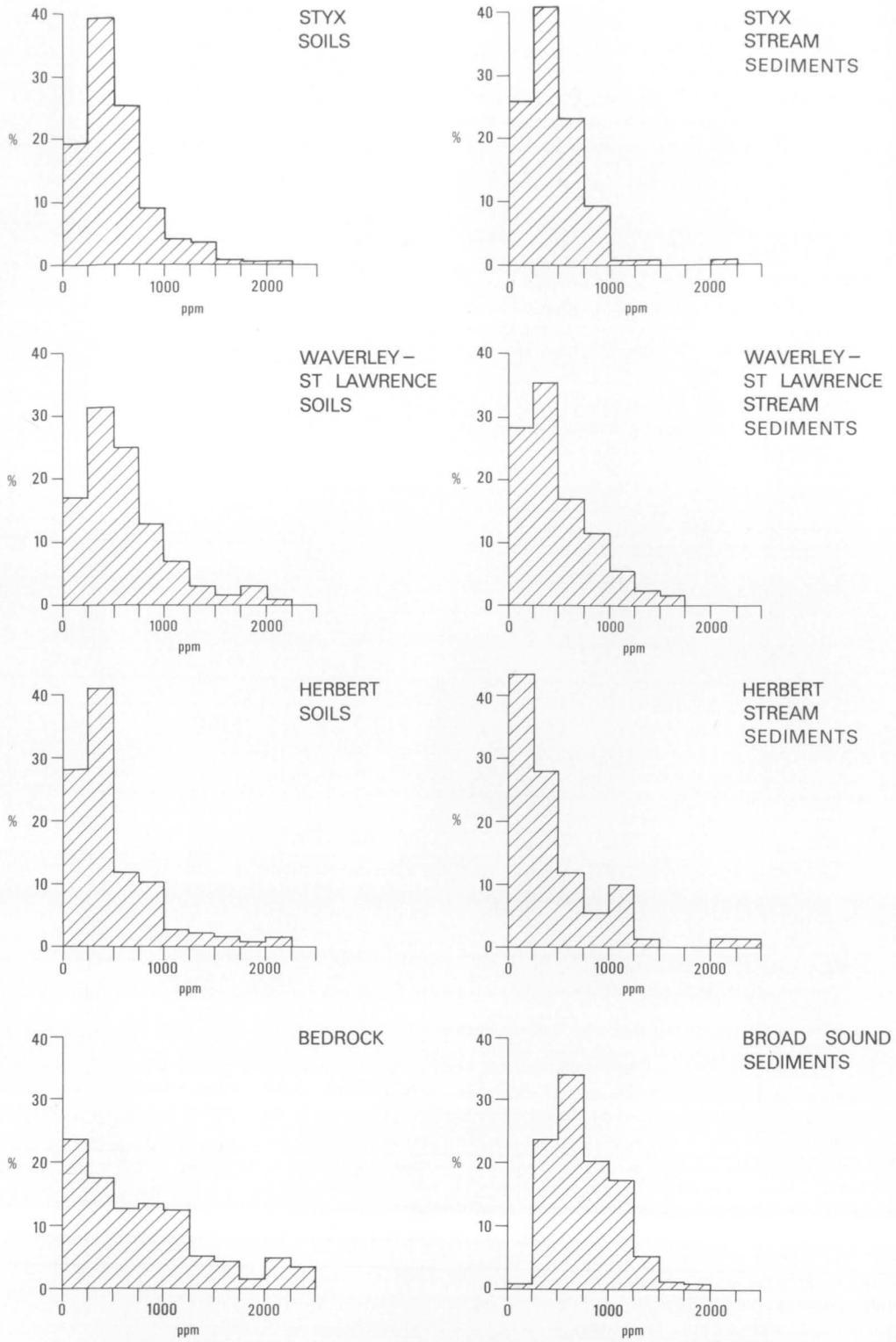


Fig. A5. P_2O_5 concentration: frequency distribution in Broad Sound catchments and estuarine sediments.

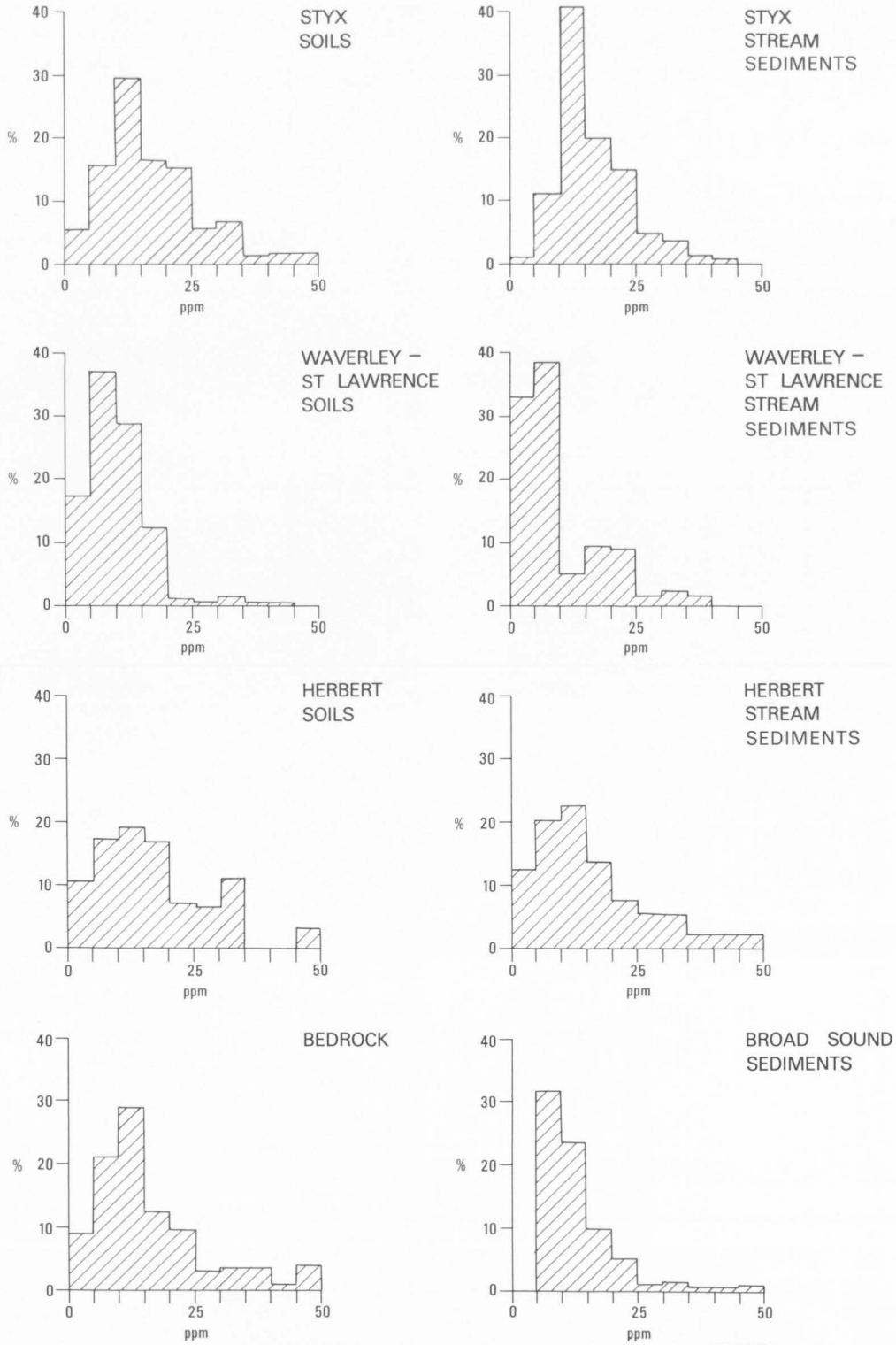


Fig. A6. Cu concentration: frequency distribution in Broad Sound catchments and estuarine sediments.

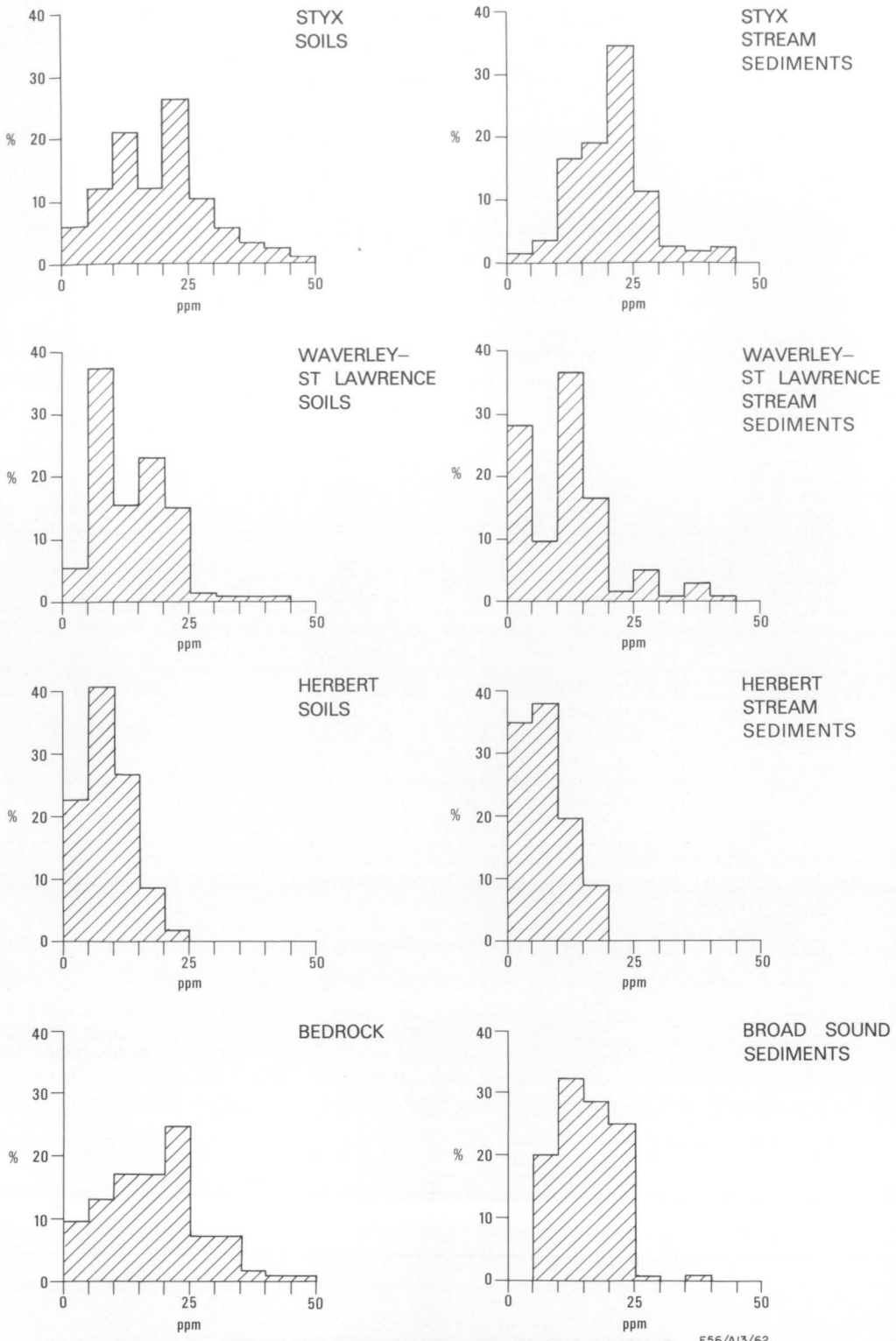


Fig. A7. Pb concentration: frequency distribution in Broad Sound catchments and estuarine sediments.

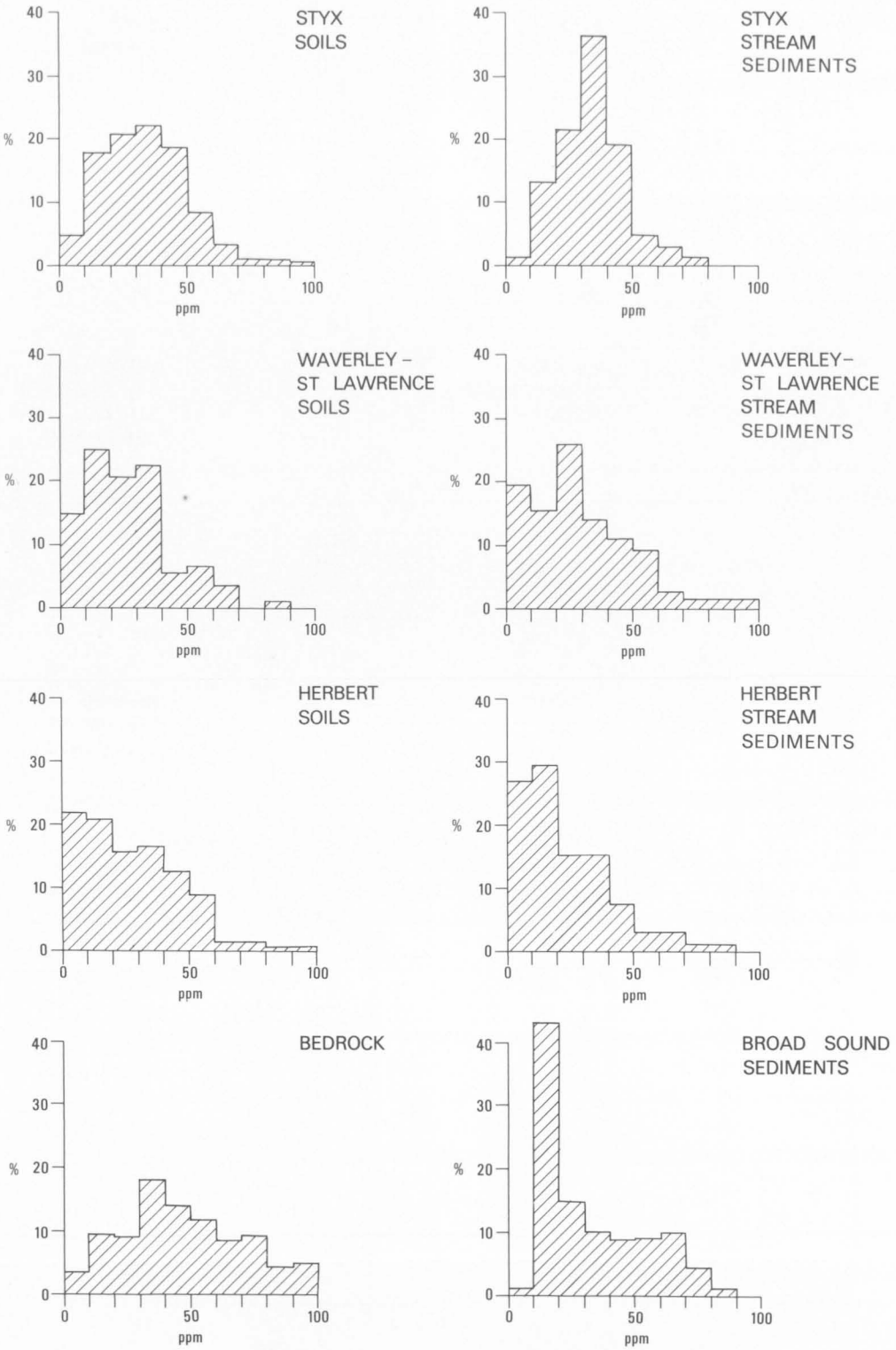


Fig. A8. Zn concentration: frequency distribution in Broad Sound catchments and estuarine sediments. F56/A13/63

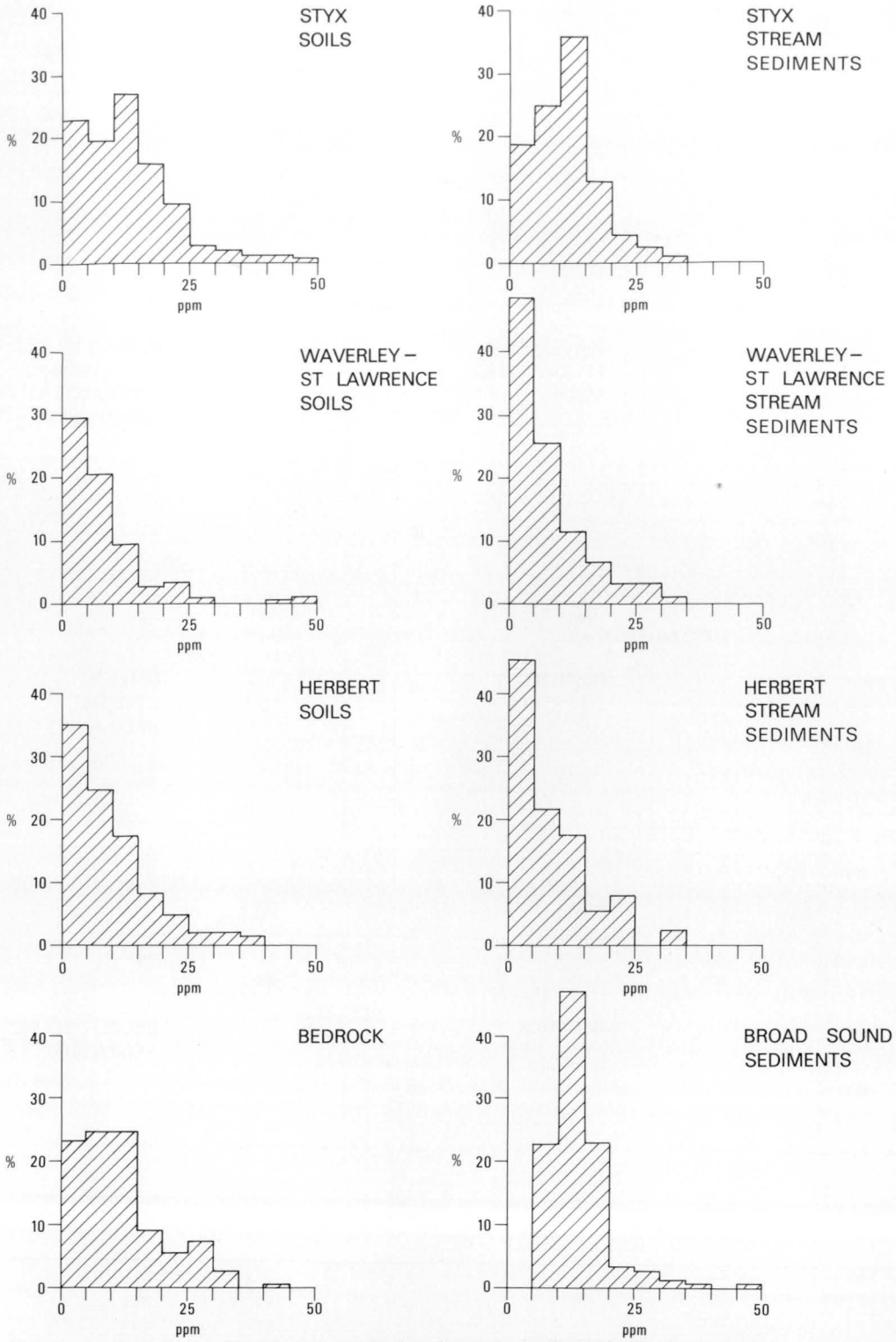


Fig. A9. Co concentration: frequency distribution in Broad Sound catchments and estuarine sediments. F56/AI3/64

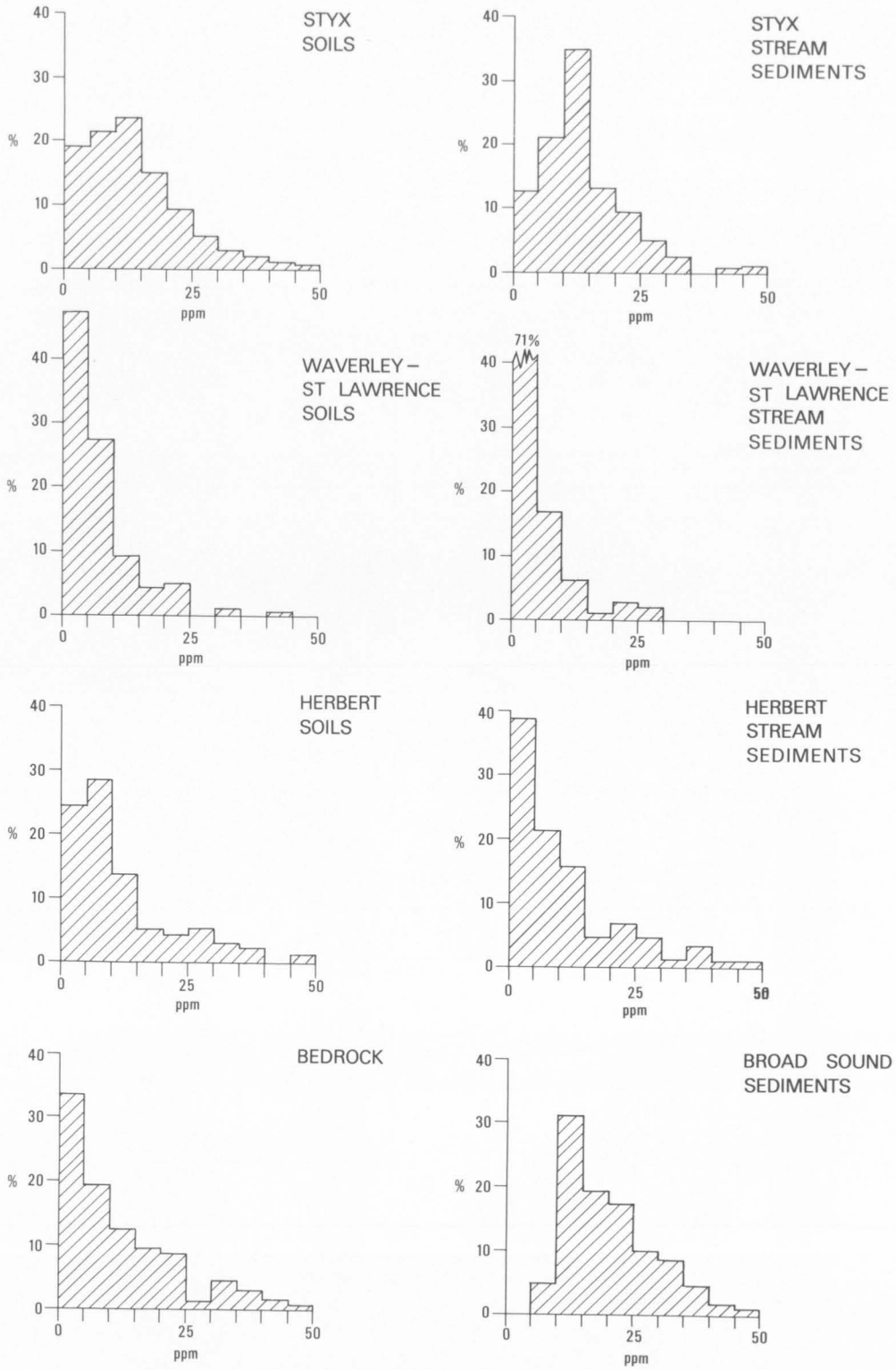


Fig. A10. Ni concentration: frequency distribution in Broad Sound catchments and estuarine sediments.

F56/AI3/65

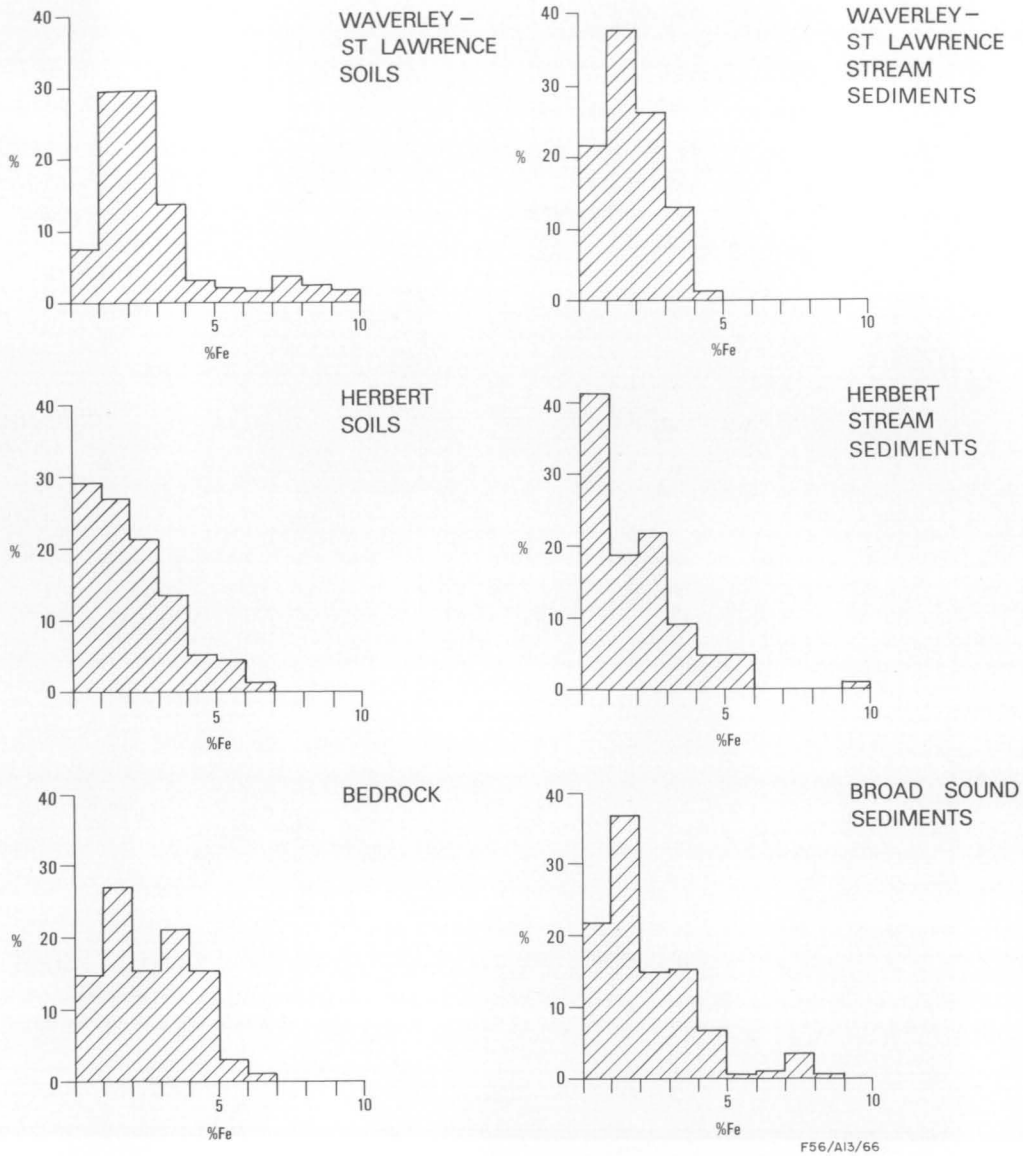


Fig. A11. Fe concentration: frequency distribution in Broad Sound catchments and estuarine sediments.

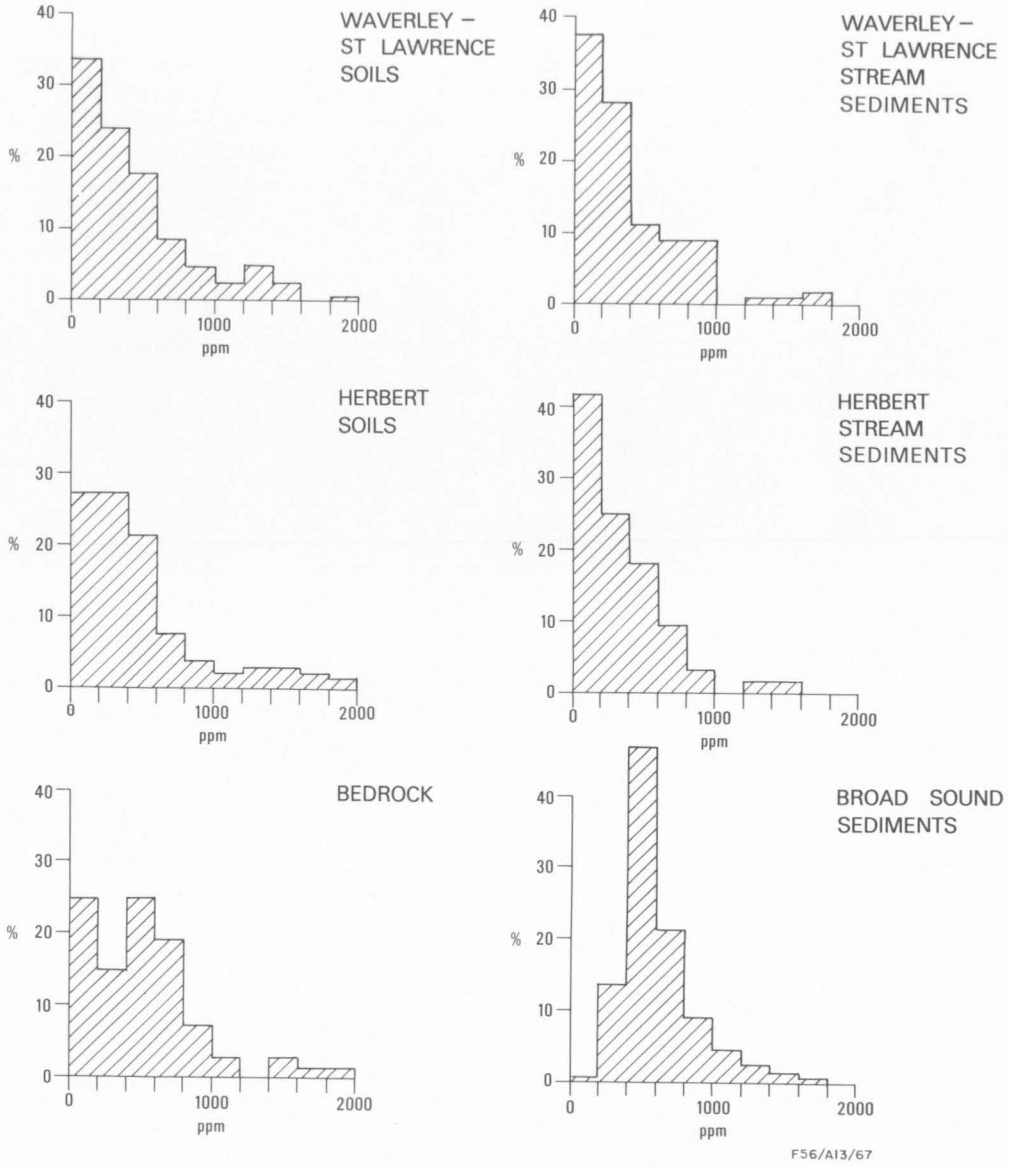


Fig. A12. Mn concentration: frequency distribution in Broad Sound catchments and estuarine sediments.

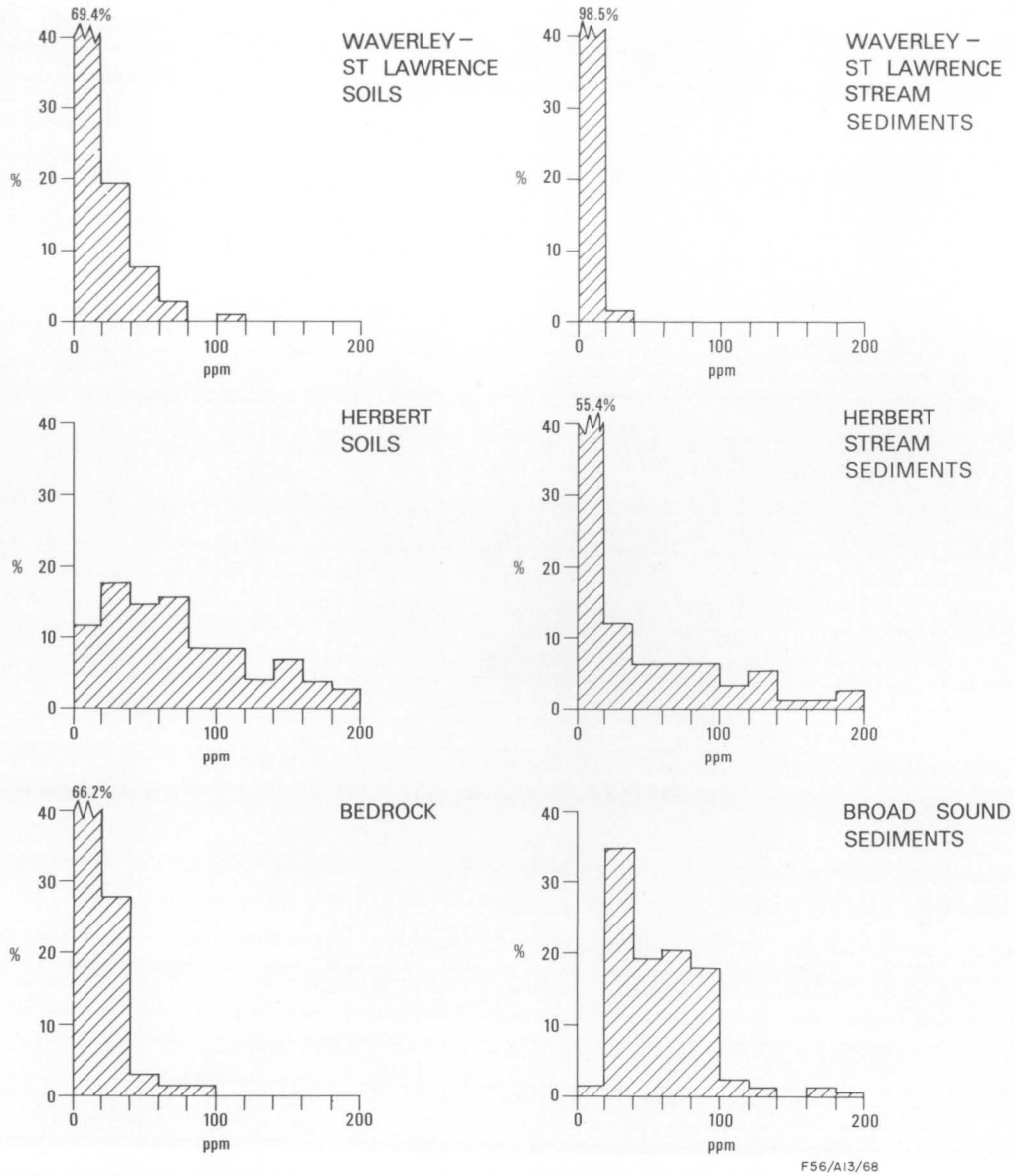


Fig. A13. Cr concentration: frequency distribution in Broad Sound catchments and estuarine sediments.

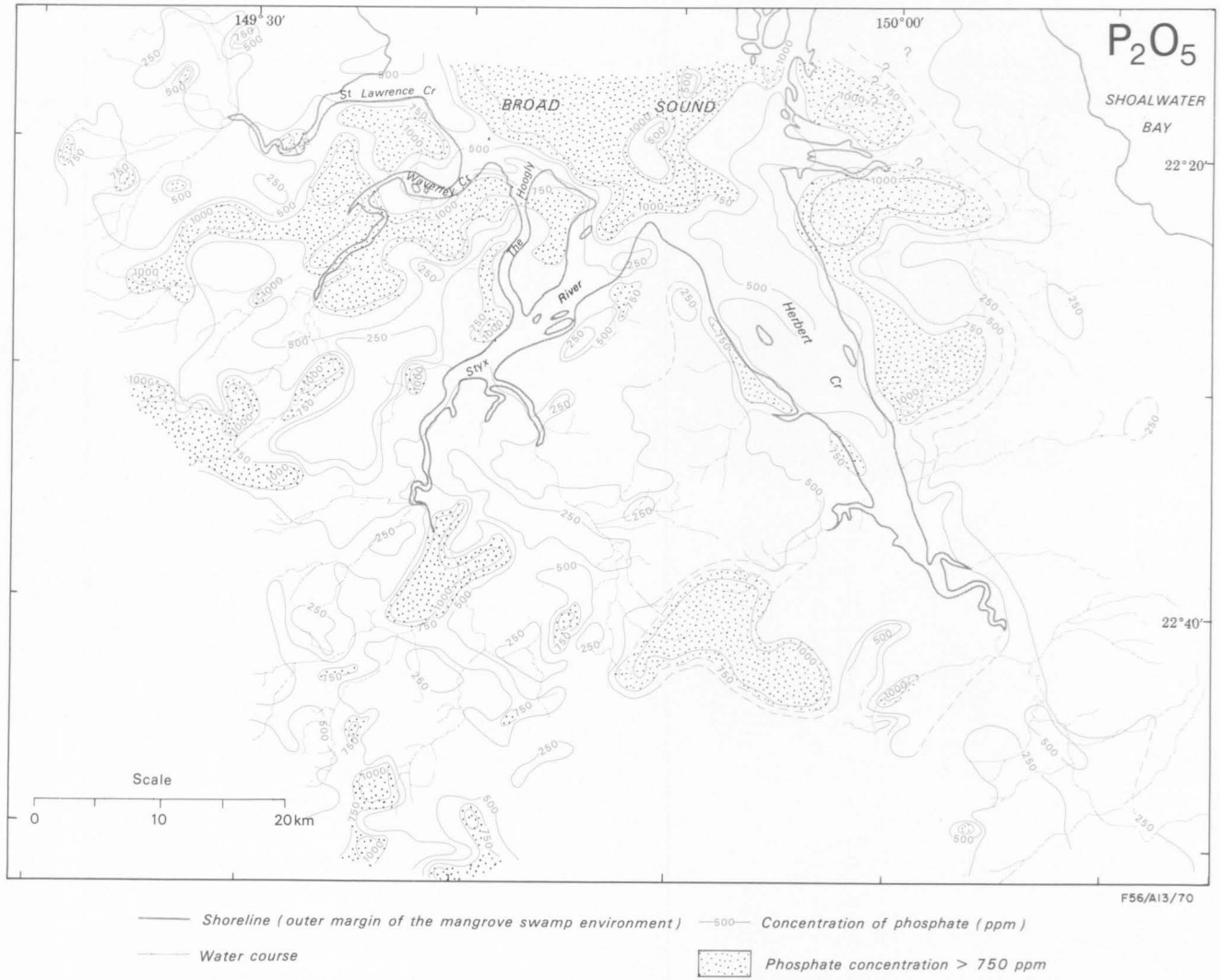


Fig. A14. P_2O_5: distribution in Broad Sound catchment and estuary

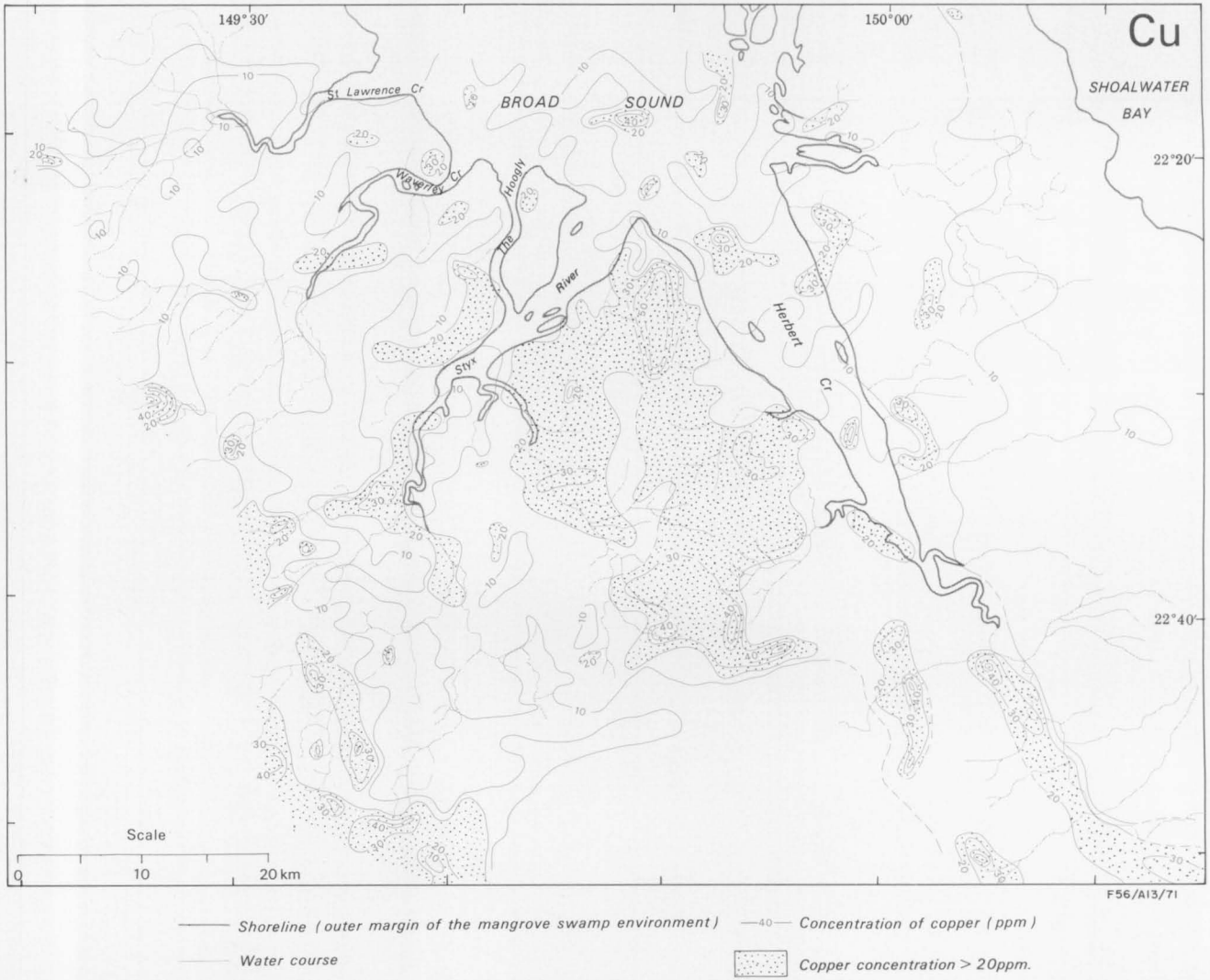


Fig. A15. Cu: distribution in Broad Sound catchment and estuary



Fig. A16. Pb: distribution in Broad Sound catchment and estuary



Fig. A17. Zn: distribution in Broad Sound catchment and estuary



Fig. A18. Co: distribution in Broad Sound catchment and estuary

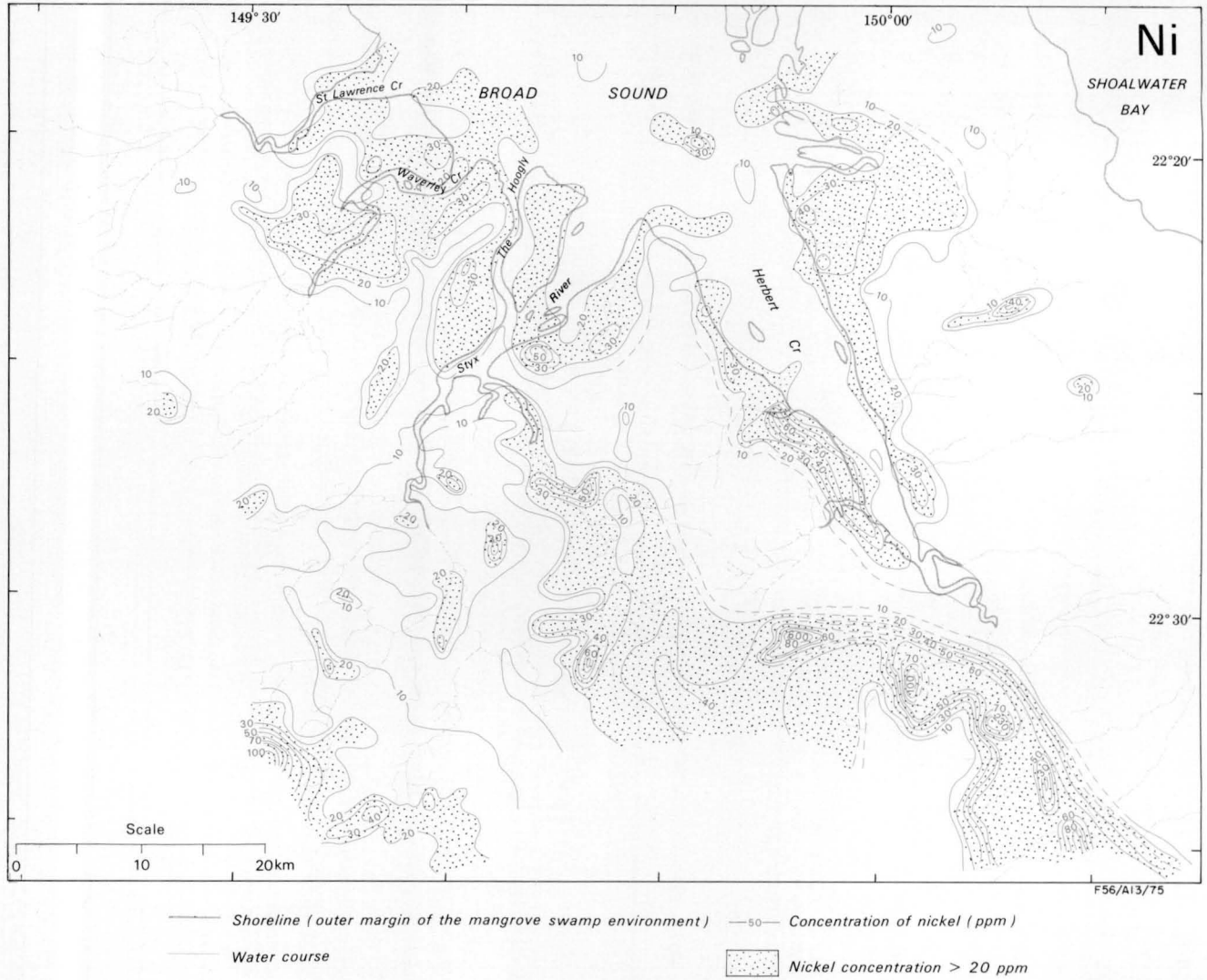


Fig. A19. Ni: distribution in Broad Sound catchment and estuary

side of Broad Sound. On the west side of Broad Sound high Cu values are generally found in soils overlying Palaeozoic rocks, particularly the volcanogenic Carmila Beds and to a lesser extent the Carboniferous-Mesozoic acid intrusive rocks. Therefore in general, the pattern conforms with high background values for Cu in volcanic (or volcanogenic) rocks in the Broad Sound catchment.

Lead

Like Cu, Pb (Fig. A16) also shows low values in the modern estuarine sediments. High Pb values most commonly occur in the catchment on the west side of Broad Sound; there is some association between high Pb and (a) cracking clays, (b) soils which overlie the volcanogenic Carmila Beds, and (c) the Styx Coal Measures (perhaps a reflection of the carbonaceous sediments in this sequence). However, in general the correlation between Pb distribution and geology or soils is poor.

Zinc

A striking feature of the contour map (Fig. A17) is the excellent correlation between areas of high Zn and the supratidal flats and coastal grassland (cracking clays), probably a result of the association of Zn with the clays. There also appears to be a correlation (though less well developed) between high Zn, and soils overlying Carboniferous-Mesozoic intrusive rocks and Tertiary sediments. Conversely the massive red earths are associated with low values.

Cobalt

Figure A18 shows similarities between the distribution of Co and those of Cu and Zn; except in the supratidal zone, values for estuarine sediments are generally low. In the catchment, the anomaly pattern is rather diffuse, though there is a correlation between high Co and areas of cracking clays. High Co values appear to be more common in soils overlying the Permian Carmila Beds than elsewhere.

Nickel

High Ni values (Fig. A19) are clearly associated with the supratidal flats and coastal grasslands cracking clays, and with a sinuous elongate belt trending roughly northwest across the area. This belt of anomalies is particularly well developed to the west of Herbert Creek, in soils above Tertiary sediments. A similar though less well-defined northwesterly trend is also apparent for Co, Cu, and Zn. The occurrence of this elongate Ni anomaly with values of up to 600 ppm Ni in soils above Tertiary sediments is at first sight puzzling, as these concentrations are much higher than those in the Tertiary sediments themselves; they are also much higher than those in sediments in general, which, according to Turekian & Wedepohl (1961), range from 2 to 68 ppm Ni. It is normally only in soils overlying ultrabasic rocks that Ni contents of this order are found. Although no ultrabasic body is shown in Figure A2 in the vicinity of the high Ni values, there are, nevertheless, a number of serpentinite bodies to the south that trend approximately northwest. It seems either that thin Cainozoic deposits are overlying ultrabasic rocks or, less likely, that some of the Tertiary conglomerate contains ultrabasic clasts.

RELATIONSHIPS BETWEEN MINOR AND TRACE ELEMENTS

It is apparent from earlier discussion that the areal distribution of some trace elements is reflected in the distribution of others, suggesting that those elements are associated with each other, or with a common third element. In order to investigate these inter-relationships, correlation matrixes were obtained for various groups of rocks, soils, and stream sediments. Because of the log-normal distributions (Figs. A5-13), all values were transformed to log-normal because some of the statistical tests assumed that variables showed normality.

Stepwise discriminant analysis and Q-technique canonical correlation analysis both indicate that trace element results in bedrock, soil, and stream samples can each be considered as single populations. This is also supported by the frequency histograms (Figs. A5-13) which indicate single (log-normal) populations. Correlation matrixes for the entire catchment are given in Table A5, and for each of the four main catchments in Tables A6-9. Several points are apparent from the matrixes. There are relatively few significant correlations when the entire catchment is considered as a whole, but far more when the four individual catchments are considered separately. This suggests that the populations within each catchment are more homogeneous than those of the Broad Sound catchment as a whole. A second feature is that the soil and stream sediment samples show a much greater number of significant correlations than the bedrock samples. The reason for this is not clear, though it may be due to the relatively small number of bedrock samples and the geochemically heterogeneous nature of the bedrock. A third feature, not unexpectedly, is that the same correlations between elements commonly exist in bedrock, soils, and stream sediments.

TABLE A5. MATRIX OF CORRELATION COEFFICIENTS FOR PHOSPHATE, IRON, AND TRACE ELEMENTS IN ROCKS, SOILS, AND STREAM SEDIMENTS FROM THE ENTIRE BROAD SOUND CATCHMENT. All values were transformed to logarithms before correlation coefficients were determined. When $\rho = 0.5$, confidence levels of 90, 95 and 99 percent are represented by correlation coefficients of 0.587, 0.602, and 0.630 respectively for rocks, 0.566, 0.579, and 0.601 for soils, and 0.555, 0.566 and 0.585 for stream sediments. A confidence level of 95 percent or greater is indicated by an asterisk

	P_2O_5	Cu	Pb	Zn	Co	Ni	Fe	Mn	Cr
Cu									
rock	0.268	1.000							
soil	0.341	1.000							
s. sed.	0.396	1.000							
Pb									
rock	0.330	0.402	1.000						
soil	0.222	0.307	1.000						
s. sed.	0.261	0.581*	1.000						
Zn									
rock	0.178	0.351	0.123	1.000					
soil	0.454	0.682*	0.557	1.000					
s. sed.	0.496	0.678*	0.667*	1.000					
Co									
rock	0.270	0.445	0.165	0.544	1.000				
soil	0.309	0.672*	0.486	0.677*	1.000				
s. sed.	0.351	0.678*	0.621*	0.689*	1.000				
Ni									
rock	0.285	0.540	0.453	0.244	0.513	1.000			
soil	0.228	0.626*	0.271	0.546	0.688*	1.000			
s. sed.	0.262	0.614*	0.492	0.557	0.664*	1.000			
Fe									
rock	0.141	0.506	0.194	0.552	0.680*	0.439	1.000		
soil	0.651*	0.365	0.621*	0.607*	0.617*	0.313	1.000		
s. sed.	0.771*	0.621*	0.604*	0.748*	0.717*	0.460	1.000		
Mn									
rock	0.133	0.368	0.123	0.567	0.589	0.244	0.390	1.000	
soil	0.379	0.436	0.384	0.567	0.612*	0.376	0.381	1.000	
s. sed.	0.497	0.504	0.511	0.662*	0.634*	0.335	0.605*	1.000	
Cr									
rock	0.288	0.089	−0.101	−0.099	−0.079	0.017	−0.093	−0.131	1.000
soil	−0.126	0.143	−0.261	−0.205	0.104	0.454	−0.147	0.007	1.000
s. sed.	0.167	0.448	−0.032	0.028	0.246	0.557	0.121	0.058	1.000

Phosphate

P_2O_5 is widely distributed in most rocks but generally is present only in small amounts mainly in accessory minerals such as apatite and monazite or, more rarely, as collophane in sedimentary rocks. There are few significant trace-element correlations evident with P_2O_5, particularly in the bedrock samples. The only correlations evident in several of the sample groups are P_2O_5-Zn and P_2O_5-Fe. A P_2O_5-Zn correlation has been noted previously in sediments (Cook, 1974), but the reason for the association is not certain. It may in fact result from a P_2O_5-Fe-Zn correlation, both the Zn and P_2O_5 being adsorbed on Fe oxides. Alternatively, all three components may be adsorbed on clays. This would seem to be consistent with the obvious correlation of high P_2O_5 and Zn (Figs. A14, A17) with areas of cracking clays and coastal grassland where there are fine clayey soils. The fact that the Fe-P_2O_5 correlation is far more prominent in the soils and stream sediments of the Waverley and Herbert catchments than in bedrock is consistent with the suggestion made by Goldschmidt (1954) that the oxidation of Fe from ferrous to ferric favours the fixation of phosphorus as an insoluble basic ferric phosphate.

Copper, lead, zinc

These three, being chalcophile elements, are commonly associated. However, correlations of Cu, Pb, and Zn in bedrock samples are almost completely lacking. Despite this absence, in soils and stream sediments a number of correlations between these elements (and with other elements) are evident. Those between Zn and Cu and Zn and Pb are particularly prominent (Table A5) probably reflecting the similarity of the ionic radii of these elements (Fig. A20). Why these correlations should be evident in these superficial deposits, yet not in bedrock, is less certain. Under the highly oxidising conditions prevailing

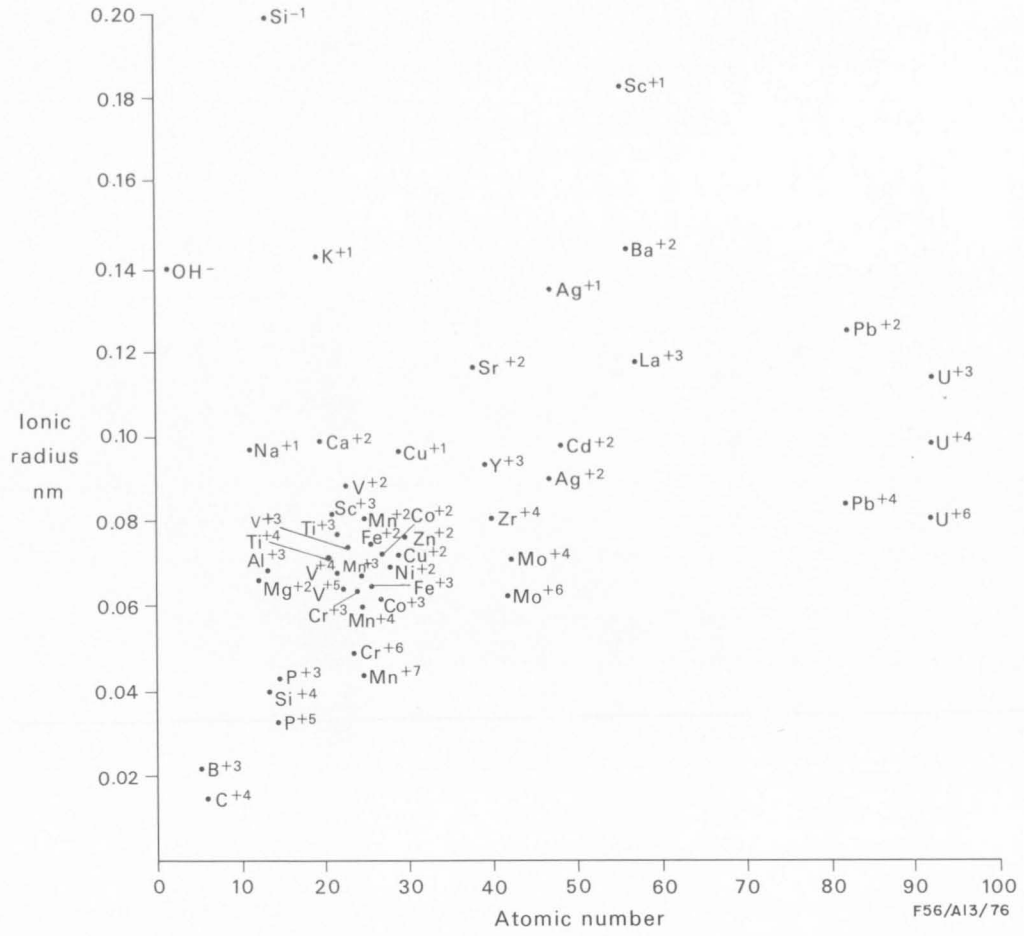


Fig. A20. Ionic radii

during weathering it is most unlikely that these elements are associated as sulphides. It is much more probable that they are linked through ionic exchange with clay anions. Alternatively they may be adsorbed by ferric oxide or hydroxide; this is supported by the fact that Cu, Pb, and Zn all correlate with Fe to varying extents in the soils and stream sediments. When discussing Cu, Wedepohl (1970) makes the point that . . . 'A positive correlation of copper and iron oxides has often been observed. Adsorption or desorption of copper on iron oxide coatings of minerals occurs in relation to copper concentration, strength of available organic chelates, pH, etc'. The same could also be said for Pb and Zn.

It is also evident that there are numerous statistically significant correlations of Cu, Pb, and Zn with Co (Tables A6-9), although the low concentration of Co makes it an unlikely 'carrier' element. It is much more probable that Co is accompanying Fe and that the correlation of the chalcophile elements with Co is secondary. Comparison of mean values for Cu, Pb, and Zn (Tables A1-2) shows that in every case the abundances of these metals in soils and stream sediments are less than their abundances in bedrock, although the ratios vary. Cu, Pb, and Zn are easily weathered, mobile elements (Goldschmidt, 1954), though with different solubilities. Consequently it might be expected that Cu/Pb and Cu/Zn ratios would vary as the degree of weathering varies. Table A10 shows that in fact the relative abundance of Cu generally increases with weathering, possibly as a result of its preferential fixation in clays.

Manganese, chromium, iron, cobalt, nickel

All these transition metals have similar ionic radii (Fig. A20) and will substitute for each other. However, their behaviour, particularly

TABLE A6. WAVERLEY CATCHMENT: MATRIX OF CORRELATION COEFFICIENTS FOR PHOSPHATE, IRON, AND TRACE ELEMENTS IN ROCKS, SOILS, AND STREAM SEDIMENTS. All values were transformed to logarithms before correlation coefficients were determined. Correlations significant at a confidence level of 95 percent or higher ($\rho = 0.3$) are indicated by an asterisk

	P_2O_5	Cu	Pb	Zn	Co	Ni	Fe	Mn	Cr
Cu									
rock	−0.052	1.000							
soil	0.448	1.000							
s. sed.	0.468	1.000							
Pb									
rock	0.173	0.342	1.000						
soil	0.471*	0.445	1.000						
s. sed.	0.427	0.452	1.000						
Zn									
rock	−0.147	0.514	0.120	1.000					
soil	0.578*	0.700*	0.644*	1.000					
s. sed.	0.593*	0.721*	0.630*	1.000					
Co									
rock	0.297	0.669*	0.127	0.524	1.000				
soil	0.454	0.506*	0.509*	0.546*	1.000				
s. sed.	0.458	0.526*	0.514*	0.527*	1.000				
Ni									
rock	0.155	0.606	0.149	0.243	0.614	1.000			
soil	0.491*	0.570*	0.463	0.654*	0.730*	1.000			
s. sed.	0.476*	0.593*	0.440	0.626*	0.714*	1.000			
Fe									
rock	0.185	0.508	0.194	0.309	0.564	0.363	1.000		
soil	0.637*	0.442	0.717*	0.529*	0.578*	0.502	1.000		
s. sed.	0.588*	0.507*	0.738*	0.568*	0.597*	0.509*	1.000		
Mn									
rock	−0.112	0.534	0.069	0.814*	0.607	0.446	0.284	1.000	
soil	0.338	0.488*	0.359	0.617*	0.564*	0.422	0.246	1.000	
s. sed.	0.398	0.525*	0.422	0.693*	0.556*	0.450	0.345	1.000	
Cr									
rock	0.360	−0.256	0.293	−0.230	−0.106	−0.206	−0.214	−0.148	1.000
soil	0.133	−0.016	0.277	0.058	0.251	0.249	0.430	−0.008	1.000
s. sed.	0.048	−0.012	0.242	0.085	0.287	0.293	0.346	0.080	1.000

under weathering conditions, varies considerably, depending on their oxidation state. In addition, pH, particularly of soils, can have a marked influence on the fixation or mobilisation of metals such as Mn. Weathering is reflected in the varying ratios of some of the elements (Table A11). The Fe/Mn ratio in particular increases markedly with increasing oxidation state, probably in part the result of the conversion of the relatively soluble divalent Fe to the highly insoluble trivalent Fe, which is then preferentially precipitated in the soils. Mn on the other hand is less readily oxidised than Fe and therefore much of it remains in solution as the divalent ion. There is also an increase in the Co/Ni ratio with increased weathering, though this may be due to the preferential incorporation of Ni in clays rather than to the oxidation state of the ions.

As was previously noted for Cu, Pb, and Zn, most of the metals investigated decrease in concentration as a result of weathering (Tables A1, A2), though Fe and Cr are notable exceptions. The increase in Fe is probably a reflection of its increased oxidation resulting in lowered solubility, and its ultimate precipitation within the soil profile. In the case of Cr the higher-valence ions are more soluble and therefore oxidation might be expected to produce a depletion of Cr. However, it is also possible that Cr is being concentrated in the soil by organo-metallic fixation.

Because of the similarity in the ionic radii of Mn, Cr, Fe, Co, and Ni, a number of inter-element correlations might be expected and it is apparent from Tables A5-9 that this is so. Common associations in bedrock include Co-Ni and Co-Fe. However, such associations are far more numerous in the soils and stream sediments and include Co-Ni, Co-Fe, Co-Mn, and Fe-Mn. In addition, Fe, Co, Ni, and Mn all show significant correlations with Cu and Zn, a likely consequence of the adsorption of all these metals by clays, or alternatively their common association with Fe oxides. The lack of any significant correlations with Cr is puzzling in view of the close similarity between the ionic radius of Cr and the other transition elements. However, under strongly oxidising conditions the formation

TABLE A7. HERBERT CATCHMENT: MATRIX OF CORRELATION COEFFICIENTS FOR PHOSPHATE, IRON, AND TRACE ELEMENTS IN ROCKS, SOILS, AND STREAM SEDIMENTS. All values were transformed to logarithms before correlation coefficients were determined. Correlations significant at a confidence level of 95 percent or higher ($\rho = 0.3$) are indicated by an asterisk

	P_2O_5	Cu	Pb	Zn	Co	Ni	Fe	Mn	Cr
Cu									
rock	0.596	1.000							
soil	0.705*	1.000							
s. sed.	0.702*	1.000							
Pb									
rock	0.322	0.370	1.000						
soil	0.304	0.290	1.000						
s. sed.	0.183	0.166	1.000						
Zn									
rock	0.855*	0.618	0.476	1.000					
soil	0.651*	0.721*	0.597*	1.000					
s. sed.	0.644*	0.733*	0.579*	1.000					
Co									
rock	0.657	0.654	0.611	0.721*	1.000				
soil	0.541*	0.755*	0.505*	0.706*	1.000				
s. sed.	0.544*	0.757*	0.473	0.794*	1.000				
Ni									
rock	0.253	0.539	0.626	0.388	0.757*	1.000			
soil	0.347	0.531*	0.325	0.482*	0.717*	1.000			
s. sed.	0.335	0.468	0.241	0.505*	0.627*	1.000			
Fe									
rock	0.667	0.613	0.448	0.721*	0.721*	0.577	1.000		
soil	0.673*	0.735*	0.576*	0.742*	0.785*	0.528*	1.000		
s. sed.	0.672*	0.695*	0.516*	0.736*	0.778*	0.453	1.000		
Mn									
rock	0.755*	0.632	0.345	0.687	0.727*	0.437	0.749*	1.000	
soil	0.452*	0.566*	0.589*	0.630*	0.749*	0.536*	0.666*	1.000	
s. sed.	0.435	0.489*	0.586*	0.685*	0.739*	0.508*	0.631*	1.000	
Cr									
rock	−0.253	0.045	−0.320	−0.245	−0.057	0.080	−0.210	−0.261	1.000
soil	−0.284	−0.207	−0.354	−0.383	−0.143	−0.293	−0.269	−0.150	1.000
s. sed.	−0.299	−0.297	−0.441	−0.520	−0.340	0.189	−0.392	−0.263	1.000

of the relatively small hexavalent Cr ion (Fig. A20) may possibly decrease the extent to which substitution takes place.

Therefore, although most of the elements behave in accordance with normal geochemical rules, some (such as Cr) nevertheless deviate from this because of the complexity of some of the elemental inter-relationships. This point is admirably expressed by Hawkes & Webb (1962) who state . . . 'The factors controlling the mobility of an element in the cycle of weathering are numerous and extremely complex. They are so complicated [that] . . . it is still difficult to say on theoretical grounds whether an element is likely to be mobile or immobile'. This statement is still true, 17 years later.

INFLUENCE OF CATCHMENT GEOCHEMISTRY ON ESTUARY GEOCHEMISTRY

One of the objectives of the Broad Sound project was to determine the extent to which the geochemistry of estuarine sediments is influenced by the geochemistry of the drainage basin. Earlier discussions have clearly shown (Table A4) that the mean concentrations of a number of elements vary significantly between the four major catchment areas. Therefore, if the geochemistry of an individual estuary is influenced by that of its catchment, then many of the same significant differences in mean compositional values should also be apparent in estuarine sediments. In addition it was hoped to determine differences in elemental behaviour in order to ascertain how inter-element association and elemental mobility vary in the estuarine, fluvial, and subaerial (soil) environments. Both these aims proved difficult to achieve because of the abundance of biogenic carbonate in most of the sediments. This had the dual effect of influencing the inter-element correlations and of making the absolute concentration of most trace metals a function of the extent of dilution by calcium carbonate. If trace metals could be allocated solely to the terrigenous or to the calcareous

TABLE A8. ST LAWRENCE CATCHMENT: MATRIX OF CORRELATION COEFFICIENTS FOR PHOSPHATE, IRON, AND TRACE ELEMENTS IN ROCKS, SOILS, AND STREAM SEDIMENTS. All values were transformed to logarithms before correlation coefficients were determined. Correlations significant at a confidence level of 95 percent or higher (ρ = 0.3) are indicated by an asterisk

	P_2O_5	Cu	Pb	Zn	Co	Ni	Fe	Mn	Cr
Cu									
rock	0.424	1.000							
soil	0.396	1.000							
s. sed.	0.387	1.000							
Pb									
rock	0.083	0.281	1,000						
soil	−0.002	0.037	1.000						
s. sed.	0.038	0.048	1.000						
Zn									
rock	0.625*	0.300	0.107	1.000					
soil	0.463	0.454	0.225	1.000					
s. sed.	0.429	0.457	0.179	1.000					
Co									
rock	0.598*	0.370	0.194	0.587	1.000				
soil	0.182	0.188	0.375	0.550*	1.000				
s. sed.	0.136	0.185	0.347	0.533*	1.000				
Ni									
rock	0.419	0.368	0.307	0.319	0.637*	1.000			
soil	0.311	0.371	0.091	0.242	0.145	1.000			
s. sed.	0.312	0.395	0.116	0.271	0.148	1.000			
Fe									
rock	0.597*	0.559	0.186	0.636*	0.695*	0.598*	1.000		
soil	0.396	0.227	0.211	0.378	0.604*	0.155	1.000		
s. sed.	0.378	0.218	0.227	0.382	0.613*	0.115	1.000		
Mn									
rock	0.531	0.015	0.119	0.293	0.434	0.129	0.181	1.000	
soil	0.375	0.177	0.229	0.481	0.399	−0.094	0.189	1.000	
s. sed.	0.351	0.162	0.209	0.458	0.383	−0.113	0.183	1.000	
Cr									
rock	0.257	0.362	0.011	0.121	0.109	0.135	0.216	0.000	1.000
soil	0.118	−0.072	−0.039	−0.282	−0.129	0.277	0.123	−0.133	1.000
s. sed.	0.117	−0.072	−0.024	−0.285	−0.136	0.230	0.094	−0.134	1.000

TABLE A9. STYX CATCHMENT: MATRIX OF CORRELATION COEFFICIENTS FOR PHOSPHATE, IRON, AND TRACE ELEMENTS IN ROCKS, SOILS, AND STREAM SEDIMENTS. All values were transformed to logarithms before correlation coefficients were determined. Correlations significant at a confidence level of 95 percent or higher (ρ = 0.3) are indicated by an asterisk

	P_2O_5	Cu	Pb	Zn	Co	Ni
Cu						
rock	0.159	1.000				
soil	0.335	1.000				
s. sed.	0.285	1.000				
Pb						
rock	0.008	−0.041	1.000			
soil	0.147	0.281	1.000			
s. sed.	0.186	0.460*	1.000			
Zn						
rock	0.503*	0.307	0.144	1.000		
soil	0.384	0.723*	0.452*	1.000		
s. sed.	0.327	0.727*	0.637*	1.000		
Co						
rock	0.433	0.398	−0.039	0.547*	1.000	
soil	0.248	0.695*	0.334	0.688*	1.000	
s. sed.	0.157	0.692*	0.484*	0.686*	1.000	
Ni						
rock	0.256	0.341	0.029	0.289	0.508*	1.000
soil	0.211	0.582*	0.109	0.596*	0.574*	1.000
s. sed.	0.303	0.436*	0.361	0.554*	0.483*	1.000

TABLE A10. Cu/Pb, Cu/Zn, AND Pb/Zn RATIOS (MEAN VALUES) IN ROCKS, SOILS, AND STREAM SEDIMENTS, ENTIRE BROAD SOUND CATCHMENT

	bedrock	soils	stream sediments
Cu/Pb	0.92	1.11	0.82
Cu/Zn	0.36	0.54	0.48
Pb/Zn	0.40	0.49	0.57

TABLE A11. Fe/Mn, Co/Ni, Fe/Ni RATIOS (MEAN VALUES) IN ROCKS, SOILS, AND STREAM SEDIMENTS, ENTIRE BROAD SOUND CATCHMENT

	bedrock	soils	stream sediments
Fe/Mn	39.1	71.4	44.5
Co/Ni	0.488	0.637	0.828
Fe/Ni	405.0	791.7	1151.5

TABLE A12. MEAN COMPOSITION (ppm) OF LOW-CARBONATE SEDIMENTS (LESS THAN 5 PERCENT $CaCO_3$) IN COMPONENT ESTUARIES, COMPARED WITH BROAD SOUND ESTUARY AS A WHOLE.

	Herbert estuary	Styx estuary	Waverley estuary	Broad Sound
P_2O_5	887.4	638.3	765.8	746.2
Cu	18.7	22.4	18.8	19.9
Pb	16.1	16.7	17.5	16.2
Zn	62.3	57.1	65.9	60.1
Co	15.9	18.4	18.7	17.2
Ni	35.7	29.2	33.2	32.0
Fe*	4.01	3.55	3.76	3.76
Mn	497.7	513.1	684.6	532.7
Cr	94.6	81.1	81.7	84.7

* percent

fraction, then values could be recalculated on a carbonate-free basis. However, this partition of elements could not in most cases be made with any confidence. Therefore it was decided to use only the slightly calcareous sediments (arbitrarily taken as those sediments with 5 percent or less of $CaCO_3$) for comparing estuarine and drainage-basin geochemistry.

The mean composition of this low-carbonate fraction for Broad Sound as a whole and also for the Herbert, Styx, and Waverley estuaries is given in Table A12. No mean value is given for the St Lawrence estuary, because of lack of low-carbonate sediments in that estuary (in part an artifact of the sampling grid). Comparison of the geochemistry of the Broad Sound estuarine sediments (Table A12) with the drainage basin geochemistry (Table A1) (particularly the soils and stream sediments) shows that in the case of P_2O_5, Cu, and Pb, values in the estuary are similar to those found in the drainage basin, whereas Zn, Co, Ni, Fe, Mn, and Cr show variable but definite concentration increases in the estuary. The low-carbonate Broad Sound sediments are exclusively fine-grained muds which are finer grained than the soils or the minus-80-mesh fraction of the stream sediments. Therefore there is likely to be increased adsorption due to the greater abundance of clays. Some cations retain much the same ratio in the estuarine sediments as in the drainage basin, e.g. the average Fe/Mn ratio in the estuary is 70.4, whereas in the soils of the drainage basin it is 71.4. Similarly the Fe/Ni ratio in the estuarine sediments is 1175 and in stream sediments 1152.

As with the catchment data, the inter-element associations may be investigated by determining correlation coefficients. The correlation matrix (Table A13) indicates several elemental associations, including P_2O_5-Zn, Co-Ni, and Co-Mn which were also present in the catchment. However, a number of other associations are not apparent in the estuary, particularly between Cu, Pb, and Zn; and still other associations, particularly Ni-Fe, Ni-Mn, Ni-Cr, and Fe-Cr, are evident in the estuarine sediments, yet not in the drainage basin. This suggests different patterns of elemental dispersion and concentration in estuarine and continental environments. The difference cannot be due to a subaqueous versus a subaerial environment, as the fine-grained low-carbonate sediments are

TABLE A13. BROAD SOUND ESTUARY: MATRIX OF CORRELATION COEFFICIENTS FOR PHOSPHATE, IRON, AND TRACE ELEMENTS IN FINE-GRAINED, LOW-CARBONATE, ESTUARINE SEDIMENTS. All analyses were log-transformed before correlation coefficients were determined. Correlations significant at a confidence level of $\geq$ 95 percent (ρ = 0.3) are indicated by an asterisk.

	P_2O_5	Cu	Pb	Zn	Co	Ni	Fe	Mn	Cr
P_2O_5	1.000								
Cu	−0.151	1.000							
Pb	0.035	0.234	1.000						
Zn	0.632*	0.056	0.435	1.000					
Co	0.105	0.449	0.533	0.354	1.000				
Ni	0.251	0.280	0.536	0.476	0.639*	1.000			
Fe	0.346	0.424	0.265	0.366	0.372	0.752*	1.000		
Mn	0.157	0.128	0.423	0.354	0.581*	0.597*	0.448	1.000	
Cr	0.169	0.178	0.312	0.301	0.373	0.796*	0.706*	0.480	1.000

almost exclusively from supratidal locations which are covered by sea water for no more than a few hours in every month. Despite this, they are generally in contact with hypersaline pore waters (see pp. 108-116), whereas the moisture content of the soils and the stream sediments is low for most of the year. It is likely that the hypersaline pore waters, which are not static but move through the fine-grained supratidal sediments, provide ample opportunity for a higher level of metal adsorption by the clays, thus producing much higher metal contents in the estuarine sediments than are found in the catchment material being supplied to the estuary. The clay mineralogy may also have some influence on the metal content. Gibson (*in* Cook & Mayo, 1978, p.146) has shown that the clay mineralogy of the estuarine sediments differs to some extent from that of the drainage basin soils, partly because of the degradation of montmorillonite to mixed-layer clays and illite in the supratidal zone.

It has already been pointed out that some catchment areas have higher metal contents than others, and it might be expected that these differences would be reflected in the composition of the sediments of the corresponding estuary. However, although the phosphate and trace-metal contents of the three estuaries (Herbert, Styx, and Waverley) do vary somewhat, F and *t*-tests on the mean concentrations (Table A4) suggest that few of these differences are statistically significant. Comparison of Table A4 with Table A14 shows that the drainage basin composition is far more heterogeneous than that of the estuarine sediments. Thus it appears from the elemental composition, that the estuarine sediments have been largely homogenised and that the sediments of individual estuaries do not reflect the composition of their corresponding drainage basin. This seems reasonable in view of the large-scale movement of sediment within the estuary as a result of tides and currents (Cook & Mayo, 1978).

In conclusion, then, the composition of Broad Sound low-carbonate sediments as a whole (Table A12) is somewhat similar to that of the drainage basin as a whole, particularly in the case of Cu, Pb and P_2O_5. However, depositional and especially post-depositional chemical processes have effects on Zn, Co, Ni, Fe, Mn and Cr concentration that are at least as important and probably more important than the composition of the drainage basin.

TABLE A14. COMPARISONS OF TRACE-ELEMENT, PHOSPHATE, AND IRON MEANS IN THE LOW-CARBONATE SEDIMENTS OF THE HERBERT (1), STYX (2), AND WAVERLEY (3) ESTUARIES

	Estuaries being compared		
	1 with 2	1 with 3	2 with 3
P_2O_5	>	=	=
Cu	=	=	>
Pb	=	=	=
Zn	=	=	=
Co	=	=	=
Ni	>	=	=
Fe	=	=	=
Mn	=	<	<
Cr	X	=	=

X F-test indicates different populations (therefore *t*-test not applied)
1>2 *t*-test indicates the mean for the Herbert estuary is greater than the mean for the Styx estuary at a confidence level of 95 percent.
1<2 *t*-test indicates the mean for the Herbert estuary is less than the mean for the Styx estuary at a confidence level of 95 percent.
1=2 *t*-test indicates means are the same.

GEOCHEMISTRY OF THE ESTUARINE SEDIMENTS

In Part B, Mayo, using a variety of mathematical techniques (particularly multivariate analysis) considers the geochemistry of the estuarine sediments in some detail. This chapter, using more intuitive procedures, attempts to answer some of the same questions. The determination of phosphorus concentration in the water column, the sediments, and associated pore waters was obviously an important aspect of the Broad Sound estuary analytical program. Because the behaviour of other elements can greatly influence the distribution of phosphorus, it was decided to undertake a comprehensive program of geochemical analysis, in order to better understand the geochemical factors influencing the concentration and dispersal of phosphorus. With a wide range of elemental analyses available it is then possible to consider a number of broader questions such as the extent of inter-element association in estuarine sediments. This chapter also considers the effect of depositional environment on the geochemistry of sediments, and, conversely, the extent to which the geochemistry of sediments might be used to identify depositional environments. A further purpose of this chapter is to provide basic documentation of the composition of Broad Sound estuarine sediments. This, together with the sedimentological data given in the previous Bulletin (Cook & Mayo, 1978) should then make Broad Sound a useful modern analogue for environmental

reconstruction. However, an equally important function of the Broad Sound geochemical results is to act as a yardstick against which to measure future geochemical changes in tropical estuarine environments, resulting from modifications by man.

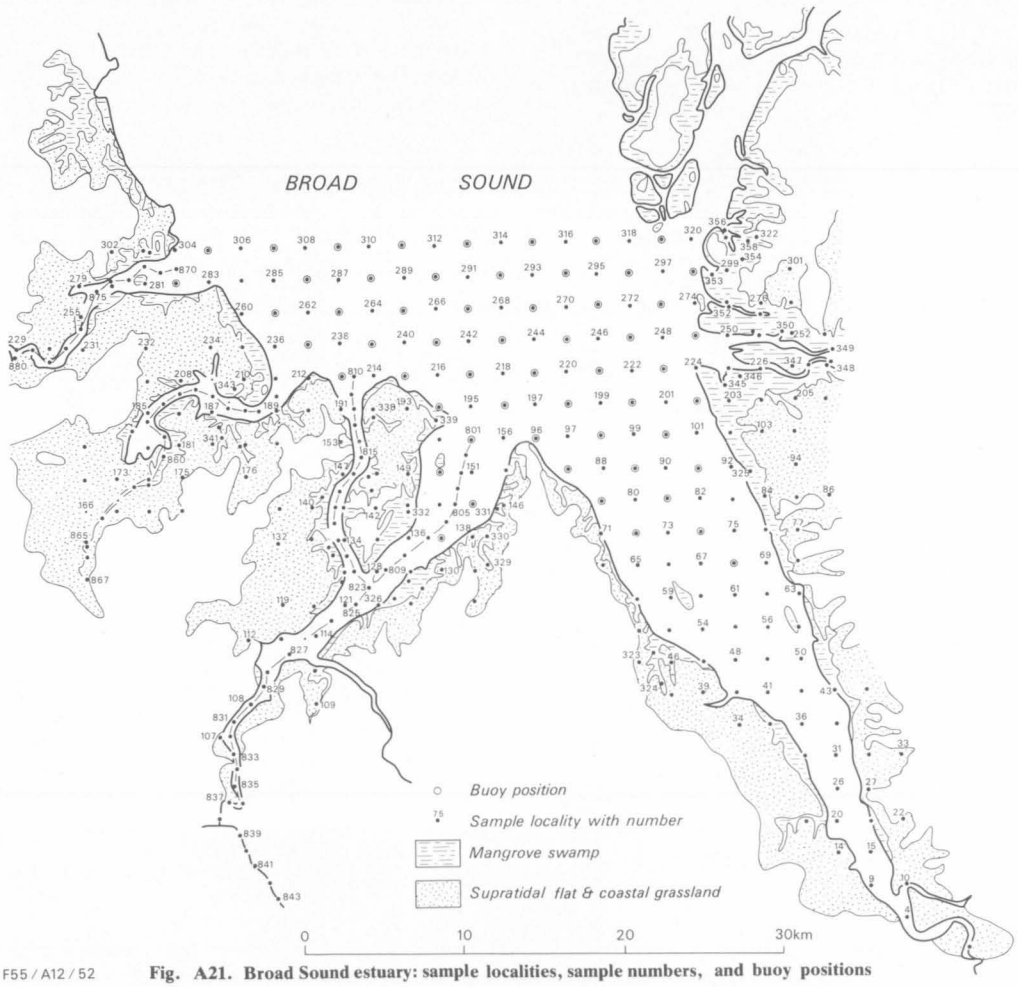
ANALYTICAL TECHNIQUES

Approximately 350 samples were collected from the estuary (Fig. A21). As it was necessary to analyse these sediment samples for a large number of parameters, a standardised sample preparation scheme was adopted (Pl. A2). Grainsize and mineralogical analyses are discussed by Cook & Mayo (1978), who also describe the sampling scheme and techniques. In order to minimise contamination, all grinding was carried out with agate or porcelain mortars and sieving was through nylon mesh.

Phosphate analyses were undertaken by AMDEL using the colorimetric phosphovanadomolybdate method, following perchloric acid digestion.

$CaCO_3$ content was determined at BMR by one of two methods discussed in detail by Armstrong (1973). The weight-loss method, involving digestion with dilute hydrochloric acid, was used for most samples. However, for samples containing gypsum (supratidal-flat and mangrove-swamp sediments), a volumetric method employing the Collins calcimeter was used. Precision for this method was within 3 percent.

Atomic absorption spectroscopy (by AMDEL), following hydrochloric-perchloric extraction, was used for Pb, Zn, Co, and Mo.



F55 / A12 / 52 **Fig. A21. Broad Sound estuary: sample localities, sample numbers, and buoy positions**

Precision for these analyses was estimated (by AMDEL) at ± 5 percent.

Ba, Ca, Co, Cr, Cu, Fe, La, Mg, Mn, Ni, Sc, Sr, Ti, V, and Y, together with loss on ignition, were determined in the BMR laboratories by direct-reading optical emission spectroscopy. The analytical method used was adapted from Ahrens & Taylor (1961). One part of the sample was mixed with two parts of graphite. This mixture was then loaded into a pre-formed graphite electrode, and arced as the anode in a constant DC current for 130 seconds. Both internal and rock-standard control were used. Precision for this method has been determined at about ± 10 percent.

A combination of X-ray fluorescence, direct-reading optical spectroscopy, and wet-chemical procedures was used by AMDEL for whole-rock silicate analyses; precisions determined from replicate analyses were: SiO_2, ± 1%; Al_2O_3 ± 1%; total Fe as Fe_2O_3, ± 17%; CaO, ± 2%; MgO, ± 7%; Na_2O, ± 16%; K_2O, ± 10%; MnO, ± 3%; P_2O_5, ± 10%; TiO_2, ± 4%; CO_2, ± 5%; H_2O-, ± 2%; H_2O+, ± 3%.

THE SEDIMENTS OF BROAD SOUND

Broad Sound is a mixed ephemeral estuarine complex (Cook & Mayo, 1978) characterised by shallow water, complete vertical mixing of the water column, a very large tidal range (10 m), and strong tidal currents (up to 4 knots). Water depths in the study area range from zero to about 20 m.

Depositional environments

A five-fold classification of depositional environments is used, based on morphology and location within the tidal range (Fig. A22). The distribution of the depositional environments is shown in Figure A23. The *shallow-marine environment* is defined as entirely subtidal; sediments range from muds on the west side of the Sound, to sands in areas flanking the intertidal sand ridges, and gravels in the more seaward portion. Gravels predominate in the shallow-marine environment, and are composed mainly of calcareous nodules and shells, overlying a hard indurated pavement; much of the gravel is believed to be a lag deposit derived by winnowing from pre-Holocene or early

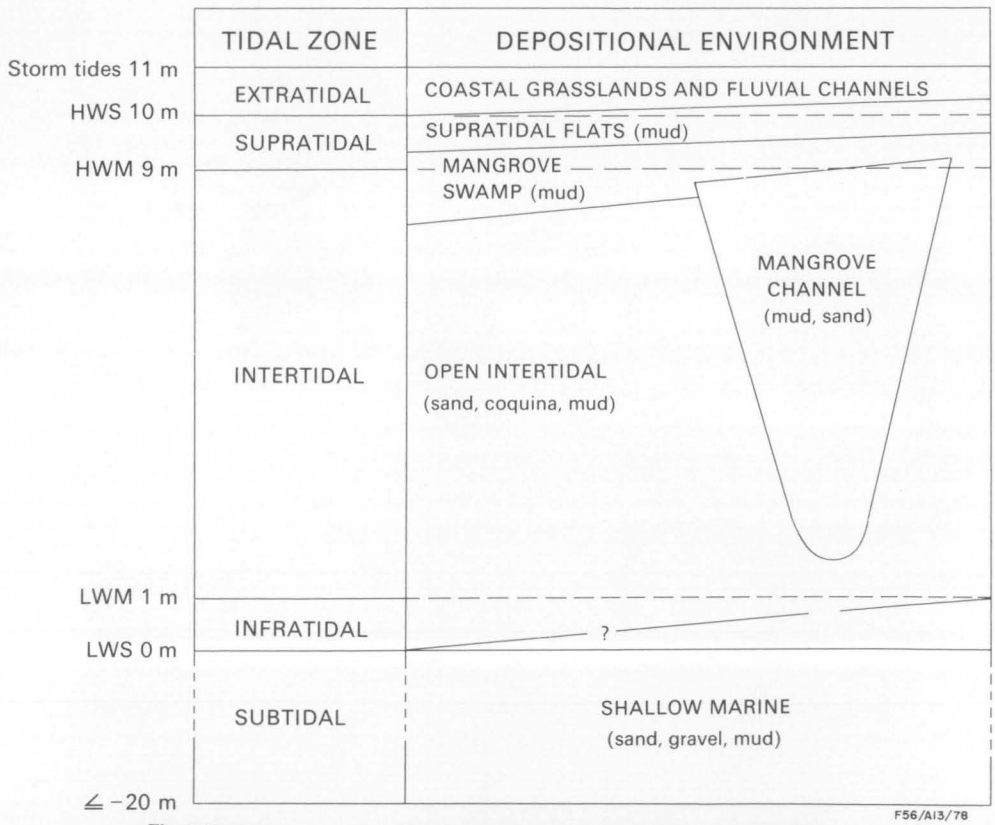
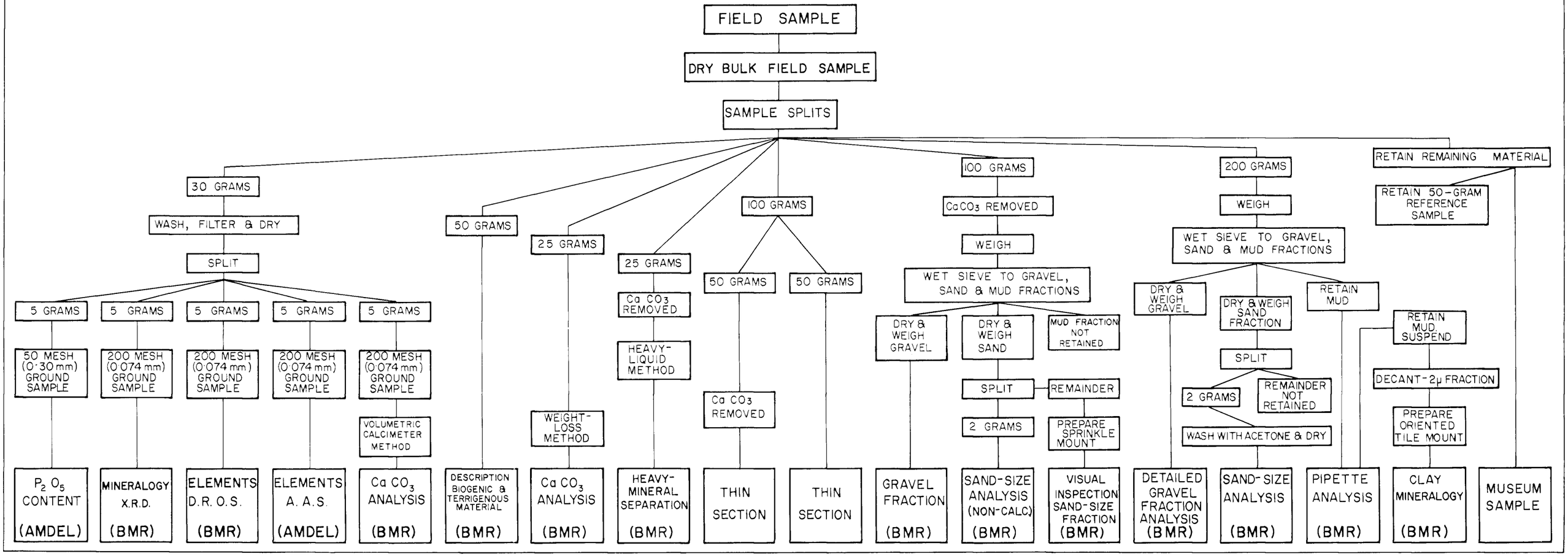


Fig. A22. Schematic relationship of tidal zones and depositional environments

PLATE A2

SAMPLE TREATMENT FLOWSHEET, BROAD SOUND ESTUARY SAMPLES



F52 / A13-143

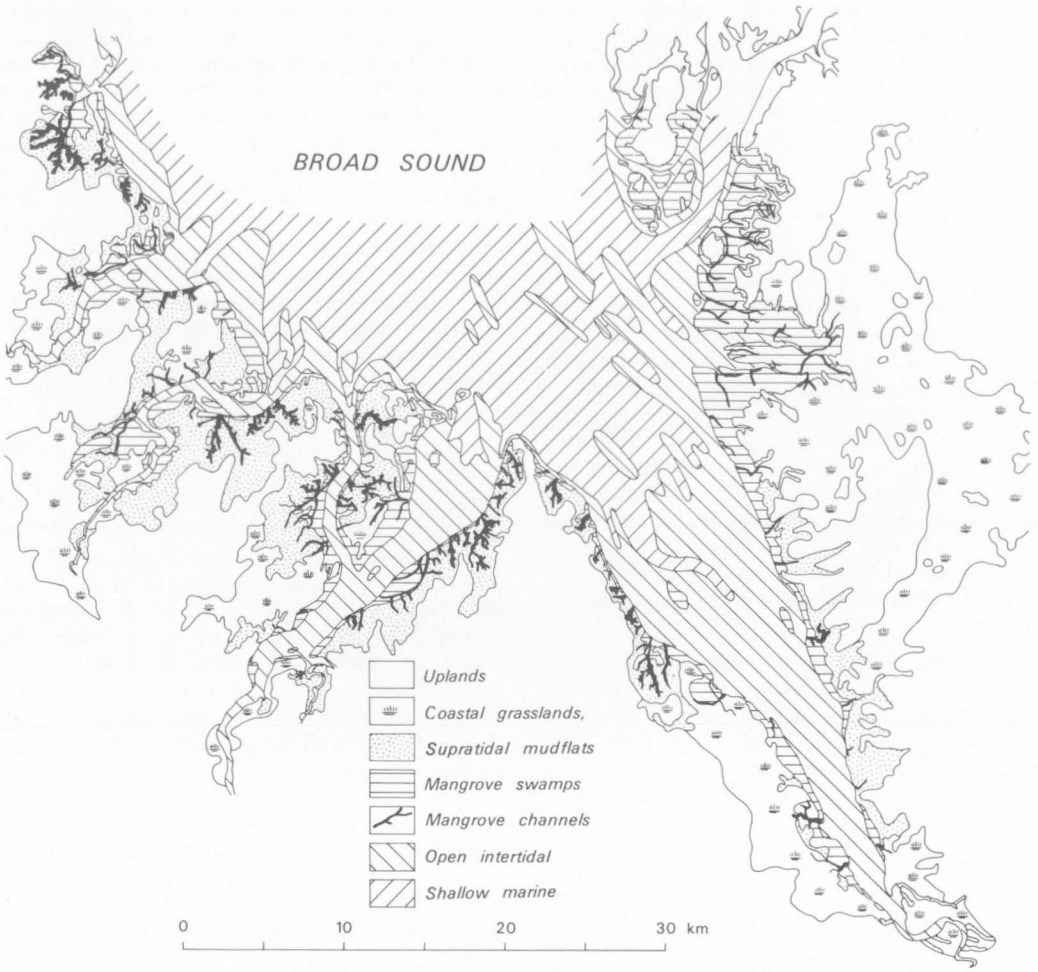


Fig. A23. Distribution of depositional environments

Holocene subaerial sediment. Many of the calcareous nodules are probably of pedogenic origin but some are calcareous intraclasts.

The *open-intertidal environment* occupies the infratidal zone and most of the intertidal zone. It interdigitates seaward with the shallow-marine environment. A few relict gravels are present in the intertidal zone; high in the zone there are a few coarse beach deposits, cemented in places to form beachrock. The sandy facies dominates the open-intertidal environment. These sands are medium to fine-grained, well sorted, and contain an average of about 40 percent $CaCo_3$, mainly in the form of shells and shell fragments. There is a seaward trend of increasing grain size in the open intertidal sands. Features of these sands include abundant mud balls, intraformational breccias (resulting from the break-up of fine mud and sand laminae), and cross beds. There is extensive bioturbation, particularly by crabs. Current ripples, oscillation ripples, and interference ripples are common. Magaripples, generally showing an ebb-orientation, are a particularly prominent feature of these sands; they are generally oriented at right angles to the axis of the large sand ridges and have an amplitude of up to 1.5 m and a wavelength of up to 30 m. Flanking the sand facies of the open-intertidal environment is a narrow facies of mud and sandy mud. This facies is particularly well developed in areas where the adjacent mangrove swamp is being actively eroded, thus providing a ready supply of mud. The surface of this mud zone is generally covered with a thin veneer of algae; the sediments are finely laminated and have a marked seaward depositional dip ranging from 4° to 10°. The muds are invariably strongly reducing.

Mangrove channels are mainly situated within the intertidal zone though they do extend into the supratidal zone in places. These channels characteristically have a steep V-shaped profile with slumping commonly taking place on the banks. Sediments are generally mud and sandy mud, though in a few places the channels, where they have been incised into the indurated surface, are floored by relict gravel.

The *mangrove-swamp environment,* which ranges from high in the intertidal zone into the supratidal zone, occurs either as a narrow belt flanking each mangrove channel or as a wide area up to several kilometres across. The swamps are inundated by sea water during spring tides or exceptional storm tides. The sediments are mainly low-carbonate muds, though a few sandy muds and sands are present on the seaward side of the environment in places. The sediments are grey and fetid on the seaward edge of the environment but become increasingly bioturbated, mottled, and oxidised landward. Stratification is totally absent due to infaunal and root activity.

On the landward side of the mangrove-swamp environment are extensive *supratidal flats,* which are inundated by the sea only during spring tides or exceptional storm tides. The sediments of this environment are mostly very fine muds, though on their landward edge there are patches of locally derived sand and gravel washed onto the flats during the summer wet season. Conditions on the supratidal flats are generally hypersaline, and discoid gypsum crystals are common, forming layers up to 20 cm thick in places. Algal fibres are important sediment binders, producing finely though irregularly laminated muds. The muds contain on average only 4 percent $CaCO_3$. Despite this, dolomite nodules have formed on these flats within the last 3000 years, probably in response to the hypersaline conditions. Further accretion and progradation finally results in the removal of the supratidal flats from the marine regime. They are then colonised by grasses to form coastal grasslands, which ultimately are overlain by fluvial sands and gravels.

Grainsize variations

There is a marked seaward increase in grainsize, on both a total-sediment and carbonate-free basis. Calculation of means and standard deviations produced a significant separation into four sample groups which are referred to by Cook & Mayo (1978) as (1) the unsorted unit (found mainly in the shallow-marine environment and comprising the polymodal gravel-sand-mud), (2) a pre-sorting unit comprising sand and mud from the upper reaches of the estuaries and the mangrove channels, (3) a high-energy sorted unit composed mainly of sands of the open-intertidal and shallow-marine environment, and (4) a low-energy sorted unit made up of muds of the mangrove-swamp and supratidal-flat environ-

TABLE A15. MEAN COMPOSITION (MAJOR AND MINOR OXIDES) OF SEDIMENT TYPES FROM VARIOUS DEPOSITIONAL ENVIRONMENTS IN THE BROAD SOUND ESTUARY

	1	2	3	4	5	6	7
SiO_2	17.4	44.1	54.5	53.0	53.0	54.4	63.0
Al_2O_3	2.2	2.8	4.0	9.0	11.6	10.8	13.9
Fe_2O_3	1.8	1.5	1.3	2.4	4.2	3.1	5.6
CaO	40.1	25.0	18.4	13.6	9.6	10.3	1.0
MgO	2.0	1.7	1.5	1.8	2.2	1.9	2.8
Na_2O	0.33	0.70	1.1	1.4	1.3	1.4	0.9
K_2O	0.5	0.5	0.6	1.07	1.6	1.4	1.8
MnO	0.13	0.10	0.10	0.05	0.10	0.06	0.12
P_2O_5	0.14	0.12	0.10	0.11	0.12	0.13	0.13
TiO_2	0.15	0.28	0.33	0.64	0.77	0.80	0.92
Cr_2O_3	0.1	0.1	0.1	0.1	0.1	0.1	0.1
V_2O_5	0.05	0.05	0.05	0.05	0.05	0.05	0.05
CO_2	32.5	20.6	15.2	10.7	8.7	7.7	0.33
H_2O-	0.35	0.32	0.42	1.39	2.41	1.97	2.83
H_2O+	1.86	1.94	1.75	3.50	4.80	3.70	6.18
Total	99.7	99.8	99.6	98.9	100.6	97.7	99.48

1. Gravel from the shallow-marine environment (4 analyses)
2. Sand from the shallow-marine environment (6 analyses)
3. Sand from the open-intertidal environment (7 analyses)
4. Mud from the open-intertidal environment (3 analyses)
5. Mud from the mangrove-channel environment (5 analyses)
6. Mud from the mangrove-swamp environment (7 analyses)
7. Mud from the supratidal-flat environment (5 analyses)

ments. Most of the terrigenous sediment is believed to be brought into Broad Sound by summer floods. During the remainder of the year, tidal currents sort it into the two end members of sand and mud. It is likely that the sediment sampled in the fluvial channels in this study may be rather different from the sediment carried into Broad Sound during major floods.

Mineralogy and petrology of the Holocene sediments

The mineralogy and petrology of the sediments supports the concept of a net seaward movement of terrigenous sediment, coupled with a net landward movement of calcareous sediment. Variations in carbonate mineralogy are dependent in part on changes in the biota and the abundance of carbonate nodules. The sediments in general contain approximately equal amounts of high-Mg and low-Mg calcite; aragonite is sparse and shows a net seaward decrease. Diagenesis appears to have modified to some extent the carbonate mineralogy, with low-Mg calcite being less abundant in those sediments most subject to subaerial weathering. The dolomite nodules of the Charon Point area were found to range in composition from $Ca_{0.65}Mg_{0.35}CO_3$ to $Ca_{0.59}Mg_{0.41}CO_3$. The important feature of the Broad Sound dolomites is that, unlike previously-recorded occurrences of Holocene dolomites, they have formed in essentially non-calcareous terrigenous muds.

The terrigenous sand fraction of Broad Sound sediments is composed mainly of quartz. There is a marked seaward decrease in the abundance of feldspar. There is also a marked seaward trend of increasing stability in the heavy-mineral assemblage, but whether this is due to progressive loss of seaward-moving immature grains or progressive dilution by landward-moving mature grains is uncertain. In general, the heavy-mineral content of Broad Sound sediments is low, because of extensive dilution by biogenic calcareous material. In the mud fraction kaolinite, illite, and montmorillonite (plus mixed-layer clays) are present in approximately equal amounts. There appears to be some degradation of montmorillonite to illite or mixed-layer illite-montmorillonite as a result of the high salinity prevailing in the supratidal-flat environment. This same illite-montmorillonite clay is also abundant in the sediments of the mangrove-channel environment, indicating that much of the mud in this environment has been derived from the supratidal flats.

TABLE A16. WORLDWIDE AVERAGE SEDIMENTARY ROCK COMPOSITIONS.

Average sandstone analysis after Pettijohn (1963); average mudstone after Shaw (1956); average limestone after Clarke (1924)

	Average sandstone	Average mudstone	Average limestone
SiO_2	77.6	63.5	5.2
Al_2O_3	7.1	17.4	0.8
Total Fe (as Fe_2O_3)	3.4	7.3	0.5
CaO	3.1	1.2	42.6
MgO	1.2	2.3	7.9
Na_2O	1.2	2.0	0.05
K_2O	1.3	3.4	0.33
MnO	—	—	0.05
P_2O_5	0.1	—	0.04
TiO_2	0.4	0.8	0.06
CO_2	2.5	0.2	41.6
Total H_2O	2.1	2.4	0.77

MAJOR-ELEMENT COMPOSITION OF BROAD SOUND SEDIMENTS

The major and minor-oxide composition of the sediments is given in Appendix A1, and is summarised in Table A15. The sediments have compositions approximating to mudstones, siliceous limestones, and calcareous sandstones. Table A16 lists commonly-cited worldwide average values for sandstone, mudstone, and limestone. The Broad Sound carbonates (Table A15, column 1) are clearly more siliceous (quartzose) than the worldwide average limestone. This is to be expected, as the world average value includes many pure limestones containing little or no terrigenous detritus, whereas the Broad Sound carbonates are calcareous sands and gravels containing abundant allochthonous material. Much of the gravel-sized nodular carbonate was originally marine, but during the last glaciation, when sea-level was much lower, it was modified in the soil profile. The high MnO and relatively high Fe_2O_3 values of these marine gravels probably reflect supergene processes that operated when the gravels were subaerially exposed (see pp. 86-90).

The likely pedogenic origin of at least some of the nodules is supported by the similarities in composition between the shallow-marine nodule and an undoubted pedogenic nodule collected from a soil profile about 3 m above the tidal limit (Table A17). The Fe and Mn content of the marine nodule is significantly higher than that of the pedogenic nodule, probably because the marine nodules were subaerially exposed for many thousands of years before the Holocene sea-level rise, whereas the pedogenic nodule analysed has probably formed only within the last

few thousand years. Other analyses provided for comparison (Table A17) show that there are few, if any, similarities between the marine nodules and dolomitic nodules which have formed in the supratidal zone during the Holocene (Cook & Polach, 1973b), or lateritic ferruginous nodules which probably formed during the late Tertiary phase of lateritic weathering.

The sands of the shallow-marine and open-intertidal environments are composed primarily of biogenic calcite (with minor aragonite) and terrigenous quartz. This is reflected in the CaO, CO_2, and SiO_2 values for these sediments, corresponding to 'impure limestones'. Such limestones are a common feature of many sedimentary sequences, though most geochemists tend to analyse the less typical 'pure' limestone or sandstone. This point is illustrated by Figure A24 which logarithmically plots $Na_2O + CaO/K_2O$ against SiO_2/Al_2O_3. The Broad Sound sediments for the most part plot outside the three main sediment fields delineated by Garrels & Mackenzie (1971). This results from the mixed nature of the Broad Sound sediments and is perhaps also an indication that the compositional fields for sediments are not as discrete as Garrels & Mackenzie suggest; the carbonate field in particular is probably far more extensive than has previously been suggested. However, the mudstone field would also seem to extend into less siliceous, more aluminous fields.

The Broad Sound sediments may be regarded as consisting of three basic components; (1) biogenic carbonate ($CaCO_3$), (2) terrigenous quartz (SiO_2), (3) terrigenous aluminosilicates, particularly kaolinite ($Al_2Si_2O_5(OH)_4$), montmorillonite ($(\frac{1}{2}Ca, Na)_{0.7}(Al, Mg, Fe)_4((SiAl)_6O_{20})(OH)_4nH_2O$), and illite (approximately $KAl_3Si_3O_{10}(OH)_2$). Because few elements are absorbed by or substitute in quartz to any significant extent, the system can virtually be regarded as a two-component carbonate-aluminosilicate geochemical system, the relative elemental concentrations generally being a function of the ratio of these two components. The $CaCO_3$ content of the estuarine sediments varies considerably among the depositional environments, the shallow-marine environment being the most calcareous and the supratidal flats the least calcareous (Fig. A25). The contour map for $CaCO_3$ (Fig. A26) also clearly shows the trend of increasing carbonate in a seaward direction, though there are local increases in $CaCO_3$ in the upper reaches of some of the estuaries, probably as a result of the prolific calcareous microfauna there. It is apparent from subsequent diagrams that many elemental distributions are a reflection of this $CaCO_3$

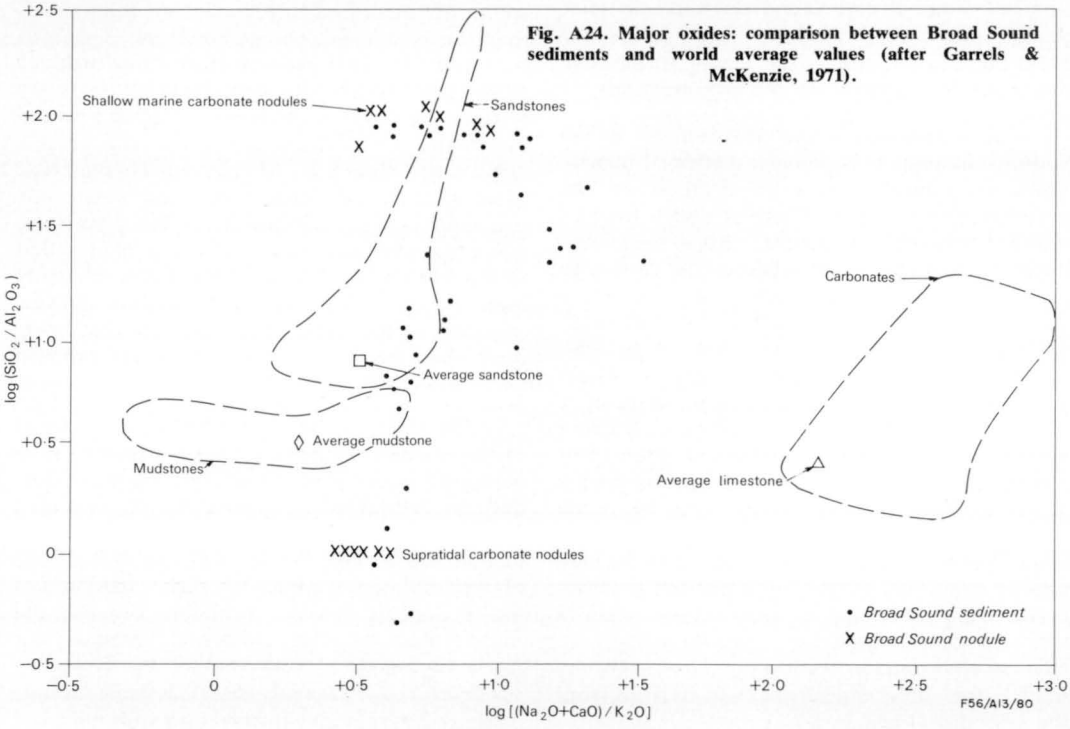


Fig. A24. Major oxides: comparison between Broad Sound sediments and world average values (after Garrels & McKenzie, 1971).

distribution, whereas others closely follow the pattern of mud abundance. It should also be remembered that these two variables show a strong negative correlation (Fig. A27) which further complicates the task of unravelling the discrete meaningful first-order correlations from the less significant second-order correlations.*

TABLE A17. COMPOSITION OF CALCAREOUS NODULES FROM THE SHALLOW-MARINE ENVIRONMENT AT BROAD SOUND, COMPARED WITH THAT OF AN UNDOUBTED PEDOGENIC NODULE (Sample No. 71636003, collected from 3 m above HWS), DOLOMITIC NODULES (mean of five analyses given by Cook (1973); Samples No. 70636720A-F), AND A FERRUGINOUS NODULE

	marine nodule	pedogenic nodule	dolomitic nodule	ferruginous nodule
	%	%	%	%
SiO_2	13.3	7.9	13.5	40.0
Al_2O_3	2.7	2.4	3.4	11.4
Fe_2O_3	3.5	0.95	2.0	36.0
CaO	41.6	48.0	33.5	0.40
MgO	1.7	1.5	8.6	0.14
Na_2O	0.3	0.2	0.4	0.82
K_2O	0.5	0.5	0.5	0.08
MnO	0.26	0.03	0.14	0.03
P_2O_5	0.19	0.08	0.55	0.11
TiO_2	0.19	0.14	0.23	1.08
Cr_2O_3	0.1	0.1	0.1	0.1
V_2O_5	0.05	0.05	0.05	0.05
L.O.I.	35.3	37.7	36.2	7.95
Total	99.04	98.9	98.4	98.0
Total H_2O	2.30	2.30	4.93	9.00
Cl	—	0.01	0.08	—
SO_4	—	—	0.47	—
	ppm	ppm	ppm	
Sr	400	350	660	—
Cu	10	10	11	—
Pb	5	5	7	—
Zn	15	20	40	—
Co	20	20	12	—
Ni	20	10	14	—

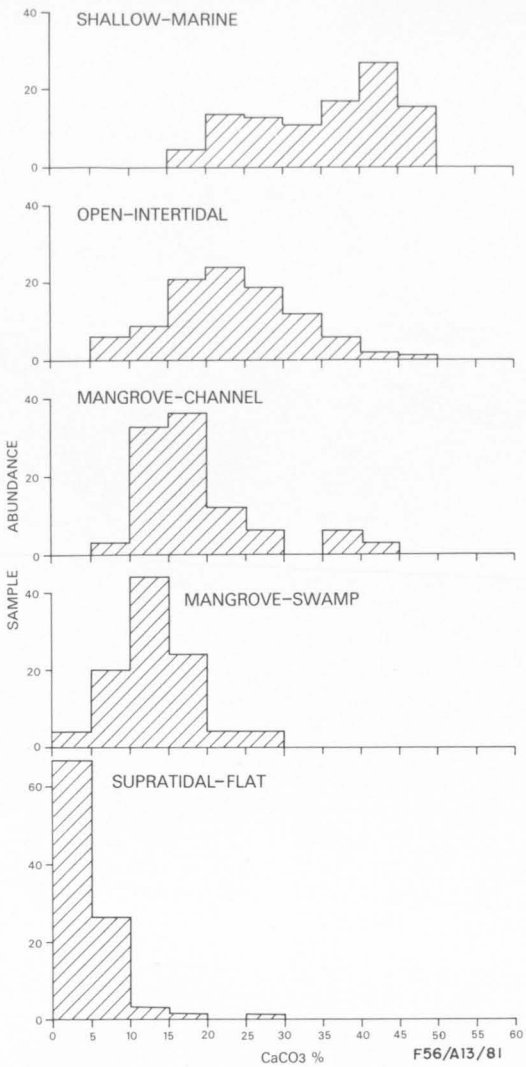


Fig. A25. $CaCO_3$ concentration: frequency distribution in estuarine depositional environments

MINOR AND TRACE-ELEMENT GEOCHEMISTRY

The average minor and trace-element composition of Broad Sound sediments, together with world average values for shales, sandstones, and carbonates (after Turekian & Wedepohl, 1961), are given in Table A18. These figures show that most Broad Sound concentrations are intermediate between the carbonate and shale values. This is to be expected, for, as already pointed out, the Broad Sound sediments range from carbonates in the shallow-marine environment to non-calcareous muds in the supratidal-flat environment. Notable departures from the general trace-element picture are shown by Cd and Zr, which are present in higher concentrations in the Broad Sound sediments than in the 'world average' sediments of Turekian & Wedepohl.

The content of trace elements and other components of the sediments from the various depositional environments is given in Table A19. There are clearly major differences in concentrations in the various environments, which in many

* A 'second-order' correlation is one in which the two variables are considered to be not directly related (i.e. not substituting for each other), but related through a third variable with which the two variables in question are significantly correlated.

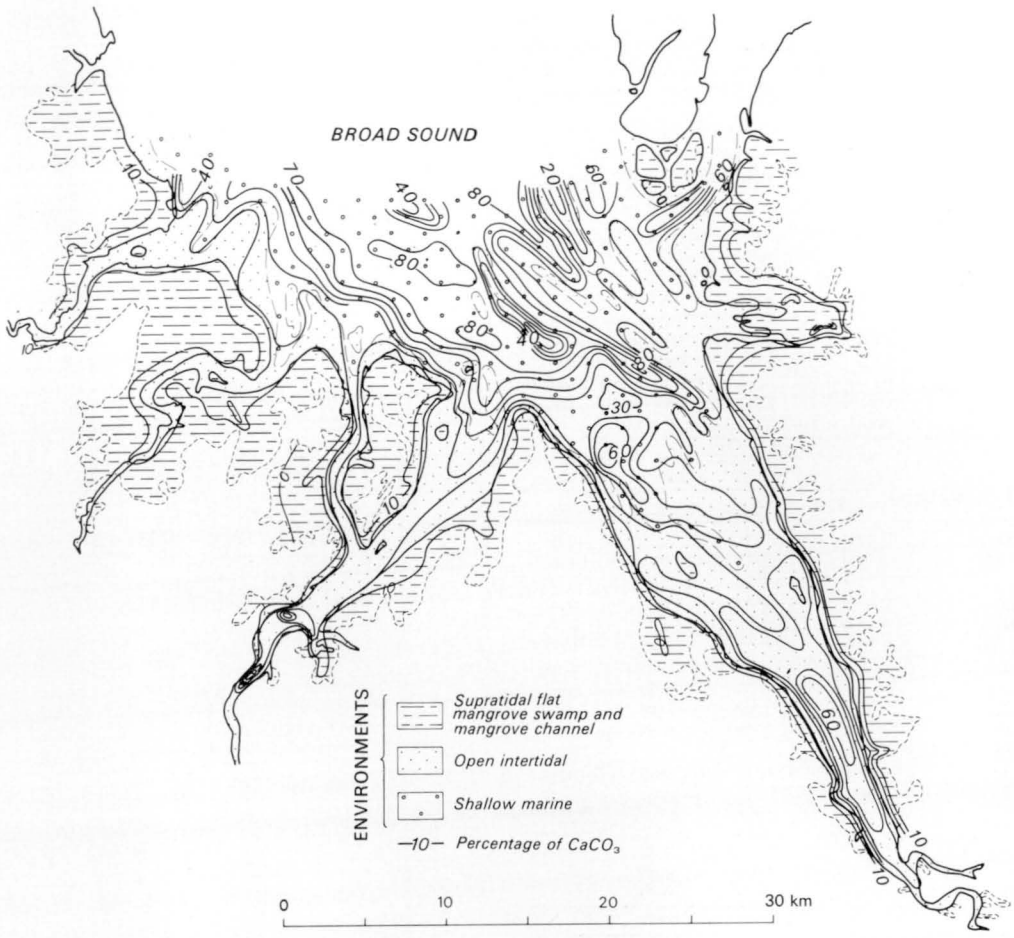


Fig. A26. $CaCO_3$: distribution in estuarine sediments

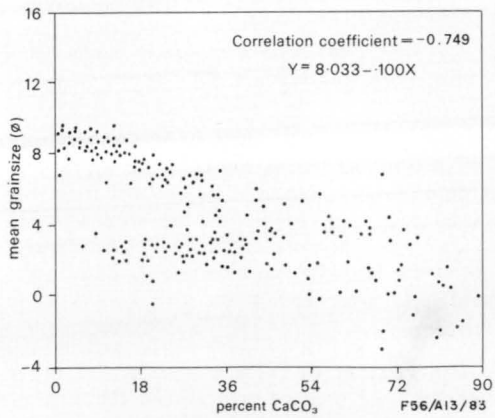


Fig. A27. Relationship between mean grainsize (phi) and $CaCO_3$ content in estuarine sediments

cases are likely to reflect the relative abundance of carbonate or terrigenous mud in the sediments of that environment. This in turn has the effect of producing positive or negative correlations which may not be a true reflection of the interrelationships between elements. Spencer, Degens & Kulbicki (1968) deal with this problem in some detail and conclude that the use of factor analysis is most likely to provide meaningful solutions. Factor analysis is used extensively by Mayo in Part B of this volume but is not employed here; here, the simpler procedures of correlation coefficients coupled with intuitive deduction are used instead.

Correlation coefficients for the whole estuary (i.e. all samples that were collected from the grid-pattern sampling program) are given in Table A20A and Figure A28. Log-normal

TABLE A18.
MINOR AND TRACE-ELEMENT COMPOSITION (ppm) OF WORLDWIDE AVERAGE SHALES, SANDSTONES, AND CARBONATES, COMPARED WITH THE AVERAGE BROAD SOUND ESTUARINE SEDIMENT COMPOSITION. Worldwide values after Turekian & Wedepohl (1961), except for organic carbon values after Ronov & Migdisov (1971)

	Worldwide average sandstone	Worldwide average shale	Worldwide average carbonate	Broad Sound average sediment
Ba	—	580	10	184
Cd	0	0.3	0.035	1
Co	0.3	19	0.1	13
Cr	35	90	11	58
Cu	—	45	4	16
Fe	9800	47 200	3800	22 000
La	30	92	—	c. 100
Mg	7000	15 000	47 000	11 300
Mn	—	850	1100	594
Mo	0.2	2.6	0.4	3
Ni	2	68	20	21
P_2O_5	390	1600	920	740
Pb	7	20	9	12
Sc	1	13	1	13
Sr	20	300	610	450
Ti	1500	4600	400	3200
V	20	130	20	50
Y	40	36	30	28
Zn	16	95	20	31
Zr	40	26	30	310
C (org	3600	9400	4700	6500

transforms were carried out routinely for drainage basin analyses, and for this reason were also initially undertaken for the total estuary results. In addition, frequency distribution histograms for major and trace elements indicated log-normal distributions for the estuary as a whole. Therefore the values were log-transformed when the total estuary was considered. However, when the samples are split into the various environments, the distributions appear to be normal. Consequently, for analyses concerned with individual environments, values were not log-transformed. Correlation matrixes for the individual environments are given in Table A21. In addition, for comparison of the overall estuary with individual environments, it was important to determine correlation coefficients for the entire estuary assuming a normal distribution (Table A20B). Comparison of part A with part B of Table A20 shows that in fact there is little difference in the level of significant correlations in the estuary as a whole, whether a normal or a log-normal distribution is assumed, and therefore, for consistency, discussion here is based on an assumed normal distribution, unless otherwise stated.

Although correlation coefficients are given for both mean grainsize (phi) and percentage mud, these two parameters correlate at a confidence level of 99.9 percent and in almost every case show identical correlations with other variables; therefore it is not necessary to consider these two parameters separately. Similarly, Ca and $CaCO_3$ need not be considered separately. Although coefficients are given for percentage sand and percentage gravel in Table A20, these two are so closely related to mean grainsize that it is unnecessary to deal with them as separate variables. Organic carbon is given in the correlation matrix only for the estuary as a whole (parts A and B, Table A20) because an insufficient number of analyses was undertaken for the depositional environments to be considered separately. The inter-relationships between organic carbon, Eh, pH, and grainsize are considered by Mayo (1976).

Tables A20 and 21 and Figure A28 show quite clearly, and not unexpectedly, that there are two groups of elements: (1) those which correlate positively with $CaCO_3$ and negatively with grainsize, e.g. Cr, and (2) those which correlate negatively with $CaCO_3$ and positively with phi grainsize (or percentage mud), e.g. Zn. Within each group, elements show positive correlations, whereas between the groups the elements tend to correlate negatively. However, the extent to which two elements correlate varies significantly from one environment to the next. Furthermore, there are some elements which have rather more complex correlation patterns, such as P_2O_5, which shows a positive correlation in one depositional environment, yet a negative correlation with the same variable in a different environment. In such cases there are obviously complex inter-relations.

Phosphate

The P_2O_5 content of Broad Sound sediments ranges from 140 to 1900 ppm, with a mean value of 740 ppm. This is similar to values normally found in sediments (Table A18). Both the mean, the mode, and the range of values vary somewhat between environments (Fig. A29). The highest mean concentration (915 ppm) is found in the shallow-marine environment (Table A19). However, the distribution of P_2O_5 in the estuarine sediments (Fig. A14) shows that there are in fact two preferred locations for high phosphate values: one is at the northern end of Broad Sound where the gravel facies of the shallow-marine environment is best developed; the other is flanking Broad Sound in the muds of the supratidal-flat environment and extending into the coastal grasslands which have formed over Holocene supratidal flats.

These relationships may be considered more closely by examining the correlation matrixes and

TABLE A19. MEANS AND STANDARD DEVIATIONS OF MAJOR AND TRACE-ELEMENT CONCENTRATIONS IN SEDIMENTS FROM BROAD SOUND DEPOSITIONAL ENVIRONMENTS.

	Shallow-marine		Open-intertidal		Mangrove-channel		Mangrove-swamp		Supratidal-flats		Broad Sound estuary average	
	mean	s.d.	mean	s.d.	mean	s.d.	mean	s.d.	mean	s.d.	mean	s.d.
mean grain-size (phi)	2.22	2.16	3.38	1.38	6.88	1.42	7.74	1.13	8.77	0.76	5.11	3.01
Mud (%)	19.0	23.1	13.8	24.0	76.0	23.2	89.7	15.9	97.3	4.7	47.7	5.12
Ba (ppm)	105	47.3	189.8	57.4	205.8	28.1	197.7	28.2	221.0	52.0	184.2	98.0
Ca (%)	17.0	8.57	11.0	4.9	9.3	4.7	6.7	1.9	2.0	2.1	9.75	7.50
Co (ppm)	11.0	3.3	12.4	4.6	11.0	2.3	12.2	3.3	17.4	6.8	13.0	5.2
Cr (ppm)	39.6	15.4	48.8	27.2	57.3	11.3	64.8	17.8	86.0	26.4	57.8	28.3
Cu (ppm)	15.2	11.2	12.8	7.3	17.8	7.6	14.7	3.3	20.5	6.0	15.9	8.4
Fe (%)	1.57	1.11	1.28	1.01	2.30	0.83	2.68	0.99	3.88	1.26	2.20	1.44
La (ppm)	c. 100	—	c. 100	—	100	—	100	—	100	—	100	
Mg (%)	1.26	0.60	0.80	0.48	0.78	1.81	1.09	0.45	1.65	0.74	1.13	0.65
Mn (ppm)	769.5	321.0	578.6	247.7	363.3	120.1	448.8	109.3	550.9	180.0	594.0	343.1
Mo (ppm)	3	—	>3	—	>3	—	>3	—	3	—	>3	—
Ni (ppm)	15.2	5.4	16.3	7.3	20.1	5.1	23.4	7.3	32.6	11.0	20.9	10.4
Pb (ppm)	9.9	5.6	9.7	4.2	11.4	3.2	13.1	4.0	16.0	4.0	11.7	5.1
Sc (ppm)	12.0	2.1	12.6	3.4	13.0	2.5	14.1	2.7	16.7	3.1	13.4	3.5
Sr (ppm)	560.0	189.9	556.9	414.1	461.3	114.0	373.0	99.9	205.9	158.4	449.5	307.7
Ti (ppm)	2180	1237	2483	1498	3652	607	4020	738	4709	1424	3205	1656
V (ppm)	43.4	10.8	37.4	13.9	53.8	14.0	55.1	12.9	68.4	20.6	49.5	19.4
Y (ppm)	26.6	8.0	30.2	10.4	25.4	4.4	25.6	5.3	28.8	4.8	28.2	8.1
Zn (ppm)	20.1	10.3	16.7	8.0	36.6	11.3	41.4	14.3	57.1	12.6	31.1	19.4
Zr (ppm)	292.6	290.2	344.0	316.6	222.1	27.3	232.3	39.7	280.5	80.5	305.8	304.3
$CaCO_3$ (%)	56.7	19.3	31.6	14.2	24.2	13.6	18.3	6.1	4.5	5.5	29.2	22.7
P_2O_5 (ppm)	914.8	294.0	497.8	143.3	803.1	137.9	873.8	139.3	841.5	295.0	738.9	285.3

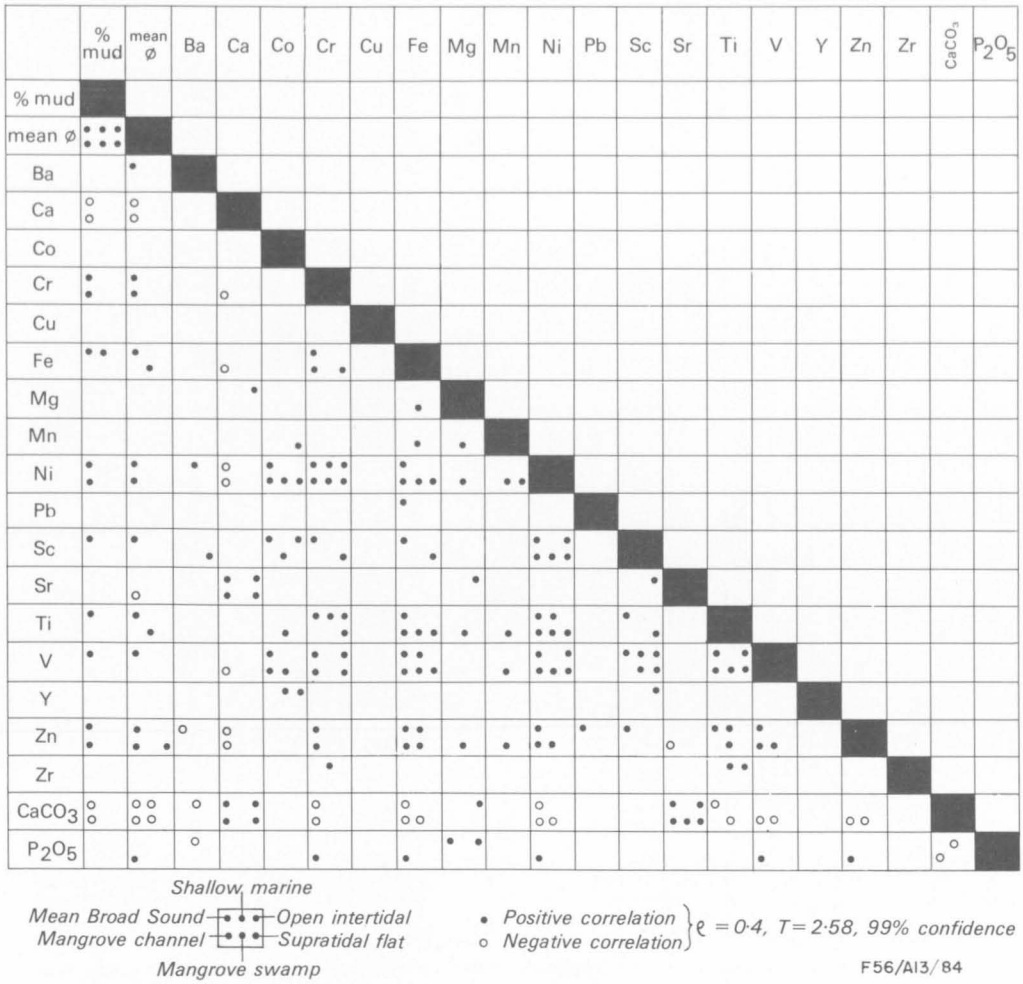


Fig. A28. Matrix of statistically significant correlation coefficients between variables in Broad Sound estuarine depositional environments

Figures A30-33. Considering the estuary as a whole (Fig. A30), there is no statistically significant correlation between P_2O_5 content and $CaCO_3$ content, nor between P_2O_5 content and mean grainsize (or percentage mud). It is obvious from both these diagrams that there is no simple straight-line relationship between these variables, although, in the case of the $CaCO_3/P_2O_5$ correlation there appear to be two correlation lines, one negative, the other positive. However, if the sediments in each of the depositional environments are examined in turn (Fig. A31) there is a strong positive correlation between $CaCO_3$ and P_2O_5 in the shallow-marine environment, a positive though less significant correlation in the open-intertidal environment, and negative correlations in the mangrove-channel and mangrove-swamp environments. There is no significant correlation in the supratidal-flat environment. Thus P_2O_5 shows a positive correlation with mean grainsize (or percentage mud) in some environments (Table A21A) and a correlation with $CaCO_3$ in others.

Looking more closely at the nature of the relationship with $CaCO_3$, one can see from Table A20 that a positive correlation exists between P_2O_5 and percentage gravel. However, a far better fit results if the relationship is taken as non-linear, as in Figure A32. The gravel-sized material is primarily carbonate nodules with some gravel-sized shells and shell fragments. This correlation may be a consequence of phosphat-

TABLE A20. MATRIXES OF CORRELATION COEFFICIENTS, FOR TRACE-ELEMENTS AND OTHER COMPONENTS OF THE ESTUARINE SEDIMENTS (AVERAGES OF ENTIRE BROAD SOUND ESTUARY) (A) calculated from log-transformed values, (B) calculated from actual values. In (A) all variables, except gravel, sand, and mud percentages, mean phi, and $CaCO_3$, were log-transformed before determination of the correlation coefficients. When $P = 0.4$, the limiting correlation coefficients corresponding to confidence levels of 90, 95, and 99 percent are 0.481, 0.496, and 0.524 respectively. Correlation coefficients significant at a confidence level equal to or greater than 99 percent are asterisked

A. Calculated from log-transformed values

	% gravel	% sand	% mud	mean phi	Ba	Ca	Co	Cr	Cu	Fe	Mg	Mn	Ni	Pb	Sc	Sr	Ti	V	Y	Zn	Zr	$CaCO_3$	P_2O_5	Organic C
% gravel	1.000																							
% sand	0.000	1.000																						
% mud	−.307	−.952*	1.000																					
mean phi	−.562*	−.809*	0.942*	1.000																				
Ba	−.633*	−.220	0.404	0.559*	1.000																			
Ca	0.364	0.554*	−.638*	−.711*	−.471	1.000																		
Co	−.281	1.310	0.381	0.448	0.432	−.514	1.000																	
Cr	−.317	−.622*	0.689*	0.718*	0.440	−.554*	0.540*	1.000																
Cu	−.151	−.407	0.434	0.428	0.174	−.375	0.327	0.407	1.000															
Fe	−.108	−.829*	0.822*	0.755*	0.307	−.632*	0.460	0.704*	0.451	1.000														
Mg	0.144	−.546*	0.476	0.358	−.195	−.170	0.132	0.346	0.278	0.544	1.000													
Mn	0.410	0.125	−.245	−.343	−.291	0.176	0.178	−.148	−.025	0.043	0.152	1.000												
Ni	−.339	−.631*	0.704*	0.751*	0.505	−.646*	0.695*	0.813*	0.462	0.725*	0.273	−.086	1.000											
Pb	−.169	−.538*	0.564*	0.543*	0.284	−.413	0.377	0.476	0.291	0.564*	0.364	−.000	0.504	1.000										
Sc	−.117	−.594*	0.601*	0.570*	0.332	−.440	0.622*	0.679*	0.384	0.576*	0.451	0.060	0.776*	0.493	1.000									
Sr	0.282	0.431	−.497	−.559*	−.308	0.833*	−.379	−.381	−.208	−.504	−.031	0.167	−.474	−.252	−.187	1.000								
Ti	−.269	−.613*	0.665*	0.680*	0.462	−.487	0.392	0.794*	0.378	0.675	0.262	−.140	0.750*	0.470	0.579*	−.303	1.000							
V	−.048	−.716*	0.696*	0.624*	0.353	−.520	0.593*	0.711*	0.410	0.788	0.432	0.161	0.808*	0.556*	0.824*	−.296	0.696*	1.000						
Y	−.172	0.090	−.033	0.047	0.287	−.133	0.585*	0.353	0.113	−.029	−.170	0.095	0.453	−.000	0.509	−.038	0.228	0.325	1.000					
Zn	−.252	−.835*	0.872*	0.845*	0.365	−.666*	0.394	0.645*	0.482	0.826*	0.469	−.142	0.729*	0.631*	0.596*	−.536*	0.661*	0.728*	0.008	1.000				
Zr	−.199	−.073	0.130	0.198	0.275	−.189	0.147	0.494	0.097	0.161	−.174	−.238	0.413	0.030	0.156	−.174	0.486	0.204	0.416	0.164	1.000			
$CaCO_3$	0.657*	0.412	−.593*	−.750*	−.728*	0.770*	−.507	−.571*	−.278	−.507	0.079	0.305	−.659*	−.343	−.360	0.745*	−.525*	−.403	−.225	−.599*	−.333	1.000		
P_2O_5	0.441	−.569*	0.406	0.197	−.391	−.059	0.001	0.128	0.210	0.501	0.687*	0.244	0.130	0.317	0.258	−.043	0.119	0.403	−.304	0.420	−.293	0.228	1.000	
Organic C	−.437	−.595*	0.701*	0.657*	0.582*	−.415	0.032	0.431	0.130	0.443	−.321	−.563*	0.231	0.370	−.015	−.349	0.497	0.207	−.186	0.598*	−.097	−.599*	−.206	1.000

TABLE A20. (cont'd) MATRIXES OF CORRELATION COEFFICIENTS, FOR TRACE-ELEMENTS AND OTHER COMPONENTS OF THE ESTUARINE SEDIMENTS (AVERAGES OF ENTIRE BROAD SOUND ESTUARY) (A) calculated from log-transformed values, (B) calculated from actual values. In (A) all variables, except gravel, sand, and mud percentages, mean phi, and $CaCO_3$, were log-transformed before determination of the correlation coefficients. When $\rho = 0.4$, the limiting correlation coefficients corresponding to confidence levels of 90, 95, and 99 percent are 0.481, 0.496, and 0.524 respectively. Correlation coefficients significant at a confidence level equal to or greater than 99 percent are asterisked

B. Calculated from actual values

	% gravel	% sand	% mud	mean phi	Ba	Ca	Co	Cr	Cu	Fe	Mg	Mn	Ni	Pb	Sc	Sr	Ti	V	Y	Zn	Zr	$CaCO_3$	P_2O_5	Organic C
% gravel	1.000																							
% sand	0.020	1.000																						
% mud	−.313	−.956*	1.000																					
mean phi	−.560*	−.820*	0.944*	1.000																				
Ba	0.544*	−.260	0.408	0.524*	1.000																			
Ca	0.566*	0.409	−.555*	−.684*	−.523	1.000																		
Co	−.207	−.251	0.300	0.359	0.392	−.384	1.000																	
Cr	−.292	−.560*	0.618*	0.652*	0.468	−.495	0.507	1.000																
Cu	−.062	−.285	0.289	0.274	0.185	−.174	0.242	0.302	1.000															
Fe	−.151	−.709	0.718*	0.698*	0.364	−.518	0.497	0.736*	0.333	1.000														
Mg	0.140	−.397	0.336	0.256	−.138	0.011	0.179	0.296	0.222	0.443	1.000													
Mn	0.455	0.183	−.308	−.405	−.223	0.301	0.202	−.116	−.033	0.024	0.202	1.000												
Ni	−.279	−.565*	0.619*	0.668*	0.498	−.548*	0.665*	0.827*	0.342	0.788*	0.294	−.039	1.000											
Pb	−.173	−.475	0.502	0.503	0.287	−.295	0.391	0.458	0.198	0.524*	0.292	0.024	0.503	1.000										
Sc	−.124	−.541*	0.550*	0.537*	0.439	−.305	0.613*	0.708*	0.277	0.613*	0.406	0.056	0.777*	0.463	1.000									
Sr	0.191	0.307	−.348	−.393	−.066	0.643*	−.170	−.198	0.029	−.345	0.075	0.113	−.282	−.145	0.035	1.000								
Ti	−.283	−.607*	0.660*	0.681	0.500	−.471	0.394	0.853*	0.302	0.709*	0.239	−.163	0.794*	0.452	0.624*	−.201	1.000							
V	−.077	−.664*	0.653*	0.609*	0.457	−.381	0.569*	0.767*	0.322	0.798*	0.352	0.119	0.828*	0.491	0.834*	−.141	0.757*	1.000						
Y	−.138	0.139	−.092	−.020	0.267	−.110	0.503	0.272	0.045	−.039	−.080	0.124	0.332	−.003	0.483	0.150	0.169	0.248	1.000					
Zn	−.273	−.802*	0.842*	0.853*	0.357	−.615*	0.427	0.621*	0.352	0.777*	0.387	−.166	0.716*	0.619*	0.592*	−.450	0.652*	0.705*	−.038	1.000				
Zr	−.128	0.144	−.098	−.022	0.073	−.144	0.043	0.292	−.003	−.043	−.186	−.117	0.168	−.053	0.013	−.111	0.348	0.009	0.360	−.069	1.000			
$CaCO_3$	0.640*	0.434	−.601*	−.749	−.651*	0.856*	−.422	−.550*	−.151	−.534*	0.040	0.325	−.596*	−.360	−.369	0.630*	−.536*	−.438	−.146	−.167	−.132	1.000		
P_2O_5	0.470	−.527*	0.362	0.173	−.370	0.125	0.007	0.094	0.161	0.386	0.558*	0.263	0.130	0.217	0.210	−.045	0.101	0.341	−.284	−.289	−.259	0.197	1.000	
Organic C	−.437	−.595*	0.701*	0.657*	0.581*	−.530*	0.001	0.328	0.032	0.347	−.332	−.541*	0.113	0.359	−.026	−.377	0.371	0.160	−.183	0.494	−.097	−.599*	−.206	1.000

TABLE A21. MATRIXES OF CORRELATION COEFFICIENTS FOR TRACE ELEMENTS AND OTHER COMPONENTS OF SEDIMENTS IN THE VARIOUS DEPOSITIONAL ENVIRONMENTS, CALCULATED FROM ACTUAL VALUES: (A) shallow-marine, (B) open-intertidal, (C) mangrove-channel, (D) mangrove-swamp, (E) supratidal-flat. When $\rho = 0.4$, the limiting correlation coefficients corresponding to confidence levels of 90, 95, and 99 percent are 0.481, 0.496, and 0.524 respectively. Correlation coefficients significant at a confidence level equal to or greater than 99 percent are asterisked

A. Shallow-marine sediments

	% mud	mean phi	Ba	Ca	Co	Cr	Cu	Fe	Mg	Mn	Ni	Pb	Sc	Sr	Ti	V	Y	Zn	Zr	$CaCO_3$	P_2O_5
% mud	1.000																				
mean phi	0.807*	1.000																			
Ba	0.188	0.553	1.000																		
Ca	−.212	−.479	−.501	1.000																	
Co	−.063	0.111	0.413	−.253	1.000																
Cr	−.445	0.458	0.364	−.280	0.099	1.000															
Cu	−.200	−.080	−.056	−.048	−.156	−.003	1.000														
Fe	0.751*	0.495	0.105	−.119	−.018	0.466	−.133	1.000													
Mg	−.006	−.230	−.609	0.316	−.289	−.105	0.023	0.104	1.000												
Mn	−.120	−.368	−.380	0.375	0.168	−.300	−.166	0.159	0.284	1.000											
Ni	0.334	0.490	0.652*	−.359	0.518	0.657*	−.005	0.401	−.346	−.267	1.000										
Pb	0.197	0.204	0.130	0.031	−.005	0.314	−.120	0.244	0.016	−.027	0.225	1.000									
Sc	−.013	−.154	−.018	0.215	0.455	0.199	−.192	0.232	0.339	0.315	0.424	0.251	1.000								
Sr	−.169	−.329	−.459	0.487	−.322	−.142	0.266	−.106	0.503	0.224	−.283	0.059	0.228	1.000							
Ti	0.464	0.455	0.392	−.210	−.018	0.732*	0.052	0.500	−.171	−.234	0.628*	0.767	0.086	−.067	1.000						
V	0.377	0.158	0.205	0.161	0.285	0.363	−.193	0.66*	0.163	0.392	0.500	0.272	0.674*	0.203	0.456	1.000					
Y	−.226	−.033	0.400	−.124	0.809*	0.217	−.037	−.137	−.272	0.128	0.617	−.024	0.574	−.127	0.117	−.318	1.000				
Zn	0.604	0.610	0.469	−.259	−.060	0.569	0.025	0.652*	−.084	−.325	0.558	0.499	0.117	−.121	0.620*	0.457	−.085	1.000			
Zr	0.197	0.324	0.457	−.274	0.034	0.674*	0.106	0.095	−.266	−.404	0.556	0.165	0.011	−.201	0.703*	0.124	0.245	0.314	1.000		
$CaCO_3$	−.126	−.550	−.826*	0.525	−.338	−.324	0.072	0.028	0.508	0.415	−.509	−.150	0.110	0.566	−.268	0.044	−.280	−.327	−.401	1.000	
P_2O_5	0.170	0.155	−.695*	0.456	−.344	−.118	−.015	0.430	0.548	0.512	−.304	−.004	0.281	0.407	−.059	0.370	−.329	−.054	−.332	0.736*	1.000

TABLE A21. (cont'd) MATRIXES OF CORRELATION COEFFICIENTS FOR TRACE ELEMENTS AND OTHER COMPONENTS OF SEDIMENTS IN THE VARIOUS DEPOSITIONAL ENVIRONMENTS, CALCULATED FROM ACTUAL VALUES: (A) shallow-marine, (B) open-intertidal, (C) mangrove-channel, (D) mangrove-swamp, (E) supratidal-flat. When $\rho = 0.4$, the limiting correlation coefficients corresponding to confidence levels of 90, 95 and 99 percent are 0.481, 0.496, and 0.524 respectively. Correlation coefficients significant at a confidence level equal to or greater than 99 percent are asterisked

B. Open-intertidal sediments

	% mud	mean phi	Ba	Ca	Co	Cr	Cu	Fe	Mg	Mn	Ni	Pb	Sc	Sr	Ti	V	Y	Zn	Zr	$CaCO_3$	P_2O_5
% mud	1.000																				
mean phi	0.928*	1.000																			
Ba	0.173	0.154	1.000																		
Ca	0.205	0.139	−.070	1.000																	
Co	0.138	0.154	0.290	−.102	1.000																
Cr	0.465	0.527	0.120	−.105	0.349	1.000															
Cu	0.244	0.156	0.231	0.178	0.168	0.199	1.000														
Fe	0.376	0.328	0.167	−.155	0.162	0.383	0.106	1.000													
Mg	0.408	0.350	−.096	0.664*	0.030	0.198	0.214	0.209	1.000												
Mn	−.279	−.458	0.233	−.077	0.238	−.065	0.151	0.113	0.030	1.000											
Ni	0.396	0.463	0.327	−.231	0.479	0.634*	0.157	0.355	0.074	0.000	1.000										
Pb	0.290	0.218	0.158	0.288	0.134	0.155	0.150	0.114	0.184	0.158	0.098	1.000									
Sc	0.462	0.488	0.343	0.207	0.605*	0.537	0.339	0.196	0.410	0.050	0.690*	0.256	1.000								
Sr	0.267	0.270	0.325	0.728*	0.160	0.168	0.288	0.040	0.638*	−.033	0.175	0.300	0.598*	1.000							
Ti	0.453	0.524	0.173	−.082	0.170	0.771*	0.102	0.354	0.174	−.058	0.586	0.135	0.393	0.150	1.000						
V	0.499	0.440	0.441	0.018	0.521	0.650*	0.294	0.462	0.366	0.293	0.770*	0.309	0.788*	0.397	0.598*	1.000					
Y	0.018	0.074	0.225	−.120	0.606*	0.379	0.139	−.080	−.015	0.098	0.576	−.042	0.680*	0.253	0.243	0.492	1.000				
Zn	0.573	0.516	0.155	0.010	0.036	0.261	0.274	0.294	0.215	0.068	0.326	0.356	0.348	0.065	0.350	0.448	0.043	1.000			
Zr	−.046	0.079	−.081	−.316	0.080	0.480	−.005	0.028	−.245	−.054	0.399	−.141	0.094	−.207	0.633*	0.168	0.400	0.023	1.000		
$CaCO_3$	0.149	0.089	−.173	0.917*	−.192	−.139	0.132	−.132	0.061*	−.150	−.257	0.260	0.150	0.691*	−.161	−.022	−.164	−.091	−.375	1.000	
P_2O_5	0.383	−.328	−.145	0.478	0.032	0.096	0.215	0.310	0.628*	0.345	−.005	0.340	0.147	0.246	0.031	0.328	−.223	0.231	−.316	0.486	1.000

TABLE A21. (cont'd) MATRIXES OF CORRELATION COEFFICIENTS FOR TRACE ELEMENTS AND OTHER COMPONENTS OF SEDIMENTS IN THE VARIOUS DEPOSITIONAL ENVIRONMENTS, CALCULATED FROM ACTUAL VALUES: (A) shallow-marine, (B) open-intertidal, (C) mangrove-channel, (D) mangrove-swamp, (E) supratidal-flat. When $\rho = 0.4$, the limiting correlation coefficients corresponding to confidence levels of 90, 95, and 99 percent are 0.481, 0.496, and 0.524 respectively. Correlation coefficients significant at a confidence level equal to or greater than 99 percent are asterisked

C. Mangrove-channel sediments

	% mud	mean phi	Ba	Ca	Co	Cr	Cu	Fe	Mg	Mn	Ni	Pb	Sc	Sr	Ti	V	Y	Zn	Zr	$CaCO_3$	P_2O_5
% mud	1.000																				
mean phi	0.944*	1.000																			
Ba	0.123	0.164	1.000																		
Ca	−.901*	−.903*	−.303	1.000																	
Co	0.443	0.430	0.435	−.574	1.000																
Cr	0.748*	0.799*	0.269	−.858*	0.550	1.000															
Cu	0.246	0.226	0.323	−.338	0.571	0.251	1.000														
Fe	0.642	0.636	0.382	−.833*	0.709	0.722*	0.429	1.000													
Mg	0.229	0.174	0.147	−.199	0.260	0.331	0.081	0.271	1.000												
Mn	0.196	0.186	0.215	−.180	−.037	0.018	0.057	0.050	0.000	1.000											
Ni	0.713*	0.772*	0.322	−.849*	0.736*	0.789*	0.485	0.855*	0.188	−.028	1.000										
Pb	0.430	0.431	0.508	−.437	0.545	0.453	0.087	0.388	0.321	0.220	0.453	1.000									
Sc	0.550	0.612	0.109	−.676	0.597	0.632	0.185	0.572	−.052	−.106	0.751*	0.278	1.000								
Sr	0.635	−.721*	−.058	0.741*	−.379	−.537	−.034	−.604	−.142	−.190	−.637	−.292	−.606	1.000							
Ti	0.574	0.578	0.379	−.681	0.682	0.650	0.616	0.749*	0.218	0.042	0.796*	0.407	0.466	−.378	1.000						
V	0.574	0.576	0.391	−.781*	0.727*	0.730*	0.409	0.936*	0.214	−.070	0.851*	0.347	0.672	−.568	0.731*	1.000					
Y	0.233	0.179	0.112	−.178	0.525	0.192	0.415	0.004	0.000	−.035	0.301	0.301	0.495	−.056	0.256	0.176	1.000				
Zn	0.791*	0.868*	0.286	−.908*	0.549	0.810*	0.280	0.827*	0.128	0.078	0.880*	0.364	0.674	−.770*	0.659	0.789*	0.070	1.000			
Zr	0.028	−.032	0.017	−.023	0.033	0.049	0.089	−.091	0.127	−.010	−.071	0.138	0.066	0.196	0.069	−.118	0.265	−.204	1.000		
$CaCO_3$	−.813*	−.806*	−.261	0.896*	−.512	−.782*	−.235	−.828*	−.303	−.143	−.759	−.331	−.571	0.754*	−.544	−.772*	−.010	−.847*	0.174	1.000	
P_2O_5	0.563	0.654*	0.262	−.703	0.491	0.710*	0.065	0.776*	0.220	−.087	0.779	0.285	0.629	−.602	0.549	0.808*	−.079	0.834*	−.246	−.736*	1.000

TABLE A21. (cont'd) MATRIXES OF CORRELATION COEFFICIENTS FOR TRACE ELEMENTS AND OTHER COMPONENTS OF SEDIMENTS IN THE VARIOUS DEPOSITIONAL ENVIRONMENTS, CALCULATED FROM ACTUAL VALUES: (A) shallow-marine, (B) open-intertidal, (C) mangrove-channel, (D) mangrove-swamp, (E) supratidal-flat. When $\rho = 0.4$, the limiting correlation coefficients corresponding to confidence levels of 90, 95 and 99 percent are 0.481, 0.496, and 0.524 respectively. Correlation coefficients significant at a confidence level equal to or greater than 99 percent are asterisked

D. Mangrove-swamp sediments

	% mud	mean phi	Ba	Ca	Co	Cr	Cu	Fe	Mg	Mn	Ni	Pb	Sc	Sr	Ti	V	Y	Zn	Zr	$CaCO_3$	P_2O_5
% mud	1.000																				
mean phi	0.850*	1.000																			
Ba	0.028	−.186	1.000																		
Ca	0.141	−.285	0.133	1.000																	
Co	0.276	0.533	0.149	−.569	1.000																
Cr	0.412	0.618	−.404	−.340	0.583	1.000															
Cu	0.153	0.511	−.451	−.484	0.381	0.381	1.000														
Fe	0.460	0.812*	−.430	−.544	0.653	0.739	0.676	1.000													
Mg	0.327	0.706	−.521	−.543	0.502	0.723	0.506	0.905*	1.000												
Mn	0.248	0.622	−.354	−.584	0.713	0.735	0.478	0.835*	0.796*	1.000											
Ni	0.295	0.620	−.229	−.643	0.830*	0.753*	0.549	0.855*	0.762*	0.841*	1.000										
Pb	0.049	0.293	−.164	−.597	0.521	0.310	0.360	0.523	0.367	0.534	0.560	1.000									
Sc	0.318	0.466	0.200	−.426	0.847*	0.519	0.188	0.549	0.464	0.562	0.753*	0.325	1.000								
Sr	−.408	−.598	0.418	0.526	−.507	−.668	−.252	−.705	−.718	−.626	−.694	−.422	−.466	1.000							
Ti	0.545	0.787*	−.218	−.407	0.771*	0.720	0.561	0.919*	0.770*	0.776*	0.877*	0.524	0.695	−.669	1.000						
V	0.314	0.600	0.043	−.509	0.882*	0.686	0.430	0.785*	0.650	0.787*	0.895*	0.465	0.858*	−.488	0.861*	1.000					
Y	−.098	−.125	0.345	−.126	0.523	0.215	−.183	−.081	−.130	0.125	0.310	0.011	0.622	−.116	0.106	0.377	1.000				
Zn	0.374	0.727	−.351	−.657	0.717	0.740	0.659	0.941*	0.833*	0.845*	0.915*	0.635	0.645	−.713	0.908*	0.840*	0.017	1.000			
Zr	0.304	−.032	0.150	0.430	0.042	0.015	−.333	−.262	−.358	−.193	−.050	−.189	0.137	−.180	−.039	−.108	0.556	−.241	1.000		
$CaCO_3$	−.546	−.776*	0.221	0.560	−.720	−.664	−.620	−.840*	−.653	−.731	−.864*	−.587	−.598	0.767*	−.881*	−.753*	−.103	−.904*	−.087	1.000	
P_2O_5	−.022	0.429	−.376	−.662	0.329	0.459	0.588	0.653	0.671	0.623	0.485	0.442	0.110	−.389	0.410	0.415	−.235	0.590	−.576	−.437	1.000

TABLE A21. (cont'd) MATRIXES OF CORRELATION COEFFICIENTS FOR TRACE ELEMENTS AND OTHER COMPONENTS OF SEDIMENTS IN THE VARIOUS DEPOSITIONAL ENVIRONMENTS, CALCULATED FROM ACTUAL VALUES: (A) shallow-marine, (B) open-intertidal, (C) mangrove-channel, (D) mangrove-swamp, (E) supratidal-flat. When $\rho = 0.4$, the limiting correlation coefficients corresponding to confidence levels of 90, 95, and 99 percent are 0.481, 0.496, and 0.524 respectively. Correlation coefficients significant at a confidence level equal to or greater than 99 percent are asterisked

E. Supratidal-flat sediments

	% mud	mean phi	Ba	Ca	Co	Cr	Cu	Fe	Mg	Mn	Ni	Pb	Sc	Sr	Ti	V	Y	Zn	Zr	$CaCO_3$	P_2O_5
% mud	1.000																				
mean phi	0.715*	1.000																			
Ba	−.165	−.258	1.000																		
Ca	−.039	−.455	0.147	1.000																	
Co	−.121	0.106	0.269	−.170	1.000																
Cr	0.070	0.099	0.566	0.136	0.420	1.000															
Cu	0.036	0.144	0.295	0.050	0.374	0.359	1.000														
Fe	0.020	0.264	0.319	−.039	0.552	0.851*	0.404	1.000													
Mg	0.022	0.083	−.082	0.083	0.037	0.091	0.062	0.221	1.000												
Mn	0.054	0.160	0.371	−.070	0.673*	0.540	0.205	0.591	0.184	1.000											
Ni	0.076	0.259	0.401	−.033	0.637*	0.856*	0.407	0.877*	0.094	0.634*	1.000										
Pb	0.120	0.267	0.093	−.221	0.487	0.316	0.243	0.380	0.074	0.458	0.480	1.000									
Sc	0.107	0.178	0.646*	0.043	0.421	0.815*	0.177	0.645*	0.079	0.491	0.738*	0.318	1.000								
Sr	−.041	−.366	0.469	0.777*	0.039	0.407	0.210	0.186	0.028	0.149	0.137	−.097	0.314	1.000							
Ti	0.111	−.134	0.611	0.161	0.377	0.871*	0.352	0.760*	0.047	0.500	0.804*	0.339	0.807*	0.398	1.000						
V	0.081	0.188	0.588	0.001	0.504	0.834*	0.263	0.686*	−.093	0.531	0.782*	0.220	0.883*	0.268	0.811*	1.000					
Y	0.005	−.013	0.439	−.013	0.491	0.383	0.064	0.211	−.099	0.414	0.270	0.177	0.518	0.284	0.308	0.468	1.000				
Zn	0.265	0.711*	−.301	−.551	0.373	0.133	0.103	0.339	0.099	0.293	0.327	0.429	0.220	−.400	0.121	0.237	0.029	1.000			
Zr	−.348	−.472	0.424	0.035	0.064	0.278	−.013	0.144	−.061	0.082	0.109	−.123	0.106	0.239	0.022	0.105	0.337	−.517	1.000		
$CaCO_3$	−.003	−.458	0.034	0.935*	−.220	−.048	0.010	−.187	0.096	−.128	−.201	−.247	−.116	0.708*	−.019	−.163	−.099	−.538	−.025	1.000	
P_2O_5	0.089	0.311	−.494	−.069	0.015	−.089	−.086	0.115	0.430	−.006	−.021	−.008	−.083	−.151	−.189	−.088	−.194	0.557	−.414	0.021	1.000

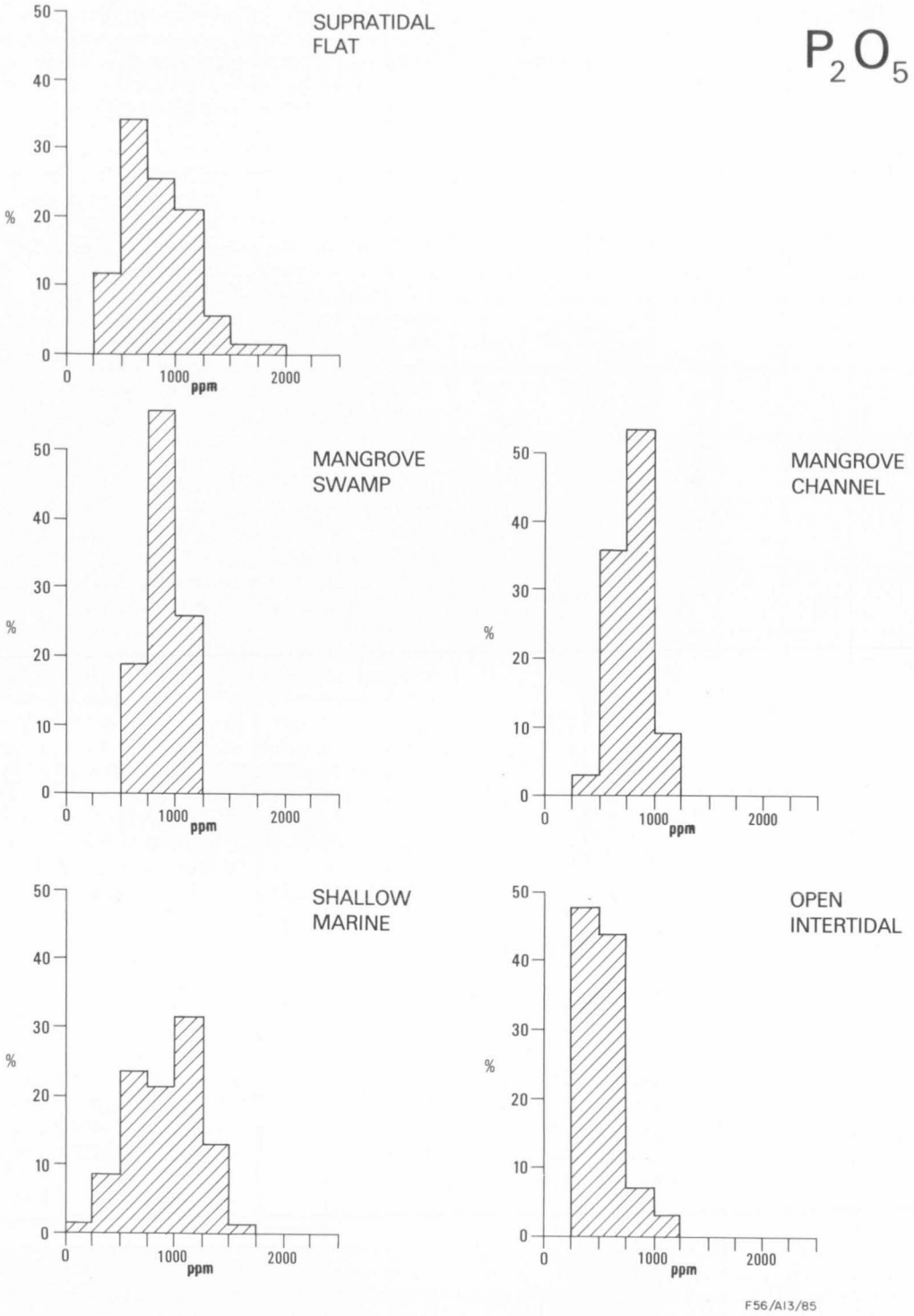


Fig. A29. P_2O_5 concentration: frequency distribution in estuarine depositional environments

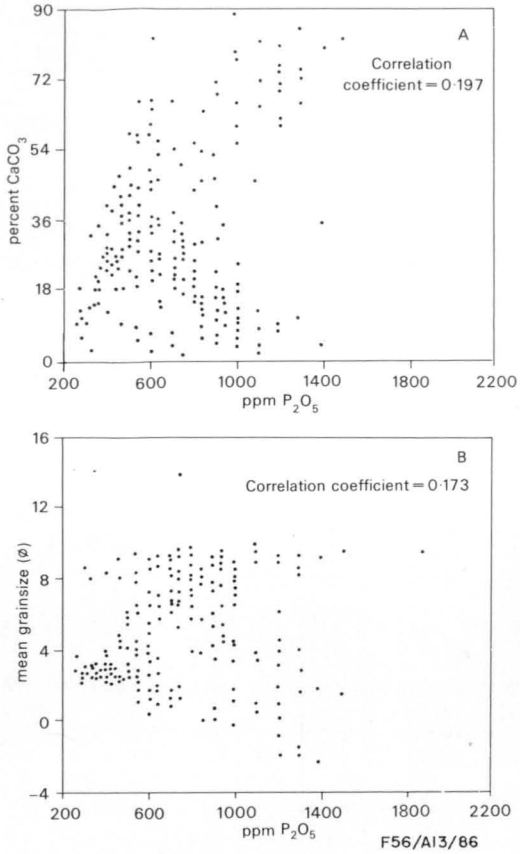


Fig. A30. Relationships of P_2O_5 with mean grainsize (phi) and $CaCO_3$, all estuarine sediments.

isation of calcareous material. Looking at other correlations involving P_2O_5 (Fig. A28) it is apparent that relatively few are significant. In the mangrove-channel environment, P_2O_5 shows significant positive correlations with Cr, Fe, Ni, V, and Zn. These relationships are likely to be the result of metal (and phosphate) fixation by clays.

The positive correlation of P_2O_5 with Mg may be somewhat deceptive (Fig. A33). As Mg^{++} has a much smaller ionic radius than Ca^{++}, there is likely to be some ionic substitution of Mg for Ca in the apatite structure. As is evident from Figure A33 there is a distinct linear relation between Mg and P_2O_5, particularly if the data are log transformed. Alternatively, it may be a second-order correlation: Mg correlates with $CaCO_3$ in a manner almost identical with the P_2O_5-$CaCO_3$ correlation (compare Figure A30A with Figure A37), both plots showing a bimodal correlation, one positive, the other negative. Similarly, Mg correlates positively with percentage mud. Therefore Mg, like P_2O_5 has two sites, one $CaCO_3$, the other clay particles, and it is possibly this similarity of association that is producing the apparent Mg-P_2O_5 correlation, rather than a true ionic association.

A positive correlation was expected between organic carbon content and P_2O_5, but it is apparent from Table A20 that this is not so. Similarly, because of the abundance of living plants in the mangrove-swamp environment it might be expected that the sediments of that environment would be rich in phosphate, but again this is not so. This may be because most of the phosphate is in the living plant material and is constantly recycled as organic phosphate within the biota, with little opportunity for it to form high concentrations within the sediments. Another possible cause is the strongly acid conditions within mangrove swamp deposits, particularly the older deposits (see p. 110), which not only restrict the uptake of phosphate by clays (Walsh, 1967), and prevent the precipitation of phosphate, but also actually cause phosphate to be leached from the sediments and the associated plant material. This in turn results in phosphate-rich pore waters. In some circumstances these phosphate-rich waters are capable of some localised phosphatisation. The Holocene dolomite nodules of the Charon Point area, which are believed to have formed as a result of post-deposition dolomitisation (Cook, 1973), contain up to about 0.5% P_2O_5, and in this case there appears to be an association between phosphatisation and dolomitisation. Generally, however, there is only limited phosphatisation and most of the phosphate-rich pore water eventually finds its way into the mangrove channels. Again, despite the high phosphate content of these channel waters the phosphate content of the sediments is generally less than that in most of the other Broad Sound environments. This suggests that in the estuarine environment the phosphate content of the overlying water column does not have an appreciable effect on the phosphate content of the bottom sediments. A far more significant factor is probably the rate of sedimentation. Thus, in the mangrove-channel environment, where there is a high rate of sediment movement and deposition, there is little opportunity for phosphatisation at the sediment-water interface by the phosphate-rich channel waters. Conversely, in the shallow-marine environment the sea water has a low phosphate content and therefore is potentially a far less vigorous phosphatising agent than the channel waters. Nevertheless, because of the slow rate of sedimentation and the high rate of water flow over the sediment-water

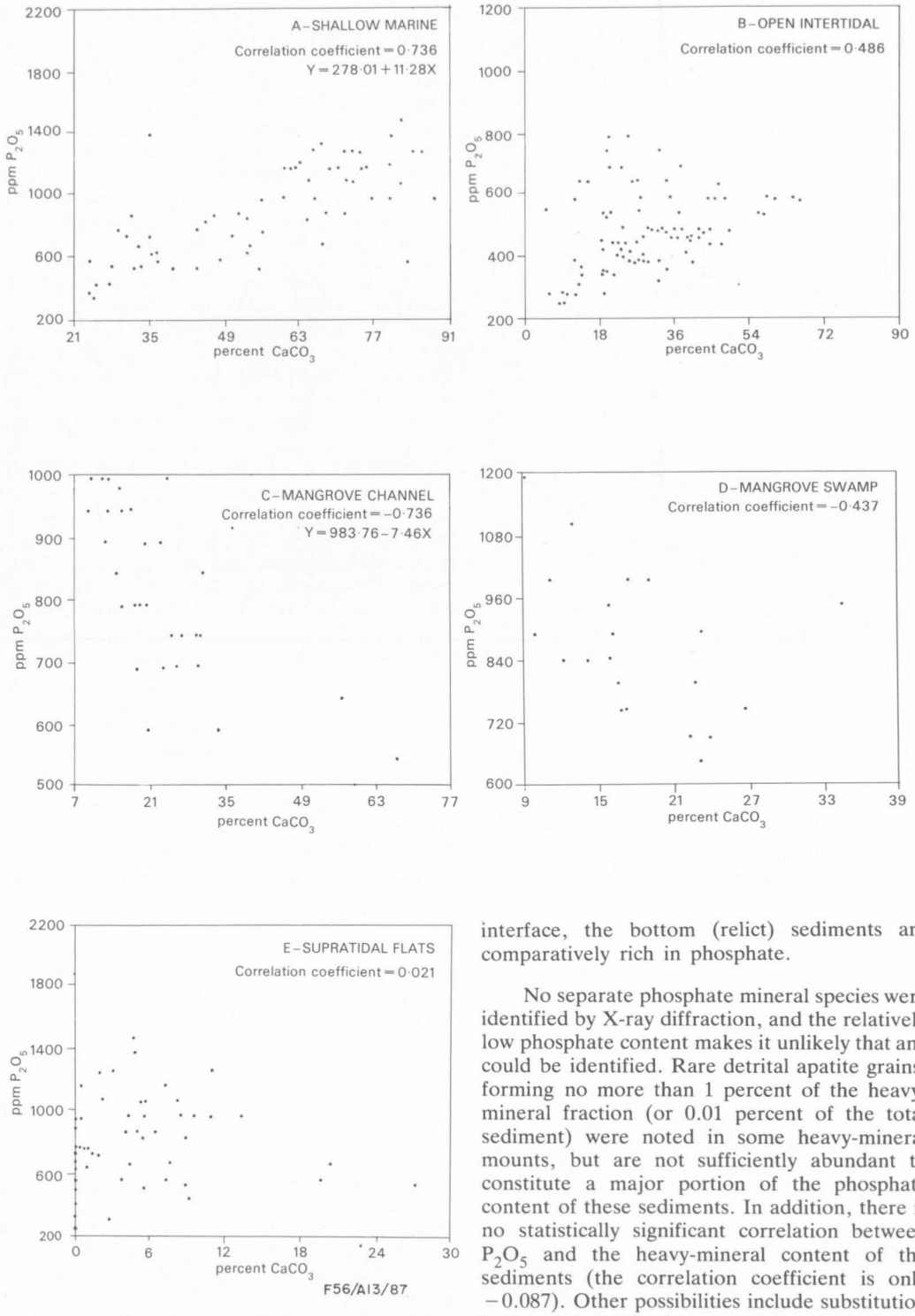


Fig. A31. Relationship betwen P_2O_5 and $CaCO_3$ in the several estuarine depositional environments

interface, the bottom (relict) sediments are comparatively rich in phosphate.

No separate phosphate mineral species were identified by X-ray diffraction, and the relatively low phosphate content makes it unlikely that any could be identified. Rare detrital apatite grains, forming no more than 1 percent of the heavy-mineral fraction (or 0.01 percent of the total sediment) were noted in some heavy-mineral mounts, but are not sufficiently abundant to constitute a major portion of the phosphate content of these sediments. In addition, there is no statistically significant correlation between P_2O_5 and the heavy-mineral content of the sediments (the correlation coefficient is only -0.087). Other possibilities include substitution in the calcite lattice (though this is unlikely to any great extent because of crystallographic con-

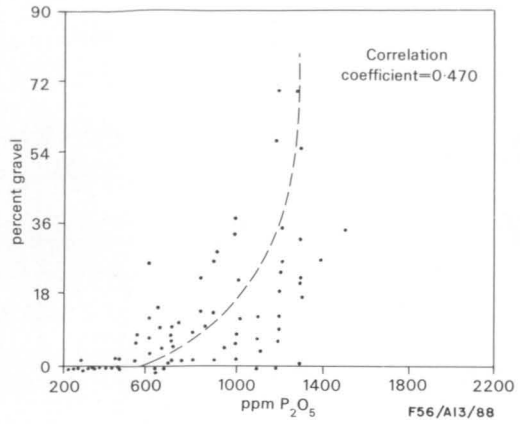


Fig. A32. Relationship between P_2O_5 and gravel content in estuarine depositional environments

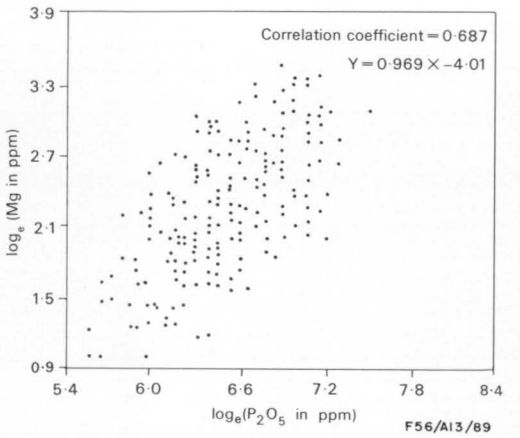


Fig. A33. Relationship between P_2O_5 and Mg in estuarine depositional environments.

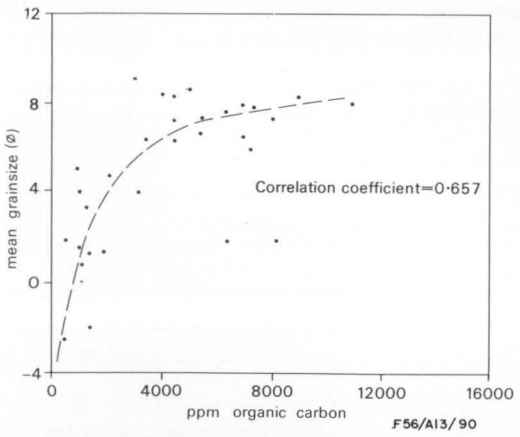


Fig. A34. Relationship between mean grainsize (phi) and organic carbon in estuarine depositional environments

straints), or the formation of phosphates such as vivianite, though the lack of a significant P_2O_5-Fe correlation in the carbonate-rich sediment also makes this unlikely. Therefore it must be concluded that the most likely mode of occurrence of the phosphate in the calcareous sediments is as trace amounts of apatite (probably carbonate fluorapatite). Some of it may be original biogenic phosphate, but much is believed to result from post-depositional phosphatisation at the sediment-water interface.

In the muds of the mangrove-channel, mangrove-swamp, and supratidal-flat environments the phosphate is probably fixed on the clays. Stout (1939) showed that phosphate fixation increases with decreasing clay particle size. Clay mineralogy also has a significant effect on phosphate fixation (Grim, 1968). However, the precise location of the phosphate is still uncertain. There may be ionic exchange with Al within the lattice, but some may be fixed by surface adsorption or be in a relatively loose inter-layer location. The high phosphate in the pore waters suggests that at least some of the phosphate is not strongly bound to the clays. The presence of the Fe-P_2O_5 correlation, particularly in the mangrove channel environment, suggests that some iron phosphates may also be forming at or below the sediment-water interface in the relatively acid conditions prevailing in this environment.

Organic carbon

The range and mean values for organic carbon in the various environments are given in Table A22. These values are of the same order as those given by Ronov & Migdisov (1971) for Mesozoic and Cainozoic sandstones (3600 ppm), mudstones (9400 ppm), and carbonates (4700 ppm). They are however, significantly lower than values given for many other estuaries (e.g. Biggs, 1967). This is particularly so for the intertidal and subtidal environments and is a reflection of the strongly oxygenated state of the Broad Sound estuarine waters in these environments. The sediment colours are closely related to the abundance of organic carbon: shallow-marine and open-intertidal sediments, which are low in organic carbon, are pale brown, supratidal flat muds are olive-grey, and organic-rich mangrove-channel and mangrove-swamp sediments are dark grey to black. Because only a small number of samples were analysed for organic carbon, it is not possible to comment on organic carbon relationships within the various depositional environments, and comments here refer to the estuary as a whole.

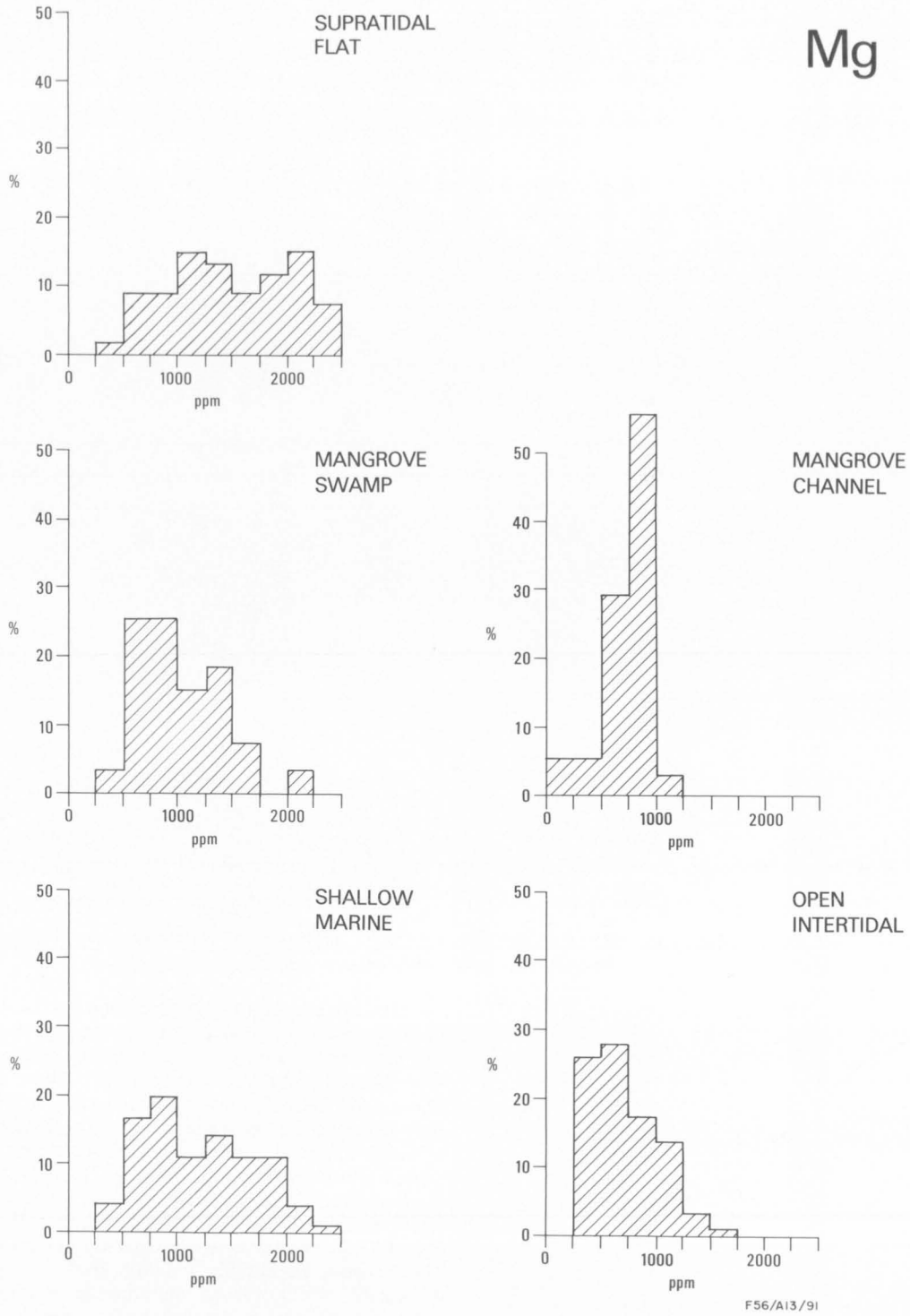


Fig. A35. Mg concentration: frequency distribution in estuarine depositional environments

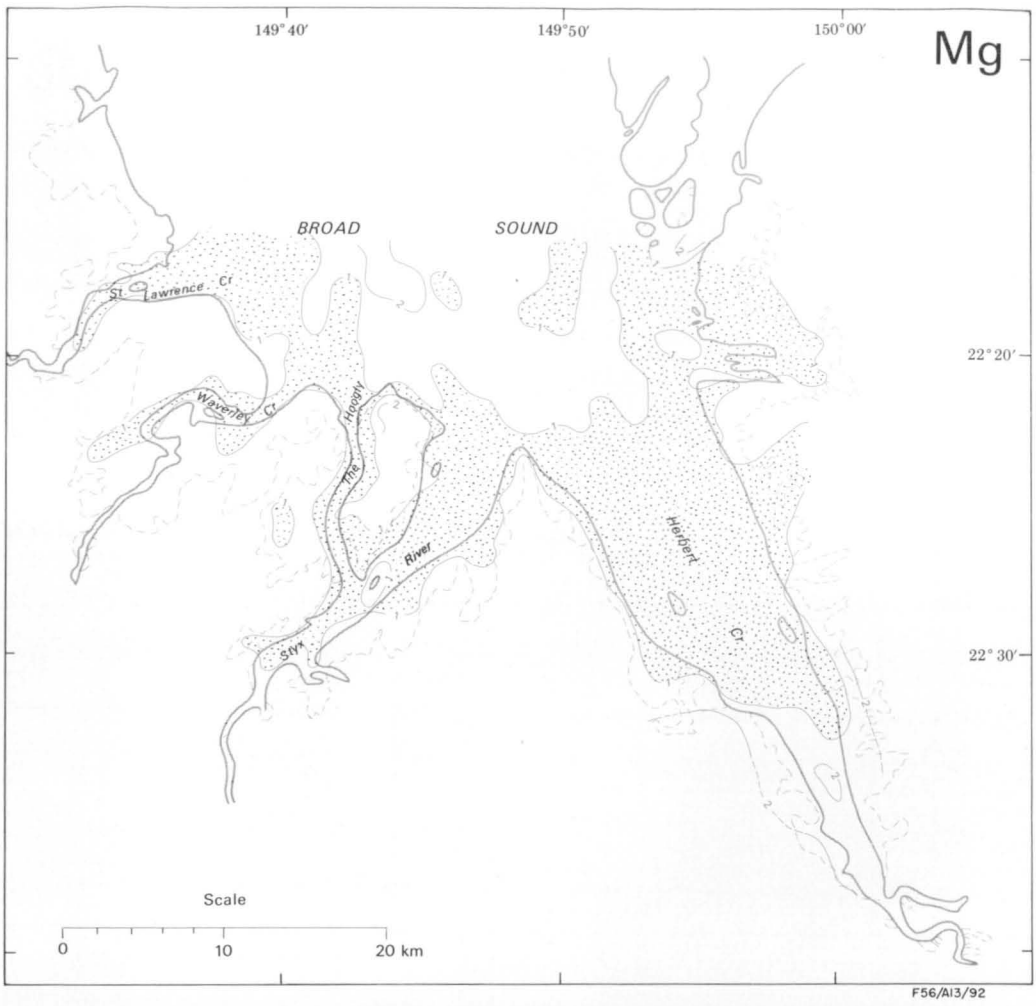


Fig. A36. Mg: distribution in estuarine sediments

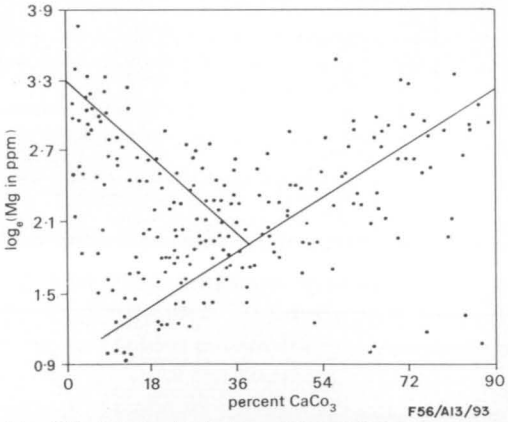


Fig. A37. Relationship between Mg and $CaCO_3$ in estuarine sediments

The abundance of organic carbon is related to grainsize. It is apparent from Figure A34 that organic carbon increases with increasing abundance of mud and decreasing grainsize. There is also a statistically significant negative correlation between organic carbon and $CaCO_3$ (Table A20) although this relationship is a consequence of a 'closed array' correlation (Fig. A27) between grainsize and $CaCO_3$ content. More significant relationships include the positive correlations Ba-C and Zn-C, and the negative correlation Mn-C. The elements Ba and Zn are both known to be associated with organic material in marine sediments. However, the correlations may also result in part from the adsorption of these metals by clay particles, coupled with the tendency for

TABLE A22. ABUNDANCE OF TOTAL ORGANIC CARBON AND EXTRACTABLE ORGANIC MATTER IN SEDIMENTS FROM BROAD SOUND DEPOSITIONAL ENVIRONMENTS. NUMBERS IN BRACKETS INDICATE THE NUMBER OF ANALYSES AVAILABLE FROM EACH ENVIRONMENT

Depositional environment	Total organic carbon (ppm)			Extractable organic matter (ppm)		
	minimum	maximum	mean	minimum	maximum	mean
Shallow-marine (11)	500	3000	1300			
Open-intertidal (9)	500	5500	2100			
Mangrove-channel (5)	4500	7000	6400	26	290	197
Mangrove-swamp (7)	3500	12000	9200	127	888	409
Supratidal-flat (5)	4000	9000	5600	170	619	357

organic carbon to be more abundant in the finer-grained sediments. The negative correlation comes about probably because the more organic-rich sediments typically are acidic reducing muds, leading to the formation of divalent Mn and the attendant dissolution of Mn from the sediments.

The organic carbon in Broad Sound sediments is derived almost entirely from plant material, especially mangrove fragments. In the intertidal and subtidal environments a minor amount derived from marine animal remains is mixed with the allochthonous plant material. In the mangrove-swamp environment the organic material is almost exclusively autochthonous mangrove detritus, whereas in the supratidal-flat environment, allochthonous plant litter, mainly from the adjacent mangrove-swamp environment but including some land plant material, is mixed with autochthonous halophytic plant material and algal fibres.

An indication of the relative abundance of the various organic components was obtained by T. G. Powell (BMR, personal communication). Geolipid concentrations in sediments from three of the environments studied are given in Table A22. Hydrocarbons (saturated and aromatic) comprised less than 5 percent of the geolipid extracts. Alkane (saturated hydrocarbon) yields were generally less than 2 ppm. Analysis of this fraction by gas chromatography (D. M. McKirdy, BMR, personal communication) has shown that saturated hydrocarbons in the supratidal-flat environment consist mainly of n-alkanes in the range C_{17}-C_{25} (maximum at C_{25}), with a predominance of odd-numbered carbon molecules, testifying to the essentially non-marine nature of the organic material. In a few cases the n-C_{17} peak is prominent, suggesting a significant algal contribution. The saturated hydrocarbon patterns in the mangrove-channel sediments are much more complex, owing largely to a higher proportion of branched and cyclic compounds. The n-alkanes range between C_{15} and C_{27}, with maxima at either C_{22}, or C_{25}, or C_{27}, and in some cases the odd-over-even predominance is lacking. Organic matter in the mangrove-swamp sediments gives alkane profiles intermediate in complexity between the supratidal-flat and mangrove-channel environments. The more heterogeneous nature of the organic detritus in the channel sediments is probably a reflection both of the influx of marine-derived organic material and also of the sedimentary mixing which occurs in the environment, perhaps coupled with some bacterial activity within the sediments.

Magnesium

In general, Broad Sound sediments are relatively low in Mg compared to average values given for shales and carbonates (Table A18). There are marked differences in Mg content between the various environments (Fig. A35), with relatively high concentrations in the supratidal-flat and shallow-marine sediments. Abundance patterns also differ widely among the various depositional environments, e.g. concentrations are bimodal in sediments of the supratidal-flat environment (Fig. A36). The distribution pattern throughout the estuary (Fig. A36) is complex: the concentration increases towards the northern (seaward) end of the Sound and also to landward in the supratidal flats, as with P_2O_5 (Fig. A14).

As mentioned previously, the $CaCO_3$-Mg correlation is clearly bimodal (Fig. A37), the positive correlation reflecting the Mg-Ca association in the calcareous sediments, and the negative correlation reflecting the Mg-mud correlation in the low-carbonate sediments. Mg has an ionic radius of 0.066 nm, and will substitute for Ca in the calcite structure, forming the magnesian calcite series. Previous work by Cook & Mayo (1978) showed that low-Mg calcite ($Ca_{0.965}Mg_{0.035}$) and high-Mg calcite ($Ca_{0.850}Mg_{0.150}$) are present in approximately equal amounts but with a tendency for high-Mg calcite to increase in abundance seawards (possibly a function of the relict nature of these sediments). This is consistent with the increase in Mg shown in Figure A36. The correlation with Ca is probably also responsible for a second-

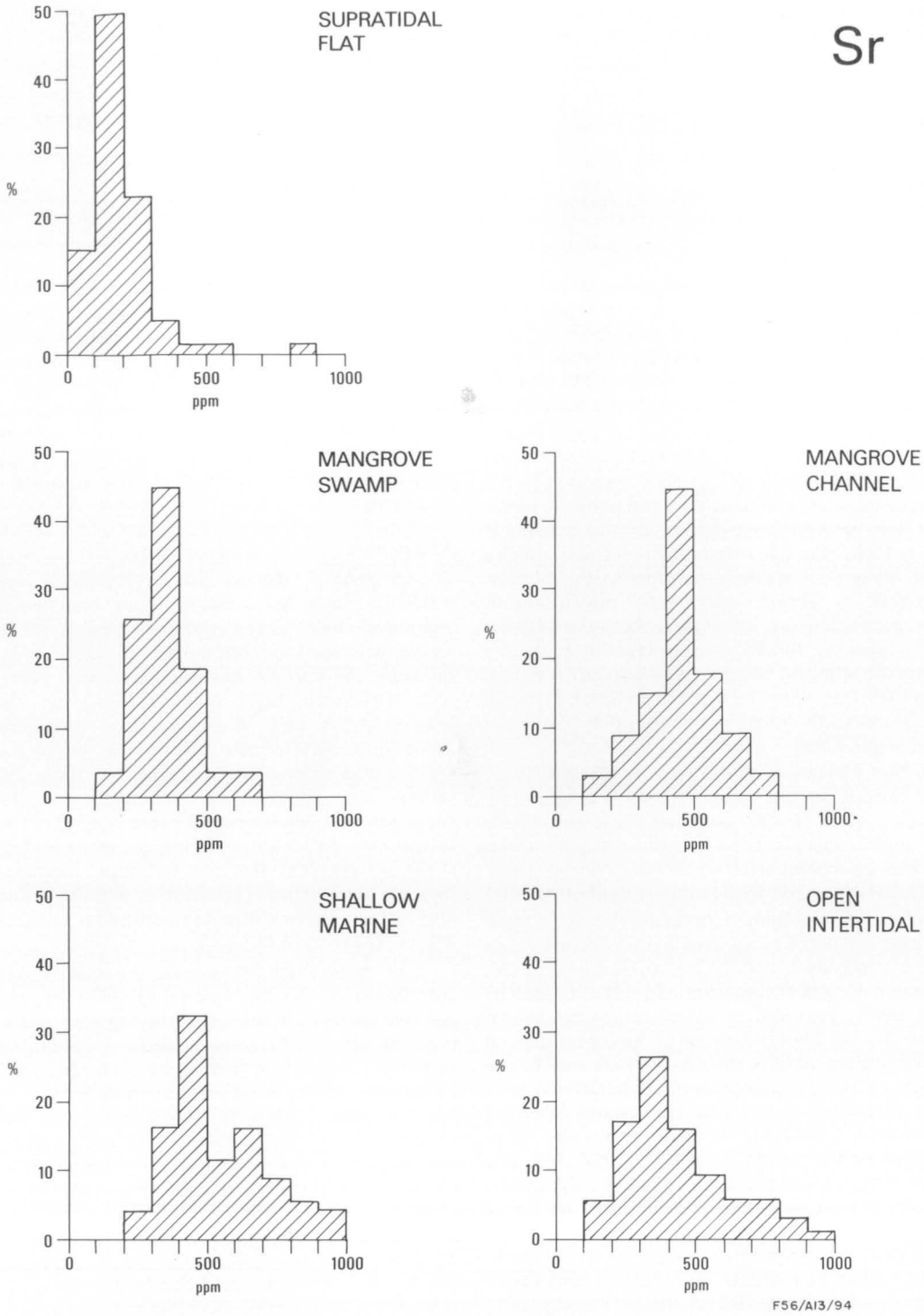


Fig. A38. Sr concentration: frequency distribution in estuarine depositional environments

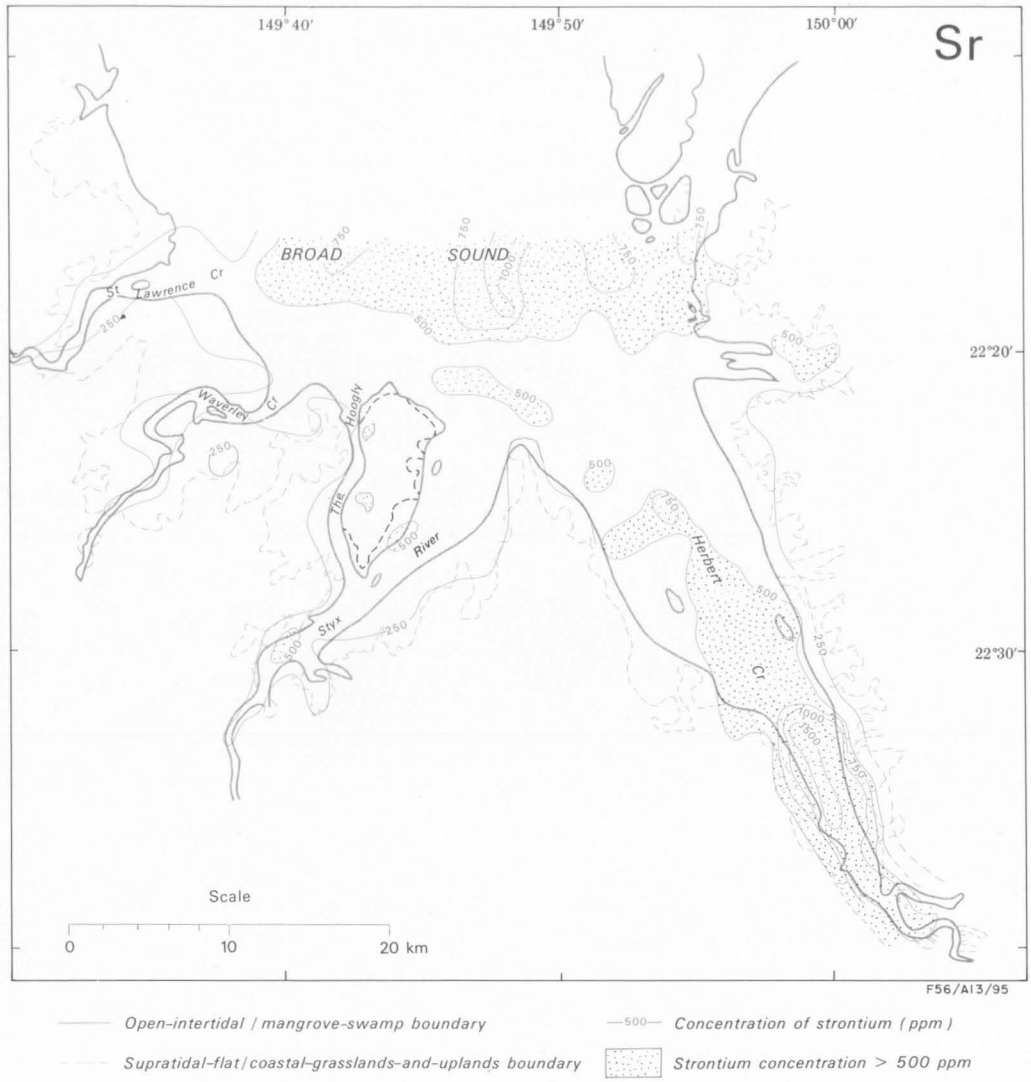


Fig. A39. Sr: distribution in estuarine sediments

order correlation between Mg and Sr in the open-intertidal environment.

Most correlations evident from Tables A20 and 21 and Figure A28, including Mg-Fe, Mg-Mn, Mg-Ni, Mg-Ti, and Mg-Zn are a result of the association of Mg with clays (especially, it would appear, those of the mangrove swamp environment). Mg is present in clays, particularly montmorillonite, though it probably also substitutes to a limited extent for K in illite and other clays when they enter the estuary. There is, however, evidence of additional uptake of Mg in the estuary, as is suggested by comparing the Mg content of the muds from the supratidal-flat environment with muds from the mangrove-channel and mangrove-swamp environments (Table A19). For instance, the abundance of mud in the supratidal-flat environment is 26 percent greater than in the mangrove channels, yet the Mg content is 110 percent greater. Also, a limited amount of dolomite forms in the supratidal-flat environment (Cook, 1973), which will locally contribute to the total Mg content of these sediments. The pore waters of the supratidal-flat environment contain two to three times as much Mg as sea water, because of the crystallising of gypsum out of solution. It appears likely some of this Mg is then being taken up by

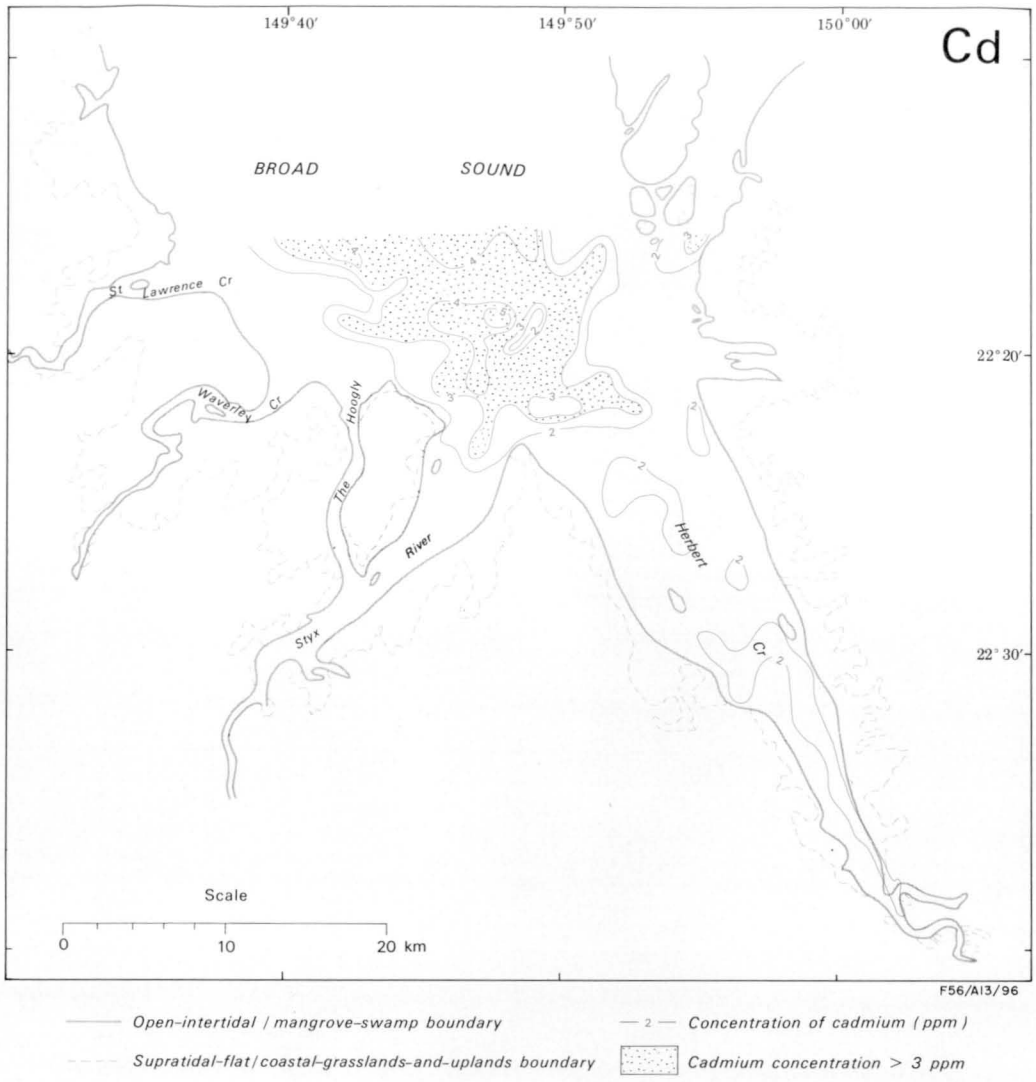


Fig. A40. Cd: distribution in estuarine sediments

the clays, either by lattice substitution or by adsorption.

Strontium

The mean Sr concentration in Broad Sound sediments is intermediate between the value for average shales and that for average limestones (Table A18). Concentrations range between about 150 and 2500 ppm, most falling between 200 and 800 ppm (Fig. A38). Highest concentrations are found in the calcareous sediments of the shallow-marine and open-intertidal environment (Table A19). Lowest concentrations occur in the supratidal-flat sediments. This is reflected in the distribution pattern for Sr within the estuary (Fig. A39), which shows a marked seaward increase in abundance. Comparison with Figure A26 shows that the Sr distribution pattern is very similar to that of $CaCO_3$.

Sr (ionic radius 0.116 nm) will substitute isomorphously for Ca (ionic radius 0.103 nm) in the eight-fold co-ordination position, as in aragonite (in preference to calcite). Thus the aragonite/calcite ratio also has a significant effect on the distribution pattern of Sr (see Cook & Mayo, 1978). Most of the correlations involving Sr (Tables A20 and 21, Fig. A28) are a direct result of the close association of Sr and Ca. Nevertheless, the positive correlation between Sr and Sc in sediments of the open-intertidal

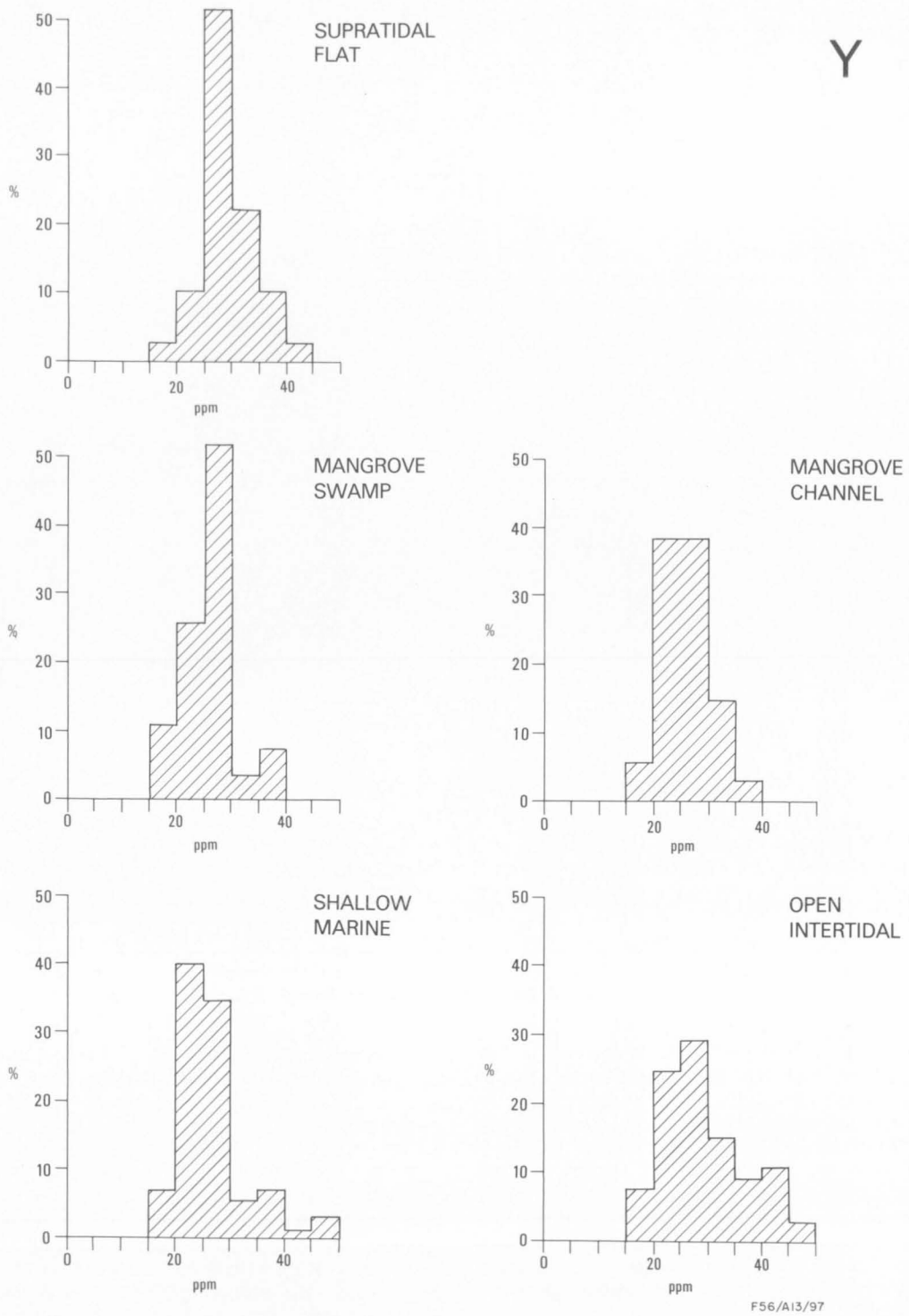


Fig. A41. Y concentration: frequency distribution in estuarine depositional environments

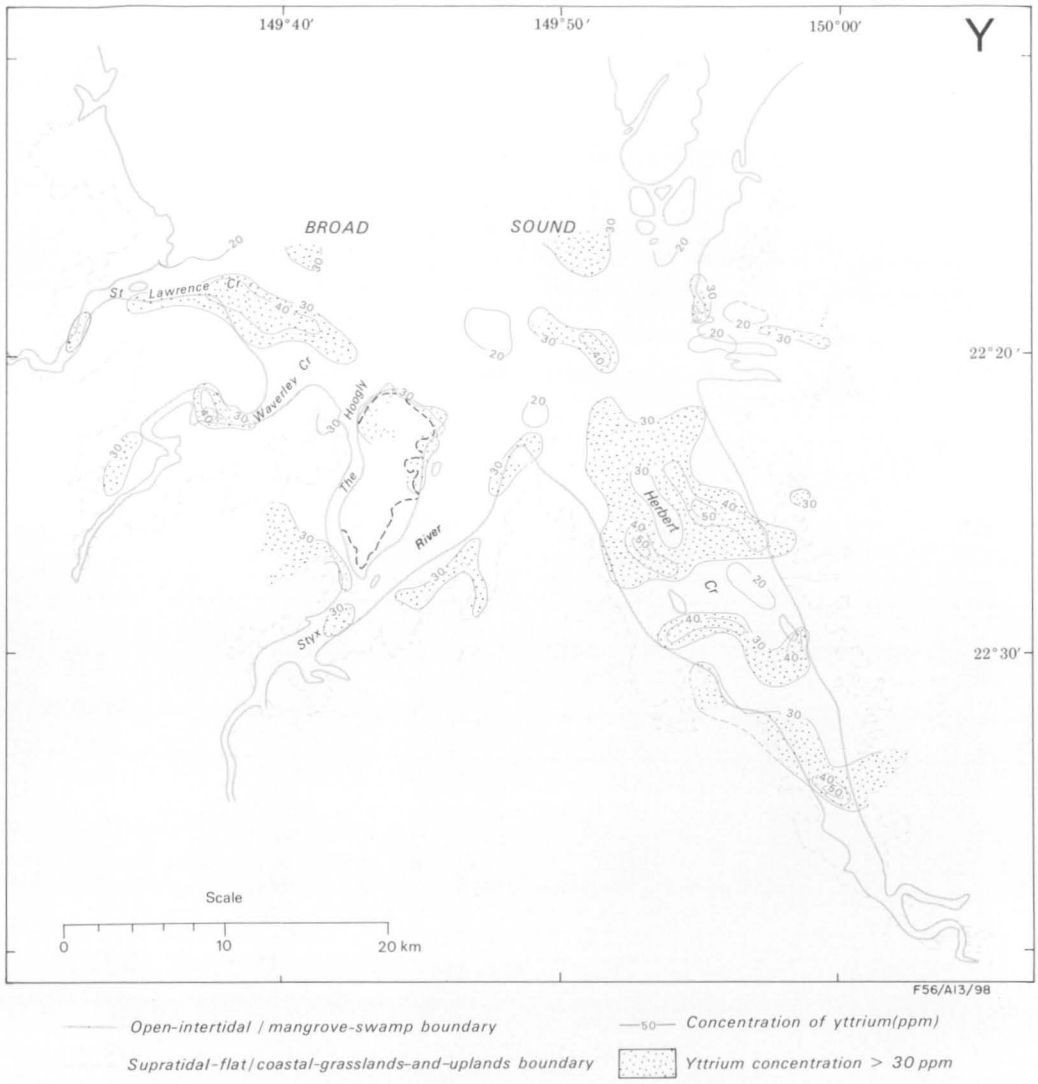


Fig. A42. Y: distribution in estuarine sediments

environment and the negative correlation between Sr and Zn in the mangrove-channel sediments (Table A19) cannot be the result of the Sr-Ca association. Trivalent Sc (ionic radius 0.081 nm) is unlikely to substitute for the large trivalent Sr ion, and the reason for this correlation is not clear. The Sr-Zn relationship in the mangrove-channel sediments is probably a second-order negative correlation resulting from the positive correlation of Zn with the mean grainsize and the negative correlation of Sr and grainsize.

Although the Sr-Ca relationship dominates the geochemistry of Sr, quite clearly not all of the Sr is substituting for Ca in $CaCO_3$. The fact that the supratidal-flat sediments contain only 4 percent $CaCO_3$ yet have a Sr concentration of about 200 ppm (Table A19) suggests that some of the Sr is associated with the clays. The Sr/Ca ratio in the Broad Sound supratidal flat sediments is about 0.04 which is intermediate between the value of 0.02 for Gulf of Paria sediments (Hirst, 1962b) and 0.06 given by Turekian & Kulp (1956) for shales. It is also about twice the Sr/Ca ratio for sea water (Turekian, 1964). Possibly, then, the Sr has been concentrated preferentially in the clays, either as a result of the hypersaline conditions on the

supratidal flats, or by the incorporation of recycled Sr-bearing terrigenous clay in the sediments. There may be limited substitution of Sr for K in the clays, so providing a lattice location for the Sr. Alternatively, it may be absorbed on the clay-particle surface.

Cadmium, lanthanum, yttrium

Because many of the Cd and La concentrations are below the detection limits, it was not possible to determine means and other statistical parameters, although concentrations do appear to be somewhat above those normally encountered in sediments (Table A18). Highest concentrations of La and Y are found in the shallow marine sediments (Table A19). In addition there is a very marked seaward increase in Cd (Fig. A40) which is very similar to the distribution shown by $CaCO_3$(Fig.A26). Such a relationship could be anticipated from the ionic radius of Cd (0.101 nm) which is very similar to that of Ca (0.103 nm), thus allowing ready substitution of Cd in $CaCO_3$ and other Ca-bearing minerals. There is no evidence of Cd substitution in, or absorption by, Broad Sound clays.

La (ionic radius 0.118 nm) also substitutes for Ca in $CaCO_3$. There is, of course, scope for other substitutions, such as La for Sr or Cd for Zn, but such substitutions are very minor in Ca-rich environments such as Broad Sound. Although Y is commonly associated with the rare earths and therefore might be expected to behave similarly to La, its affinities, because of its ionic radius (0.092 nm), are more with the heavier lanthanides than with lanthanum itself. This difference is reflected in Table A19 and also in Figure A42 which together demonstrate that there is no marked increase in Y in the more calcareous sediments. There is a high secondary mode in the shallow-marine and open-intertidal environment at about 45 ppm (Fig. A41) which may be a reflection of some substitution of Y for Ca. Other factors probably influence the distribution of Y, as the areas of highest Y concentrations (Fig. A42) do not always coincide with areas of highest $CaCO_3$. The Herbert estuary in particular has high Y concentrations. This might be in part a reflection of the catchment geochemistry, though this is generally not reflected in the geochemistry of individual estuaries in the Broad Sound system.

The correlation matrixes (Tables A20-21, and Fig. A28) also show a general lack of association between Y and Ca, and between Y and most other variables. One of the few statistically significant correlations is between Co and Y in both shallow-marine and open-intertidal environments. This does not appear to be a function of a Co-Ca correlation. Moreover the Co ion is too small to allow significant substitution of Y in Co-bearing minerals. For the present, one can only conclude that the processes controlling the distribution of Y in Broad Sound are unclear. Whilst the processes may be related to some extent to the distribution of Ca, this is obviously not the only factor.

Molybdenum

Most Mo values are below the detection limit of 3 ppm; consequently the statistical techniques normally used in the Broad Sound study could not be applied to Mo, and only the most general trends can be established. The mean values for the depositional environments are all less than 3 ppm, except for the shallow-marine environment (Table A19). A single value of 360 ppm (sample 70636216) is of doubtful validity, although some concentrations as high as 22 ppm were noted in shallow-marine sediments. Tetravalent Mo has an ionic radius of about 0.07 nm, and hexavalent Mo about 0.06 nm. Thus, despite the fact that the highest Mo concentrations are found in the most calcareous sediments, there is unlikely to be a Mo-Ca substitution. A much more likely possibility is that Mo is associated with Fe. Hirst (1962b) suggests that under oxidising conditions $(MoO_4)^{2-}$ will form and that Fe $(OH)_3$ sols, which have a slightly positive charge, will attract molybdate anions. Thus, the association of high Mo concentrations with shallow-marine sediments probably results from the enrichment of Mo in the ferruginous coating on the calcareous nodules. In view of this, the lack of Mo in the iron-rich muds of the supratidal zone is perhaps surprising. However, the subaerial conditions prevailing in the supratidal zone are likely to have a marked influence on Mo mobility, perhaps resulting in leaching of Mo from these sediments. The low Mo content of the low-Eh sediments of the mangrove channels and mangrove swamps conflicts with the observed association between Mo and sediments formed in reducing environments (e.g. Goldschmidt (1954) reports that there is up to 200 ppm Mo in the black shales of the Kupferschiefer). This suggests that redox conditions are by no means the most important factor in Mo mobility.

Barium

The concentration of Ba in Broad Sound sediments ranges from 40 to 1400 ppm, with a mean of about 180. Concentrations are lowest in the shallow-marine sediments and highest in supratidal-flat sediments (Fig. A43), and generally decrease seaward (Fig. A44). The average Ba content of 105 ppm (Table A19) for the shallow-marine calcareous sediments is considerably higher than the average carbonate value of 10 ppm given by Turekian & Wedepohl (1961). This may be a feature of nearshore impure carbonates, such as those of Broad Sound.

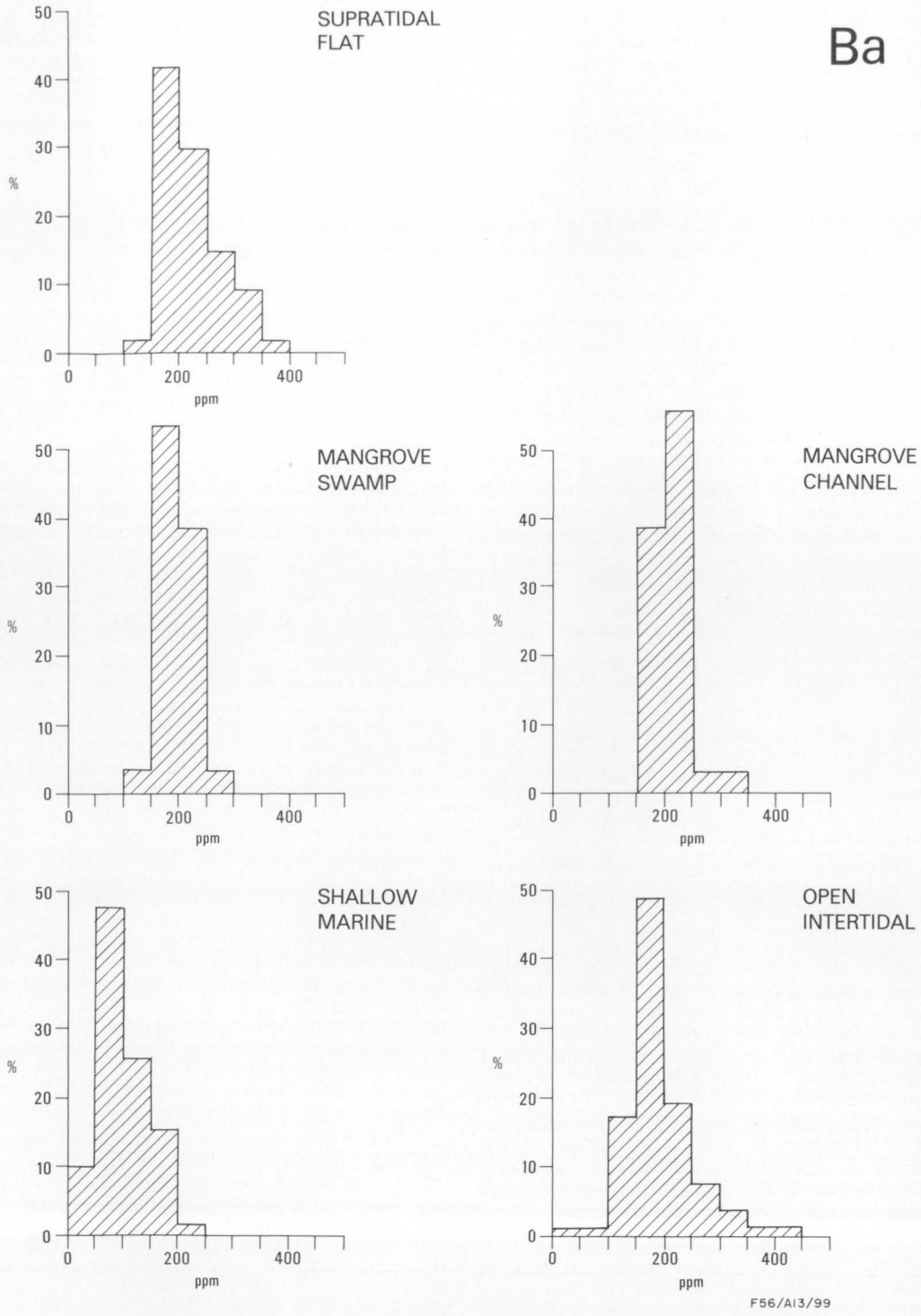


Fig. A43. Ba concentration: frequency distribution in estuarine sediments

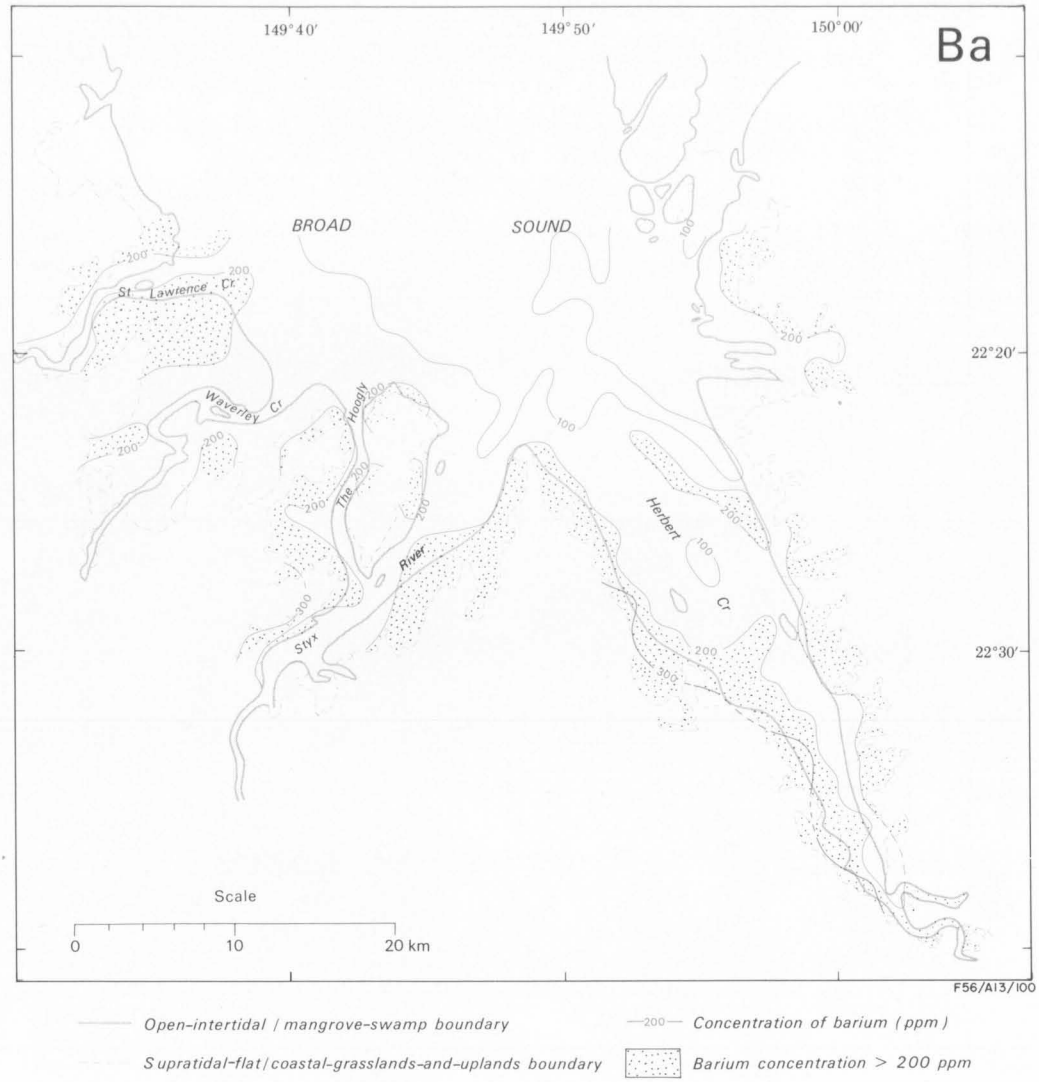


Fig. A44. Ba: distribution in estuarine sediments

Ba^{++}, with an ionic radius of 0.146 nm, has the potential to substitute for K^{+}, whose ionic radius is 0.145 nm. The higher charge may also lead to some preferential adsorption in clays. Either or both of these features may be responsible for the positive correlation between Ba and phi mean grainsize (see Fig. A28) and the sympathetic negative correlation with $CaCO_3$. However, there are few other Ba correlations. The Ba-Ni correlation in the open-intertidal environment is inexplicable for the present, as is the negative Zn-Ba correlation. The Ba-Sc positive correlation in the supratidal-flat sediments may result from ionic capture of the smaller, more highly charged Ba ion; however, this is difficult to reconcile with the low Sc concentrations. The negative P_2O_5 correlation in the shallow-marine environment (Table A21A) is also of unknown cause.

Therefore the geochemistry of Ba in Broad Sound sediments is not understood, though for the most part Ba appears to be associated with the clay fraction, probably substituting for interlayered K.

Copper, lead, zinc

Cu, Pb, and Zn concentrations in Broad Sound sediments are generally in the range

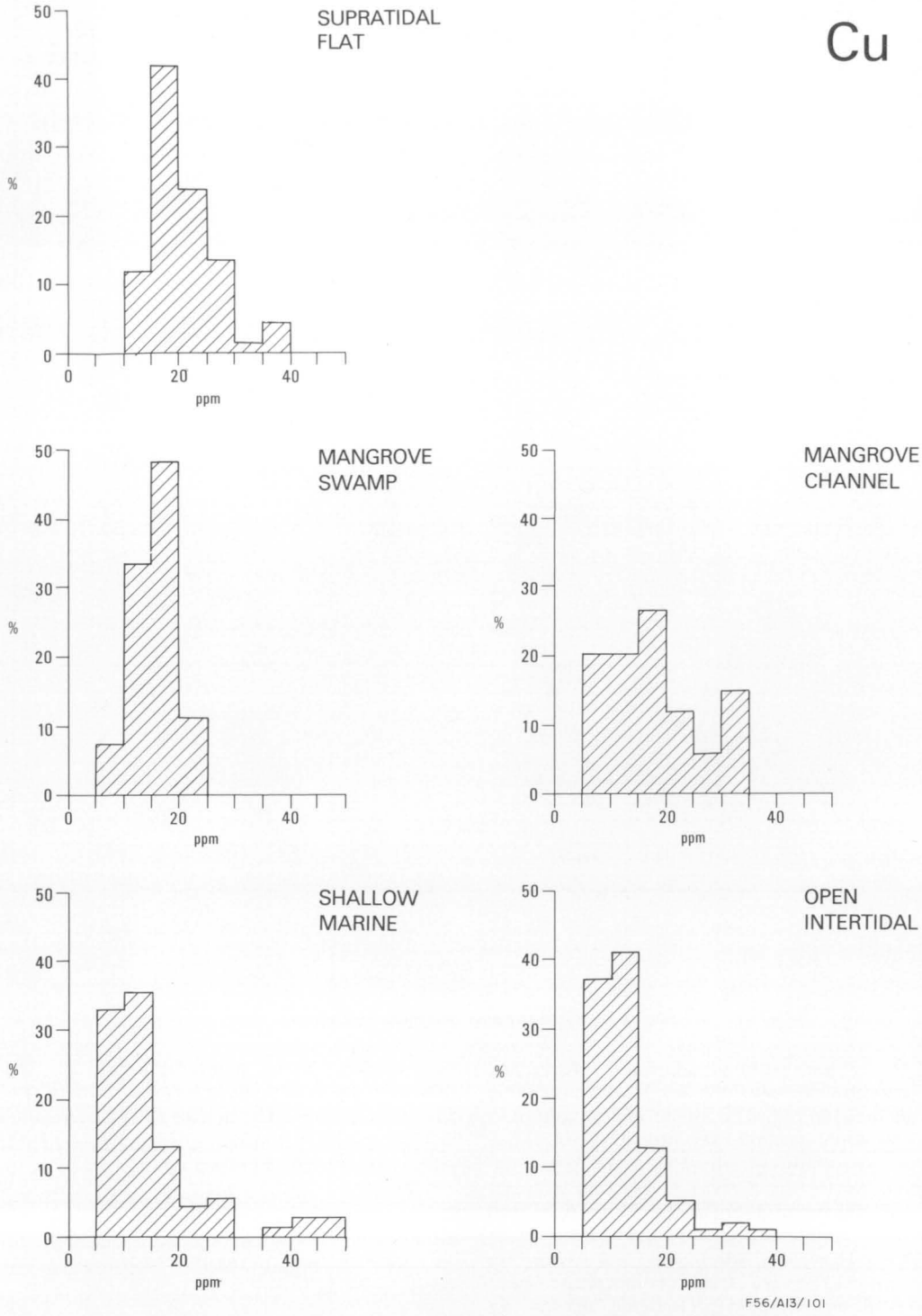


Fig. A45. Cu concentration: frequency distribution in estuarine depositional environments

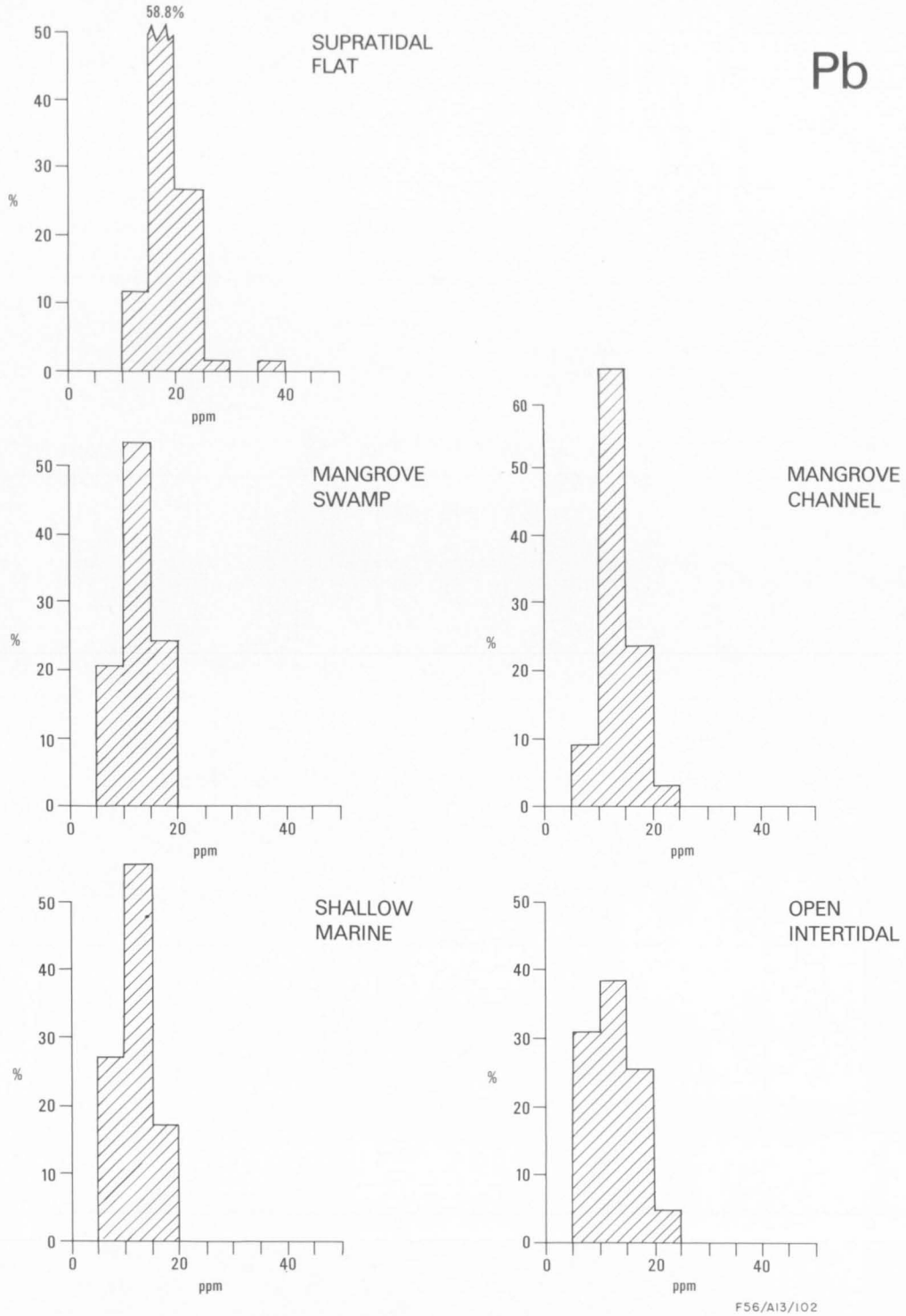


Fig. A46. Pb concentration: frequency distribution in estuarine depositional environments

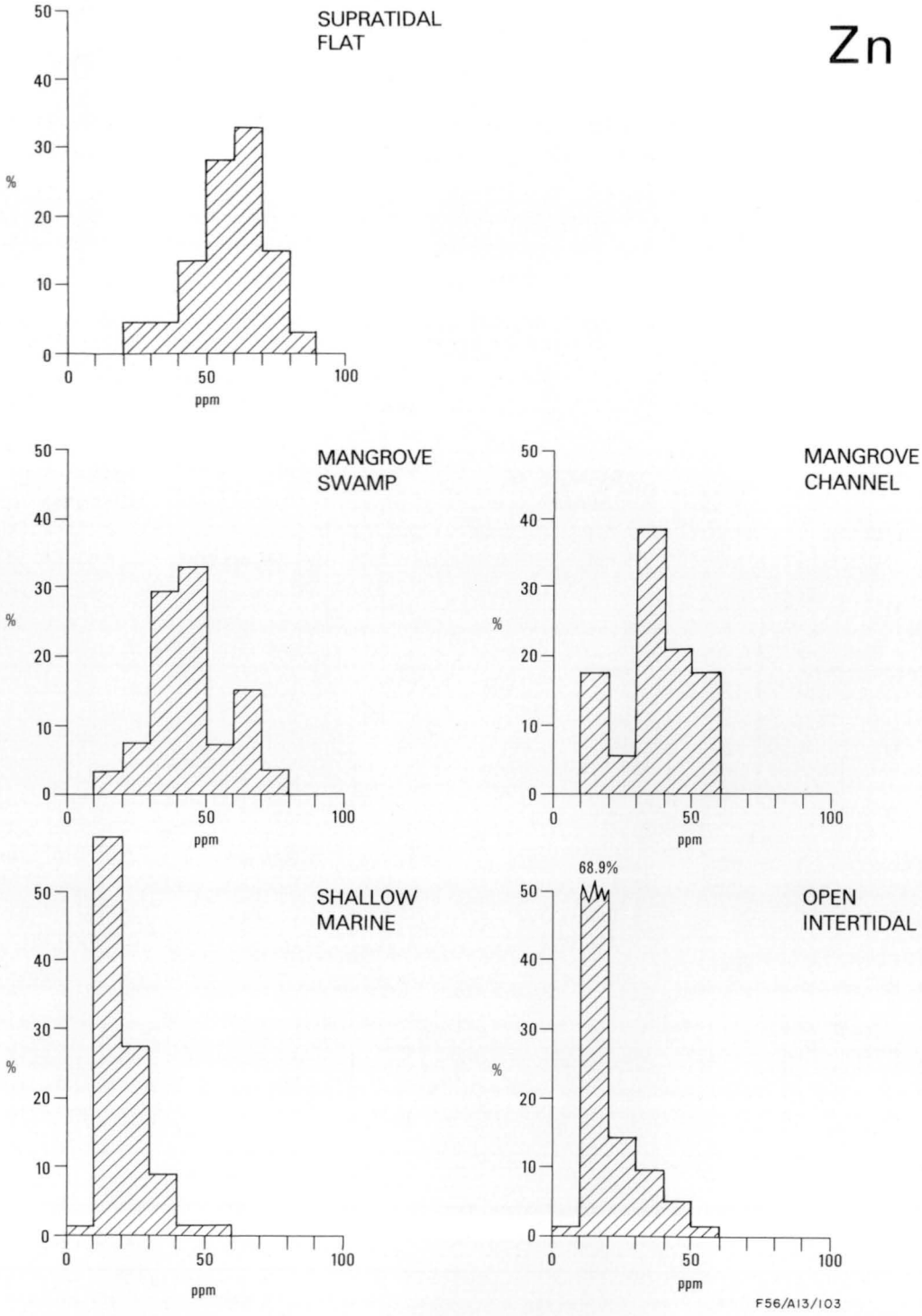


Fig. A47. Zn concentration: frequency distribution in estuarine depositional environments

normally encountered in sediments (Table A18), though the muds of the mangrove-channel, mangrove-swamp, and supratidal-flat environments (Table A19) have somewhat lower concentrations of all these metals than those normally encountered in shales. The frequency distribution of concentrations for the estuary as a whole is log-normal for both Cu and Zn (Figs. A45, 47) but there is an ill-defined distribution for Pb (Fig. A46). Similarly, when individual depositional environments are considered (Figs. A45-47), the Cu and Zn frequency distribution histograms are similar in form and are approximately log-normal, whereas Pb distributions are rather different, being much more peaked and approximating to a normal distribution.

Regional variations in the distribution patterns of these trace metals are shown in Figures A15 to 17. Concentrations are for the most part uniformly low in the intertidal and subtidal portions of the Sound, although high for Cu in a number of localised areas. However, all three trace metals are markedly concentrated in the supratidal portion of the Sound. This is particularly so for Zn — a belt of high Zn concentrations flanks most of the Sound. Cu, Pb, and Zn have similar ionic radii (depending on valence state), and are commonly associated in rocks. Although limited substitution of some of these metal ions for Ca could be expected, this form of substitution is likely to provide only a very minor proportion of the total base-metal content.

Wedepohl (1970) suggests that for Cu at least, adsorption on iron oxides is the major process of accumulation and dispersion. However, the total lack of Cu-Fe and Pb-Fe correlations suggests that this may not be a major mechanism in Broad Sound sediments. A much more likely site for Cu, Pb, and Zn would seem to be adsorption (perhaps with some very limited lattice substitution) by clay particles, particularly illite (Hirst, 1962a). The Zn-percent mud correlation would seem to support this, although there is no significant correlation between Cu and Pb, Cu and percent mud, or Cu and phi grainsize. There is in fact an almost total lack of any significant correlation between Pb, Cu, and other variables. Zn on the other hand shows a variety of significant positive correlations with percent mud, phi, grainsize, Cr, Fe, Mg, Mn, Ni, Pb, Sc, Ti, V, and P_2O_5 (Fig. A28). Most of these are probably second-order correlations resulting from a common association of these elements with clays. There is also a Zn-organic carbon correlation; whether it is also merely a second-order correlation or of first-order significance is not known, though at least some of the Zn is probably associated with the organic matter.

Goldschmidt (1954) points out that, under normal conditions of weathering, Cu is more readily oxidised than either Pb or Zn, and therefore is more strongly leached. This is reflected in the Cu/Pb and Cu/Zn ratios (Table A23), which show a marked decrease in the relative abundance of Cu as the environments become less marine. There is a similar decrease

TABLE A23. TRACE-ELEMENT RATIOS IN SEDIMENTS FROM BROAD SOUND DEPOSITIONAL ENVIRONMENTS

	Shallow-marine	Open-intertidal	Mangrove-channel	Mangrove-swamp	Supratidal-flat
Mn/Fe	0.055	0.054	0.019	0.018	0.016
Co/Ni	0.762	0.815	0.565	0.537	0.546
Ca/Mg	15.4	15.6	13.5	7.63	1.34
Cu/Pb	1.90	1.56	1.65	1.23	1.32
Pb/Zn	0.44	0.50	0.30	0.30	0.27
Cu/Zn	0.84	0.78	0.49	0.37	0.36

of Pb relative to Zn. It may be possible to use these ratios to establish where the shoreline was in unweathered ancient marine sediments, i.e. decreasing Cu/Pb, Cu/Zn, and Pb/Zn ratios in the direction of the shoreline. However, further work is obviously required on this topic before it can be regarded as a reliable criterion for locating ancient shorelines.

Scandium, titanium, zirconium

Sc, Ti, and Zr are present in Broad Sound sediments in somewhat higher-than-average abundances (Table A18), the Zr concentrations being particularly high. However, comparison of the Turekian & Wedepohl (1961) world average values with Zr values from elsewhere (e.g. Hirst, 1962b), suggests that the Turekian & Wedepohl values are too low. In the case of Ti there is a marked increase in concentration in the muddier sediments (Table A19, Fig. A48), but there is no such well-defined trend for Sc (Fig. A49) or Zr (Fig. A50): Sc^{+3} has an ionic radius of 0.081 nm, Ti^{+3} is 0.076 nm, Ti^{+4} 0.068 nm, Zr^{+4} about 0.080 nm. Consequently one would expect that all three elements would substitute extensively for each other and would have similar distribution patterns. In fact, however, the regional distribution patterns are rather dissimilar. Ti concentration decreases markedly (Fig. A51), with particularly high values over the supratidal environments. Sc (Fig. A52) shows this trend to a limited extent but is not nearly so well defined. Zr (Fig. A53) shows a different pattern, with highest values in the intertidal and subtidal environments.

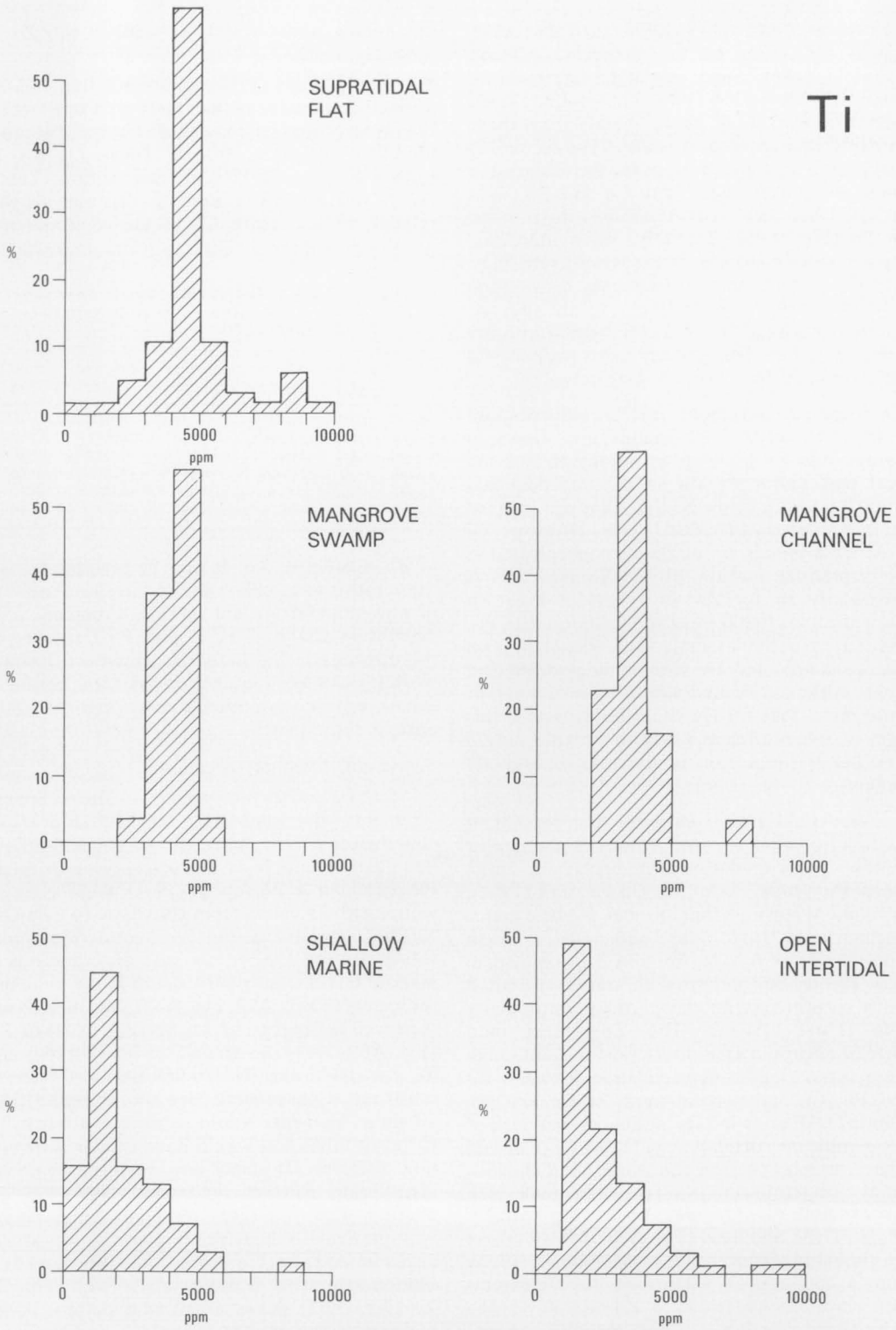


Fig. A48. Ti concentration: frequency distribution in estuarine depositional environments

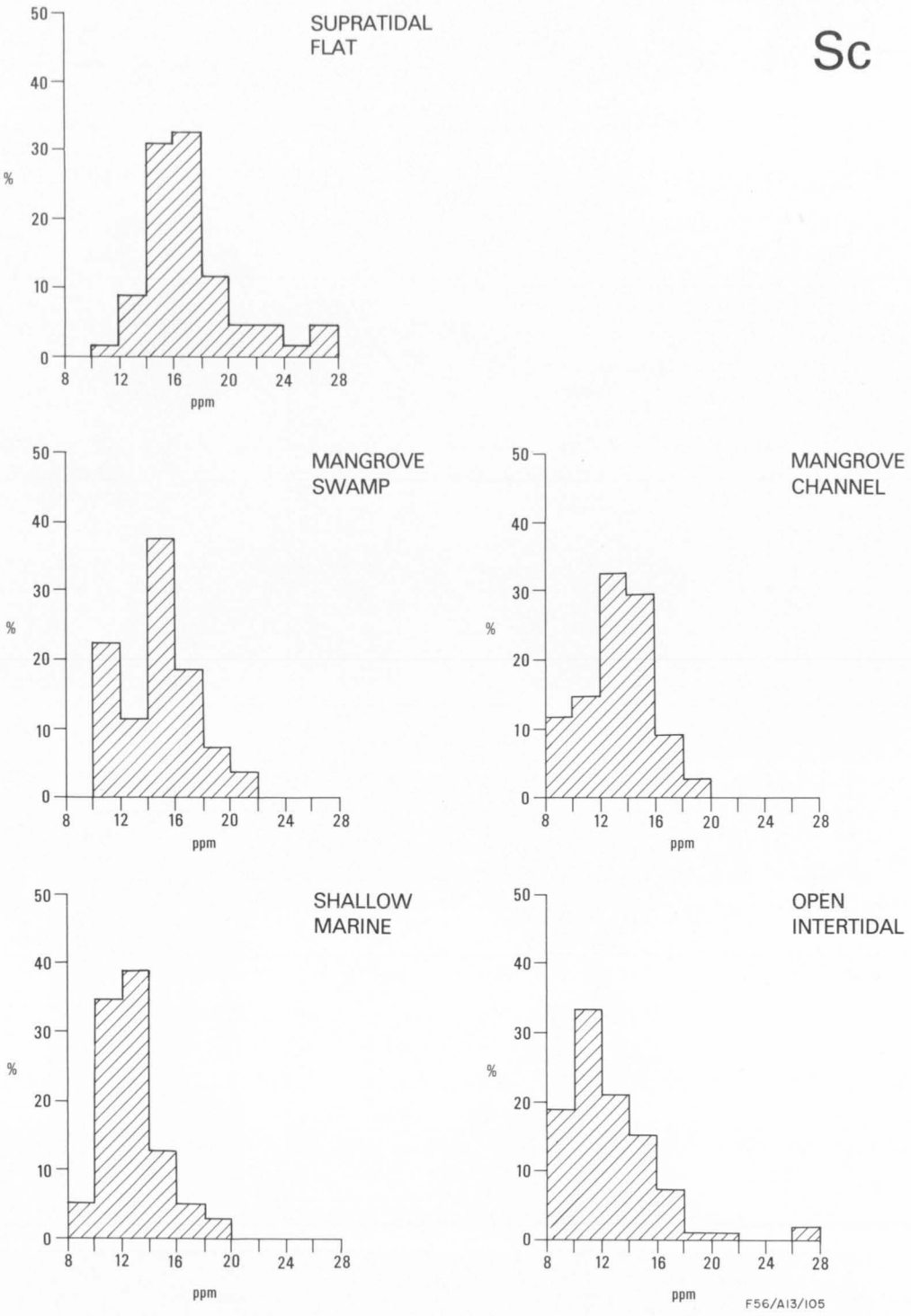


Fig. A49. Sc concentration: frequency distribution in estuarine depositional environments

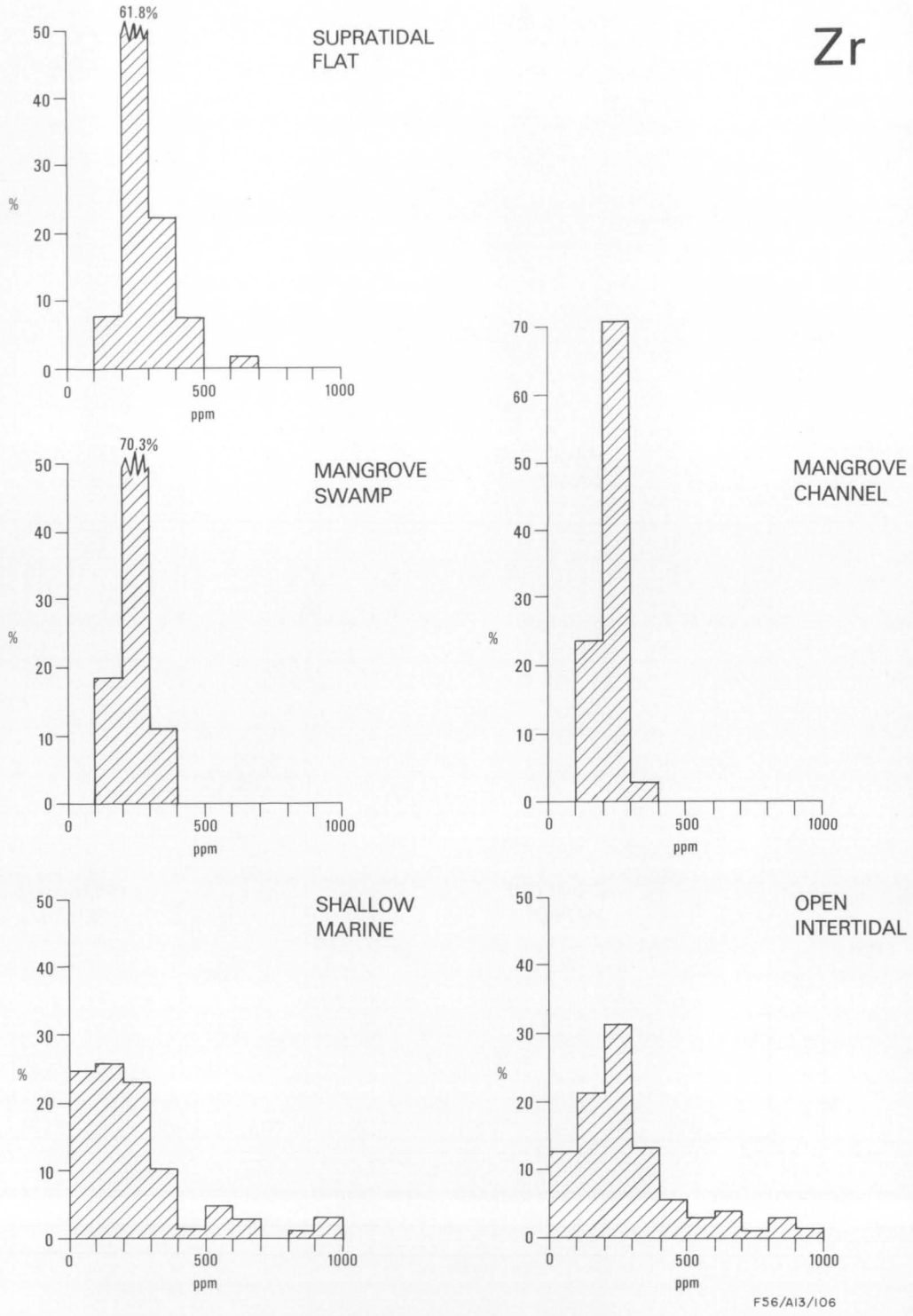


Fig. A50. Zr concentration: frequency distribution in estuarine depositional environments

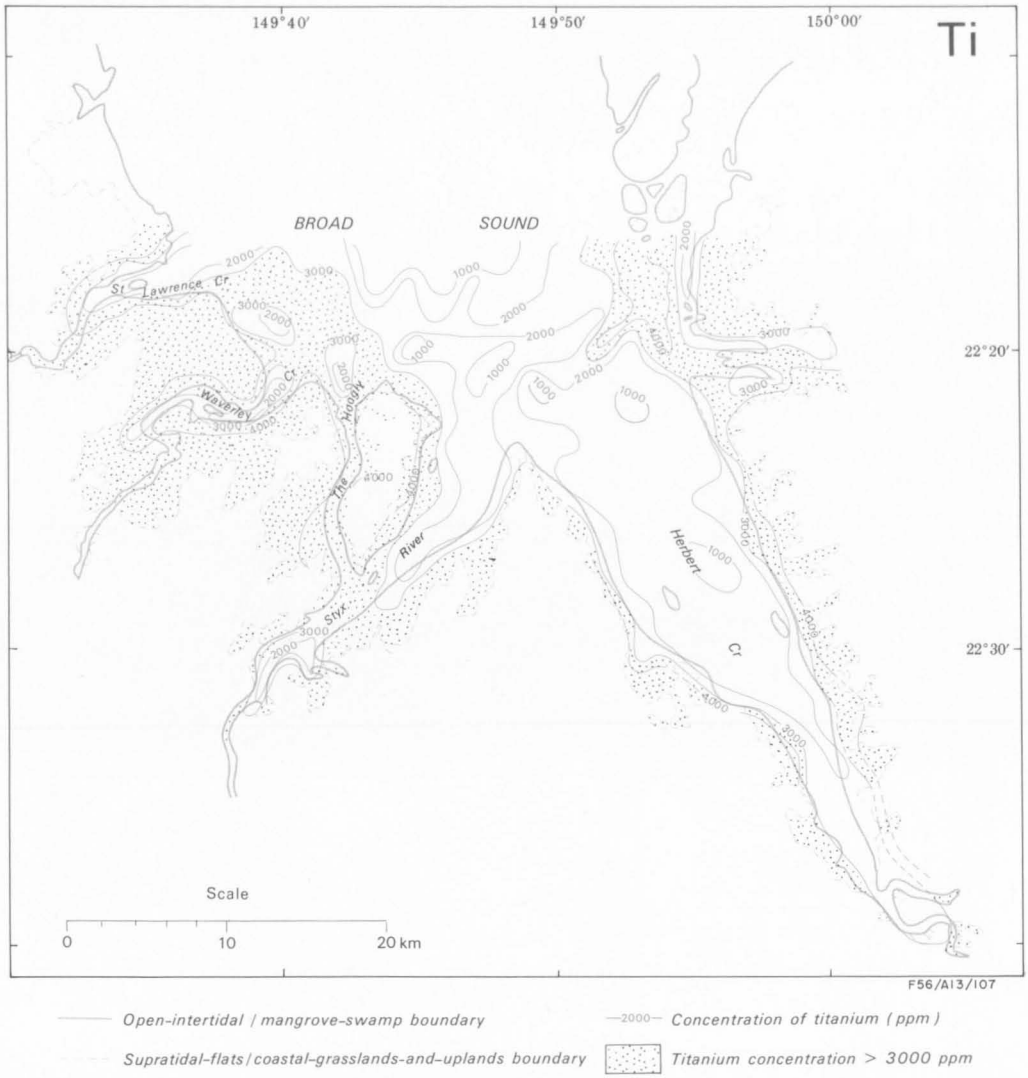


Fig. A51. Ti: distribution in estuarine sediments

These distribution patterns are in turn reflected in the correlation coefficients. There is a significant Sc-Ti correlation in the estuary as a whole and also in the supratidal-flat environment. There is a Zr-Ti correlation in the shallow-marine and open-intertidal environments, yet not in any of the muddier environments. There is no Sc-Zr correlation in any of the environments.

It might reasonably be predicted that Ti and Zr would show a positive correlation with each other and with the percentage of heavy minerals, owing to the location of Ti and Zr in detrital heavy minerals such as zircon, rutile, and ilmenite. Despite this, a Zr-Ti correlation does not exist (Fig. A28), nor is there any correlation with the percentage of heavy minerals.

In the fine-grained sediments of the mangrove swamps, mangrove channels, and supratidal flats, recognisable heavy minerals are less abundant, and Ti in particular appears to be associated with clays. This is indicated both by the positive correlation between Ti and phi grain-size (and % mud), and also by the many positive correlations with other trace metals that are thought to be associated with the clay fraction (Fig. A28). Goldschmidt (1954) suggests that very little of the Ti is chemically or physically bonded to clay minerals, and points out that Ti is

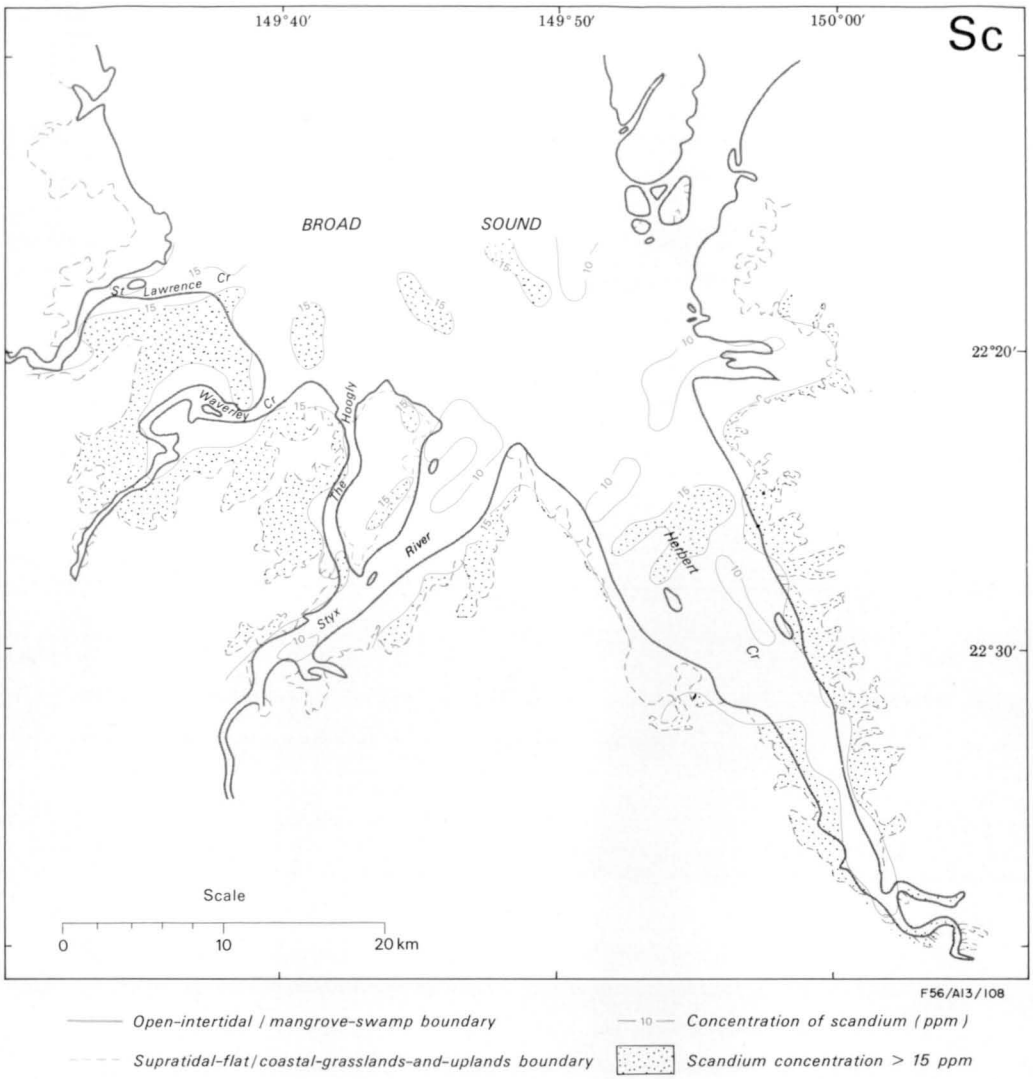


Fig. A52. Sc: distribution in estuarine sediments

virtually insoluble in sea water and therefore would not be precipitated to any significant extent. Hirst (1962a) found, in the Gulf of Paria sediments, that Ti remains associated with the clay fraction throughout weathering and transportation, though he does not indicate whether the Ti is substituting in the clay mineral, or is absorbed, or is present in minute Ti-bearing crystals such as rutile. With the Broad Sound sediments it seems likely that all the Ti is detrital, being associated with heavy minerals in the sands and with clay minerals in the muds.

Vanadium, chromium

V and Cr concentrations in Broad Sound sediments lie in the range normally found in sediments (Table A18). Their frequency distribution histograms (Figs. A54, 55) are similar in shape, and both elements are concentrated in the finer-grained sediments of the mangrove-channel, mangrove-swamp, and supratidal-flat environments. These trends are in turn reflected to some extent in the regional distribution pattern. Cr concentration (Fig. A56) decreases very markedly seaward. The same goes for V

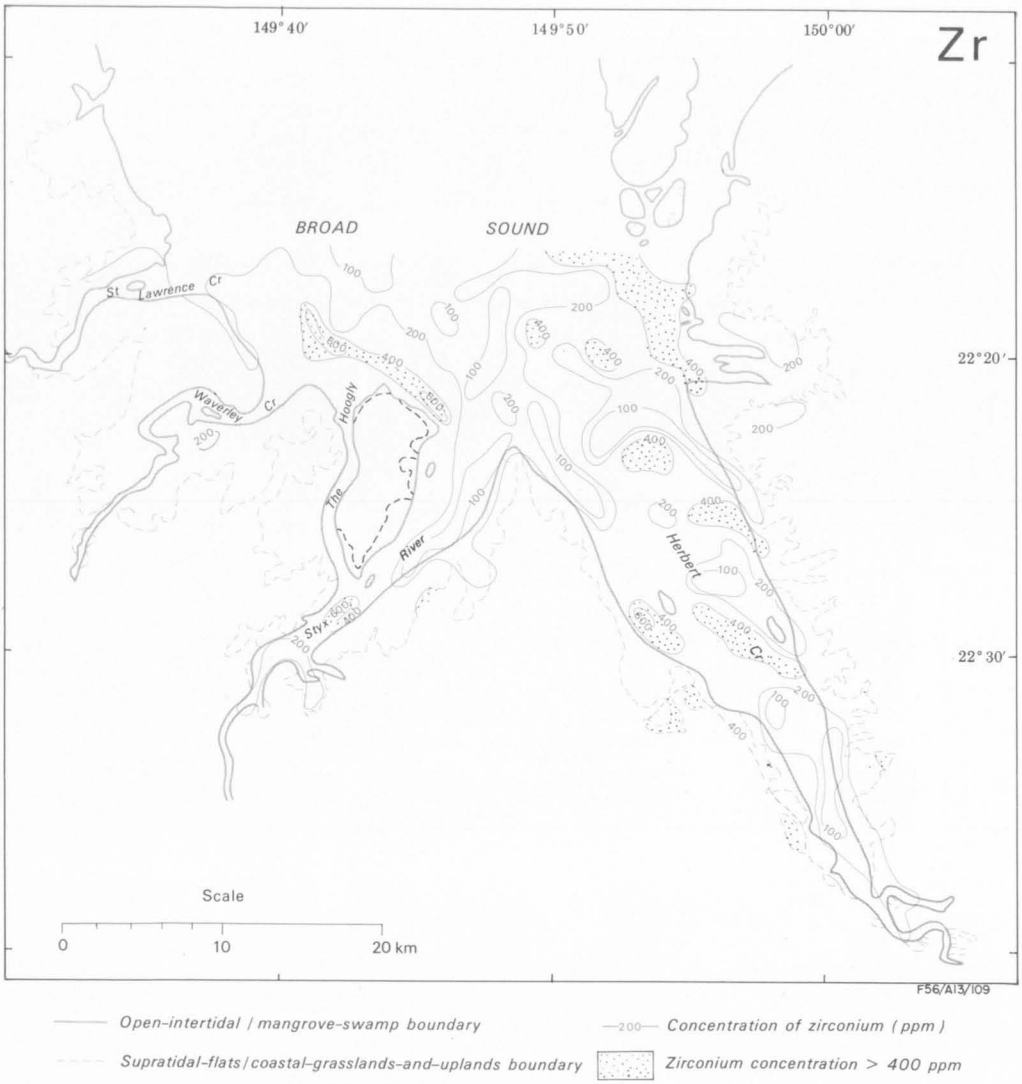


Fig. A53. Zr: distribution in estuarine sediments

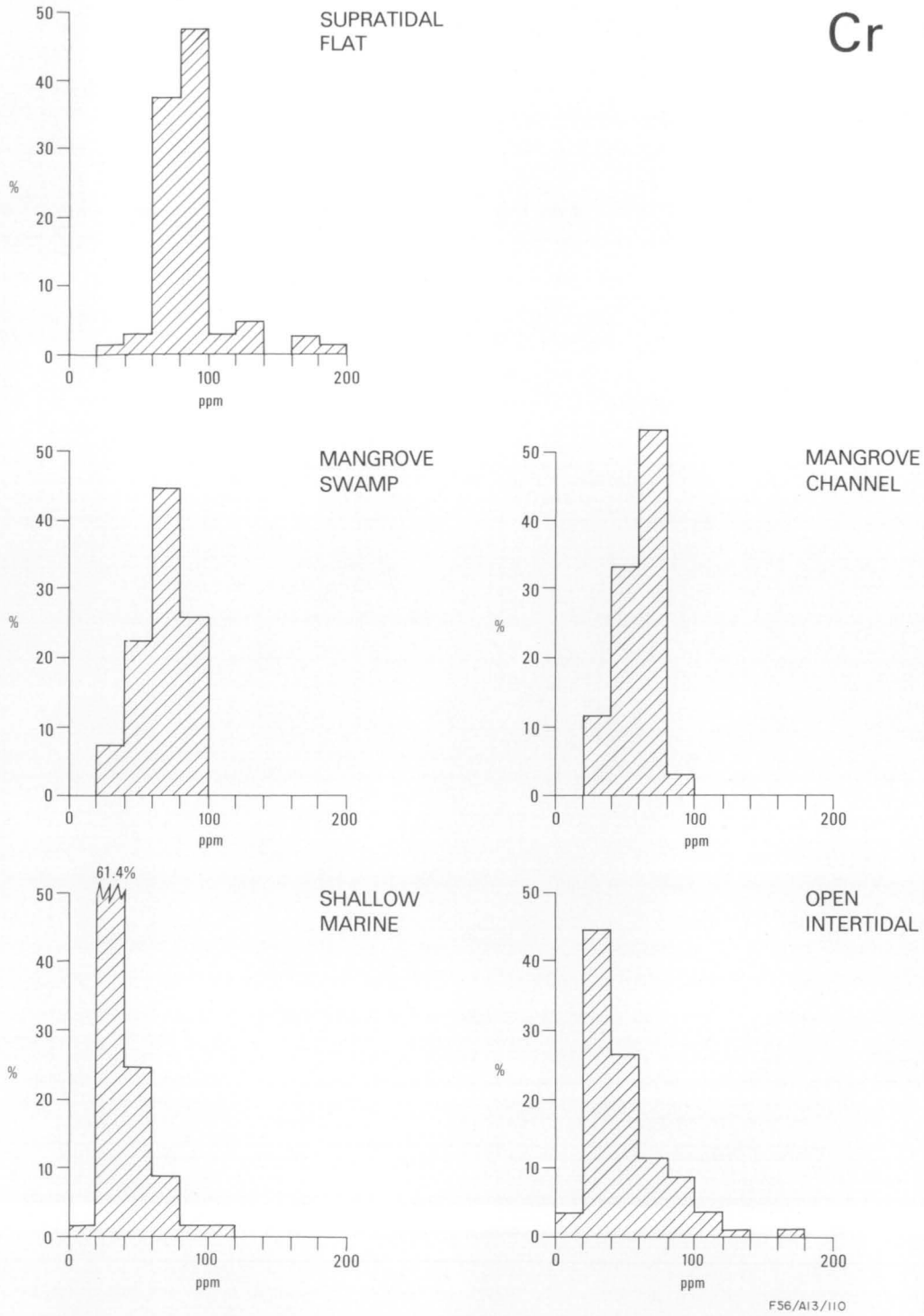


Fig. A54. Cr concentration: frequency distribution in estuarine depositional environments

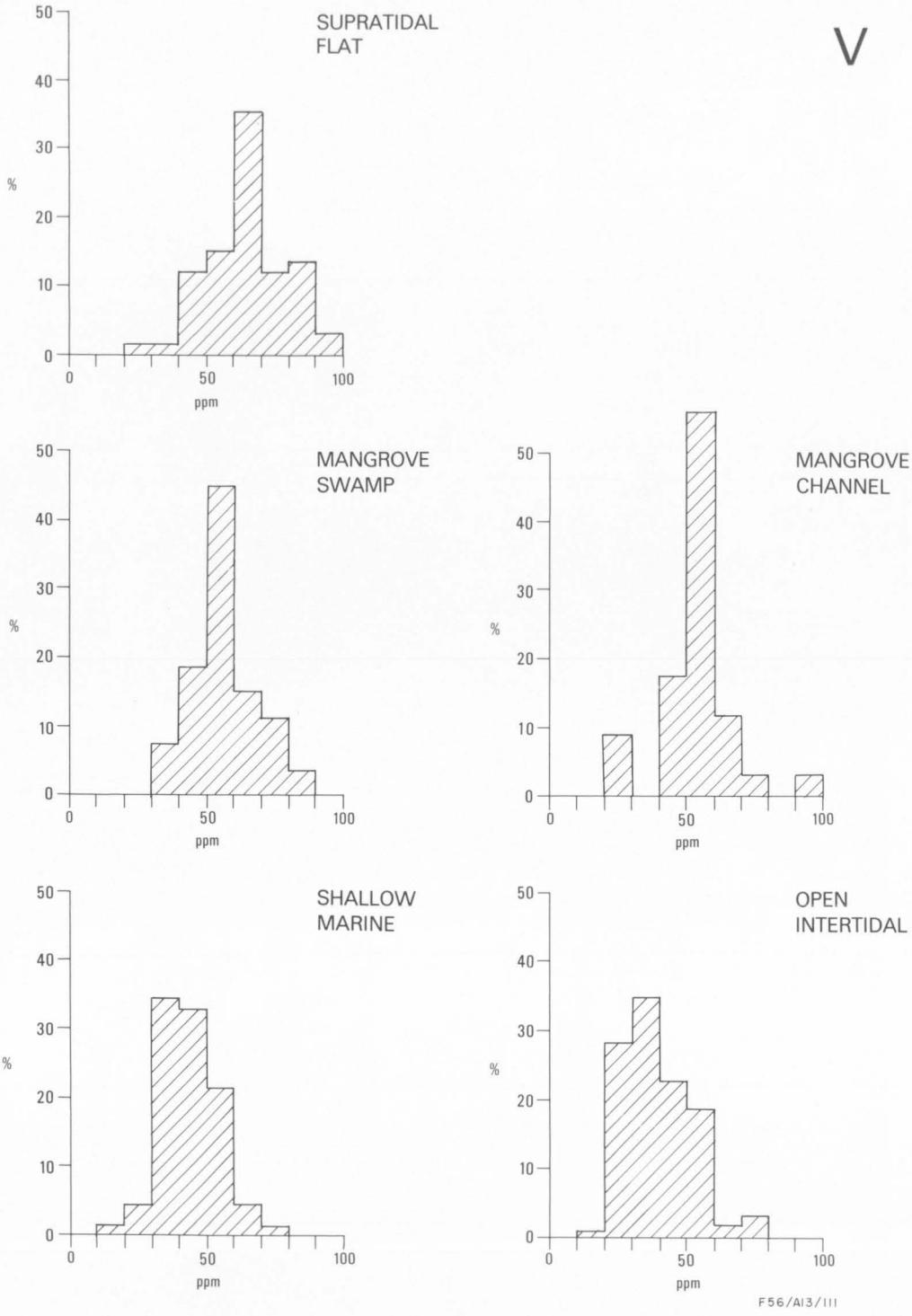


Fig. A55. V concentration: frequency distribution in estuarine depositional environments

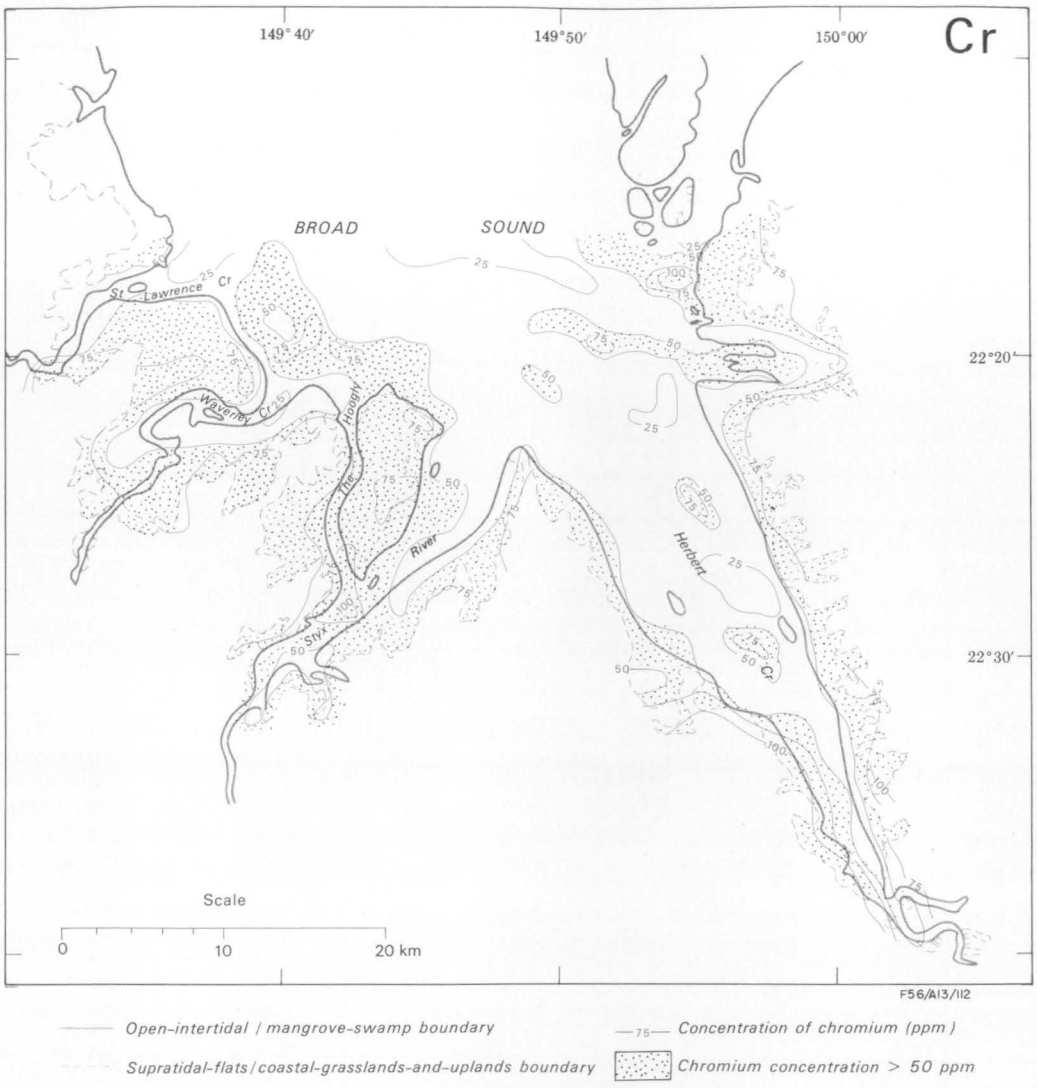


Fig. A56. Cr: distribution in estuarine sediments

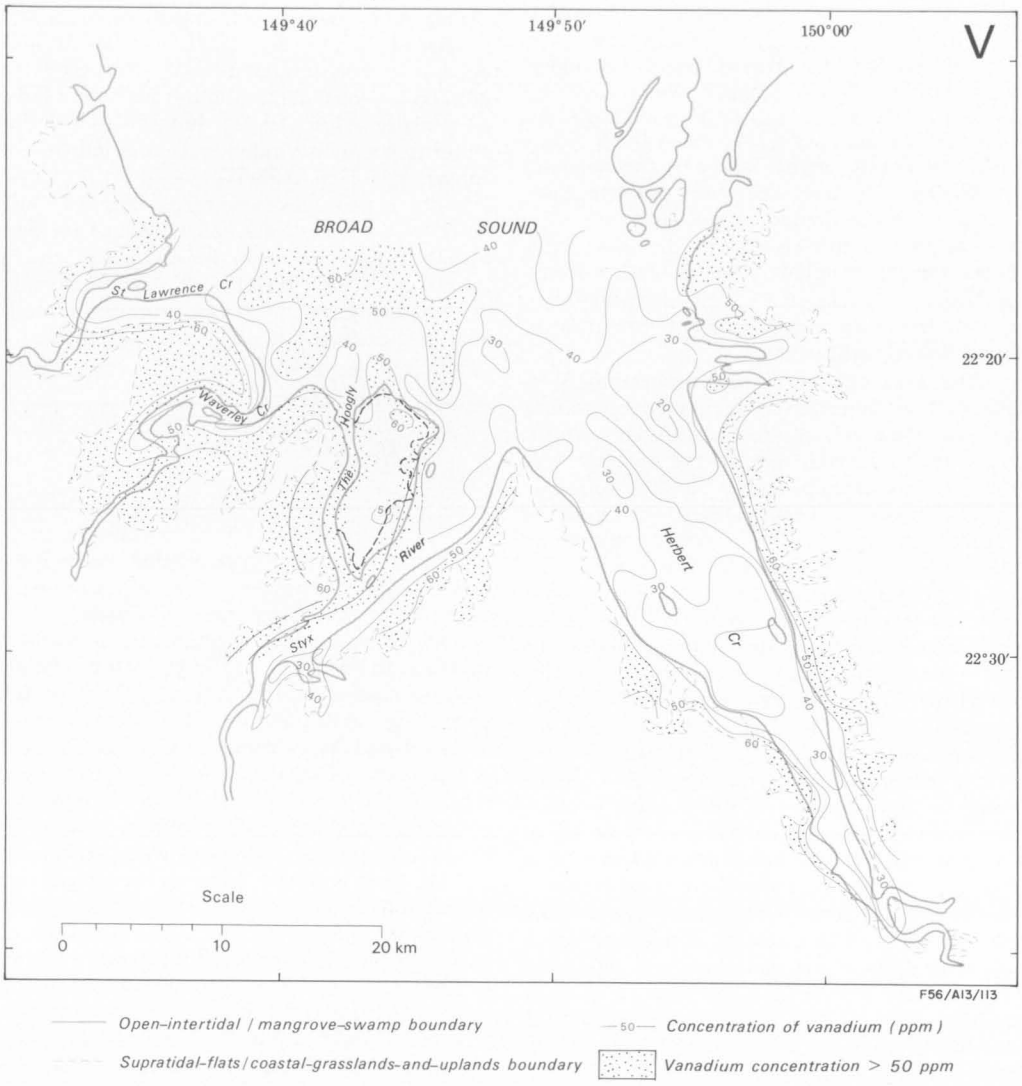


Fig. A57. V: distribution in estuarine sediments

(Fig. A57), though the decrease is less marked and there are some areas of high V content even in the subtidal zone.

The ionic radii of Cr and V are similar (Fig. A20), and there is a strong Cr-V correlation, indicating substitution. Also, both metals show significant positive correlation with percent mud, phi mean grainsize, Fe, Ni, Sc, Ti, and Zn. These metals all have ionic radii similar to those of V and Cr. In the strongly oxidising conditions generally prevailing in Broad Sound, the higher valence states (and smaller ions) will be dominant. Therefore substitution will for the most part be confined to Fe, Co, and Ni. Some substitution in the apatite lattice by the vanadate ion $(VO_4)^{3-}$ is possible, and perhaps also, though to a more limited extent, substitution by the chromate ion. However, the low P_2O_5 concentration, coupled with the lack of any significant V-P_2O_5 or Cr-P_2O_5 correlations, suggests that such reactions are unimportant in Broad Sound sediments.

The presence of some non-detrital V is suggested by the relatively high V concentration in some of the calcareous depositional environments at the seaward end of the estuary (Fig. A57). The V is unlikely to be substituting in $CaCO_3$; however, in the southern area many of the calcareous nodules have ferruginous coatings and it is possible that some V (as vanadate ions) is fixed by the iron oxide and hydroxide coatings on the late Pleistocene carbonate nodules. V and also Cr are commonly associated in sediments with organic carbon, in part as organo-metallic complexes. The highest V and Cr concentrations occur in those Broad Sound depositional environments that have the highest organic carbon contents (Table A22, Figs. A54, A55). However, although there are positive correlations between organic carbon and V or Cr at Broad Sound, they are not considered statistically significant and therefore there is no evidence from the Broad Sound study of any relationship between them. The reducing conditions which prevail in parts of the mangrove and supratidal environments may reduce the ions to a lower valence state, in which they are much less soluble, resulting in the fixation of V and Cr in these reducing sediments.

Results from Broad Sound and elsewhere (e.g. Le Riche, 1959) indicate a close association between V and Cr and clays. Hirst (1962b) discusses in some detail the question of whether or not these ions occupy a lattice position.

He suggests that the anions may be removed by adsorption onto clay minerals that are flocculating as a result of changing salinity. This also seems a likely explanation for Broad Sound, as the highest concentrations of V and Cr are found in the most saline depositional environments, where clays are likely to flocculate.

Iron, cobalt, nickel

The ionic radii of Fe, Co, and Ni are very similar (Table A24), resulting in similar chemical behaviour. Their abundances are different (Table A18), but the concentrations of all three at Broad Sound are of the order normally encountered in sediments. All three show well defined log-normal distribution for Broad Sound as a whole (Figs. A9-11), but less-well defined patterns when the individual environments are considered (Figs. A58-61).

The regional distribution pattern of Fe (Fig. A61) shows a very marked landward increase, with the highest values in the supratidal zone (an area of moderately high Fe at the northern end of the Sound presumably results from the presence of iron-stained residual Pleistocene sediments).

TABLE A24. IONIC RADII OF Fe, Co, AND Ni (AFTER GREEN, 1959)

	Ionic radius (nm)
Fe^{++}	0.074
Fe^{+++}	0.064
Co^{++}	0.072
Co^{+++}	0.063
Ni^{++}	0.069

Thus at this stage it appears that Fe in Broad Sound sediments has two chemical locations: (1) as ferruginous coatings on calcareous nodules, and (2) accompanying clay minerals, probably by substitution for Al or Mg in the lattice. Ni also shows a marked concentration in the supratidal zone (Fig. A19). A similar though less well defined trend also occurs with Co. The similarity in ionic radii of Fe, Co, and Ni with other ions (Fig. A20) results in a large number of significant positive correlations with elements such as Cr, Mn, Ti, V, and Zn, as well as with percent mud and phi mean grainsize. Many of these significant correlations result from the common association with clays, either through substitution in the lattice or through adsorption. However, some are probably due partly to an association with iron oxides and hydroxides. In the Broad Sound sediments only total Fe (as Fe_2O_3) was determined and therefore relative abundance of the two oxidation states is not known, though it is reasonable to assume that the trivalent state is generally dominant. However, pyrite is present in small amounts in some sediments of the mangrove-channel and mangrove-swamp environments. It is particularly common in the old mangrove swamp deposits which underlie the supratidal flats. The pyrite is believed to result from the reducing conditions and from the action

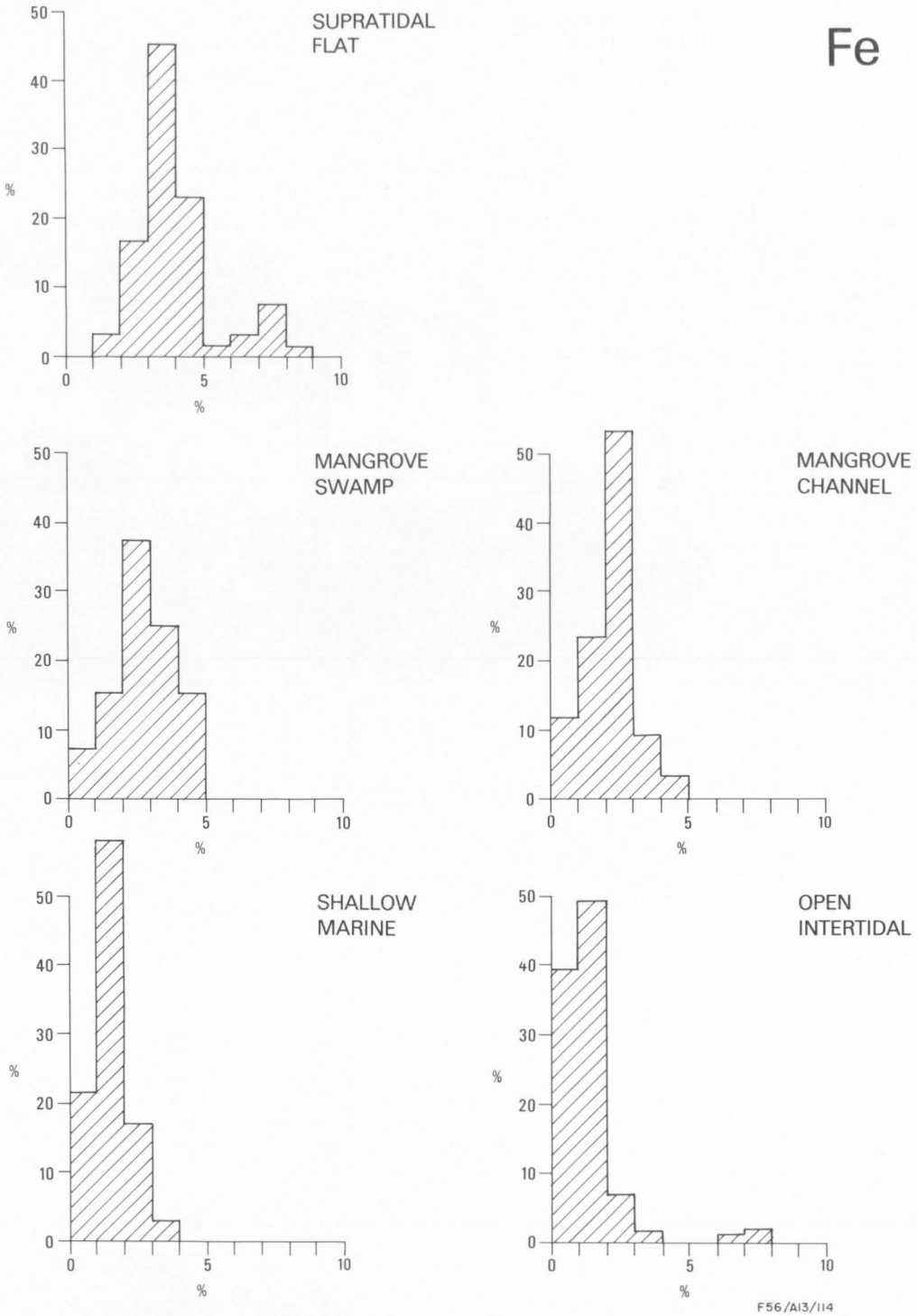


Fig. A58. Fe concentration: frequency distribution in estuarine depositional environments

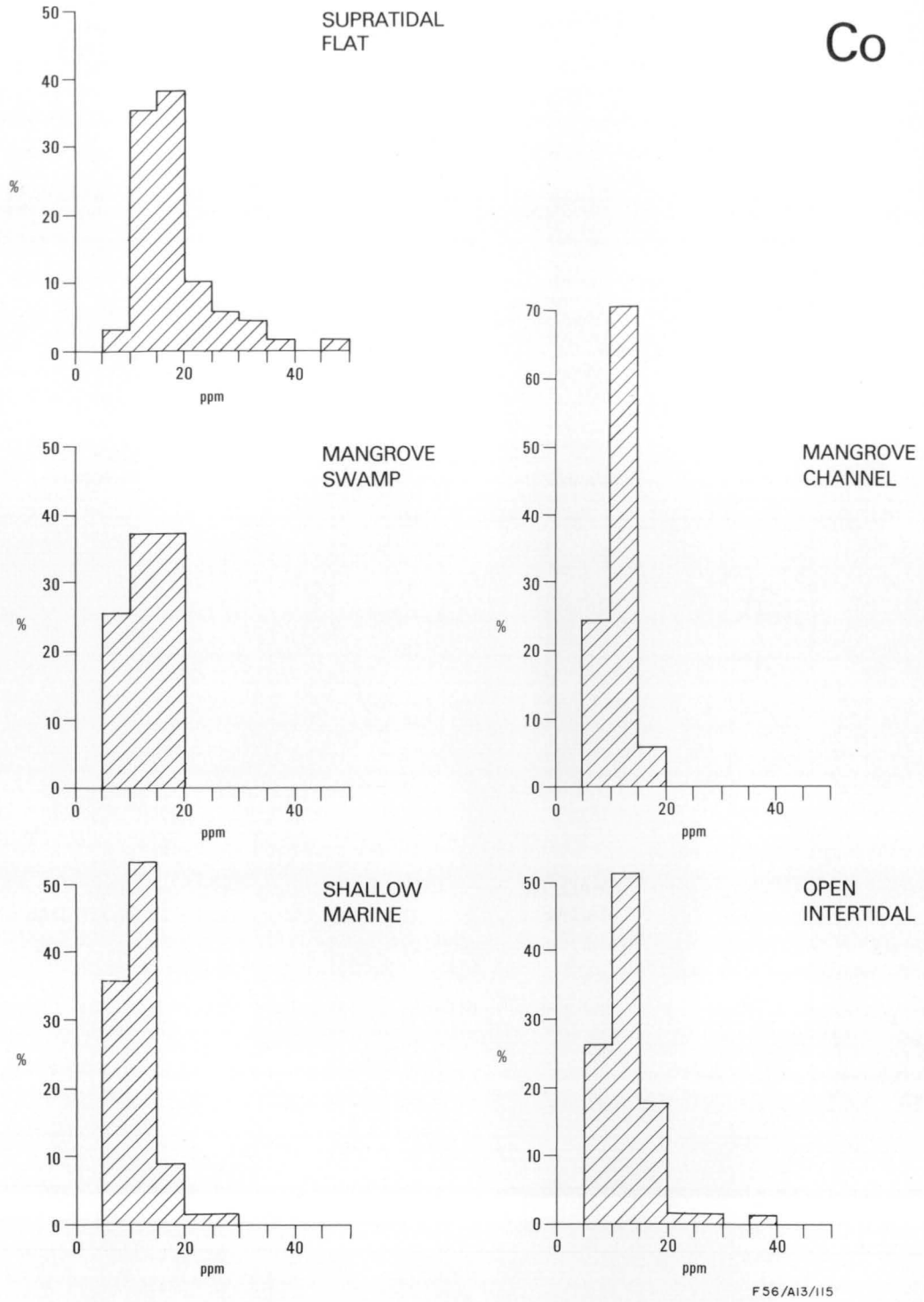


Fig. A59. Co concentration: frequency distribution in estuarine depositional environments

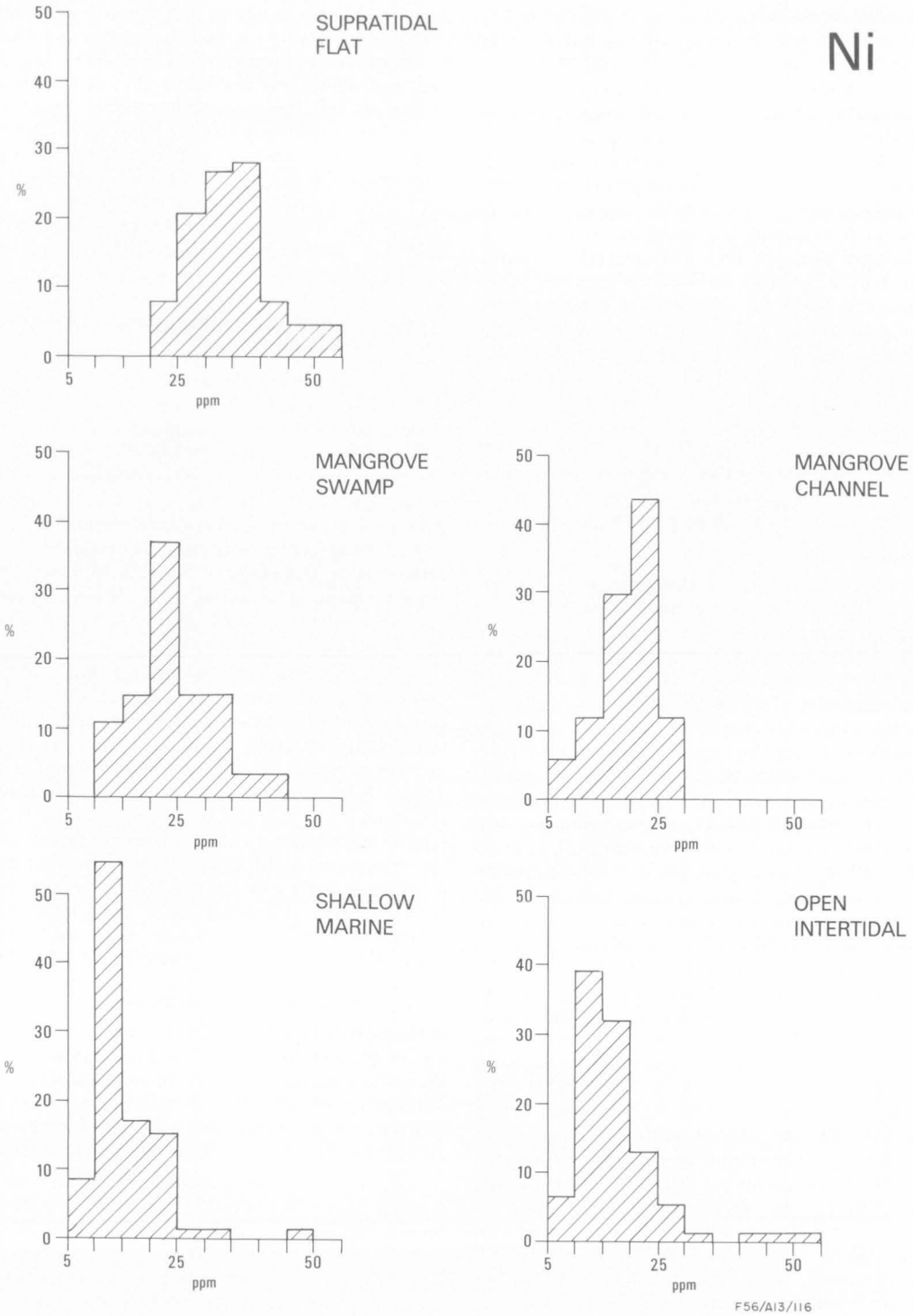


Fig. A60. Ni concentration: frequency distribution in estuarine depositional environments

of sulphate-reducing bacteria, as pointed out on p.113.There may be limited incorporation of Co and Ni into the pyrite under these conditions.

Nicholls & Loring (1962) report a strong correlation of Ni and Co with organic carbon. However, such a relationship was not found in Broad Sound sediments. Despite the similarity in behaviour of Co and Ni, it is apparent from Table A23 that there is preferential loss of Co in the change from subtidal to supratidal environments. The sediments of the open-intertidal environment have a Co/Ni ratio of 0.815, whereas the ratio is 0.546 in the sediments of the supratidal-flat environment. This may be the result of the greater stability of Ni during weathering (see earlier), leading to its preferential enrichment. It is conceivable that the Co/Ni ratio may be of value in establishing where shorelines lay in ancient sediments, though, as in the case of the Cu/Zn and other ratios, much more work is needed before the value of the ratio as a shoreline indicator can be proved or disproved.

Manganese

The Mn content of Broad Sound sediments is comparatively low compared with that of average carbonates and shales (Table A18). The distribution appears to be log-normal in the estuary as a whole and also in the individual environments (Fig. A63). However, the mode varies somewhat; maximum concentrations are found in the shallow-marine environment (Fig. A62), with minimum values in the mangrove-channel environment. The regional distribution pattern of Mn (Fig. A63) appears complex, with some highs in the mouths of estuaries (e.g. Styx) and other, more prominent, ones probably associated with shallow-marine gravels in the northern part of the Sound. There is clearly no association of Mn with supratidal clays, in contrast with for instance Fe (Figs. A58, A63). Three of the Mn ions have ionic radii similar to those of many other metals (i.e. within about 15%), particularly Fe, Co, and Ni. Therefore one would naturally expect correlations of Mn with Fe, Mg, Ni, Ti, V, and Zn (Fig. A28). The surprising feature, however, is that these correlations are almost entirely restricted to sediments of the mangrove-swamp environment. In this environment the Mn may be substituting for lattice ions, such as Mg, or it may be associated with Fe oxides, but, if such reactions are taking place in the mangrove-swamp environment, then why not also in the other environments characterised by fine-grained sediments? Clearly there are physico-chemical factors such as redox conditions which are affecting the behaviour of Mn. An indication of these processes is given by the Mn/Fe ratio, which shows a very marked change from subtidal to supratidal environments (Table A23). Under the acid conditions prevailing in, for instance, sediments of the mangrove-channel environment, Mn is relatively soluble (Garrels & Christ, 1965) and is leached from the sediments at the expense of the less soluble Fe, thus producing a lower Mn-Fe ratio. This ratio may likewise be of some value in ancient sediments for determining shoreline locations. Again, further work is required.

GEOCHEMISTRY AND DEPOSITIONAL ENVIRONMENTS

From previous discussion it is evident that different sediment types and sediments from various sedimentary environments can have very different chemical compositions. Previous workers, such as Degens (1958) and Ernst (1970), have attempted to use the trace-element geochemistry of sediments to determine ancient depositional environments. Therefore it is important to determine the extent to which the trace-element geochemistry of Broad Sound sediments can be used as an environmental indicator.

One method of attempting this is by determining, using *t*-tests, whether the mean composition of sediments in one environment is significantly different from the composition in another environment. This has been attempted in Table A25, from which it is immediately apparent that there are many statistically significant differences between environments. At the 95 percent confidence level it appears that the dominance of Ba could be used for distinguishing between shallow-marine and open-intertidal sediments, and the abundance of Cr could be used for distinguishing between mangrove-channel and mangrove-swamp sediments. In reality, however, such differences, though perhaps statistically significant, are geologically meaningless in most cases, for they largely reflect the gross changes in $CaCO_3$ or mud content (or phi mean grainsize). Therefore the concentration of trace elements in Broad Sound sediments gives no real indication of depositional environment.

If either the terrigenous or the carbonate fraction alone had been analysed, the environmental significance could perhaps have been more rigorously tested. This was not done for Broad Sound sediments. However, an alternative method is to recalculate compositions on a carbonate-free or clay-free basis. This would be satisfactory if ions were located entirely in one or the other of these components, but this is not so,

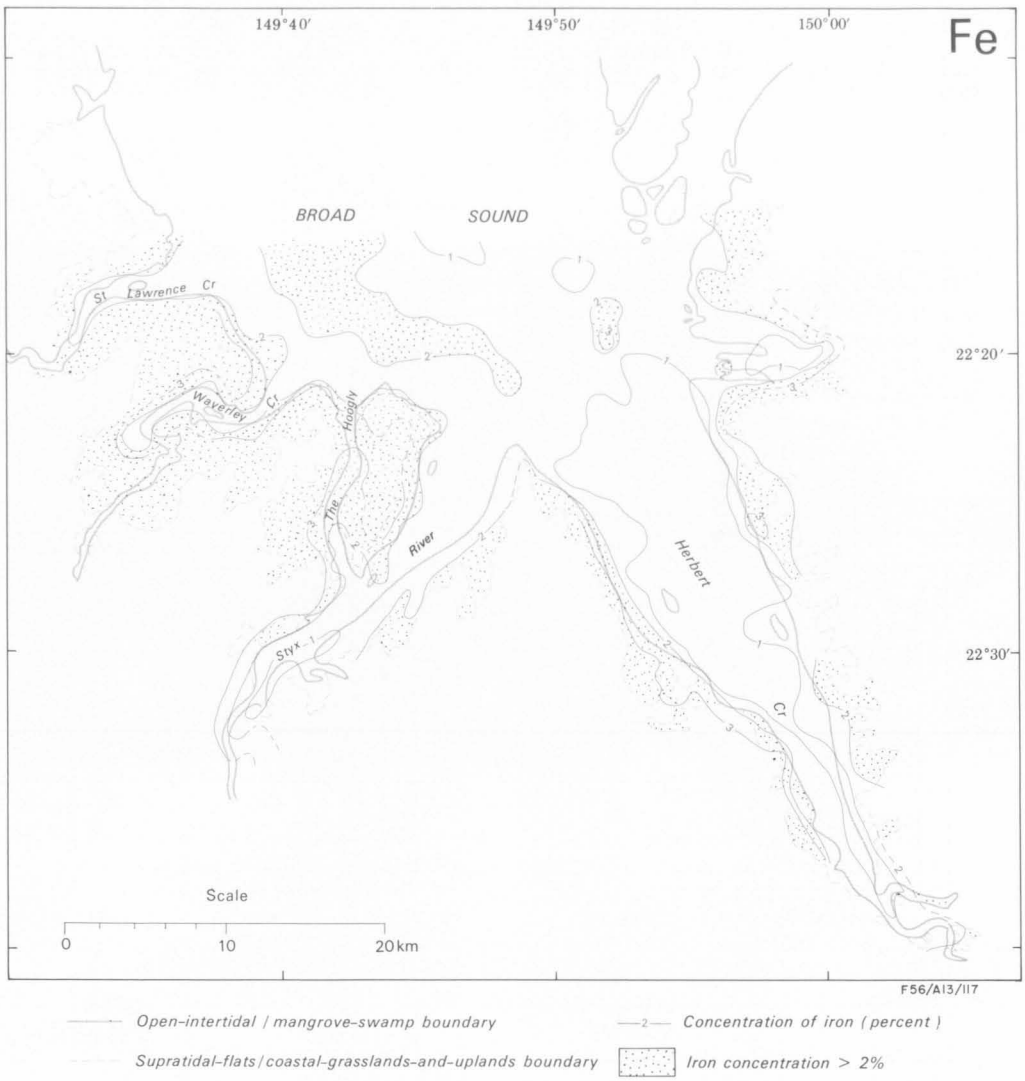


Fig. A61. Fe: distribution in estuarine sediments

and thus the procedure is somewhat questionable. Nevertheless, this procedure has been followed for a number of elements where the particular element is located primarily in either the carbonate or non-carbonate fraction (Table A26). The procedure used was to calculate concentrations on a carbonate-free basis for those elements likely to be located primarily in the detrital fraction, and on a 100-percent carbonate basis for those elements likely to be located primarily in the carbonate fraction (Tables A25, A27). Where some elements (e.g. P, Mg) were known to be located in both components their concentrations were not recalculated.

It is immediately apparent that there are far fewer statistically significant differences in Table A27 than in Table A25. It appears that Ba, Cr and Ti content could be useful in distinguishing between the terrigenous fractions in shallow-marine and open-intertidal environments. But surprisingly few differences exist between the shallow-marine and the mangrove and supratidal environments, perhaps as a result of subaerial influences on the relict sediments of the shallow-marine environment. Distinction between the open-intertidal sediments and the mangrove-channel, mangrove-swamp, and supratidal-flat sediments might be possible using Ba, Cr, Fe, Ni, Ti, and Zn, though the grainsize of the original

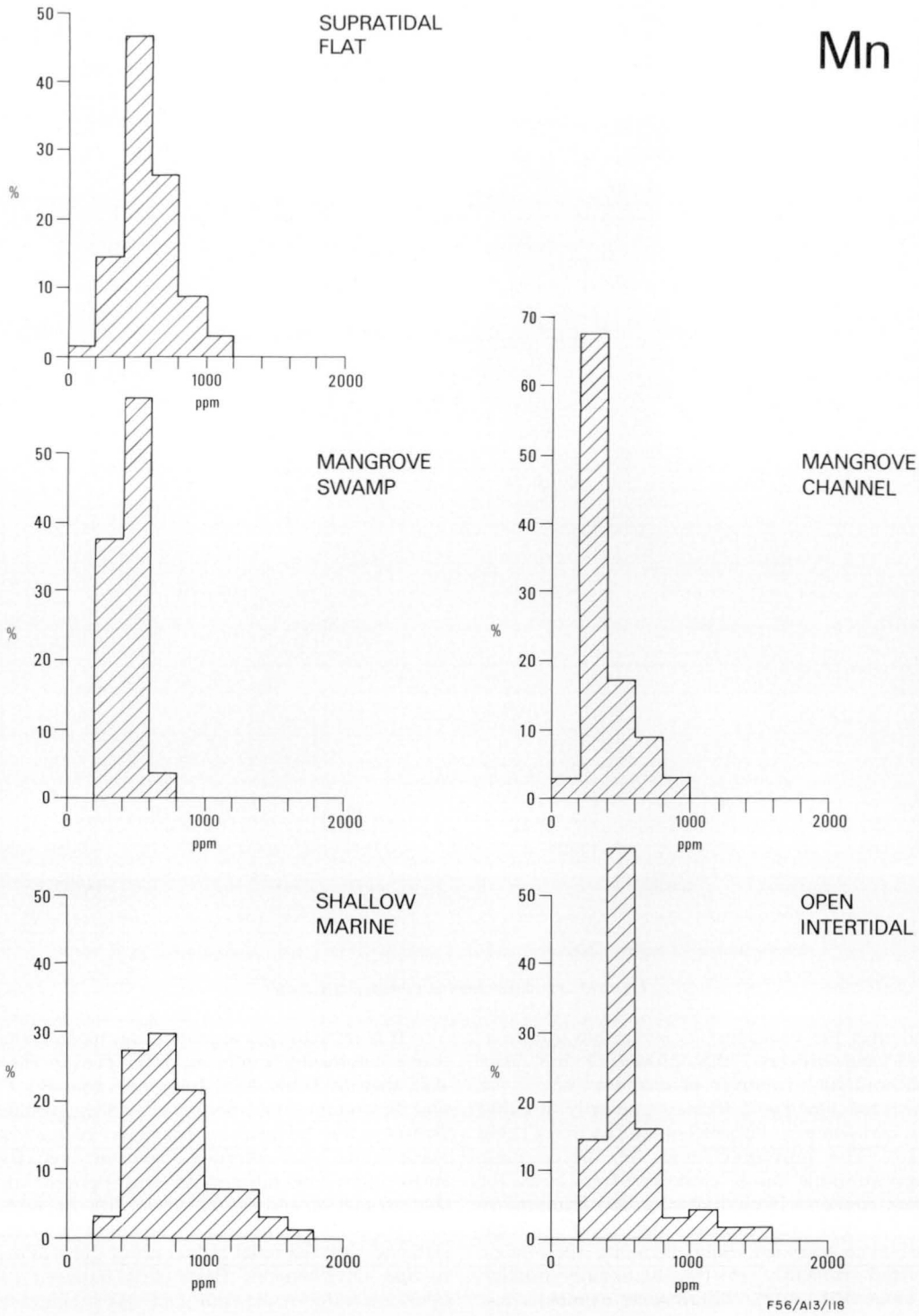


Fig. A62. Mn concentration: frequency distribution in estuarine depositional environments

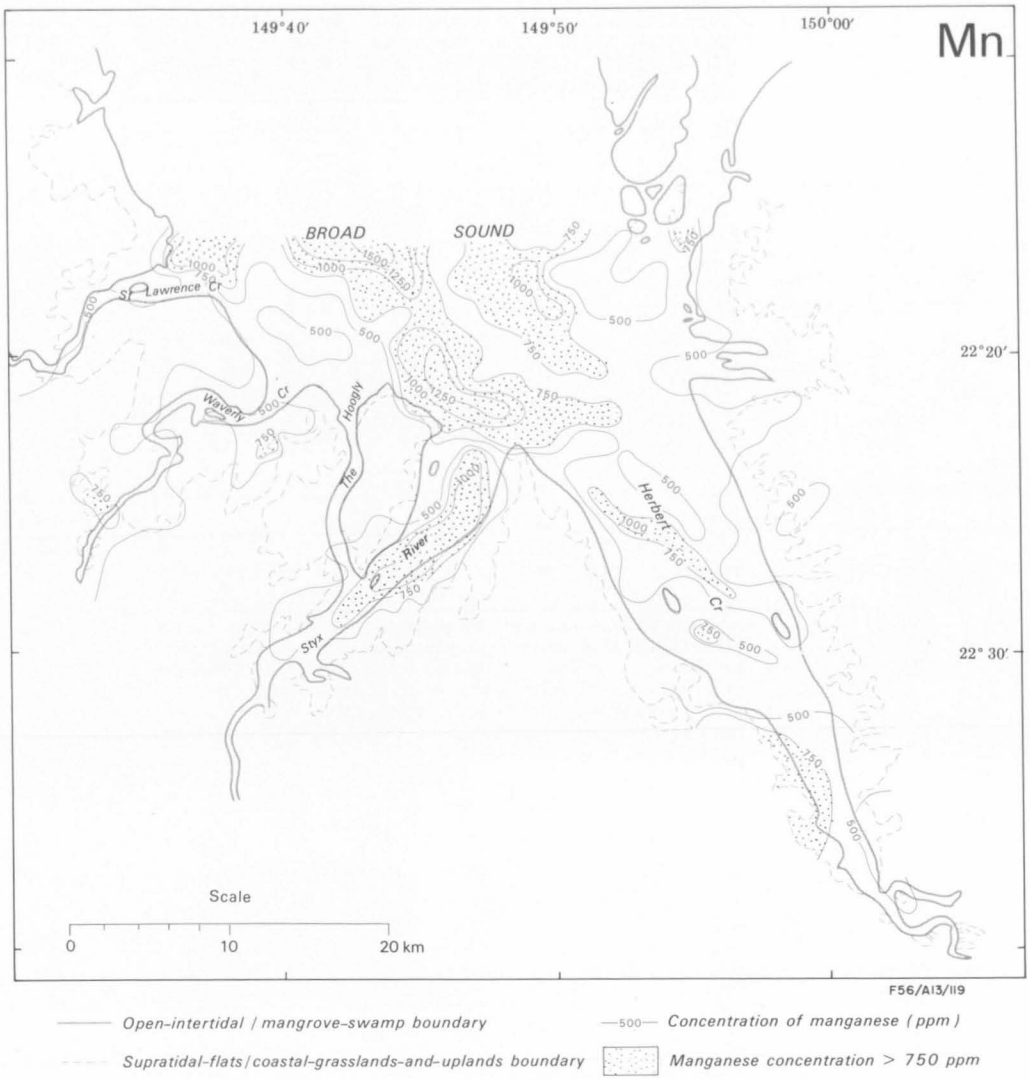


Fig. A63. Mn: distribution in estuarine sediments

sediment would undoubtedly be a far better criterion.

It is more difficult to use grainsize to distinguish between the muds of the mangrove-channel, mangrove-swamp, and supratidal-flat environments, though the abundance of organic matter (which was not statistically tested here) might be the most useful indicator. However, alternative criteria include Mn and Zn for distinguishing between mangrove-channel and supratidal-flat sediments, and Cr, Fe, Ni, and Zn for distinguishing between mangrove-swamp and supratidal-flat sediments.

In the carbonate fraction, Sr appears to be of only limited use as an environmental indicator; also, some Sr is undoubtedly associated with the clay fraction, making the calculation on a 100-percent-$CaCO_3$ basis dubious.

In conclusion, then, the Broad Sound data suggest that absolute concentrations of trace metals are of questionable use for distinguishing between depositional environments. Zn appears to be potentially a useful indicator, and Ba, Cr, Ni, and Ti perhaps also have some value. Possibly the most useful indication may be elemental ratios; Mn/Fe, Cu/Pb, and Cu/Zn ratios offer the greatest potential, because of the environmentally sensitive nature of the ions and the preferential concentration or leaching arising from environmental changes.

TABLE A25. COMPARISONS OF MEANS OF TRACE-ELEMENT COMPOSITIONS AND OTHER PARAMETERS OF BROAD SOUND DEPOSITIONAL ENVIRONMENTS: (1) shallow-marine, (2) open-intertidal, (3) mangrove-channel, (4) mangrove-swamp, (5) supratidal-flat

	1-2	1-3	1-4	1-5	2-3	2-4	2-5	3-4	3-5	4-5
Grainsize (phi)	X	<	<	X	<	<	X	<	X	<
% Sand	>	>	>	X	>	>	X	>	X	X
% Mud	=	<	<	X	<	<	X	<	X	X
Ba	<	<	<	<	X	X	<	=	X	<
Ca	>	>	X	X	>	X	X	X	X	>
Co	<	=	=	X	X	=	<	=	X	X
Cr	X	<		X	<	<	<	<	X	<
Cu	X	=	X	X	<	X	<	X	<	<
Fe	>	<	<	X	<	<	<	=	<	<
Mg	>	X	=	X	X	<	X	X	X	<
Mn	>	X	X	X	X	X	=	<	<	<
Ni	=	<	<	X	<	<	<	<	X	<
Pb	=	X	<	<	<	<	<	<	<	<
Sc	X	<	<	<	<	<	<	<	<	<
Sr	X	>	>	>	X	X	X	>	>	>
Ti	=	X	<	<	X	X	<	<	X	<
V	>	<	<	X	<	<	<	=	<	<
Y	<	X	=	X	X	X	X	=	<	<
Zn	>	<	<	<	<	<	<	=	<	<
Zr	=	X	X	X	X	X	X	=	X	X
$CaCO_3$	>	>	X	X	>	>	X	X	X	>
P_2O_3	X	X	X	=	<	<	X	<	X	X

'X' ..... F-test indicates different variances, thus preventing the application of a *t*-test.
'1>2' ..... *t*-test indicates that the mean for the shallow-marine environment is greater than the mean for the open-intertidal environment, at a confidence level of 95-percent.
'1<2' ..... *t*-test indicates that the mean for the shallow-marine environment is less than the mean for the open-intertidal environment, at a confidence level of 95-percent.
'1=2' ..... *t*-test indicates that the means are the same, at the 95-percent confidence level.

TABLE A26. MEAN TRACE-ELEMENT, IRON, AND PHOSPHATE CONTENT OF SEDIMENTS IN BROAD SOUND DEPOSITIONAL ENVIRONMENTS, CALCULATED ON A CARBONATE-FREE BASIS (ppm)

	Shallow marine	Open intertidal	Mangrove channel	Mangrove swamp	Supratidal flat
Ba	257.5	288.9	284.5	244.0	251.1
Co	31.0	18.9	14.9	14.8	18.1
Cr	110.8	74.1	76.4	78.6	90.3
Cu	45.7	20.5	24.2	17.9	21.5
Fe(%)	4.56	1.96	2.96	3.22	4.10
Mg	4129	1433	1059	1310	1737
Mn	2372	960	496	545	575
Ni	41.5	24.6	26.6	28.2	33.9
Pb	28.3	15.5	15.5	15.9	16.8
Sc	35.6	19.0	17.6	17.3	17.4
Ti	5911	3754	4972	4888	4932
V	127.4	59.0	71.0	66.9	72.0
Y	75.6	46.6	35.3	31.5	30.1
Zn	54.0	26.0	47.4	49.8	59.4
Zr	760.9	486.0	310.9	285.5	295.2
P_2O_5	2942	820	1079	1071	886

TABLE A27. COMPARISONS OF TRACE-ELEMENT MEANS IN BROAD SOUND DEPOSITIONAL ENVIRONMENTS, CALCULATED ON A CARBONATE-FREE BASIS (except for Sr, which was calculated on a 100-percent $CaCO_3$ basis): (1) shallow-marine, (2) open-intertidal, (3) mangrove-channel, (4) mangrove-swamp, (5) supratidal-flat

	1-2	1-3	1-4	1-5	2-3	2-4	2-5	3-4	3-5	4-5
Ba	<	=	X	X	=	X	>	X	X	X
Co	X	X	X	X	X	X	=	=	X	X
Cr	>	X	X	X	X	X	<	=	X	<
Cu	X	X	X	X	=	X	X	X	X	X
Fe	X	X	X	X	X	<	<	=	X	<
Mn	X	X	X	X	X	X	X	X	<	X
Ni	X	X	X	X	X	=	<	=	X	<
Pb	X	X	X	X	X	X	X	=	=	=
Sc	X	X	X	X	X	X	X	=	=	=
Sr	X	X	<	X	<	X	X	=	X	X
Ti	>	X	X	X	<	X	<	X	=	X
V	X	X	X	X	X	X	X	=	=	=
Y	X	X	X	X	X	X	X	=	X	=
Zn	X	X	=	X	<	<	<	=	<	<
Zr	X	X	X	X	X	X	X	X	=	=

'X' ..... F-test indicates different variances, thus preventing the application of a *t*-test.
'1>2' ..... *t*-test indicates the mean for the shallow-marine environment is greater than the mean for the open-intertidal environment, at the 95-percent confidence level.
'1<2' ..... *t*-test indicates the mean for the shallow-marine environment is less than the mean for the open-intertidal environment, at the 95-percent confidence level.
'1=2' ..... *t*-test indicates that the means are the same, at the 95-percent confidence level.

GEOCHEMISTRY OF HOLOCENE OYSTER SHELLS

Well developed chenier sequences flank the mouths of several of the estuaries in Broad Sound. Fossil oyster shells were collected from some of the cheniers during the study. Radiocarbon dating of the shells showed that the cheniers are aged from about 1000 to 5500 years B.P. and are progressively older landward (Cook & Polach, 1973a). Having discovered this order of succession of cheniers, we considered that chemical analyses of the fossil shells, once tied into the time framework, might be capable of revealing the effects and trends of chemical weathering over the last several thousand years.

Shell samples were collected from twelve separate cheniers (Fig. A64) in the Charon Point, Hoogly-Waverley, and Torilla Plains areas. Each sample was obtained by digging a hole 30 cm deep (to get below the poorly developed A soil horizon) and a grab sample was taken from the bottom of the hole. The oyster shells *(Saccostrea* sp.*)* were then hand-picked from the shell hash. In addition, shells were collected from live oysters in the intertidal zone at Charon Point. The live and fossil oysters differed in appearance in that the old shells were surfaced-stained, probably by iron. This surface staining was removed by cleaning in an ultrasonic bath for 30 minutes. Bulk samples were then prepared for analysis from 20-30 whole and broken shells, each 1-2 cm in diameter. Although the possibility of reworking shells from older cheniers undoubtedly exists, the internal consistency of the individual chenier ages suggests that such reworking is minor. Obviously dating and analysis would ideally have been undertaken on individual shells but this was not possible because insufficient material is available in a single shell. The alternative of a bulk sample to provide a good average value was therefore taken.

ANALYSES

Analyses, by AMDEL, were carried out for Ca (titration-EDTA), Mg, Pb, Zn, Co, Ni, Cu, Cd, Mn, Ag, Mo, V, Fe, Cr (atomic absorption spectroscopy), P_2O_5, B (colorimetry), and U (fluorimetry). The mineralogy of the shells was determined by the author by X-ray diffraction, using calcined fluorite as an internal standard, and by measuring the position of the 211 peak. H. A. Polach of the Radiocarbon Laboratory of the Australian National University and R. Gillespie of the Radiocarbon Laboratory of Sydney University determined the radiocarbon ages.

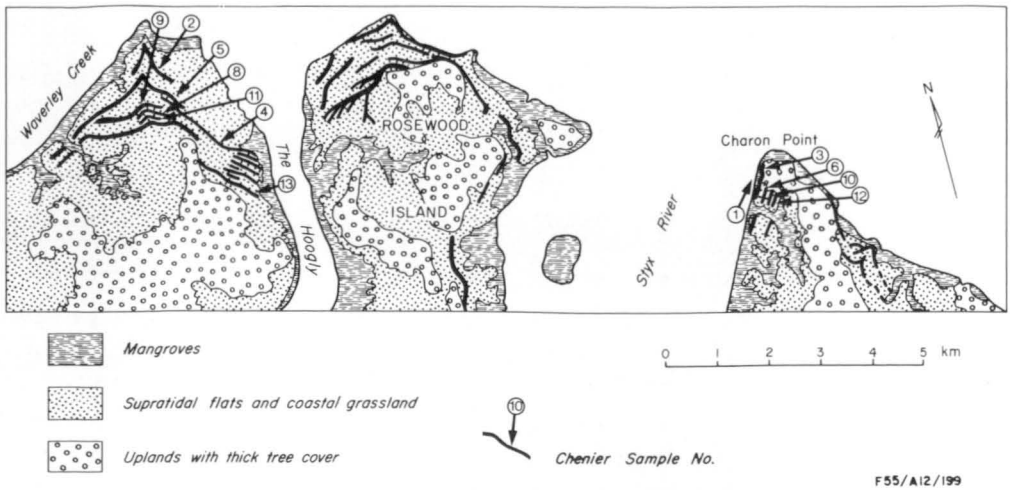


Fig. A64. Positions of chenier samples in the southwest part of Broad Sound. Sample numbers refer to table A28

RESULTS

The results of the chemical analyses are given in Table A28, except for those elements sought but not detected; these were Co (<3.5 ppm), Ni (<3.5 ppm), Cd (<1 ppm), Ag (<0.5 ppm), Mo (<2 ppm), V (<3 ppm), Ba (<50 ppm), Nb (<20 ppm), and La (<100 ppm). The precision of analyses is indicated in Table A28. All shells were found to be composed of low-magnesium calcite. In general, the chemical composition of the shells appears similar to that found in other studies (Table A29), though the range of available analyses from other localities is more limited. Sr and Mg concentrations in both modern and fossil oyster shells at Broad Sound are very similar to other published results. In Fe and Mn the modern shells from Broad Sound are similar to the Georgia shells of Pilkey & Goodell (1963), but both groups of modern shells have a significantly lower Fe and Mn content than the fossil Broad Sound shells. Such differences are to be expected as these old shells have been exposed to a long period of tropical weathering.

One might reasonably expect from this that elements which are concentrated in shell material during weathering will show a positive correlation with age; however, changes in temperature (Pilkey & Goodell, 1963), variation in location within the intertidal zone (Pilkey & Harriss, 1966), and changes in salinity (Rucker & Valentine, 1961) also give rise to changes in the shell composition of mulluscs. Changes in the depositional environment, then, could complicate any simple relationship between age and composition.

In order to test for significant correlations between elements, and also between elements and radiocarbon age, PROGRAM VARPLOT (Mayo & Long, 1976) was applied to the data. This provided an x-y plot for all data combinations, together with various statistical parameters. A matrix of correlation coefficients for all variables is given in Table A30; correlations with a confidence level of 95 percent or greater are considered to be significant. From Table A30 it is possible to establish two groups of relationships: (1) the variation of radiocarbon age with major-element, trace-element, and isotope geochemistry; and (2) the inter-element associations.

Significant inter-element correlations evident in the correlation matrix (Table A30) are few. Those present are of two types: iron-associated elements, and calcium-associated elements.

VARIATION OF COMPOSITION WITH AGE

Table A30A contains several correlations between age and trace-element content. However, despite the relatively high confidence level of the correlations, the variation of elemental content with radiocarbon age, if examined graphically (Fig. A66), is rather less than convincing. The statistically significant correlation between Pb and radiocarbon age is geologically meaningless, as it results from a

TABLE A28. AGE AND COMPOSITION (ppm) OF OYSTER SHELLS, BROAD SOUND. 'I.S.' indicates insufficient sample available. Precision of analyses: Pb ± 2 ppm, Zn ± 1 ppm, Cu ± 0.5 ppm, Mn ± 10 ppm, Sr ± 30 ppm, Fe ± 20 ppm, U ± 0.2 ppm, P_2O_5 ± 20 ppm, B ± 2 ppm, Mg ± 0.01%, Ca ± 0.1%.

Location (Fig. A64)	Sample No. (71636-)	Age (years B.P.)	Pb	Zn	Cu	Mn	Sr	Fe	U	P_2O_5	B	Mg (%)	Ca (%)
1	205	002	3.0	5	2.0	20	910	100	1.6	720	17	0.21	38.5
2	100	1170	3.0	4	2.5	320	840	550	9.3	380	15	0.23	39.0
3	141	1640	3.0	7	1.5	340	790	500	2.5	330	16	0.26	39.1
4	103	2100	3.0	5	1.5	250	800	540	4.5	340	16	0.18	39.5
5	138	2140	5.0	10	1.0	170	780	320	5.7	340	15	0.20	39.0
6	202	2480	3.5	3	1.5	170	760	250	3.8	310	15	0.25	38.9
7	039	2910	3.0	4	1.5	110	760	450	0.4	240	17	0.13	38.7
8	139	2930	3.0	5	5.5	190	760	650	4.9	370	14	0.25	38.8
9	106	2960	3.5	2	1.5	220	800	430	7.9	260	13	0.20	39.2
10	203	3465	3.5	1	1.5	280	1500	420	0.7	270	12	0.32	38.5
11	107	4060	3.0	2	1.5	370	790	800	2.8	310	14	0.22	38.9
12	204	4520	3.0	7	8.0	430	750	650	1.0	300	12	0.24	39.0
13	108	5450	10.0	20	10.0	300	490	I.S.	I.S.	270	I.S.	0.28	40.2

TABLE A29. COMPOSITION (ppm) OF SHELLS OF LIVE AND FOSSIL OYSTERS FROM BROAD SOUND *(Saccostrea* sp.*)* AND OF LIVE OYSTERS *(Crassostrea virginica)* FROM USA. The Georgia results are from Pilkey & Harriss (1966); those from eastern USA in general are from Rucker & Valentine (1961)

	Broad Sound				Georgia (live)			Eastern USA (live)		
	live	fossil								
	(one sample)	minimum	maximum	average	minimum	maximum	average	minimum	maximum	average
Sr	910	490	1500	818	871	1081	977	1142	1648	1436
Mg	2100	1300	3200	2300	1320	2540	1739	1964	2388	2169
Fe	100	250	800	505	159	432	270	—	—	—
Mn	20	110	430	263	18	50	31	21	228	70

single high Pb value (the correlation is geologically no more meaningful than any straight line drawn between two points). Similarly with Cu. The correlations shown of Mn and Fe with radiocarbon age are also of questionable validity if plotted graphically. From these it is clear that there is a wide spread of data points. Nevertheless, there does appear to be a trend, albeit poorly defined, of increasing Fe and Mn with increasing age. Such a trend may reasonably be taken to result from tropical weathering during the Holocene. The phosphorus content of the shells is seen to decrease with increasing age (Fig. A66). The decrease clearly cannot be represented by a simple regression line. It corresponds rather more closely to an asymptotic curve, with much of the decrease in P_2O_5 content occurring in the first 1000 years. This pattern is a reflection of the comparatively soluble nature of phosphorus, and the ease with which it can be leached from calcareous shell material in the course of tropical weathering. A well defined negative correlation previously discussed by the writer (Cook, 1976) exists between B and radiocarbon age (Table A28). Over a period of about 5000 years the mean boron content decreases uniformly from 17 ppm to 12 ppm. The concentration of boron in sediments is frequently taken as an indicator of palaeosalinity; consequently the decrease in B with increasing radiocarbon age could be taken to indicate a progressive increase in salinity. However, as shown by the present study (Cook & Mayo, 1978) there is little prolonged 'freshening' of the estuary even during the summer months. Consequently, to get the degree of freshening indicated, a very major increase in rainfall would have been necessary. Kershaw (1975), on the other hand, has shown that whilst the climate of north Queensland between 6000 and 3000 years B.P. was somewhat warmer and probably also wetter than at present, the greater rainfall inferred from Kershaw's work is likely to have been insufficient to give rise to a major lowering of the salinity of Broad Sound. The writer (Cook, 1976) concludes that the decrease in boron is likely to have resulted from the weathering of the shells, and associated leaching of boron from the shells.

In conclusion, there is no evidence of enrichment or depletion of most trace elements in oyster shells over a period of about 5000 years. The poorly developed trend of increasing Mn and Fe with increasing age may reasonably be expected in view of the visible increase in iron-staining in older shells. The decrease in P might similarly be expected because of the relative solubility of P, though the leaching of more than 50 percent of the P in the shells over a period of less than 1000 years represents a more rapid rate of leaching than might normally be expected. The decrease of B with increasing age is an important observation in view of the fact that the abundance of boron in sediments is frequently taken as an indicator of palaeosalinity. The Broad Sound investigations suggest that erroneous conclusions on palaeosalinity may be drawn from the boron contents of calcareous sequences that have been subaerially weathered.

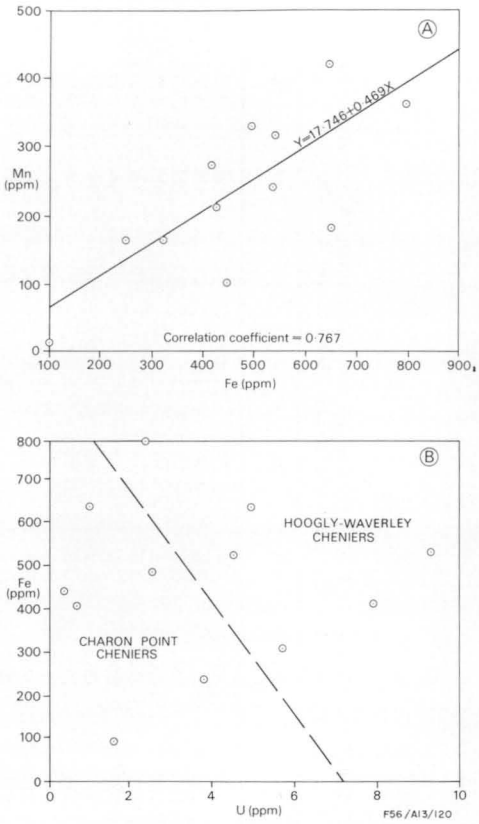


Fig. A65. Relationships of Fe with Mn and U in Holocene oyster shells

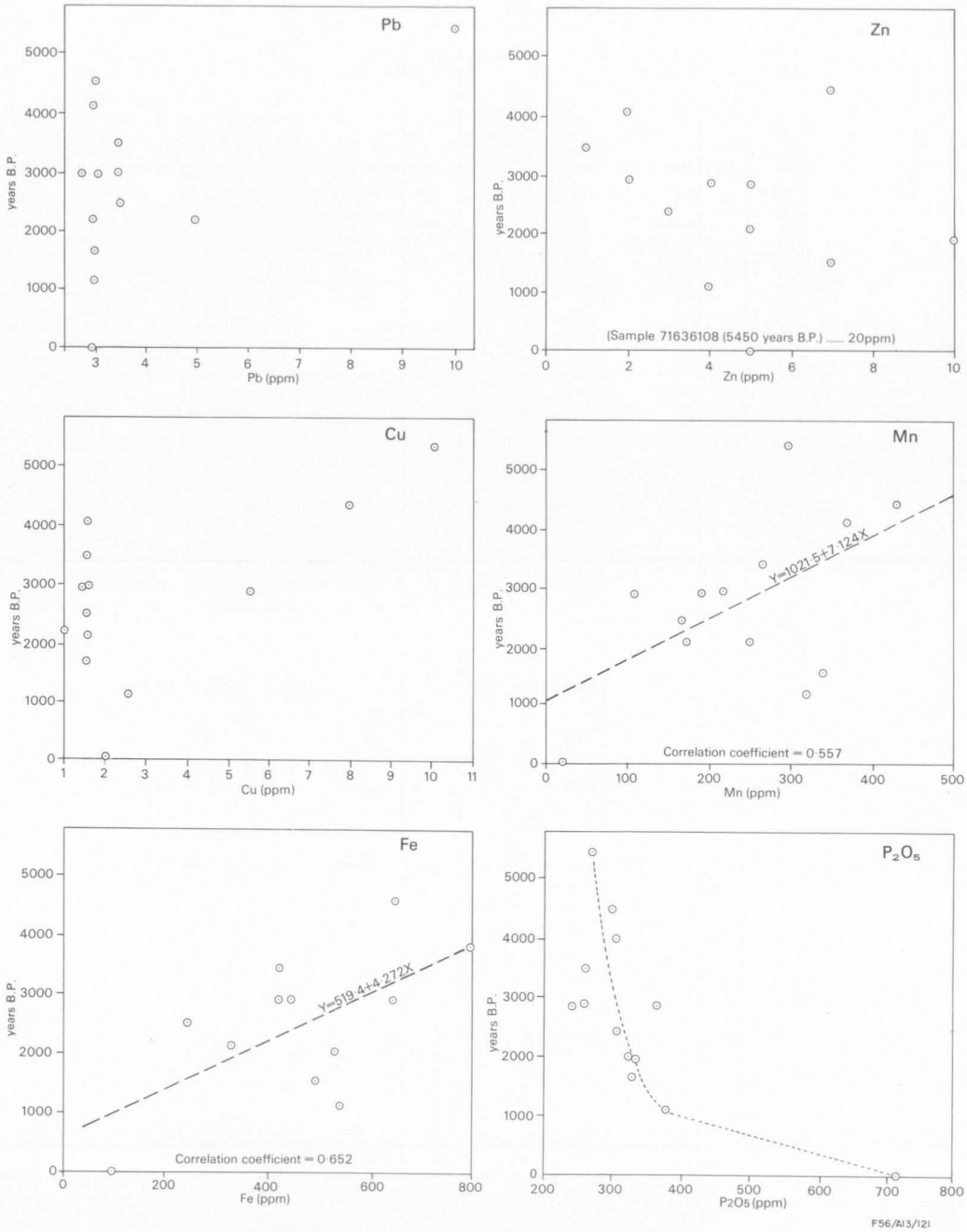


Fig. A66. Relationships between radiocarbon age of Holocene oyster shells and their content of Pb, Zn, Cu, Mn, Fe, and P_2O_5

TABLE A30. MATRIX OF CORRELATION COEFFICIENTS FOR TRACE-ELEMENTS, PHOSPHATE, AND CALCIUM, IN BROAD SOUND OYSTER SHELLS. Significance at confidence levels of 90, 95, and 99 percent is indicated by one, two, and three asterisks respectively

A. Live and fossil shells

	Age	Pb	Zn	Cu	Mn	Sr	Fe	U	P_2O_5	Mg	Ca	B
Age	1.000											
Pb	.534*	1.000										
Zn	−.241	.428	1.000									
Cu	.644**	.626**	.243	1.000								
Mn	.577**	.082	−.023	.375	1.000							
Sr	−.197	−.412	−.545	−.452	−.044	1.000						
Fe	−.652**	−.378	.418	.418	.767***	−.185	1.000					
U	−.282	−.244	.026	−.150	.051	−.299	.068	1.000				
P_2O_5	−.699***	−.211	.192	−.127	−.517	.068	−.514*	−.050	1.000			
Mg	.310	.312	−.213	.365	.427	.377	.059	−.101	−.078	1.000		
Ca	.474	.766***	.256	.559**	.365	−.636**	.338	.514*	−.349	.088	1.000	
B	−.731***	−.121	.277	−.468	−.600**	−.394	−.414	−.048	.453	−.599**	.019	1.000

B. Fossil shells only

	Age	Pb	Zn	Cu	Mn	Sr	Fe	U	P_2O_5	Mg	Ca	B
Age	1.000											
Pb	.569*	1.000										
Zn	−.476	−.328	1.000									
Cu	.715***	.621**	−.177	1.000								
Mn	.326	.009	−.049	.390	1.000							
Sr	−.162	−.404	−.162	−.445	.030	1.000						
Fe	.426	−.610**	−.106	.478	.634	−.169	1.000					
U	−.583*	.215	.040	−.172	−.116	−.288	−.104	1.000				
P_2O_5	−.564*	−.271	.491	−.175	.153	−.113	.241	.531*	1.000			
Mg	.300	.302	−.323	.357	.448	.369	.001	−.128	.092	1.000		
Ca	.354	.778***	−.214	.561*	.194	−.641*	.068	.469	−.057	.051	1.000	
B	−.658**	−.060	.282	−.486	−.476	−.478	.213	.062	−.168	.620**	.276	1.000

HYDROGEOCHEMISTRY

METHODS

Water samples were taken in the estuary during 1970, at each of the sediment sampling stations in turn. At each station a vertical water profile was obtained by pumping water at 5-m intervals between the surface and the bottom. Water temperatures were measured at the same time. Turbidity, salinity, and nitrate and phosphate contents were then measured on-shore. Salinity was measured with a conductivity meter standardised with a saturated KCl solution of known conductivity. During the 1971 program, some in-situ temperature and salinity measurements were taken, using a Beckman salinometer. Also in 1971 a Metrohm Eh-pH meter was used, and proved to be more reliable than the Jones instrument used during 1970. Nitrate and phosphate levels were determined colorimetrically on the filtered samples in the base camp laboratory, though some water samples were subsequently sent to AMDEL for additional phosphate analyses. Turbidity was measured with a turbidimeter, and is expressed as percentage transmittance.

Because of the large tidal range at Broad Sound, a true picture of the lateral variation of any of the variables can only be obtained by taking readings simultaneously throughout the Sound; therefore the picture of lateral variations obtained for the Sound at large during this study can only be a broad approximation.

In the 1971 season, a *Baroid* filter press was employed to obtain pore-water samples from the estuarine sediments. Nitrogen at a pressure of 9 kg/cm^2 was used to express the fluid. The pH and Eh values were determined immediately after expressing the fluid; in addition, 'in-situ' determinations of Eh and pH were made by placing the electrodes directly into the sediment. Salinity was subsequently determined with a *Radiometer* conductivity meter. Phosphate was determined colorimetrically by AMDEL using the molybdenum blue method. Analysis for Mg, Ca, and K, also by AMDEL, was by atomic absorption spectroscopy. Cu, Zn, Fe, Ni, Cd, and Mn were also determined by AMDEL by atomic absorption, following the solvent extraction procedure of Nix & Goodwin (1970). However, some of the results showed that there had been metal contamination from the Baroid filter. Therefore the trace-metal results for the pore waters have been discarded.

BROAD SOUND WATERS

Runoff data are not available for any of the Broad Sound catchment areas. Climatic information and runoff data for rivers in nearby catchment areas such as the Isaac River (Fig. A67) indicate major runoff during the summer months and negligible runoff throughout the remainder of the year. Because of the much smaller, more mountainous catchment areas of the main estuaries entering Broad Sound, the runoff maximum is probably more pronounced and shorter-lived than indicated in Figure A67. Not surprisingly, then, there was no significant runoff from any of the major rivers entering the Sound during either of the winter field seasons. Consequently there was no measurable dilution of the Sound water, except locally in mangrove channels for a short period after heavy rain. During the winter months it is likely that hypersaline runoff from the supratidal flats, particularly after spring tides, is more important than freshwater runoff. Therefore locally, particularly in mangrove channels, inverse estuarine conditions prevail at times. Local residents report that for short periods after heavy summer rains the major estuaries become markedly less saline at low water, as far down as their mouths. Whether there is also some salinity stratification at this time is not known.

At the time of the 1970 and 1971 surveys there was no measurable salinity stratification anywhere within the estuary, nor was there any lateral variation. It appears that because of the lack of runoff, the large tidal range (up to 10 m), and the strong tidal currents, Broad Sound waters are vertically and laterally homogeneous, with the salinity (during the winter) ranging throughout from about 35.5 to 36.5 parts per thousand (ppt).

The P_2O_5 and NO_3 contents of the open water in the Sound were at or below the detection limit of 0.01 ppm throughout. Therefore the Sound must be regarded as a nutrient-poor area compared with normal ocean water, which ranges from about 0.01 to 0.1 ppm P_2O_5, and with estuarine areas which commonly attain even higher values (during the grid sampling a single anomalously high phosphate value was obtained in a mangrove channel — see 'Mangrove Channel Waters', below).

The pH of the seawater in the Sound generally ranges from 7.9 to 8.1, with a mean

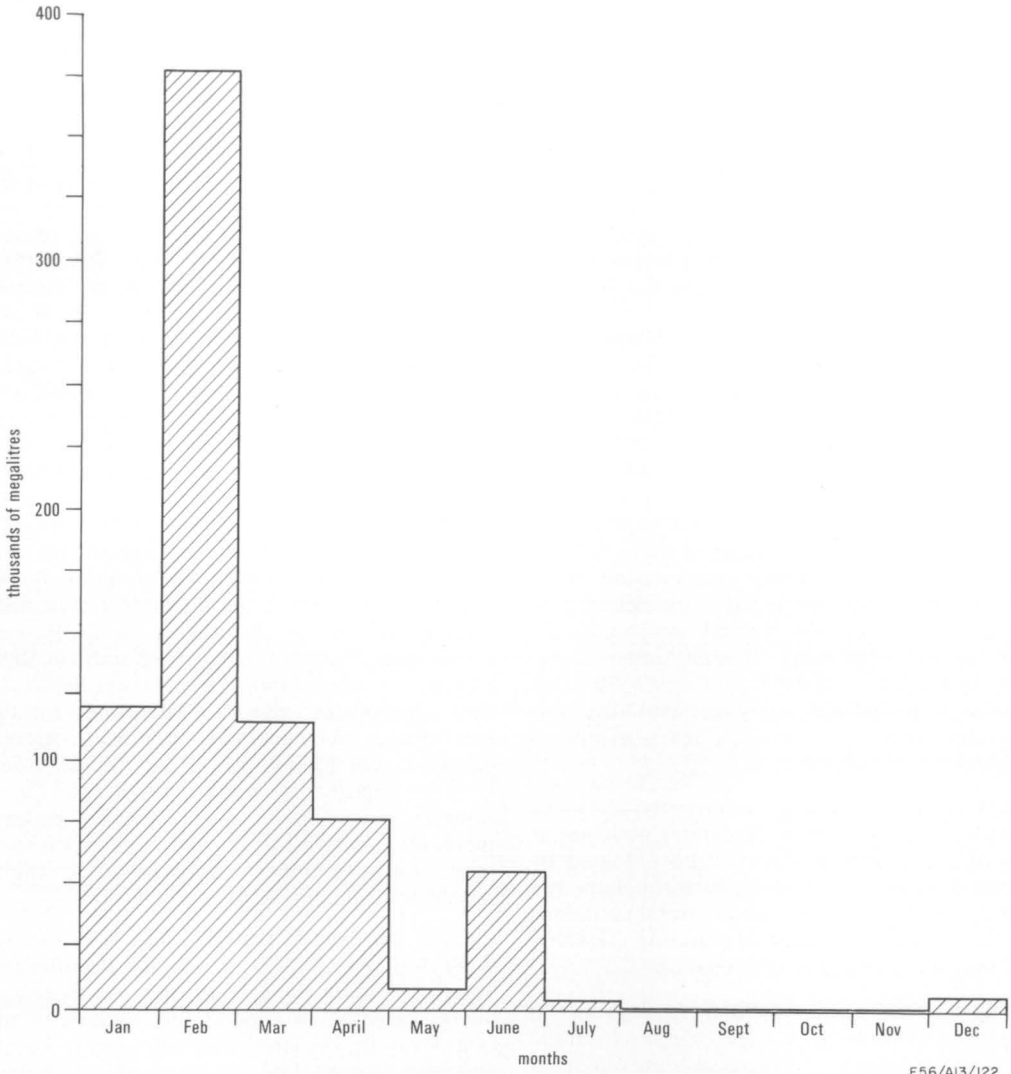


Fig. A67. Isaac River: average monthly discharge at Yatton (50 km west of Ogmore)

value of about 8.0 (although there are marked variations from this range in the mangrove channels). As in all marine systems (Park & others, 1958) the pH of Broad Sound water varies diurnally — the pH is highest at 2-3 p.m. and lowest between about 8 p.m. and 5 a.m. As it was not possible to measure pH or Eh in situ (the sample had to be pumped up before the measurement was taken) the value obtained may deviate from the true value and theoretically a correction factor should be applied. Culberson & Pytkowicz (1968) have shown that the pH value may be corrected by the formula

$$pH = pH\ (measured) - 4 \times 10^{-4} P$$

where P is the water pressure. However, as the water depth nowhere exceeds 30 m, it can be seen that the relevant correction factor for Broad Sound is relatively small, and may be ignored.

The measured Eh ranged from +190 to +250 mV, with a mean of about +210 mV. Therefore the Broad Sound waters are strongly oxygenated.

Turbidity (Fig. A68) at any one point is highly variable, depending on whether the tide is flooding (bringing in clearer sea water from the continental shelf) or ebbing (carrying turbid water from nearshore environments, particularly the mangrove swamps). Turbidity is also influenced by the tidal range (it is greatest during

an ebbing spring tide) and by wave activity. Consequently the turbidity values which were obtained over a period of several days at various states of the tide and were used to compile Figure A68, only provide an approximation to the true picture at any one time. The difference in turbidity between surface waters and bottom waters is only slight — on average, the transmittance of bottom waters is 2 percent less than that of surface waters. The surface turbidity pattern (Fig. A68) clearly shows the increase in turbidity up the estuaries, with a maximum in Herbert Creek. A similar pattern is visible in the Landsat photograph on the cover.

No temperature stratification was detected in the estuary; the temperatures range between 20°C and 22°C during the winter months, with no consistent lateral or vertical change.

In conclusion then, the Eh, pH, salinity, and temperature of the water in Broad Sound throughout most of the year are comparable with those normally prevailing in tropical or sub-tropical nearshore marine waters. The water is completely mixed vertically as a result of the strong tidal currents, the large tidal range, and, during the dry season, the lack of significant freshwater input. Turbidity shows some lateral variations, and for short periods after heavy rains there may be some lateral salinity changes. Only in the mangrove channels did the conditions show any measurable variation from normal marine conditions.

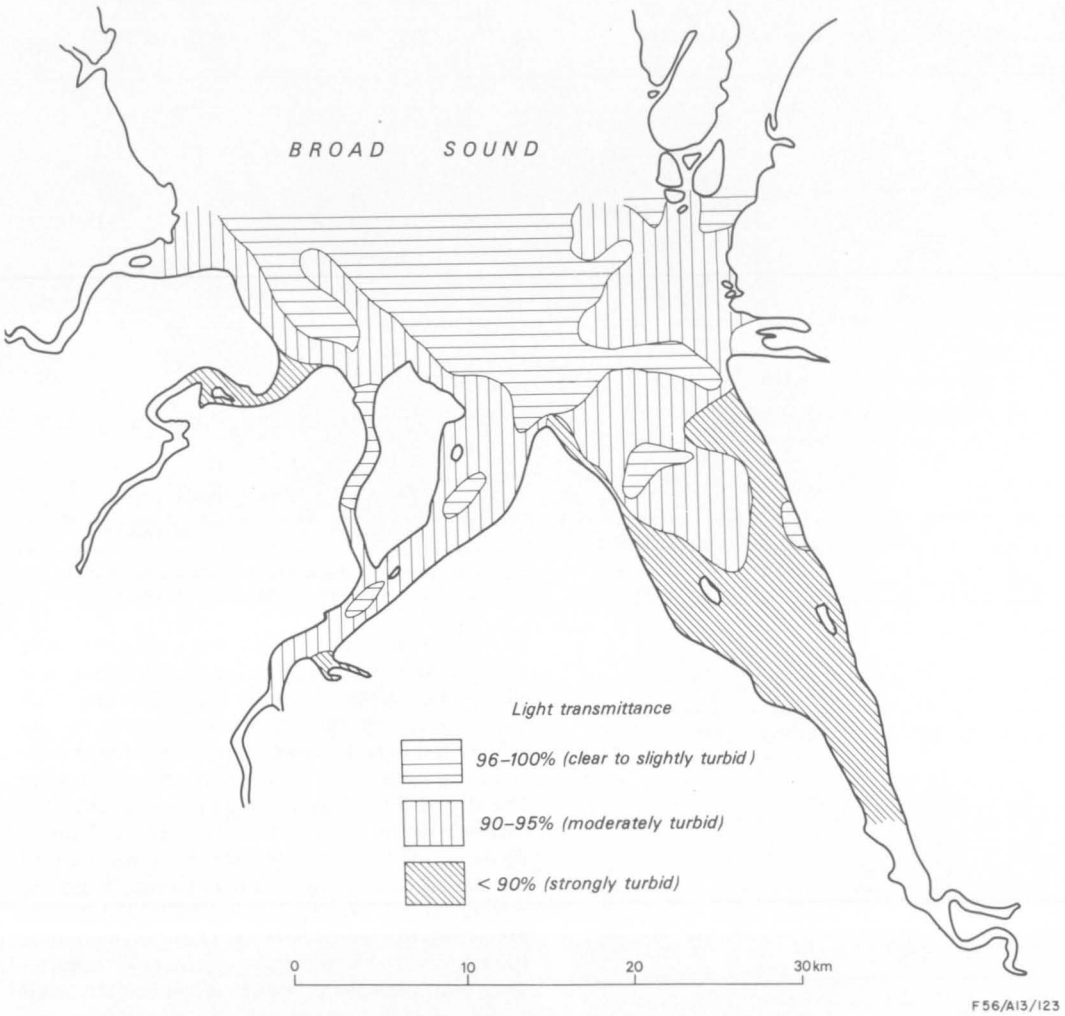


Fig. A68. Turbidity of Broad Sound surface waters

MANGROVE-CHANNEL WATERS

Mangrove channels range from the subtidal zone to the supratidal zone, but are mainly in the intertidal zone. They extend inland up to 5 km and vary in width from a few metres to 500 m. The sediments of the channels are generally dark grey to olive muds, derived mainly by slumping from the adjacent mangrove swamps. The walls of the channels are extensively bioturbated. Diurnal tides flush most channels. Some channels are completely dry at low water; most retain water up to 1 m deep even at low water.

During the grid sampling, a single anomalously high phosphate value was obtained from a mangrove channel. Several other channels were subsequently sampled but proved to have low phosphate values. Possibly, then, the tidal cycle was influencing the phosphate content of the water, and to test this we undertook a continuous sampling program in a mangrove channel close to the Broad Sound base camp. It was decided to measure water depth, salinity, pH, and phosphate content. Continuous sampling was carried out during three periods, each of about 36 hours, during August and September 1970. The results are shown in Figures A69-71. There is an obvious though somewhat irregular, cyclicity in salinity, pH, and phosphate which is related to tidal cycles: at high tide pH is high, salinity low, and phosphate content low, and vice versa at low tide. The phosphate content varied greatly

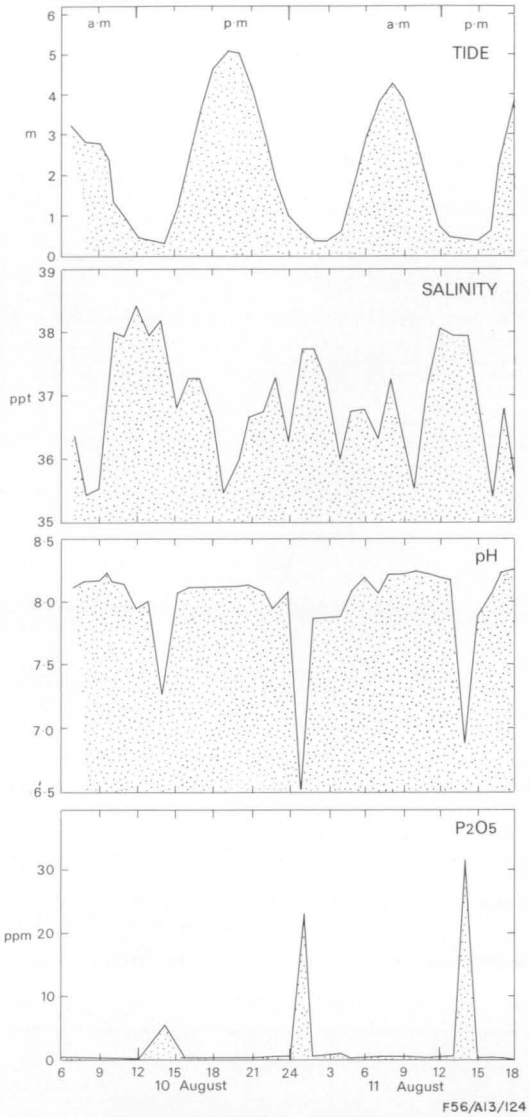


Fig. A69. Mangrove-channel waters: relationship of P_2O_5, pH, and salinity with state of tide, 10-11 August 1970

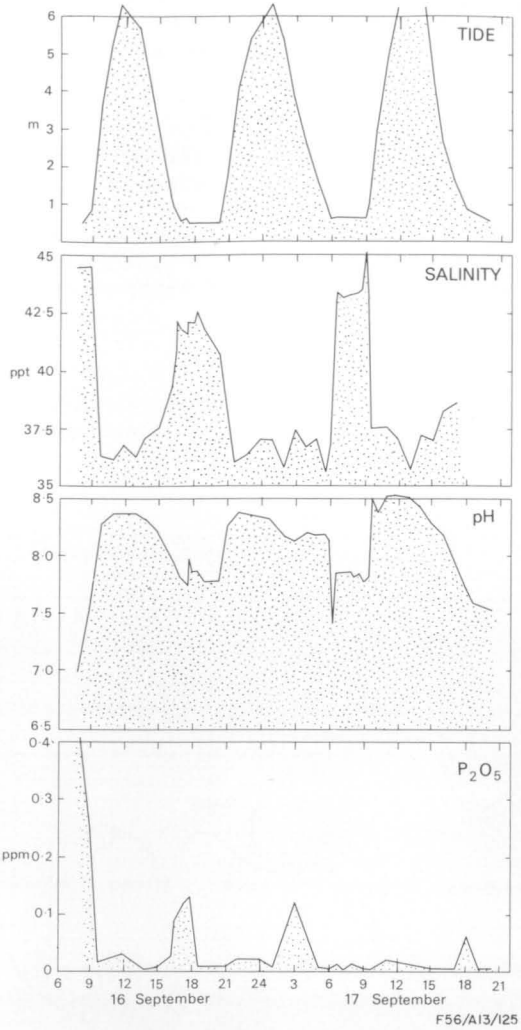


Fig. A70. Mangrove-channel waters: relationship of P_2O_5, pH, and salinity with state of tide, 16-17 September 1970

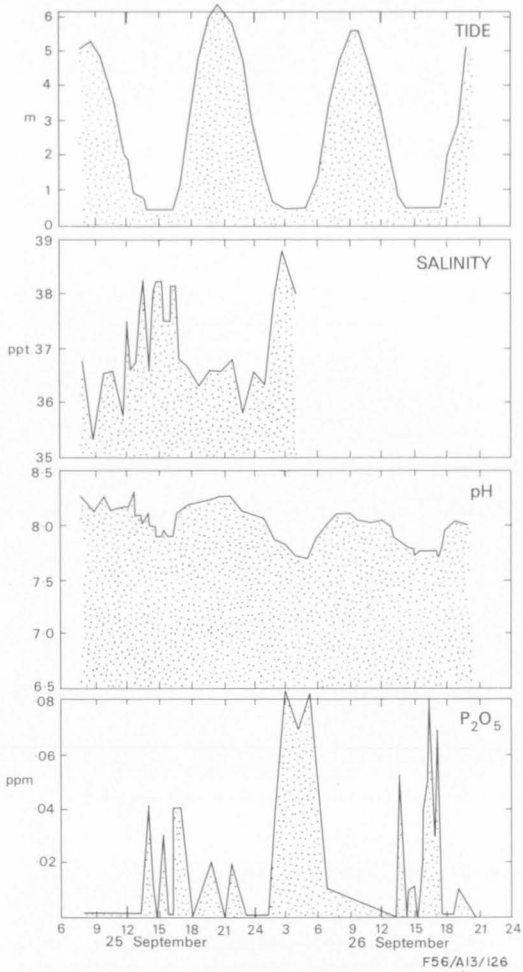


Fig. A71. Mangrove-channel waters: relationship of P_2O_5, pH, and salinity with state of tide, 25-26 September 1970

during the observed tidal cycles, and the maximum on 11 August (32 ppm) was over three hundred times the maximum on 26 September (0.09 ppm). Both of these values are much higher than those found in any other Broad Sound waters. The salinity also varied; it was 38.1 ppt on 11 August whereas on 17 September (Fig. A70) it reached 45.3 ppt. This change in the maximum value appears to be related to the tidal range: maximum salinity (16 and 17 September) occurred at low tide during spring tides when the saline supratidal flats had been inundated. Also, the time of day has a marked effect on the pH value, which is up to 0.4 units lower at night than during the day, at the same state of the tide. Phosphate solubility is considerably affected by pH (Kramer, 1964: Roberson, 1966); a plot of pH versus total phosphate content using the mangrove channel data (Fig. A72) demonstrates this and given an approximate solubility curve. There is a marked increase in phosphate solubility below a pH of about 7.4.

The pH, salinity, and phosphate values in the mangrove channels depart quite markedly from those of open Broad Sound waters in the lower part of the tidal cycle. Although only one mangrove channel was studied in detail, probably all mangrove channels in Broad Sound contain low-pH/high-salinity/high-phosphate waters for a significant portion of each tidal cycle. A similar phenomenon was observed (though not explained) in Queensland mangrove swamps by Orr & Moorhouse (1933), who noted in particular that there was a rise in salinity and a fall in pH (and oxygen saturation) at low tide.

Possibly some oxidation of dead organic matter in the water may take place, lowering the pH:

$$C + O_2 \rightarrow CO_2 \qquad (1)$$

$$CO_2 + H_2O \rightleftharpoons H_2CO_3 \rightleftharpoons H^+ + HCO_3^- \qquad (2)$$

Skirrow (1965) points out that oxidation of dead organic matter is accompanied by liberation of phosphate and hence an increase in the total phosphate content of the water. However, at low water, when pH is lowest, the waters of the mangrove channel stagnate and conditions probably become euxinic for a limited period. Although under such conditions extensive oxidation is not possible, microbial fermentation can still produce CO_2(Berner, 1971). The likely reaction is represented by Berner by the formula

$$C_6H_{12}O_6 \rightarrow 3CO_2 + 3CH_4$$
(carbohydrate)

This, in turn, would lower the pH. However, the strongly buffered nature of sea water makes it unlikely that the observed large drop in pH can be attributed to this reaction alone. Furthermore, the in-situ development of anoxic conditions could obviously in no way be responsible for the observed high salinities. Therefore it seems likely that there is a major influx of high-salinity water from another environment. An obvious source is the supratidal flats, which are commonly covered by a veneer of salt. Although this salt would readily dissolve during inundation by the infrequent high spring tides, the pH of standing water on the supratidal flats is even higher than that of sea water, values of up to 9 having been measured (probably as a result of algal photosynthesis). Therefore the available surface waters cannot account for all of the particular physico-chemical conditions observed in mangrove channels.

The composition of the pore water of the present-day supratidal flats and of the mangrove

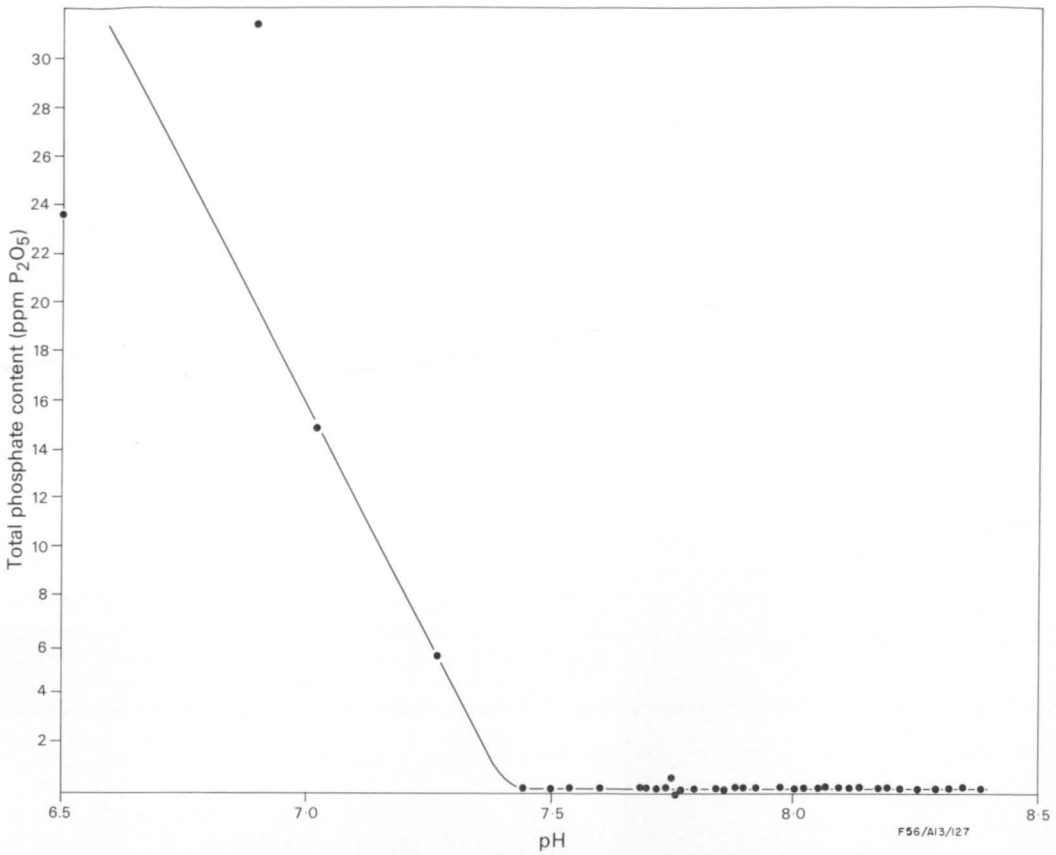


Fig. A72. Mangrove-channel waters: relationship between phosphate content and pH

swamp sediments was determined. In both environments the pore waters had high salinities and low pH values. The pore waters of the old mangrove deposits, which underlie both the mangrove-swamp and supratidal-flat environments, were particularly saline and acid. Therefore it appears that at least some of the interstitial water in nearby depositional environments is entering the mangrove channels. Some of this water is no doubt contributed by the immediately-preceding high tide, but a significant amount must be 'old' water, because a residence time of several tidal cycles would be necessary for it to acquire the observed low pH and high salinity.

The mechanism may perhaps be considered as a modified version of the refluxion process of Adams & Rhodes (1960) (Fig. A73). At Broad Sound the capillary rise of sea water in the mangrove swamps and, especially in the supratidal flats, increases salinity and forms a relatively dense brine which then tends to move downwards and seaward, eventually reaching the mangrove channels. At high water the hydrostatic pressure is such that there is some entry of sea water (with a normal salinity) into the sediments flanking the channel. However, at low tide the highly saline water flows relatively freely into the channels via crab burrows and roots, which have the effect of making the clayey sediment highly permeable.

In its passage through the sediments the pore water also acquires a low pH. It is noticeable that whilst the highest salinities (Fig. A73) (up to 45.3 ppt) are found in the mangrove channels during low spring tides (acquired from dissolution of surface salts), this does not coincide with the lowest-pH/highest-phosphate waters. These are found during neap and intermediate tides when the supratidal flats are not inundated and the high salinities (up to about 38 ppt) result only from the influx of pore waters. Thus there are three types of saline waters mixing to varying degrees in the mangrove-channel environment: (i) normal sea water with a salinity of 35-36 ppt, a pH of about 8, and a P_2O_5 content of about 0.01 ppm; (ii) supratidal surface water with a high salinity, a pH of 8 or higher, and a

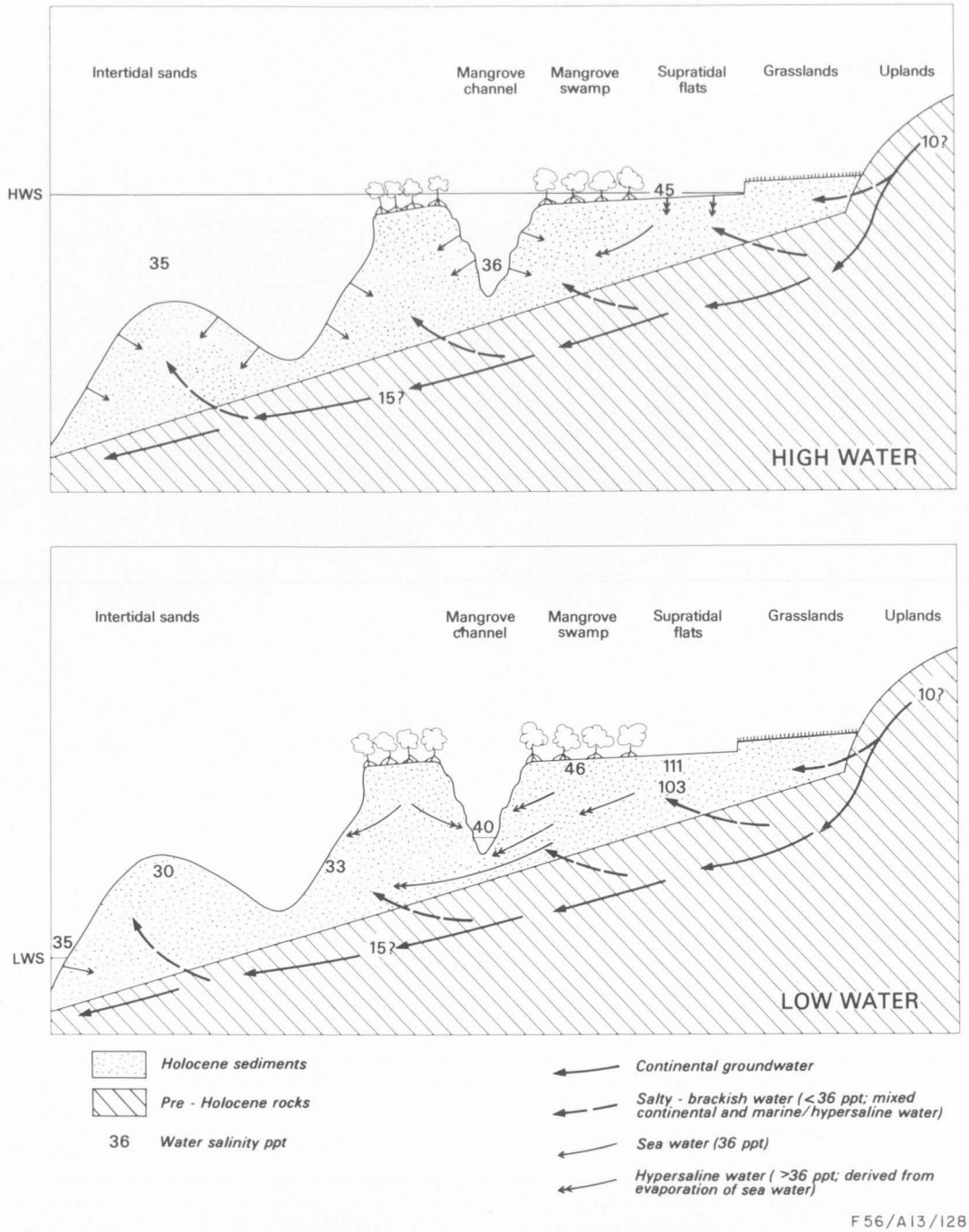


Fig. A73. Probable groundwater movement through intertidal and supratidal sediments, at high water and low water

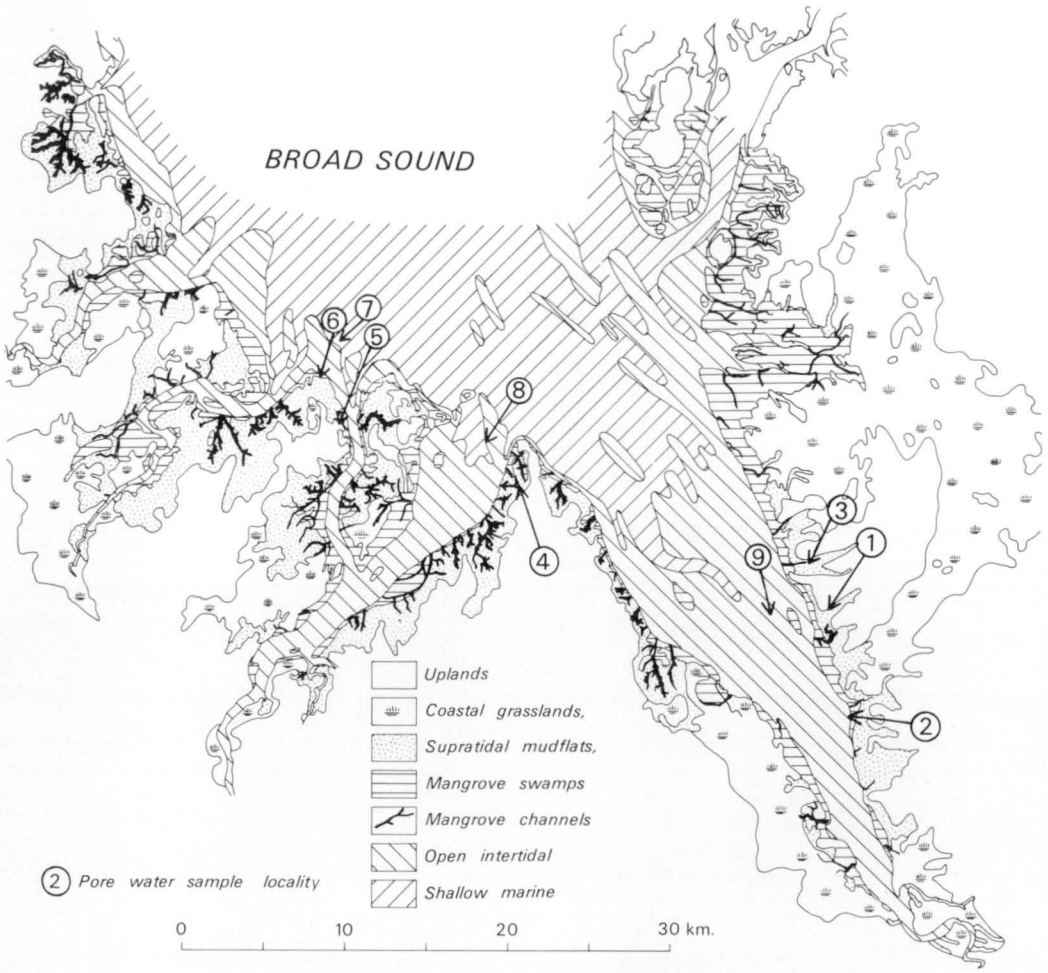


Fig. A74. Broad Sound: pore-water sample localities F56/A13/129

P_2O_5 content of up to 0.5 ppm; (iii) pore waters with a high salinity, a low pH of 7.5-6.5, and a high P_2O_5 content of up to 30 ppm.

PORE WATERS

Pore waters were expressed from sands and muds of the supratidal-flat, mangrove-swamp, and open-intertidal environments; several samples were also obtained from old mangrove-swamp deposits underlying the supratidal-flats at a depth of 30-60 cm. In-situ measurements were also made. The localities sampled are shown in Figure A74. The physical and chemical properties of the pore waters are given in Appendix 2, and are summarised in Table A31. It is apparent that the physico-chemical parameters vary markedly, and, in most environments, deviate significantly from those of sea water.

Salinity

Predictably, the pore waters of the mangrove swamps and supratidal flats, which are exposed subaerially for most of the time are hypersaline. The salinity varies partly with the time elapsed since the last tidal inundation. Salt encrustations are common. Gypsum is abundant, particularly in the subsurface, where it occurs as abundant flat discoid crystals up to 1 cm across. Halite is present as an ephemeral surface encrustation, and there are small quantities of bischofite ($MgCl_2.6H_2O$) and bassanite ($CaSO_4.½H_2O$). Minor calcite and aragonite are also present, probably mainly as reworked biogenic material, though trace amounts may be of evaporitic origin; dolomite has formed in places, probably as a result of early diagenetic dolomitisation of calcite (Cook, 1973).

TABLE A31. SUMMARY OF PHYSICO-CHEMICAL CHARACTERISTICS OF PORE WATERS AND ASSOCIATED SEDIMENTS, BROAD SOUND (LOWEST, HIGHEST, AND MEAN VALUES)

	Open-intertidal		Mangrove-swamp		Supratidal-flat	Broad Sound sea water
	Sand	Mud	Modern	Old		
Eh, in situ (mV)						
lowest	+130	−150	−120	−360	+80	
highest	+210	+200	+270	+270	+290	
mean	+160	+3	+138	+132	+180	
pH, in situ						
lowest	7.2	6.9	6.6	3.5	6.6	
highest	7.9	7.3	7.0	6.9	7.8	
mean	7.6	7.1	6.8	5.2	7.1	
Eh, pore water (mV)						
lowest	+130	−30	+60	−120	−10	+190
highest	+190	+210	+210	+200	+160	+250
mean	+152	+105	+142	+98	+54	+210
pH, pore water						
lowest	7.4	7.0	7.1	5.7	6.9	7.9
highest	7.9	7.8	8.4	7.8	8.5	8.1
mean	7.6	7.5	7.8	6.9	7.6	8.0
Salinity(ppt)						
lowest	24.8	28.9	34.3	44.5	58.8	34.6
highest	33.5	37.9	70.3	122.0	128.6	36.6
mean	30.0	32.6	45.8	98.1	102.3	35.8
Mg (ppm)						
lowest	1080	1140	1640	1650	5260	1300
highest	1410	1620	2520	7160	7000	1400
mean	1245	1148	2173	5739	6193	1340
Ca (ppm)						
lowest	300	340	310	500	880	410
highest	420	450	1110	860	1290	450
mean	361	397	621	714	978	430
K (ppm)						
lowest	280	320	455	1380	1320	400
highest	365	420	660	1640	1840	460
mean	323	368	572	1537	1514	430
P_2O_5 pore water (%)						
lowest	0.01	0.02	0.13	0.06	0.2	0.01
highest	0.02	0.28	0.18	0.8	1.4	0.05
mean	0.01	0.13	0.16	0.42	0.5	0.01
P_2O_5, sediment (%)						
lowest	410	440	730	380	370	
highest	520	720	1150	990	1000	
mean	454	600	923	687	716	

The salt encrustation may in some instances form by the evaporation to dryness of a standing body of shallow water, particularly where there is a localised depression. However, field observation suggests that generally most of the surface water returns to the estuary via channels, with some percolating into the underlying mud. Subsequently the water in the mud rises by capillary action ultimately evaporating at the surface and producing brine. At a locality near the Torilla Plains base camp (locality 1, Fig. A74; sample 71636068, Appendix 2), supratidal-flat deposits in which the pore waters have a salinity of 58.8 ppt are immediately underlain by old mangrove-swamp deposits with a salinity of 103.3 ppt. How much of this difference in salinity is due to downward movement of dense brines and how much to the dilution of upper brines by the influx of lower-salinity seawater is not certain. However, at a second locality nearby, close to the landward edge of the supratidal flats, (locality 3, Fig. A74), the salinity decreases progressively downwards (Fig. A75). Locality 3 is far removed from all but exceptionally high tides; consequently there is no dilution of the upper pore waters. A further complication, when evaluating the effects of evaporation at Broad Sound on the salinity of pore water and its subsequent movement, is that there is likely to be dilution of the hypersaline water by seaward-moving fresh or brackish groundwater. The groundwater is predominantly within the pre-Holocene gravels and rocks, but there is probably some upward leakage into the Holocene sediments owing to hydrostatic pressure, resulting in progressive dilution towards the base of the Holocene sequence (Fig. A73).

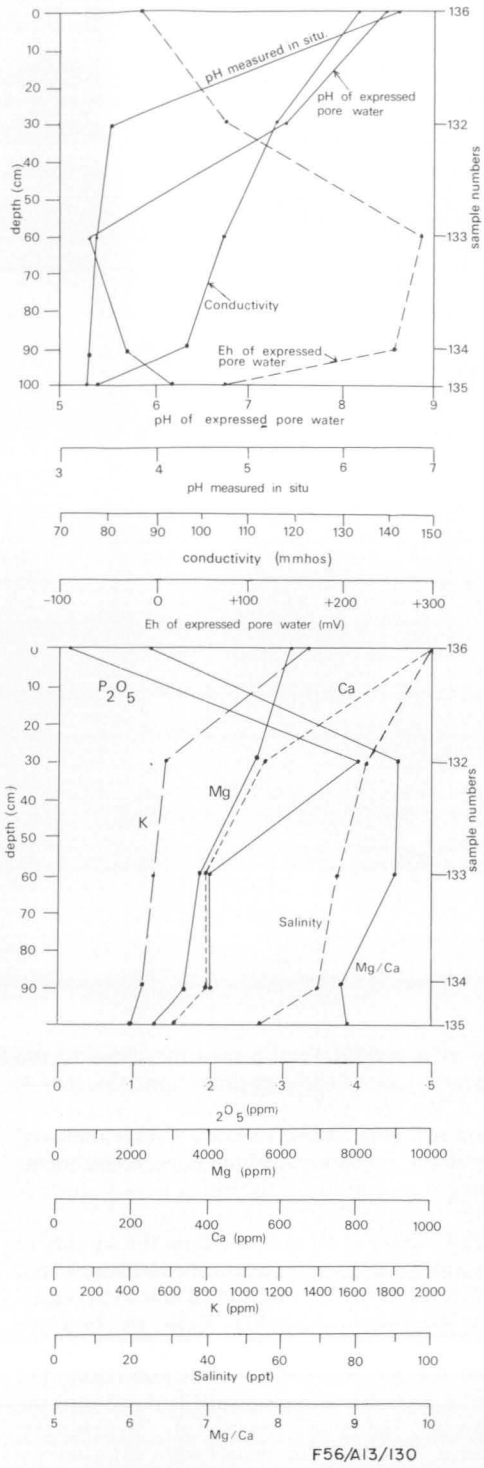


Fig. A75. Supratidal sediments, locality 3, Fig. A74: vertical variation in pore-water geochemistry

Abundant low-salinity pore water is also indicated by the surprisingly low pore-water salinities found in the sands, and to a lesser extent in some of the muds in the open-intertidal environment. The intertidal sands were sampled at low water, 60 to 70 cm below the surface and 1-2 km from the edge of the mangrove swamps; at all of the 18 points sampled (Appendix 2) the salinity (averaging 30 ppt) was substantially below that of normal Broad Sound water (35-36 ppt), which had been overlying the sands only a few hours previously (Table A31). Similarly, the sediments of the muddy facies have an average pore-water salinity of 32.6 ppt, ranging as low as 28.9 ppt. Clearly this dilution is most likely to be due to groundwater inflow, because there is no salinity stratification in the waters of Broad Sound or its associated estuaries.

Eh and pH

One of the first features evident from Table A31 and Appendix 2 is that in many cases there are marked differences between the Eh and pH measured in situ and the Eh and pH measured on the expressed pore water. This is shown in Figures A76 & A77, and perhaps more clearly in Figures A78 & A79, where the spreads of values are shown as fields. The difference may be the result of the 'suspension' or Pallmann effect (Bates, 1964), caused by abnormal junction potentials in colloidal systems. Any attempt, therefore, to evaluate the Eh and pH data must be considered in the knowledge that there is uncertainty over which value is closest to the true value. Stability of Eh and pH over time is also an important consideration. Mayo (1976) considered this question in some detail and found that in-situ Eh and pH readings are stable over prolonged periods in the intertidal and supratidal sediments. Both the 'in-situ' and the 'expressed' values indicate that conditions are generally less oxidising and more acid than those prevailing in seawater. Maximum Eh-pH separation between environments is shown by the in-situ results (compare Figures A76 and A77). It is apparent in Figure A78 that the old mangrove-swamp sediments in particular form a more clearly defined group. Analogous fields are less coherent in Figure A79 than in Figure A78. Whether the 'in-situ' or the 'expressed' values are taken, most samples fall into the bicarbonate-sulphate stability field, though there is some extension of the old mangrove-swamp sediments into the carbonic acid field. The apparent absence of any extension into the sulphide field would seem to be at odds with the fact that gaseous hydrogen sulphide was commonly present in the old mangrove-swamp muds and the muds of the open-intertidal

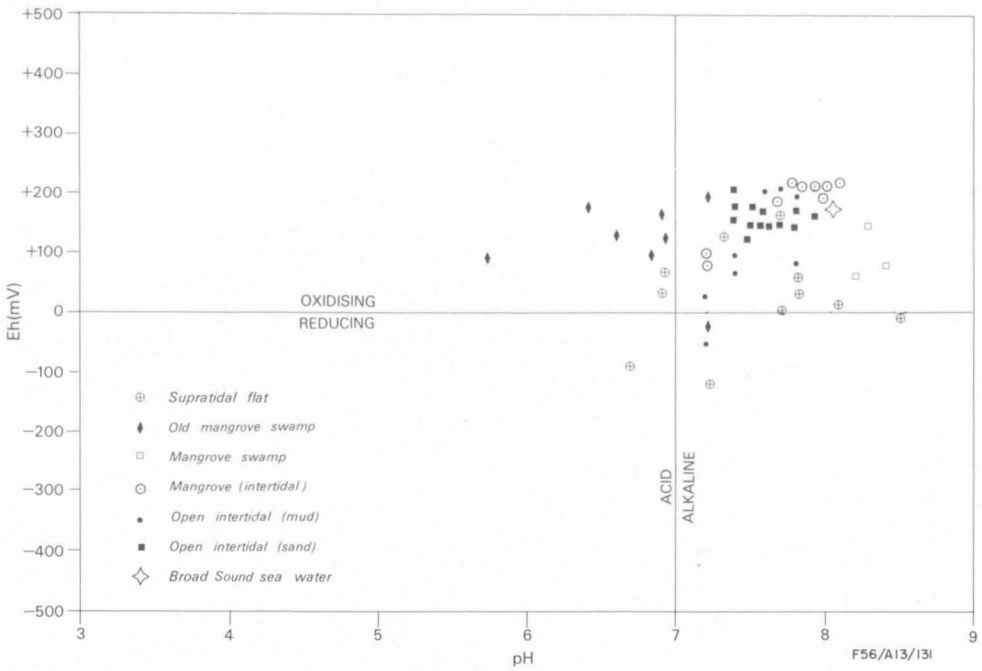


Fig. A76. Eh and pH of expressed pore waters, estuarine depositional environments

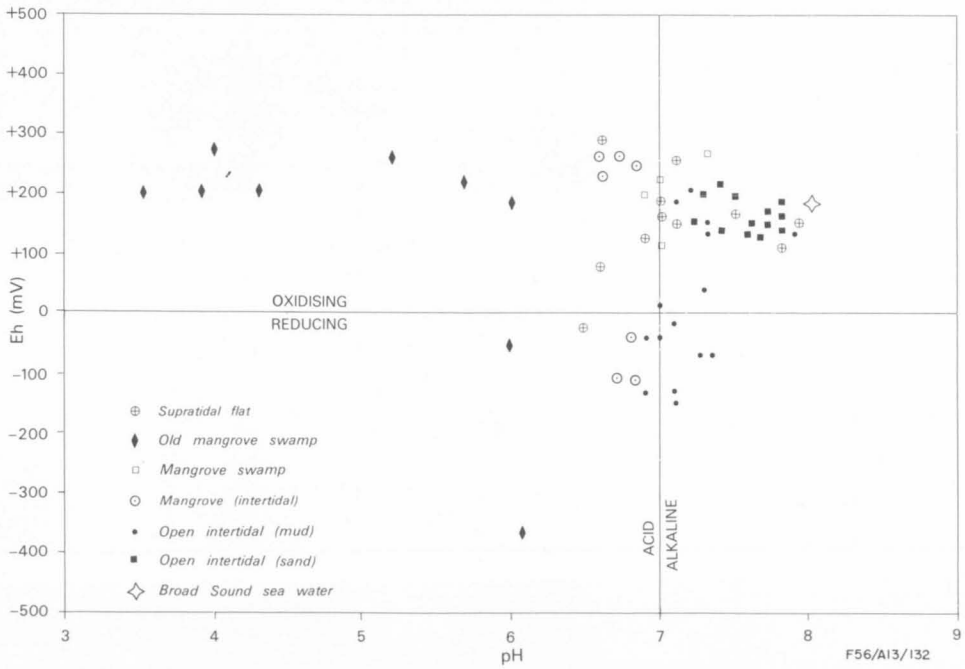


Fig. A77. Eh and pH of pore waters measured in situ, estuarine depositional environments

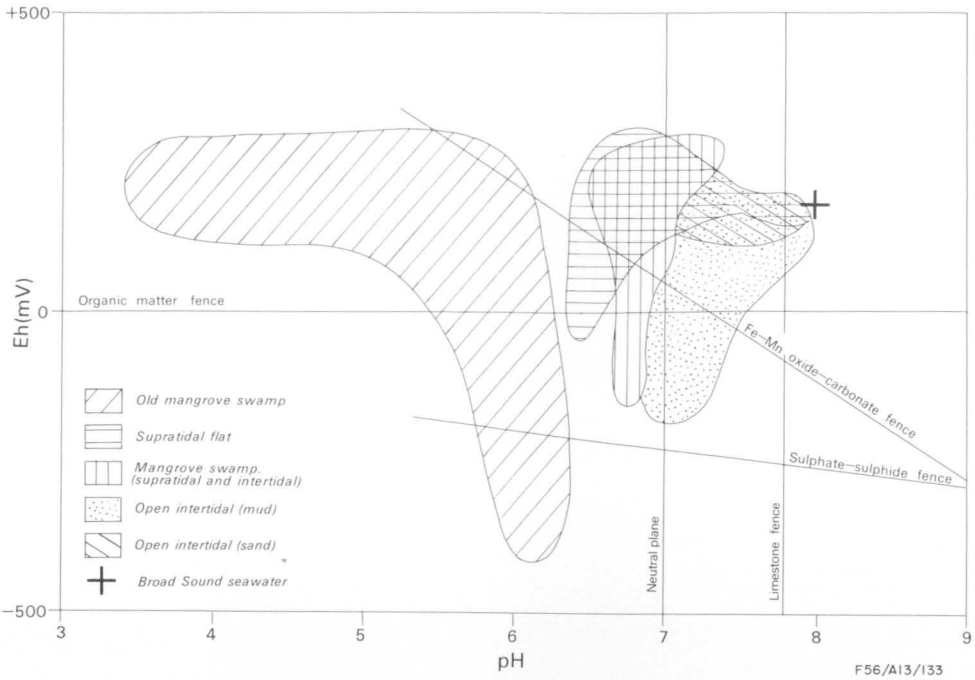


Fig. A78. Eh and pH fields of pore waters in estuarine depositional environments, measurements made in situ. The classical Eh and pH 'fences' of Krumbein & Garrels (1952) are indicated

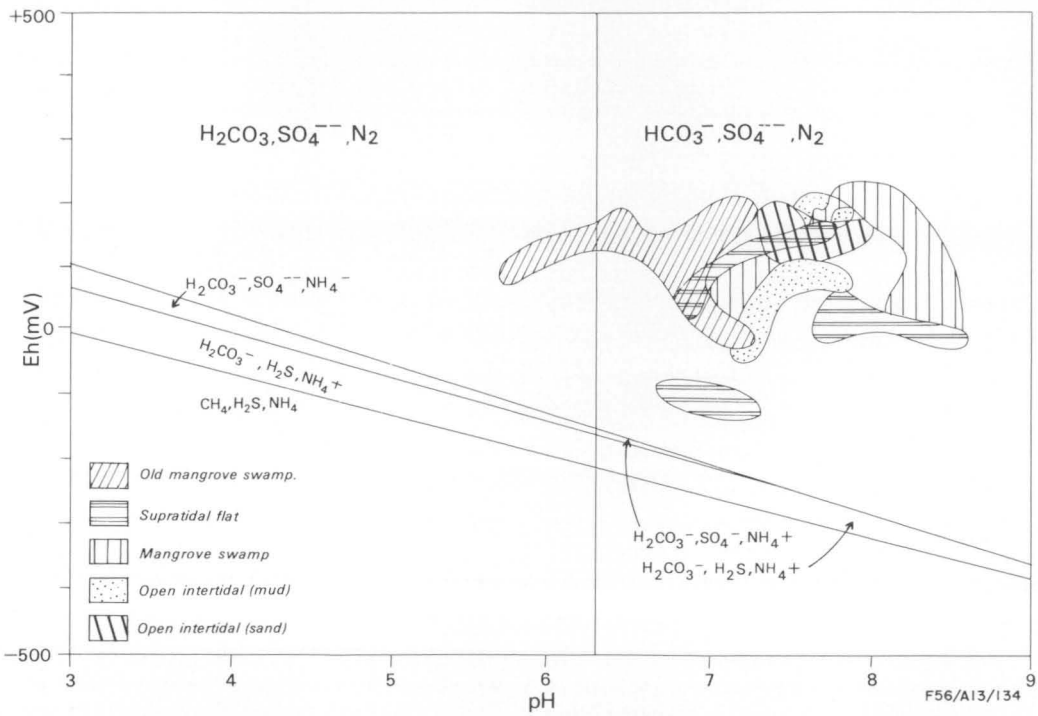


Fig. A79. Eh and pH fields of expressed pore waters, estuarine depositional environments. Stability fields are indicated for dissolved species in the C-N-S-H-O system (after Berner, 1971, pp. 116-117)

environment. In addition, pyrite was a common feature of both these environments. Therefore, either the Eh-pH values obtained are not truly indicative of the conditions prevailing in the Broad Sound depositional environments, or, alternatively, small-scale localised conditions, possibly associated with microbiological activity, are responsible for the formation of H_2S and FeS.

In the sulphate-rich brines (as evidenced by the abundance of gypsum crystals in the supratidal zone) bacterial sulphate reduction is likely to be an important mechanism. Likely reactions may be represented by the approximate equations

$$SO_4^{--} + 2C \rightleftharpoons S^{--} + 2CO_2, \text{ and}$$
$$SO_4^{--} + CH_4 \rightleftharpoons HS^- + HCO_3^- + H_2O,$$

or, alternatively

$$Na_2SO_4 + 4CH_3COCOONa + 2H_2O \rightarrow H_2S + 2NaOH + 4CO_2 + 4CH_3COONa.$$

However, all of these reactions involving sulphate reduction will cause an increase in pH, whereas the pore waters of the mangrove swamp are acid. Strongly acid soils have been noted elsewhere in mangrove swamps (Thornton & Giglioli, 1965). Hart (1962) has suggested that this results from the formation of sulphuric acid, following the oxidation of sulphur by *Thiobacillus thio-oxidans*. More recent work by Goldhaber & Kaplan (1974) has shown that the oxidative reaction for sulphur is fairly complex, producing not only the sulphate, but also thiosulphate, polythionate, and sulphite, which they represent by the following equations:

$$S + O_2 + H_2O \rightleftharpoons SO_3^{--} + 2H^+ \quad \ldots\ldots (1)$$
$$SO_3^{--} + S \rightleftharpoons S_2O_3^{--} \quad \ldots\ldots\ldots\ldots (2)$$
$$2S_2O_3 + H_2O + \tfrac{1}{2}O_2 \rightleftharpoons S_4O_6^{--} + 2OH^- \quad (3)$$

But, whatever the mechanism, it would seem that biological or abiological sulphur oxidation is potentially capable of producing strongly acid conditions. However, it was noted that, in the open-intertidal muds flanking the mangrove swamps, where conditions are also acid, the most strongly acid conditions are found in the fine-grained organic-rich anaerobic bands, which are an unsuitable environment for thiobacilli and other aerobic bacteria. Some sulphuric acid may also be formed by atmospheric oxidation of sulphide ion and elemental sulphur, but again such a reaction seems incompatible with the prevailing reducing conditions. An alternative source of acidity is organic acids, such as fulvic acid, derived from the breakdown of plant fragments. However, these organic acids are generally weak and are unlikely to produce any major decrease in pH. In addition, the formation of pyrite can also produce a strongly acid reaction involving the products of earlier oxidation (Berner, 1964; Rickard, 1969, 1970). The reaction may be represented as:

$$Fe^{++} + S + H_2S \rightleftharpoons FeS_2 + 2H^+$$

This, and other reactions involving sulphate reduction, is consistent with the observed anaerobic condition below the sediment-water interface in the mangrove-swamp, old mangrove-swamp, and open-intertidal mud deposits, and with the presence of abundant pyrite and hydrogen sulphide. The work of Thorstenson (1970), Ben-Yaakov (1973), and others has shown that using up all the available sulphate in anoxic marine sediments during the course of sulphate reduction will lower the pH only to 6.9 from the normal value of about 8. However, in the old mangrove sediments underlying the supratidal flats, pH values below 6 were recorded at a number of localities (Appendix 2, Figs. A76, A77). Mayo (1976) suggests that the low pH values in the old mangrove sediments are due to the oxidation of FeS_2 deposited originally under reducing conditions. There is undoubtedly a need for more detailed chemical and biochemical studies of these sediments.

So far, this discussion has dealt primarily with sediments having a low pH and a negative Eh. However, not all of the Broad Sound sediments are of this type. The sands of the open-intertidal environment have pH and Eh values only slightly below those of normal Broad Sound water. In some circumstances in supratidal-flat muds both pH and Eh may be above that of normal sea water. As mentioned previously, high pH values can be reached in standing bodies of water on the supratidal flats, probably as a result of removal of CO_2 from the water through algal activity. When this water filters down into the underlying muds, it imparts (though probably only for a short time) a high pH to the uppermost pore waters.

In addition, the subaerial condition may reasonably be expected to imprint a high redox potential on the pore waters. However, a complication to this relatively simple picture is that in places conditions are more strongly oxidising 1 m below the surface than at the surface. This is exemplified by the values for samples 71636132-6136 (Appendix 2 and Fig. A75), and indicates that in places there probably is some input of highly oxygenated groundwater. The decrease in salinity with increasing depth (Figs. A75, A76) would also seem to support this suggestion.

Cations

Only the cations Ca^{++}, Mg^{++}, and K^{+} were determined (by atomic absorption spectroscopy). Values are given in Appendix 2; summary values are given in Table A31.

It has been pointed out earlier that the salinities of the interstitial waters differ significantly from normal sea water salinity. One would expect cation concentration to vary sympathetically with the salinity, but in fact the ratios of cation concentration to total salinity do not remain constant. There is in particular a marked change in the Mg/Ca ratio, despite the fact that the Mg/K ratio remains constant (see Cook, 1973, fig. 6). It is apparent from Figure A80 that Ca is depleted relative to Mg in many of the pore waters, particularly in the old mangrove-swamp and supratidal-flat samples. It can be seen from Figure A81 that this variation is clearly related to increasing salinity; the Mg/Ca ratio remains relatively stable at between 3 and 4 (about equal to that of ordinary sea water) up to a salinity of 80-90 ppt, and then deviates significantly. A similar phenomenon has been found in other hypersaline environments (Kinsman, 1969) and may be ascribed to the preferential removal of Ca in gypsum, as follows:

$$Ca^{++} + SO_4^{--} \rightleftharpoons CaSO_4$$

This is supported by the abundance of large gypsum crystals in the sediments underlying the supratidal flats. The nett effect of this is to produce Mg-rich pore fluids, which may be responsible for dolomitisation in the Charon Point area.

A second feature apparent from Figure A80 is that, whereas most pore waters show a marked

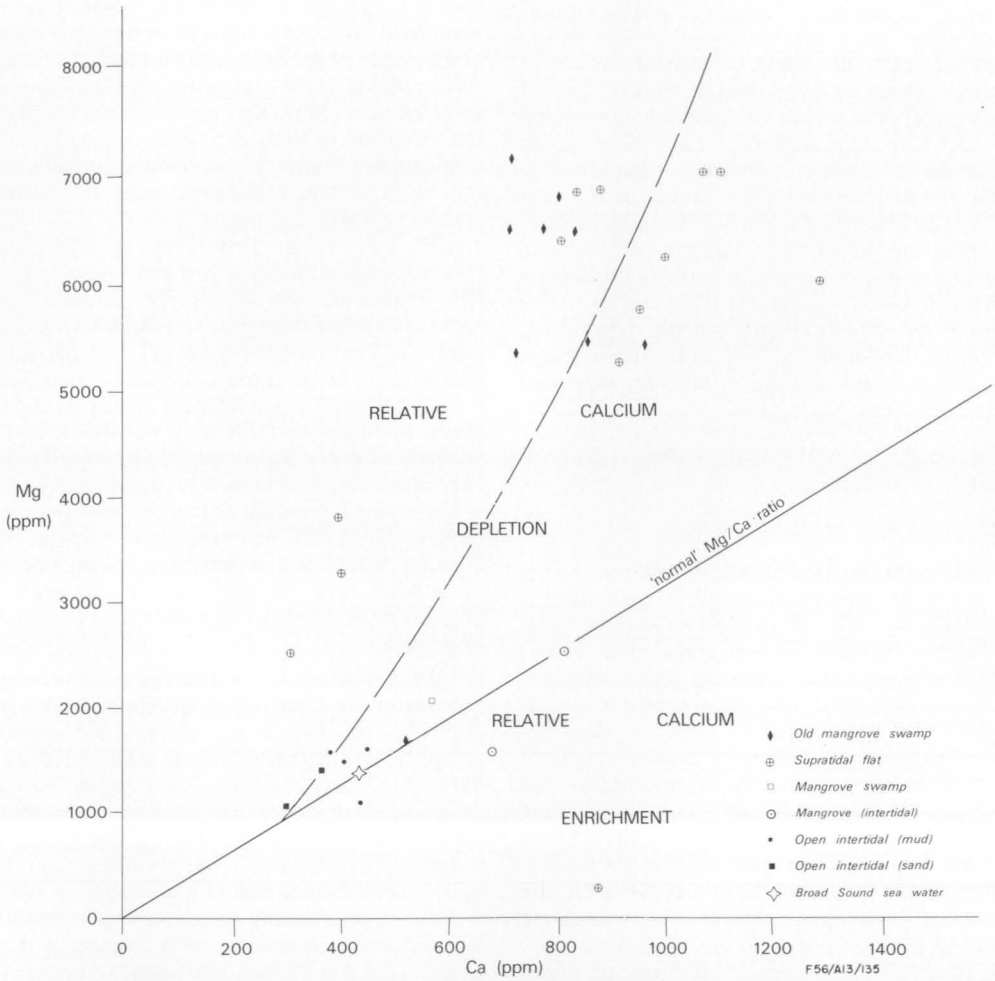


Fig. A80. Abundance of Mg and Ca in expressed Broad Sound pore waters

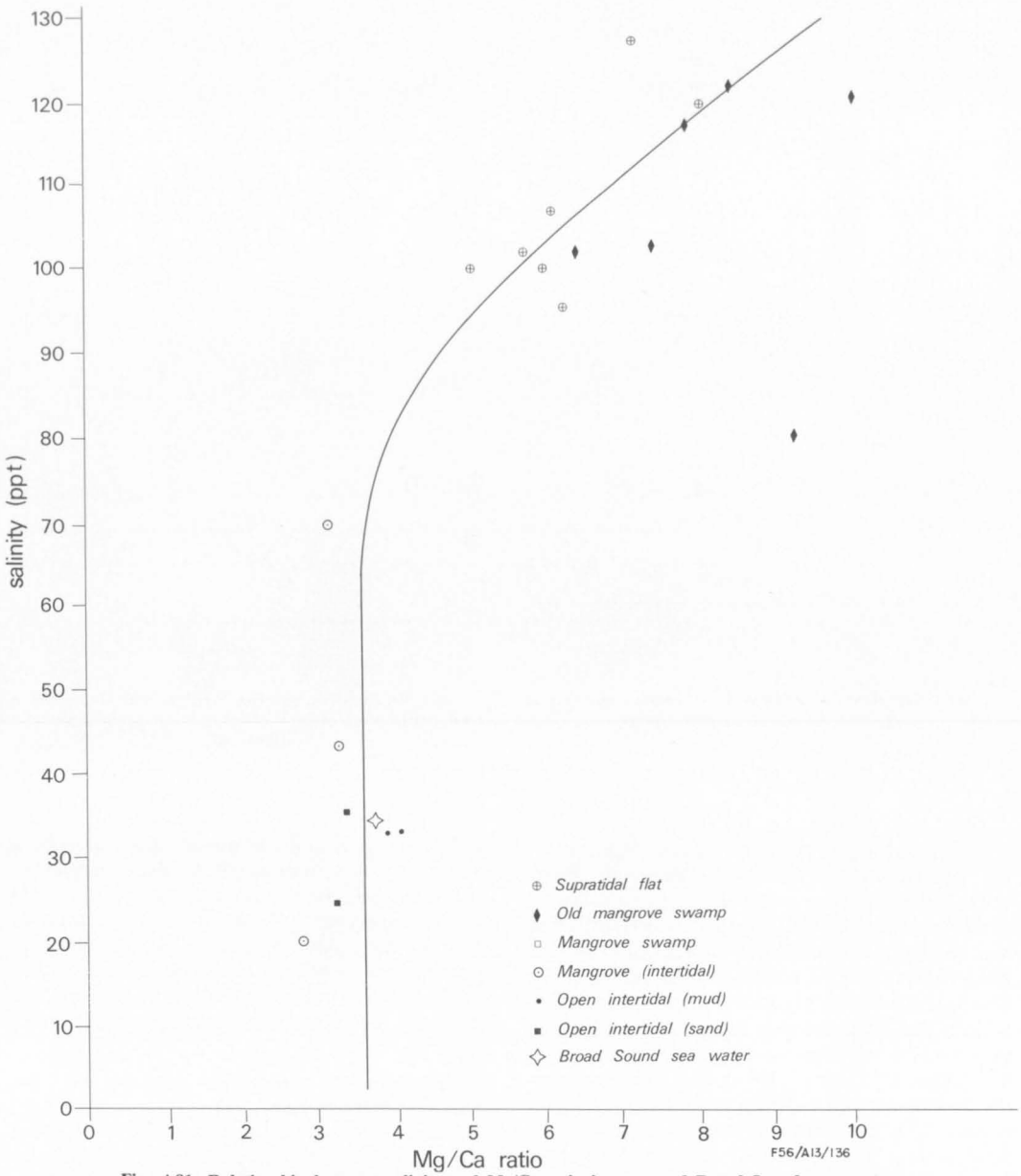


Fig. A81. Relationship between salinity and Mg/Ca ratio in expressed Broad Sound pore waters

relative depletion of calcium, a few samples, particularly those from the open-intertidal sands and intertidal mangrove sediments, show a relative depletion of Mg. Wiedemann (1969) has pointed out that the Mg/Ca ratio in rain water is very much lower than that in sea water; thus, dilution of sea water by rain water (and some groundwater) will lower the Mg/Ca ratio. This is consistent with the observation that the lowest Mg/Ca ratios are found in water with salinities below that of sea water. However, a low Mg/Ca ratio is also found in some waters with salinities greater than that of normal sea water. The reason for this is not known.

Phosphate

The phosphate content of pore waters, and of the sediments from which these waters were expressed, is given in Appendix 2; summary values for the various depositional environments are given in Table A31.

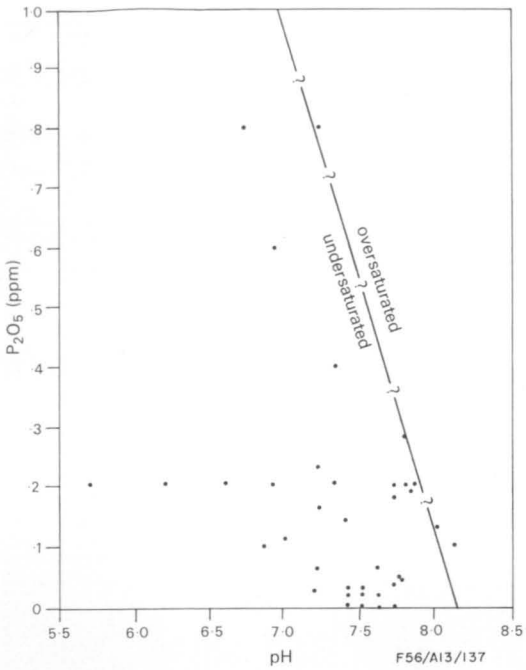


Fig. A82. Relationship between P_2O_5 content and pH in expressed Broad Sound pore waters

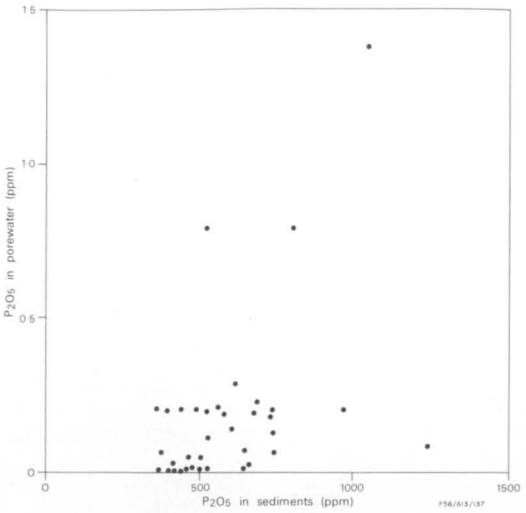


Fig. A83. Relationship between P_2O_5 content of expressed Broad Sound pore waters and P_2O_5 content of associated sediments

The phosphate content of the pore waters in the depositional environments varies considerably. Values for pore waters from open-intertidal sands are close to that of normal Broad Sound sea water, whereas the values in the old mangrove-swamp deposits are, on average, 50 times higher than those found in normal sea water. The phenomenon of high phosphate in pore waters has been noted in subtidal marine environments (Cook, 1974) but has not been previously documented for supratidal-zone sediments. The presence of these high-phosphate pore waters has potentially important implications for diagenetic phosphatisation and the formation of phosphorites in the intertidal-supratidal zone. It has been proposed that pH is the controlling factor in phosphate solubility (Kazakov, 1938), and the results in the mangrove channels (Fig. A72) indicate a well-defined pH phosphate-solubility relationship. If the phosphate content of the pore waters is plotted against pH (Fig. A82) there is no such well-defined relationship. Cook (1974) has suggested from deep-sea data that alkalinity is an important controlling factor in phosphate solubility in pore waters; however, alkalinity was not determined in the Broad Sound sediments. The phosphate content of the sediments could also conceivably influence the phosphate content of the pore waters. However, when the two phosphate contents are plotted (Fig. A83) there is no apparent relationship. Therefore it seems that the phosphate content of the sediments does not influence the phosphate content of the pore water.

The mean phosphate content of the mangrove-swamp and old mangrove-swamp sediments is 923 $\pm$ 139 ppm and 687 $+$ 210 ppm respectively. A student's *t*-test gives a greater than 99 percent probability that the difference between these two means is statistically significant. As the original depositional environment is the same in both cases, changes in depositional conditions are unlikely to account for this difference. Therefore it is possible that the difference results from post-depositional conditions, with acid waters removing a significant amount of phosphate from these sediments over the last 1000-5000 years. Thus, mangrove deposits are likely to be important contributors of phosphate to the estuarine system at Broad Sound and elsewhere.

IMPLICATIONS OF THE BROAD SOUND GEOCHEMICAL STUDY

The Broad Sound study has answered some of the questions asked earlier, such as the influence of drainage basin geochemistry on estuarine geochemistry, the effectiveness of geochemistry as an environmental indicator, and the extrapolation of Broad Sound geochemical processes to ancient sedimentary environments. Additional points that have come out of the study include information drawn from our resulting knowledge of the geochemistry of the drainage basin that may be useful in geochemical exploration, information on the influence of tropical weathering processes on element mobility, and a general understanding of geochemical processes in a modern tropical estuary, particularly the processes relevant to pollution and the ecosystem. Although some of these points have been discussed earlier, all are briefly re-examined below in order to establish the overall implications of the study.

GEOCHEMICAL EXPLORATION IN THE BROAD SOUND DRAINAGE BASIN

Before considering the implications of the present study to any future geochemical exploration, several points should be made.

(1) The drainage basin is, overall, a fairly 'average' provenance area, with no obvious signs of major mineralisation, with the possible exception of Ni.

(2) The correlation between metal content in the soil and in the underlying rock varies: Cu, Zn, Ni, and Mn show significant correlation; P_2O_5, Pb, Co (?), and Cr show no significant correlation.

(3) The extent to which stream-sediment geochemistry reflects the geochemistry of the adjacent bedrock is not clear.

(4) The geochemistry of the bedrock is more homogeneous than that of the soils or stream sediments, suggesting that processes governing element dispersion vary within the drainage basin, and that such processes are likely to mask, to varying degrees, geochemical anomalies in bedrock.

(5) Some elements show quite marked correlations with particular soils, e. g., high P_2O_5 and Zn concentrations in the cracking soils and high Cu in the massive red earths. Some soil types are related to bedrock, but many are not, and in such cases again there is masking of the bedrock anomalies.

(6) Some relative element abundances are strongly affected by the amount of weathering (and associated oxidation). Examples of this include Fe/Mn and Co/Ni. This, too, may serve to obscure significant anomalies.

It can be seen from all these points that attempts to determine significant geochemical anomalies from the soil geochemistry are fraught with dangers, the anomalies produced by secondary processes commonly being greater than those in the underlying bedrock. It was not possible to evaluate stream-sediment geochemistry. Probably it too has some of the problems encountered in the soils, although it possibly provides a better indication of bedrock geochemistry.

Despite the difficulties, geochemical contouring shows a strong, elongate NW-trending Ni anomaly (also present though less well-defined for Co, Cu, and Zn). This trend parallels that of ultrabasic bodies further to the south and it is reasonable to suggest that it reflects a non-outcropping ultrabasic body. Again, this anomaly is considered to be worth investigating further because of the possibility of associated Ni mineralisation.

INFLUENCE OF CATCHMENT GEOCHEMISTRY ON ESTUARINE GEOCHEMISTRY

Worldwide, there are various examples of mineral deposits in inferred estuarine sequences, such as the phosphorites of the east coast of the United States (Pevear, 1966) and the uranium deposits of the Texas Gulf coast. Some of the deposits may have formed diagenetically, but others have formed as a result of depositional conditions, including the influence of the associated drainage basin. One must ask, under what conditions are high Cu, Pb, and Zn values in the catchment likely to lead to correspondingly high Cu, Pb, and Zn values in the estuarine sediments? This is hard to answer at Broad Sound because of the addition of biogenic carbonate to the estuarine system. However, when the non-calcareous fraction of the sediments is considered as a whole, the average Broad Sound terrigenous sediment has a trace-element composition somewhat similar to that of the Broad Sound catchment in the case of P_2O_5, Cu, and Pb, whereas Zn, Co, Ni, Fe, Mn, and Cr increase markedly in the estuary. Some ratios, such as Fe/Mn and Fe/Ni, are similar in both the

estuary and the catchment. The increased concentration is probably due partly to the finer grainsize of the estuarine muds, though there may too be some scavenging of metals from solution when the clays flocculate on reaching the sea. Thus, patterns of elemental dispersal and concentration are rather different in the estuary compared with in the catchment. This is supported by the observation that many inter-element correlations that are apparent in the estuarine sediments (such as Ni-Fe, Ni-Mn, and Fe-Cr) are not evident in the drainage-basin soils, stream sediments, or bedrock.

It might be supposed that, despite this, differences in elemental concentration in the individual catchments will be reflected in the corresponding estuary. However, when this was statistically tested for Broad Sound estuaries it was found not to be true: the estuarine sediments were found to be far more homogeneous than the catchment soils. It appears, then, that at Broad Sound, depositional environment and post-depositional conditions exert a much greater influence on the geochemistry of estuarine sediments than does catchment geochemistry. In the general context of the formation of non-detrital mineral deposits in estuarine sediments it seems fair to conclude that, although the geochemistry of the regional hinterland has a broad general influence, the immediate catchment of a local estuary has little if any specific influence on the geochemistry of that estuary, because of sediment homogenisation and other depositional and post-depositional processes.

It could be argued that the processes which have caused sediments to homogenise in modern estuaries are the result of the Holocene sea-level rise, and consequently are atypical of the geological past as a whole. Similarly, estuaries themselves may be abnormally common at the present time as a result of the Holocene sea-level rise. Nevertheless it is reasonable to extrapolate from Broad Sound to ancient estuarine sequences and consider that their geochemistry will owe little to the geochemistry of the immediate drainage basin. Similarly, where ore deposits of non-detrital minerals exist in fossil estuarine sequences the Broad Sound evidence suggests that they too are far more likely to have been the product of depositional and post-depositional processes than of provenance.

TRACE ELEMENTS AS INDICATORS OF DEPOSITIONAL ENVIRONMENTS

The Broad Sound study has shown that absolute trace element concentrations are of little or no use as environmental indicators, because of input of biogenic carbonate. If the non-calcareous fraction is considered alone (i.e. recalculated on a carbonate-free basis), then a measure of discrimination between some of the depositional environments seems possible. There are, for instance, statistically significant differences in the Cr, Ni, and Zn concentrations in mangrove-swamp muds and supratidal-flat muds. Zn similarly distinguishes between the open-intertidal environment and the mangrove-channel environment (which is also intertidal), whereas Ba, Cr, and Ti will separate shallow-marine and open-intertidal sediments. Whether these findings at Broad Sound can be applied to similar environments elsewhere is not known. There is obviously a need for more studies of this type.

Elemental ratios may be of more general application, particularly where the ratios are between elements that are differentially sensitive to physico-chemical conditions. The Broad Sound study suggested that Mn/Fe, Cu/Pb, and Cu/Zn are potentially the most useful ratios for distinguishing between depositional environments, and perhaps also for the determination of ancient shorelines, but again far more work is necessary before these ratios can really be regarded as useful environmental indicators.

All in all, a far more reliable environmental reconstruction may be made for Broad Sound (and comparable) sediments, if the overall sedimentary sequence is considered, using grainsize, mud/sand/gravel ratios, carbonate abundance, faunal and floral assemblage, and sedimentary structures, rather than employing only geochemical parameters.

THE WEATHERING OF SHELLS

Weathering is rapid under tropical or sub-tropical conditions, though it is generally not possible to measure the rate because of the lack of material which can be dated absolutely. However, the dating of shells in the Broad Sound cheniers, with ages ranging up to 5500 years BP, offered an excellent opportunity to determine fairly precisely the rate of subaerial leaching or concentration of some elements from shells. For instance the Broad Sound data show that over a period of 5000 years P_2O_5 decreased from 720 to 270 ppm and Sr from 910 to 490 ppm. In this same period the Fe and Mn contents tended to increase. Therefore, using these observations it may be possible to predict the order of magnitude of mobility of these elements in shelly calcareous sediments, during subaerial weathering. A related feature is the loss of B. B is commonly used as an indicator of palaeosalinity;

however, the Broad Sound results suggest that in subaerial weathering it is comparatively mobile, and may not always be a reliable palaeosalinity indicator in carbonate rocks which have been weathered subaerially.

A further implication of the work is in the use of shells to establish pollution levels in estuaries. Modern oyster shells in some of the Tasmanian estuaries have much higher metal contents than those from aboriginal middens in the same area (S. J. Thrower, CSIRO Division of Food Research, personal communication). The Tasmanian middens are up to several thousand years old and it could perhaps be argued that their lower metal contents are the result of metal leaching during weathering. However, the Broad Sound work shows that no such trend results from weathering. This suggests that the high metal content of some modern shells in, for instance, Tasmania, is a recent phenomenon, perhaps related to present-day pollution. Conversely, it also suggests that unburnt shells from aboriginal middens may provide excellent base-level material against which to measure present-day levels of pollution; chemical changes occurring as a result of weathering over the past few thousand years appear to be relatively minor when compared with chemical changes likely to result from pollutants.

PHOSPHATE DEPOSITS IN THE ESTUARINE ENVIRONMENT

A major reason for the Broad Sound study was to determine processes responsible for mobilising and concentrating phosphorus in an estuarine environment, and in turn to speculate on the relevance of these processes to the formation of phosphate deposits in the Georgina Basin. Significant findings from the present study and from Cook & Mayo (1978), include:

(1) The phosphate content of the catchment has little influence on the phosphate content of the estuarine sediments. Depositional and post-depositional processes appear to be far more important than provenance.

(2) The phosphate content of Broad Sound waters is generally low, indicating that this estuary is not a high-phosphate site.

(3) The phosphate content of the overlying water is not necessarily the most important control on the phosphate content of estuarine sediments: the waters at the northern end of Broad Sound have the lowest phosphate content, yet the sediments of this same area have the highest phosphate content.

(4) The rate of sedimentation is an important control over phosphate content: the northern end of the Sound, where the sedimentation rate is lowest and the abundance of relict sediments highest, is the area with the highest phosphate contents in the sediments.

(5) The phosphate is located in two sites: in the calcareous sediments and in the clays, though whether it is absorbed or occupies a lattice position in the clays is uncertain.

(6) High phosphate contents are found in the interstitial waters of the supratidal environments.

(7) The phosphate-rich pore waters are a potent agent for phosphatisation. Phosphatisation of dolomite appears to occur most readily, the highest phosphate contents being found in the Holocene dolomite nodules.

In the Georgina Basin, there appear to be two types of phosphorite deposits — pelletal phosphorites which were formed under submarine conditions, and fine-grained phosphorites formed partly subaerially (Cook, 1972). If the depositional environment was a bay or estuary, then there must have been a low rate of terrigenous input, as the Broad Sound study has clearly shown that a high rate of terrigenous or calcareous sedimentation is incompatible with a high phosphorus content. An additional process is the winnowing of fine material at the northern end of Broad Sound. In this area, phosphate levels in the sediment are relatively high. Therefore, by implication, winnowing is likely to have been an important process in the formation of the Georgina Basin pelletal phosphorites. Winnowing has been shown to have been important in the formation of the pelletal and nodular phosphorites of the Stairway Sandstone of the Amadeus Basin (Cook, 1967). The winnowing currents also transport more water across the surface of the sediment, thus resulting in enhanced phosphatisation. One further point arising from the pattern of sediment dispersal at Broad Sound is that most of the carbonate is derived from the continental shelf, Broad Sound merely having the role of a trap. By analogy, the Georgina Basin phosphorites may have been formed on the outer part of the continental shelf, and may then have been swept shoreward into estuarine locations where the phosphatic sediment was trapped to form a phosphate deposit.

Perhaps one of the more important implications for phosphate from the Broad Sound study is the discovery of high phosphate in the pore

waters of the supratidal zone, and the associated phosphatisation. The sediments of this zone are primarily terrigenous clays with a low carbonate content. There is no positive evidence of phosphatisation of clays, though the clays do have a relatively high phosphate content, and information from elsewhere (Baturin, 1971) suggests that phosphatisation of clays can occur fairly readily in continental-shelf deposits. There is, however, evidence from Broad Sound of the phosphatisation of dolomite. In some of the fine-grained phosphorites of the Georgina Basin there is clear evidence of the phosphatisation of dolomite rhombs (as well as of clay particles), and it is apparent from Broad Sound data that a likely site for such a mechanism is the supratidal zone. Supratidal phosphorites have seldom been described, in part because of the difficulty in recognising these fine-grained sediments as phosphorites (those of the Georgina Basin look like kaolinitic mudstones). However, they are probably rather more common than has previously been supposed, forming as a result of early-diagenetic phosphatisation of calcareous or clayey, high-intertidal or supratidal sediments by phosphate-rich pore waters. But it should be emphasised that, despite the high phosphorus content of the pore waters, no separate apatite mineral phase was in fact identified. The reason for this may lie in the high Mg/Ca ratio of the Broad Sound pore waters. Martens & Harris (1970) have shown that Mg^{++} ions inhibit the precipitation of apatite from solution. Where a decrease in the Mg/Ca ratio can be induced by mixing of pore waters with for instance low-Mg groundwaters, then precipitation of apatite may occur. Further work is required in hypersaline depositional systems, such as the Broad Sound supratidal flats, in order to test this hypothesis.

ESTUARINE GEOCHEMICAL PROCESSES

Estuaries are vitally important to man. Lauff (1967) points out that 'Estuaries are significant to human welfare through their role in transportation, production of food, waste disposal, and various recreational pursuits. Many of the world's largest metropolitan areas have developed near estuaries and these waters have become adversely affected by human activities'. One of the major adverse changes has been in the input of metals, with concentrations reaching toxic levels in some cases. Therefore an understanding of the geochemical processes in estuaries is essential for estuarine management. Studies such as those carried out at Broad Sound help in two ways. They provide basic data on elemental levels in unpolluted estuaries. These data can then be used to measure future changes in that estuary, or alternatively, by inference, to determine the changes which have already taken place in similar estuaries that have been subjected to human activity. They also provide information on the processes which fix or mobilise metals. The Broad Sound study shows that there is a high level of metal fixation by the estuarine sediments, particularly in the supratidal zone. There are two conclusions which may be drawn from this. Firstly, if the muds of the supratidal zone are 'reclaimed', this will lead to a major change in the hydrology of these sediments and might lead to some release of metals from them. Secondly, if there is a decrease in the amount of clay entering the estuary (perhaps due to future damming of the headwaters) yet no corresponding decrease in the input of metals in solution, then there is likely to be a build-up of metals both in the water of the estuary and in the sediments, because of the smaller amount of clay available for metal scavenging.

The nutrient level in estuaries is also important. If the input is artifically high, eutrophication may result; if it is depleted, fish catches may decline. The Broad Sound study was concerned with an unpolluted estuary with a negligible input of phosphate from agricultural or domestic sources. It was found that by far the highest phosphate level in the water column was found in the mangrove channels. This input into the main body of the estuary is likely to be of very great importance to the whole Broad Sound ecosystem. This input could be upset by, for instance, building dams across the channels, or by 'reclaiming' the mangrove swamps and associated environments, effectively withdrawing them from the estuarine system. Such 'reclamation' has not been done at Broad Sound, but is happening in many other coastal areas. The Broad Sound study suggests that unless such a loss of nutrients is balanced by increased man-induced input, it could conceivably produce a significant reduction in estuarine biomass. Clearly such environmental modification should only be undertaken after all the implications have been evaluated.

REFERENCES

ADAMS, J.E., & RHODES, M.C., 1960 — Dolomitization by seepage refluxion. *Bulletin, American Association of Petroleum Geologists* 44(2), 1912-20.

AHRENS, L.H., & TAYLOR, S.R., 1961 — SPECTROCHEMICAL ANALYSIS. *Addison-Wesley, Massachusetts.*

ARMSTRONG, K.J., 1973 — Methods of sample preparation and analysis used in the Broad Sound estuary study project. *Bureau of Mineral Resources, Australia, Record* 1973/73 (unpublished).

BATES, R.G., 1964 — DETERMINATION OF pH: THEORY AND PRACTICE. *John Wiley & Sons Inc., New York.*

BATURIN, G.N., 1971 — Stages of phosphorite formation on the ocean floor. *Nature* (Physical Sciences), 232(29), 61-62.

BEN-YAAKOV, S., 1973 — pH buffering of pore water of recent anoxic marine sediments. *Limnology and Oceanography,* 18, (1), 85-94.

BERNER, R.A., 1964 — Iron sulfides formed from aqueous solution at low temperatures and atmospheric pressure. *Journal of Geology,* 72, 293-306.

BERNER, R.A., 1971 — PRINCIPLES OF CHEMICAL SEDIMENTOLOGY. *McGraw-Hill, New York.*

BIGGS, R.B., 1967 — The sediments of Chesapeake Bay. *In* LAUFF, G.H. (Editor) — ESTUARIES. *American Association for the Advancement of Science, Publication* 83, 239-60.

BURGIS, W.A., 1974 — Cainozoic history of the Torilla Peninsula, Broad Sound. *Bureau of Mineral Resources, Australia, Report* 172.

CLARKE, F.W., 1924 — Data of geochemistry. *United States Geological Survey Bulletin* 770.

COOK, P.J., 1967 — Winnowing — an important process in the concentration of the Stairway Sandstone (Ordovician) phosphorites of Central Australia. *Journal of Sedimentary Petrology,* 37(4), 818-828.

COOK, P.J., 1972 — Petrology and geochemistry of the phosphate deposits of northwest Queensland, Australia. *Economic Geology,* 67, 1193-1213.

COOK, P.J., 1973 — Supratidal environment and geochemistry of some recent dolomite concretions, Broad Sound, Queensland, Australia. *Journal of Sedimentary Petrology,* 43(4), 998-1011.

COOK, P.J., 1974 — Geochemistry and diagenesis of interstitial fluids and associated calcareous oozes, Deep Sea Drilling Project, Leg 27, Site 262. *In* VEEVERS, J.J., & HEIRTZLER, J.M. & OTHERS — INITIAL REPORTS OF THE DEEP SEA DRILLING PROJECT, VOLUME 27. *U.S. Government Printing Service, Washington,* 463-480.

COOK, P.J., 1976 — Mobility of boron during diagenesis and possible implications for the determination of palaeosalinity. *Nature,* 268, 426.

COOK, P.J., & MAYO, W., 1978 — Sedimentology and Holocene history of a tropical estuary (Broad Sound, Queensland). *Bureau of Mineral Resources, Australia, Bulletin* 170.

COOK, P.J., & POLACH, H.A., 1973a — A chenier sequence at Broad Sound, Queensland, and evidence against a Holocene high sea level. *Marine Geology,* 14, 253-68.

COOK, P.J., & POLACH, H.A., 1973b — Discovery of recent supratidal dolomite at Broad Sound, Queensland. *Search,* 4(3), 78-79.

CULBERSON, C., & PYTKOWICZ, R.M., 1968 — Effect of pressure on carbonic acid, boric acid and the pH in sea water. *Limnology & Oceanography,* 13, 403-417.

DAVIS, J.C., 1973 — STATISTICS AND DATA ANALYSIS IN GEOLOGY. *John Wiley & Sons Inc., New York.*

DEGENS, E.T., 1958 — Environmental studies of Carboniferous sediments, 2. Application of geochemical criteria. *Bulletin, American Association of Petroleum Geologists,* 42, 987-998.

DE KEYSER, F., & COOK, P.J., 1972 — Geology of the Middle Cambrian phosphorites and associated sediments of northwest Queensland. *Bureau of Mineral Resources, Australia, Bulletin* 138.

DEPARTMENT OF NATIONAL DEVELOPMENT, 1965 — Fitzroy Region, Queensland: Climate. *Department of National Development, Canberra, Resources Series.*

ERNST, W., 1970 — GEOCHEMICAL FACIES ANALYSIS. *Elsevier, Amsterdam.*

GARRELS, R.M., & CHRIST, C.L., 1965 — SOLUTIONS, MINERALS AND EQUILIBRIA. *Harper, New York.*

GARRELS, R.M., & MACKENZIE, F.T., 1971 — EVOLUTION OF SEDIMENTARY ROCKS. *Norton, New York.*

GIBSON, D.L., 1972 — Clay mineralogy of recent sediments of the Broad Sound area. *Bureau of Mineral Resources, Australia, Record* 1972/75 (unpublished).

GOLDHABER, M.B., & KAPLAN, I.R., 1974 — The sulfur cycle. *In* GOLDBERG, E.D. (Editor) — THE SEA, 5, 569-655. *John Wiley & Sons Inc., New York.*

GOLDSCHMIDT, V.M., 1954 — GEOCHEMISTRY. *Clarendon Press, Oxford.*

GREEN, J., 1959 — Geochemical table of the elements for 1959. *Bulletin, Geological Society of America,* 70, 1127-84.

GRIM, R.E., 1968 — CLAY MINERALOGY. *McGraw-Hill, New York.*

GULYAYEVA, L.A., & PUNANOVA, S.A., 1974 — Trace elements in sedimentary rocks, formation water and oil. *Doklady* (Earth Sciences Section), 218, 180-82.

GUNN, R.H., 1972 — Soils of the Shoalwater Bay area. *CSIRO Division of Land Research, Technical Memoir* 72/10, 70-84 (unpublished).

HART, M.G.R., 1962 — Observations on the source of acid in empoldered mangrove soils. 1. Formation of elemental sulphur. *Plant & Soil,* 17, 87-98.

HAWKES, H.E., & WEBB, J.S., 1962 — GEOCHEMISTRY IN MINERAL EXPLORATION. *Harper, New York.*

HIRST, D.M., 1962a — The geochemistry of modern marine sediments from the Gulf of Paria. I — The relationship between the mineralogy and the distribution of minor elements. *Geochimica et Cosmochimica Acta* 26, 309-34.

HIRST, D.M., 1962b — The geochemistry of modern marine sediments from the Gulf of Paria. II — The location and distribution of trace elements. *Geochimica et Cosmochimica Acta* 26, 1147-87.

ISBELL, R.F., & HUBBLE, G.D., 1967 — Fitzroy Region, Queensland: Soils. *Department of National Development, Canberra, Resources Series.*

JARDINE, F., 1928 — The Broad Sound drainage in relation to the Fitzroy River. *Report to Great Barrier Reef Committee* 2, 88-92.

KAZAKOV, A.V., 1938 — The phosphorite facies and the genesis of phosphorites. *17th International Geology Congress, Moscow*, 95-113.

KEITH, M.L., & DEGENS, E.T., 1959 — Geochemical indicators of marine and freshwater sediments. *In* ABELSON, P.H., (Editor) — RESEARCHES IN GEOCHEMISTRY. *John Wiley & Sons, Inc., New York.*

KERSHAW, A.P., 1975 — Late Quaternary vegetation and climate in northeast Australia. *In* SUGGATE, R.P. & CRESSWELL, M.M. (Editors) *Quaternary Studies, Royal Society of New Zealand, Wellington*, 181-187.

KINSMANN, D.J.J., 1969 — Modes of formation, sedimentary associations, and diagenetic features of shallow water and supratidal evaporites. *Bulletin, American Association of Petroleum Geologists*, 53, 830-40.

KIRKEGAARD, A.G., SHAW, R.D. & MURRAY, C.G., 1970 — Geology of the Rockhampton and Port Clinton 1:250 000 Sheet areas. *Geological Survey of Queensland, Report* 38.

KRAMER, J.R. 1964 — Seawater: saturation with apatites and carbonates. *Science* 146, 637-38.

KRUMBEIN, W.C., & GARRELS, R.M., 1952 — Origin and classification of chemical sediments in terms of pH and oxidation reduction potentials. *Journal of Geology*, 60, 1-33.

LAUFF, G.E. (Editor), 1967 — ESTUARIES. *American Association for the Advancement of Science, Publication* 83.

LE RICHE, H.H., 1959 — The distribution of certain trace elements in the Lower Lias of Southern England. *Geochimica et Cosmochimica Acta*, 16, 101-22.

McALPINE, J.R., 1972 — Climate of the Shoalwater Bay area. *CSIRO Division of Land Research Technical Memoir*, 72/10, 44-56 (unpublished).

MALONE, E.J., OLGERS, F., & KIRKEGAARD, A.G., 1969 — The geology of the Duaringa and Saint Lawrence 1:250 000 Sheet areas, Queensland. *Bureau of Mineral Resources, Australia, Report* 121.

MARTENS, C.S., & HARRISS, R.C., 1970 — Inhibition of apatite precipitation in the marine environment by magnesium ions. *Geochimica et Cosmochimica Acta*, 238, 863-879.

MAXWELL, W.G.H., 1968 — ATLAS OF THE GREAT BARRIER REEF. *Elsevier, Amsterdam.*

MAYO, W., 1972 — A computer program for calculating statistical parameters of grainsize distribution derived from various analytical methods. *Bureau of Mineral Resources, Australia,* Record 1972/140 (unpublished).

MAYO, W., 1974 — Determining the distribution and classification of the Broad Sound surficial sediments using numerical techniques. *Bureau of Mineral Resources, Australia, Record* 1974/85 (unpublished).

MAYO W., 1976 — Numerical techniques applied to the geochemistry of some estuarine sediments from Broad Sound, Queensland. *BMR Journal of Australian Geology & Geophysics*, 1(3).

MAYO, W., & LONG, K.A., 1976 — Documentation of BMR Geological Branch computer programs. *Bureau of Mineral Resources, Australia, Record* 1976/82 (unpublished); *BMR Microform* MF4.

MEYERS, P.A., & QUINN, J.G., 1974 — Organic matter on clay minerals and marine sediments — effect on adsorption of dissolved copper, phosphate, and lipids from saline solutions. *Chemical Geology*, 13, 63-68.

NICHOLLS, G.D., & LORING, D.H., 1962 — The geochemistry of some British Carboniferous sediments. *Geochimica et Cosmochimica Acta*, 26, 181-223.

NIX, J., & GOODWIN, T., 1970 — The simultaneous extraction of Fe, Mn, Cu, Co, Ni, Cr, Pb, and Zn from natural water for determination by AAS. *Atomic Absorption Newsletter*, 9(6).

ORR, A. P., — MOOREHOUSE, F. W., 1933 — Physical and chemical conditions in mangrove swamps. *Great Barrier Reef Expedition 1928-29. Science Report* 2, 102-110.

PARK, K. D., HOOD, D. W., & ODUM, H. T., 1958 — Diurnal pH variation in Texas bays, and its application to primary production estimation. *Publications of the Institute of Marine Science, Texas*, 6, 47-64.

PETTIJOHN, F. J., 1963 — Chemical composition of sandstones — excluding carbonate and volcanic sands. *In* FLEISCHER, M. (Editor), Data of Geochemistry *U.S. Geological Survey Professional Paper* 440-S.

PEVEAR, D. R., 1966 — The estuarine formation of United States Atlantic coastal plain phosphorites. *Economic Geology*, 61(2), 251-256.

PILKEY, O. H., & HARRISS, R. C., 1966 — The effect of intertidal environment on the composition of calcareous skeletal material. *Oceanography*, 11(3), 381-85.

PILKEY, O. H., & GOODELL, H. G., 1963 — Trace elements in recent mollusc shells. *Limnology & Oceanography* 8(2), 137-48.

REINSON, G. E., 1975 — Geochemistry of muds from a shallow restricted estuary, Australia. *Marine Geology*, 19, 297-314.

REINSON, G. E., 1977 — Hydrology and sediments of a temperature estuary — Mallacoota Inlet, Victoria. *Bureau of Mineral Resources, Australia, Bulletin* 178.

RICKARD, D. T., 1969 — The chemistry of iron sulphide formation at low temperatures. *Stockholm Contributions in Geology*, 20, 67-95.

RICKARD, D. T., 1970 — The origin of framboids. *Lithos*, 3, 269-293.

ROBERSON, C. E., 1966 — Solubility implications of apatite in seawater. *US Geological Survey, Professional Paper*, 550-D, 178-85.

RONOV, A. B., & MIGDISOV, A. A., 1971 — Geochemical hvxtry of the crystalline basement and the sedimentary cover of the Russian and North American platforms. *Sedimentology*, 16, 137-85.

RUCKER, J. B., & VALENTINE, J. W., 1961 — Salinity response of trace element concentration in *Crassostrea virginica. Nature*, 190, 1099-1100.

SHAW, D. M., 1956 — Geochemistry of pelitic rocks, Part III. Major elements and general geochemistry. *Bulletin, Geological Society of America*, 67, 919-934.

SKIRROW, G., 1965 — The dissolved gases — carbon dioxide. *In* RILEY, J.P., & SKIRROW, G. (Editors) — CHEMICAL OCEANOGRAPHY. *Academic Press, London*, 1, 227-322.

SPENCER, D. W., DEGENS, E. T., & KULBICKI, G., 1968 — Factors affecting element distributions in sediments. *In* L.H. AHRENS (Editor) — ORIGIN AND DISTRIBUTION OF THE ELEMENTS, *Pergamon Press, Oxford*, 981-998.

STOUT, P. P., 1939 — Alterations in the crystal structure of the clay minerals as a result of phosphate fixation. *Proceedings, Soil Science Society of America*, 4, 177-182.

THORNTON, I., & GIGLIOLI, M. E. C., 1965 — The mangrove swamps of Keneba, Lower Gambia River Basin. *Journal of Applied Ecology*, 2, 257-69.

THORSTENSON, D. C., 1970 — Equilibrium distribution applied to small organic molecules in natural waters. *Geochimica et Cosmochimica Acta*, 34, 745-70.

TUREKIAN, K. K., 1964 — The marine geochemistry of strontium. *Geochimica et Cosmochimica Acta*, 28, 1479-96.

TUREKIAN, K. K., & KULP, J. L., 1956 — The geochemistry of strontium. *Geochimica et Cosmochimica Acta*, 10, 245-96.

TUREKIAN, K. K., & WEDEPOHL, K. H., 1961 — Distribution of the elements in some major rock units of the Earth's crust. *Bulletin, Geological Society of America*, 72, 175-92.

WALSH, G. E., 1967 — An ecological study of a Hawaiian mangrove swamp. *In* LAUFF, G. H. (Editor) — ESTUARIES. *American Association for the Advancement of Science, Publication* 83, 420-31.

WEDEPOHL, K. H. (Editor), 1970 — HANDBOOK OF GEOCHEMISTRY. *Springer-Verlag, Berlin.*

WIEDEMANN, H. V., 1969 — Solutions in intertidal and supratidal environments of modern carbonate sedimentation: their implication on diagenesis. *Chemical Geology*, 4, 393-409.

APPENDIX A1
TABLES LISTING MAJOR AND MINOR OXIDE COMPOSITION (PERCENT) OF SEDIMENT SAMPLES FROM THE ESTUARY

TABLE A32. GRAVEL FACIES, SHALLOW-MARINE ENVIRONMENT

	70636 266	70636 290	70636 308	70636 315
SiO_2	15.6	15.2	27.4	11.5
Al_2O_3	1.9	2.2	3.0	1.8
Fe_2O_3 (total)	2.0	1.7	1.75	1.9
CaO	41.0	43.0	34.0	42.5
MgO	2.0	1.3	1.55	3.2
Na_2O	0.13	0.36	0.45	0.39
K_2O	0.5	0.5	0.5	0.5
MnO	0.11	0.10	0.19	0.11
P_2O_5	0.13	0.14	0.14	0.15
TiO_2	0.12	0.16	0.19	0.11
Cr_2O_3	0.1	0.1	0.1	0.1
V_2O_5	0.05	0.05	0.05	0.05
CO_2	33.9	33.5	28.0	34.4
H_2O-	0.26	0.28	0.47	0.39
H_2O+	1.88	1.48	2.30	1.79
Total	99.68	100.07	100.09	98.89
Loss on ignition	35.7	35.6	29.7	37.6

TABLE A33. SANDY FACIES, SHALLOW-MARINE ENVIRONMENT

	70636 072	70636 215	70636 246	70636 262	70636 266	70636 313
SiO_2	49.0	52.0	66.0	63.5	15.6	18.4
Al_2O_3	2.2	4.0	4.1	3.3	1.9	1.5
Fe_2O_3 (total)	2.2	1.1	1.4	0.81	2.0	1.2
CaO	22.0	20.0	12.3	14.6	41.0	40.0
MgO	1.2	1.3	1.2	1.5	2.0	3.0
Na_2O	0.89	1.1	1.0	0.77	0.13	0.36
K_2O	0.05	0.5	0.6	0.6	0.5	0.5
MnO	0.13	0.08	0.04	0.07	0.11	0.14
P_2O_5	0.13	0.15	0.05	0.11	0.13	0.14
TiO_2	0.19	0.47	0.48	0.35	0.12	0.08
Cr_2O_3	0.1	0.1	0.1	0.08	0.1	0.1
V_2O_5	0.05	0.05	0.05	0.05	0.05	0.05
CO_2	19.3	16.8	10.0	11.8	33.9	31.5
H_2O-	0.14	0.36	0.38	0.52	0.26	0.26
H_2O+	1.65	2.40	1.85	1.96	1.88	1.92
Total	100.13	100.41	99.55	100.02	99.68	99.15
Loss on ignition	20.9	18.9	12.0	13.4	35.7	33.9

TABLE A34. SANDY FACIES, OPEN-INTERTIDAL ENVIRONMENT

	70636 065	70636 113	70636 137	70636 152	70636 226	70636 229	70636 320
SiO_2	74.0	41.0	72.0	65.0	55.0	54.5	20.0
$A1_2O_3$	2.1	4.0	5.75	3.7	3.4	7.8	1.5
Fe_2O_3 (total)	0.9	0.64	2.3	1.0	0.54	1.5	2.0
CaO	10.2	25.0	8.2	13.5	19.0	15.0	38.0
MgO	0.76	1.95	0.70	1.03	1.4	1.55	3.1
Na	0.62	1.2	1.6	1.25	0.90	1.55	0.44
K_2O	0.5	0.5	1.15	0.6	0.65	1.17	0.5
MnO	0.07	0.08	0.19	0.08	0.07	0.03	0.16
P_2O_5	0.13	0.14	0.12	0.03	0.12	0.05	0.14
TiO_2	0.36	0.26	0.36	0.34	0.36	0.56	0.09
Cr_2O_3	0.1	0.1	0.1	0.1	0.1	0.1	0.1
V_2O_5	0.05	0.05	0.05	0.05	0.05	0.05	0.05
CO_2	8.3	20.8	6.35	10.7	16.5	12.2	31.6
H_2O-	0.18	1.43	0.11	0.17	0.17	0.66	0.25
H_2O+	0.83	0.94	1.23	1.35	1.85	4.10	1.99
Total	99.10	98.09	100.21	97.91	100.11	101.82	99.92
Loss on ignition	98.6	23.3	7.30	12.5	17.8	15.5	34.1

TABLE A35. MUDDY FACIES, OPEN-INTERTIDAL ENVIRONMENT

	70636 122	70636 150	70636 214
SiO_2	54.0	55.0	50.0
Al_2O_3	9.3	7.95	9.8
Fe_2O_3 (total)	3.2	1.45	2.6
CaO	12.5	14.0	14.2
MgO	1.54	1.9	2.05
Na_2O	1.6	1.25	1.42
K_2O	0.6	1.45	1.15
MnO	0.06	0.07	0.03
P_2O_5	0.14	0.09	0.09
TiO_2	0.63	0.59	0.70
Cr_2O_3	0.1	0.1	0.1
V_2O_5	0.05	0.05	0.05
CO_2	10.1	11.3	10.8
H_2O-	1.41	1.23	1.52
H_2O+	3.30	3.05	4.15
Total	98.53	99.48	98.66
Loss on ignition	14.3	15.0	16.0

TABLE A36. MANGROVE-CHANNEL ENVIRONMENT

	70636 332	70636 336	70636 338	70636 341	70636 343
SiO_2	51.0	52.0	56.0	52.0	54.0
Al_2O_3	9.3	11.5	11.2	13.4	12.5
Fe_2O_3 (total)	2.5	5.8	3.7	5.1	4.1
CaO	14.1	9.3	8.4	7.9	8.2
MgO	2.2	2.0	2.3	2.2	2.4
Na_2O	1.2	1.4	1.2	1.4	1.25
K_2O	1.45	1.2	1.7	1.7	2.0
MnO	0.06	0.22	0.08	0.07	0.09
P_2O_5	0.12	0.09	0.14	0.12	0.12
TiO_2	0.64	0.76	0.71	0.88	0.86
Cr_2O_3	0.1	0.1	0.1	0.1	0.1
V_2O_5	0.05	0.05	0.05	0.05	0.05
CO_2	10.2	8.90	7.25	5.55	11.6
H_2O-	1.50	2.30	2.45	2.75	3.05
H_2O+	4.15	4.85	4.45	5.60	4.95
Total	98.57	100.47	99.73	98.82	105.27
Loss on ignition	15.7	12.9	11.4	11.9	11.7

TABLE A37. MANGROVE-SWAMP ENVIRONMENT

	70636 127	70636 138	70636 146	70636 275	70636 276	70636 299	70636 321
SiO_2	56.0	53.0	59.0	52.0	53.0	53.0	55.0
Al_2O_3	11.0	12.7	12.5	10.5	10.4	7.9	10.3
Fe_2O_3 (total)	2.9	4.8	3.75	2.6	2.8	1.5	3.0
CaO	9.5	7.8	6.1	12.1	10.7	15.7	10.2
MgO	1.95	2.1	1.7	2.0	1.9	1.7	1.6
Na_2O	1.3	1.5	1.7	1.2	1.3	1.3	1.4
K_2O	1.7	1.4	1.7	1.2	1.2	1.45	1.4
MnO	0.09	0.07	0.06	0.05	0.06	0.05	0.03
P_2O_5	0.14	0.11	0.09	0.15	0.17	0.14	0.11
TiO_2	0.83	0.94	1.0	0.72	0.75	0.58	0.75
Cr_2O_3	0.1	0.1	0.1	0.1	0.1	0.1	0.1
V_2O_5	0.05	0.05	0.05	0.05	0.05	0.05	0.05
CO_2	7.0	5.7	4.35	9.10	8.30	11.6	7.60
H_2O-	1.98	2.3	2.15	1.99	2.15	1.10	2.15
H_2O+	3.25	4.90	4.05	4.15	4.05	3.30	2.10
Total	97.79	97.47	98.30	97.91	96.93	99.47	95.79
Loss on ignition	12.7	12.7	10.5	14.8	14.4	15.7	13.8

TABLE A38. SUPRATIDAL-FLAT ENVIRONMENT

	70636 019	70636 033	70636 190	70636 232	70636 302
SiO_2	67.0	58.0	62.0	66.0	62.0
Al_2O_3	13.3	14.8	14.7	14.0	12.8
Fe_2O_3 (total)	5.0	6.8	5.3	4.8	5.9
CaO	0.86	0.87	1.36	0.48	1.25
MgO	1.6	4.0	3.9	2.3	2.0
Na_2O	0.32	0.8	0.95	0.3	2.3
K_2O	2.15	1.7	1.73	1.5	1.73
MnO	0.13	0.15	0.14	0.13	0.06
P_2O_5	0.13	0.12	0.11	0.15	0.12
TiO_2	0.86	0.91	0.92	0.96	0.93
Cr_2O_3	0.15	0.25	0.1	0.1	0.1
V_2O_5	0.05	0.05	0.05	0.05	0.05
CO_2	0.25	0.40	0.23	0.27	0.39
H_2O-	2.45	3.05	2.25	3.0	3.4
H_2O+	5.15	7.55	6.10	6.25	5.85
Total	99.04	99.45	99.84	100.19	98.90
Loss on ignition	5.85	8.45	6.70	6.85	7.90

TABLE A39. NODULES, SHALLOW-MARINE ENVIRONMENT

	70636 220N	70636 266N	70636 289N	70636 308N	70636 311N
SiO_2	13.6	11.7	15.6	15.0	10.6
Al_2O_3	2.4	2.6	2.7	3.3	2.7
Fe_2O_3 (total)	3.1	3.2	3.2	3.5	4.7
CaO	42.0	43.0	40.0	41.0	42.0
MgO	1.6	1.8	1.8	1.4	1.75
Na_2O	0.52	0.07	0.15	0.53	0.34
K_2O	0.5	0.5	0.5	0.5	0.5
MnO	0.18	0.22	0.23	0.27	0.42
P_2O_5	0.17	0.20	0.21	0.22	0.16
TiO_2	0.18	0.17	0.19	0.22	0.17
Cr_2O_3	0.1	0.1	0.1	0.1	0.1
V_2O_5	0.05	0.05	0.05	0.05	0.05
CO_2	33.0	33.1	32.7	32.0	35.0
H_2O-	0.21	0.32	0.46	0.61	0.37
H_2O+	1.77	1.98	1.92	1.91	1.95
Total	99.98	99.01	100.70	100.60	100.81
Loss on ignition	35.9	36.0	34.4	33.9	36.3

APPENDIX A2
PHYSICO-CHEMICAL CHARACTERISTICS OF ESTUARINE SEDIMENTS AND THEIR EXPRESSED PORE WATERS

Sample localities are shown in Figure A74.

Sample No. 71636—	Depth (cm)	IN-SITU		EXPRESSED PORE FLUIDS							P_2O_5 of sediments (ppm)
		Eh (mV)	pH	Eh (mV)	pH	Salinity (ppt)	Mg (ppm)	Ca (ppm)	K (ppm)	P_2O_5 (ppm)	
OPEN-INTERTIDAL (SAND)											
048	60	+130	7.6	+150	7.6	30.0	—	380	—	—	480
047	60	+210	7.4	+160	7.6	31.0	—	390	—	0.01	430
049	60	+140	7.7	+170	7.4	25.8	—	320	—	0.01	—
050	60	+200	7.3	+150	7.7	24.8	1080	300	280	0.01	—
051	60	+150	7.2	+190	7.4	28.0	—	340	—	0.01	—
052	60	+140	7.4	+160	7.4	33.0	—	370	—	0.02	—
053	30	+150	7.3	+140	7.5	31.5	1410	360	365	0.01	430
054	30	+190	7.5	+150	7.6	31.0	—	350	—	0.01	410
055	30	+170	7.7	+130	7.5	28.0	—	330	—	0.01	500
056	60	+150	7.7	+130	7.5	28.5	—	320	—	0.01	450
057	30	+170	7.7	+140	7.5	30.5	—	370	—	0.01	430
058	30	+130	7.6	+140	7.5	28.4	—	360	—	0.02	410
090	30	+170	7.8	+140	7.8	31.5	—	390	—	—	440
091	30	+160	7.8	+160	7.9	33.5	—	400	—	—	480
092	30	+140	7.9	+170	7.5	32.0	—	—	—	—	440
093	30	+150	7.6	—	—	—	—	—	—	—	440
094	30	+170	7.9	+160	7.8	31.5	—	370	—	—	500
095	30	+160	7.9	+140	7.6	31.6	—	420	—	—	520
Mean		+160	7.6	+152	7.6	30.0	1245	361	323	0.01	454
OPEN-INTERTIDAL (MUD)											
021	15	+140	7.3	+200	7.7	33.4	1530	380	365	0.2	440
022	15	+20	7.0	+190	7.8	28.9	—	340	—	0.28	610
023	30	+200	7.2	+210	7.8	31.8	—	410	—	0.19	670
024	40	+40	7.3	+190	7.7	30.3	—	350	—	0.03	520
025	15	+130	7.0	+210	7.8	31.2	—	410	—	0.04	470
026	15	+180	7.1	+200	7.6	35.5	1620	450	420	0.06	650
062	30	−20	7.1	+110	7.0	31.5	—	380	—	0.11	530
063	30	−40	7.0	+70	7.8	30.0	1140	435	—	—	650
064	30	−40	6.9	+90	7.4	31.7	—	400	—	0.14	600
074	15	−150	7.1	−30	7.2	—	1500	400	320	0.16	—
075	15	−70	7.3	+20	7.2	34.8	—	410	—	0.23	680
076	15	−70	7.3	+60	7.4	—	—	—	—	—	—
077	10	−140	7.1	−20	7.2	4.3	—	380	—	0.2	660
078	10	−140	6.9	−30	7.3	37.9	—	410	—	—	720
Mean		+3	7.1	+105	7.5	32.6	1148	397	368	0.13	600

Sample No. 71636—	Depth (cm)	IN-SITU		EXPRESSED PORE FLUIDS							P_2O_5 of sediments (ppm)
		Eh (mV)	pH	Eh (mV)	pH	Salinity (ppt)	Mg (ppm)	Ca (ppm)	K (ppm)	P_2O_5 (ppm)	
MANGROVE-SWAMP (MUD)											
027	15	—	—	+190	8.0	—	1640	675	455	0.13	740
028	15	+270	6.7	+210	8.1	—	—	—	—	—	780
030	15	+260	6.8	+190	8.0	—	—	1110	—	—	890
031	15	+260	6.6	+200	7.9	48.5	2400	—	660	—	880
032	15	+240	6.6	+190	7.7	70.3	2520	810	—	0.18	730
079	10	−40	6.8	+90	7.2	34.3	—	420	—	—	1150
080	10	−120	6.8	+80	7.2	36.4	—	310	—	—	1100
081	10	−120	6.7	+140	7.1	43.5	—	450	—	—	—
082	10	+270	7.3	+60	8.2	44.5	—	—	—	—	1050
083	10	+240	7.0	+70	8.4	45.6	2130	—	600	—	950
084	10	+120	7.0	+140	8.3	43.0	—	570	—	—	960
Mean		+138	6.8	+142	7.8	45.8	2173	621	572	0.16	923
SUPRATIDAL-FLAT (MUD)											
068A	60	+190	7.0	+30	6.9	58.8	—	880	—	0.8	—
071	25	+260	7.1	+40	7.8	103.0	5440	950	1520	0.2	570
072	25	+150	7.1	0	7.7	107.4	5760	950	1520	—	520
073	25	+190	7.0	+60	7.8	102.0	5260	910	1380	0.2	520
101	30	+130	6.9	+160	7.7	—	6900	840	—	1.4	1050
105	15	+80	6.5	+70	6.9	128.6	7000	1100	1840	0.2	730
109	10	+180	7.5	+130	7.3	121.0	6980	880	1640	0.2	970
110	20	+150	7.8	+10	8.1	101.0	6000	1290	1380	—	1000
136	62	+290	6.6	−10	8.5	96.3	6200	1000	1320	—	370
Mean		+180	7.1	+54	7.6	102.3	6193	978	1514	0.5	716
OLD MANGROVE-SWAMP (MUD)											
033	250	+200	6.9	+150	7.8	44.5	1650	510	—	—	630
041	30	+200	3.5	+90	5.7	118.6	6500	830	1640	—	530
042	30	+220	5.7	+90	6.8	123.0	6500	780	1580	—	890
043	30	+200	4.3	+150	6.9	81.7	6500	710	1580	—	990
044	60	+200	3.9	+130	6.6	122.0	7160	720	1580	0.2	570
045	30	+260	5.2	+200	7.2	—	—	—	—	0.06	750
046	30	+270	4.0	+130	6.9	116.7	6800	800	—	0.6	380
059	60	+190	6.0	+180	6.4	103.2	5360	720	1380	—	430
060	60	−360	6.1	−120	7.2	69.8	—	500	—	—	900
068B	90	−60	5.7	−20	7.2	103.3	5440	860	1460	0.8	800
Mean		+132	5.2	+98	6.9	98.1	5739	714	1537	0.42	687
SUPRATIDAL-FLAT (vertical sequence)											
136	62	+290	6.6	−10	8.5	96.3	6200	1000	1320	–	370
132	32	+380	3.5	−70	6.2	82.3	5240	550	560	0.4	290
133	60	+30	3.35	+290	5.3	74.6	3800	400	500	0.2	500
134	90	+360	3.3	+260	5.7	68.0	3300	400	440	0.2	390
135	100	+380	3.3	+70	6.2	53.5	2500	300	380	–	360

Samples 71636021-71636068, 71636108-71636109, and 71636132-71636136 are from the vicinity of the Torilla Plains Base Camp. Samples 71636071- 71636084 are from the vicinity of the Hoogly Base Camp. Samples 71636090-71636095 are from the sand banks at the mouth of the Styx River, opposite Charon Point.

PART B

A numerical approach to the geochemistry of the estuarine sediments

BY

W. MAYO

Page 130 is blank.

INTRODUCTION

The following account describes the results of a numerical approach to the study of the geochemistry of the Broad Sound estuarine sediments, which were sampled in 1970-71. The sedimentology and Holocene history of the estuary system have been discussed by Cook & Mayo (1978).

The analysis of the sediment grainsize parameters resulted in a model of terrigenous sediment movement in the estuary system (Cook & Mayo, 1978, p. 112; Mayo, 1974). The estuarine sediments are classified here into separate sedimentary units using mathematical and statistical techniques; the classification obtained is linked to this sedimentation model to aid in the geochemical interpretations. The detailed geochemistry of each sedimentary unit is analysed separately using further statistical and mathematical techniques and then generalised for the total estuarine system. 'Geochemistry' as used here means the study of the distribution and circulation of some selected chemical elements, and as such is somewhat more restrictive than the definition by Goldschmidt (1954).

The overall strategy of the study was to measure as many chemical elements as possible on each sample, together with as many other variables as was practicable, and to determine subsequently all the relevant geochemical relations between the variables. This 'fishing expedition' strategy aims at revealing general geochemical relations within the estuarine sediments which in turn may point to certain aspects worthy of further, more detailed study.

Within this overall strategy, the data were analysed using a series of mathematical and statistical techniques (1) to classify the sediments into separate groups reflecting a distinct set of geological processes, and (2) to determine the interrelations between the variables within each of the sediment groups identified by this classification.

Although the primary aim of this study was to clarify the geochemical relations within the estuarine complex, some comparison of different numerical techniques also was possible during the analysis of the data. Detailed discussions of individual mathematical and statistical techniques are contained in Appendix B1.

In contrast to the 'fishing expedition' strategy, a small additional set of samples was collected in the estuary in 1971 to determine the geological processes controlling the concentrations of P_2O_5, Cu, Pb, and Zn (Mayo 1976). This specific study included measurement of pH, Eh, and organic carbon (measurements of which were not practicable with the major study). The results of the two studies complement each other in some aspects.

DEPOSITIONAL ENVIRONMENTS

The *shallow-marine environment* is in the subtidal zone — its lower limit is about 10 m below the low-water spring tide level and it grades upwards into intertidal sand banks. Because the tidal currents are stronger at the surface than at depth the average maximum energy of the depositing currents is lower in the subtidal zone than in the intertidal zone. Therefore, in the shallow-marine environment, mud deposited from suspension coexists not only with early Holocene relict gravels, but also with sand and gravel dumped from the intertidal zone. The Holocene relict gravels appear to consist of intraclasts formed from subaerial weathering of calcareous sediments, nodules of pedogenic origin, and subaerially weathered biogenic particles.

The lower limit of the *open-intertidal environment* grades into the shallow-marine environment and its upper limit is the mangrove swamp boundary. For the most part it is represented by a sand facies forming as sheets and ridges. A muddy facies occurs next to the mangrove-swamp environment, and a gravel facies, much of which consists of early Holocene relict sediment, is present in the lower part of the open-intertidal environment.

The *mangrove-swamp environment* straddles the boundary between the intertidal and supratidal zones (the supratidal zone is completely above normal high-tide level), whereas the *supratidal-flat environment* lies entirely in the supratidal zone and grades landwards into coastal grasslands. Spring tides flood the supratidal areas almost every month. They deposit mainly silt and clay in the mangrove swamps and supratidal mudflats under relatively low energy conditions, more clay being deposited in the mudflats than in the mangrove swamps. *Mangrove channels,* which are mainly within the intertidal zone, extend through the mangrove swamp environment to the mudflats; the sediment in the channels is also mainly silt and clay.

SAMPLING

The shallow-marine, open-intertidal, mangrove-swamp, and supratidal-flat depositional environments were sampled on a 2-km grid; the mangrove-channel environment was sampled at regular intervals along the total length of all of the major channels (Fig. A22 in Part A). This produced 305 sediment samples. More details of the sampling strategy are given by Cook & Mayo (1978). Triplicate sampling was done at about every tenth locality to enable the significance of the combined analytical and sampling error to be tested.

ANALYTICAL METHODS

Details of the analytical methods employed in determining the grainsize and mineralogy of the estuarine samples (including the heavy-mineral content) are given in Cook & Mayo (1978). Sieves (for the gravel), a settling tube (for the sand), and a pipette (for the mud) were used to determine grainsize; total carbonate content was determined by the weight-loss method; X-ray diffraction was used to determine the more abundant minerals (carbonate and terrigenous); and the heavy minerals were separated with bromoform and identified optically.

Closed arrays in the data arise because groups of variables measured by these analytical methods sum to 100 percent. These may adversely affect the results of numerical data analysis and are considered where relevant in these analyses.

The elements Ba, Ca, Co, Cu, Fe, Mg, Mn, Ni, Sc, Sr, Ti, V, Y, and Zr were determined by direct-reading optical spectrograph at BMR in Canberra. Pb and Zn were determined using atomic absorption spectrophotometry and P_2O_5 by wet chemical analysis at the Australian Mineral Development Laboratories (AMDEL), in Adelaide, SA.

All chemical analyses performed were on the total sample. Subsequent selected analyses on different sediment fractions would have enabled corroboration of some of the conclusions and, in some instances, allowed more detailed interpretations. Nevertheless, to some extent, a numerical sample classification that groups the samples into distinct sediment types overcomes the interpretation difficulties resulting from only analysing the total sample.

ACKNOWLEDGEMENTS

I express my appreciation to Mr K. J. Armstrong and Mr D. E. Hunter for their field and laboratory work throughout the Broad Sound project, and to Messrs F. L. Stevenson, G. Burgis, A. Lewis, and C. Madden for their assistance in the field. The considerable amount of X-ray diffraction work carried out by Mr G. Berryman was an important contribution to the Broad Sound work. Mr G. Oke, Captain of the M.V. *Bali Hai,* was helpful with various phases of the investigations. The hospitality of Mr & Mrs G. Burrill of 'Bald Hills' and Mr & Mrs A. Mace of 'Torilla' was much appreciated. I am grateful to Professor A. C. Cook for his valuable comments and suggestions. The illustrations were drawn by Mr G. Butterworth and Miss C. Hynson.

NUMERICAL SAMPLE CLASSIFICATION

BACKGROUND

In order to determine the detailed geochemical interrelations from a set of geological data, the first step must be to classify the samples into distinct populations, each representing the effects of a set of geological processes. The geochemical interrelations within each of these populations can then be clarified. Using the total data set to attempt to clarify the geochemical interrelations would mainly emphasise the relations *between* the populations, and the detailed interrelations *within* each population would be masked.

Cook & Mayo (1978, p. 103) showed that an X-Y phi-units plot (Fig. B1) of two grainsize parameters — mean, and standard deviation — measured on each of the estuarine samples without the carbonate removed, could be used to classify the samples into four geologically significant *basic sedimentary units: unsorted gravel, unsorted muddy sand, sorted sand,* and *sorted mud.* The four basic units were delineated on the X-Y plot by comparing the grainsize frequency distributions of the samples. The comparison is summarised in Table B1.

These four basic sedimentary units were linked with an idealised model of the Holocene terrigenous sedimentation which is illustrated in Figure B2 and described in Figure B3. The model postulates that:

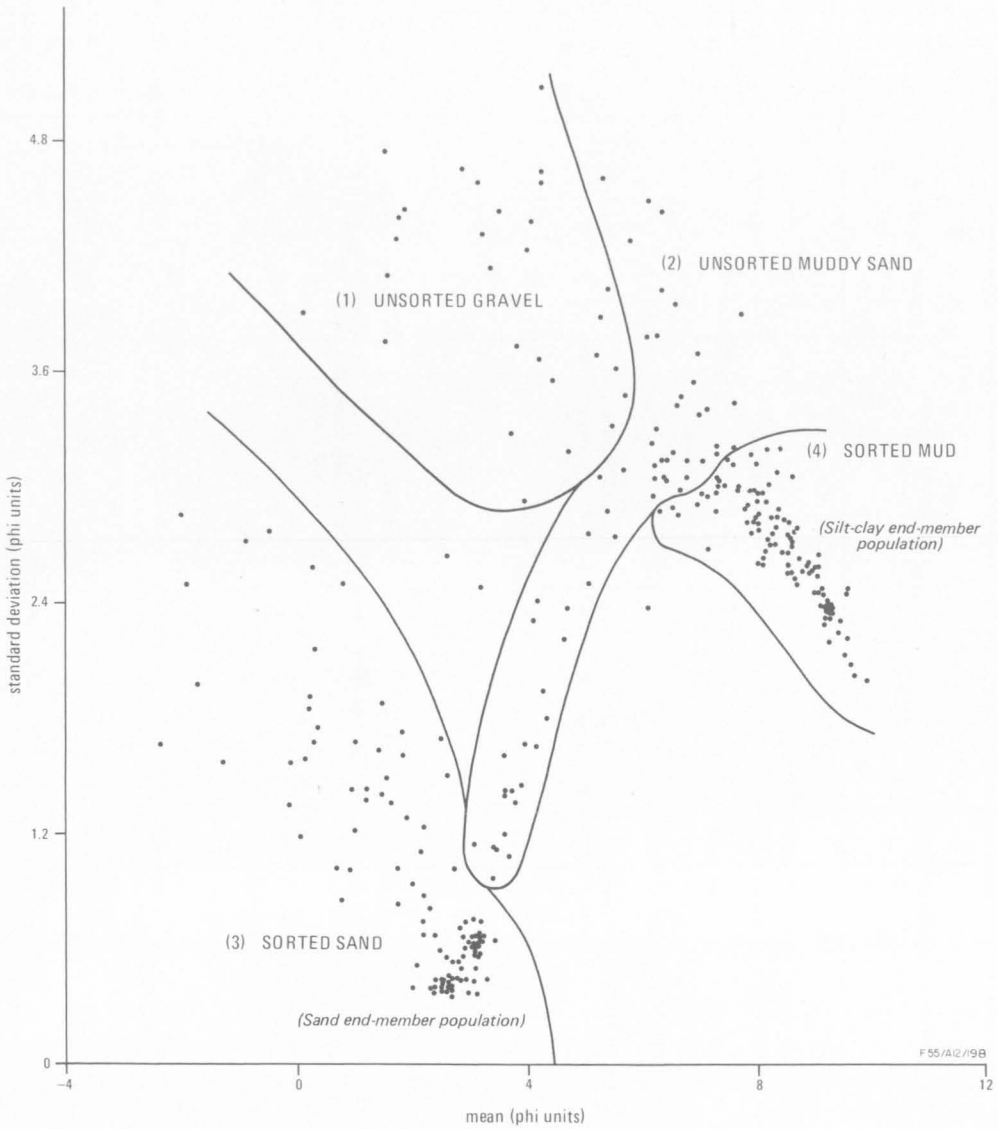


Fig. B1. The four basic sedimentary units, classified by mean and standard deviation of grainsize.

TABLE B1 — COMPARISON OF THE FOUR BASIC SEDIMENTARY UNITS

BASIC SEDIMENTARY UNIT (with mean and standard deviation grouping)	Corresponding field environment	Relative maximum energy (and equilibrium of sediment)	Typical grainsize distribution	Gravel	Sand	Mud	Geological interpretation with decreasing standard deviation and increasing mean (phi) (except for unsorted muddy sand)
UNSORTED GRAVEL							
Coarse to fine mean; moderate to very high standard deviation	Shallow-marine	Low (not in equilibrium)	Multimodal	Variable amounts of all fractions			Decreasing proportion of shells, nodules, terrigenous gravel
UNSORTED MUDDY SAND							
Medium to very fine mean; moderate to very high standard deviation	Intertidal, mangrove-channel	High (not in equilibrium)	Bimodal (dominant mode in very-fine-sand/coarse-silt range)		Minor to equal	Major to equal	Decreasing standard deviation with decreasing mean (phi) indicates decreasing mud content as sorting process continues
SORTED SAND							
Coarse to medium mean; low to high standard deviation	Intertidal, shallow-marine	High (in equilibrium)	Unimodal or bimodal (dominant mode in fine-sand fraction)	Minor or absent	Major		Moving from shallow-marine to intertidal zone associated with decreasing proportion of calcareous shells and nodules
SORTED MUD							
Very fine mean; high standard deviation	Mangrove-channel, supratidal-flat	Low (in equilibrium)	Bimodal (dominant mode in medium-silt or clay fraction)		Minor	Major	With decreasing carbonate, indicates movement from near-intertidal zone to supratidal flats; otherwise from near-land zone to supratidal flats

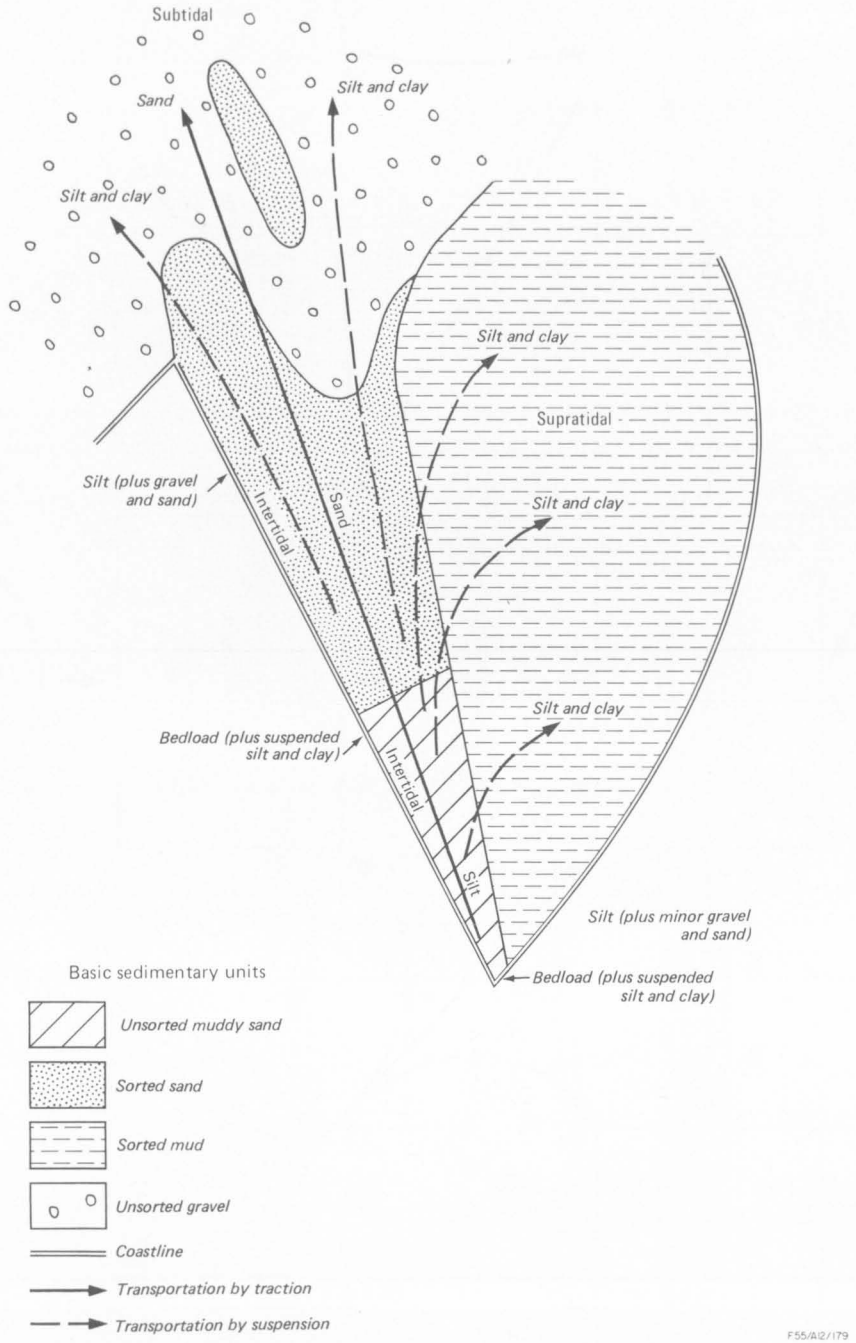


Fig. B2. Idealised model of Holocene non-carbonate sedimentation in Broad Sound.

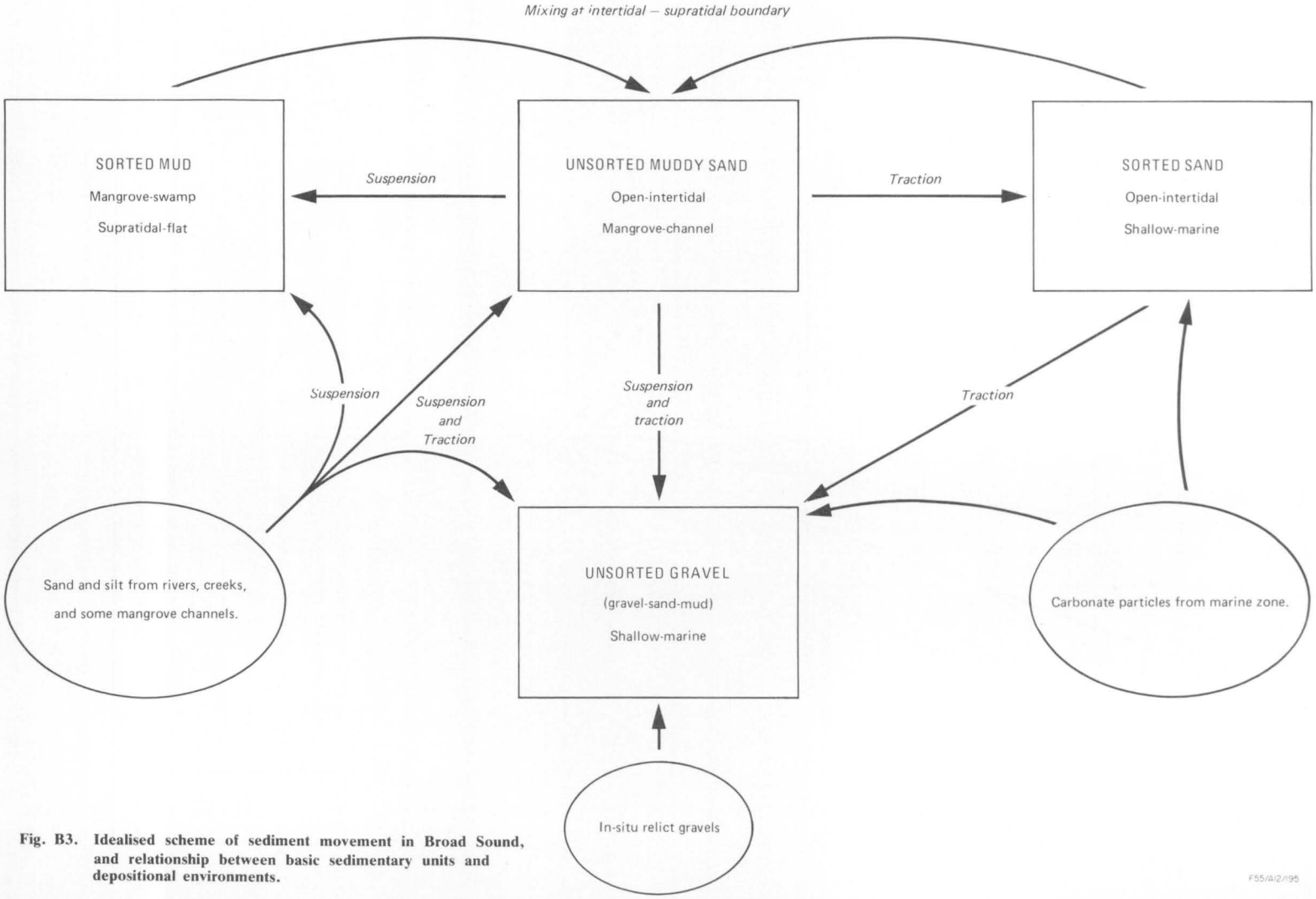


Fig. B3. Idealised scheme of sediment movement in Broad Sound, and relationship between basic sedimentary units and depositional environments.

F55/A/2/195

1. The catchment sediment is transported into the estuary mainly during annual floods; very fine sand and coarse silt are deposited initially in the upper reaches of the estuarine watercourses, whereas much of the silt and clay remains in suspension.
2. Between floods, silt and clay, both winnowed from the bedload and already in suspension, are deposited in the supratidal zone to form the *sorted-mud basic sedimentary unit* and to some extent in the subtidal zone combining with sand, in-situ shells, and relict sediments to form the *unsorted-gravel basic sedimentary unit.*
3. The *sorted-sand basic sedimentary unit* consists of 2-3-phi sand particles which are moved more rapidly seaward than the coarser sand and gravel. The sand mixes with biogenic material (both in-situ and derived from the marine shelf zone) to form current-orientated sandbanks overlying relict sediments.
4. Mixing of the sorted-sand and sorted-mud sediments takes place continuously in the mangrove channels and at the mangrove-swamp/open-intertidal boundary, to form the *unsorted-muddy-sand basic sedimentary unit.*

It was clear that further subdivision of the sorted-sand unit, the sorted-mud unit, and the unsorted-muddy-sand unit would be required before the detailed geochemical relations could be described throughout the estuary (Cook & Mayo, 1978). Although this classification into four *basic sedimentary units* was useful for explaining the overall sediment movement in Broad Sound, this rather coarse grouping would probably mask some important geochemical information. Accordingly, Q-mode factor analysis was used to effect a more detailed classification.

Q-MODE FACTOR ANALYSIS CLASSIFICATION

Q-mode factor analysis determines relations between samples and has been used to differentiate depositional environments (Klovan, 1966). In addition, all of the variables measured on a set of samples may be included in the analysis to obtain a classification that reflects all geological processes affecting these variables. Such a classification of the Broad Sound sediments should be much more refined than a classification based only on grainsize parameters. Details of the Q-mode factor analysis method and the use of the technique for classification of geological samples are given in Appendix B1a.

Factor analysis does not require a knowledge of the distribution, nor of the independence, of the variables, but with the Q-mode analysis, transformation of the original data is required so that changes in all of the variables have equal weighting (Harbaugh & Demirmen, 1964). In this study, a percentage-of-range transformation was used for each variable.

Further, with the Q-mode analysis, variables which are not statistically independent (for example, measurements of both Ca and $CaCO_3$) give extra weight to the geological processes associated with these variables. Therefore, variables which were obviously not independent, as well as variables not measured in certain

TABLE B2. Q-MODE FACTOR SCORES

Variable	*Factor 1*	*Factor 2*	*Factor 3*
Mean grainsize (phi)	2.14	−0.89	−0.01
Grainsize std dev.	1.35	0.57	2.03
% Gravel } carbonate	−0.23	0.26	1.33
% Sand } retained	−1.03	−4.13	−0.11
% Mud	2.83	0.96	0.41
Dolomite	0.10	−0.13	−0.12
Mg-calcite	−0.21	−0.90	1.69
Plagioclase	1.68	−1.18	−1.05
Orthoclase	0.22	−0.74	−0.38
Aragonite	0.07	−1.39	2.10
Quartz	1.21	−1.67	−1.33
Ba	0.32	−0.38	−0.22
Co	0.45	−0.44	−0.31
Cr	0.87	−0.34	−0.13
Cu	0.55	−0.26	0.21
Fe	0.98	0.04	0.06
Mg	0.52	−0.08	0.92
Mn	0.05	−0.27	0.23
Ni	0.78	−0.23	−0.25
Pb	0.58	−0.16	0.13
Sc	0.98	−0.41	0.26
Sr	−0.06	−0.38	0.90
Ti	1.06	−0.38	−0.01
Va	0.52	−0.08	0.12
Y	0.32	−0.80	−0.19
Zn	1.54	0.03	−0.03
Zr	0.15	−0.36	−0.09
Carbonate	−0.49	−0.66	2.79
P_2O_5	0.63	0.20	1.65

Factor 'composition'

Factor 1	*Factor 2*	*Factor 3*
1. % mud	1. % sand	1. Carbonate
2. Mean grainsize (phi)	2. Quartz	2. Aragonite
3. Plagioclase	3. Aragonite	3. Grainsize std dev.
4. Zn	4. Plagioclase	4. Mg-calcite
5. Grainsize std dev.		5. P_2O_5
6. Quartz		6. % gravel
		7. Quartz

environments or having concentrations below the detection limit, were omitted from the analysis. Consequently, 29 variables (Table B2) and 289 samples were used in the factor analysis. Although the gravel, sand, and mud percentages are directly related to the mean grainsize measure and are also dependent on each other, they were included because their contribution to the final interpretations was considered to outweigh these disadvantages.

Three rotated Q-mode factors account for 91.53 percent of the variation in the 29 variables observed on each sample (see Appendix B1). Only an extra 1.74 percent of the variance is explained by including the fourth factor, and the important variables (indicated from the factor scores) for the first three factors do not change. Consequently, three factors adequately control the structure of the data.

Alternatively, with each factor representing a set of distinct geological processes, the three factors adequately represent all the geological processes affecting the samples. Using three factors, the analysis results in three factor loadings for each sample, each loading representing the influence each factor has on that sample.

A triangular plot of the three normalised varimax factor loadings for each sample is shown in Figure B4. The position of each sample reflects the effects of the three controlling factors on that sample and may be imagined to be determined by the net effect of the 'pull' of each factor from the corresponding apex of the triangle. The more similar the effect of the three factors on each

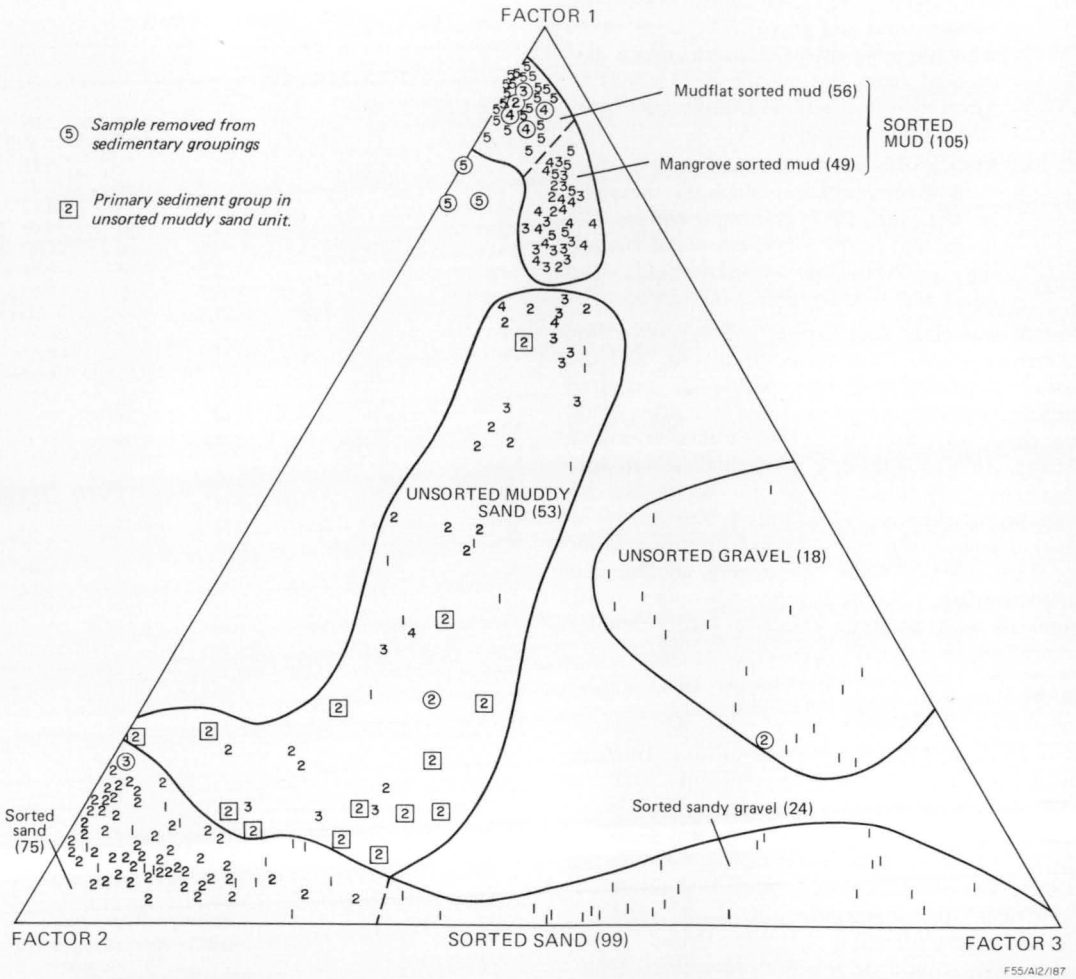


Fig. B4. Triangular plot of the three normalised factor loadings from the Q-mode factor analysis. Samples are numbered according to sedimentary environment: 1 — shallow marine, 2 — open-intertidal, 3 — mangrove-channel, 4 — mngrove-swamp, 5 — supratidal-flat (some samples have been omitted from the plot in areas of high concentration).

sample, the closer are the samples in the triangular plot and the more similar are the samples, based on the measured variables.

With only a few exceptions, the same samples in each of the four *basic sedimentary units* formed separate groupings in Figure B4, illustrating the importance of the grainsize parameters — mean and standard deviation — in this numerical sample classification. Consequently, the three factors used in the analysis would be expected to represent similar geological processes to those postulated in the sedimentation model.

Geological interpretation

The nature of each controlling factor may be interpreted from the factor scores which indicate the important variables in each factor. The scaled varimax factor scores (Appendix B1a) for the three rotated factors are given in Table B2. A cut-off value of 1.1 was used to isolate those variables which are important contributors to each factor, and these variables are listed in decreasing order of importance in Table B2. In Figure B5, changes in these variables are linked with the changes in the factor loadings in order to determine the relations between these variables and the factors.

Increasing Factor-1 loadings reflect increasing mud percentage, associated with a corresponding decrease in mean grainsize (i.e., increase in phi values). This factor then probably represents the low-energy sorting process that results in mud concentrations in the sorted-mud *basic unit* and the unsorted-gravel *basic unit*. Factor 2 appears to represent the intertidal high-

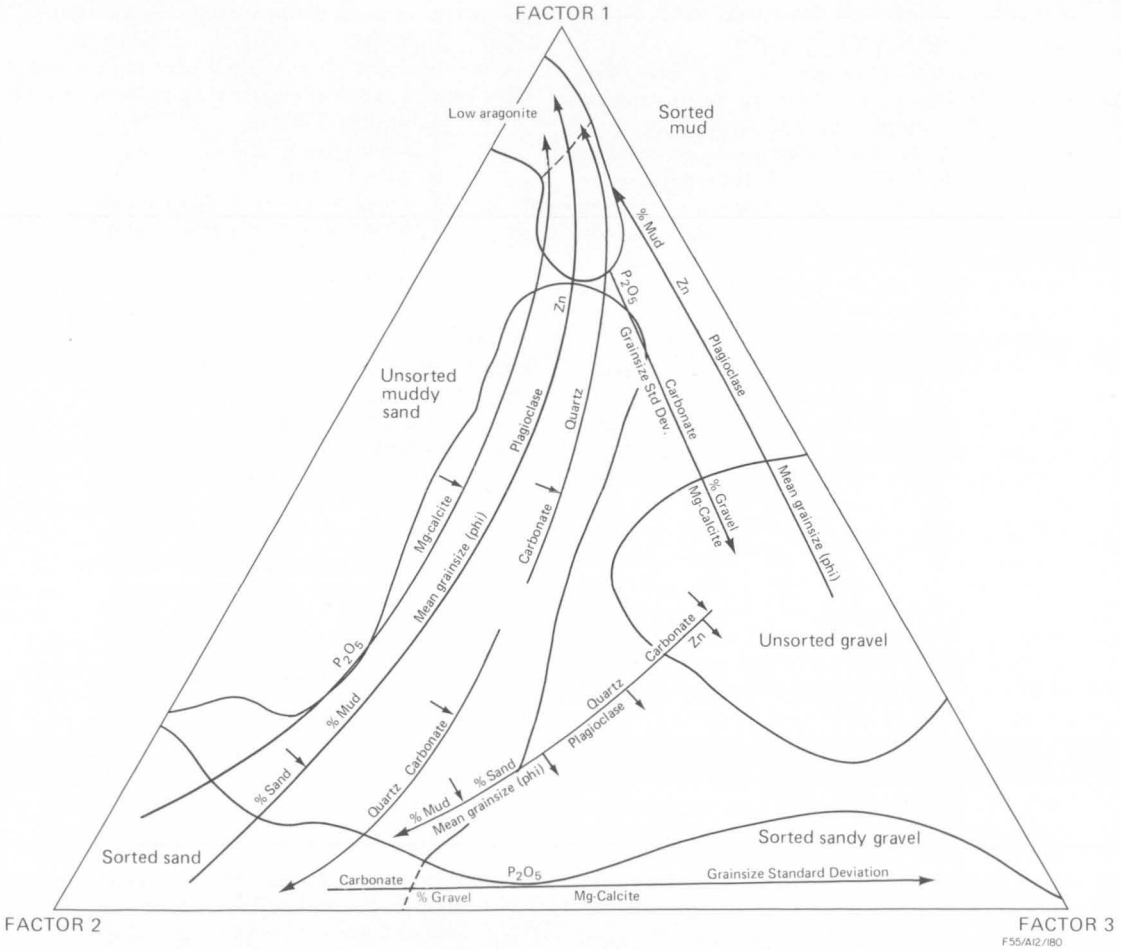


Fig. B5. Contrasts between sedimentary units as reflected by the variables significant in the Q-mode factor analysis. Values of variables increase in direction of long arrows; short perpendicular arrows indicate a contrasting decrease in values in the same direction.

energy sorting process responsible for forming the sorted-sand *basic unit*, the factor loadings increasing with increasing percentage of sand and quartz. Factor 3 reflects a lack of sorting in samples either containing in-situ shells and nodules or consisting of mud-sand-gravel mixtures, the loadings increasing with increasing $CaCO_3$, grainsize standard deviation, and percentage of gravel.

The above geological interpretations of the three factors coincide with processes identified in the sedimentation model summarised above. Furthermore, these interpreted geological processes directly affect the grainsize distributions of the estuarine sediments, thus explaining the similar sample groupings obtained from the grainsize mean/standard-deviation plot and the Q-mode factor analysis. No doubt the inclusion of the three variables — percent gravel, sand, and mud — reinforced this effect, but it did not change the basic interpretations.

In addition to separating the four *basic sedimentary units*, the Q-mode factor analysis enables the sorted-sand and sorted-mud *basic units* each to be subdivided into two separate sample groupings. Factor 3 distinguishes the sorted-sand samples with significant in-situ coarse shells and nodules — the sorted-sandy-gravel group — from the rest of the sorted-sand samples. All of the sorted sandy gravel samples are marine, whereas the rest of the sorted-sand samples are both intertidal and marine.

The Q-mode factor analysis also subdivides the sorted-mud *basic unit* into two separate groups — supratidal-flat and mangrove-swamp — because Factor 1 reflects the higher proportion of mud and clay in the supratidal flats than in the mangrove swamps. This is due to sorting processes described by Cook & Mayo (1978, p. 104). The supratidal-flat group consists almost entirely of samples from the supratidal-flat environment; however, because of the similarity of certain supratidal-flat, mangrove-swamp, mangrove-channel, and open-intertidal samples, all of these environments are represented in the mangrove-swamp group.

From an areal plot of the unsorted-muddy-sand sample locations (Cook & Mayo, 1978, figure 58) two distinct groupings are apparent. One group is restricted to the upper reaches of the estuaries, the other to a zone between the sorted-mud and the sorted-sand basic units; the former represents primary source sediment, the latter a re-mixing of previously sorted mud and sand. Because the primary sediment entering the estuaries as bedload was found to be mainly fine sand and coarse silt (Cook & Mayo, 1978, p. 93), whereas the sorted-mud *basic unit* contains a large proportion of clay, the silt:clay ratio was expected to distinguish the primary from the mixed sediment. In fact, a silt:clay ratio greater than 2.0 distinguished the primary source sediment from the mixed sediment, and the samples corresponding to the primary group are identified in Figure B4.

Therefore, using the triangular factor loading plot in conjunction with the classification derived from the mean/standard-deviation plot, as well as areal distribution considerations, seven separate sample groups have been recognised. Each sample group represents sediment resulting from a different set of geological processes. As the sorted-sandy-gravel group, the unsorted-gravel group and the mixed-unsorted-muddy-sand group do not represent deposition under one set of uniform conditions, these groups cannot be termed sedimentation units (Otto, 1938). Therefore the more general term, 'sedimentary unit', will be used here to describe these groups. The *sedimentary units*, then, are:

1. unsorted gravel
2. sorted sandy gravel
3. sorted sand
4. primary unsorted muddy sand
5. mixed unsorted muddy sand
6. mangrove sorted mud
7. mudflat sorted mud

Appendix B2 lists the classification of the samples into each of these units, together with those anomalous samples which were removed completely from any of the units because of isolated plot positions in Figure B4. Fourteen anomalous samples were removed, leaving a total of 275 samples. Typical grainsize frequency distributions for five of the sedimentary units are shown in Figures B6 to B10.

The triangular plot (Fig. B4) illustrates the sedimentological relationships between the seven sedimentary units. The unsorted-muddy-sand units link the sorted-mud and sorted-sand units, reflecting the sorting of the primary-unsorted-muddy-sand unit into the two sorted end-members and also the re-mixing of these two end-member units to form the mixed-unsorted-muddy-sand unit. The graphical subdivision of the sorted-mud basic unit was discussed earlier. Much of the biogenic material in the estuary system is derived from the continental shelf and is mixed with the locally derived terrigenous material (Cook & Mayo, 1978), but the unsorted-gravel unit and the sorted-sandy-gravel unit are separated from the rest in Figure B4 because of a high content of carbonate gravel (Table B5 and Fig. B5). Much of this gravel consists of in-situ

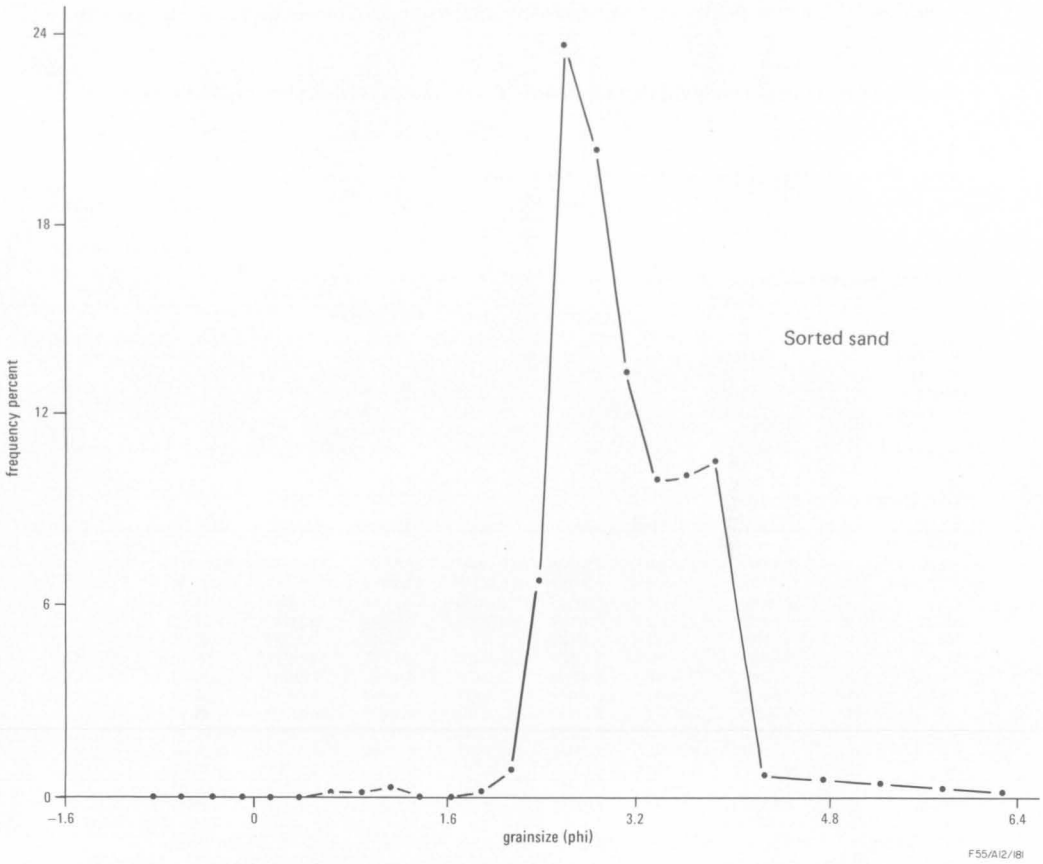


Fig. B6. Typical grainsize distribution of sedimentary units — *sorted sand*. Sample no. 70636055, environment INTERTIDAL, mean 3.09 phi, standard deviation 0.63 phi, carbonate retained.

shells and relict nodules that are out of equilibrium with the depositional regime (Cook & Mayo, 1978, pp. 45, 107). The separation of the unsorted-gravel unit from the sorted-sandy-gravel unit reflects the relatively high mud content of the unsorted gravel and its lack of sorting.

STATISTICAL AND MATHEMATICAL CHECK BY STEPWISE DISCRIMINANT ANALYSIS

Unfortunately, the statistical theory of factor analysis does not at present enable the distribution of the factor loadings to be identified. Therefore the samples cannot be classified at a known confidence level. Further, as explained in Appendix B1a, there are certain basic philosophical objections to the Q-mode approach. Consequently, a multiple discriminant analysis carried out in a stepwise manner (Appendix B1b) was used to test statistically the factor analysis sample classification. The seven sample groupings were used in the discriminant analysis with the same 29 variables as in the factor analysis. With each step in the analysis, a variable is entered or removed until no more variables are suitable for entry as sample discriminators.

Discriminant analysis assumes normality and independence of the variables, but, as shown in Appendix B3, many of the 29 variables do not approach a normal or log-normal distribution and, as explained earlier, several of these variables are not independent. Despite these problems, the analysis is still useful as a check on the Q-mode factor analysis results.

Table B3 shows the last step in the stepwise discriminant analysis and includes the final 14 discriminatory variables and the matrix of F values for comparison of each pair of groups. The critical F value for the comparisons, F (14, 255, 0.95), is 1.69. An F value (in the matrix of F values) greater than 1.69 shows that statistically

TABLE B3 — LAST STEP IN STEPWISE DISCRIMINANT ANALYSIS (Step number 14, variable entered 24)

VARIABLES INCLUDED AND F VALUE FOR REMOVAL — Degrees of freedom: 6, 255 (Supplied F Value — 1.83)

1. 6.8836	3. 3.4376	7. 5.5531	10. 12.0168	17. 6.4377	24. 3.1701	27. 3.7018
2. 48.6822	5. 16.1176	8. 10.0612	11. 7.7725	18. 15.4575	25. 4.3398	28. 15.9491

VARIABLES NOT INCLUDED AND F VALUE FOR ENTRY — Degrees of freedom: 6, 254

4. 1.7268	12. 0.5755	15. 2.1742	19. 0.9785	23. 1.5319	
6. 0.2169	13. 0.4449	16. 1.2480	20. 0.0981	25. 0.8467	
9. 1.7073	14. 1.1358	18. 1.0258	21. 2.1877	29. 2.6659	

F VALUE MATRIX — Degrees of freedom: 14, 255

	GROUP GRAV	SAND G	SAND	PRIM*		
GROUP						
SAND G	39.91696					
SAND	78.93606	58.94207				
PRIM	30.70991	31.28749	20.22300			
MIXED	22.39141	69.19900	69.39742	16.60310		
MANG	53.87664	123.24270	152.01104	40.02206	25.29944	
MUD Fl	95.44720	179.07160	230.87060	63.96063	75.15948	37.84474

DISCRIMINANT FUNCTION

		GRAV	SAND G	SAND	PRIM	MIXED	MANG	MUD FL
VARIABLE								
MEAN (phi)	1.	15.49711	8.48480	13.43666	15.29991	15.66323	14.63924	16.82548
STD DEV	2.	21.45756	8.56035	7.39392	10.69157	16.57056	13.82067	12.82130
GRAV	3.	0.99960	1.40711	1.23726	1.23468	1.14780	1.24933	1.36144
MUD	5.	−0.68189	−0.47522	−0.76849	−0.71095	−0.61057	−0.23225	−0.33747
MG-CAL	7.	1.12762	1.68727	1.48027	1.46817	1.50921	1.55357	1.66085
PLAG	8.	1.91681	2.08864	2.14529	2.40160	2.39441	2.43415	2.69416
ARAG	10.	1.91501	2.58416	2.44490	2.14462	2.49643	2.60284	1.42863
QTZ	11.	1.60116	1.88691	1.90457	1.90457	1.90373	1.88026	2.29143
Mg	17.	0.70277	0.93499	0.61050	0.72062	0.58517	0.63208	0.98197
Sr	22.	−0.01535	−0.01856	−0.01139	0.00587	−0.00912	−0.00938	−0.01145
Va	24.	0.21131	0.30146	0.25535	0.16091	0.18892	0.22176	0.28365
Zn	26.	0.15763	0.17526	0.05032	0.07552	0.12283	0.14005	0.26442
Zr	27.	0.00918	0.00437	0.00257	0.00561	0.00962	0.00803	0.00759
CARB	28.	1.60628	1.51087	1.01340	1.24429	1.24342	1.09513	1.19519
CONSTANT		−161.11934	−143.19462	−109.23441	−145.42786	−156.26818	−171.04812	−208.18834

THEORETICAL CLASSIFICATION *(using D^2 statistic)*

Number of cases classified into sedimentary unit

	GRAV	SAND G	SAND	PRIM	MIXED	MANG	MUD FL	MISCLASSIFIED
GROUP								
GRAV	16	0	0	0	2	0	0	2
SAND G	2	22	0	0	0	0	0	2
SAND	0	0	75	0	0	0	0	0
PRIM	0	0	1	11	2	0	0	3
MIXED	0	0	2	3	28	6	0	11
MANG	0	0	0	0	1	48	0	1
MUD FL	0	0	0	0	0	4	52	4

* *Abbreviations:* GRAV — Unsorted gravel; SAND G — Sorted sandy gravel; SAND — Sorted sand; PRIM — Primary unsorted muddy sand; MIXED — Mixed unsorted muddy sand; MANG — Mangrove-sorted mud; MUD FL — Mudflat-sorted mud; MEAN — Mean grainsize; STD DEV — Grainsize standard deviation; $GRAV_1$ — Gravel, carbonate retained; MUD_1 — Mud, carbonate retained; Mg-CAL — Mg-calcite; PLAG — Plagioclase; ARAG — Aragonite; QTZ — Quartz; CARB — Carbonate

The numbering of the variables corresponds to the order given in Table B2.

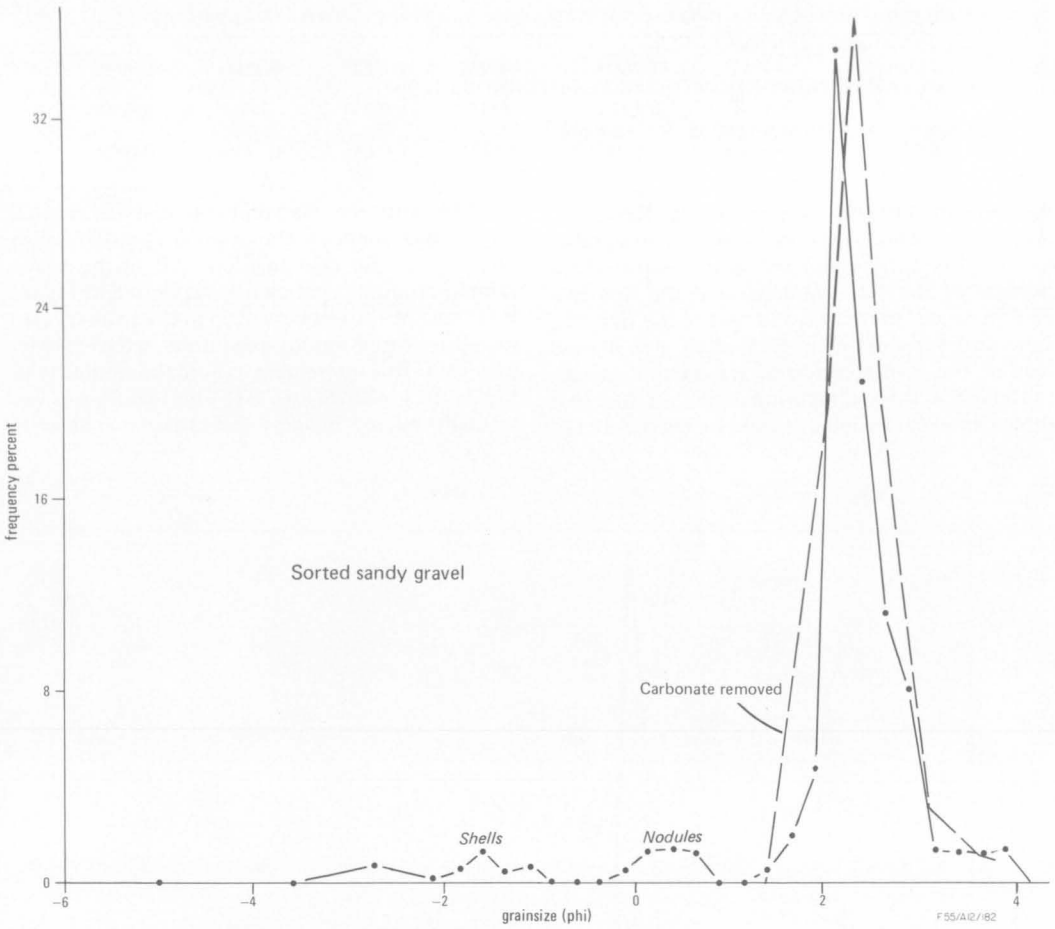


Fig. B7. Typical grainsize distribution of sedimentary units — *sorted sandy gravel*. Sample no. 70636199, environment SHALLOW-MARINE, mean 1.96 phi, standard deviation 1.28 phi, $CaCO_3$ 36.5 percent.

the corresponding two groups are different at the 95-percent confidence level (or at a higher level). In fact, all of the F values are greater than 1.69, confirming that each group classified by the factor analysis is significantly different from all of the others.

Table B3 also shows the theoretical statistical classification of each sample using the D^2 statistic (see Appendix B1b). This statistic, used as a chi-square variable, indicates which individual samples differ significantly from the average for the group into which they were classified. Only 23 out of the 275 samples are classified differently from the factor analysis grouping by this test and 11 of these had been classified into the mixed-unsorted-muddy-sand unit, from which many marginal samples would be expected.

Removal of the differently classified samples to make both classification schemes compatible was not done, because of the normality and independence problems with the discriminant analysis. Nevertheless, the excellent agreement between the two different classification techniques strongly supports the use of the Q-mode factor analysis classification results.

Q-TECHNIQUE CANONICAL CORRELATION ANALYSIS

Q-technique canonical correlation analysis (Appendix B1c) gives further useful support to the factor analysis sample classification. The results for the 275 samples, classified into the seven groups by the factor analysis and using the same 14 discriminatory variables from the

TABLE B4. RESULTS OF Q-TECHNIQUE CANONICAL CORRELATION ANALYSIS

EIGENVALUES (see Appendix B1c)						
17.68199	5.37177	2.27534	1.01803	0.77533	0.16555	0.00000
CUMULATIVE PROPORTION OF TOTAL DISPERSION						
0.64798	0.84483	0.92821	0.96552	0.99393	1.00000	1.00000
CANONICAL CORRELATIONS (see Appendix B1c)						
0.97287	0.91818	0.83348	0.71026	0.66085	0.37688	0.00000

discriminant analysis, are shown in Table B4. Although six canonical correlations seem significant, the first three canonical vectors explain 92.8 percent of the total variance and the first two 84.5 percent. Therefore, the plot of the first two canonical variables (Fig. B11) does give a good idea of the configuration of the sample groups (although a three-dimensional plot of the first three canonical variables would be even better).

As with the discriminant analysis results, Figure B11 supports the original Q-mode factor analysis sample classification. All of the seven sample groupings are clearly separated in Figure B11, except for some overlap in the primary and mixed-unsorted-muddy-sand units, which is to be expected. It is interesting to note the similarity of Figure B11 with Figure B1. The two figures are virtually mirror images, indicating that despite

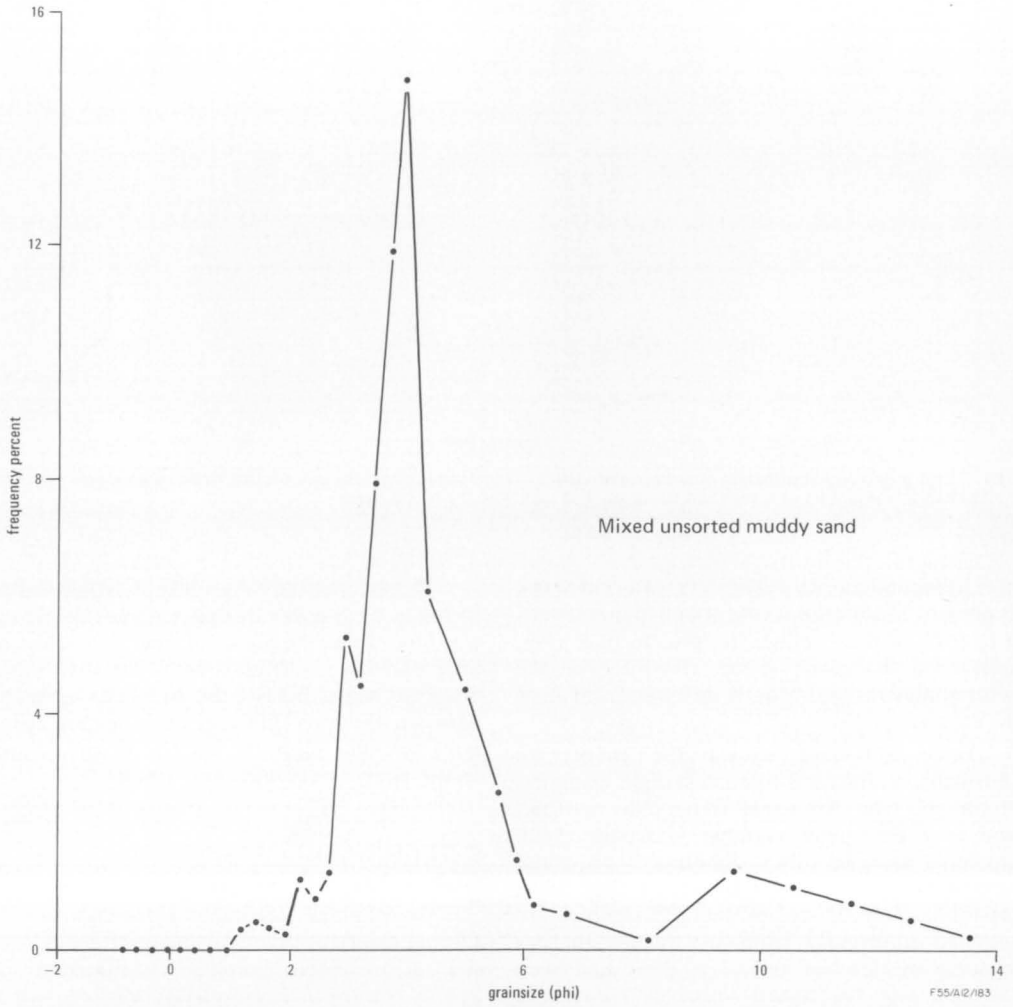


Fig. B8. Typical grainsize distribution of sedimentary units — *mixed unsorted muddy sand*. Sample no. 70636224, environment INTERTIDAL, mean 5.19 phi, standard deviation 2.77 phi, carbonate retained.

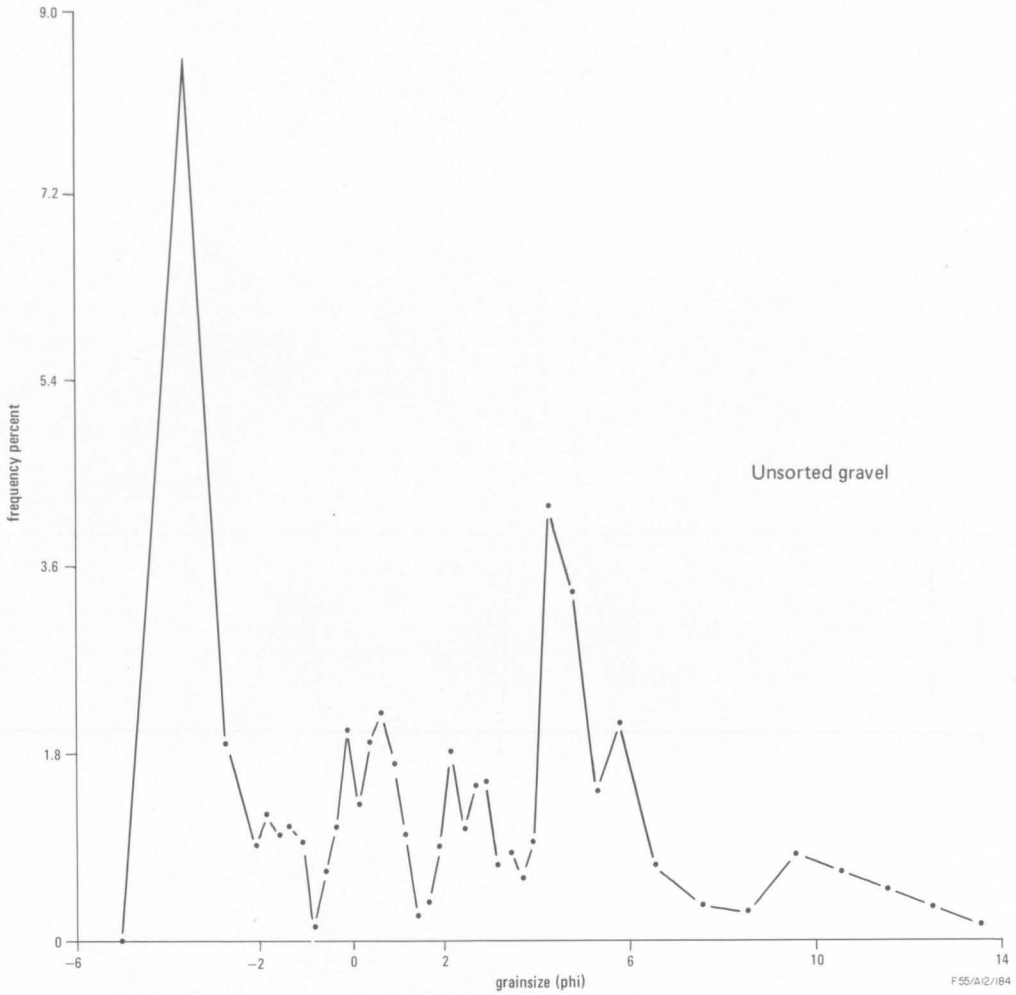


Fig. B9. Typical grainsize distribution of sedimentary units — *unsorted gravel*. Sample no. 70636220, environment SHALLOW-MARINE, mean 1.66 phi, standard deviation 4.76 phi, carbonate retained.

the inclusion of 14 variables in the canonical analysis, the two grainsize parameters, mean and standard deviation, are the most important discriminatory variables. The importance of the mean and standard deviation as discriminatory variables also explains the similarity of the sample groupings using the mean/standard-deviation plot and the Q-mode factor analysis.

Both the stepwise discriminant analysis and the Q-technique canonical analysis support the sample classification obtained from the Q-mode factor analysis. This implies also that a similar classification would have been obtained if either of these techniques had been used instead of the factor analysis. The factor analysis, though, has the advantage of not requiring an initial grouping of samples before the analysis.

Q-MODE CLUSTER ANALYSIS

Although comparison of numerical analytical techniques was not a primary aim of this study, after the close agreement using factor analysis, discriminant analysis, and canonical correlation analysis, sample classification using Q-mode cluster analysis (see Appendix B1d) was also examined. The particular computer program used limited to 250 the number of estuary samples that could be clustered. Therefore, 25 samples were removed at random from the seven previously classified units, the number removed from each unit depending on the total number of samples representing that unit.

Perhaps the most useful characteristic of cluster analysis is the wide range of similarity measures available for use with the technique.

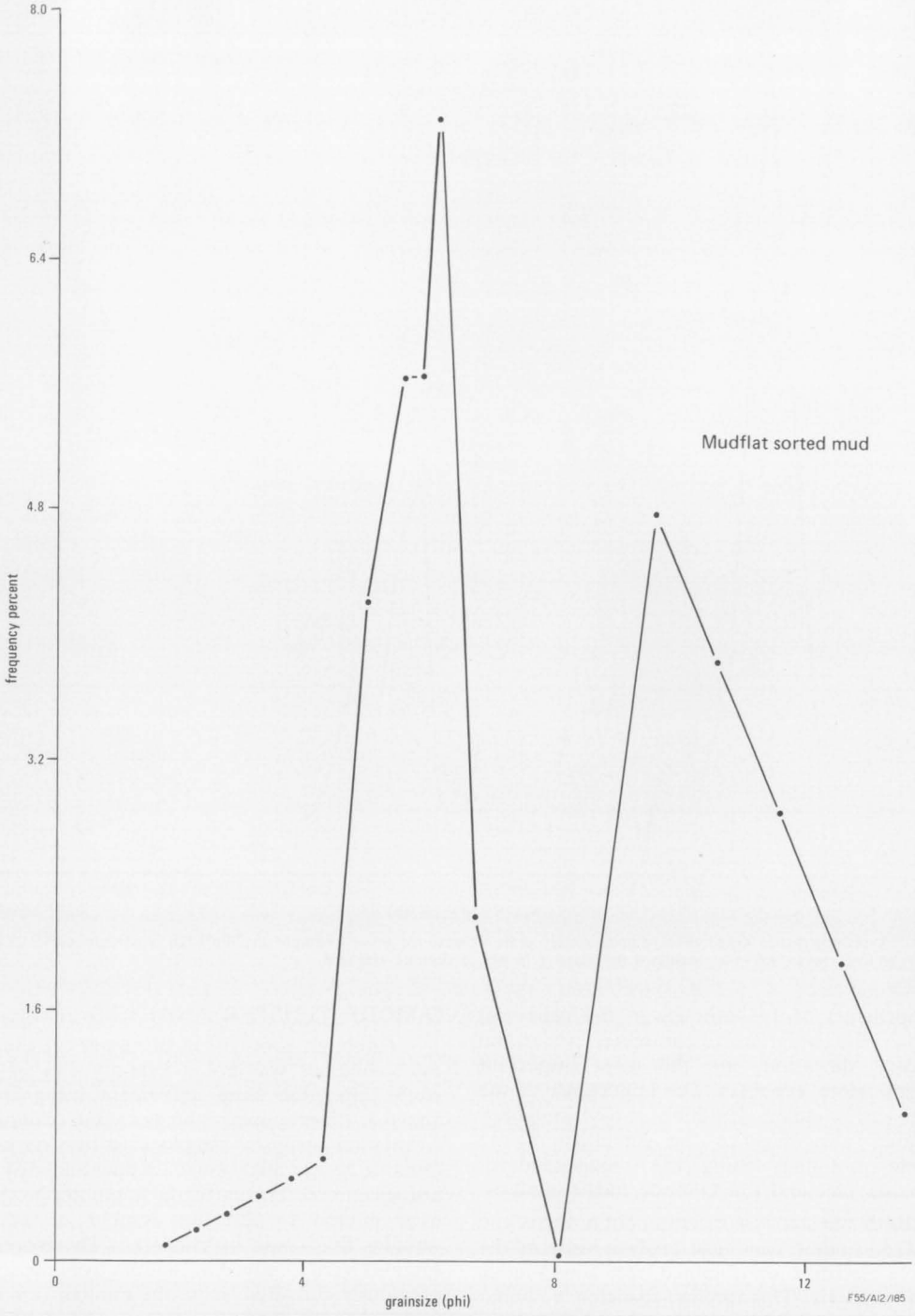


Fig. B10. Typical grainsize distribution of sedimentary units — *mudflat sorted mud*. Sample no. 70636019, environment SUPRATIDAL-FLAT, mean 8.54 phi, standard deviation 2.90 phi, carbonate retained.

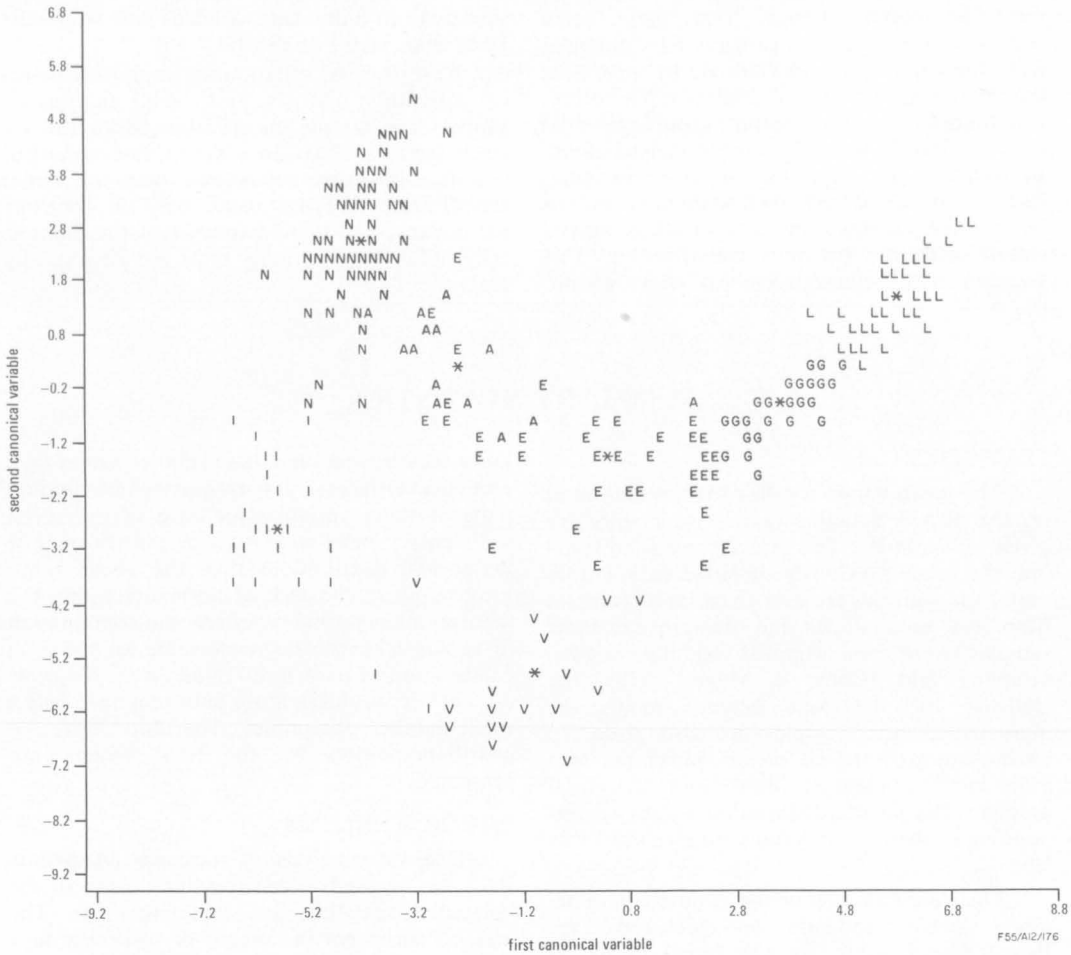


Fig. B11. First two canonical variables, Q-technique canonical correlation analysis. * — group mean, V - unsorted gravel, I - sorted sandy gravel, N - sorted sand, A - primary unsorted muddy sand, E - mixed unsorted muddy sand, G - mangrove sorted mud, L - mudflat sorted mud.

Despite the fact that other similarity measures may have been more suitable for the estuarine data (Appendix B1d) the same measure used in Q-mode factor analysis — the coefficient of proportional similarity (Appendix B1a) — was used with the cluster analysis for comparison. The unweighted group average (Appendix B1d) was selected to obtain more intense clustering. Percent-of-the-range transformation was again used to ensure equal weighting of each variable. As the cluster analysis was done simply for comparison, redundant variables were not removed using R-mode cluster analysis, and the same 29 variables were used, as before.

Plate B1 shows the dendrogram from the Q-mode cluster analysis, using the 29 variables; the sedimentary unit of each sample is also indicated on the plot. Although this plot indeed shows a tendency to group the samples into the same sedimentary units, in Plate B2 the tendency is even more marked. To produce Plate B2 the same 14 variables as were found significant in the stepwise discriminant analysis were used, instead of the entire 29 original variables.

There is close agreement between the sample grouping in Plate B2 and the Q-mode factor analysis plot (Figure B4). The differences are probably mainly due to the fact that the dendrogram is only a one-directional representation of the relations between the samples, whereas the triangular plot of the normalised factor loadings is a three-dimensional representation (in that the sample plot positions are affected by movement in three directions). It

must be noted, though, that these same sedimentary unit groupings cannot be obtained from the dendrogram in Plate B2 by separating the clusters at one level of similarity. Therefore, it is doubtful if the same sample groupings would have resulted by using the cluster analysis alone. In addition, the most discriminatory variables had to be obtained from the discriminant analysis before the dendrogram classification agreed closely with the previous classification. This suggests that cluster analysis has greater sensitivity to redundant variables (see Appendix B1d) than factor analysis.

Nevertheless, discriminant analysis, canonical correlation analysis, and cluster analysis all support the sample classification from the Q-mode factor analysis. In addition, this numerical classification corresponds well with the initial classification that was based only on grainsize parameters, and demonstrates that the numerically defined sedimentary units are geologically real.

SUMMARY STATISTICS

STATISTICS

The mean values for 46 variables measured on the Broad Sound estuarine sediments are given in Table B5. The samples are subdivided into the seven previously classified sedimentary units, and statistics are also given for all samples from the estuary. As the mangrove-channel samples were not sampled on the original sampling grid (Cook & Mayo, 1978), the statistics for the total estuary minus the mangrove-channel samples are also given, to enable comparisons of mean values between individual sedimentary units and the total estuary. The standard deviation values corresponding to these mean values are given in Table B6.

The determination of the grainsize parameters — skewness and kurtosis — measured on the Broad Sound sediments was found to be ill-conditioned (Cook & Mayo, 1978, p. 99), in that small changes in the original data could result in unacceptably large changes in the value of these parameters. Consequently, realistic geological interpretations from these two parameters could not be made, and the statistics for these two variables are not included in the Tables.

Figures B14 to B21 (Appendix B3) contain the frequency distributions of each of these 46 variables throughout the estuary. The main conclusion to be drawn from these plots is that although a few variables may approach a log-normal distribution (such as Ba, Cu, Mg, and Mn), none of the distributions appears to represent sampling from a single normal or log-normal population. Chi-square tests of normality were not considered necessary with these distributions.

As the numerical results of each sedimentary unit were to be analysed separately with statistical techniques, it was thought necessary to know the distribution of the variables within each unit. Nevertheless, the frequency distribution plots of these variables for each of the seven sedimentary units were no closer to normal or log-normal distributions than the above total-estuary plots. The lack of normality within the separate units probably reflects the combination of geological processes responsible for the final composition of each unit. In addition, the plots are not very useful in those units that have only a small number of samples. Therefore, only the distribution plots for the total estuary are presented.

ERROR ANALYSIS

One-way analysis of variance (Appendix B1e) can be used to test the significance of the combined analytical and sampling error. The method compares the means of several groups simultaneously, each group being repeat samples at individual localities when the technique is used to analyse these combined errors. If there is no significant difference between the groups of repeat samples from different localities for a particular variable, then the combination of errors masks any variation in that variable, i.e. there is no significant variation in that variable from locality to locality. Analysis of variance assumes both normality of the variable and equality of the variance of that variable for each group of repeat samples.

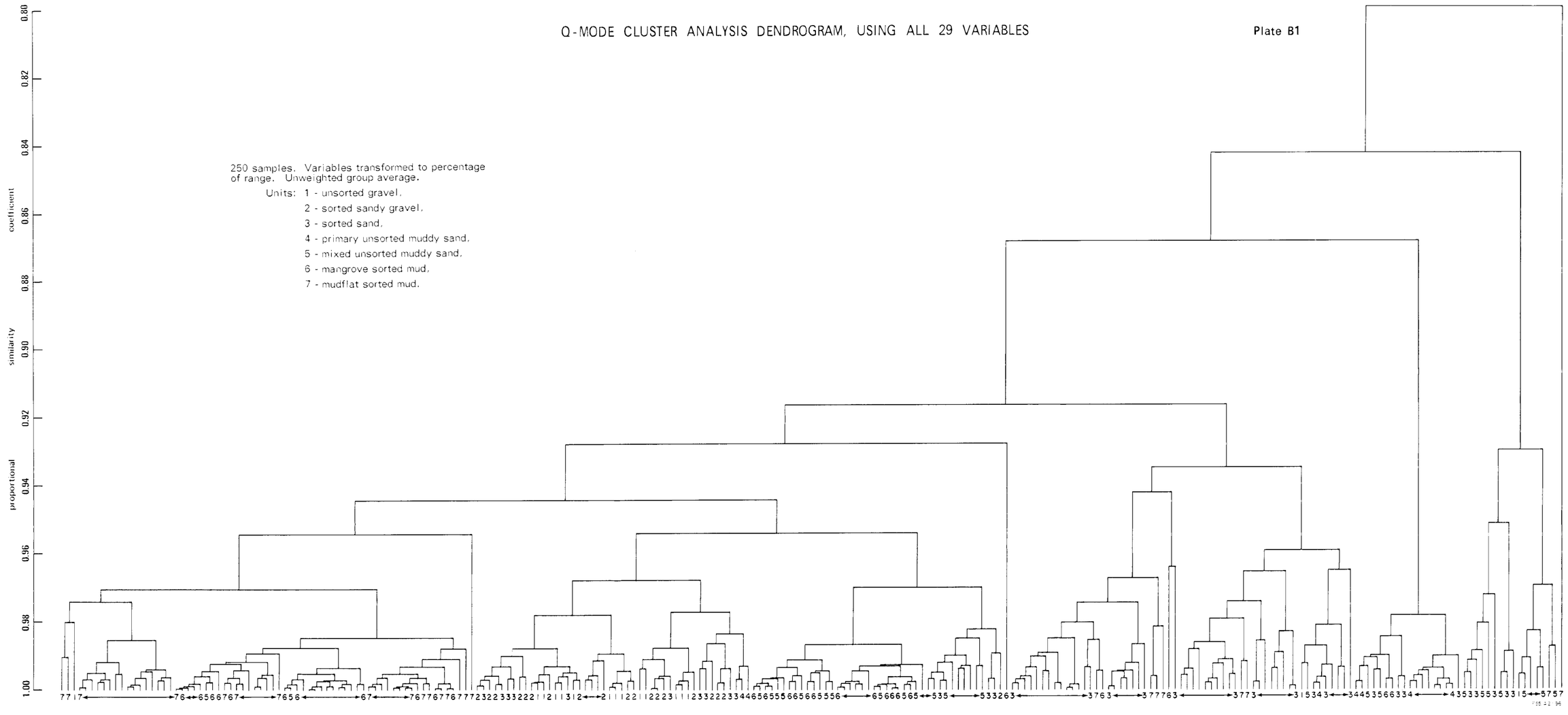
As the seven sedimentary units are considered separately in later numerical analyses, the error analysis was carried out separately on the results from individual units. Five of the seven sedimentary units had sufficient (three or more) localities with triplicate sampling for the analysis of variance test (see Appendix B1e). Table B7 lists the chi-square value of Bartlett's test for the equality of variances, and the F distribution value from the analysis of variance (see Appendix

Q-MODE CLUSTER ANALYSIS DENDROGRAM, USING ALL 29 VARIABLES

Plate B1

250 samples. Variables transformed to percentage of range. Unweighted group average.

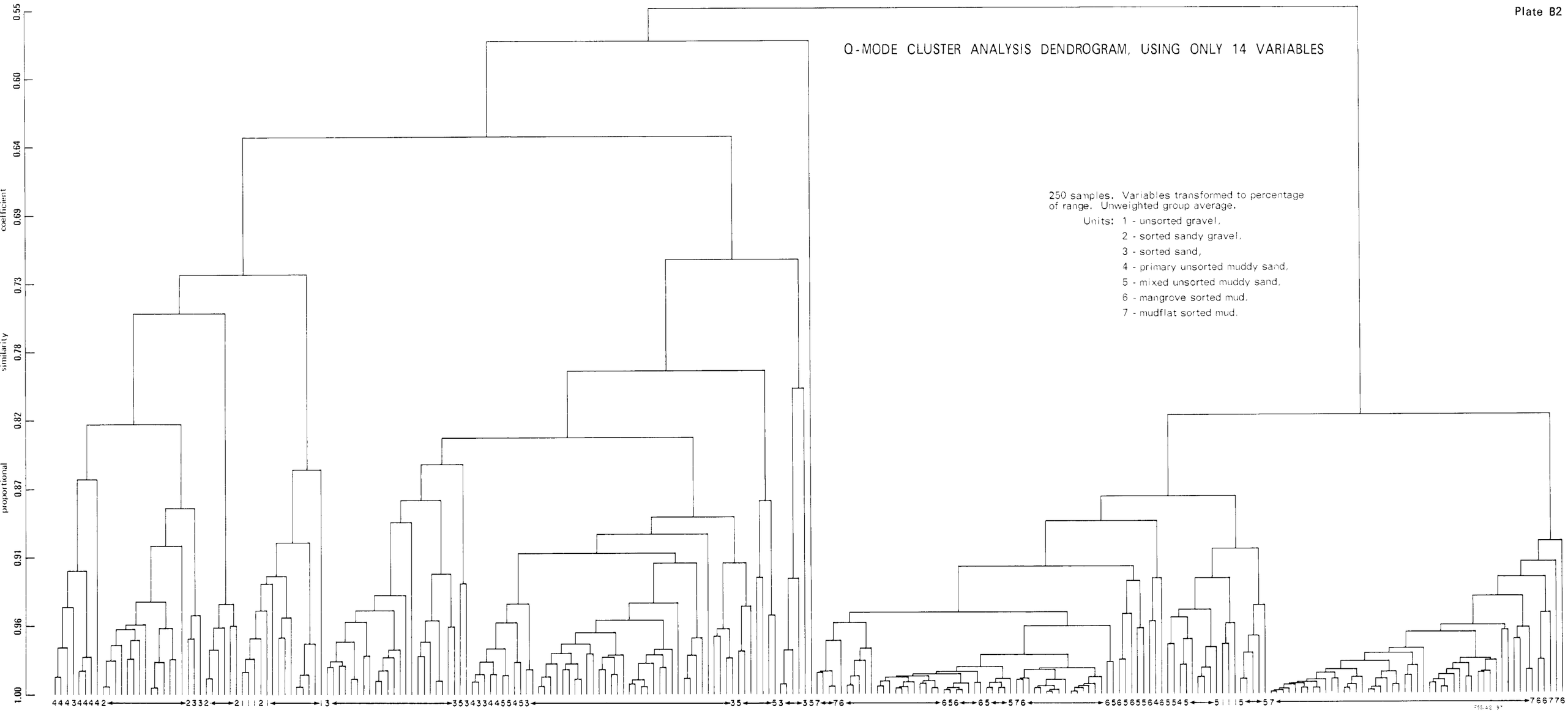
Units: 1 - unsorted gravel.
2 - sorted sandy gravel.
3 - sorted sand.
4 - primary unsorted muddy sand.
5 - mixed unsorted muddy sand.
6 - mangrove sorted mud.
7 - mudflat sorted mud.



Q-MODE CLUSTER ANALYSIS DENDROGRAM, USING ONLY 14 VARIABLES

250 samples. Variables transformed to percentage of range. Unweighted group average.

Units: 1 - unsorted gravel,
2 - sorted sandy gravel,
3 - sorted sand,
4 - primary unsorted muddy sand,
5 - mixed unsorted muddy sand,
6 - mangrove sorted mud,
7 - mudflat sorted mud.



B1e), for 19 variables measured on the estuary repeat samples.

Table B7 indicates that, at the 95-percent confidence level, many of the 19 variables in each of the units do not differ significantly between localities, suggesting that errors are masking the variation of that variable throughout the corresponding unit. Therefore, it could be argued that these variables should be left out of any numerical analyses carried out on the results from the corresponding sedimentary unit. However, many of the variables which have significant error do not satisfy the equality-of-variance requirement (Table B7), and also none of the variables satisfy the normality assumption, as was indicated above. Further, even if these two statistical assumptions were satisfied, the small number of repeat sampling localities in each sedimentary unit makes it difficult to justify completely removing variables from subsequent study. One or two localities in a particular unit that give results significantly different from the rest of the unit may be very important geologically. Consequently, a variable could only be removed completely from the results for a unit, using analysis of variance, if each locality in the unit had repeat results on that variable. Nevertheless, the analysis-of-variance results for the estuary were included for information, and Table B7 indicates that all 19 variables show significant differences in some of the sedimentary units.

Three samples were taken at each of the 28 localities in the intertidal and supratidal zones at Broad Sound by Mayo (1976). Analysis of variance showed that except for grainsize mean and standard deviation values in the supratidal sediments, all variables measured varied significantly from locality to locality. Because of the triplicate sampling at every locality in the study, the grainsize mean was able to be confidently replaced by percent clay as a surrogate measure of grainsize. Analysis of variance in this study by Mayo (1976) was also used to test for analytical error separately, as well as to test for the stability of pH and Eh readings over time.

INTERRELATIONS BETWEEN VARIABLES IN THE ESTUARINE SEDIMENTARY UNITS

The estuarine samples were classified into geologically meaningful sedimentary units to enable the detailed geochemical relations to be studied within each unit. Without this classification the relations between the variables would be on an inter-unit basis and much of the detail would be lost.

One-way analysis of variance (Appendix B1e) was usee to compare the means of each variable (Table B5) between all seven sedimentary units simultaneously. Ignoring the problem of lack of normality with these variables, this analysis showed that at the 99-percent level the only variable with no significant difference between the sedimentary units was the percentage of gravel with carbonate removed. Geological reasons for these differences between the units could have been discussed for each variable. However, to avoid this somewhat tedious approach, the inter-unit relations indicated from the Q-mode factor analysis are summarised, and further details of the inter-unit effects are considered as required when analysing each individual unit.

As explained earlier, the factor scores from the Q-mode factor analysis indicate the variables which most distinguish the sedimentary units in the factor analysis classification. The important variables corresponding to each of the three factors (or the 'composition' of each factor) in the analysis are shown in Table B2. Some of the variables are common to more than one factor and, in all, the analysis indicates that 12 variables are significant in discriminating the sedimentary units. Using the means of these 12 variables in each of the sedimentary units, as well as actual values of individual samples, the broad relations between the sedimentary-unit variables were determined and are illustrated diagramatically in Figure B5, where they are superimposed on the triangular factor loading plot of Figure B4.

The 14 most significant discriminatory variables indicated by the discriminant analysis (Table B3) differed somewhat from these 12 variables: P_2O_5 and percent sand were not included; the chemical elements Mg, Sr, V, and Zr were additional inclusions. Because the factor analysis was the basis of the classification, only the 12 significant variables from that analysis were studied in this way.

The following general points can be made from the relations shown in Figure B5:

(a) P_2O_5 is concentrated in the sorted-mud, unsorted-gravel, and sorted-sandy-

TABLE B5: MEAN VALUES OF THE VARIABLES IN EACH SEDIMENTARY UNIT

Variable		Units of Measurement	Unsorted Gravel (18)	Sorted Sandy Gravel (24)	Sorted Sand (75)	Primary Unsorted Muddy Sand (14)	Mixed Unsorted Muddy Sand (39)	Mangrove Sorted Mud (49)	Mudflat Sorted Mud (56)	Total Estuary (275)	Total Estuary (Minus Mangrove Channel Samples) (244)
Mean grainsize		phi	3.68	0.128	2.61	4.03	5.43	7.84	8.83	5.13	4.92
Grainsize standard deviation		phi	4.29	1.96	0.734	1.44	2.94	2.97	2.65	2.21	2.10
Gravel	carbonate retained	%	17.50	33.40	1.97	0.064	0.878	0.625	0.056	4.85	5.26
Sand	carbonate retained	%	39.4	64.00	96.7	74.9	49.2	6.70	2.90	47.1	50.22
Mud	carbonate retained	%	43.1	2.59	1.30	25.0	49.9	92.7	97.0	48.0	44.5
Silt	carbonate retained	%	21.7	1.41	1.29	20.5	24.1	38.3	28.5	19.0	17.3
Clay	carbonate retained	%	21.3	1.18	0.007	4.47	25.9	54.2	68.6	29.0	27.1
Gravel	carbonate removed	%	3.03	2.15	0.408	n.d.	0.380	0.321	0.209	0.652	0.613
Sand	carbonate removed	%	51.7	65.40	92.5	46.9	31.4	3.09	2.35	42.2	46.5
Mud	carbonate removed	%	45.2	32.50	7.12	53.1	68.2	96.5	97.4	57.2	52.8
Dolomite	percent of X.R.D. peak areas (0.426-nm quartz peak used, and the major peak for the others)		0.074	n.d.	0.299	0.248	0.147	0.207	0.447	0.248	0.254
Mg-Calcite	percent of X.R.D. peak areas (0.426-nm quartz peak used, and the major peak for the others)		18.3	28.9	16.3	25.3	18.1	12.6	4.16	15.1	15.2
Calcite	percent of X.R.D. peak areas (0.426-nm quartz peak used, and the major peak for the others)		51.0	49.7	16.0	16.5	17.8	16.5	4.73	19.3	19.6
Plagioclase	percent of X.R.D. peak areas (0.426-nm quartz peak used, and the major peak for the others)		9.04	3.30	8.16	22.1	23.3	28.1	37.9	23.0	22.5
Orthoclase	percent of X.R.D. peak areas (0.426-nm quartz peak used, and the major peak for the others)		3.40	1.90	11.2	8.46	7.77	6.20	7.77	7.65	7.76
Aragonite	percent of X.R.D. peak areas (0.426-nm quartz peak used, and the major peak for the others)		7.8	8.40	7.08	8.03	8.64	8.35	1.22	6.52	6.29
Quartz	percent of X.R.D. peak areas (0.426-nm quartz peak used, and the major peak for the others)		10.71	7.76	31.0	19.4	24.1	28.0	43.8	28.2	28.4

TABLE B5 (cont'd): MEAN VALUES OF THE VARIABLES IN EACH SEDIMENTARY UNIT

Variable	Units of Measurement	Unsorted Gravel (18)	Sorted Sandy Gravel (24)	Sorted Sand (75)	Primary Unsorted Muddy Sand (14)	Mixed Unsorted Muddy Sand (39)	Mangrove Sorted Mud (49)	Mudflat Sorted Mud (56)	Total Estuary (275)	Total Estuary (Minus Mangrove Channel Samples) (244)
Ba	ppm	96.3	65.3	179	208	184	206	244	184	181
Ca	ppm	16.9	22.5	9.51	17.9	11.8	6.65	1.45	9.73	9.79
Co	ppm	10.6	9.50	12.5	12.3	11.2	12.6	17.8	13.1	13.3
Cr	ppm	41.7	33.1	42.3	49.2	58.2	68.7	87.3	57.9	58.0
Cu	ppm	11.3	17.0	12.5	15.1	15.1	17.7	20.4	15.9	15.6
Fe	ppt	21.4	13.2	11.3	10.7	17.7	28.5	40.3	22.0	21.9
Mg	ppt	12.6	17.4	6.14	13.3	9.05	10.8	16.5	11.3	11.7
Mn	ppm	847	894	636	507	392	512	555	593	622
Ni	ppm	15.6	11.5	15.2	14.8	20.2	23.8	33.5	20.9	21.0
Pb	ppm	10.6	9.4	8.60	11.1	11.5	13.0	16.3	11.7	11.7
Sc	ppm	11.8	12.3	11.0	14.5	12.7	14.3	16.9	13.4	13.5
Sr	ppm	539	697	410	1171	520	399	178	449	446
Ti	ppt	2.75	1.57	2.11	2.33	3.51	4.04	4.82	3.21	3.16
V	ppm	47.7	42.8	34.6	39.3	45.7	58.1	70.8	49.5	49.1
Y	ppm	23.7	24.6	30.6	31.5	28.1	26.3	28.8	28.2	28.6
Zn	ppm	24.2	15.0	14.1	16.8	29.2	42.0	58.8	31.2	30.6
Zr	ppm	272	167	349	185	480	245	281	306	316
Carbonate	%	61.4	73.6	28.6	50.0	32.7	17.2	2.97	29.1	29.7
P_2O_5	ppm	1073	1079	473	528	680	854	836	739	732
Heavy minerals	% of non-carbonate fraction	0.959	0.694	0.816						
Opaque	% of heavy minerals	57.4	56.4	42.7						
Non-opaque		42.6	43.6	57.3						
Zircon	% of non-opaque heavy-mineral fraction	34.8	36.9	8.98						
Epidote		50.7	46.9	70.7	*	*	*	*		
Tourmaline		4.59	4.25	4.31						
Rutile		3.51	3.26	1.52						
Hornblende		4.42	6.43	10.4						
Garnet		0.970	0.736	0.709						
Zoisite		0.679	1.22	3.08						

* Heavy-mineral results not available
n.d. not detected

TABLE B6: STANDARD DEVIATION VALUES OF THE VARIABLES IN EACH SEDIMENTARY UNIT

Variable		Unsorted gravel	Sorted sandy gravel	Sorted sand	Primary unsorted muddy sand	Mixed unsorted muddy sand	Mangrove sorted mud	Mudflat sorted mud	Total estuary	Total estuary (minus mangrove -channel samples)
Mean grainsize (phi)		1.27	1.20	0.608	0.745	1.29	0.840	0.719	3.01	3.09
Grainsize standard deviation		0.422	0.815	0.402	0.478	0.719	0.446	0.325	1.18	1.17
Gravel	carbonate retained	11.3	23.3	3.98	0.241	2.75	2.256	0.418	12.5	13.1
Sand	carbonate retained	11.3	24.3	4.21	20.2	24.4	6.69	5.09	40.1	40.8
Mud	carbonate retained	12.3	5.66	2.37	20.2	24.3	7.67	5.24	42.3	42.8
Silt	carbonate retained	13.8	3.05	2.36	15.7	13.3	10.97	8.54	17.0	16.9
Clay	carbonate retained	7.95	3.28	0.044	4.61	14.7cc	12.5	11.6	29.3	29.8
Gravel	carbonate removed	6.32	3.14	1.89	nd	2.05	1.09	0.984	2.43	2.42
Sand	carbonate removed	13.6	19.6	7.29	25.0	28.4	5.33	4.66	39.6	39.9
Mud	carbonate removed	14.5	19.9	6.87	25.0	28.2	6.24	5.30	39.8	40.1
Dolomite		0.248	nd	0.494	0.414	0.290	0.419	1.25	0.677	0.705
Mg-calcite		8.33	10.2	7.27	7.67	3.83	3.22	5.18	9.44	9.95
Calcite		18.0	12.8	7.50	3.66	5.21	3.20	5.69	16.0	17.0
Plagioclase		5.63	2.37	7.95	5.42	6.46	3.80	6.41	11.9	12.5
Orthoclase		2.64	2.26	3.95	3.81	3.51	3.06	4.18	4.52	4.66
Aragonite		2.50	2.58	2.67	2.13	1.48	1.94	2.57	3.59	3.72
Quartz		4.42	5.32	8.86	4.93	4.19	3.89	9.26	12.8	13.5
Ba		33.2	21.8	56.7	50.1	25.7	39.7	165	97.7	103
Ca		8.98	8.68	3.45	3.65	4.01	1.79	1.35	7.47	7.76
Co		2.03	1.87	3.73	5.25	4.76	3.09	6.91	5.17	5.37
Cr		7.54	13.6	22.9	20.6	21.9	19.8	26.8	28.2	29.7
Cu		3.72	14.8	7.32	13.1	6.33	5.80	6.04	8.37	8.43
Fe		4.88	4.33	3.16	3.29	7.78	9.56	13.1	14.3	14.9
Mg		3.00	7.61	2.47	4.63	3.46	4.72	7.55	6.49	6.72
Mn		355	303	260	125	81.2	556	187	342	350
Ni		3.40	2.00	4.76	5.78	8.55	7.30	11.0	10.3	10.8
Pb		3.79	2.68	3.84	4.46	6.60	3.21	4.18	5.05	5.24
Sc		1.29	2.10	2.41	4.64	2.35	2.89	3.10	3.46	3.57
Sr		151	195	174	656	164	173	118	307	323
Ti		0.932	0.776	1.40	0.606	1.39	0.959	1.36	1.65	1.73
V		8.80	11.2	8.63	16.1	11.4	15.3	20.6	19.3	19.9
Y		3.24	4.52	9.56	18.1	7.57	4.87	4.65	8.06	8.34
Zn		9.28	2.55	6.30	3.17	11.90	10.6	11.0	19.3	20.1
Zr		206	120	352	85.9	569	49.3	81.7	303	320
Carbonate		11.8	10.2	11.3	11.5	11.2	4.83	3.18	22.6	23.5
P_2O_5		212	232	120	74.7	159	162	295	284	297
Heavy minerals		0.746	0.564	0.688						
Opaque		11.4	16.2	13.4						
Non-opaque		11.4	16.2	13.4						
Zircon		19.5	24.3	9.30						
Epidote		19.4	23.2	14.1	*	*	*	*		
Tourmaline		3.54	2.37	3.67						
Rutile		2.08	3.22	1.71						
Hornblende		4.37	5.97	6.60						
Garnet		1.11	0.894	0.971						
Zoisite		1.02	1.62	3.01						

* Heavy-mineral results not available.
nd: not detected.

gravel units, revealing its association with the clay fraction and with the biogenic and carbonate-nodule material.

(b) Zn is closely associated with the clay fraction.

(c) Mg-calcite is associated with the shells and carbonate nodules.

(d) Although there is a suggestion (Table B5) that some aragonite is being converted to dolomite in the mudflat zone, the low aragonite values in this zone probably simply reflect the overall decrease in carbonate and the corresponding increase in quartz and plagioclase in the mudflat-sorted-mud unit. The low carbonate in turn reflects the preferential removal of the sand and silt-sized carbonate by the low-energy sorting process (Cook & Mayo, 1978, p. 104) and the proximity of the supratidal mudflat zone to the land.

METHODS OF DATA ANALYSIS

The relations between the variables within each of the sedimentary units were analysed using R-mode factor analysis (Appendix B1f), multiple stepwise linear regression (Appendix B1g), and R-technique canonical correlation analysis (Appendix B1c). The strategy with the

TABLE B7: ONE-WAY-ANALYSIS-OF-VARIANCE RESULTS FOR TRIPLICATE SAMPLING

	UNSORTED GRAVEL		SORTED SAND		MIXED UNSORTED MUDDY SAND		MANGROVE SORTED MUD		MUDFLAT SORTED MUD	
	λ^2_2	F(2,6)	λ^2_7	F(7,16)	λ^2_4	F(4,10)	λ^2_7	F(7,16)	λ^2_5	F(5,12)
Ba	7.02*	2.76**	31.32*	14.55	5.08	1.93**	16.40*	1.25**	41.36*	2.79**
Ca	9.94	0.18**	13.67	12.13	5.93	9.19	31.52*	5.59	52.93*	3.34
Co	1.31	9.88	7.04	2.53**	0.32	2.30**	25.74*	0.84**	9.59	87.96
Cr	0.90	3.15**	25.38*	3.47	7.63	2.95**	18.13*	0.86**	5.78	2.31**
Cu	6.63*	7.84	>100*	0.70**	2.38	1.64**	13.89	0.57**	33.48*	1.69**
Fe	0.37	1.54**	26.50*	18.44	11.48**	1.62**	35.19*	1.43**	5.86	26.48
Mg	6.45*	1.96**	15.79*	4.40	6.04	1.63**	11.60	10.93	23.94*	2.41**
Mn	10.00*	13.22	>100*	44.72	12.31**	11.38	74.91*	0.72**	22.84*	46.17
Ni	1.50	13.03	23.80*	1.30**	9.00	2.10**	34.81*	1.37**	6.84	52.85
Pb	3.63	0.64**	>100*	3.93	>100**	>100	3.60	0.91**	>100*	8.90
Sc	1.37	5.44	8.24	0.89**	0.91	1.50**	27.02*	0.77**	>100*	3.06**
Sr	2.09	12.93	6.07	10.91	6.58	1.57**	48.14*	3.07	21.80*	5.65
Ti	9.08*	2.95**	28.75*	3.83	4.89	4.64	35.35*	0.82**	25.14*	5.01
V	1.81	9.75	>100*	1.00**	6.60	1.63**	39.18*	1.04**	6.58	11.97
Y	0.81	1.60**	18.18*	3.58	4.14	2.49**	10.11	1.13**	18.95*	2.97**
Zn	8.43*	7.14	>100*	0.96**	7.89	9.88	44.05*	5.96	>100*	5.90
Zr	1.15	0.09**	>100*	2.52**	11.24**	9.50	18.21*	0.59**	3.87	2.93**
Carbonate	4.59	6.09	12.39	11.31	15.29**	7.00	43.98**	5.10	8.59	0.95**
P_2O_5	1.17	9.43	13.08	7.61	0.13	13.53	>100*	17.11	9.43	28.13
Theoretical distribution value at 95% level	5.99	5.14	14.1	2.66	9.5	3.48	14.1	2.66	11.1	3.11
No. of repeat localities	3	3	8	8	5	5	8	8	6	6

* Bartlett's test for the equality of variance between localities with repeat sampling rejected, indicating the analysis of variance is not valid for that variable.

** Hypothesis for equality of means of the localities with repeat sampling accepted at the 95% level, indicating significant error for that variable.

λ^2 stands for the chi-square distribution.

Broad Sound estuarine samples was to measure as many variables as time and facilities would permit so that all possible relations between these variables could be determined. It can be argued that this 'fishing expedition' or 'shotgun' approach (Browner & Veinus, 1974) lacks the scientific rigour of having one pre-defined problem and measuring the variables best suited to the techniques that are to be used to solve that problem. Nevertheless, the 'shotgun' approach often produces useful results which would not have been obtained using a more restrictive approach. Given that the aim of the numerical analysis of the estuarine data was to obtain the overall relations between the variables to enable general geological interpretation, with the expectation that these results could point to certain aspects worthy of more detailed study, this strategy was warranted.

It should be emphasised that the geochemical observations made with the aid of these numerical techniques could well be interpreted differently by other researchers. For this reason, the most important results from these techniques are given in Appendix B1 and the original data set may be obtained as indicated in Appendix B4.

R-mode factor analysis.

Much of the intuitive discussion of R-mode factor analysis in Appendix B1f links the resulting mathematical factors with geological processes. It is also suggested there that careful selection of the variables included in the analysis is required to enable the final factors in an actual study to be linked to corresponding geological processes. The 'fishing expedition' strategy for variable selection meant that this controlled geological interpretation of the factors was not possible. This limitation, as well as the closed array problems with the grainsize fraction percentage data, the mineralogical data, and the heavy-mineral percentages, reduced the results from the R-mode factors to a general geological classification of several groups of associated variables. Nevertheless, geological interpretation of these factors was still possible.

The variables shown in Table B6 were used in the factor analyses, the heavy-mineral results being unavailable for the unsorted-muddy-sand and the sorted-mud units. In addition, dolomite and gravel (with the carbonate removed) were not detected in the samples from the sorted-sandy-gravel and primary-unsorted-muddy-sand units respectively, and were therefore not included in the factor analysis for those units. In an attempt to overcome the closed array problems, an R-mode factor analysis was also carried out on each of the sedimentary units using the following 24 variables: mean grainsize, grainsize standard deviation, Mg-calcite, aragonite, quartz, Ba, Ca, Co, Cr, Cu, Fe, Mg, Mn, Ni, Pb, Sc, Sr, Ti, V, Y, Zn, Zr, carbonate, and P_2O_5.

No significant differences in the associations of these variables resulted, and in addition, the geological interpretations were made more difficult. Therefore the results with all variables included were used.

Appendix B1f discusses in detail how the 'ideal number of rotated factors was selected for each analysis and how the significant factor loadings were identified. The oblique factor matrixes for all of the sedimentary units with the silnificant loadings distinguished are given in Tables B25-31 (Appendix B1f), and a working summary of the results of each analysis is given for each sedimentary unit later in this chapter.

Multiple linear stepwise regression

Full details of the stepwise regression procedures and the associated assumptions are given in Appendix B1g. With the data for each sedimentary unit, stepwise regression analyses were carriee out using each chemical element (including P_2O_5) in turn as the dependent variable, and the variables shown in Table B8 as the explanatory, or 'independent' variables. To minimise the likelihood of mutually correlated variables beinl included in the final regression equations, any grainsize analysis variable which had a significant correlation with another grainsize variable was remoped from the a alysis. Most of these grainsize variables were correlated with the mean grainsize parameter and were therefore removed. Similarly, the non-opaque heavy-mineral variable was removed because of its dependence on the opaque heavy-mineral variable. Table B8 indicates the deleted variables by showing the variable remaining in the analysis which is significantly correlated with the removed variable and the sign of the correlation coefficient.

The detailed regression analysis results are given in Tables B32-39 (Appendix B1g). Diagramatic representations of these results are given below, in the discussion of each sedimentary unit. Although those regression equations which are shown, in Tables B32-39, to be poor predictors of the corresponding dependent variable (by having an excessive sum of squares remaining after the regression) may be used in general discussions, they will not be used in final interpretations. (An excessive sum of squares remaining may be due to important unmeasured variables not being included in the analysis. Therefore, conclusions based on equations which are poor predictors could be misleading. Nevertheless, the relations between the dependent and the independent variables shown in these equations are statistically significant and can still be used confidently).

Combined with the R-mode factor analysis, which groups variables associated with the same geological processes, the regression results were found to be valuable in explaining and clarifying the detailed relations of the variables measured on the estuarine samples.

R-technique canonical correlation analysis

Because of the usefulness of multiple regression in analysing the estuarine results, R-technique canonical correlation analysis was expected to be helpful too, because the technique is used to analyse the relation between two sets of variables measured on the same samples (Appendix B1c). In fact, Cooley & Lohnes (1971, p. 176) suggest that 'multiple regression analysis of each variable of each set regressed on all the variables of the other set is a useful supplement, but no substitute for, the canonical structure'.

With each analysis, all chemical elements except Fe, Mn, and P_2O_5 were included as one set of variables with Fe, Mn, P_2O_5, together with the mineralogical variables, the heavy mineral variables if applicable, and the grainsize mean and standard deviation comprising the second set. To enable valid comparison of the canonical coefficients corresponding to each variable, a percent-of-the-range transformation was carried out on each variable.

The results of the analyses again seemed to be restricted by the closed array problems in the data. This was especially so with the results from the unsorted-gravel, sorted-sandy-gravel, and sorted-sand units because of closed array problems with the mineralogical data. Although the canonical correlation analysis was certainly no substitute for the factor and regression

TABLE B8. INDEPENDENT VARIABLES: STEPWISE REGRESSION ANALYSIS

Independent Variable		Unsorted Gravel	Sorted Sandy Gravel	Sorted Sand	Primary Unsorted Muddy Sand	Mixed Unsorted Muddy Sand	Mangrove Sorted Mud	Mudflat Sorted Mud
Mean grainsize (phi)								
Grainsize std dev.		−MEAN		−MEAN	+MEAN	+MEAN	−MEAN	−MEAN
Gravel	carbonate retained	−MEAN	−MEAN	−MEAN		+GRAVEL (IN)	−MEAN	−MEAN
Sand	carbonate retained		+MEAN	+MEAN	−MEAN	−MEAN	−MEAN	−MEAN
Mud	carbonate retained	+MEAN	+STD DEV.	+MEAN	+MEAN	+MEAN	+MEAN	+MEAN
Silt	carbonate retained	+SAND (OUT)	+STD DEV.	+MEAN	+MEAN	+MEAN	−MEAN	−MEAN
Clay	carbonate retained	+MEAN	+STD DEV.		+MEAN	+MEAN	+MEAN	+MEAN
Gravel	carbonate removed			−MEAN	*		−MEAN	
Sand	carbonate removed	+MEAN	+MEAN	−MUD (IN)	MEAN	−MEAN	−MEAN	−MEAN
Mud	carbonate removed		+MEAN		+MEAN	+MEAN	+MEAN	+MEAN
Dolomite			*					
Mg-calcite								
Plagioclase								
Orthoclase								
Aragonite								
Quartz								
Carbonate								
P_2O_5								
Fe								
Mn								
Heavy minerals					*	*	*	*
Opaque					*	*	*	*
Non-opaque		−OPAQUE	−OPAQUE	−OPAQUE	*	*	*	*
Zircon					*	*	*	*
Epidote					*	*	*	*
Tourmaline					*	*	*	*
Rutile					*	*	*	*
Hornblende					*	*	*	*
Garnet					*	*	*	*
Zoisite					*	*	*	*

Variables included in the final regression equations are left blank.
Variables deleted are indicated by showing the variables remaining in the analysis which is significantly correlated with the deleted variable (and the sign of the correlation coefficient).
* No value.

analyses, the canonical correlation results were often useful in supporting interpretations based on the results from these other techniques. Full details of the R-technique canonical analysis of the mangrove and mudflat-sorted-mud units are given later.

Significance of correlation coefficients

The correlation coefficients based on the number of samples representing each sedimentary unit are used throughout the following discussions of the interrelations between the measured variables. The significance of these is tested using the transformation of this sample correlation coefficient, which results in

$$\sqrt{\frac{n-3}{2}}\left(\log_e\left[\frac{1+r}{1-r}\right]-\log_e\left[\frac{1+\rho}{1-\rho}\right]\right)$$

being approximately distributed as the normal (0, 1) distribution,

where r = sample correlation coefficient,
n = number of pairs of values (of the two variables) used to determine r,
and ρ = population correlation coefficient.

This result does not assume that the two variables follow a bivariate normal distribution as does the Student's t test that is also used for testing the significance of correlation coefficients.

The significance of r is tested at the desired confidence level by testing the hypothesis that ρ equals a selected value. Unless otherwise stated, a sample correlation coefficient called 'significant' in the following discussions reflects the rejection of the hypothesis that $\rho = 0.0$ at the 95-percent level. This corresponds to the above

mathematical expression being greater than the normal (0, 1) distribution 95-percent critical value ($\pm$ 1.96), with ρ being set to 0.0. 'Significant', then, implies a linear trend, although not necessarily an excellent one, between the two variables.

Testing the equality of means

Two different tests are commonly used to compare the means of a variable measured on two sets of geological samples. The normal distribution test is for sets with large numbers of samples (greater than about 30) because then the means may be assumed to be normally distributed and the standard deviation values obtained may be regarded as the population standard deviation values without serious error (Hoel, 1962). Student's *t* distribution test is used for small sample numbers and although this test does not require the values of any population parameters, the equality of population variances is assumed. Therefore, with this *t* test an additional F-distribution test for the equality of variance is required (Hoel, 1962).

Although three of the sedimentary units are each represented by fewer than 30 samples (Table B5), the normal distribution test was used for comparing means between all sedimentary units. Under the hypothesis that the mean value of a variable between two sedimentary units is the same,

$$\frac{\overline{x_1} - \overline{x_2}}{\sqrt{\frac{x_1^2}{n_1} + \frac{x_2^2}{n_2}}}$$

is distributed as the

normal (0, 1) distribution,

where $\overline{x_1}$ and $\overline{x_2}$ are the sample means in unit 1 and 2 respectively,
x_1^2 and x_2^2 are the population variances in units 1 and 2 respectively (which are replaced by the sample variances),
and n_1 and n_2 are the number of values of the variable in units 1 and 2 respectively.

Therefore, if the value of the above expression is greater than the normal (0, 1) distribution 95-percent critical value ($\pm$1.96), then the hypothesis that the means are equal is rejected at this level of confidence. Unless otherwise stated, the descriptions 'greater than' or 'less than', used when comparing mean values between the sedimentary units, are based on the above test at the 95-percent confidence level.

MANGROVE-SORTED-MUD UNIT

This unit represents preferential deposition of silt and clay near the boundary of the supratidal and intertidal zones, owing to sorting processes discussed in Cook & Mayo (1978) and summarised above. The numerical classification included samples from the supratidal-flat, mangrove-swamp, mangrove-channel, and open-intertidal environments in this unit because of the numerical similarity of the variables measured on these samples. This numerical similarity in turn reflects the fact that the mangrove deposits are concentrated near the boundary of the intertidal and supratidal zones, and that the open-intertidal deposits flanking the mangrove-swamp and mangrove-channel deposits consist mainly of mangrove-swamp sediment.

The mangrove-sorted-mud unit is distinguished from the mudflat-sorted-mud unit by higher silt, lower clay, and higher carbonate. These differences reflect the preferential deposition of carbonate silt in the mangrove swamps compared to the supratidal mudflats (Cook & Mayo, 1978, p. 104). Therefore, the boundary between the two sorted mud units would be expected to be gradational, which explains why the numerical classification causes several supratidal mudflat samples to be included in the mangrove-sorted-mud unit.

Table B9 shows the relevant results from the R-mode factor analysis and stepwise regression analysis for this unit. It summarises the relations between the variables with significant factor loadings in two of the five factors resulting from the factor analysis (Table B25). The correlation (or lack of it) between these variables as well as the associated multiple regression results (summarised in Table B9 from Table B33) clarify some of the geochemical relations in the mangrove-sorted-mud unit.

The interpretations associated with the grainsize/carbonate control factor in Table B9 are relatively straightforward. A significant amount of the silt fraction consists of zircon particles, and carbonate particles in which Sr partly substitutes for Ca. Zn and P_2O_5 (probably in the form of PO_4^{3-}) are adsorbed on the clay-sized particles and are also possibly attached to ferric-hydroxide colloids deposited on the sediment. The suggested association of both Zn and P_2O_5 with ferric-hydroxide colloids implies both negatively and positively charged ferric-hydroxide particles. This implication is discussed in more detail below.

The trace-element factor has significant factor loadings (Table B9) for 10 of the 17 elements in the factor analysis, including Fe. Although organic carbon was not a variable in this analysis, Mayo (1976) found no association of trace elements with organic carbon in the Broad Sound supratidal deposits, and therefore this factor probably reflects the attraction of the trace elements to ferric-hydroxide colloids. Ferric-hydroxide colloids may be either positively or negatively charged depending on the presence of excess H^+ or OH^- (Krauskopf, 1967). The alkaline estuarine environment would be expected to result in negatively charged ferric-hydroxide colloids which would tend to attract the trace-element cations.

Stumm & Morgan (1970, ch. 10) state that in view of the fact that the ion exchange capacities of hydrous manganese and ferric oxides are large, it is to be expected that these oxides will profoundly modify the distribution of trace elements such as Cu, Co, Ni, Zn, and Sr which can be adsorbed on these oxides. Goldberg (1954) indicated that the concentrations of trace elements in the ocean sediments depend on the Fe or Mn content of the sediments. Cation adsorption capacities of the hydrous oxides are comparable on a per-weight basis with those of clays (Stumm & Morgan, 1970) and the main difference in the adsorption process between the oxides and clays is that the trace elements are released from the oxides under acid or reducing conditions. This cation release was noted under reducing conditions in the Broad Sound intertidal zone by Mayo (1976).

Because of the suggested trace-element association with hydrated oxide colloids, Fe and Mn were included as response variables in the multiple regression analyses, and Fe proved to be an important predictor for Co, Cr, Ni, Sc, Sr, Ti, and V. The regression equation for each of these elements includes a negative P_2O_5 term which seems to contradict the positive linear relation between P_2O_5 and Fe (Table B9). These relations suggest that P_2O_5 adsorbed on the Fe colloids is being exchanged for the trace elements, either before or after deposition of the colloids. Mayo (1976) found an association between P_2O_5 and organic carbon in the Broad Sound supratidal sediments, and the inclusion of organic carbon in this study may have clarified these interrelations.

Ferric-hydroxide colloids probably form in the Broad Sound catchment under slightly acid conditions (Krauskopf, 1967) and so would be positively charged and as such could attract phosphate ions. Under alkaline marine conditions the colloids could tend to become negatively charged and the P_2O_5 could tend to be replaced by the trace elements. The suspended Fe particles would be expected to be preferentially deposited as the tidal currents enter the mangrove-swamp environment, but whether the ion exchange occurs before or after deposition is uncertain. Probably the exchange takes place in both situations. The importance of this Fe colloid deposition in this unit is shown by the fact that the Fe concentration is significantly greater in this unit than in all other units except mudflat-sorted mud.

TABLE B9. SUMMARY OF FACTOR AND REGRESSION ANALYSES RESULTS, MANGROVE-SORTED-MUD UNIT

A. GRAINSIZE/CARBONATE CONTROL FACTOR

GROUP 1	GROUP 2
Mean grainsize (phi)	Silt
Clay	Ca
Zn	Sr
P_2O_5	Zr
	Carbonate
	(no significant correlation: Zr-Sr, Zr-carbonate)

RELEVANT REGRESSIONS:

Zn = mean grainsize (phi), P_2O_5, Fe
P_2O_5 = Fe, mean grainsize.

B. TRACE-ELEMENT FACTOR

Ba, Cr, Co, Fe, Ni, Sc, Sr, Ti, V, Y
(no significant correlation: Fe-Ba, Fe-Y, Ni-Y, Ti-Y, V-Y)

RELEVANT REGRESSIONS:

Co = Fe
Cr = Fe, $-P_2O_5$
Ni = Fe, $-P_2O_5$, mean grainsize (phi), orthoclase
Sc = Fe, $-P_2O_5$
Sr = Fe, $-P_2O_5$, mean grainsize (phi)
Ti = Fe, $-P_2O_5$
V = Fe, $-P_2O_5$, orthoclase.

Notes:

1. The variables with significant factor loadings in Factor A are split into two groups on the sign of the loadings. Each variable in one of these groups of variables is negatively correlated with each variable in the other group, but not necessarily significantly.

2. The significant Factor B loadings all had the same sign.

3. All pairs of variables in each group of variables have a significant positive correlation (i.e. $H_0 : \rho = 0.0$ rejected at the 95-percent confidence level), except as indicated above.

4. The dependent variable in each regression equation is shown to the left of the 'equals' sign, and the independent variables, with the appropriate sign, to the right. The independent variables are listed in decreasing order of importance as predictors of the dependent variable (from the 'increase in RSQ' values in Table B33).

Fe, apart from being included in the regression equations for the seven trace elements shown in Table B9, is also included in the equations for Ba (and again with negative P_2O_5), but the linear regression in this case is not an adequate predictor of the changes in Ba. Nevertheless, this explains the inclusion of Ba in the trace-element factor. The inclusion of Y in the trace element factor cannot be adequately explained.

The mangrove-sorted-mud then represents deposition of

(1) silt and clay sorted under low-energy conditions, Zn and P_2O_5 being adsorbed on the clay-sized particles, Sr replacing Ca in the carbonate silt fraction, and the terrigenous silt fraction containing significant amounts of zircon;
(2) ferric-hydroxide colloids with adsorbed P_2O_5 ; P_2O_5 being exchanged for Co, Cr, Ni, Sc, Sr, Ti, and V.

TABLE B10. SUMMARY OF FACTOR AND REGRESSION ANALYSES RESULTS, MUDFLAT-SORTED-MUD UNIT

A. TRACE-ELEMENT FACTOR

Fe, Mn, Co, Cr, Ni, Sc, Ti, V
All are significantly correlated (positively) at the 99-percent level.

RELEVANT REGRESSIONS:

Co = Mn
Cr = Fe, orthoclase, −gravel (carbonate removed)
Ni = Fe, Mn, −plagioclase, −gravel (carbonate removed)
Sc = Fe, plagioclase, Mn
Ti = Fe, $-P_2O_5$, −plagioclase, mean grainsize (phi)
V = Fe, orthoclase

B. GRAINSIZE CONTROL FACTOR

GROUP 1	GROUP 2
Zn	Silt
P_2O_5	Orthoclase

RELEVANT REGRESSIONS:

Zn = P_2O_5, mean grainsize (phi), −Mg-calcite, Mn

C. OTHER TRACE-ELEMENT REGRESSIONS

Ba = gravel, −mean grainsize (phi), Fe, plagioclase
Sr = aragonite, Fe, $-P_2O_5$, Mg-calcite
Zr = −mean grainsize (phi), $-P_2O_5$, Fe

Notes:

1. The variables with significant factor loadings in Factor B are split into two groups on the sign of the loadings. Each variable in one of these groups of variables is negatively correlated with each variable in the other group, but not necessarily significantly, and each pair of variables in each group has a significant positive correlation ($H_o : \rho = 0.0$ rejected at the 99% level).
2. The dependent variable in each regression equation is shown to the left of the 'equals' sign, and the independent variables (with the appropriate sign) to the right. The independent variables are listed in decreasing order of importance as predictors of the dependent variables (from the 'increase in RSQ' values in Table B34).

MUDFLAT-SORTED-MUD UNIT

All the samples representing this sedimentary unit are from the supratidal mudflats. The unit reflects low-carbonate and high-mud deposition under low-energy sorting conditions (Table B1). Higher mud and clay content, and lower sand, silt, and carbonate distinguish this unit from the mangrove-sorted-mud unit. These mostly physical differences are a result of preferential estuarine deposition of carbonate and non-carbonate sand and silt in the mangrove swamps rather than on the supratidal mudflats. In addition, most of the sand and minor amounts of silt and clay in the unit are locally derived terrigenous sediment.

As with the mangrove unit, two factors are geochemically important out of the six final factors from the R-mode factor analysis (Table B26): one trace-element factor and one grainsize-control factor. The variables controlled by these factors are summarised in Table B10. Notably the trace-element factor includes both Fe and Mn with this unit, whereas Fe but not Mn was included in the mangrove unit's trace-element factor. The contrasting geochemical relations of Fe and Mn between the mangrove and mudflats unit is well illustrated in Table B11. The correlations between Fe and the other elements only differ markedly with Ca, Zn, P_2O_5, and Mn from the mangrove to the mudflat units, whereas with Mn there are no significant correlations in the mangrove unit, and all elements except seven are positively correlated in the mudflat unit.

As a result of these observations both Fe and Mn were included as response variables in the stepwise regression analysis for all sedimentary units. The multiple regression equations relevant to each of the two R-mode factors of geochemical importance to the mudflat-sorted-mud unit, as well as those for three trace elements not included in these two factors, are summarised in Table B10 from Table B34.

The grainsize control factor again reflects the affinity of P_2O_5 and Zn for the clay-sized particles. Although 'clay' was not included in the grainsize control factor, the silt content is inversely related to the clay content in this unit (correlation coefficient = −0.909), and Table B8 indicates that the mean grainsize parameter in the regression equation for Zn would reflect decreasing silt and increasing clay. The adsorption of P_2O_5 and Zn on the clay particles dominates any adsorption on Fe colloids, but Zn is probably also adsorbed to a limited extent on Mn colloids deposited in the mudflat sediments. These differences with the Zn and P_2O_5

associations between the mudflat and mangrove-sorted muds are also reflected in the correlations of these variables with Fe and Mn in the two units (Table B11).

The geological process represented by the trace-element factor is probably cation adsorption on both Fe and Mn colloidal particles and the regression analysis results (Tables B10 and B34) reveal the details of the relations of the cations with these two types of colloids. Co is associated with the Mn colloids; Cr, Ti and V are associated with Fe colloids; and Ni and Sc have affinity for both the Fe and Mn colloids, the Fe association being dominant. These differences in colloidal affinity must be considered somewhat arbitrary, though, because of the close association of Mn and Fe in this unit (correlation coefficient 0.538). Ti is the only adsorbed cation displaying a negative relation with P_2O_5, and this, coupled with the lack of any significant Fe-P_2O_5 relation in the mudflat unit, indicates that the suggested colloidal ionic exchange of the trace elements for P_2O_5 in the mangrove unit is effected more completely after deposition in the mudflat unit.

The importance of the Mn colloids in the mudflat unit compared with the mangrove unit may be due to the greater stability of Mn in ionic solution compared with Fe (Keith & Degens, 1959). Whereas much of the Fe reaching the estuarine complex is probably in the form of ferric-hydroxide colloids, a large percentage of the Mn enters the estuaries in the dissolved divalent form (Murata, 1939). Consequently, the Fe colloids may be expected to be deposited readily in the low-energy conditions in the estuarine supratidal zone (which encompasses the mangrove swamps and supratidal mudflats), perhaps with some preference for the mangrove swamp environment adjacent to the intertidal zone.

Stumm & Morgan (1970) also note that Mn^{2+} does not oxidise as readily as Fe^{2+}, and dissolved Mn would be expected to be carried through the mangroves to the supratidal mudflats where oxidation and formation of negatively charged manganese hydroxide colloids may occur with the associated attraction of trace-element cations. This process could be particularly important in the pools of surface water remaining on the mudflats after the spring tides recede. Mn^{2+} oxidation can occur close to surfaces with higher pH than the bulk of the surface water (Stumm & Morgan, 1970), and the pH of water just above algal mats on the supratidal mudflats was commonly close to 9.

TABLE B11. COMPARISON OF THE CORRELATIONS OF Fe AND Mn WITH THE OTHER ELEMENTS, BETWEEN MANGROVE-SORTED-MUD AND MUDFLAT-SORTED-MUD UNITS

Variable	Fe correlation		Mn correlation	
	Mangrove	Mudflat	Mangrove	Mudflat
Ba	0.266*	0.369	−0.066*	0.046*
Ca	−0.436	0.269*	0.141*	0.036*
Co	0.723	0.490	0.034*	0.670
Cr	0.715	0.844	0.149*	0.522
Cu	0.333	0.393	0.044*	0.245*
Fe	1.000	1.000	0.002*	0.538
Mg	0.589	0.220*	0.102*	0.169*
Mn	0.002*	0.538	1.000	1.000
Ni	0.789	0.823	0.026*	0.656
Pb	0.334	0.370	−0.047*	0.429
Sc	0.591	0.607	0.007*	0.483
Sr	0.317*	0.435	0.026*	0.259*
Ti	0.646	0.773	0.041*	0.528
V	0.748	0.709	0.021*	0.514
Y	0.135*	0.144*	−0.021*	0.413
Zn	0.610	0.179*	−0.027*	0.279*
Zr	0.072*	0.166*	0.091*	0.065*
P_2O_5	0.505	0.116*	−0.190*	−0.024*

* no significant linear trend.

The limiting sample-correlation coefficient value for significance, under the hypothesis that the population correlation coefficient, ρ , is 0.0 at the 95% level, is 0.329 for the mangrove unit with 49 samples, and 0.272 for the mudflat unit with 56 samples.

The multiple regression equations for the elements Ba, Sr, and Zr, which were not included in the two R-mode factors are also given in Table B10. Ba is concentrated in the sand and gravel fraction of these sediments and this is also reflected in the fourth factor in Table B26. The inclusion of Fe and plagioclase in the Ba regression equation could indicate that the Ba is adsorbed on Fe oxide coatings on locally derived terrigenous plagioclase sand and gravel particles. Zr is probably deposited as locally derived zircon sand grains and as adsorbed ions on Fe colloids. Sr substitutes for Ca in aragonite and to a lesser extent in Mg-calcite, as well as being adsorbed on Fe colloids. Both the Sr and Zr equations reflect the suggested ionic exchange with P_2O_5 on the Fe colloids.

In summary, in the mudflat-sorted-mud unit,

1) Zn and P_2O_5 are adsorbed on the clay-sized particles;
2) Cr, Ni, Sc, Ti, and V are adsorbed on colloidal Fe particles, Ni and Sc being also adsorbed on Mn colloids;
3) Co is adsorbed on Mn colloids;
4) Sr substitutes for Ca in aragonite, and Ba and Zr are associated with locally derived terrigenous sand and gravel particles.

R-TECHNIQUE CANONICAL CORRELATION ANALYSIS OF THE MANGROVE AND MUDFLAT RESULTS

Because of the interesting contrast in the colloidal affinities of the trace elements between the mangrove and mudflat-sorted mud units, the canonical correlation results for these two units are included for comparison. Tables B12 and B13 summarise the R-technique canonical correlation analyses for the mangrove and mudflat units. Both tables show that the first three canonical correlations are significant (ignoring the normality assumption associated with the chi-square test discussed in Appendix B1c). Despite the high values of these significant canonical correlations, the redundancy measures for the correlations are very low, indicating that the corresponding canonical vectors only 'extract' a low proportion of the variance of the data sets (Appendix B1c), and that the amount of overlap of the data sets is not great. Only the first canonical correlation with the mangrove results (Table B12) and the first two canonical correlations with the mudflat results (Table B13) have at least one of the two corresponding redundancy measures greater than 0.10. Therefore, taking 0.10 as the cut-off redundancy level, only the first pair of canonical vectors is used for interpretations with the mangrove unit results, and the first two pairs of canonical vectors with the mudflat results.

Assuming that the absolute values of the canonical coefficients in Tables B12 and B13 are significant if greater than 0.20, the canonical correlation results for the mangrove unit (Table B12) substantially support the factor analysis and regression results in Table B9. Increasing Co, Ni, Sr, Ti, Zn, and Zr and decreasing Y in set 2 reflect decreasing mean grainsize and Fe with decreasing P_2O_5 in set 1. Apart from Zr and Y which have the opposite expected sign of the coefficient, these results support the previous interpretations that Co, Ni, Sr, and Ti are being exchanged for P_2O_5 on Fe colloids, and Zn is adsorbed on fine-grained particles. The importance of the colloidal adsorption process is indicated by the very high (0.92) coefficient for Fe in Table B12. The canonical correlation results support these previous interpretations, but it would have been impossible to make all the geochemical interpretations relevant to the mangrove unit from the canonical correlation analysis alone.

With the mudflat results (Table B13) both Fe and Mn have significant coefficients with canonical correlation 1, contrasting the mangrove results where only Fe is significant and thus supporting the previously observed differences in colloidal deposition between the mangrove and mudflat units. In addition, the significant positive Cr, Ni, Ti, and V (set 2) coefficients with canonical correlation 1 in Table B13 confirm the association of these anions with the Fe and Mn colloids in the mudflat unit (Table B11). In contrast, the second pair of canonical vectors reflects the relation of the trace elements with that part of the system not concerned with the Fe and Mn colloids.

TABLE B12. SUMMARY OF R-TECHNIQUE CANONICAL CORRELATION ANALYSIS RESULTS, MANGROVE-SORTED-MUD UNIT

A. CHI-SQUARE TESTS WITH SUCCESSIVE CANONICAL PAIRS REMOVED (first pair removed first, followed by second, etc.)

No. of Pairs Removed	Chi-Square Value	Degrees of Freedom	95-Percent Chi-Square Critical Value
0	325.43	168	200
1	227.79	143	171
2	155.69	120	147
3	113.46	99	123*
4	81.31	80	
5	54.88	63	
6	34.52	48	
7	22.42	35	
8	12.89	24	
9	6.85	15	
10	1.87	8	

Significant correlations from chi-square test:
Canonical correlation 1 = 0.9700
Canonical correlation 2 = 0.9361
Canonical correlation 3 = 0.8402

* With the critical value greater than the chi-square value, the canonical correlation is not significant. This applies to all successive removal of canonical pairs.

B. CANONICAL COEFFICIENTS

Canonical correlation 1

SET 1		SET 2	
Variable	Coefficient	Variable	Coefficient
Mean grainsize (phi)	0.249	Ba	−0.148
Standard deviation	−0.183	Co	0.274
Dolomite	−0.049	Cr	−0.107
Mg-calcite	−0.183	Cu	−0.016
Calcite	−0.041	Mg	0.112
Plagioclase	−0.133	Ni	0.218
Orthoclase	−0.010	Pb	−0.051
Aragonite	−0.131	Sc	−0.023
Quartz	−0.065	Sr	0.276
P_2O_5	−0.218	Ti	0.400
Fe	0.919	V	−0.168
Mn	0.020	Y	−0.231
		Zn	0.672
		Zr	0.279

Redundancy of SET 1 given SET 2 = 0.197
Redundancy of SET 2 given SET 1 = 0.299

TABLE B13: SUMMARY OF R-TECHNIQUE CANONICAL CORRELATION ANALYSIS RESULTS, MUDFLAT-SORTED-MUD UNIT

A. CHI-SQUARE TESTS WITH SUCCESSIVE CANONICAL PAIRS REMOVED (first pair removed first, followed by second, etc.)

NO. OF PAIRS REMOVED	CHI-SQUARE VALUE	DEGREES OF FREEDOM	95-PERCENT CHI-SQUARE CRITICAL VALUE
0	367.61	168	200
1	253.65	143	171
2	166.98	120	147
3	110.42	99	123*
4	72.40	80	
5	45.59	63	
6	27.13	48	
7	16.11	35	
8	6.56	24	
9	1.17	15	
10	0.35	8	

Significant correlations from chi-squares test:
Canonical correlation 1 = 0.9674
Canonical correlation 2 = 0.9360
Canonical correlation 3 = 0.8626

* With the critical value greater than the chi-square value, the canonical correlation is not significant. This applies to all successive removal of canonical pairs.

B. CANONICAL COEFFICIENTS

Variable	SET 1 Coefficient		Variable	SET 2 Coefficient	
	Canonical correlation 1	Canonical correlation 2		Canonical correlation 1	Canonical correlation 2
Grainsize mean (phi)	−0.043	−0.221	Ba	0.100	0.565
Grainsize Std dev.	−0.102	0.562	Co	0.099	0.868
Dolomite	0.040	0.090	Cr	0.234	0.555
Mg-calcite	0.488	−0.469	Cu	−0.106	0.025
Calcite	−0.098	−0.353	Mg	0.236	−0.164
Plagioclase	0.100	−0.254	Ni	0.430	−0.782
Orthoclase	0.215	−0.526	Pb	0.051	−0.160
Aragonite	0.169	−0.176	Sc	−0.358	0.366
Quartz	0.323	−0.872	Sr	0.055	0.021
P_2O_5	−0.021	−0.315	Ti	0.314	0.273
Fe	0.840	0.188	V	0.253	−0.804
Mn	0.244	−0.162	Y	−0.076	−0.322
			Zn	0.112	−0.573
			Zr	0.111	0.096

Canonical correlation 1
Redundancy of SET 1 given SET 2 = 0.115;
Redundancy of SET 2 given SET 1 = 0.312
Canonical correlation 2
Redundancy of SET 1 given SET 2 = 0.137;
Redundancy of SET 2 given SET 1 = 0.078.

The significant coefficients of canonical correlation 2 in Table B13 (negative mean grainsize with positive standard deviation in set 1, and positive Ba and negative Zn in set 2) support the previously observed associations of Ba with sand-sized particles, and of Zn with the mud fraction. The significant coefficients for Co, Cr, Sc, and Ti in set 2 also suggest an association of these trace elements with the sand and silt fractions of the mudflat sediments. Ths regression equations for Cr and Sc in Table B10 which include orthoclase and plagioclase respectively, and the significant correlation of orthoclase with silt (0.293) and of plagioclase with sand (0.295), confirm this interpretation for Cr and Sc. The regression equations in Table B10, though, do not support the association of Co and Ti with the coarser grainsizes in the mudflat unit.

R-technique canonical correlation analysis then seems generally to support previous geochemical observations made on the mangrove and mudflat-sorted mud units. However, it did not supply the detail available through the combined use of R-mode factor analysis and multiple regression analysis. Nevertheless, the discussions have shown the potential of the R-technique canonical correlation analysis for use either in a supporting role or as the major interpretive technique, perhaps with data resulting in much higher redundancy measures than obtained in this study.

PRIMARY-UNSORTED-MUDDY-SAND UNIT

As indicated earlier and in Cook & Mayo (1978), most of the sediment from the Broad Sound catchments is transported into the estuarine complex during the annual floods. In the upper reaches of the estuarine waterways, the bed-load portion consisting mostly of fine sand and coarse silt is called the primary-unsorted-muddy-sand unit. Between floods, particles finer than 3 phi are removed from this unit by waves and tides and the remaining 2-phi to 3-phi sand particles are transported seaward and tend to form sand banks overlying pre-Holocene relict sediments. This net seaward movement is a result of complex oscillatory sediment movement which mixes marine biogenic particles (shown in Table B7 to comprise half of the sediment) and sorted-sand particles with this primary sediment.

The R-mode factor analysis (Table B27) for this unit separated all the trace elements except Zn and Pb into two factors, as summarised in Table B14 along with the corresponding multiple regression analyses. Using these regression results and the discussions of the mangrove and mudflat-sorted-mud units, the trace-element factor in this unit probably reflects adsorption of these trace elements on Fe and Mn colloids in the primary sediment. From the regression results, Ba, Co, Cr, Ni, Ti, V, and Y are associated mainly with the Fe colloids, whereas Cu, Sc, and Sr appear to be preferentially adsorbed on the Mn colloids, but the close association of Fe and Mn (correlation coefficient of 0.624) admittedly makes this division of elements on colloidal affinity somewhat arbitrary. Nevertheless, these different elemental affinities are supported by the regression results in the mangrove and mudflat-sorted-mud units.

As much of the silt and clay from this unit is winnowed out and redeposited in the supratidal zone, the geochemical relations in the unit were expected to be similar to those in the mangrove and mudflat-sorted-mud units. Comparison of Table B14 with Tables B9 and B10 in fact supports the association of Co, Cr, Ni, Ti, and V with Fe and the association of Sc with Mn. In addition, the association of Zn with the mud fraction in the primary sediment is corroborated by Tables B9 and B10. Differences are evident, however, with Ba, Cu, and Sr. Further, there is no confirmation of the previously suggested adsorption of P_2O_5 on Fe colloids entering the estuary (the correlation coefficient of P_2O_5 with Fe in the primary sediment being only 0.053). However, this relation could be masked by the dominant association of P_2O_5 and the carbonate fraction.

TABLE B14. SUMMARY OF FACTOR AND REGRESSION ANALYSES RESULTS, PRIMARY-UNSORTED-MUDDY-SAND UNIT

A. TRACE-ELEMENT FACTOR

Ba, Co, Cr, Cu, Fe, Mn, Ni, Sc, Sr, Ti, V, Y
(no significant correlations: Co-Cu, Cr-Mn, Cr-Sr, Cu-Ni, Cu-Sc, Cu-Sr, Cu-Ti, Cu-V, Cu-Y, Fe-Sr, Mn-Ti, Sr-Ti)

RELEVANT REGRESSIONS:

Ba = Fe
Co = Fe
Cr = Fe
Cu = Mn
Fe = Mn, Mg-calcite
Mn = P_2O_5, Fe, −mean grainsize (phi)
Ni = Fe
Sc = Mn
Sr = Mn, P_2O_5
Ti = Fe
V = Fe
Y = Fe

B. CARBONATE CONTROL FACTOR

GROUP 1	GROUP 2
Mg-calcite	Gravel (carbonate retained)
Calcite	Plagioclase
Ca	Quartz
Mg	Zr
Mn	
Sr	
Carbonate	
P_2O_5	

(no significant correlations: calcite-Mg, calcite-Mn, calcite-Sr)

RELEVANT REGRESSIONS:

Mg = Mn, Mg-calcite
Mn = P_2O_5, Fe, −mean grainsize (phi)
Sr = Mn, P_2O_5
P_2O_5 = Mg-calcite, Mn
Zr = −calcite, quartz

Other regressions:

Zn = mean grainsize (phi), −Fe.

Notes:

1. The variables with significant factor loadings in the trace-element factor (Factor A) are split into two groups on the sign of the loadings. Each variable in one of these groups of variables is negatively correlated with each variable in the other group, but not necessarily significantly.
2. All pairs of variables in each group of variables have a significant positive correlation (i.e. H_0: $\rho = 0.0$ rejected at the 95-percent confidence level), except as indicated above.

Sr and Mn are also included in the carbonate control factor (Table B14), suggesting substitution of these elements in the carbonate lattice. The factor analysis results point to the dual mode of occurrence of both Sr and Mn, illustrating an advantage of factor analysis compared with the multiple regression analysis which only emphasises the carbonate association of Sr and Mn (although this is the dominant mode of occurrence of these elements). The dual mode of occurrence of Mn in the primary sediment also explains the lack of significant correlation of Mn with clay (-0.116) compared with the correlation of Fe with clay (0.504, which is significant at the 90% level). This dual mode of occurrence of Sr partly explains the relatively high concentration of Sr in the primary-unsorted-muddy-sand unit (1171 ppm, Table B5), and perhaps Sr has a higher concentration in the carbonate of the foraminifera tests (which are very abundant in the upper reaches of the estuarine creeks and rivers (Cook & Mayo, 1978)) than in the shallow-marine biogenic material (Table B20; 910 ppm). Table B14 also indicates that most P_2O_5, as well as Mg, is concentrated in the carbonate fraction, in contrast with Zr which is associated with the non-carbonate fraction, doubtless in the form of zircon.

The geochemistry of the primary-unsorted-muddy-sand unit may be summarised as follows:

1) Mn is mainly concentrated in the biogenic fraction, as is Sr, but is also present as colloidal particles with adsorbed Cu, Sr, and Sc cations.
2) Ba, Co, Cr, Ni, Ti, V, and Y are associated primarily with Fe colloids.
3) Mg and P_2O_5 are concentrated in the biogenic fraction, whereas Zr is associated with the non-carbonate fraction.

SORTED-SAND UNIT

In contrast to the low-energy conditions prevailing in the supratidal environment, the open-intertidal and shallow-marine sandbanks in the estuarine complex are associated with relatively high maximum energy conditions. Under these relatively high energy conditions, most of the silt and clay particles are winnowed from the sediment, to be subsequently deposited in the supratidal environment, or in the quieter, deeper parts of the shallow-marine environment (Fig. B2).

This sorting process results in a unimodal sediment averaging 30 percent carbonate and almost 100 percent sand, with one dominant mode in the 2-phi to 3-phi range in equilibrium with the prevailing conditions (Tables B1, B5). This unit may be considered as the sand end-member grainsize population in the Broad Sound estuary, whereas the mudflat and mangrove-sorted-mud units represent the silt-clay end-member population (Fig. B1, and Cook & Mayo, 1978, p.111).

Table B15 summarises the geochemically relevant results from the factor matrix for this unit shown in Table B28. The results of the carbonate and feldspar control factor reflect the substitution of Mg and Sr for Ca in the carbonate minerals and the association of Ba with the feldspars. The association of Ba with plagioclase sand particles as well as Fe was noted in the mudflat-sorted-mud unit, and these same relations are also evident here. These associations probably indicate adsorption of Ba on Fe-oxide coatings on feldspar sand particles. Given the observation of these relations in both the mudflat and sorted sand units, the adsorption probably occurred before or during transportation of the sand grains to the estuarine complex, implying that this ionic bonding, once effected, is very stable.

As an aid to geological interpretation of the trace-element factor, the independent variables with positive coefficients in the regression equation corresponding to each of the eight trace elements in this factor are listed in Table B16. For overall interpretation, the results for those regressions with an excessive sum of squares remaining (Table B36) were also included in Table B16. The independent variable common to all the eight trace elements except Co and Sc is 'heavy minerals', and each set of independent variables (except that for Ni) includes either Fe or Mn.

The main geological processes controlling these eight trace elements are then probably *adsorption* on Mn and Fe-oxide coatings on sand grains and heavy mineral grains and *substitution* within certain heavy minerals present in the sorted sands. Stumm & Morgan (1970) observe that the common occurrence of Fe and Mn as grain coatings allows them to exert surface adsorption far out of proportion to their total concentration. Because the mean grainsize (phi) variable is included with three of the trace elements (Table B16) adsorption on minor silt and clay particles is probably still a significant process within this unit. P_2O_5 is known to be concentrated in the relict calcareous nodules with high Fe and Mn content that are present in the Broad Sound sediment (Table B20), and this is reflected in the P_2O_5 regression (Table B15) where calcite is the most important independent

TABLE B15. SUMMARY OF FACTOR AND REGRESSION ANALYSES RESULTS, SORTED-SAND UNIT

A. TRACE-ELEMENT FACTOR

Co, Cr, Ni, Sc, Ti, V, Y, Zr
(no significant correlation: Co-Cr, Co-Ti, Co-Zr, Sc-Ti)
Relevant regressions:

- Co = Mn, quartz, −zircon, orthoclase, aragonite
- Sc = tourmaline, quartz, hornblende, Mn, mean grainsize (phi)
- Ti = mean grainsize (phi), Fe, −orthoclase, heavies, $-P_2O_5$, −quartz
- V = Mn, tourmaline, $-P_2O_5$, heavies
- Fe = Mn, plagioclase, −zoisite, calcite
- Mn = Fe, −mean grainsize (phi), heavies, −clay.

Other regression:

- P_2O_5 = calcite, mean grainsize, heavies, quartz, tourmaline.

B. CARBONATE AND FELDSPAR CONTROL FACTOR

Group 1: Plagioclase, Orthoclase, Ba
Group 2: Mg-calcite, aragonite, carbonate, hornblende, Ca, Sr, Mg
(no significant correlation: Mg-hornblende)
Relevant regressions:

- Ba = plagioclase, $-P_2O_5$, Fe, zoisite
- Sr = tourmaline, −quartz, −heavies, −orthoclase

Notes:

1. The variables with significant factor loadings in Factor B are split into two groups on the sign of the loadings. Each variable in one of these groups is negatively correlated with each variable in the other group, but not necessarily significantly.
2. The significant Factor-A loadings all had the same sign.
3. All pairs of variables in each group of variables have a significant positive correlation (i.e. H_0: $\rho = 0.0$ rejected at the 95-percent confidence level), except as indicated above.
4. In each regression equation the dependent variable is shown to the left of the 'equals' sign, and the independent variables, with the corresponding sign, to the right, in decreasing order of importance as predictors.

variable. However, because P_2O_5 was not included as an independent variable with any of the eight trace elements, any association of trace elements with Fe and Mn in the carbonate nodules was not considered important in this unit.

A summary of the regression variables associated with four of the eight elements in the trace-element factor — Co, Sc, Ti, and V — (as well as the variables associated with Fe and Mn) is given in Table B15. The independent variables for each trace element are listed in decreasing order of importance as predictors of the element. The relative importance is obtained from the square of the multiple correlation coefficient, RSQ, in Table B36.

Cr, Ni, Y, and Zr will not be discussed in detail as the excessive sum of squares remaining in the corresponding regression analysis indicates that certain important processes controlling these elements were not reflected in the independent

TABLE B16. RESPONSE REGRESSION VARIABLES HAVING POSITIVE COEFFICIENTS, SORTED-SAND UNIT

Dependent variable	Independent variables included in the regression with positive coefficients
Co	1. Mn, quartz, orthoclase
	2. Aragonite
Cr*	1. Fe, heavy minerals
	2. Mean grainsize (phi)
Ni*	1. Heavy minerals
Sc	1. Mn, quartz
	2. Hornblende, tourmaline
	3. Mean grainsize (phi)
Ti	1. Fe, heavy minerals
	2. Mean grainsize (phi)
V	1. Mn, heavy minerals
	2. Hornblende
Y*	1. Mn, quartz
	2. Hornblende
Zr*	1. Fe, heavy minerals

* Excessive sum of squares remaining in the corresponding regression equation

The independent variables associated with each dependent variable are grouped according to geological process (i.e. 1, 2, etc.).

variables in the analysis. Nevertheless, the geological processes relevant to the other four trace elements also apply to these, as can be seen from Table B16.

Apart from occurring in combination in rutile and ilmenite as expected, Ti is also adsorbed on the minor mud particles in the sediment, as was found in the mudflat-sorted-mud unit. Because of the negative regression coefficients with quartz and orthoclase in the Ti equation, the inclusion of Fe in the equation probably reflects the presence of ilmenite and not an association of Ti with Fe-oxide grain coatings. This interpretation is simpler than suggesting that the Ti is adsorbed on Fe-oxide coatings restricted to heavy minerals.

The regression equation for Fe in fact suggests that Fe-oxide coatings are most common on plagioclase grains, and perhaps Ba is the only element adsorbed to a significant extent on these coatings. With microscopic inspection, Fe coatings proved to be very common on sand-sized grains from open intertidal sediments, especially on quartz and heavy-mineral grains. The Fe equation also reflects the ferruginisation of the calcareous nodules in the sediment, although these nodules are present in this unit only in minor amounts.

In contrast, the Mn regression equation does suggest Mn coatings are common on heavy-mineral grains, and the correlation coefficient of heavy minerals with Mn (0.516) is higher than

that between Mn and any other variable in the analysis, except for Fe. Even though Mn commonly replaces Ca, Ba, Mg, Al, and Fe in various minerals (Read, 1947), the high positive correlation of Mn with the heavy-mineral variable, the fact that epidote is the only individual heavy mineral having a positive correlation with Mn (0.493) and the inclusion of the heavy-mineral variable in the Mn regression equation all support the suggestion of Mn-oxide coatings on heavy-mineral grains.

The regression equations for Co, Sc, and V suggest that these three elements are adsorbed on Mn-oxide coatings on sand grains. V appears to be associated preferentially with these Mn coatings on heavy minerals, whereas Co and Sc are probably associated with Mn coatings mainly on quartz grains, and, in the case of Co, to some extent on orthoclase. It is also worthwhile noting (Table B36) that with the Sc regression the heavy-mineral variable was initially included, but removed at a later step in the analysis. These differences in affinities of the trace elements may be due to different provenances of these mineral grains, and suggests, as with Ba, that the adsorption occurred before deposition in this unit.

Rather than suggest that the Mn coatings are restricted to tourmaline and hornblende in the case of Sc adsorption and to tourmaline with the V adsorption, it seems more likely that the elements were included in these minerals at the time of formation or substituted later (perhaps for ferrous ions). This also seems a possibility with Sr (Table B15) but in this case substitution for Ca is more likely. In addition, some Sc is probably adsorbed on mud particles, and there is also a link between Co and aragonite.

The most important observed geochemical relations within the sorted-sand unit are that

1) Ba is adsorbed on Fe-oxide coatings on feldspar minerals.

2) Ti is adsorbed on mud particles, as well as being present in rutile and ilmenite.

3) V is adsorbed on Mn coatings on heavy-mineral grains, and is substituted in tourmaline.

4) Sc and Co are adsorbed on Mn coatings on quartz grains, and Sc is substituted in hornblende and tourmaline.

5) Sr and Mg substitute for Ca in the carbonate minerals.

MIXED-UNSORTED-MUDDY-SAND UNIT

The mixed-unsorted-muddy-sand unit forms as a result of the mixing of sediment from the sorted-sand and mangrove-sorted-mud units near the boundary of the open-intertidal and mangrove-swamp environments. Consequently, the mud fraction of the sediment is out of equilibrium with the high (relative to the mangrove environment) maximum energy of the open-intertidal environment. This mixing of two distinct populations was expected to make interpretation of the numerical results for this unit less clear, while at the same time reducing the analysis to one which merely reflects the differences between the two mixing sediment types.

The summary of the factor and regression analyses (Tables B29 and B37) for this unit is shown in Table B17. In the R-mode factor analysis, most trace elements are split into two factors. By comparing the correlation coefficients of the elements in each of these factors with relevant grainsize variables (Table B18), the reasons for this split can be generalised. Increasing phi mean grainsize and standard deviation in this unit represent increasing proportions of mud from the sorted-mud unit; Sc, V, Zn, and Cr increase correspondingly. In addition, the significant correlation between these four elements and clay indicates that these elements are mainly associated with the clay fraction.

TABLE B17. SUMMARY OF FACTOR AND REGRESSION ANALYSES RESULTS, MIXED-UNSORTED-MUDDY-SAND UNIT

A. CLAY-FRACTION FACTOR

Group 1: Mn, Pb, Sc, V, Zn, quartz
(no significant correlation: Mn-quartz, Pb-quartz, Sc-quartz, V-quartz, Zn-quartz)

Group 2: Carbonate, Ca

RELEVANT REGRESSIONS:

V = Fe, quartz

Zn = Fe, Mn, P_2O_5

B. SAND-FRACTION FACTOR

Cr, Ni, Ti, Y, Zr
(no significant correlation: Cr-Y)

RELEVANT REGRESSIONS:

Ni = Fe, quartz, −mean grainsize (phi), $-P_2O_5$

Zr = $-P_2O_5$, Fe, −mean grainsize (phi)

Fe = mean grainsize, Mn, calcite, P_2O_5

Notes:

1. The variables with significant factor loadings in Factor A are split into two groups on the sign of the loadings. Each variable in one of these groups is negatively correlated with each variable in the other group.
2. All pairs of variables in each group of variables have a significant positive correlation (i.e. H_0: $\rho = 0.0$ rejected at the 95-percent confidence level), except as indicated above.
3. The independent variables in the regression equations are given in decreasing order of importance.

TABLE B18. SIGNIFICANT CORRELATION COEFFICIENTS BETWEEN TRACE ELEMENT AND GRAINSIZE PARAMETERS, MIXED-UNSORTED-MUDDY-SAND UNIT

	Mean grainsize	Grainsize standard deviation	Clay	Sand (carbonate in)	Sand (carbonate out)
Mn					0.282
Pb					
Sc		0.427	0.312		
V	0.427	0.684	0.607		
Zn	0.389	0.593	0.585		
Cr	0.386	0.485	0.431		
Ni		0.267			0.353
Ti					
Y	−0.298			0.311	0.434
Zr	−0.336			0.345	0.507

Significance is determined under the hypothesis that $\rho = 0.0$ at the 90% confidence level.

In contrast, Ni, Y, and Zr are related to the sand fraction, which is mainly derived from the sorted-sand unit. Therefore, the elements in Factor A are probably related to the clay fraction of the sediment, whereas those in Factor B (except for Cr) are related to the sand fraction. The correlation of Mn with the other trace elements in Factor A probably indicates some concentration of Mn in the clay fraction, although this relation is masked by the presence of Mn as coatings on sand-sized particles. In fact, the grouping of the elements in Factor A seems to depend on this correlation with Mn, probably explaining the placing of Cr (which is not correlated with Mn) in Factor B when it is clearly associated with the clay fraction.

The regression equations (Table B17) support this broad division into clay-related and sand-related elements, but the somewhat blurred effect caused by the mixing of two separate populations is also evident in these regression results. For example, with the Fe regression, calcite is included because of the presence of sand-sized calcareous nodules (Table B15), and P_2O_5 is included with mean grainsize because of higher Fe, P_2O_5, and lower mean grainsize in the mangrove mud compared to the sorted sand (Table B5 and B9). Despite this blurring effect, the regression results indicate that Ni and Zr are primarily associated with the sand fraction in this mixed-unsorted-muddy-sand unit, whereas V and Zn are associated with the mud fraction. The negative coefficients of P_2O_5 and mean grainsize (in phi units) with Ni and Zr, compared with the positive P_2O_5 coefficient with Zn and the significant correlation coefficient (0.379) of V with P_2O_5 (although P_2O_5 was not included in the regression equation for V), indicate these different affinities for the two pairs of elements. The Zn and V affinity for the clay fraction was discussed with the mangrove-sorted-mud unit (and Table B9). Although Ni was also shown to be associated with the clay fraction in the mangrove-sorted-mud unit (Table B9), in this unit the regression result emphasises the association of Ni with Fe oxides present as coatings on sand grains. Given the higher average Ni concentration in the mangrove-sorted-mud unit compared with the sorted-sand unit (Table B5), this emphasis on the association of Ni with oxide coatings seems strange, and Fe included in the Ni equation probably also reflects the association of Ni with Fe colloids in the mud fraction. Zr, though, appears to be associated with the sand-sized heavy-mineral fraction, as expected.

Apart from illustrating the problems associated with analysing mixed populations numerically, the only new geochemical information added from this discussion of the mixed-unsorted-muddy-sand unit is the concentration of Mn in the clay fraction in this unit. The significant linear relations between Mn and the other four elements in the clay-fraction factor contrast sharply with the fact that, with the mangrove-sorted-mud unit, dolomite is the only variable with a significant correlation coefficient (0.334) with Mn. It has been previously suggested that Mn-oxide colloids are preferentially deposited in the mudflats after bypassing the mangroves during spring tides. It seems likely that these colloids (and the absorbed cations) are also deposited in the intertidal zone during the quiescent period at normal high tides. This colloidal deposition in the mixed-unsorted-muddy-sand unit is supported by the significant correlation coefficients of Mn with Pb, Sc, V, and Zn in the mudflat-sorted-mud unit (Table B11) and the inclusion of Mn in the regression equations for Pb, Sc, and Zn in that unit (Table B10).

SORTED-SANDY-GRAVEL UNIT

The sorted-sandy-gravel unit is distinguished texturally from the sorted-sand unit by a much higher carbonate-gravel content (Table B5). The samples representing this unit are all from the shallow-marine sand banks and, although most of the sediment, including much of the carbonate, is in equilibrium with the prevailing conditions (as with the sorted-sand), significant amounts of

shelly molluscs and ferruginised carbonate nodules are also present in the samples. The carbonate nodules are probably relict pedogenic nodules and intraclasts from carbonate beds (Cook & Mayo, 1978).

As the differences in the numerical results between this unit and the sorted-sand unit are expected to be due mainly to the presence of nodules and shells, a comparison of the chemical composition of typical nodular and shell material is given in Table B20, to aid in the following interpretations. Although the proportions of the carbonate minerals present in the biogenic fraction vary considerably, a comparison of the calcite (low Mg-calcite):Mg-calcite (high Mg-calcite) ratio between the sedimentary units (Table B5) indicates that, on average, calcite is dominant in the nodules whereas Mg-calcite and calcite occur in approximately equal proportions in the biogenic fraction. This conclusion is based on the observation that the carbonate nodules are mainly confined to the unsorted-gravel and sorted-sandy-gravel units, and with these units the calcite:Mg-calcite ratio is much higher than in the other units.

Two factors from the R-mode factor analysis (Table B30) are useful geochemically, and the results of these two factors and the associated stepwise regression results from Table B38 are summarised in Table B19. Factor A in Table B19 seems to reflect the mineralogical maturity of the sediments in this unit. The concentration of P_2O_5 in the carbonate nodules (Table B20) and the association of P_2O_5 with the stable heavy minerals, zircon and rutile, in this maturity factor, suggest a link between the occurrence of the carbonate nodules and increasing mineralogical maturity.

This supports the conclusion of Cook & Mayo (1978) that most of the carbonate nodules formed part of an early Holocene weathering profile. An increasing grainsize standard deviation on this unit represents increasing in-situ shell and nodule content (Table B1), and as no monazite or apatite was identified in the opaque-mineral fraction, the regression equation for P_2O_5 in Table B19 also reflects the association of

TABLE B20. CHEMICAL ANALYSES OF CARBONATE NODULES (Sample 70636310) AND SHELLS (Sample 70636205)

Variable	Units	70636310 Nodules	70636205 Shells
Ca	%	30.7	38.5
Co	ppm	20	<3.5
Cu	ppm	10	2.0
Fe	ppt	42.7	0.1
Mg	%	1.2	0.21
Mn	ppm	2960	<20
Ni	ppm	20	<3.5
Pb	ppm	5	<3.5
Sr	ppm	400	910
Zn	ppm	20-55*	5
P_2O_5	ppm	2100	720
SiO_2	%	8.4	

* Analyses for Zn were obtained separately on six nodules from this sample; the results were: 20, 20, 25, 45, 40, 55.

TABLE B19: SUMMARY OF FACTOR AND REGRESSION ANALYSES RESULTS, SORTED-SANDY-GRAVEL UNIT

A. MINERALOGICAL MATURITY FACTOR

GROUP 1	GROUP 2
Opaque heavies	Non-opaque heavies
Zircon	Epidote
Rutile	Hornblende
V	Plagioclase
Zn	Orthoclase
Mg	Quartz
Sc	(no significant
P_2O_5*	correlation:
	epidote-plagioclase)

(no significant correlation: Mg-zircon, Mg-rutile, Sc-P_2O_5, V-Mg, Zn-Zircon)

* Included although factor loading (−0.584) was just below the 0.6 cut-off (see Table B30).

RELEVANT REGRESSIONS:

V = Mn, −epidote, heavies, −quartz, zoisite
Zn = rutile
Mg = Mg-calcite, Mn, −quartz
Sc = rutile, −quartz, zoisite
P_2O_5 = opaque heavies, grainsize standard deviation, −orthoclase, −tourmaline

B. TRACE-ELEMENT FACTOR

Cr, Ni, Ti, Zr

RELEVANT REGRESSIONS:

Ti = grainsize standard deviation, zircon, mean grainsize (phi), Fe.

C. OTHER REGRESSION

Ba = quartz, Mn

Notes:

1. The variables in Factor A are grouped according to the sign of the loadings. Each variable in one of these groups is negatively correlated with each variable in the other group, but not necessarily significantly.
2. All pairs of variables in each group of variables have a significant positive correlation (i.e. H_0: ρ 0.0 rejected at the 95-percent confidence level), except as indicated above.
3. The independent variables to the right of the 'equals' sign are given in decreasing order of importance as predictors of the dependent variable.

the carbonate nodules with the mineralogically mature fraction of the sediments.

V, Zn, Mg, and Sc, in addition to P_2O_5, are also associated with the mineralogically mature portion of the sorted sandy gravel. Because calcite has a significant positive correlation with rutile and Sc (0.427 and 0.409 respectively), and because P_2O_5 is significantly correlated with rutile and Zn (0.404 and 0.614 respectively), both Sc and Zn are probably concentrated to some extent in the carbonate nodules. This suggestion is supported by the high relative values (see Table B5) for Zn shown for the nodules in Table B20. The relation between the carbonate nodules and the mature heavy minerals discussed above, in turn explains the inclusion of rutile in the regression equations for both Zn and Sc. However, the mechanism of the concentration of the Zn and Sc in the nodules is not clarified by the regression equations. Perhaps Zn is concentrated in mud layers in the intraclast type of nodule.

In contrast, the regression equation for V suggests that V is associated with Mn in the calcareous nodules. Table B20 shows that Mn is concentrated in the nodules, and as the correlation of Mn with Fe is 0.734, this Mn and associated V concentration would probably have occurred during the ferruginisation of the nodules when they were subaerially exposed. Although both Mn and heavy minerals are included in the regression equation for V, as in the sorted-sand unit, the significant positive correlation of V with P_2O_5 (0.559) and the lack of correlation with Mn and heavy minerals in the sorted-sandy-gravel unit, reinforces this different interpretation for V in this unit. With the sorted-sand results, Mn and heavy minerals were significantly correlated and P_2O_5 was included in the regression equation for V, but with a negative coefficient. Obviously, the high relative Mn values in the carbonate nodules have masked any effects of the Mn heavy-mineral-grain coatings in this unit.

The in-situ biogenic fraction consists of relict ferruginised and abraded material as well as recent sediments. The regression equation for Mg indicates, as expected, that Mg substitutes for Ca in this biogenic calcite. In addition, the equation suggests that Mg is probably also associated with the Mn concentrated in the carbonate nodules. This Mg concentration in the nodules is also indicated in Table B20.

As the grainsize-standard-deviation variable is included in the regression equations for Cr and Ti, and calcite is included with Ni, the trace-element factor (Table B19) seems also to reflect the presence of the relict carbonate nodules in this sedimentary unit. Ti again occurs in rutile and ilmenite which are concentrated in the relict, mature fraction of the sorted sandy gravel. As with the sorted-sand unit, Ti is also associated with mud-sized particles in these sediments.

The inclusion of Mn in the regression equation for Ba suggests an association with the carbonate nodules, though the inclusion of quartz with a positive coefficient does not confirm this. Removal of Mn from the regression analysis for Ba resulted in quartz, grainsize standard deviation, and rutile being included in the regression equation, thus supporting the relation of Ba with the nodules but not clarifying the nature of its association with quartz. As quartz and plagioclase are significantly correlated (0.451), the relation with quartz and Ba could be a reflection of the adsorption of Ba on Fe-oxide coatings on plagioclase grains, or possibly of the presence of Ba feldspars. This possible association of Ba with Fe-oxide coatings was noted previously, but in this unit the concentration of Fe in the carbonate nodules would be expected to mask this relation.

The geochemical relations within the sorted sandy gravel may be summarised as follows:

(1) V, Mg, and Ba are associated with Mn in the relict carbonate nodules; Mg also substitutes for Ca in the biogenic fraction.

(2) P_2O_5, Zn, and Sc are concentrated in the carbonate nodules.

(3) Ti is adsorbed on mud particles, as well as being present in rutile and ilmenite.

UNSORTED-GRAVEL UNIT

The unsorted gravel sediment occurs in the deeper zones of the shallow-marine environment. This sediment is a variable mixture of relict carbonate nodular gravel and coarse sand, relict non-carbonate gravel and coarse sand, in-situ gravel and sand-sized biogenic particles, sorted sand transported from the sand banks, and silt and clay particles winnowed from elsewhere in the estuary. This shows that the sediment is out of equilibrium with the relatively low energy of the environment (Cook & Mayo, 1978). The original numerical classification of all the estuarine samples was carried out to overcome the problem of attempting to analyse numerically mixed sediment populations by grouping the samples into sedimentary units, each reflecting a distinct set of geological processes. The unsorted gravel unit, though, is a mixture of several components. Because the total sediment was analysed rather than the separate sediment

fraction, the mixing of the components in the unsorted-gravel unit makes it harder to identify geochemical relations within the unit. This was also the case with the mixed-unsorted-muddy sand.

Again the R-mode factor analysis (Table B31) was useful in partitioning the trace elements into two geologically meaningful groups — Factors A and B in Table B21. Factor A suggests that Ba, Cr, Cu, Ni, Ti, and Zn are associated with the clay fraction of the sediments and that in contrast Mg, Mn, and P_2O_5 are associated with the carbonate gravel fraction. These broad interpretations are supported (and, indeed, the reasons for the composition of the factors are also indicated) by the correlation coefficients between the trace elements in Factor A and relevant grainsize variables (Table B22) and the concentration of Mn, Mg, and P_2O_5 in the carbonate nodules (Table B20).

The associations of the trace elements in Factor A are further clarified by the associated multiple regression equations also given in Table B21. The close agreement between the factor analysis and these regressions is obvious from the significant correlations between the mean grainsize (in phi units), clay, sand, plagio-clase, and P_2O_5 variables (Table B22). Clearly Ba, Cr, Ni, Ti, and Zn are mainly concentrated in the clay fraction, probably through adsorption. In addition, the regression equations for Ti and Cr reflect the occurrence of these elements in ilmenite and chromite, and the relation of Fe with both Ni and Zn probably reflects the adsorption of Ni and Zn on Fe colloids in the sediments.

The elements in Factor B (Table B21) appear to be partitioned there because of their relation with Fe. This is illustrated clearly in Table B22 where the elements in Group 1 of Factor B all have significant positive correlations with Fe. In contrast, Zr, which has the opposite factor loading sign to Group-1 elements, is negatively correlated with Fe. Zr is probably concentrated in zircon but the four Group-1 elements Co, Sc, V and Zn do not appear to have a common mode of occurrence. From the regression equations in Table B21 and the significant correlation coefficients in Table B22, Co and Sc appear to be associated with the Fe concentrated in the carbonate nodules, whereas V and Zn are probably associated with Fe colloids deposited in the finer sediment. In fact, the dual mode of occurrence of Fe in both the carbonate nodules and the fine fraction of the unsorted-gravel unit probably explains the lack

TABLE B21: SUMMARY OF FACTOR AND REGRESSION ANALYSES RESULTS, UNSORTED-GRAVEL UNIT

A. GRAINSIZE/CARBONATE CONTROL FACTOR

GROUP 1	GROUP 2
Mean grainsize (phi)	Gravel (carbonate in)
Clay	Calcite
Aragonite	Mg
Plagioclase	Mn
Quartz	Carbonate
Ba	P_2O_5
Cr	(no significant correlation:
Cu	Mn-carbonate, Mn-gravel,
Ni	Mg-Mn, Mg-calcite, Mg-P_2O_5,
Ti	calcite-carbonate, gravel-Mg,
Zn	gravel-carbonate)

(no significant correlation: mean grainsize-Cu, clay-plagioclase, clay-Cr, aragonite-Cr, aragonite-Cu, aragonite-Ni, aragonite-Ti, plagioclase-Cr, plagioclase-Cu, quartz-Cu, quartz-Ni, quartz-Zn)

RELEVANT REGRESSIONS

- Ba = plagioclase, sand(carb. in), −Mg-calcite, rutile
- Cr = $-P_2O_5$, −Mg-calcite, −zircon, aragonite, carbonate, Fe
- Ni = plagioclase, Fe, sand(carb. in), −Mg-calcite
- Ti = plagioclase, $-P_2O_5$, zoisite, opaque heavies, Fe
- Zn = Fe, plagioclase, sand(carb. in)
- Mg = carbonate, zircon
- Mn = −plagioclase, dolomite
- P_2O_5 = quartz, tourmaline

B. Fe CONTROL FACTOR

GROUP 1	GROUP 2
Co	Zr
Fe	hornblende
Sc	zoisite
V	
Zn	

(no significant correlation: Co-Sc, Co-V, Co-Zn, Sc-Zn)

RELEVANT REGRESSIONS

- Co = dolomite, −Mg-calcite, aragonite
- V = Fe, −epidote
- Zn = Fe, plagioclase, sand (carb. in)
- Zr = $-P_2O_5$, zoisite
- Sc = −quartz, tourmaline, −heavy minerals, −garnet

Notes:

1. Each variable in one of the groups of variables in each factor is negatively correlated with each variable in the other group, but not necessarily significantly.
2. All pairs of variables in each group of variables have a significant positive correlation (i.e. $H_0 : \rho = 0.0$ rejected at the 95-percent confidence level), except as indicated above.
3. The independent variables in the regression equation are given in decreasing order of importance.

TABLE B22. SIGNIFICANT CORRELATION COEFFICIENTS USED IN INTERPRETING UNSORTED-GRAVEL UNIT RESULTS

(a) TRACE-ELEMENT CORRELATIONS

		Variable	Mean grainsize	Gravel	Sand	Clay	Fe
FACTOR A	Group 1	Ba	0.553	−0.569	0.552	0.760	
		Cr	0.501	−0.468			
		Cu				0.509	
		Ni	0.506	−0.534	0.510	0.573	0.550
		Ti	0.652	−0.634		0.595	
	Group 2	Mg	−0.407	0.40		−0.460	
		Mn					
		P_2O_5		0.594		−0.404	
FACTOR B	Group 1	Co			−0.428		0.540
		Fe					1.000
		Sc	−0.412	0.402			0.480
		V					0.657
		Zn	0.478	−0.524	0.501	0.521	0.569
	Group 2	Zr					−0.492

(b) MATRIX OF GRAINSIZE/MINERALOGICAL CORRELATIONS

		Mean grainsize	carbonate in Clay	carbonate in Sand	Plagioclase	P_2O_5
Carbonate retained	Mean grainsize		0.653		0.580	−0.599
	Clay			0.487		
	Sand				0.439	
	Plagioclase					−0.570

Only correlation coefficients significant at the 90% level are shown.

of significant correlation of Fe with the grainsize variables (Table B22).

In spite of the mixing of different sediment types in the unsorted-gravel unit, meaningful geochemical relations can nevertheless be discerned. This is partly due to the much greater content of mud (with carbonate not removed) with associated trace elements in the unsorted-gravel unit compared to the other units. The overall geochemical relations in the unsorted gravel unit are as follows:

(1) Ba, Cr, Ni, Ti, Zn, and V are concentrated in the clay fraction, the Ni, Zn, and V probably being associated with Fe colloids in the sediment.

(2) Mg, Mn, P_2O_5, Co, and Sc are concentrated in the carbonate nodules, Co and Sc being associated with the Fe in the nodules.

(3) Zr occurs mainly in the heavy-mineral fraction.

GEOCHEMICAL MODEL

In the immediately preceding discussions of the geochemistry of each sedimentary unit, different possible modes of occurrence of the chemical elements were often indicated. In the summation for each unit, though, only dominant modes of occurrence of the elements were given. These final interpretations include only those geochemical relations (supported by both the factor analysis associations and regression equations) which satisfactorily predicted the relevant dependent variables (by explaining a significant amount of the total variation of these variables).

The final geochemical interpretations from all the sedimentary units, except the mixed-unsorted-muddy-sand unit, are summarised in Table B23, from which six main modes of occurrence of the chemical elements are evident. The interpretations from the mixed-unsorted-muddy-sand unit were not included because these merely supported the geochemical interpretations within each of the two mixed

sediment types comprising that unit: the sorted-sand and mangrove-sorted-mud units. An idealised geochemical model of the estuarine complex (Fig. B12) was constructed by using the summary of associations in Table B23 and the sedimentation model diagram (Fig. B2) to link the geochemical results with the sediment movement in the estuary.

Figure B12 summarises the dominant geochemical associations within each sedimentary unit, although it does not show the influence of these associations on the absolute concentration of the chemical elements throughout the estuary. The relative importance of the processes (reflected in these associations) which concentrate the various elements is clarified by Table B24, showing the units in which each chemical element is most concentrated, and the dominant association modes of each unit. For example, although Figure B12 shows that P_2O_5 is associated with both the clay and the relict carbonate nodules, Table B24 indicates, from the higher P_2O_5 values in the sorted-sandy-gravel and unsorted-gravel units than in the sorted-mud units, that the carbonate nodules are relatively more important for concentrating P_2O_5.

The dominance of colloids and clay particles in concentrating most of the trace elements at Broad Sound is clearly shown in Table B24, where the concentration of ten elements (Co, Cr, Cu, Fe, Ni, Pb, Sc, Ti, V, and Zn) is shown to be highest in the mudflat-sorted-mud unit. Nevertheless, interest is not confined to the processes resulting in the highest concentrations, but to all the significant geochemical associations of the chemical elements shown in Table B23 and Figure B12.

Figures B2 and B12 together convey an overall summary of the sediment movement and geochemical associations in Broad Sound. Sand, silt, clay, and Fe and Mn colloids are transported into the estuarine system from the catchment, mainly during floods. The Fe and Mn colloids bear Co, Cr, Ni, Sc, and V ions, and the clay particles carry adsorbed Zn and P_2O_5. An appreciable amount of the silt is zircon, and the sand grains are commonly coated with Fe and Mn oxides bearing adsorbed Ba, Co, Sc, and V. Ti is present in chromite and zircon, and is adsorbed on clay particles and attached to Fe and Mn colloids.

Much of the silt, clay, and colloidal material not initially deposited in the upper areas of the estuary is later deposited in the mangrove-swamp and mudflat environments. Silt (including appreciable zircon) is preferentially deposited in the mangrove swamps, whereas clay and Fe colloids are somewhat more abundant in the mudflats. The Mn colloids with the attached cations are transported through the mangroves and are also preferentially deposited on the mudflats. Evidence from the regression analyses suggests that perhaps the above colloidal cations are actually exchanged in the mangrove swamp for P_2O_5, which was originally attached to some of the Fe colloids entering the estuary. Some of the silt and clay and colloidal particles are also deposited in the quiet zones of the shallow-marine environment.

The silt and clay dumped in the upper reaches of the waterways is winnowed out from the unsorted sediment by waves and currents, and is also redeposited in the supratidal and marine zones. The remaining sand bedload, with the Ba, Co, Sc, and V adsorbed on oxide grain coatings, is transported seawards and deposited on the pre-Holocene relict sediments. Ba, Co, Mg, Sc, Zn, and P_2O_5 are associated with the carbonate nodules in these relict sediments.

Mixing of the sand and mud end-member populations in the mangrove channels and at the mangrove swamp/open intertidal boundary takes place continuously. It is in this zone that Mayo (1976) showed that with decreasing pH more P_2O_5 is adsorbed on the clay particles and with decreasing pH and Eh metal ions are released and form metal sulphides or metallo-organic complexes.

Biogenic carbonate material from the shallow-marine zone, with Sr and Mg substituting for Ca, is mixed with the terrigenous sediment in the estuary. Only a relatively small amount of carbonate silt is deposited in the supratidal zone, and most of this is preferentially deposited in the mangrove swamps.

CONCLUSIONS

Using a 'fishing expedition' type of strategy, important geochemical associations were detected and interpreted in each sedimentary unit in the Broad Sound estuary. In fact, some of the geochemical observations could well have been missed, had a more restrictive strategy with limited, predetermined aims been used. Meaningful interpretation was possible, first because of the numerical sample classification which grouped the samples into sedimentary units, and

TABLE B23. MODES OF OCCURRENCE OF CHEMICAL ELEMENTS

	Clay-fraction adsorption	Colloidal association				Biogenic carbonate substitution/ replacement	Carbonate nodule association		Sand-oxide-coating adsorption		Heavy-mineral combination
		Mainly Fe		Mainly Mn					Mainly Fe	Mainly Mn	
MANGROVE-SORTED MUD	Zn P_2O_5	Cr Sc Ti Co	Ni Sr V			Sr					Zr
MUDFLAT-SORTED MUD	Zn P_2O_5	Ni, Sc Cr V	Ti		Co	Sr			Ba		Zr
PRIMARY UNSORTED MUDDY SAND		Ba Cr Ti Y	Co Ni V	Cu Sc	Sr	Mn Mg	Sr P_2O_5				Zr
SORTED SAND	Ti					Sr	Mg		Ba	V Co Sc	Ti
SORTED SANDY GRAVEL	Ti					Mg	Ba Mn V P_2O_5	Mg Sc Zn			Ti
UNSORTED GRAVEL	Ba Ni Zn	Cr Ti V	Ni V	Zn			Co Mn P_2O_5	Mg Sc			Zr

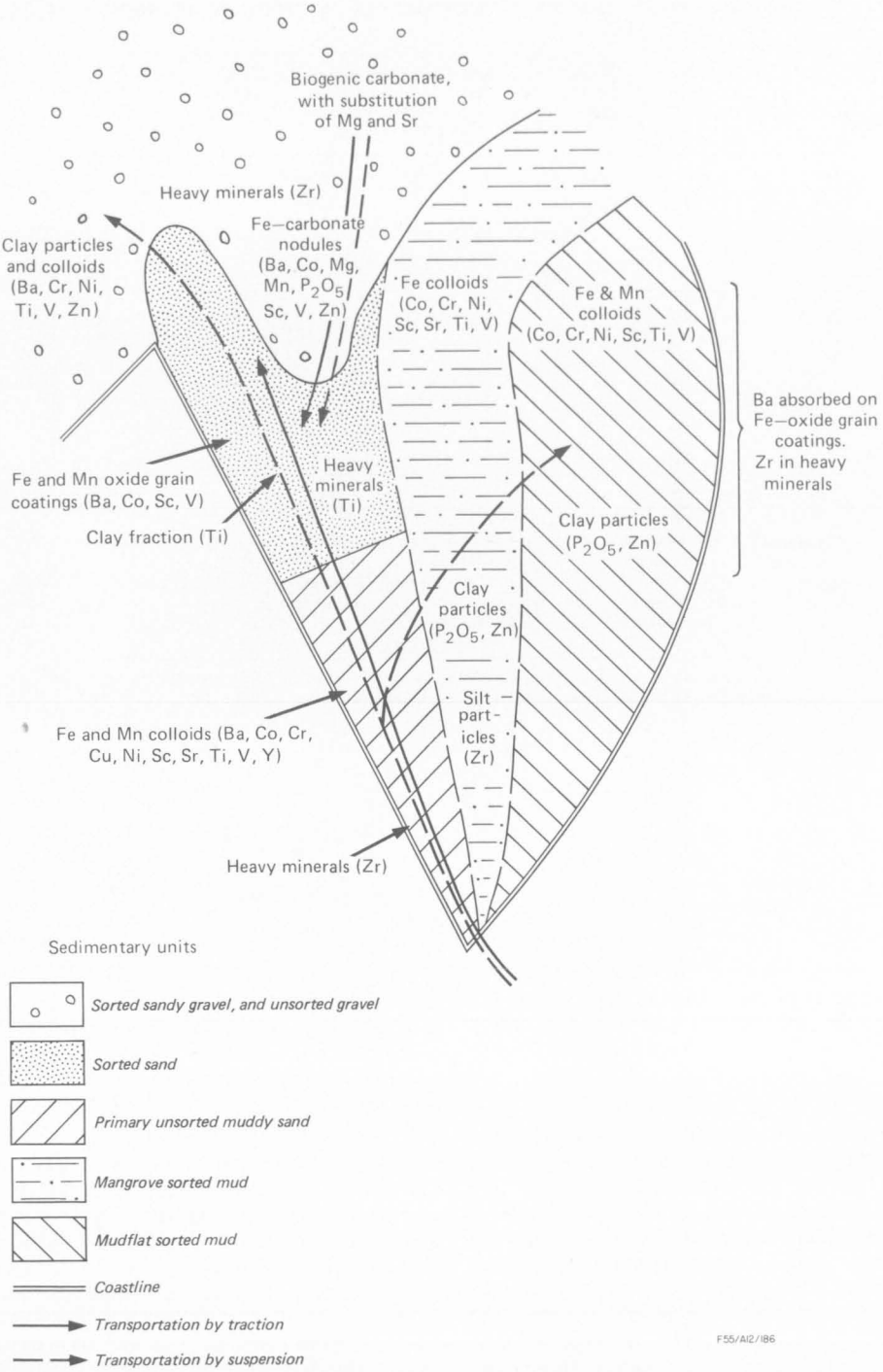


Fig. B12. Idealised geochemical model of the Broad Sound estuarine complex, showing trace-element associations in components of the sedimentary units.

TABLE B24. SEDIMENTARY UNITS: DIFFERENCES IN CHEMICAL-ELEMENT CONCENTRATIONS

	Unsorted gravel	Sorted sandy gravel	Sorted sand	Primary unsorted muddy sand	Mangrove sorted mud	Mudflat sorted mud
Ba				*	*	* Ba
Co						* Co
Cr						* Cr
Cu						* Cu
Fe						* Fe
Mg		*				* Mg
Mn	*	*				Mn
Ni						* Ni
Pb						* Pb
Sc						* Sc
Sr					*	Sr
Ti						* Ti
V						* V
Y			*		*	* Y
Zn						* Zn
Zr			*			Zr
P_2O_5	*	*				P_2O_5
Dominant association mode	1. Carbonate nodules 2. Biogenic carbonate		1. Grain coatings 2. Heavy mins.	1. Colloidal 2. Biogenic carbonate	1. Colloidal 2. Clay	

* Indicates the mean in this unit is significantly greater than that in the other units (using the normal distribution test at the 90-percent level with the results in Tables B5 and B6).

second, because several of these units consist almost entirely of one sediment population. For example, the sorted-sand unit and the sorted-mud units consist of over 90 percent sand and 90 percent mud respectively.

Once the Broad Sound samples had been first classified into separate units using Q-mode factor analysis, R-mode factor analysis then isolated groups of associated variables, and stepwise multiple regression clarified the detail of the geochemical association within each sedimentary unit. From these broad geochemical observations more detailed and selective studies, aimed at clarifying some of the geochemical associations, especially in relation to the colloids, and the actual mechanism causing these, can easily be identified. Chemical analysis of the separate sediment fractions would be essential for a more detailed geochemical study of the sedimentary units consisting of mixed sediment types, such as the mixed-unsorted-muddy sand and the unsorted gravel. Once the overall strategy becomes more restrictive and the chemical analyses more complex, the need for such 'shot gun' techniques as R-mode factor analysis would be expected to decrease with increasing use of more rigorous statistical tests.

Apart from the geochemical associations discussed above, the general importance of Fe and Mn in any geochemical study was certainly shown here. At Broad Sound, Fe and Mn occur as colloidal particles, as coatings on sand grains, and as concentrations in relict carbonate nodules; various chemical elements are associated with the Fe and Mn in these three modes of occurrence. In fact, the chemical element associations with Fe and Mn in these three forms, and with the clay fraction in the sediment, constitute the more important geochemical relationships in the Broad Sound sediments.

REFERENCES

BROWNER, J. C., & VEINUS, J., 1974 — The statistical zap versus the shotgun approach. *Mathematical Geology*, 6(4), 311-32.

COOK, P. J., & MAYO, W., 1978 — Sedimentology and Holocene history of a tropical estuary (Broad Sound, Queensland). *Bureau of Mineral Resources, Australia, Bulletin 170.*

COOLEY, W. W., & LOHNES, P. R., 1971 — MULTIVARIATE DATA ANALYSIS. *Wiley, International.*

GOLDBERG, E. D., 1954 — Marine Geochemistry 1. Chemical scavengers of the sea. *Journal of Geology*, 62(2), 249-65.

GOLDSCHMIDT, V. M., 1954 — GEOCHEMISTRY. *Oxford, Clarendon Press.*

GOLDSMITH, J. R., 1959 — Some aspects of the geochemistry of carbonates. *In* ABELSON, P. H. (Editor) — RESEARCHES IN GEOCHEMISTRY. *Wiley, New York.*

HARBAUGH, J. W., & DEMIRMEN, F., 1964 — Application of factor analysis to petrologic variations of Americus Limestone (Lower Permian), Kansas and Oklahoma. *Kansas Geological Survey Special Distribution Publication* 15.

HOEL, P. G., 1962 — INTRODUCTION TO MATHEMATICAL STATISTICS. *Wiley, International.*

KEITH, M. L., & DEGENS, E. T., 1959 — Geochemical indicators of marine and fresh-water sediments. *In* ABELSON, P. H. (Editor) — RESEARCHES IN GEOCHEMISTRY. *Wiley, New York.*

KLOVAN, J. E., 1966 — The use of factor analysis in determining depositional environments from grainsize distributions. *Journal of Sedimentary Petrology*, 36, 115-25.

KRAUSKOPF, K. B., 1967 — INTRODUCTION TO GEOCHEMISTRY. *McGraw-Hill, International.*

MAYO, W., 1976 — Numerical techniques applied to the geochemistry of some estuarine sediments from Broad Sound, Queensland. *BMR Journal of Australian Geology & Geophysics*, 1, 193-203.

MURATA, K. J., 1939 — Exchangeable manganese in river and ocean muds. *American Journal of Science*, 237, 725-30.

OTTO, G. H., 1938 — The sedimentation unit and its use in field sampling. *Journal of Geology*, 46, 569-82.

READ, H. H., 1947 — RUTLEY'S ELEMENTS OF MINERALOGY. *Thomas Murby & Co., London.*

STUMM, W., & MORGAN, J. J., 1970 — AQUATIC CHEMISTRY. *Wiley-Interscience.*

APPENDIX B1

MATHEMATICAL AND STATISTICAL TECHNIQUES USED IN THE BROAD SOUND STUDY

(a) FACTOR ANALYSIS

Principal components analysis

Principal components analysis may be used to clarify the structure of a matrix, X, consisting of r observations on c variables. When the analysis is to be used to clarify the relationships between variables, the matrix X is represented geometrically in c-dimensional space, each set of c observations being one point in this space. The analysis transforms the original variables to new independent variables by

$$Y = AX \qquad (1)$$

where A is a $c \times c$ matrix of coefficients, and Y is the transformed matrix.

The matrix A consists of the eigenvectors of the matrix of correlation coefficients derived from X. Geometrically, each eigenvector is positioned such that the sum of squares of distances of sample points from it is a minimum and each pair of eigenvectors is perpendicular.

The eigenvalue corresponding to each eigenvector represents the proportion of the total variance explained by that eigenvector. If every element of each eigenvector is multiplied by the square root of the corresponding eigenvalue, the coefficients are weighted in proportion to the amount of variance explained. The coefficients (then termed factor loadings) may be regarded as reflecting the effect of the underlying factors controlling the structure of the data.

R-mode factor analysis

Factor analysis attempts more than a study of the underlying structure of a data set. This analysis assumes that the original variables are linear functions of a set number of underlying controlling factors. If there were c such factors the analysis would be equivalent to a principal components analysis. However, the task of clarifying the structure of the data is simplified if the number of transformed independent variables is reduced from c to m. That is, for each variable,

$$x_i = \sum_{k=1}^{m} l_{ij} z_k + e_i \qquad (2)$$

where x_i is the ith original variable,
l_{ij} is the factor loadings representing the effect each structural factor has on the ith variable,

z_k is the kth factor controlling the structure of the data, and
e_i is the error term,

under the assumptions that,

(1) structural factors, z, are independent normal variables with zero mean and unit variance, and
(2) each e_i is independent (both independent of the other error terms, and independent of the structural factors).

A mathematical comparison of principal components analysis and factor analysis is given in Kendal & Stuart (1976).

With this factor analysis model, factor loadings (l_{ij} in equation (2)) for each original variable and the corresponding eigenvalue, may be determined from the correlation coefficient matrix as with the principal components analysis but with the diagonal terms replaced by estimates of the communalities of each variable (the communality of each variable is the sum of the factor loadings of that variable, and is normally unknown).

By initially carrying out a principal components analysis (with unit communalities), the number of factors to be included can be decided and the communalities estimated for the factor analysis. The number of factors, m, which cumulatively 'explain' a specified proportion of the total variance, as shown by the eigenvalues, can be selected. Given the value of m, the variance of the discarded c-m factor loadings for each variable from the component analysis may be used to estimate the communalities for the factor analysis. Various other methods, including iterative methods, are commonly used for this communality estimation (Dixon, 1971).

Various methods may be used to rotate orthogonally the resulting scaled eigenvectors to achieve more meaningful results. One method is to maximise the varimax criterion (Kaiser, 1958). This tends to minimise the low loadings and maximise the high loadings by associating the variables with fewer and more different factors. This orthogonal rotation may be followed by an oblique (non-orthogonal) rotation such as the Promax method (Hendrickson & White, 1964).

Q-mode factor analysis

The factor analysis model given in equation (2) is designed to clarify the relationships between variables and is termed R-mode analysis. Specifying the model as

$$w_i = \sum_{k=1}^{m} l_{ij} z_k + e_i \qquad (3)$$

where w_i is the original case (i.e. observations on c variables), and
m is the number of controlling factors (less than n),

enables the between-case relationships to be studied. This is Q-mode factor analysis. In contrast to R-mode analysis, the factor loadings with a Q-mode analysis are determined from the eigenvectors and eigenvalues of a matrix of coefficients of proportional similarity (cosine theta coefficients). This coefficient is defined for each pair of cases as

$$\cos\theta_{12} = \frac{\sum_{k=1}^{m} x_{k1}\, x_{k2}}{\sqrt{\sum_{k=1}^{m} x_{k1}^2\, x_{k2}^2}} \qquad (4)$$

where m is the number of variables associated with each case,
x_{k1} is the value of the kth variable with case 1, and
x_{k2} is the value of the kth variable with case 2.

Q-mode analysis results in a factor loading corresponding to each controlling factor for each case. Intuitively, the factor loadings indicate the influence each of these structural factors has on the corresponding case. The nature of each structural factor may be interpreted from the factor scores which indicate the important variables in each factor.

Using the Q-mode analysis the values of c variables for each case are reduced to m factor loadings which reflect the influence of each structural factor on each case. Consequently, classification of the cases into separate groups of populations is simplified by comparing the factor loadings, rather than the original variables, of each case. Interpretation of the factors in terms of the original variables may lead to a meaningful explanation of the differences in these populations.

The problem of deciding how many factors to include in the analysis was discussed earlier. Unlike R-mode analysis, Q-mode analysis commonly results in a high cumulative proportion of the total variance being 'explained' with only a small number of factors. Very often only three factors 'explain' around 90 percent of the total variance of large data matrixes.

Limitations of Q-mode factor analysis

The cosine theta coefficient gives the cosine of the angle between the two vectors to the points representing the two cases (equation (4)) in *m*-dimensional space. Consequently, other distance measures, such as a simple Euclidean distance, could result in a better separation of dissimilar cases with some data sets.

There is, however, a more basic philosophical objection to the Q-mode approach: it requires the computation of 'variances' across variables. What the coefficient is actually measuring is somewhat obscure. Nevertheless, it has been shown that if the same transformation is used on both rows and columns of the data set, then the factor loadings in Q-mode are proportional to factor scores in R-mode, and vice-versa.

Consequently, a classification resulting from plots of the scores from an R-mode analysis (which is not subject to the above objections) should be equally reflected in an analysis of the loadings from the Q-mode analysis. Because of this, and because with a Q-mode analysis interpretation is simplified by only a small number of factors 'explaining' a high proportion of the total variance, the Q-mode approach was used to classify the Broad Sound samples. Doubts as to the validity of computing correlation coefficients, with the R-mode analysis, across different populations of geological samples also reinforced this decision.

Application of Q-mode factor analysis

Program CABFAC (Klovan & Imbrie, 1971), which was used in this study, rotates the initial factors to satisfy the varimax criterion (Kaiser, 1958) so that only a few high loadings remain on each factor. Although these mathematical factors need not necessarily represent geological processes, intuitively the factor loadings indicate the effect which that factor has on each sample. The degree of representation of the effects of all the factors on each sample is given by the sum of squares of the factor loadings for that sample (the 'communality'). Therefore, differing factor loadings may indicate differing geological effects on the Broad Sound samples.

Factor scores, which are also produced by CABFAC, can be used to interpret the geological significance of each of these factors. The initial factor scores are scaled (by multiplying by the square root of the number of variables) so that the maximum absolute value possible (when all the other variables 'contribute nothing to a factor' and have zero scores) is equal to the square root of the number of variables. 'If all variables in a study are equally important in a factor, then each scaled score equals unity' (Klovan & Imbrie, 1971, p. 63). Once the important variables for each factor have been found, the relationship between these variables and the corresponding factor can be determined from the relative factor loadings of the individual samples, and from the changing values of the important variables with these samples.

If only three factors are rotated using the varimax criterion, it is possible to make a graphical comparison of the effect on each sample of these three factors (which may represent three geological processes) by normalising the three factor loadings for each sample and plotting these values on a triangular diagram. The loadings are normalised for plotting by squaring each loading, multiplying by 100 percent, and dividing by the communality for that row. Similarly, the relative positions of the samples may be plotted along a straight line with only two factors rotated. Two limitations with these plots are that (1) the plot positions of any loadings which are of opposite sign to most loadings (bipolar loadings) in that factor will be incorrect, and (2) 'low' communality values for individual samples mean that the plot positions for these samples do not represent all the geological processes affecting them. These were not problems with the Broad Sound samples.

The orthogonal varimax rotation may be followed by an oblique rotation which selects the most extreme samples (one for each factor) and expresses the other samples in terms of these (Mason & Imbrie, 1964). A program has been developed at BMR incorporating the oblique rotation in program CABFAC and adding:

1) triangular or line plots of normalised varimax loadings,
2) graphs of varimax or oblique factor loadings against grid reference values, and
3) areal distribution plots of classified oblique loadings (Mayo & Long, 1976).

(b) STEPWISE DISCRIMINANT ANALYSIS

Discriminant analysis is a well known technique (Davis & Sampson, 1966) for testing differences between populations on the basis of multivariate measurements. This technique computes a linear function of the variables measured on the samples from two populations, and the function may be used to test statistically whether the two groups of samples are in fact from different populations.

The Mahalanobis generalised distance (D^2) is determined by substituting the difference

between the variable means into the discriminant function. D^2 is a measure of the distance between two points in any number of dimensions (Rao, 1952). The statistic

$$\frac{n_1 \quad n_2}{(n_1+n_2)\ (n_1+n_2-2)} \cdot \frac{n_1+n_2-K-1}{K} \cdot D^2$$

where n_1 is the number of samples in the first group, n_2 the number of samples in the second group and K the number of variables, is distributed as the F distribution with K, $n_1 + n_2 - K - 1$ degrees of freedom. This statistic is used to test whether the multivariate means of the two groups are significantly different.

A stepwise analysis allows for entry or removal of a variable in a series of steps before the discriminant function is determined. Control can be kept of the variables entering the discriminant analysis by using likelihood ratio tests for the equality of the conditional distribution of each variable, given the variables not yet entered (Dixon, 1971). The likelihood ratios are distributed as the F distribution and may be used to select the next variable to be entered, and to indicate when no further variables are suitable for entry.

Program BMDO7M (Dixon, 1971) was used with the Broad Sound estuary samples grouped by the Q-mode factor analysis. At each step the variable entered has the highest likelihood ratio but also a variable may be deleted if its likelihood ratio (given the variables entered) becomes too small later in the analysis. When no more variables are suitable for entry, a matrix of the F values is printed, to test the difference between each pair of sample groups statistically, as described above.

The program then checks the original grouping of the samples by determining the D^2 between the point representing each sample and the mean point of each of the original groupings. With this check, D^2 is used as a chi-square variable to determine statistically the critical value for classifying each sample. This is, in fact, a much more sensitive test of the original classification than the discriminant analysis.

(c) CANONICAL CORRELATION ANALYSIS

R-technique

Canonical correlation analysis (Hotelling, 1936) is used to analyse the relations between two sets of variables measured on the same samples (Browner & Veinus, 1974). Used in this way, the technique is termed R-technique canonical correlation analysis and the relationship between the two sets of variables is given by

$$U = a_i X_i,$$
$$\text{and } V = b_i Y_i,$$

where coefficients are chosen to give the largest possible correlation between the canonical variates, U and V. The type of the relationship is indicated by the size and sign of the coefficients a_i and b_i of the two canonical vectors (Lee, 1969). To enable comparison of the absolute size of these coefficients, the data for each variable should be transformed in some appropriate way, such as to the percent-of-the-range of the corresponding variable.

After the first pair of canonical variates with the maximum correlation are obtained, further pairs of canonical variates may be obtained, with the restriction that each pair of variates must have no correlation with any previous variates. As a general rule, canonical correlations less than 0.30 indicate that the corresponding pair of variates probably does not add significantly to the information on the relationship between the two sets of variables (Cooley & Lohnes, 1971). Assuming that the variables in the two sets follow a multivariate normal distribution, a chi-square test incorporating all the positive canonical correlations, followed by tests with successive removal of each canonical relationship, enables the number of significant canonical relationships to be determined statistically (Cooley & Lohnes, 1971). The test is carried out under the hypotheses that the two sets of variables are unrelated.

A further aid in the interpretation of the R-technique results is the redundancy measure, which shows what proportion of the variance in each set is found (for each canonical correlation) to be redundant, given the other set of variables. Redundancy is the proportion of variance of one set extracted by a canonical vector, times the proportion of shared variance (i.e. the square of the canonical correlation) between the two corresponding canonical vectors (Cooley & Lohnes, 1971). The use of the redundancy measure overcomes the problem of a high canonical correlation being obtained between two sets of variables which do not actually overlap to a great extent. That is, the canonical correlation measures the overlap of the two canonical variates, but does not necessarily give a measure of the overlap of the two data sets.

Both the chi-square tests of canonical correlation significance and the redundancy measure of each set for each canonical correlation have been added to program

BMD06M (Dixon, 1971) in the BMR Geological Branch program set (Mayo & Long, 1976).

Q-technique

Q-technique canonical correlation analysis (Lee, 1969) may be used to compare different groups of samples, the same set of variables being measured on each sample. This analysis determines the extent to which the individual samples occupy the same relative positions in one measurement space.

The problem here is to find the linear functions of the measured variables which maximise (Rao, 1952) the sum of all possible D^2 values (see under discriminant analysis) that are computed for a number of sample groupings, using these variables and linear functions. If the variables are transformed to an uncorrelated set, the problem is reduced to finding the eigenvalues and eigenvectors of the between product-sum matrix of the transformed variables (Rao, 1952; Dixon, 1971). These eigenvectors are then the canonical vectors, and the eigenvalues indicate the amount of variance of the data explained by the corresponding canonical vector.

Using these canonical vectors the first two canonical variable values for each sample may be computed (Dixon, 1971) and plotted on an X-Y graph; the cumulative proportion of the total variance explained by the first two vectors indicates the degree of representation of the configuration of the groups in this plot. The canonical correlations relative to the sample groups in this Q-technique analysis also indicate the importance of each of the vectors for contrasting the position of the groups in multi-dimensional space.

Q-technique canonical correlation analysis is conceptually very similar to Q-mode factor analysis, but uses a different basis for positioning the vectors. An important difference between the two techniques is that the Q-mode factor analysis does not require any preliminary grouping of the samples before the analysis.

The actual computations follow on from the stepwise discriminant analysis, and program BMD07M also carries out a Q-technique canonical analysis using the discriminatory variables included in the last step of the discriminant analysis.

(d) CLUSTER ANALYSIS

Many different similarity measures and fusion strategies have been used for agglomerative classifications (Cheetham & Hazel, 1969; Lance & Williams, 1967). The Broad Sound estuary samples were analysed using a computer program adapted from Bonham-Carter (1967) which uses the group average clustering strategy. This program (Program CLUSTER, Mayo & Long, 1976) allows both Q-mode and R-mode analyses, with the option of seven different similarity measures with qualitative or semi-quantitative data, and either the correlation coefficient or the proportional similarity coefficient with quantitative data (Mayo & Long, 1976). In addition, percent-of-range transformation of the data may be carried out to ensure equal weighting of the variables in a Q-mode analysis.

At each cycle of the clustering, the similarity matrix is scanned to obtain the largest values between each pair of objects, and objects corresponding to these values are linked, each pair being represented by a single object of intermediate composition in the subsequent cycle. 'Similarity values are calculated between groups of objects by taking the arithmetical average of the similarity coefficients between their component members' (Bonham-Carter, 1967). The program allows for two different methods of calculating the group averages. With the 'weighted' method equal weight is given to each group being linked, whereas with the 'unweighted' method each object has equal importance, so that larger groups are given more weight.

The end result of the cluster analysis is a dendrogram in which all the objects (or variables) and groups are linked in a hierarchical way, thus classifying the objects/variables. As the positions of the objects/variables along one axis are fixed, the dendrogram is only a one-dimensional representation of the relationships between the samples. A second dimension can be added by including the relationships between the groups of objects/variables in the analysis and producing a dendrograph (McCammon, 1968) but this is not yet available with Program CLUSTER. A further limitation of cluster analysis is that clustering is produced even when completely independent and uniformly distributed variables are used (McCammon, 1968), although the initial clustering does occur at low similarity levels. In addition, the amount of information excluded from the dendrogram is not known — in contrast with the factor and canonical correlation analyses.

As with the Q-mode factor analysis, variables which are not independent may bias the results, as the corresponding environmental process will have an extra weighting in the cluster

analysis. This is the problem of redundancy among the variables, and R-mode cluster analysis can be used to identify and remove the redundant variables before classifying objects by means of the Q-mode cluster analysis (Parks, 1966; Park, 1974, pp. 333-352). Those variables with high similarity compared to the other similarity levels in the R-mode analysis are the redundant variables.

It was shown with the Broad Sound results that only after the redundant variables were removed from the Q-mode cluster analysis using stepwise discriminant analysis (after the samples were classified by means of Q-mode factor analysis) did the sample groupings obtained from the cluster analysis correspond well with those from the original factor analysis. This illustrated the greater sensitivity of the cluster analysis to redundant variables than the factor analysis.

Despite the advantages of Q-mode factor analysis over cluster analysis, there is one major advantage of the cluster analysis: the similarity measure can be chosen to suit the particular data set, and the disadvantages of the cosine theta coefficient can be avoided (see Part 'a' of this Appendix).

For example, with the Broad Sound data, the Lance & William's Canberra metric,

$$D_{XY} = \sum_{i=1}^{m} \frac{|x_i - y_i|}{|x_i + y_i|}$$

where m is the number of variables,

x_i is the value of the ith variable measured on sample X, and

y_i is the value of the ith variable measured on sample Y,

would be most suitable to use with a Q-mode cluster analysis, and this measure tends to minimise the structure it imposes on the data (Lance & Williams, 1967).

(e) ANALYSIS OF VARIANCE

One-way analysis of variance (Ehrenfeld & Littauer, 1964) is a method for testing k means of one variable simultaneously. Under the hypothesis that the k means are equal, the expression

$$\frac{(N-k)\sum_{i=1}^{k} n_i(\bar{x}_i - \bar{\bar{x}})^2}{(k-1)\sum_{i=1}^{k}\sum_{j=1}^{n_i}(x_{ij} - \bar{\bar{x}})^2}$$

(where N is the total number of observations, n_i is the number of observations in the ith group, $\bar{x}_i$ is the mean of the ith group, x_{ij} is the jth observation in the ith group, and $\bar{\bar{x}}$ is the grand mean of all sample values) is distributed as an F distribution with $k-1$, $n-k$ degrees of freedom. The analysis assumes normality of the variable x, and that the variance of x in each group is equal.

If the above calculated F value is greater than the critical value for the theoretical F distribution at the selected confidence level, then the hypothesis of equal means is rejected. When the technique is used for total error analysis and the groups are actually repeat samples at one locality, rejection indicates that differences between localities are still significant and therefore that the errors are not significant enough to mask all the differences between localities. Similarly, repeat analyses of one sample from k localities can be used to test the significance of the analytical error.

Bartlett's test (Hoel, 1962, p. 227) may be used to test the equality of the k variances by comparing the weighted arithmetic and geometric means of the k variances. With this test, the expression

$$\frac{2.303}{C}\left[f \log\left(\frac{1}{f}\sum_{i=1}^{k} f_i S_i^2\right) - \sum_{i=1}^{k} f_i \log S_i^2\right],$$

where f is the total number of observations, f_i is the number of observations in the ith group, S_i^2 the variance of the ith group, and

$$C = 1 + \frac{1}{3(k-1)}\left[\sum_{i=1}^{k}\left(\frac{1}{f_i}\right) - \frac{1}{f}\right]$$

is distributed as a chi-square distribution with $k-1$ degrees of freedom. Although the analysis of variance may be carried out with only two observations in each group, Bartlett's test is only

valid with three or more observations in each group. That is why triplicate sampling for error analysis was conducted at Broad Sound.

Using one-way analysis of variance with Bartlett's test, the error analysis of the Broad Sound estuary and catchment samples was carried out by program ANOVAI (Mayo & Long, 1976). This program also computes a 'least significant difference', which indicates those groups which are different when a significant F value is obtained in the analysis of variance.

(f) R-MODE FACTOR ANALYSIS

As explained in Part (a) of this Appendix, both R-mode and Q-mode factor analyses follow the same computational procedure, down to and including the orthogonal varimax rotation, except that the R-mode analysis initially computes the correlation coefficient

$$r = \frac{\sum_{i=1}^{n} (x_i - \bar{x})\,(y_i - \bar{y})}{n\,S_x\,S_y}$$

where, for each pair of variables, n is the number of samples, x_i the ith value of the 1st variable, x the mean of the 1st variable, y_i the ith value of the 2nd variable, y the mean of the 2nd variable, S_x is the standard deviation of the 1st variable, and S_y is the standard deviation of the 2nd variable. The R-mode analysis is therefore determining variable-to-variable relations. Every element in each eigenvector of the matrix of correlation coefficients with the diagonal replaced by communality estimates is multiplied by the square root of the corresponding eigenvalue to obtain the initial factor matrix, which is rotated orthogonally using the varimax criterion (Kaiser, 1958).

This orthogonal rotation may be followed by an oblique (non-orthogonal) rotation, which tends to minimise the low loadings and maximise the high loadings in each factor. Whereas the oblique rotation method of Manson & Imbrie (1964) is appropriate for Q-mode factor analysis, the Promax method (Hendrickson & White, 1964) is suited to the R-mode analysis. Other methods have been used for both the orthogonal and oblique rotation in R-mode and Q-mode factor analysis; some of them are indicated in Garrett (1967).

Theoretically, factor analysis requires that the number of factors to be obtained should be known before the analysis (Davis, 1973). However, in practice, any number of factors may be specified for each analysis. The use of R-mode factor analysis in the Broad Sound study corresponds to the description of a 'fishing expedition' by Davis (1973, p. 503) because the number of factors was not known before each analysis, but the method used in the Broad Sound study to determine the ideal number of factors to be used in the rotations is discussed in detail below.

Once the selected factors have been rotated, the sum of squares of the loadings in each row of the factor matrix (the communality) indicates the amount of variance of the corresponding variable explained by all the factors. Each factor may represent a geological process and in that case each loading in a factor represents the effect the process has on the corresponding variable. A significantly high loading indicates that that geological process is responsible for much of the variation in the corresponding variable. Generally, variables within one factor with significant loadings of the same sign are positively correlated and those with opposite loading signs are negatively correlated, but these relations should be checked from the matrix of correlation coefficients, especially regarding the significance of the appropriate correlation. If the changes of some variables with significant loadings within a factor can be interpreted geologically then the geological process being represented by the factor can often be deduced. Then the 'unknown' variables that also have significant loadings in that factor can be linked to that geological process or processes.

To enable geological interpretation of the factors obtained, careful selection of the variables to be measured on the collected samples is necessary, to ensure reflection of the expected geological processes which have affected these samples. Griffiths (1963) discusses these concepts in detail while attempting to obtain the critical properties of oil-bearing sands using R-mode factor analysis. In addition, this careful selection of geologically interpretable variables helps in the final decision on the number of factors to be rotated.

Linked to this selection of variables are the difficulties associated with any variables adding to a constant sum (a closed array) in the analysis. Any spurious correlations resulting from closed arrays will be reflected in the final factor loadings, and any interpretations from the analysis must be made with care. Similarly, a meaningful geological sample classification ensures that the correlations between variables used in the analysis reflect effects within a geological population and not between populations.

Broad Sound analyses

R-mode factor analysis was carried out on the results of each of the seven sedimentary units in the Broad Sound estuarine complex. Program BMD03M (Dixon, 1971) was used for the analyses, with a Promax oblique rotation addition and a facility added for obtaining a series of factor rotations, each successive rotation having one less factor (Mayo & Long, 1976). With each factor analysis a value of 1.0 was left in the diagonal of the matrix of correlation coefficients as the communality estimate. This program also computes factor scores which indicate the relative effect of each factor (geological process) on each sample. The scores can only be compared from sample to sample within each factor.

Although some variables measured on the estuarine samples can be interpreted geologically, as indicated with the grainsize-mean and standard-deviation parameters in Table B1, most variables were included as 'unknowns' with the aim of determining the overall relations between them. Closed-array effects are also a problem with these variables, with the gravimetric results, the XRD mineral results, and the heavy-mineral determinations each adding to a constant 100 percent (Table B5).

The oblique factor matrix of each sedimentary unit data set was obtained with a series of rotations using from eight down to four factors. Factor scores were not computed, as the Q-mode factor analysis results were used to obtain the required sample-to-sample relations. The first problem was to select the ideal number of rotated factors for each of the seven data sets.

Proceeding from the intuitive notion that the factors are related to geological processes, if too many factors are rotated, important relations between variables will be lost. That is, variables being affected by the same geological process may be forced into separate factors. If too few factors are used, variables related to different geological processes are forced into the one factor. From a study of the factor analysis results using a series of rotations of the Broad Sound data as well as data from various other projects, it was apparent that normally two or more contiguous rotations in the series reflected the same basic combinations of high loadings (at this stage greater than about 0.5). Commonly, rotations with more factors than these 'stable' rotations contained only one high loading, and those with fewer factors differed markedly from the 'stable' combination of variables. This 'stable' combination of variables was assumed to truly represent the geological processes affecting the samples. This assumption was applied to the series of oblique rotated matrixes of each sedimentary unit, and the matrix that reflected the same basic combination of high loadings as the matrix with one or more factors included, but which differed markedly from the matrix with one less factor included, was chosen as the 'ideal' matrix. The only constraint applied to these criteria was that the amount of variance 'explained' by the number of factors in the 'ideal' matrix had to be greater than 60 percent.

Extending this concept of the factors representing geological processes, if more than one factor represented one geological process the correlation between these factors would be expected to be significant. In fact, it was found that the selection of the 'ideal' matrix often coincided with a change from some significant correlations between the factors in the matrix with one extra factor included, to no significant correlations with the 'ideal matrix'. This gave some support to the assumption that the 'stable' variable combination does represent the geological processes affecting the samples. Significant correlations between factors in the 'ideal' matrix could also be useful in the geological interpretations of the processes represented by these factors.

It must be emphasised that there is no mathematical reason why the factors should represent geological processes, although this concept does help in interpreting the factor analysis results.

Once the 'ideal' matrix was chosen, the next problem was to select the significant variable loadings in the matrix. The statistical distribution of these loadings is not known, so no statistical method of selecting the significant loadings was possible. A simple practical technique for deleting the low insignificant loadings was required. It was found that a graph of the percent frequency of the number of loadings greater than 0.3, 0.4, 0.5, 0.6, 0.7, 0.8 and 0.9 in the selected matrix commonly levelled off over a limited range of loadings, after an initial sharp decline and before a further decline. The point at which the curve changes slope after the initial sharp decline was selected as the lower cut-off for significance. It was felt that this empirical graphical approach was more appropriate than selecting a limit of say 0.5 for significance for each of the 'ideal' matrixes from the Broad Sound sedimentary unit results.

The graphs used to determine the significant loading cut-off value for each of the sedimentary units are given in Figure B13. The cut-off value is 0.5 for five of the seven units and 0.6 for the

remaining two. This suggests that 0.5 could have been used as a general cut-off level for significance if the above graphical method had not been considered useful. Alternatively, the loadings could have been grouped into three general classes such as 0.4 to 0.6 (significant), 0.6 to 0.8 (very significant), and 0.8 to 1.0 (highly significant).

The matrix of oblique factor loadings and the associated factor correlations for the results from each sedimentary unit are given in Tables B25-31. The significant loadings which are used for geological interpretations are also indicated in these tables.

(g) MULTIPLE STEPWISE REGRESSION

Many different procedures are used to obtain the 'best' linear/multiple regression equation using a least-squares model; they include

1) all possible regressions,
2) backward elimination,
3) forward selection, and
4) stepwise regression.

A detailed coverage of all these techiniques is given in Draper & Smith (1966). For most applications, the stepwise regression procedure seems to be the best for general use.

The basic sequence of analysis with the stepwise regression technique, to select certain variables from the set of 'independent' X variables to be included in the final regression equation with the 'dependent' variable Y, is as follows:

1. The X variable with the highest absolute correlation coefficient with Y is selected.
2. The partial correlation coefficient of each remaining X variable and Y 'in the presence of' (Krumbein & Graybill, 1965) the selected X variable, is obtained.
3. Of these remaining X variables, the one with the highest partial correlation coefficient is selected for inclusion in the regression equation.
4. This process of using the partial correlation coefficients to select the variables is continued, the partial correlation of each remaining X variable and Y being calculated 'in the presence of' all the X variables included in the equation after each step.
5. A variable added at one step may be an insignificant contributor to the regression when other variables are added at later steps. Therefore, after each step the partial F-values (Draper & Smith, 1966) for each variable in the regression are computed so that the contribution made by each variable is determined as though it had been the last variable entered. Any variable not making a significant contribution (that is, a variable with an F-value below a preselected point on the appropriate F-distribution (Mayo & Long, 1976)) is removed from the equation.
6. This sequence continues until no more variables can be admitted or rejected.

As with other general least-squares regression analyses, to enable the regression equation to be examined statistically the residuals from stepwise regression analysis are assumed to be independent and normally distributed, with a zero mean and constant variance. Further, it is usually undesirable for any of the 'independent', or explanatory, variables included in the final equation to vary together in some definite way, such as may be caused by the closed array effect, but this may often be unavoidable in practical applications. Inclusion of such variables which are not independent will tend to mask the individual response of each of those variables.

Program BMDO2R (Dixon, 1971) was used to carry out a stepwise regression analysis of the Broad Sound results. Each element, as well as P_2O_5, in the set of results for each sedimentary unit was taken as the 'dependent' variable in the analysis; Fe, Mn, and P_2O_5 were also included as 'independent' variables. Several of the explanatory variables were removed from the analysis of each set of these results (Table B8), to satisfy the independence criterion.

Several graphical methods used to indicate whether the assumptions relating to the residuals appear to be violated or not are given in Draper & Smith (1966, ch. 3). One of these methods — plotting the residuals against each 'independent' variable — is incorporated in program BMDO2R and was used to check the normality assumption with the Broad Sound results. This plot may indicate a need for weighted least squares, extra non-linear terms, such as X variables, or transformation of the Y variable. However, the plots produced after each regression analysis on the Broad Sound results did not appear to violate the assumptions about the residuals.

Tables B33-39 are summaries of the stepwise regression analysis for each sedimentary unit. The abbreviations of the variable names used in these tables are given in Table B32. The

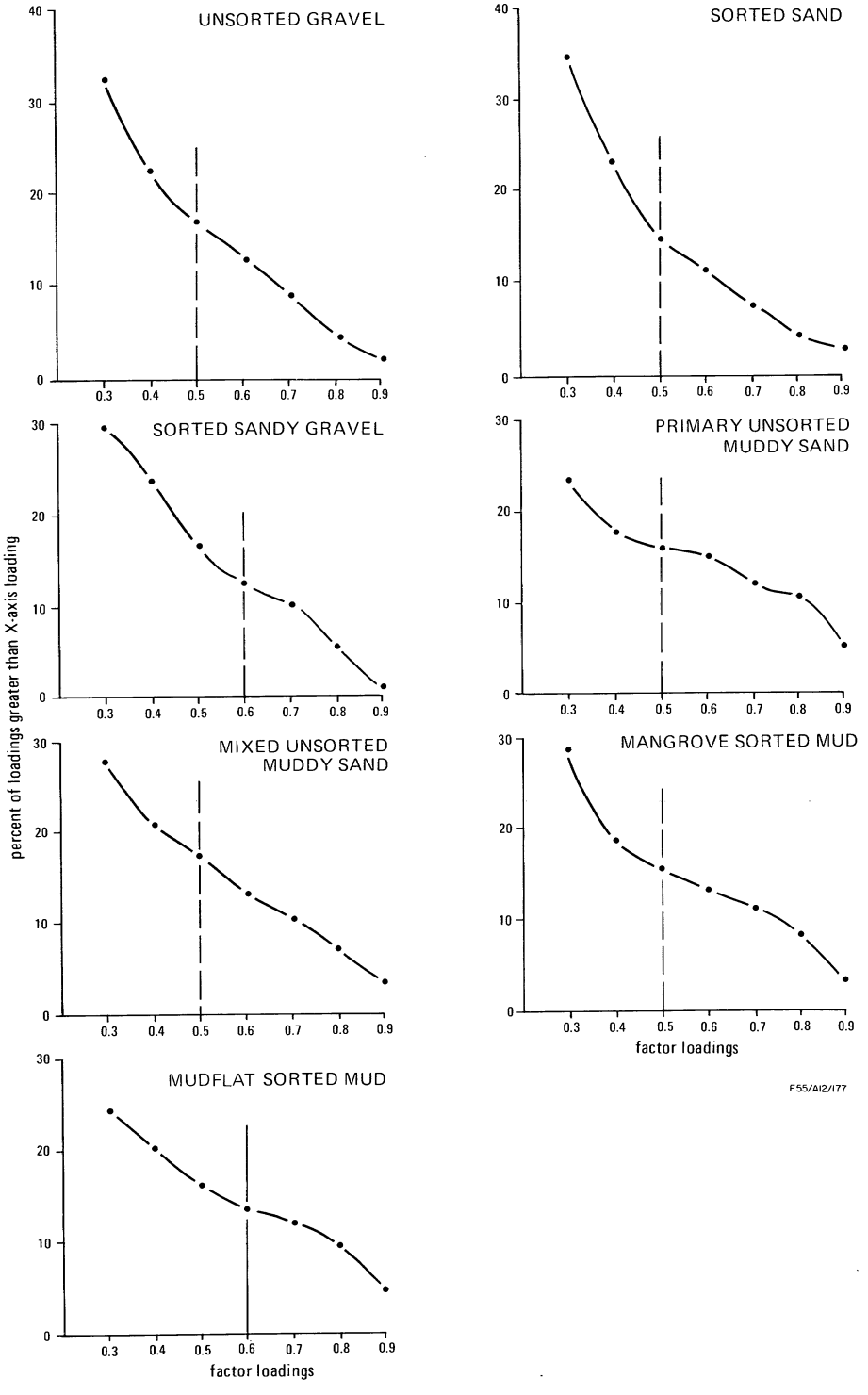


Fig. B13. Plots used to determine significant factor loadings in each selected 'ideal' matrix. Broken vertical lines mark cut-off value for significant factor loadings.

TABLE B25. OBLIQUE FACTOR MATRIX, MANGROVE-SORTED-MUD UNIT

	Factors				
Mean grainsize (phi)	−0.706**	−0.073	0.529**	−0.011	0.060
Grainsize std dev.	−0.166	−0.217	−0.745**	−0.065	0.071
Gravel (carbonate retained)	−0.157	−0.105	−0.822**	0.002	−0.129
Sand (carbonate retained)	0.394	0.214	−0.637**	0.067	0.169
Mud (carbonate retained)	−0.297	−0.156	0.797**	−0.059	−0.109
Silt (carbonate retained)	0.819**	−0.099	0.343	−0.073	−0.178
Clay (carbonate retained)	−0.881**	0.001	0.188	0.018	0.109
Gravel (carbonate removed)	−0.216	−0.137	−0.852**	−0.106	−0.081
Sand (carbonate removed)	−0.022	0.022	−0.924**	0.014	0.005
Mud (carbonate removed)	0.059	−0.012	0.939**	0.007	0.019
Dolomite	0.310	0.352	0.165	−0.077	0.329
Mg-calcite	0.316	−0.337	−0.054	0.668**	−0.068
Calcite	−0.298	−0.106	0.061	0.342	0.506**
Plagioclase	0.329	0.248	−0.087	−0.193	−0.390
Orthoclase	0.084	0.004	0.045	0.389	−0.697**
Aragonite	−0.224	−0.024	0.353	−0.221	0.465
Quartz	−0.326	0.094	−0.149	−0.834**	0.303
Ba	0.286	−0.710**	−0.344	−0.092	−0.029
Ca	0.927**	−0.061	0.107	0.278	0.100
Co	−0.181	−0.864**	−0.096	−0.124	−0.104
Cr	0.056	−0.835**	0.198	0.016	0.142
Cu	−0.121	−0.053	−0.294	−0.241	0.566**
Fe	−0.423	−0.666**	−0.132	−0.033	0.165
Mg	−0.305	−0.360	0.279	0.013	−0.108
Mn	0.216	0.011	0.096	0.018	0.370
Ni	−0.231	−0.821**	0.051	0.142	0.008
Pb	−0.453	−0.362	−0.056	−0.020	−0.474**
Sc	−0.014	−0.902**	0.122	0.157	−0.216
Sr	0.627**	−0.724**	−0.080	−0.029	0.222
Ti	0.157	−0.850**	0.037	0.205	0.168
V	−0.109	−0.867**	−0.305	0.216	0.024
Y	0.273	−0.597**	0.102	−0.357	−0.046
Zn	−0.929**	−0.105	0.049	−0.014	−0.001
Zr	0.525**	−0.385	0.236	−0.534**	0.063
Carbonate	0.939**	−0.012	0.190	0.275	0.021
P_2O_5	−0.903**	0.054	−0.103	−0.103	−0.091
Cumulative percent of total variance explained	27.1	44.1	59.3	65.7	70.4

** Significant loading.

MATRIX OF FACTOR CORRELATIONS (95% SIGNIFICANCE LIMIT = ± 0.329)					
1	1.000	0.199	−0.135	−0.087	−0.279
2	0.199	1.000	−0.070	0.060	−0.186
3	−0.135	−0.070	1.000	−0.023	0.012
4	−0.087	0.060	−0.023	1.000	0.332
5	−0.279	−0.186	0.012	0.332	1.000

usefulness of the stepwise technique is well shown in the results for Cr in Table B39 (unsorted gravel unit). In step 3, Fe is included in the regression equation, but in step 6 it is removed, because at that stage its contribution to the prediction of Cr is insignificant, given the other variables in the equation. Despite this removal, in step 8, after the inclusion of carbonate in the equation in step 7, the contribution of Fe to the regression is significant and Fe is once again included.

The square of the multiple correlation coefficient (RSQ in Tables B33-39) is equal to

$$\frac{\text{sum of squares (SS) due to the regression}}{\text{total SS about the mean}}$$

and is therefore a measure of how closely the regression equation fits the observed values. A perfect linear fit would result in an RSQ of 1.0, thus indicating that 100 percent of the total SS of the Y variable is 'explained' by the regression

TABLE B26. OBLIQUE FACTOR MATRIX, MUDFLAT-SORTED-MUD UNIT

	Factors					
Mean grainsize (phi)	−0.864**	0.082	0.053	−0.020	−0.221	0.083
Grainsize std dev.	0.284	0.435	−0.158	0.083	0.164	−0.012
Gravel (carbonate retained)	0.004	−0.004	0.049	0.924**	−0.104	0.002
Sand (carbonate retained)	0.977**	−0.040	0.131	−0.013	−0.234	−0.135
Mud (carbonate retained)	−0.970*	0.039	−0.131	−0.061	0.236	0.131
Silt (carbonate retained)	0.488	−0.068	−0.137	−0.055	0.627**	0.024
Clay (carbonate retained)	−0.797**	0.068	0.042	0.013	−0.355	0.041
Gravel (carbonate removed)	−0.214	−0.027	−0.076	0.817**	−0.005	0.038
Sand (carbonate removed)	0.213	−0.054	0.006	0.827**	−0.062	0.134
Mud (carbonate removed)	−0.147	0.052	0.009	−0.878**	0.055	−0.125
Dolomite	−0.353	−0.054	−0.061	0.106	0.293	0.479
Mg-calcite	0.015	−0.045	−0.901**	−0.077	−0.146	0.108
Calcite	−0.081	−0.093	−0.885**	0.002	0.250	−0.132
Plagioclase	−0.024	−0.081	0.271	0.246	0.211	0.558
Orthoclase	−0.151	−0.064	0.145	−0.152	0.655**	0.097
Aragonite	0.010	0.097	−0.397	−0.019	−0.111	−0.527
Quartz	0.171	0.148	0.914**	−0.069	−0.216	−0.328
Ba	0.004	0.199	0.057	0.915**	0.075	0.050
Ca	0.048	0.263	−0.726**	−0.014	0.037	−0.304
Co	0.252	0.667**	0.130	−0.191	−0.184	0.316
Cr	−0.022	0.925**	−0.016	0.039	0.078	−0.066
Cu	−0.017	0.488	−0.151	−0.167	0.037	0.387
Fe	0.099	0.831**	−0.068	0.238	−0.231	0.028
Mg	0.103	0.075	−0.588	0.005	−0.241	0.503
Mn	−0.014	0.718**	0.035	−0.072	−0.020	0.369
Ni	0.018	0.920**	−0.019	−0.141	−0.098	0.042
Pb	−0.138	0.447	0.131	0.079	−0.089	0.437
Sc	−0.167	0.845**	0.030	0.048	0.073	−0.119
Sr	0.011	0.576	−0.408	−0.017	0.177	−0.192
Ti	−0.145	0.884*	−0.104	0.015	0.081	−0.046
V	−0.105	0.859**	0.158	0.225	−0.004	−0.232
Y	0.037	0.541	0.271	−0.179	0.219	0.012
Zn	−0.212	0.150	0.226	−0.114	−0.758**	−0.048
Zr	0.439	0.252	0.132	−0.039	0.508	0.013
Carbonate	−0.028	−0.007	−0.884**	0.025	−0.009	−0.145
P_2O_5	0.128	−0.151	−0.188	0.005	−0.923**	−0.216
Cumulative percent of total variance explained	21.4	39.7	53.8	64.1	69.2	73.5

**Significant loading

MATRIX OF FACTOR CORRELATIONS (95% SIGNIFICANCE LIMIT = ± 0.329)

1	1.000	−0.035	0.009	0.406	0.281	0.114
2	−0.035	1.000	−0.073	−0.012	−0.049	−0.089
3	0.009	−0.073	1.000	0.045	−0.055	0.239
4	0.406	−0.012	0.045	1.000	0.040	0.045
5	0.281	−0.049	−0.055	0.040	1.000	−0.326
6	0.114	−0.089	0.239	0.045	−0.326	1.000

equation. In addition, if a plot of the *Y* variable against the residuals results in a linear trend, then this suggests that the linear regression equation is a poor predictor of the *Y* variable. With the Broad Sound regression results, an observable linear trend with this residual plot corresponded to an RSQ value of approximately 0.50 or less. The equations with a poor linear fit or an excessive sum of squares ('unexplained' by the regression) are indicated in Tables B33-39.

The size of the increase in the RSQ value resulting from the addition of a variable to the equation, indicates the importance of that variable in the regression given the presence of the variables previously included in the equation. Using this increase in the RSQ statistic, the reasons for the inclusion, deletion, and final repeated inclusion of Fe in the regression equation for Cr in the unsorted gravel results, as discussed above, can be seen.

TABLE B27. OBLIQUE FACTOR MATRIX, PRIMARY-UNSORTED-MUDDY-SAND UNIT

	Factors			
Mean grainsize (phi)	0.881**	−0.184	−0.227	0.012
Grainsize std dev.	0.841**	−0.176	0.320	0.081
Gravel (carbonate retained)	−0.237	−0.530**	0.054	−0.750**
Sand (carbonate retained)	−0.923**	0.112	0.193	0.005
Mud (carbonate retained)	0.925**	−0.106	−0.193	0.004
Silt (carbonate retained)	0.928**	−0.095	−0.191	−0.024
Clay (carbonate retained)	0.896**	−0.140	−0.198	0.099
Sand (carbonate removed)	−0.986**	−0.197	−0.030	0.075
Mud (carbonate removed)	0.986**	0.197	0.030	−0.075
Dolomite	0.033	−0.292	0.370	0.692**
Mg-calcite	−0.090	0.890**	0.081	−0.165
Calcite	0.177	0.858**	0.393	0.122
Plagioclase	−0.025	−0.813**	−0.060	−0.055
Orthoclase	0.041	−0.267	−0.338	0.363
Aragonite	−0.298	−0.307	−0.391	0.041
Quartz	0.129	−0.766**	0.045	−0.131
Ba	0.135	−0.031	−0.886**	−0.306
Ca	−0.081	0.909**	−0.058	−0.147
Co	−0.084	0.006	−0.946**	−0.074
Cr	−0.068	−0.298	−0.896**	0.115
Cu	−0.288	0.071	−0.599**	0.244
Fe	0.154	−0.090	−0.854**	0.362
Mg	0.012	0.859**	−0.376	0.241
Mn	−0.208	0.591**	−0.643**	0.324
Ni	0.087	−0.089	−0.955**	−0.168
Pb	0.266	0.208	−0.049	−0.817**
Sc	0.067	0.246	−0.854**	−0.075
Sr	−0.077	0.596**	−0.634**	−0.157
Ti	0.330	−0.169	−0.846**	0.042
V	0.201	0.042	−0.933**	−0.023
Y	−0.019	−0.010	−0.849**	−0.114
Zn	0.873**	0.278	0.462	0.031
Zr	−0.157	−0.981**	0.356	−0.072
Carbonate	−0.058	0.824**	−0.023	−0.241
P_2O_5	−0.019	0.919**	−0.134	−0.008
Cumulative percent of total variance explained	31.4	60.8	77.0	83.5

**Significant loading

MATRIX OF FACTOR CORRELATIONS (95% SIGNIFICANCE LIMIT = ± 0.333)

1	1.000	−0.197	−0.135	0.043
2	−0.197	1.000	−0.187	−0.260
3	−0.135	−0.187	1.000	−0.009
4	0.043	−0.260	−0.009	1.000

TABLE B28. OBLIQUE FACTOR MATRIX, SORTED-SAND UNIT

	Factors					
Mean grainsize (phi)	−0.000	−0.147	−0.077	0.401	−0.056	0.687**
Grainsize std dev.	−0.250	0.030	−0.103	−0.005	0.038	−0.793**
Gravel (carbonate retained)	0.033	−0.036	0.004	−0.098	−0.027	−0.950**
Sand (carbonate retained)	−0.008	−0.022	−0.032	−0.437	0.013	0.851**
Mud (carbonate retained)	−0.041	0.099	0.050	0.942**	0.022	0.083
Silt (carbonate retained)	−0.039	0.102	0.053	0.939**	0.023	0.092
Clay (carbonate retained)	−0.100	−0.145	−0.190	0.349	−0.038	−0.486
Gravel (carbonate removed)	−0.045	−0.266	0.170	−0.109	−0.030	−0.654**
Sand (carbonate removed)	−0.322	0.202	−0.103	−0.385	−0.081	0.361
Mud (carbonate removed)	0.355	−0.142	0.063	0.438	0.094	−0.203
Dolomite	−0.481	0.062	0.120	0.010	0.264	−0.154
Mg-calcite	0.919**	−0.043	−0.000	−0.006	−0.023	0.316
Calcite	0.469	0.072	0.095	−0.137	0.122	−0.612**
Plagioclase	−0.750**	0.125	0.203	0.123	0.440	0.095
Orthoclase	−0.540**	0.033	0.221	0.067	0.121	0.308
Aragonite	0.820**	−0.036	−0.076	0.029	0.040	0.236
Quartz	−0.468	−0.146	−0.345	−0.028	−0.560**	−0.028
Ba	−0.716**	0.037	0.052	0.428	0.370	−0.060
Ca	0.618**	0.133	0.126	0.249	0.059	−0.302
Co	−0.052	0.439	−0.650**	−0.053	−0.153	−0.033
Cr	0.148	−0.185	−0.645**	−0.082	0.0394	0.189
Cu	−0.119	−0.075	−0.297	0.116	0.094	−0.510**
Fe	−0.291	0.010	0.007	−0.151	0.724**	−0.233
Mg	0.600**	−0.096	0.242	−0.170	0.157	0.154
Mn	−0.115	0.346	−0.166	−0.278	0.421	−0.311
Ni	−0.042	−0.009	−0.860**	−0.034	0.047	−0.055
Pb	0.048	0.417	0.033	0.277	0.406	0.173
Sc	0.177	0.324	−0.840**	0.042	−0.125	0.083
Sr	0.555**	0.074	−0.095	0.362	0.247	0.076
Ti	0.105	−0.300	−0.508**	−0.005	0.622**	0.104
V	0.026	0.251	−0.777**	−0.078	0.388	−0.104
Y	0.005	0.061	−0.912**	−0.048	−0.200	−0.172
Zn	−0.238	−0.102	−0.172	0.116	0.304	−0.300
Zr	0.010	−0.417	−0.665**	−0.037	0.304	−0.068
Carbonate	0.724**	0.128	0.130	0.131	−0.060	−0.250
P_2O_5	0.328	0.419	0.223	−0.231	0.159	−0.322
Heavy minerals	−0.059	0.434	−0.360	−0.266	0.174	−0.020
Opaque	0.034	−0.932**	0.137	−0.169	−0.036	−0.062
Non-opaque	−0.304	0.932**	−0.137	0.169	0.036	0.062
Zircon	0.195	−0.758**	0.077	−0.154	0.038	0.013
Epidote	−0.461	0.551**	0.192	−0.121	0.216	0.025
Tourmaline	0.298	0.120	−0.443	0.143	−0.001	0.218
Rutile	−0.114	−0.734**	0.001	0.155	0.049	−0.040
Hornblende	0.538**	−0.040	−0.275	0.138	−0.366	−0.108
Garnet	−0.017	−0.437	0.056	−0.073	−0.341	−0.205
Zoisite	0.091	0.296	−0.032	0.493	−0.334	−0.075
Cumulative percent of total variance explained	19.8	36.2	45.8	52.4	58.6	63.5

** Significant loading
One sample (70636114) was removed before the analysis

MATRIX OF FACTOR CORRELATIONS (95% SIGNIFICANCE LIMIT = ± 0.290)

1	1.000	−0.138	0.271	0.338	−0.007	−0.200
2	−0.138	1.000	0.072	−0.209	0.090	−0.430
3	0.271	0.072	1.000	0.065	0.053	−0.282
4	0.338	−0.209	0.065	1.000	−0.088	0.088
5	−0.007	0.090	0.053	−0.008	1.000	−0.070
6	−0.200	−0.430	−0.282	0.088	−0.070	1.000

TABLE B29. OBLIQUE FACTOR MATRIX, MIXED-UNSORTED-MUDDY-SAND UNIT

	Factors					
Mean grainsize (phi)	−0.218	−0.871**	−0.133	0.045	0.137	0.028
Grainsize std dev.	−0.034	0.116	0.238	0.271	−0.024	0.101
Gravel (carbonate retained)	0.046	0.131	0.938**	−0.094	−0.106	−0.095
Sand (carbonate retained)	0.103	0.913**	−0.127	−0.023	−0.040	0.029
Mud (carbonate retained)	−0.109	−0.932**	0.021	0.033	0.052	−0.018
Silt (carbonate retained)	0.202	−0.901**	0.048	−0.083	−0.153	−0.079
Clay (carbonate retained)	−0.362	−0.724**	−0.008	0.130	0.224	0.041
Gravel (carbonate removed)	0.069	−0.111	0.885**	−0.142	−0.147	−0.044
Sand (carbonate removed)	−0.205	0.960**	0.58	0.008	0.052	0.010
Mud (carbonate removed)	0.201	−0.958**	−0.123	0.003	−0.042	−0.006
Dolomite	0.110	0.015	0.619**	−0.006	0.043	0.184
Mg-calcite	0.122	0.525**	−0.230	0.666**	0.307	0.086
Calcite	0.101	0.106	0.722**	0.177	0.371	0.077
Plagioclase	0.137	−0.606**	−0.189	−0.384	−0.294	0.058
Orthoclase	0.090	0.138	−0.343	−0.627**	0.254	−0.135
Aragonite	0.032	−0.035	−0.244	0.645**	0.146	0.029
Quartz	−0.543**	0.219	−0.067	0.062	−0.577**	0.019
Ba	−0.093	−0.301	−0.099	−0.107	−0.838**	0.066
Ca	0.848**	0.110	−0.008	0.191	−0.011	−0.039
Co	−0.378	0.157	−0.089	−0.066	−0.125	−0.118
Cr	−0.096	−0.279	−0.127	0.126	0.317	−0.602**
Cu	0.282	−0.326	−0.008	0.578**	−0.206	−0.486
Fe	−0.299	−0.292	0.023	0.021	0.598**	−0.290
Mg	0.075	−0.131	−0.229	−0.005	0.865**	−0.221
Mn	−0.705**	0.269	−0.167	−0.204	0.076	−0.092
Ni	−0.478	0.213	0.044	0.023	0.009	−0.565**
Pb	−0.600**	0.126	−0.127	0.253	−0.070	0.250
Sc	−0.787**	−0.047	−0.071	0.256	−0.353	−0.187
Sr	0.291	−0.123	0.012	0.470	−0.601**	0.081
Ti	0.097	−0.168	−0.002	−0.088	0.184	−0.912**
V	−0.533**	−0.227	0.141	0.151	0.131	−0.377
Y	−0.370	0.253	0.013	0.011	−0.459	−0.602**
Zn	−0.724**	−0.096	0.102	0.161	0.198	0.195
Zr	0.166	0.400	0.065	−0.131	0.319	−0.804**
Carbonate	0.856**	0.110	−0.028	0.365	−0.044	−0.080
P_2O_5	−0.123	−0.375	0.195	0.097	0.422	0.288
Cumulative percent of total variance explained	25.4	45.2	55.2	62.2	68.8	73.8

** Significant loading.

MATRIX OF FACTOR CORRELATIONS (95% SIGNIFICANCE LEVEL = $\pm$ 0.329)

1	1.000	0.126	−0.087	−0.085	−0.392	0.422
2	0.126	1.000	−0.127	0.027	−0.205	−0.153
3	−0.087	−0.127	1.000	0.108	0.226	0.024
4	−0.085	0.027	0.108	1.000	0.149	−0.097
5	−0.392	−0.205	0.226	0.149	1.000	−0.039
6	0.422	−0.153	0.024	−0.097	−0.039	1.000

TABLE B30. OBLIQUE FACTOR MATRIX, SORTED-SANDY-GRAVEL UNIT

	Factors					
Mean grainsize (phi)	0.065	−0.589	−0.066	0.539	−0.002	−0.539
Grainsize std dev.	0.424	0.113	0.110	0.717**	0.093	−0.009
Gravel (carbonate retained)	−0.003	0.710**	−0.008	−0.166	0.140	0.466
Sand (carbonate retained)	0.026	−0.657**	0.020	−0.062	−0.157	−0.461
Mud (carbonate retained)	−0.100	−0.106	−0.051	0.951**	0.096	0.057
Silt (carbonate retained)	−0.093	−0.193	0.049	0.783**	0.203	0.250
Clay (carbonate retained)	−0.085	−0.004	−0.133	0.913**	−0.024	−0.134
Gravel (carbonate removed)	0.121	0.263	0.192	−0.029	−0.386	0.001
Sand (carbonate removed)	0.095	0.120	−0.128	−0.094	−0.040	−0.903**
Mud (carbonate removed)	−0.113	−0.160	0.096	0.098	0.101	0.892**
Mg-calcite	−0.330	−0.943**	−0.062	0.062	0.036	0.188
Calcite	−0.335	0.880	−0.203	−0.114	0.041	−0.138
Plagioclase	0.710**	0.022	0.159	0.237	0.123	0.264
Orthoclase	0.724**	−0.028	0.198	0.094	0.009	−0.223
Aragonite	0.164	−0.836**	0.118	−0.075	−0.133	0.144
Quartz	0.736**	0.093	0.395	0.047	−0.161	−0.120
Ba	0.239	0.173	0.740**	0.199	−0.197	−0.012
Ca	−0.552	0.246	0.083	−0.554	−0.202	−0.010
Co	−0.072	−0.099	0.697**	−0.142	−0.012	0.106
Cr	0.143	0.036	−0.050	0.176	0.882**	0.140
Cu	−0.113	0.339	−0.806**	0.063	−0.147	−0.448
Fe	−0.345	0.482	0.152	0.388	−0.060	−0.078
Mg	−0.753**	−0.717**	0.147	0.011	−0.033	−0.042
Mn	−0.463	0.240	0.500	0.252	−0.293	−0.249
Ni	−0.196	0.471	0.067	−0.002	0.617**	−0.075
Pb	−0.076	−0.167	−0.030	−0.176	0.508	−0.292
Sc	−0.792**	−0.149	0.377	−0.274	0.199	0.115
Sr	−0.442	−0.201	−0.439	0.180	0.213	−0.272
Ti	−0.081	0.240	0.137	0.317	0.667**	0.041
V	−0.691**	0.185	0.476	0.103	0.047	0.011
Y	−0.383	0.072	0.411	−0.177	0.493	−0.169
Zn	−0.671**	−0.207	0.443	0.081	0.051	0.066
Zr	0.210	0.171	−0.029	0.054	0.929**	0.020
Carbonate	−0.223	0.431	−0.401	−0.042	−0.061	0.027
P_2O_5	−0.584	0.248	−0.196	0.317	−0.136	0.323
Heavy minerals	0.401	0.431	0.477	0.129	0.054	0.065
Opaque	−0.873**	0.029	−0.183	0.115	−0.053	0.119
Non-opaque	0.873**	−0.029	0.183	−0.115	0.053	−0.119
Zircon	−0.782**	0.156	−0.207	0.056	0.024	0.021
Epidote	0.727**	−0.187	0.188	−0.035	−0.164	0.118
Tourmaline	0.003	−0.029	−0.268	−0.022	0.339	−0.526
Rutile	−0.833**	0.045	0.309	−0.015	0.023	−0.175
Hornblende	0.804**	0.097	−0.030	−0.060	0.393	−0.216
Garnet	−0.031	0.084	−0.167	0.503	−0.154	0.290
Zoisite	0.148	−0.063	0.474	−0.225	0.137	−0.167
Cumulative percent of total variance explained	27.6	42.4	52.3	61.0	67.6	72.6

**Significant loading

MATRIX OF FACTOR CORRELATIONS (95% SIGNIFICANCE LIMIT = ± 0.294)

1	1.000	−0.217	0.056	−0.146	−0.267	−0.199
2	−0.217	1.000	0.276	0.215	0.140	0.321
3	0.056	0.276	1.000	0.099	0.176	−0.197
4	−0.146	0.215	0.099	1.000	0.024	0.137
5	−0.267	0.140	0.176	−0.024	1.000	0.084
6	−0.199	0.321	−0.197	0.137	0.084	1.000

TABLE B31. OBLIQUE FACTOR MATRIX, UNSORTED-GRAVEL UNIT

	Factors					
Mean grainsize (phi)	−0.770**	−0.231	−0.009	0.544**	0.014	−0.220
Grainsize std dev.	0.125	−0.140	0.317	−0.600**	0.099	0.181
Gravel (carbonate retained)	0.762**	0.247	0.040	−0.395	−0.084	0.245
Sand (carbonate retained)	−0.444	−0.081	0.024	−0.603**	0.237	−0.014
Mud (carbonate retained)	−0.286	−0.151	−0.058	0.913**	−0.141	−0.127
Silt (carbonate retained)	0.158	0.035	−0.087	0.925**	−0.169	−0.014
Clay (carbonate retained)	−0.720**	−0.295	0.061	−0.189	0.075	−0.173
Gravel (carbonate removed)	0.247	0.635**	−0.334	−0.096	−0.343	−0.266
Sand (carbonate removed)	−0.304	−0.129	0.091	0.360	−0.693**	0.171
Mud (carbonate removed)	0.178	−0.156	0.060	−0.297	0.803**	−0.045
Dolomite	0.242	−0.043	0.367	0.833**	0.039	−0.056
Mg-calcite	−0.044	−0.918**	−0.214	0.113	0.184	0.103
Calcite	0.564**	0.607**	0.172	−0.059	−0.117	−0.265
Plagioclase	−0.688**	−0.234	−0.062	0.088	0.173	0.323
Orthoclase	−0.494	−0.074	−0.188	−0.009	0.235	0.473
Aragonite	−0.534**	−0.503	0.162	−0.247	−0.103	−0.017
Quartz	−0.751**	−0.107	−0.215	−0.013	−0.177	0.203
Ba	−0.909**	0.049	0.267	−0.282	0.075	0.060
Ca	0.187	−0.097	−0.402	−0.215	0.126	−0.719**
Co	0.125	0.322	0.604**	0.614**	−0.152	−0.102
Cr	−0.810**	0.578**	0.171	0.022	−0.418	0.126
Cu	−0.596**	0.086	0.385	−0.173	−0.227	−0.062
Fe	−0.179	0.202	0.906**	0.004	0.052	0.202
Mg	0.766**	−0.423	0.247	0.143	−0.284	0.387
Mn	0.611**	0.045	0.128	0.255	0.165	−0.344
Ni	−-0.849**	0.196	0.390	−0.118	0.232	0.058
Pb	−0.013	−0.164	0.081	0.191	0.030	−0.855**
Sc	0.314	0.043	0.481	0.000	0.439	−0.173
Sr	−0.026	−0.695**	0.016	−0.057	0.024	−0.465
Ti	−0.871*	0.014	−0.199	−0.100	−0.066	0.045
V	−0.215	−0.203	0.716**	0.018	0.241	−0.281
Y	−0.199	0.115	0.053	0.203	0.365	−0.164
Zn	−0.781**	0.070	0.558**	−0.091	0.002	0.013
Zr	−0.439	0.028	−0.593**	0.024	−0.114	0.100
Carbonate	0.531**	−0.267	0.041	0.352	−0.071	0.213
P_2O_5	0.730**	−0.052	0.128	−0.016	0.461	−0.091
Heavy minerals	0.217	0.487	−0.478	−0.072	−0.080	0.255
Opaque	−0.214	−0.380	−0.124	−0.587**	−0.174	−0.179
Non-opaque	0.214	0.380	0.124	0.587**	0.174	0.179
Zircon	0.401	−0.665**	0.215	−0.374	−0.182	−0.179
Epidote	−0.341	0.760**	−0.071	0.349	0.113	0.080
Tourmaline	−0.221	−0.116	0.155	0.055	0.716**	0.207
Rutile	−0.138	−0.468	0.276	−0.335	−0.385	−0.099
Hornblende	0.043	−0.037	−0.708**	0.072	−0.194	−0.255
Garnet	−0.147	−0.480	−0.322	0.282	−0.165	−0.392
Zoisite	−0.123	0.240	−0.736**	−0.118	0.295	−0.001
Cumulative percent of total variance explained	26.2	43.4	56.9	65.5	71.1	76.2

** Significant loading

MATRIX OF FACTOR CORRELATIONS (95% SIGNIFICANCE LIMIT = ± 0.29)

1	1.000	0.227	0.068	−0.029	0.026	−0.111
2	0.227	1.000	0.075	0.199	0.218	0.090
3	0.068	0.075	1.000	−0.119	0.205	−0.260
4	−0.029	0.199	−0.119	1.000	0.015	0.273
5	0.026	0.218	0.205	0.015	1.000	−0.003
6	−0.111	0.090	−0.260	0.273	−0.003	1.000

(h) REFERENCES

BONHAM-CARTER, G.F., 1967 — FORTRAN IV program for Q-mode cluster analysis of nonquantitative data using IBM 7090/7094 computers. Computer Contribution 17. *Kansas Geological Survey.*

BROWNER, J.C. & VEINUS, J., 1974 — The statistical zap versus the shotgun approach. *Mathematical Geology* 6(4), 311-32.

CHEETHAM, A.H. & HAZEL, J.E., 1969 — Binary (presence-absence) similarity coefficients. *Journal of Paleontology,* 43(5), 1130-36.

COOLEY, W.W. & LOHNES, P.R., 1971 — MULTIVARIATE DATA ANALYSIS. *Wiley, International.*

DAVIS, J.C., 1973 — STATISTICS AND DATA ANALYSIS IN GEOLOGY. *Wiley, International.*

DAVIS, J.C. & SAMPSON, R.J., 1966 — FORTRAN II program for multivariate discriminate analysis using an IBM 1620 computer. Computer Contribution 4. *Kansas Geological Survey.*

DIXON, W.J. (Editor), 1971 — BIOMEDICAL COMPUTER PROGRAMS. *University of California Press.*

DRAPER, N.R. & SMITH, H., 1966 — APPLIED REGRESSION ANALYSIS. *Wiley, International.*

EHRENFELD, S. & LITTAUER, S., 1964 — INTRODUCTION TO STATISTICAL METHOD. *McGraw-Hill.*

GARRETT, R.G., 1967 — Two programs for the factor analysis of geologic and remote-sensing data. Northwestern University. Report No 12. *Northwestern University, Evanston, Illinois.*

GRIFFITHS, J.C., 1963 — Statistical approach to the study of potential oil reservoir sandstones. *Computers in the Mineral Industries,* 9, 637-68.

HENDRICKSON, A.E. & WHITE, P.O., 1964 — Promax: A quick method for rotation to oblique simple structure. *British Journal of Statistics and Psychology,* 2(3), 173-78.

HOEL, P.G., 1962 — INTRODUCTION TO MATHEMATICAL STATISTICS. *Wiley, International.*

HOTELLING, H., 1936 — Relations between two sets of variates. *Biometrika* 28, 321-77.

KAISER, H.F., 1958 — The varimax criterion for analytic rotation in factor analysis. *Psychometrika,* 23, 187-200.

KENDAL, M. & STUART, A., 1976 — THE ADVANCED THEORY OF STATISTICS, VOLUME 3 (DESIGN AND ANALYSIS, AND TIME SERIES), 3rd Ed., *Griffin and Co.*

KLOVAN, J.E. & IMBRIE, J., 1971 — An algorithm and FORTRAN IV program for large-scale Q-mode factor analysis and calculation of factor scores. *Mathematical Geology* 3(1), 61-8.

KRUMBEIN, W.C. & GRAYBILL, F.A., 1965 — AN INTRODUCTION TO STATISTICAL MODELS IN GEOLOGY. *Wiley, International.*

LANCE, G.N. & WILLIAMS, W.T., 1967 — A general theory of classificatory sorting strategies, I. Hierarchical systems. *Computer Journal,* 9, 373-80.

LEE, P.J., 1969 — FORTRAN IV programs for canonical correlation and canonical trend-surface analysis. Computer Contribution 32. *Kansas Geological Survey.*

McCAMMON, R.B., 1968 — The dendrograph: a new tool for correlation. *Geological Society of America Bulletin* 79, 1663-70.

MANSON, V. & IMBRIE, J., 1964 — FORTRAN program for factor and vector analysis of geologic data using an IBM 7090 or 7094/1401 computer system. *Kansas Geological Survey Special Distribution Publication* 13.

MAYO, W. & LONG, K.A., 1976 — Documentation of BMR Geological Branch computer programs. *Bureau of Mineral Resources, Australia, Record 1976/82 (unpublished); BMR Microform* MF4.

PARK, R.A., 1974 — A multivariate analytical strategy for classifying paleoenvironments. *Mathematical Geology,* 6(4), 333-52.

PARKS, J.M., 1966 — Cluster analysis applied to multivariate data. *Journal of Geology,* 74(5), 703-15.

RAO, C.R., 1952 — ADVANCED STATISTICAL MODELS IN BIOMETRIC RESEARCH. *John Wiley & Sons.*

TABLE B32. ABBREVIATIONS USED FOR VARIABLES IN TABLES B33-39.

MEAN	Mean grainsize (phi)
ST DEV	Grainsize standard deviation
GRAV 1	Gravel with carbonate in
SAND 1	Sand with carbonate in
CLAY	Clay with carbonate in
GRAV 2	Gravel with carbonate out
MUD 2	Mud with carbonate out
DOLO	Dolomite
MG-CAL	Mg-calcite
CALCIT	Calcite
PLAG	Plagioclase
ORTH	Orthoclase
ARAG	Aragonite
QTZ	Quartz
$CACO_3$	Carbonate
HEAVYS	Heavy minerals
OPAQUE	Opaque heavy minerals
EPIDOT	Epidote
TOURM	Tourmaline
HORNBL	Hornblende
ZOISIT	Zoisite
P_2O_5	Phosphate

TABLE B33. SUMMARY OF STEPWISE REGRESSION ANALYSIS, MANGROVE-SORTED-MUD UNIT

STEP NUMBER	VARIABLE ENTERED	VARIABLE REMOVED	MULTIPLE R	MULTIPLE RSQ	INCREASE IN RSQ	F VALUE TO ENTER OR REMOVE	COEFFICIENT
Ba							(CONSTANT 242.042)
1	FE		0.2658	0.0707	0.0707	3.5732	2.045
1	P_2O_5		0.4702	0.2211**	0.1505	8.8872	−0.110
Co							(CONSTANT 5.955)
1	FE		0.7228	0.5225	0.5225	51.4300	0.233
Cr							(CONSTANT 48.814)
1	FE		0.7148	0.5109	0.5109	49.0985	1.791
2	P_2O_5		0.7598	0.5773	0.0664	7.2277	−0.037
Cu							(CONSTANT 21.907)
1	ORTH		0.3559	0.1267**	0.1267	6.8173	−0.673
Fe							(CONSTANT 32.381)
1	P_2O_5		0.5054	0.2554	0.2554	16.1245	0.022
2	PLAG		0.5664	0.3208	0.0654	4.4269	−0.642
3	ORTH		0.6138	0.3767**	0.0559	4.0362	−0.751
Mg							(CONSTANT 2.513)
1	FE		0.5885	0.3464**	0.3464	24.9071	0.290
Mn							(CONSTANT 419.955)
1	DOLO		0.3340	0.1115**	0.1115	5.8999	443.662
Ni							(CONSTANT −4.743)
1	FE		0.7891	0.6227	0.6227	77.5710	0.690
2	ORTH		0.8070	0.6513	0.0286	3.7724	0.490
3	P_2O_5		0.8242	0.6793	0.0280	3.9263	−0.015
4	MEAN		0.8513	0.7247	0.0454	7.2497	2.380
Pb							(CONSTANT 9.758)
1	FE		0.3339	0.1115**	0.1115	5.8970	0.112
Sc							(CONSTANT 12.630)
1	FE		0.5912	0.3495	0.3495	25.2567	0.226
2	P_2O_5		0.6488	0.4209**	0.0714	5.6718	−0.006
Sr							(CONSTANT 979.270)
1	P_2O_5		0.3637	0.1322	0.1322	7.1626	−0.609
2	FE		0.6847	0.4688	0.3366	29.1472	13.113
3	MEAN		0.7161	0.5128	0.0440	4.0602	−55.257
Ti							(CONSTANT 6.349)
1	FE		0.6458	0.4170	0.4170	33.6204	0.088
2	P_2O_5		0.8245	0.6798	0.2627	37.7391	−0.004
3	PLAG		0.8479	0.7189	0.0392	6.2756	−0.056
V							(CONSTANT 32.696)
1	FE		0.7479	0.5593	0.5593	59.6456	1.543
2	P_2O_5		0.7913	0.6262	0.0669	8.2344	−0.029
3	ORTH		0.8105	0.6569	0.0307	4.0259	0.931
Y							(CONSTANT 27.118)
1	DOLO		0.3295	0.1086**	0.1086	5.7250	−3.832
Zn							(CONSTANT −32.267)
1	MEAN		0.7938	0.6302	0.6302	80.0802	6.241
2	P_2O_5		0.8594	0.7386	0.1085	19.0897	0.022
3	FE		0.8796	0.7736	0.0350	6.9615	0.245
Zr							(CONSTANT 400.832)
1	CALCIT		0.3446	0.1188	0.1188	6.3347	−7.565
2	ORTH		0.4396	0.1932**	0.0745	4.2465	−4.981
P_2O_5							(CONSTANT 5.037)
1	MEAN		0.6004	0.3605	0.3605	26.4912	90.033
2	FE		0.6563	0.4308	0.0703	5.6806	5.009

**Excessive sum of squares remaining.

TABLE B34. SUMMARY OF STEPWISE REGRESSION ANALYSIS, MUDFLAT-SORTED-MUD UNIT.

STEP NUMBER	VARIABLE ENTERED	VARIABLE REMOVED	MULTIPLE R	MULTIPLE RSQ	INCREASE IN RSQ	F VALUE TO ENTER OR REMOVE	COEFFICIENT
Ba							(CONSTANT 505.430)
1	GRAV 2		0.5034	0.2534	0.2534	18.3281	66.252
2	MEAN		0.5966	0.3560	0.1026	8.4409	−72.604
3	FE		0.6765	0.4576	0.1016	9.7419	4.091
4	PLAG		0.7063	0.4989	0.0413	4.2020	5.310
Co							(CONSTANT 4.079)
1	MN		0.6696	0.4483	0.4483	43.8862	0.025
Cr							(CONSTANT −0.741)
1	FE		0.8440	0.7123	0.7123	133.7145	1.920
2	ORTH		0.8724	0.7611	0.0488	10.8309	1.506
3	GRAV 2		0.8902	0.7925	0.0314	7.8562	−4.873
Cu							(CONSTANT 12.798)
1	FE		0.3927	0.1542	0.1542	9.8432	0.197
2	GRAV 2		0.4609	0.2125**	0.0583	3.9227	−1.498
Fe							(CONSTANT 26.123)
1	MN		0.5377	0.2892	0.2892	21.9675	0.036
2	ORTH		0.5866	0.3441**	0.0549	4.4356	−0.739
Mg							(CONSTANT 6.772)
1	MG-CAL		0.5187	0.2690	0.2690	19.8724	1.215
2	P_2O_5		0.5974	0.3569	0.0879	7.2454	0.009
3	CALCIT		0.6479	0.4198**	0.0629	5.6347	−0.642
Mn							(CONSTANT 245.594)
1	FE		0.5377	0.2892**	0.2892	21.9675	7.690
Ni							(CONSTANT 13.544)
1	FE		0.8232	0.6777	0.6777	113.5239	0.576
2	MN		0.8612	0.7417	0.0641	13.1474	0.018
3	PLAG		0.8894	0.7910	0.0493	12.2577	−0.343
4	GRAV 2		0.9078	0.8241	0.0331	9.5914	−2.080
Pb							(CONSTANT 10.927)
1	MN		0.4287	0.1838**	0.1838	12.1586	0.010
Sc							(CONSTANT 14.862)
1	FE		0.6073	0.3688	0.3688	31.5501	0.112
2	PLAG		0.6540	0.4278	0.0590	5.4615	0.004
3	MN		0.6859	0.4705	0.0427	4.1968	
Sr							(CONSTANT 74.408)
1	ARAG		0.4665	0.2176	0.2176	15.0173	18.019
2	FE		0.6071	0.3686	0.1510	12.6750	3.721
3	P_2O_5		0.6432	0.4136	0.0451	3.9961	−0.113
4	MG-CAL		0.6939	0.4815	0.0679	6.6780	6.249
Ti							(CONSTANT 1.590)
1	FE		0.7732	0.5978	0.5978	80.2604	0.083
2	PLAG		0.8006	0.6409	0.0431	6.3609	−0.050
3	P_2O_5		0.8375	0.7014	0.0605	10.5361	−0.001
4	MEAN		0.8539	0.7292	0.0278	5.2410	0.328
V							(CONSTANT 13.737)
1	FE		0.7089	0.5025	0.5025	54.5430	1.214
2	ORTH		0.7377	0.5442	0.0417	4.8458	1.053
Y							(CONSTANT 23.125)
1	MN		0.4129	0.1705**	0.1705	11.0987	0.010
Zn							(CONSTANT −21.283)
1	P_2O_5		0.6058	0.3669	0.3669	31.2991	0.021
2	MEAN		0.7582	0.5748	0.2079	25.9148	6.524
3	MG-CAL		0.8033	0.6453	0.0705	10.3366	−0.556
4	MN		0.8305	0.6898	0.0444	7.3054	0.013
Zr							(CONSTANT 768.639)
1	MEAN		0.5431	0.2949	0.2949	22.5870	−52.539
2	P_2O_5		0.6254	0.3911	0.0962	8.3687	−0.096
3	FE		0.6635	0.4402	0.0492	4.5670	1.393
P_2O_5							(CONSTANT 972.245)
1	ORTH		0.4118	0.1696	0.1696	11.0258	−25.666
2	CALCIT		0.4835	0.2338**	0.0642	4.4438	13.359

**Excessive sum of squares remaining.

TABLE B35. SUMMARY OF STEPWISE REGRESSION ANALYSIS, PRIMARY-UNSORTED-MUDDY-SAND UNIT

STEP NUMBER	VARIABLE ENTERED	VARIABLE REMOVED	MULTIPLE R	MULTIPLE RSQ	INCREASE IN RSQ	F VALUE TO ENTER OR REMOVE	COEFFICIENT
Ba							(CONSTANT 92.725)
1	FE		0.7094	0.5032	0.5032	12.1569	10.820
Co							(CONSTANT −0.242)
1	FE		0.7337	0.5383	0.5383	13.9922	1.173
Cr							(CONSTANT −5.168)
1	FE		0.8110	0.6578	0.6578	23.0625	5.092
Cu							(CONSTANT −19.560)
1	MN		0.6507	0.4235	0.4235	8.8136	0.068
Fe							(CONSTANT 5.128)
1	MN		0.6245	0.3899	0.3899	7.6702	0.026
2	MG-CAL		0.8776	0.7701	0.3802	18.1931	−0.310
Mg							(CONSTANT −6.023)
1	MN		0.9148	0.8369	0.8369	61.5812	0.026
2	MG-CAL		0.9725	0.9458	0.1089	22.0934	0.234
Mn							(CONSTANT −78.002)
1	P_2O_5		0.7217	0.5209	0.5209	13.0474	0.981
2	FE		0.9303	0.8654	0.3445	28.1468	29.426
3	MEAN		0.9774	0.9554	0.0900	20.1537	−61.196
Ni							(CONSTANT 0.691)
1	FE		0.7503	0.5629	0.5629	15.4561	1.320
Pb							
	NONE						
Sc							(CONSTANT 1.107)
1	MN		0.7109	0.5054	0.5054	12.2639	0.026
Sr							(CONSTANT −2327.211)
1	MN		0.8535	0.7285	0.7285	32.2019	2.768
2	P_2O_5		0.9091	0.8264	0.0979	6.2054	3.966
Ti							(CONSTANT 0.597)
1	FE		0.8784	0.7716	0.7716	40.5486	0.162
V							(CONSTANT −4.589)
1	FE		0.8473	0.7180	0.7180	30.5495	3.379
Y							(CONSTANT −4.589)
1	FE		0.6120	0.3746	0.3746	7.1878	3.379
Zn							(CONSTANT 7.740)
1	MEAN		0.5933	0.3520	0.3520	6.5177	3.799
2	FE		0.7945	0.6312	0.2792	8.3276	−0.586
Zr							(CONSTANT 177.826)
1	P_2O_5		0.8059	0.6494	0.6494	22.2286	
2	CALCIT		0.8784	0.7716	0.1221	5.8814	−11.675
3	QTZ		0.9198	0.8460	0.0745	4.8386	10.315
4		P_2O_5	0.9114	0.8307	0.0154	0.0000	
P_2O_5							(CONSTANT 246.792)
1	MG-CAL		0.8906	0.7931	0.7931	46.0083	6.883
2	MN		0.9400	0.8835	0.0904	8.5352	0.211

Dolomite was forced out of these regressions because the correlation coefficient between 'dolomite' and Mg for this unit was − 0.435, suggesting a misinterpretation of the XRD results.

TABLE B36. SUMMARY OF STEPWISE REGRESSION ANALYSIS, SORTED-SAND UNIT

STEP NUMBER	VARIABLE ENTERED	VARIABLE REMOVED	MULTIPLE R	MULTIPLE RSQ	INCREASE IN RSQ	F VALUE TO ENTER OR REMOVE	COEFFICIENT
Ba							(CONSTANT 126.206)
1	PLAG		0.5680	0.3226	0.3226	34.2917	2.883
2	P_2O_5		0.6084	0.3701	0.0475	5.3512	−0.182
3	FE		0.6615	0.4376	0.0675	8.3968	7.379
4	ZOISIT		0.6856	0.4700	0.0324	4.2238	3.781
Co							(CONSTANT −7.556)
1	MN		0.4025	0.1620	0.1620	13.9170	0.008
2	QTZ		0.5673	0.3219	0.1599	16.7404	0.252
3	ZIRCON		0.5999	0.3598	0.0380	4.1507	−0.105
4	EPIDOT		0.6311	0.3983	0.0384	4.4058	
5	ORTH		0.6598	0.4353	0.0371	4.4637	0.313
6	ARAG		0.7024	0.4933	0.0580	7.6668	0.623
7		EPIDOT	0.6873	0.4724	−0.0209	0.0000	
Cr							(CONSTANT −20.309)
1	MEAN		0.3613	0.1305	0.1305	10.8091	19.558
2	FE		0.5107	0.2608	0.1303	12.5108	3.008
3	HEAVYS		0.5585	0.3120	0.0512	5.2065	10.109
4	EPIDOT		0.5941	0.3530**	0.0410	4.3720	−0.395
Cu							(CONSTANT 20.258)
1	CLAY		0.3330	0.1109	0.1109	8.9792	50.569
2	MEAN		0.4191	0.1757**	0.0648	5.5798	−3.080
FE							(CONSTANT 3.556)
1	MN		0.6394	0.4088	0.4088	49.7956	0.005
2	PLAG		0.7039	0.4955	0.0867	12.1990	0.158
3	ZOISIT		0.7327	0.5368	0.0413	6.2392	−0.252
4	CALCIT		0.7602	0.5779	0.0411	6.7188	0.109
Mg							(CONSTANT −6.838)
1	MG-CAL		0.5231	0.2736	0.2736	27.1209	0.149
2	P_2O_5		0.5903	0.3484	0.0748	8.1503	0.011
3	OPAQUE		0.6451	0.4162	0.0678	8.1273	0.052
4	MEAN		0.6721	0.4517**	0.0355	4.4653	1.236
Mn							(CONSTANT 676.059)
1	FE		0.6394	0.4088	0.4088	49.7956	30.612
2	MEAN		0.7491	0.5611	0.1523	24.6371	−172.094
3	HEAVYS		0.8038	0.6461	0.0849	16.7974	122.900
4	CLAY		0.8164	0.6665	0.0204	4.2221	−852.382
Ni							(CONSTANT 21.428)
1	QTZ		0.3450	0.1190	0.1190	9.7257	
2	HEAVYS		0.4286	0.1837	0.0647	5.6272	3.134
3	P_2O_5		0.5392	0.2908	0.1071	10.5656	−0.018
4		QTZ	0.5333	0.2844**	0.0063	0.0000	
Pb							(CONSTANT 5.853)
1	MN		0.2888	0.0834**	0.0834	6.5496	0.004

TABLE B36 (cont'd) SUMMARY OF STEPWISE REGRESSION ANALYSIS, SORTED-SAND UNIT

STEP NUMBER	VARIABLE ENTERED	VARIABLE REMOVED	MULTIPLE R	MULTIPLE RSQ	INCREASE IN RSQ	F VALUE TO ENTER OR REMOVE	COEFFICIENT
Sc							(CONSTANT −1.168)
1	TOURM		0.3696	0.1366	0.1366	11.3883	0.214
2	HEAVYS		0.4745	0.2251	0.0886	8.1150	
3	QTZ		0.5330	0.2841	0.0590	5.7650	0.098
4	HORNBL		0.5859	0.3433	0.0592	6.2213	0.125
5	MN		0.6491	0.4214	0.0780	9.1719	0.006
6		HEAVYS	0.6377	0.4067	0.0146	0.0000	
7	MEAN		0.6802	0.4626	0.0559	7.0756	1.232
Sr							(CONSTANT 811.549)
1	MG-CAL		0.5594	0.3129	0.3129	32.7906	
2	TOURM		0.6049	0.3658	0.0529	5.9263	18.131
3	QTZ		0.6698	0.4486	0.0827	10.5013	−8.998
4	HEAVYS		0.6896	0.4755	0.0269	3.5422	−67.926
5	ORTH		0.7185	0.5162	0.0407	5.7257	−12.834
6		MG-CAL	0.7117	0.5065	0.0098	0.0000	
Ti							(CONSTANT 2.776)
1	MEAN		0.3332	0.1110	0.1110	8.9889	0.881
2	FE		0.5539	0.3068	0.1958	20.0511	0.202
3	ORTH		0.5885	0.3463	0.0396	4.2353	−0.107
4	HEAVYS		0.6168	0.3804	0.0341	3.7963	0.753
5	P_2O_5		0.6565	0.4310	0.0506	6.0441	−0.006
6	QTZ		0.7037	0.4953	0.0643	8.5329	−0.051
V							(CONSTANT 26.871)
1	MN		0.5366	0.2880	0.2880	29.1187	0.020
2	TOURM		0.6319	0.3993	0.1114	13.1622	0.577
3	P_2O_5		0.6674	0.4454	0.0460	5.8104	−0.021
4	HEAVYS		0.7013	0.4918	0.0465	6.3101	3.191
Y							CONSTANT 8.647)
1	QTZ		0.4569	0.2087	0.2087	18.9952	0.494
2	MN		0.5215	0.2720	0.0632	6.1647	0.019
3	HORNBL		0.6126	0.3753	0.1033	11.5784	0.517
4	P_2O_5		0.6510	0.4238**	0.0485	5.8045	−0.022
Zn							(CONSTANT 14.127)
1	CLAY		0.3006	0.0904	0.0904	7.1544	50.972
2	MN		0.4387	0.1924	0.1020	8.9707	0.012
3	P_2O_5		0.5148	0.2650**	0.0726	6.9099	−0.017
Zr							(CONSTANT 1394.051)
1	P_2O_5		0.3899	0.1520	0.1520	12.9056	−1.801
2	HEAVYS		0.5184	0.2688	0.1168	11.3397	208.236
3	EPIDOT		0.5616	0.3154	0.0466	4.7698	−7.537
4	FE		0.6187	0.3828	0.0674	7.5362	40.379
5	ORTH		0.6596	0.4350**	0.0522	6.2813	−22.467
P_2O_5							(CONSTANT 602.473)
1	CALCIT		0.6838	0.4676	0.4676	63.2277	5.702
2	MEAN		0.7531	0.5672	0.0996	16.3375	−58.118
3	HEAVYS		0.7865	0.6186	0.0514	9.4336	48.099
4	QTZ		0.8070	0.6512	0.0326	6.4519	−2.749
5	TOURM		0.8223	0.6762	0.0250	5.2578	−5.384

**Excessive sum of squares remaining
One sample (70636114) with anomalous Fe was removed.

TABLE B37. SUMMARY OF STEPWISE REGRESSION ANALYSIS, MIXED-UNSORTED-MUDDY-SAND UNIT

STEP NUMBER	VARIABLE ENTERED	VARIABLE REMOVED	MULTIPLE R	MULTIPLE RSQ	INCREASE IN RSQ	F VALUE TO ENTER OR REMOVE	COEFFICIENT
Ba							(CONSTANT 169.958)
1	PLAG		0.4795	0.2299	0.2299	11.0455	1.630
	FE		0.6261	0.3920**	0.1621	9.5979	−1.348
Co							
	NONE						
Cr							(CONSTANT −9.875)
1	FE		0.6388	0.4080	0.4080	25.5005	1.954
2	QTZ		0.6892	0.4750**	0.0670	4.5918	1.386
Cu							(CONSTANT 19.697)
1	ORTH		0.3261	0.1063**	0.1063	4.4015	−0.588
Fe							(CONSTANT −32.952)
1	MEAN		0.5678	0.3224	0.3224	17.6044	2.368
2	MN		0.7053	0.4975	0.1751	12.5447	0.048
3	CALCIT		0.8171	0.6677	0.1702	17.9318	0.478
4	P_2O_5		0.8542	0.7296	0.0619	7.7817	0.015
Mg							(CONSTANT 3.195)
1	FE		0.7445	0.5543	0.5543	46.0099	0.331
Mn							(CONSTANT 455.903)
1	FE		0.4259	0.1814	0.1814	8.1965	7.504
2	P_2O_5		0.6449	0.4159**	0.2346	14.4583	−0.289
Ni							(CONSTANT 2.410)
1	FE		0.5120	0.2621	0.2621	13.1437	1.030
2	QTZ		0.7158	0.5123	0.2502	18.4686	0.900
3	MEAN		0.7957	0.6331	0.1208	11.5212	−2.299
4	P_2O_5		0.8234	0.6780	0.0449	4.7394	−0.014
Pb							(CONSTANT −1.077)
1	MN		0.3953	0.1563**	0.1563	6.8530	0.032
Sc							(CONSTANT 6.688)
1	MN		0.5339	0.2850**	0.2850	14.7507	0.015
Sr							(CONSTANT 823.960)
1	FE		0.5397	0.2913	0.2913	15.2069	−11.548
2	ORTH		0.6059	0.3671**	0.0758	4.3131	−12.831
Ti							(CONSTANT 3.524)
1	FE		0.5277	0.2785	0.2785	14.2811	0.131
2	P_2O_5		0.6245	0.3900**	0.1115	6.5816	−0.003
V							(CONSTANT 11.318)
1	FE		0.8010	0.6416	0.6416	66.2291	1.232
2	QTZ		0.8227	0.6769	0.0353	3.9337	0.523
Y*							(CONSTANT 25.617)
1	P_2O_5		0.4684	0.2194	0.2194	10.4004	−0.027
2	FE		0.5543	0.3072	0.0878	4.5626	0.361
3	QTZ		0.6368	0.4055**	0.0983	5.7850	0.594
Zn							(CONSTANT −20.679)
1	FE		0.7525	0.5662	0.5662	48.2918	0.653
2	MN		0.7903	0.6245	0.0583	5.5926	0.060
3	P_2O_5		0.8172	0.6679	0.0433	4.5666	0.022
Zr*							(CONSTANT 1872.584)
1	PLAG		0.4508	0.2033	0.2033	9.4388	
2	P_2O_5		0.5329	0.2840	0.0807	4.0594	−1.543
3	FE		0.6681	0.4463	0.1623	10.2614	59.951
4	MEAN		0.7492	0.5613	0.1150	8.9115	−258.576
		PLAG	0.7366	0.5426	0.0187	0.0000	
P_2O_5							(CONSTANT 804.033)
1	FE		0.5185	0.2688	0.2688	13.6019	15.019
2	MN		0.6916	0.4783**	0.2095	14.4583	−0.993

**Excessive sum of squares remaining.
*Mn was forced out of the regression, as its inclusion resulted in a large reduction in the total RSQ value.
The regression equation for Y and Zr, with Mn included, was
$Y = 28.071 - 0.019\ P_2O_5 + 0.033$ Mn (RSQ = 0.340).
Zr = 314.523 − 36.784 Plagioclase + 2.610 Mn (RSQ = 0.341).

TABLE B38. SUMMARY OF STEPWISE REGRESSION ANALYSIS, SORTED-SANDY-GRAVEL UNIT

STEP NUMBER	VARIABLE ENTERED	VARIABLE REMOVED	MULTIPLE R	MULTIPLE RSQ	INCREASE IN RSQ	F VALUE TO ENTER OR REMOVE	COEFFICIENT
Ba							(CONSTANT 14.621)
1	QTZ		0.6501	0.4226	0.4226	16.1012	2.722
2	MN		0.7958	.6333	0.2107	12.0694	0.033
Co							
	NONE						
Cr							(CONSTANT 19.781)
1	ST DEV		0.4086	0.1669**	0.1669	4.4086	6.799
Cu							
	NONE						
Fe							(CONSTANT 0.568)
1	MN		0.7342	0.5391	0.5391	25.7334	0.007
2	P_2O_5		0.8345	0.6964	0.1573	10.8828	0.008
3	MG-CAL		0.8678	0.7531	0.0566	4.5858	−0.106
Mg							(CONSTANT −1.680)
1	MG-CAL		0.6506	0.4233	0.4233	16.1476	0.487
2	MN		0.7737	0.5986	0.1753	9.1712	0.010
3	QTZ		0.8397	0.7051	0.1065	7.2253	−0.496
Mn							(CONSTANT 216.500)
1	FE		0.7342	0.5391	0.5391	25.7334	51.360
Ni							(CONSTANT 6.759)
1	CALCIT		0.6169	0.3806**	0.3806	13.5193	0.096
Pb							
	NONE						
Sc							(CONSTANT 12.645)
1	RUTILE		0.7230	0.5228	0.5228	24.0985	0.299
2	QTZ		0.8013	0.6420	0.1192	6.9949	−0.229
3	ZOISIT		0.8385	0.7030	0.0610	4.1105	0.400
Sr							(CONSTANT 854.616)
1	QTZ		0.5559	0.3091**	0.3091	9.8410	−20.377
Ti*							(CONSTANT −1.230)
1	ST DEV		0.8234	0.6779	0.6779	39.9936	0.976
2	ZIRCON		0.9467	0.8961	0.2182	37.8213	0.012
3	MEAN		0.9579	0.9176	0.0215	4.4362	0.141
4	FE		0.9719	0.9446	0.0269	7.7793	0.044
V							(CONSTANT 35.170)
1	MN		0.7534	0.5677	0.5677	28.8874	0.018
2	EPIDOT		0.8680	0.7535	0.1858	15.8270	−0.212
3	HEAVYS		0.9134	0.8343	0.0808	9.7510	9.151
4	QTZ		0.9400	0.8836	0.0493	8.0413	−0.873
5	ZOISIT		0.9552	0.9125	0.0289	5.9491	1.393
Y							(CONSTANT 21.869)
1	RUTILE		0.6021	0.3626**	0.3626	12.5141	0.846
Zn							(CONSTANT 13.137)
1	RUTILE		0.7206	0.5192	0.5192	23.7603	0.572
Zr							
	NONE						
P_2O_5							(CONSTANT 775.307)
1	OPAQUE		0.7833	0.6136	0.6136	34.9404	5.163
2	ST DEV		0.8483	0.7197	0.1060	7.9429	98.773
3	ORTH		0.9028	0.8151	0.0954	10.3162	−5.163
4	TOURM		0.9285	0.8622	0.0471	6.4957	−21.449

** Excessive sum of squares remaining
* 3 anomalous samples (70636010, 018 and 023) removed

TABLE B39. SUMMARY OF STEPWISE REGRESSION ANALYSIS, UNSORTED-GRAVEL UNIT

STEP NUMBER	VARIABLE ENTERED	VARIABLE REMOVED	MULTIPLE R	MULTIPLE RSQ	INCREASE IN RSQ	F VALUE TO ENTER OR REMOVE	COEFFICIENT
Ba							(CONSTANT 17.557)
1	PLAG		0.6678	0.4459	0.4459	12.8755	4.831
2	SAND 1		0.8108	0.6575	0.2116	9.2648	1.280
3	MG-CAL		0.8693	0.7557	0.0983	5.6313	−1.867
4	RUTILE		0.9192	0.8450	0.0892	7.4832	5.355
Co							(CONSTANT 10.330)
1	DOLO		0.6587	0.4339	0.4339	12.2618	6.716
2	MG-CAL		0.7853	0.6167	0.1828	7.1550	−0.159
3	ARAG		0.8413	0.7078	0.0911	4.3639	0.360
Cr							(CONSTANT 63.064)
1	P_2O_5		0.6959	0.4842	0.4842	15.0221	−0.028
2	MG-CAL		0.8637	0.7460	0.2618	15.4600	−0.514
3	FE		0.9050	0.8191	0.0731	5.6528	
4	ZIRCON		0.9336	0.8716	0.0525	5.3122	−0.113
5	ARAG		0.9581	0.9180	0.0464	6.7961	1.002
6		FE	0.9445	0.8921	0.0259	0.0000	
7	$CACO_3$		0.9648	0.9307	0.387	6.6992	0.143
8	FE		0.9782	0.9568	0.0261	6.6538	0.290
Cu							
	NONE						
Fe							(CONSTANT 24.768)
1	HORNBL		0.6742	0.4545**	0.4545	13.3303	−0.753
Mg							(CONSTANT 0.988)
1	$CACO_3$		0.6168	0.3804	0.3804	9.8241	0.155
2	ZIRCON		0.7273	0.5289	0.1485	4.7281	0.059
Mn							(CONSTANT 1208.812)
1	PLAG		0.7294	0.5320	0.5320	18.1873	−44.020
2	DOLO		0.8032	0.6452	0.1132	4.7852	483.878
Ni							(CONSTANT 2.269)
1	PLAG		0.6232	0.3884	0.3884	10.1591	−0.435
2	FE		0.8511	0.7243	0.3360	18.2797	0.280
3	SAND 1		0.9073	0.8233	0.0990	7.8404	0.122
4	MG-CAL		0.9401	0.8838	0.0605	6.7641	−0.126

TABLE B39 (cont'd). SUMMARY OF STEPWISE REGRESSION ANALYSIS, UNSORTED-GRAVEL UNIT

STEP NUMBER	VARIABLE ENTERED	VARIABLE REMOVED	MULTIPLE R	MULTIPLE RSQ	INCREASE IN RSQ	F VALUE TO ENTER OR REMOVE	COEFFICIENT
Pb							(CONSTANT 13.109)
1	HEAVYS		0.5238	0.2744**	0.2744	6.0495	−2.663
Sc							(CONSTANT 14.547)
1	QTZ		0.7569	0.5729	0.5729	21.4590	−0.214
2	TOURM		0.8795	0.7735	0.2006	13.2878	0.113
3	HEAVYS		0.9459	0.8948	0.1213	16.1430	−0.719
4	GARNET		0.9671	0.9354	0.0406	8.1623	−0.263
Sr							(CONSTANT 678.815)
1	EPIDOT		0.7032	0.4945	0.4945	15.6532	−5.787
2	MEAN		0.7876	0.6203	0.1258	4.9708	62.517
3	ORTH		0.8620	0.7430	0.1227	6.6852	−22.437
Ti							(CONSTANT 1.891)
1	PLAG		0.7664	0.5874	0.5874	22.7783	0.072
2	P_2O_5		0.8621	0.7433	0.1559	9.1072	−0.002
3	ZOISIT		0.9025	0.8145	0.0713	5.3799	0.324
4	OPAQUE		0.9277	0.8607	0.0461	4.3041	0.021
5	FE		0.9542	0.9105	0.0499	6.6914	0.048
V							(CONSTANT 27.451)
1	FE		0.6573	0.4320	0.4320	12.1698	1.368
2	EPIDOT		0.7609	0.5790	0.1470	5.2372	−0.180
Y							
	NONE						
Zn							(CONSTANT −16.031)
1	FE		0.5693	0.3241	0.3241	7.6721	1.014
2	PLAG		0.8215	0.6748	0.3507	16.1801	0.896
3	SAND 1		0.8784	0.7716	0.0968	5.9313	0.263
Zr							(CONSTANT 853.079)
1	P_2O_5		0.6305	0.3976	0.3976	10.5589	−0.594
2	ZOISIT		0.7522	0.5657	0.1682	5.8093	83.130
P_2O_5							(CONSTANT 1399.738)
1	QTZ		0.7630	0.5822	0.5822	22.2940	−38.790
2	TOURM		0.8271	0.6840	0.1018	4.8350	19.314

**Excessive sum of squares remaining

APPENDIX B2
CLASSIFICATION OF SAMPLES (SAMPLE NOS. LISTED) INTO SEDIMENTARY UNITS AND DEPOSITIONAL ENVIRONMENTS
(sample locations are shown in Figure A21 in PART A)

UNSORTED GRAVEL (18)
Shallow-marine 196, 198, 215, 218, 220, 241, 242, 263, 264, 273, 286, 287, 295, 307, 308, 309, 311, 319.

SORTED SANDY GRAVEL (24)
Shallow-marine 67, 79, 101, 197, 216, 217, 221, 244, 245, 267, 268, 270, 289, 290, 291, 292, 293, 310, 312, 313, 314, 315, 317, 320.

SORTED SAND (75)
Shallow-marine 61, 66, 72, 80, 87, 88, 89, 96, 195, 199, 201, 243, 1269.
Open-intertidal 37, 41, 42, 47, 49, 50, 53, 54, 55, 56, 57, 59, 60, 62, 68, 69, 73, 75, 82, 90, 92, 98, 100, 114, 121, 129, 134, 136, 137, 144, 145, 151, 154, 156, 187, 188, 202, 209, 211, 213, 222, 223, 226, 238, 247, 248, 249, 250, 261, 274, 280, 281, 282, 284, 294, 296, 298, 304, 305, 306, 316.

PRIMARY UNSORTED MUDDY SAND (14)
Open-intertidal 4, 9, 10, 20, 21, 26, 31, 36, 40, 48, 108, 109, 111, 260.

MIXED UNSORTED MUDDY SAND (39)
Shallow-marine 97, 219, 237, 239, 246, 262, 271, 285, 318.
Open-intertidal 27, 71, 74, 76, 81, 83, 150, 214, 224, 236, 251, 272, 283, 297.
Mangrove-channel 332, 339, 342, 345, 346, 347, 348, 349, 350, 351, 352, 353, 356.
Mangrove-swamp 174, 252, 299.

MANGROVE SORTED MUD (49)
Open-intertidal 30, 122, 128.
Mangrove-channel 138, 141, 323, 324, 325, 329, 330, 331, 333, 335, 336, 337, 338, 340, 341, 343, 344, 354, 355.
Mangrove-swamp 35, 43, 46, 102, 123, 127, 140, 143, 147, 180, 203, 212, 225, 227, 228, 235, 255, 275, 276, 321.
Supratidal-flat 2, 103, 107, 162, 189, 253, 279.

MUDFLAT SORTED MUD (56)
Supratidal-flat 14, 19, 22, 32, 34, 38, 39, 44, 52, 64, 70, 77, 85, 86, 94, 104, 112, 116, 119, 120, 124, 130, 132, 133, 139, 142, 148, 149, 166, 167, 168, 169, 172, 173, 175, 176, 179, 182, 183, 184, 190, 191, 192, 193, 204, 205, 206, 208, 210, 230, 231, 232, 234, 277, 300, 302.

Samples removed
After Q-mode (14)
Open-intertidal — 58, 63, 181, 229; mangrove-channel — 326, 327, 334; mangrove-swamp — 84, 146, 303, 322; supratidal-flat — 45, 131, 153.
Before Q-mode (15)
Shallow-marine — 91, 155, 200, 240, 265, 266, 288; open-intertidal — 15, 65, 113, 152, 185, 194; supratidal-flat — 33, 207.

APPENDIX B3
FREQUENCY DISTRIBUTION PLOTS

Figures B14-21 are frequency distribution plots of 46 variables measured on the Broad Sound sediments. The distributions of the 10 variables that relate to the heavy-mineral content (Figures B20 and B21) were obtained by combining the samples from the unsorted-gravel, the sorted-sandy-gravel, and the sorted-sand units. The distributions of the other 36 variables represent the values of all the estuarine samples less the mangrove channel samples.

Each frequency distribution was plotted on the line printer using program VARPLOT (Mayo & Long, 1976), and the sample values for each variable were classified into intervals equal to ¼ of the standard deviation of that variable.

REFERENCE

MAYO, W., & LONG, K.A., 1976 — Documentation of BMR Geological Branch computer programs. *Bureau of Mineral Resources, Australia, Record* 1976/82 (unpublished); *BMR Microform* MF4.

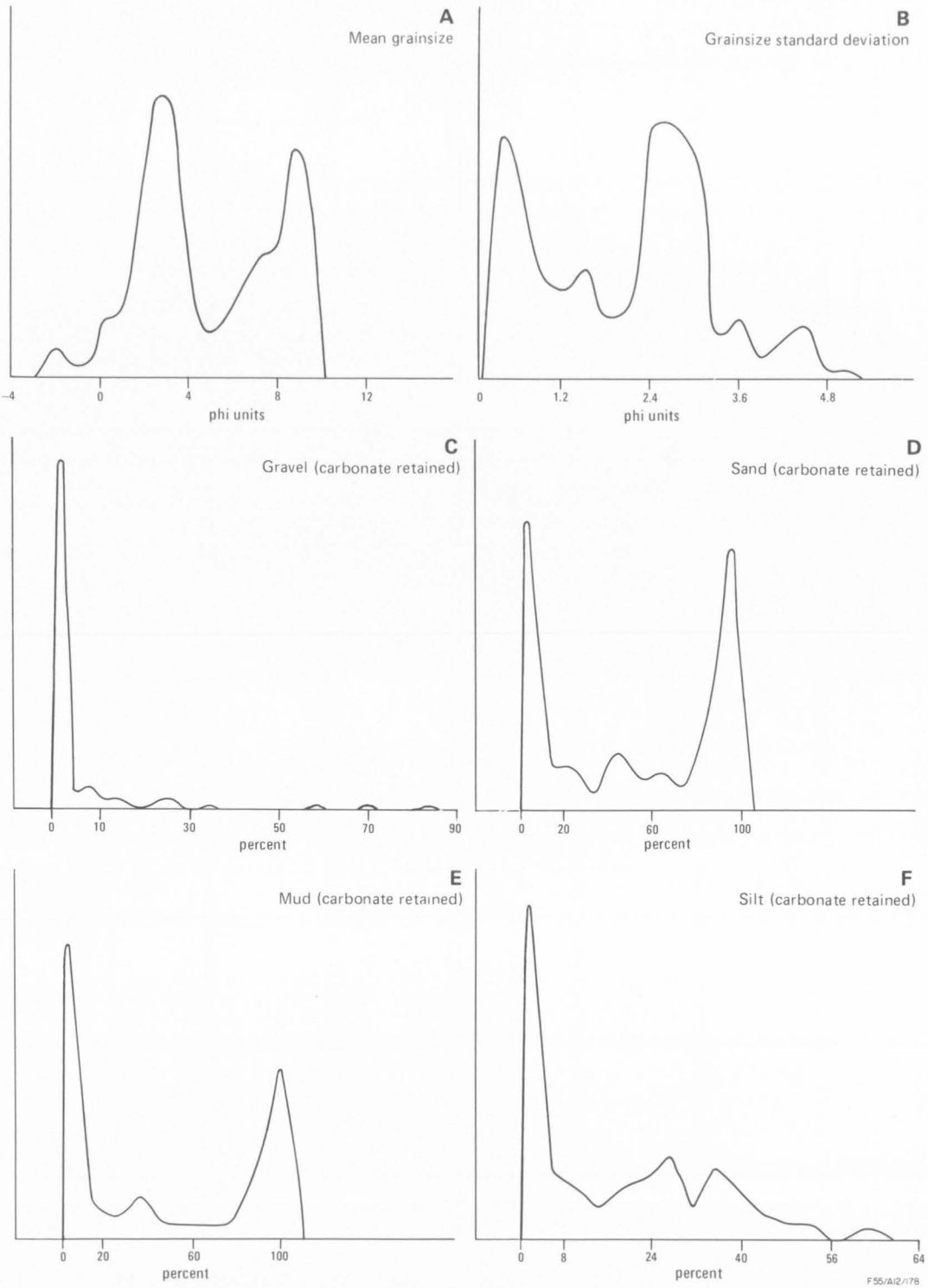


Fig. B14. Frequency-distribution plots, interpolated from computer-derived histogram data. Minimum and maximum values: A - −2.358, 10.083; B - 0.268, 5.086; C - zero, 82.99; D - zero, 100; E - zero, 100; F - zero, 65.15. The vertical axes denote frequency.

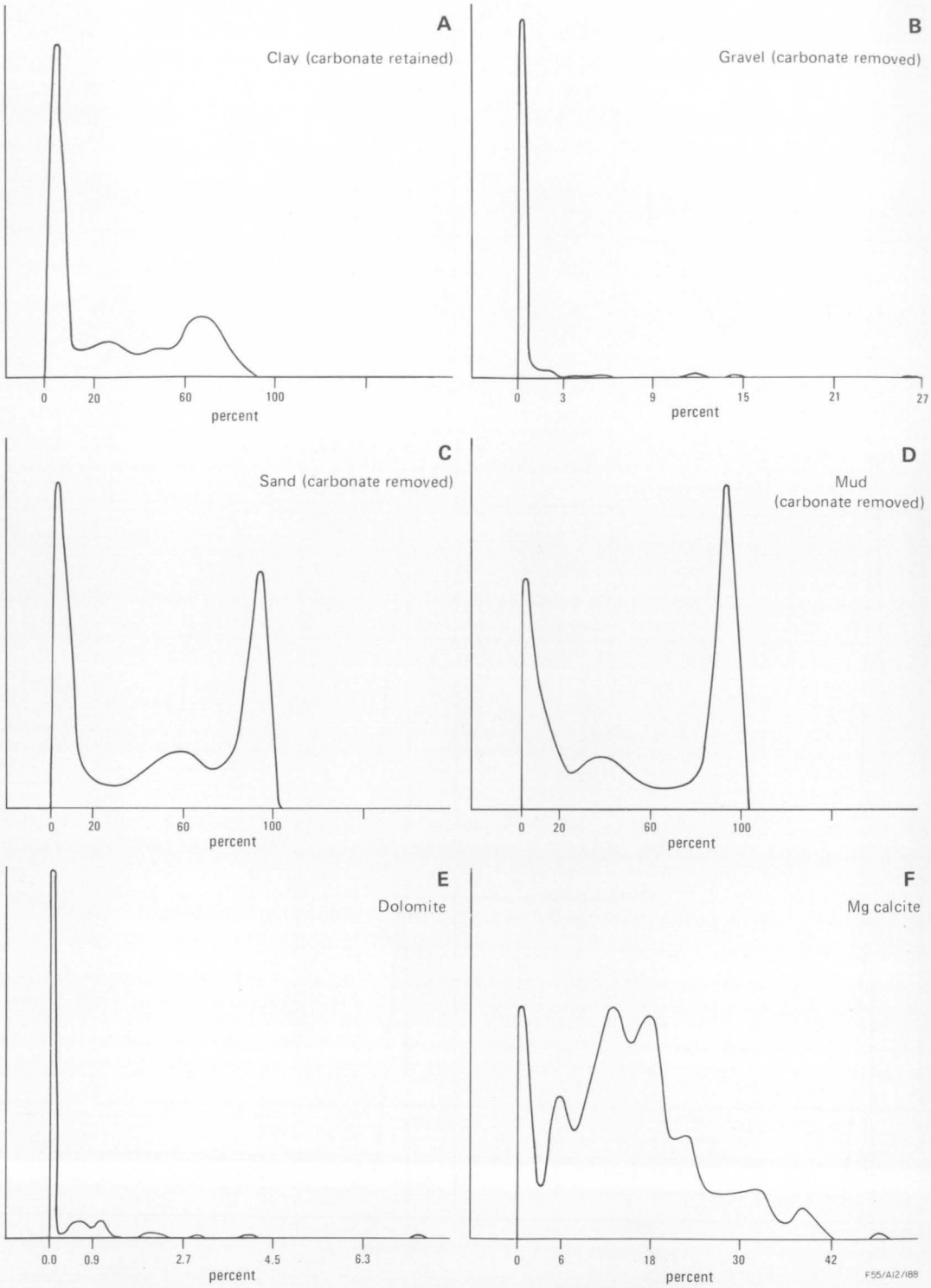


Fig. B15. Frequency-distribution plots, interpolated from computer-derived histogram data. Minimum and maximum values: A - zero, 88.65; B - zero, 26.04; C - zero, 100; D - zero, 100; E - zero, 7.47; F - zero, 49.32. The vertical axes denote frequency.

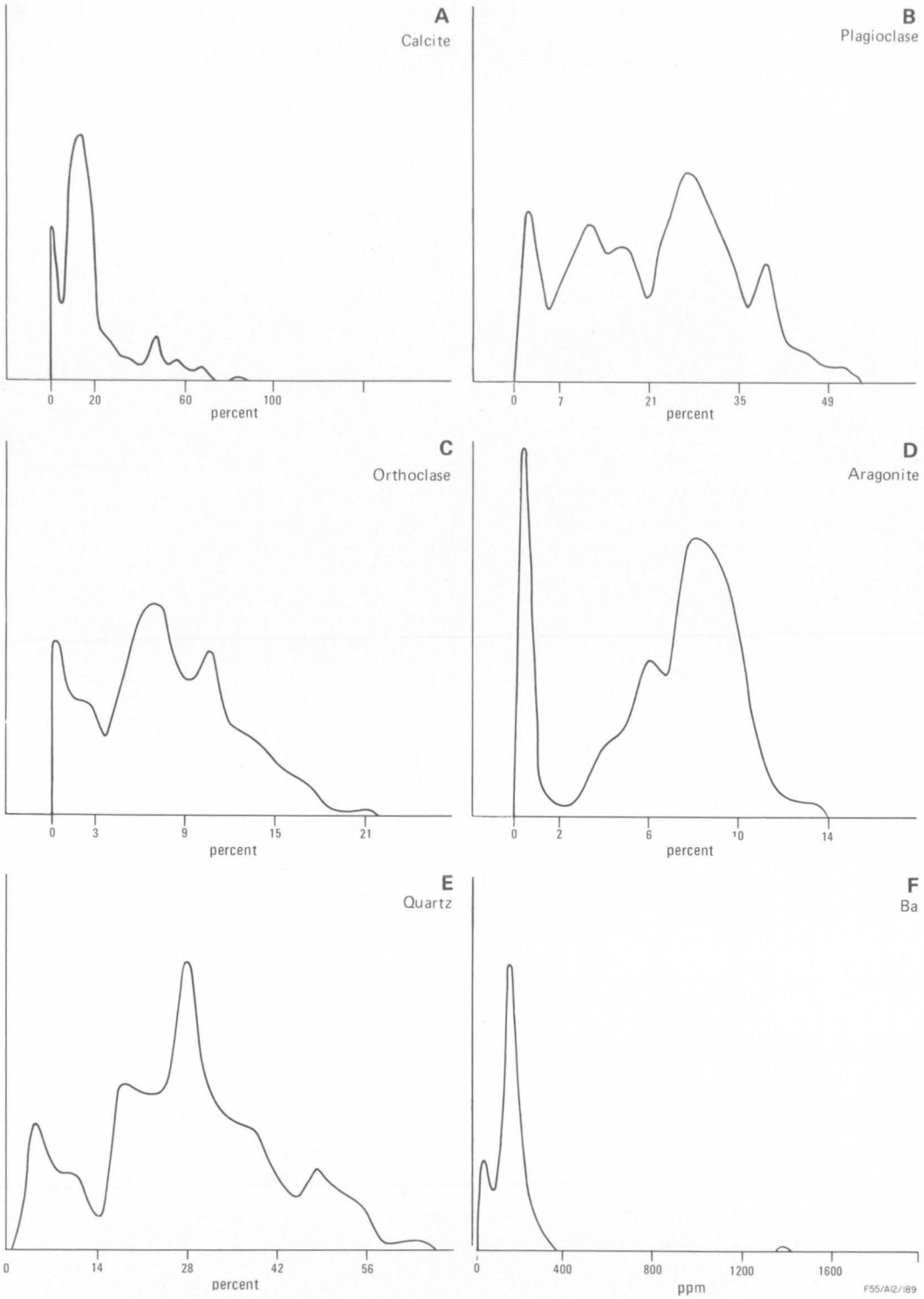


Fig. B16. Frequency-distribution plots, interpolated from computer-derived histogram data. Minimum and maximum values: A - zero, 87.15; B - 0.76, 52.21; C - zero, 22.13; D - zero, 13.26; E - 3.18, 67.04; F - 42, 1398. The vertical axes denote frequency.

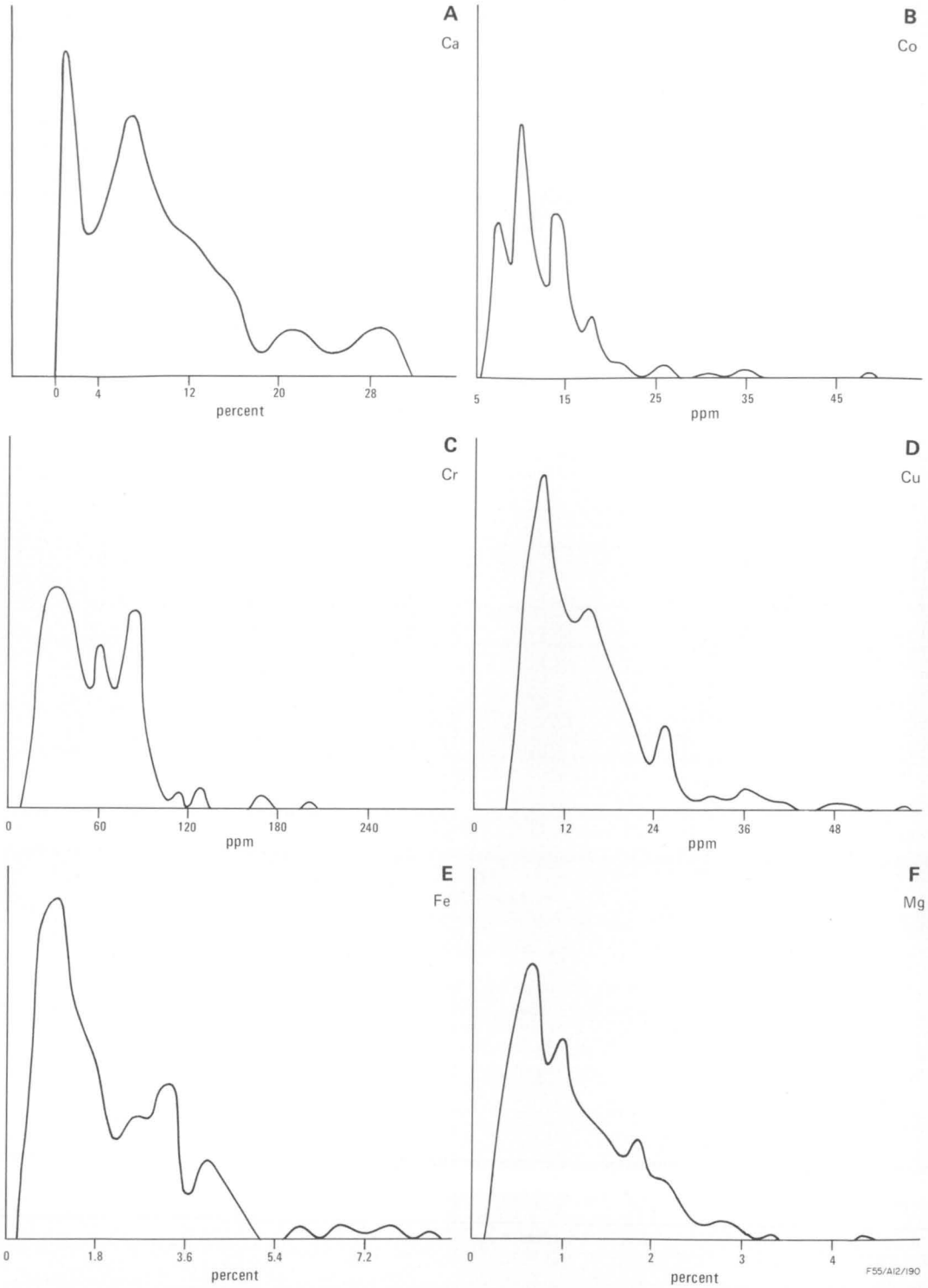


Fig. B17. Frequency-distribution plots, interpolated from computer-derived histogram data. Minimum and maximum values: A - 0.11, 30.90; B - 7.00, 49.00; C - 14.00, 200.00; D - 6.00, 57.00, E - 0.51, 8.36; F - 0.27, 4.41. The vertical axes denote frequency.

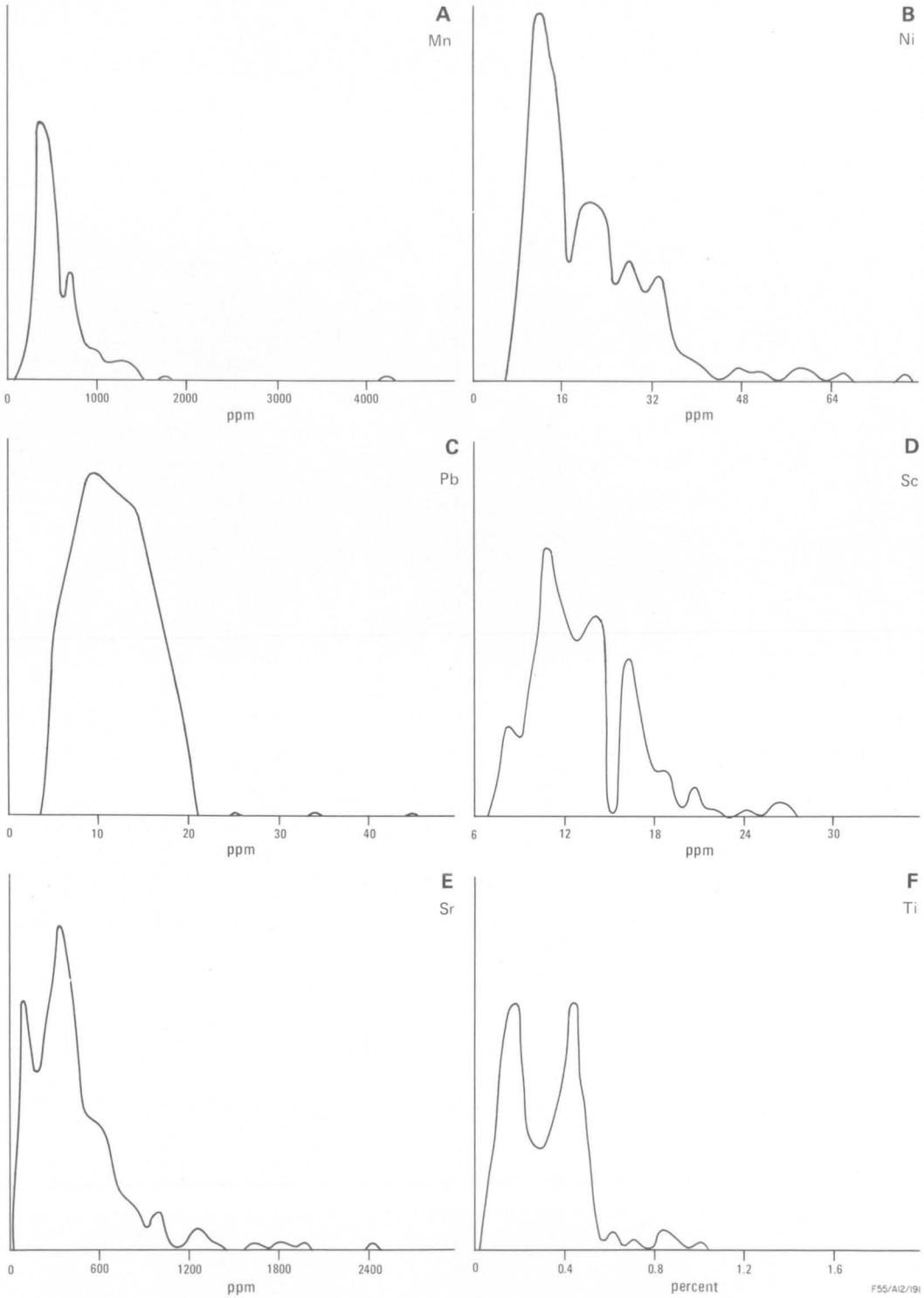


Fig. B18. Frequency-distribution plots, interpolated from computer-derived histogram data. Minimum and maximum values: A - 180, 4217; B - 8, 77; C - 5, 45; D - 7, 27; E - 72, 2486; F - 0.04, 1.01. The vertical axes denote frequency.

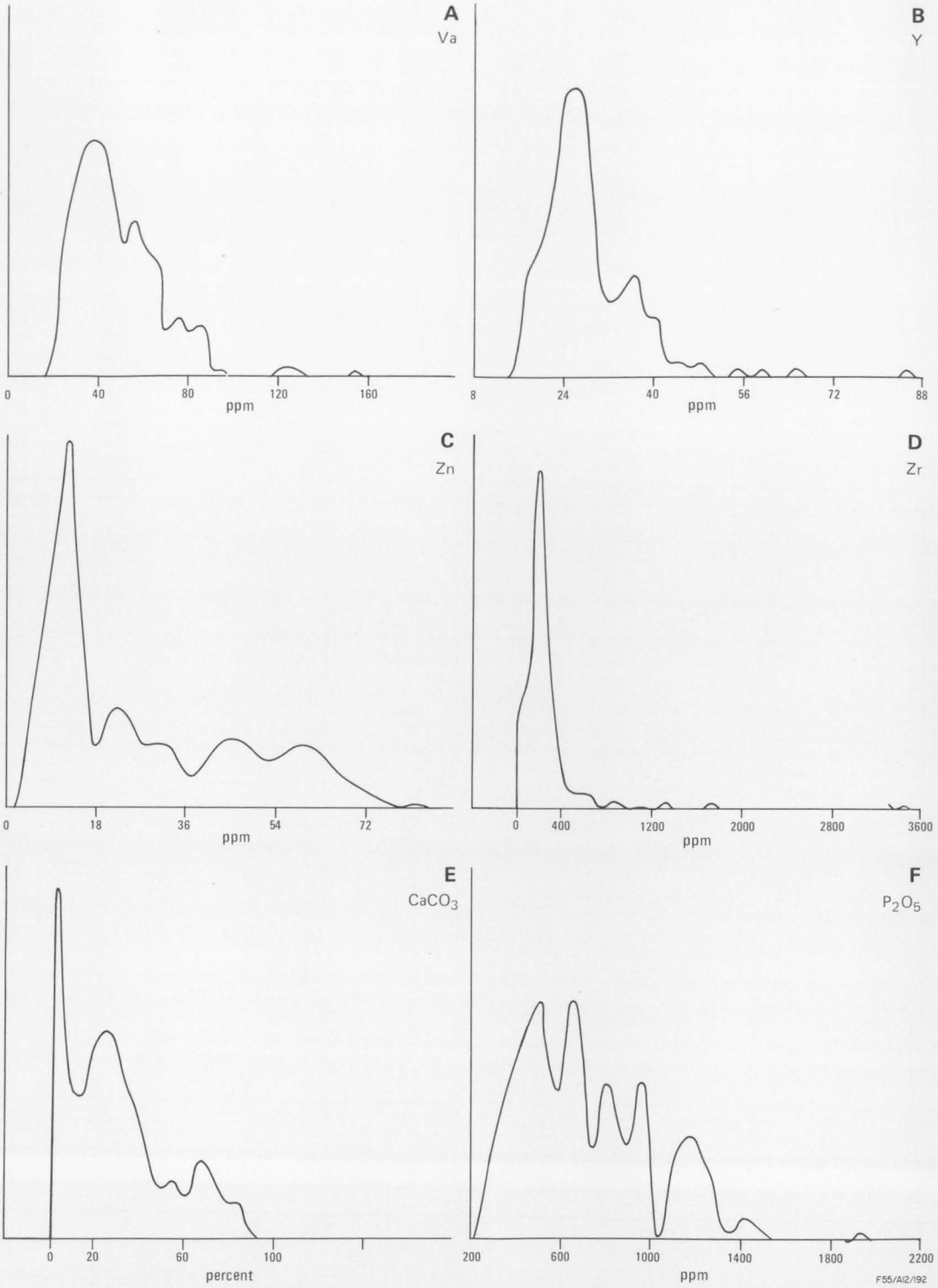


Fig. B19. Frequency-distribution plots, interpolated from computer-derived histogram data. Minimum and maximum values: A - 19, 154; B - 15, 85; C - 5, 85; D - 23, 3448; E - zero, 88.78; F - 260, 1900. The vertical axes denote frequency.

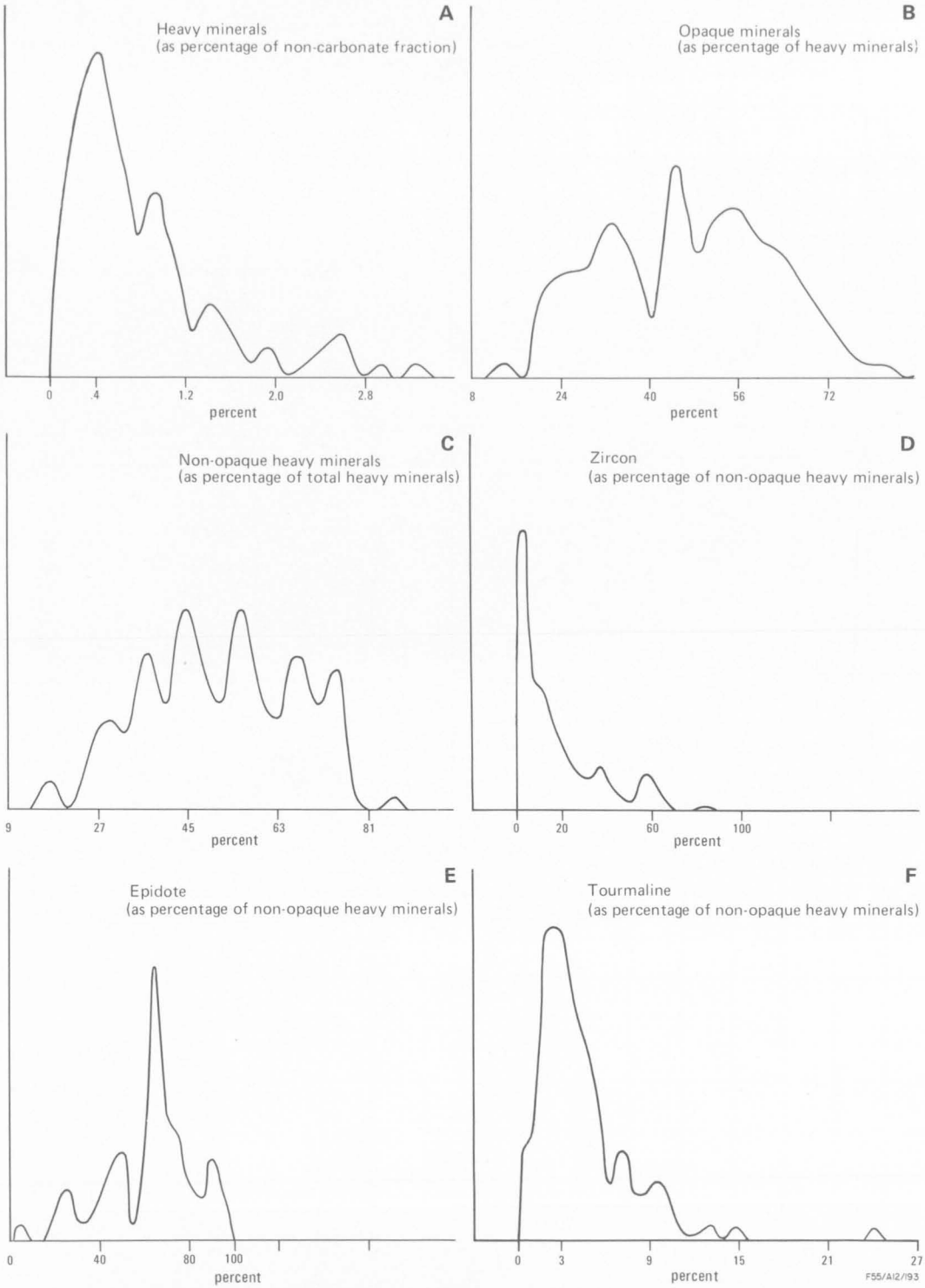


Fig. B20. Frequency-distribution plots, interpolated from computer-derived histogram data. Minimum and maximum values: A - 0.03, 3.35; B - 12.61, 83.92; C - 16.07, 87.39; D - zero, 87.18; E - 3.42, 96.58; F - zero, 24.44. O zero, 24.44. The vertical axes denote frequency.

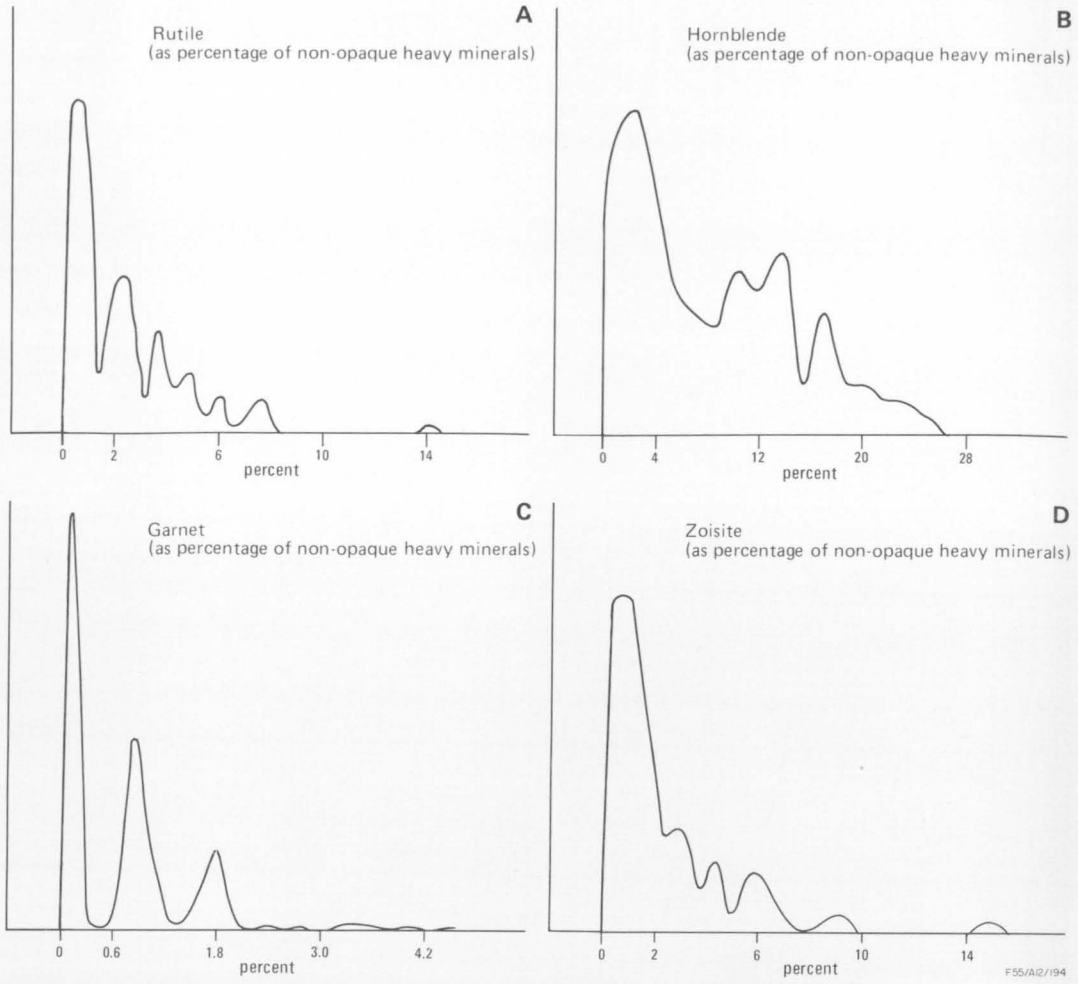


Fig. B21. Frequency-distribution plots, interpolated from computer-derived histogram data. Minimum and maximum values: A - zero, 14.04; B - zero, 25.00; C - zero, 4.46; D - zero, 15.24. The vertical axes denote frequency.

APPENDIX B4
AVAILABILITY OF DATA

The original estuarine sample data set may be obtained by writing to:

Director,
Bureau of Mineral Resources,
P.O. Box 378,
Canberra City,
A.C.T. 2601, AUSTRALIA.

In addition to the 46 variables indicated in Table B31, the original estuarine sample data set includes the following information on each sample:

SAMPLE NUMBER
GRID REFERENCE
RELATED CATCHMENT
FIELD ENVIRONMENT
SEDIMENTARY UNIT
GRAINSIZE SKEWNESS
GRAINSIZE KURTOSIS

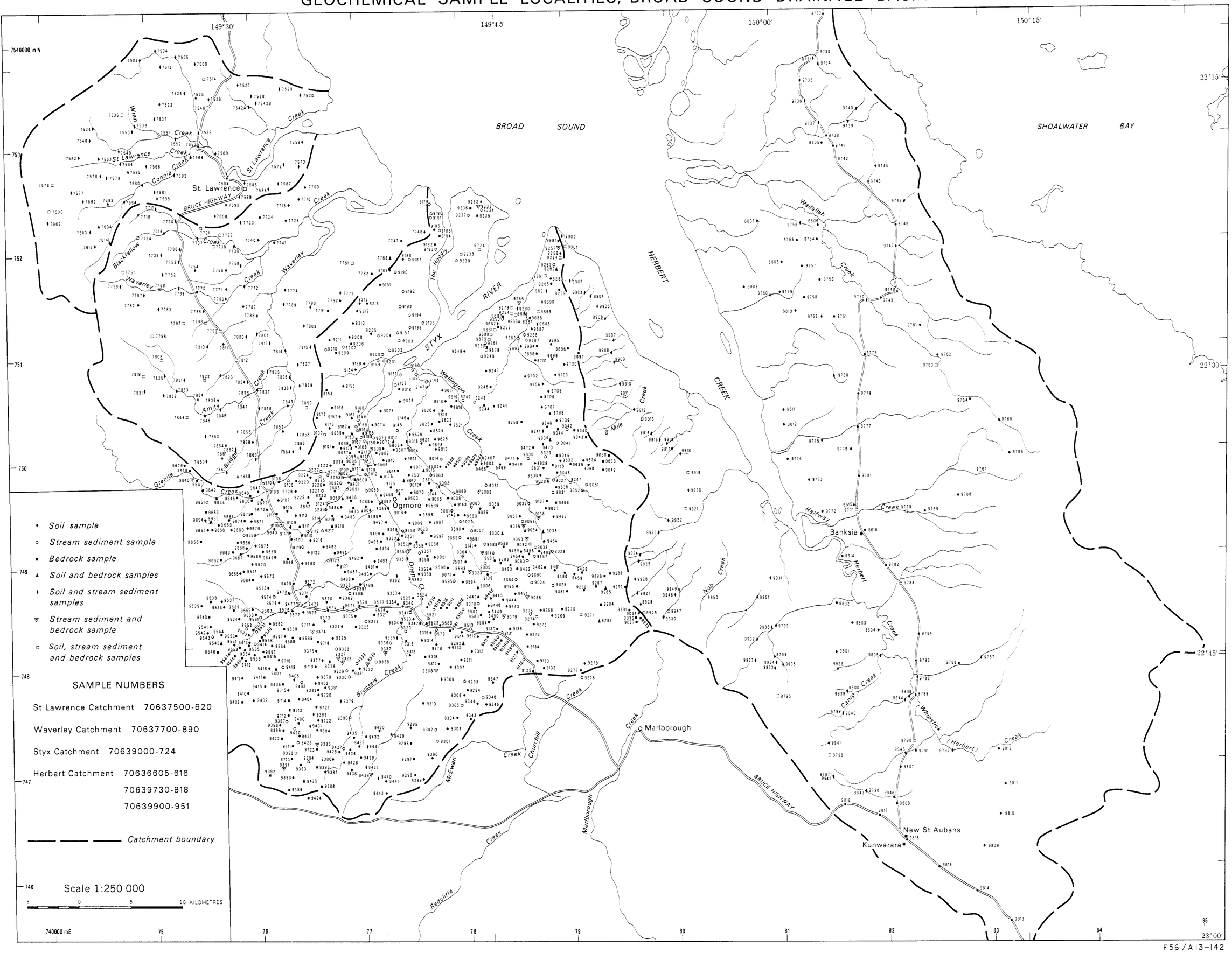
FACTOR LOADING 1
FACTOR LOADING 2
FACTOR LOADING 3
} Used in the sample classification plot (Fig. B4)

A computer listing of the correlation coefficients between each pair of variables for each sedimentary unit is also available on request.

R78/1766 Cat. No. 79 8079 6

GEOCHEMICAL SAMPLE LOCALITIES, BROAD SOUND DRAINAGE BASIN

PLATE A1


149°30′
149°45′
150°00′
150°15′
22°15′
22°30′
22°45′
23°00′
7540000 m N
753
752
751
750
749
748
747
746
740000 mE
75
76
77
78
79
80
81
82
83
84
85
BROAD SOUND
SHOALWATER BAY
HERBERT CREEK
St. Lawrence
Ogmore
Banksia
Marlborough
New St Aubans
Kunwarara
BRUCE HIGHWAY
BRUCE HIGHWAY
Warn Creek
St Lawrence Creek
Connie Creek
Creek
Blackfellow Creek
Waverley Creek
Waverley Creek
Creek
Creek

